

NSEL Report Series  
Report No. NSEL-017  
August 2009

---

# Behavior of Bolted Steel Slip-critical Connections with Fillers



**Daniel J. Borello**  
**Mark D. Denavit**  
**Jerome F. Hajjar**



Department of Civil and Environmental Engineering  
University of Illinois at Urbana-Champaign

UILU-ENG-2009-1805



ISSN: 1940-9826

The Newmark Structural Engineering Laboratory (NSEL) of the Department of Civil and Environmental Engineering at the University of Illinois at Urbana-Champaign has a long history of excellence in research and education that has contributed greatly to the state-of-the-art in civil engineering. Completed in 1967 and extended in 1971, the structural testing area of the laboratory has a versatile strong-floor/wall and a three-story clear height that can be used to carry out a wide range of tests of building materials, models, and structural systems. The laboratory is named for Dr. Nathan M. Newmark, an internationally known educator and engineer, who was the Head of the Department of Civil Engineering at the University of Illinois [1956-73] and the Chair of the Digital Computing Laboratory [1947-57]. He developed simple, yet powerful and widely used, methods for analyzing complex structures and assemblages subjected to a variety of static, dynamic, blast, and earthquake loadings. Dr. Newmark received numerous honors and awards for his achievements, including the prestigious National Medal of Science awarded in 1968 by President Lyndon B. Johnson. He was also one of the founding members of the National Academy of Engineering.

Contact:

Prof. B.F. Spencer, Jr.  
Director, Newmark Structural Engineering Laboratory  
2213 NCEL, MC-250  
205 North Mathews Ave.  
Urbana, IL 61801  
Telephone (217) 333-8630  
E-mail: bfs@uiuc.edu

*This work was supported by the American Institute of Steel Construction, W&W Steel Corporation, and the University of Illinois at Urbana-Champaign. In-kind funding was provided by Lohr Structural Fasteners. The authors thank G. A. Rassati and J. Swanson of the University of Cincinnati for conducting the ancillary bolt shear and tension tests; Prof. P. Dusicka of Oregon State University and Prof. G. Grondin of the University of Alberta for sharing data related to their research on bolted steel connections; Prof. J. Philips, Director of the 3,000,000 lb Testing Machine at the University of Illinois at Urbana-Champaign, for his extensive contributions to this research; and K. Elam, D. Foley, G. Banas, T. Prunkard, M. Bingham, and M. Parkolap of the University of Illinois at Urbana-Champaign for their pivotal contributions to the execution of the experiments. The authors also thank the members of the AISC Technical Advisory Panel (TAP) for their excellent contributions to this research, including T. Schlafly (TAP Chair and AISC Director of Research), C. J. Carter, and C. J. Duncan, AISC; S. Armbrust, T. Winneberger, and W. Lindley, W&W Steel Corporation; L. S. Muir and W. A. Thornton, Cives Engineering Corporation; L. A. Kloiber, LeJeune Steel Company; Prof. G. Grondin, U. of Alberta; G. Heathcock, FabArc Steel Supply, Inc.; and J. M. Fisher, Computerized Structural Design, S.C. Any opinions, findings, and conclusions or recommendations expressed in this material are those of the authors and do not necessarily reflect the views of the sponsors.*

*The cover photographs are used with permission. The Trans-Alaska Pipeline photograph was provided by Terra Galleria Photography (<http://www.terragalleria.com/>).*

# ABSTRACT

This document reports the results of sixteen experiments of bolted slip-critical connections with fillers. Fifteen of the connections used oversized holes and one connection used standard holes to establish a baseline comparison. Such connections with oversized holes are commonly fabricated for use with structures such as long-span trusses, since the use of oversized holes allows erection in-place rather than first assessing fit-up on the ground. Filler plates are used to connect members of different depths or widths. The *Specification for Structural Steel Buildings* of the American Institute of Steel Construction (AISC, 2005) currently requires connections with oversized holes to be designed as slip-critical at what is termed the “required strength level,” for which a resistance factor (LRFD)  $\phi$  of 0.85 and a safety factor  $\Omega$  (ASD) of 1.76 are specified. These slip strengths are typically below values that had been used for years in the *Specification for Structural Steel Buildings: Allowable Stress Design and Plastic Design* (AISC, 1989). In addition, when fillers are used in these connections, the AISC (2005) provisions do not require changes in the strength calculations, whereas if standard holes are used, options are provided for connection design that include reduction of the bolt shear strength or development of the connection.

The sixteen experiments reported herein highlight the behavior of bolted steel connections with oversized holes in which fillers are included and are undeveloped, partially developed, or fully developed. Both single-ply and two-ply filler are investigated, as are welded fillers, and specimens fabricated using either turn-of-the-nut or tension-controlled bolts. Extensive instrumentation was used on the specimens to document the flow of forces through the connection.

The results document the slip and shear strengths of these connections, propose formulas for assessing these strengths for the different conditions investigated, provide revised recommendations for design of these types of connections, and include suggestions for further work.

# Contents

CHAPTER 1 INTRODUCTION .....	1
1.1 Background .....	1
1.2 Objectives .....	4
1.3 Prior Work .....	5
CHAPTER 2 EXPERIMENTAL SPECIMENS.....	12
2.1 Specimen Description .....	12
2.2 Testing Machine and Procedure.....	17
2.3 Specimen Instrumentation .....	18
CHAPTER 3 ANCILLARY TESTS .....	22
3.1 Turn-of-Nut Bolts .....	22
3.2 Tension-Controlled Bolts.....	26
3.3 Slip Coefficient Tests.....	27
3.4 Material Properties.....	32
CHAPTER 4 EXPERIMENTAL RESULTS .....	33
4.1 Summary of Experimental Results .....	33
4.2 Typical Behavior.....	36
4.3 Slip Strength.....	60
4.4 Shear Strength.....	70
4.5 Development .....	80
CHAPTER 5 CONCLUSIONS .....	87
5.1 Slip .....	87
5.2 Shear .....	87
5.3 Development .....	88
5.4 Recommended Design Provisions .....	88
5.5 Recommendations for Future Work.....	90

REFERENCES .....	92
APPENDIX A CALCULATIONS OF NOMINAL, DESIGN, AND PREDICTED STRENGTHS .....	94
APPENDIX B INDIVIDUAL SPECIMEN RESULTS .....	120
APPENDIX C DETAILED COMPARISON OF SPECIMEN BEHAVIOR .....	294
APPENDIX D STATISTICAL ANALYSIS OF SLIP STRENGTH .....	308
APPENDIX E STEEL AND BOLT MATERIAL AND CALIBRATION REPORTS .	316
APPENDIX F 3,000,000-LB SOUTHWARK-EMERY TESTING MACHINE CALIBRATION REPORT .....	352

## INTRODUCTION

### 1.1 Background

Filler plates are used in bolted steel connections where hot-rolled structural steel members of different depths are joined. Filler plates are commonly found in long span truss connections, steel girders splices, and column splices. Figure 1 shows a typical bolted splice connection between two wide flange members of different depths, requiring filler plates. Limited research has been conducted on the effect of filler plates on the slip-critical resistance and shear strength in bearing of the connection. This report summarizes research conducted at the University of Illinois at Urbana-Champaign exploring the influence of filler plates on the behavior of bolted splice connections.

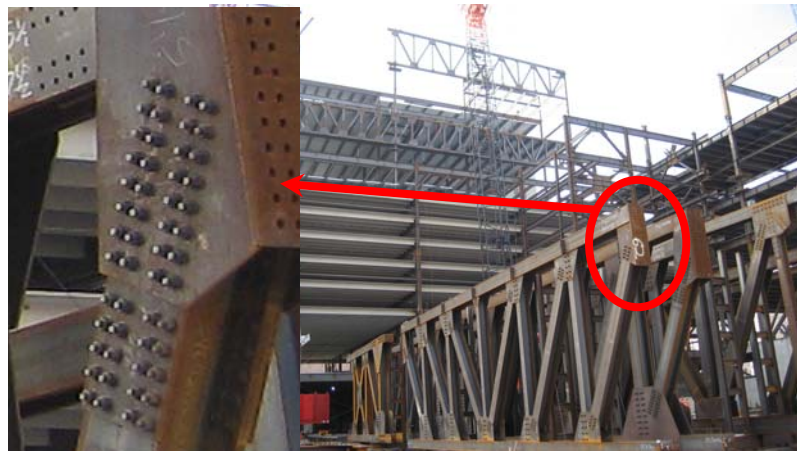


**Figure 1 – Example of filler plate connection in steel truss (from W&W Steel)**

Typical filler plate thicknesses range from 1/4 in. to 4 in. or larger. For long-span trusses in particular, recent fabrication and erection practices have favored the use of oversized holes in connections with fillers so that the trusses may be erected in place without first checking fit-up through a trial erection on the ground.

#### 1.1.1 AISC Design Provisions for Bolted Slip Critical Connections

The *Specification for Structural Steel Buildings* of the American Institute of Steel Construction (AISC) specifies in Section J3.8 on “High-Strength Bolts in Slip-Critical Connections” that all connections with oversized bolt holes must be designed as slip-critical connections (AISC, 2005). This section also distinguishes between connections designed as a “serviceability limit state,” for which a resistance factor (LRFD)  $\phi$  of 1.0 and a safety factor  $\Omega$  (ASD) of 1.5 are specified, and connections designed at the “required strength level”, for which a resistance factor (LRFD)  $\phi$  of 0.85 and a safety factor  $\Omega$  (ASD) of 1.76 are specified. The section indicates that connections with

oversized holes or slots parallel to the direction of force must be designed to prevent slip at the required strength level. For connections with standard holes, it would often be customary to design the connection as a serviceability limit state. The slip critical strength of bolted connections is given in these provisions as:

$$R_n = \mu h_{sc} D_u T_b N_s \quad (1)$$

where  $R_n$  is the slip-critical strength of a single bolt;  $\mu$  is the slip coefficient, equal to 0.33 for Class A surfaces and 0.5 for sand-blasted Class B surfaces (which is the value typically used for the bolted connections considered in this research);  $D_u$  equals 1.13 and is a multiplier that reflects the ratio of the mean installed bolt pretension to the specified minimum bolt pretension from Table J3.1;  $h_{sc}$  is a hole factor that equals 1.0 for standard holes, 0.85 for oversized holes, and 0.70 for long slotted holes and accounts for the potentially detrimental effects to the structure and attached non-structural elements after a connection slips into bearing;  $T_b$  is the specified minimum bolt pretension from Table J3.1 of AISC (2005); and  $N_s$  is the number of slip planes (implicitly, this is taken as the minimum number of primary slip planes, i.e., for the specimens tested in this research,  $N_s$  would be taken as 2, regardless of the number of fillers used in the connection).

Section J5 of the 2005 AISC *Specification* on “Fillers” then states the following regarding fillers:

In welded construction, any *filler* 1/4 in. (6 mm) or more in thickness shall extend beyond the edges of the *splice* plate and shall be welded to the part on which it is fitted with sufficient weld to transmit the splice plate *load*, applied at the surface of the filler. The welds joining the splice plate to the filler shall be sufficient to transmit the splice plate load and shall be long enough to avoid overloading the filler along the toe of the weld. Any filler less than 1/4 in. (6 mm) thick shall have its edges made flush with the edges of the splice plate and the weld size shall be the sum of the size necessary to carry the splice plus the thickness of the filler plate.

When a bolt that carries load passes through fillers that are equal to or less than 1/4 in. (6 mm) thick, the shear strength shall be used without reduction. When a bolt that carries load passes through fillers that are greater than 1/4 in. (6 mm) thick, one of the following requirements shall apply:

1. For fillers that are equal to or less than 3/4 in. (19 mm) thick, the shear strength of the bolts shall be multiplied by the factor  $[1 - 0.4(t - 0.25)]$  [S.I.:  $[1 - 0.0154(t - 6)]$ ], where  $t$  is the total thickness of the fillers up to 3/4 in. (19 mm);
2. The fillers shall be extended beyond the *joint* and the filler extension shall be secured with enough bolts to uniformly distribute the total *force* in the connected element over the combined cross section of the connected element and the fillers;

3. The size of the joint shall be increased to accommodate a number of bolts that is equivalent to the total number required in (2) above; or
4. The joint shall be designed to prevent *slip* at required strength levels in accordance with Section J3.8.

The AISC 2005 Specification Commentary for Section J5 states:

The practice of securing fillers by means of additional fasteners, so that they are, in effect, an integral part of a shear-connected component, is not required where a connection is designed for slip at member required strength levels. In such connections, the resistance to slip between the filler and either connected part is comparable to that which would exist between the connected parts if no filler were present. Filler plates may be used in lap joints of welded connections that splice parts of different thickness, or where there may be an offset in the joint.

The first of the four options listed for bolted connections is based on research by Frank and Yura (1981), who examined fillers that were between 1/4 in. and 3/4 in. thick. Therefore, this equation is not applicable for fillers larger than 3/4 in., currently eliminating the possibility of using the first option for large fillers. The second and third options pertain to developing the filler, which ensures that the filler acts integrally with one of the connected members. Developing the filler is accomplished by providing additional bolts to provide a more uniform stress distribution throughout the combined section of the connecting member and the filler plates. Fillers are considered to be fully developed if they secure the filler to the connected part using a number of bolts (or equivalent amount of weld) equal to or greater than the number of bolts in the connection times the ratio of the filler thickness to the total thickness of the filler and the connected part. The fourth option indicates that if connections are designed as slip critical at the required strength level, no further development or strength reductions are required. This fourth option would often require extra bolts for typical connections with standard holes, but is satisfied automatically for connections with oversized holes that satisfy the provisions of Section J3.8. Options 2 through 4 are available for connections with thick fillers. The research summarized in this report explores the effect of large fillers on the slip and shear strengths of a connection, as well as the effect of developing the filler plate.

The 1989 AISC *Specification for Structural Steel Buildings: Allowable Stress Design and Plastic Design* (AISC, 1989) had similar provisions to those in AISC (2005) with two important differences. First, the slip strength per bolt of surfaces with standard or oversized holes and Class B surfaces is based on multiplying the nominal area of the bolt shank by an allowable slip-critical stress obtained from the 1989 RCSC Specification (RCSC, 1989). These stress values equal 34 ksi for standard holes and 29 ksi for oversized holes (the ratio between the two approximately equaling 0.85). As will be seen in the calculations later in this report, the nominal slip-critical strength of connections with oversized holes provided by the 1989 AISC *Specification* is larger (approximately 24% larger for the case of the connections studied herein) than that provided in the 2005

AISC *Specification* using the ASD approach. Second, the fourth option available for connections with fillers in the 2005 *Specification* was worded in the 1989 *Specification* such that slip-critical connections did not need further development or strength reductions when using fillers.

The net result of these two changes is that a) connections with oversized holes require more bolts when designed using the 2005 *Specification* as compared to the 1989 *Specification*; and b) if a designer wants to avoid developing or reducing the bolt shear strength on a connection with standard holes, that connection must be designed at the required strength level; for this case, connections with standard holes that could be designed using 34 ksi in the 1989 *Specification* would thus need to be designed at the required strength level in the 2005 *Specification*. Similar to the slip-critical strength differences for oversized holes, for the connections studied in this work, designing the connections as slip-critical in the 1989 *Specification* using standard holes provides approximately 24% more strength than designing the connection in the 2005 *Specification* at the required strength level.

In addition, very few prior tests had been conducted on connections with fillers thicker than 3/4 in., or on connections that compared fully developed, partially developed, and undeveloped connections. It was thus unclear whether slip-critical connections with thick fillers need to be developed, whether slip-critical strength reductions are needed for connections with single-ply or multiple-ply fillers, and whether there is a difference between the behavior of slip-critical connections with standard and oversized holes, or with turn-of-the-nut (TN) versus tension-controlled (TC) bolts, in connections that use thick fillers.

## 1.2 Objectives

The objectives of this research include:

1. Assess the slip-critical strength of connections with thick fillers (single ply and multi-ply) using oversized holes. In particular, it will be investigated whether it is necessary both to have a hole factor,  $h_{sc}$ , and design connections with oversized holes at the required strength level (e.g.,  $\phi = 0.85$ ,  $\Omega = 1.76$ ) versus as a serviceability limit state (e.g.,  $\phi = 1.0$ ,  $\Omega = 1.50$ ). Only Class B surfaces are tested in this work, although some specimens from the literature that are studied include Class A surfaces.
2. Assess the bolt shear strength of bearing connections with thick fillers (single ply and multi-ply) using oversized holes, and update the bolt shear strength reduction equation of Section J5 if appropriate (recognizing that, as the AISC 2005 provisions are currently written, the formula is only appropriate for use with connections with standard holes).
3. Determine if connection development affects the slip-critical or bolt shear strength of connections with thick fillers using oversized holes (recognizing that, as the AISC 2005 provisions are currently written, development does not

affect slip-critical strength and for bearing connections is appropriate for consideration only for connections with standard holes).

Through comparisons with prior research (e.g., Lee and Fisher, 1968; Frank and Yura, 1981; Dusicka and Lewis, 2007; Grondin et al., 2008), this research will be extended to connections with thinner fillers, standard holes, or up to three plies of fillers.

### **1.3 Prior Work**

Early research on the effect of fillers in bolted connections included a series of tests conducted at Dorman Long and Company in 1965 in which washers were used as fillers in a bolted splice connection. These tests were described in a report by Lee and Fisher (1968), who conducted experiments on the slip behavior of bolted connection with fillers.

The study by Lee and Fisher (1968) was originally intended to determine the effect of contact area on slip resistance. The test specimens consisted of two central pull plates and two outer lap plates loaded in tension until the bolts came into bearing. The contact area was controlled by the size of washer added between the two plates. In the first phase of research, it was concluded that contact area had little effect on the slip strength of these connections but there was a significant decrease in slip strength between the specimens with washers added and control specimens without washers. In the second phase of testing, this unexpected decrease in strength was investigated further. The testing included four sets of triplicate specimens with filler plates, rather than washers, and one set of triplicate specimens without fillers. The specimens with washers will be excluded from this discussion.

A typical specimen is shown in Figure 2. All specimens had standard size bolt holes with four 7/8 in. A325 bolts in line, which were tightened to a specified pretension based on torqued tension curves. Filler plates of three different thicknesses (1/16 in., 1/2 in. and 1 in) in addition to control connections without fillers were tested. For three of the specimens with 1/2 in. thick filler plates, the filler plate was tack welded to one of the connecting plates. The slip load was defined as the load at which a sudden definite slip occurred, or in the cases without sudden slip, the load at which the load vs. elongation response deviated from linear. The experimental results are summarized in Table 1. The values of predicted slip strength were calculated as the product of the published clamping force, an average slip coefficient for blast-cleaned surfaces, 0.525 (Grondin et al., 2008), the number of slip planes (equal to 2, independent of the number of filler plates), and the number of bolts. The slip strength of the specimens with fillers was found to be approximately 20% less than that of the control specimens (Specimens SCA1), independent of filler thickness or tack welding.

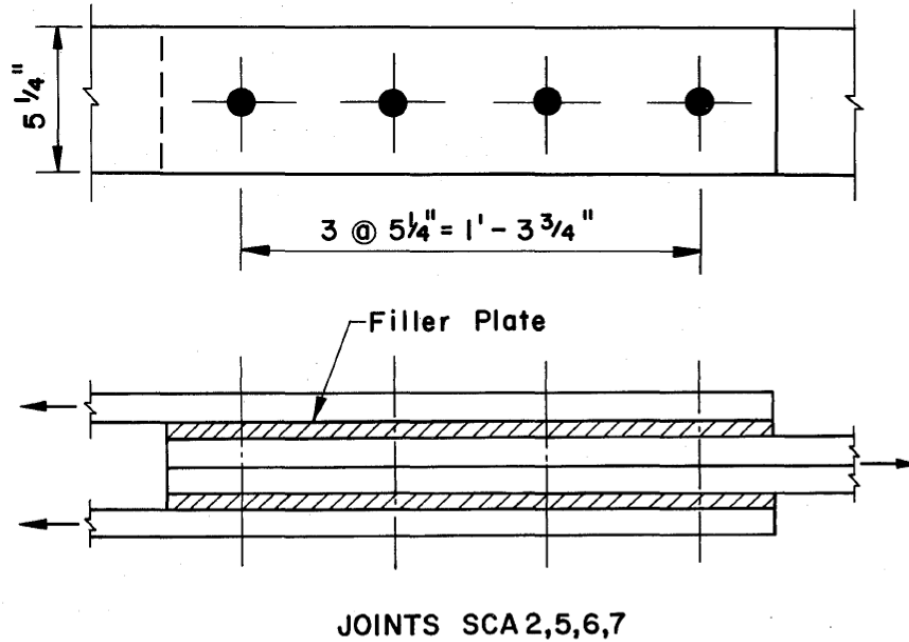


**Figure 2 – Lee and Fisher (1968) typical test specimen [from Lee and Fisher, 1968]**

**Table 1 – Lee and Fisher (1968) test results**

Specimen Name	Description	Predicted Slip Strength (kips)	Measured Slip Strength (kips)	Slip Test-to-Predicted Ratio
SCA1-1	Blast-cleaned faying surface	151	170	1.12
SCA1-2		151	200	1.32
SCA1-3		151	190	1.26
SCA2-1	Blast-cleaned with 1/2 in. filler plate	151	120	0.79
SCA2-2		151	100	0.66
SCA2-3		151	100	0.66
SCA5-1	Blast-cleaned with 1/2 in. filler plate tack-welded	151	110	0.73
SCA5-2		151	130	0.86
SCA5-3		151	80	0.53
SCA6-1	Blast-cleaned with 1/16 in. filler plate	151	135	0.89
SCA6-2		151	165	1.09
SCA6-3		151	160	1.06
SCA7-1	Blast-cleaned with 1 in. filler plate	151	163	1.08
SCA7-2		151	147	0.97
SCA7-3		151	155	1.03

As part of a larger research effort, Frank and Yura (1981) studied the effect of undeveloped fillers on the connection slip strength and bolt shear strength. They conducted five sets of duplicate tests with varying filler thickness using standard size bolt holes and Class A slip surfaces. The test specimens (shown in Figure 3) consisted of two central pull plates and two outer splice plates. One side had two bolts in line with an undeveloped filler and the other had three bolts in line with a fully developed filler. The tests were conducted in tension and all significant behavior occurred on the two bolt side. The filler plates were of lower strength than the other plates so as to increase connection flexibility and provide lower ultimate loads. The five sets of duplicates represented different filler thicknesses: no fill, 0.075 in., 0.25 in., 0.75 in. made of a single plate, and 0.75 in. made of three 0.25 in. plates (i.e., multiple plies). The experimental results are summarized in Table 2. The values of predicted slip strength were calculated as the product of the published clamping force, an average slip coefficient for clean mill scale surfaces, 0.338 (Grondin et al., 2008), the number of slip planes (equal to 2, independent of the number of filler plates), and the number of bolts. The values of predicted shear were calculated as the product of the measured shear strength for the bolt (from their ancillary bolt shear tests) and the number of bolts.

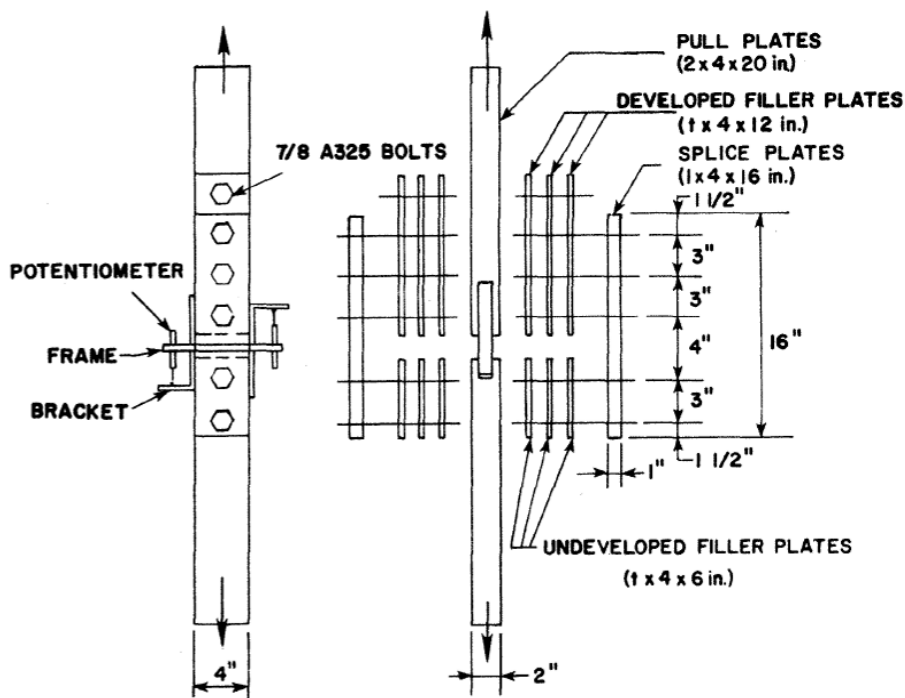


Figure 3 – Frank and Yura (1981) typical test specimen [from Frank and Yura, 1981]

**Table 2 – Frank and Yura (1981) test results**

<b>Filler Thickness (in)</b>	<b>Number of Plies on One Side of Connection</b>	<b>Predicted Slip Strength (kips)</b>	<b>Measured Slip Strength (kips)</b>	<b>Slip Test-to-Predicted Ratio</b>	<b>Predicted Shear Strength (kips)</b>	<b>Measured Shear Strength (kips)</b>	<b>Shear Test-to-Predicted Ratio</b>
0	0	58.5	52	0.89	184.0	190.1	1.03
0	0	60.2	62	1.03	184.0	178.9	0.97
0.075	1	-	-	-	184.0	174.6	0.95
0.075	1	-	-	-	184.0	183.8	1.00
0.25	1	58.9	44	0.75	181.6	178.9	0.99
0.25	1	58.8	50	0.85	181.6	180.2	0.99
0.75	3	72.2	41	0.57	198.4	169.9	0.86
0.75	3	70.0	32	0.46	198.4	172.6	0.87
0.75	1	-	-	-	198.4	177.3	0.89
0.75	1	-	-	-	198.4	170.8	0.86

The 0.075 in. and 0.75 in thick plates did not have clean mill scale surfaces, as all other surfaces did, thus the slip behavior of only the no fill, 0.25 in., and 3x0.25in. connections were reported. Consistent with the observations of Lee and Fisher (1968), the addition of a filler plate reduced the slip resistance by approximately 17%. However, the specimens with multiple ply filler plates experienced a more drastic reduction in slip resistance, 46% below that of no fillers. A direct comparison of slip strengths of connections with fillers of different thicknesses could not be performed.

A reduction in the shear strength of the connection due the presence of fillers was also noted. The shear strength of the connections without fillers was predicted well by the results of ancillary bolts shear tests. The shear strength of connections with fillers decreased with increasing filler thickness. The reduction in shear strength was attributed to bolt bending. Of the specimens with 0.75 in thick fillers, the multiple ply filler showed slightly lower shear strength. It was hypothesized that the solid, single plate filler offered more resistance to bolt bending, and therefore the behavior was less detrimental to the bolt. It was further noted that significant bearing deformations occurred in the 0.75 in. thick fillers and that if the filler was of higher strength steel, more resistance to bolt bending would have been achieved, resulting in a higher ultimate load.

Based on these observations, an empirical equation for the shear strength reduction was developed as a linear function of filler thickness. However, rather than using the ultimate strength of the connection as the measured response, the applied load at a deformation of 0.25 in. was used to develop the equation. This equation is the basis for the bolt shear strength reduction formulation in Section J5 of the *AISC Specification* (AISC, 2005).

The limit of applicability of this equation (0.25 in. to 0.75 in.) is based on the range of filler thicknesses in this series of experiments.

Since all significant behavior occurred on the side of the specimen with undeveloped filler plates, no quantitative comparisons could be made between undeveloped and developed fillers.

In recent work by Dusicka and Lewis (2007), a series of bolted connections with filler plates were tested. A total of 28 sets of duplicate tests were performed with various filler thicknesses, hole sizes, bolt grades, surface preparations, numbers of bolts, and numbers of filler plies. A typical specimen is shown in Figure 4. The specimens consisted of two central pull plates and two outer splice plates, all made from ASTM A709 HPS70W high strength steel to investigate the effect of using high strength steel on the bearing strength of connections with fillers. One side of the specimen had four bolts in line and a developed filler, while the other side had either a single bolt or three bolts in line and an undeveloped filler. All fillers were made from ASTM A709 Grade 50W steel. The tests were conducted in tension and all significant behavior occurred on the side with the undeveloped filler. The experimental results are summarized in Table 3. The predicted slip strength was calculated as the product of the expected pretension from the torque tension curves, a average slip coefficient for blast-cleaned surfaces, 0.525 (Grondin et al., 2008), the number of slip planes (equal to 2, independent of the number of filler plates), and the number of bolts. Ancillary bolt shear tests were not conducted on the lots of bolts, but ancillary torqued tension tests were conducted on each lot of bolts. Without ancillary bolt shear tests, the predicted shear strength of one bolt was taken as the average of the two no-filler, standard hole, single bolts tests. Since multiple lots of bolts were used, this value was then adjusted by the ratio of the plateau force from the torqued tension test of the specific lot to the plateau force from the torqued tension test of the lot from which the bolts in the no-filler, standard hole, single bolts specimen came. This value was then multiplied by the number of bolts in the specimen to determine the predicted bolt shear strength. Since the data presented in Dusicka and Lewis is reported in a preliminary fashion and includes limited ancillary data, results and figures in this report are presented with and without the work by Dusicka and Lewis (2007).

Consistent with the prior experiments, a reduction in both slip strength and shear strength was observed in the presence of a filler. However, the lowest ultimate strength was observed for the 1 in. thick filler; the 2 in. thick filler achieved a higher ultimate strength. This indicates that there is likely to be a thickness (or relation between thickness and hole diameter) that provides a worst case for prematurely failing the bolt, and at that point the strength reduction does not continue to increase with increasing filler thickness. This was attributed to restraint of the bolt within the large thickness of the filler. It was noted that if multiple plies were used, that restraint would not be as significant, and the degradation would continue with an increase in filler thickness. Slip strengths were consistently lower for connections with fillers, with a larger decrease for multiple plies. Further investigation was suggested to determine the cause of the lower slip strength.

Earlier work published in Japanese by Miyachi and Koeda (1999), Takizawa et al. (1999), Sugiyama et al. (2001), and Kanda et al. (2006) compliments the studies

summarized herein. Each of these studies included a series of tests similar to those already presented. The tests were all conducted in tension. The specimens consisted of two central pull plates, outer splice plates, and undeveloped fillers with thicknesses varying between 0.126 in. (3.2 mm) and 0.866 in. (22 mm).

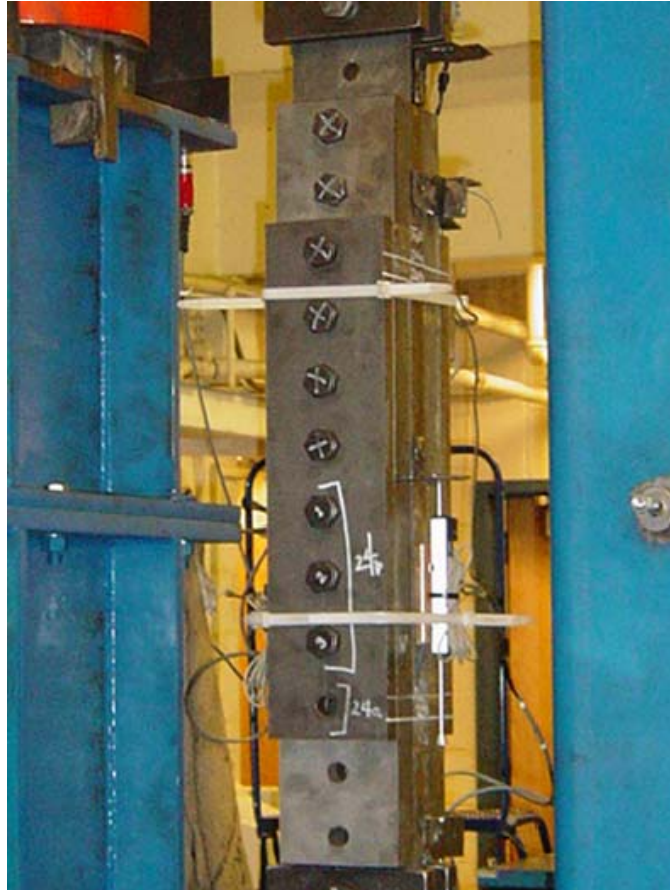


**Figure 4 – Dusicka and Lewis (2007) typical test specimen [from (Dusicka and Lewis, 2007)]**

**Table 3 – Dusicka and Lewis (2007) test results**

Filler Thickness (in)	Hole Size	Number of Bolts	Predicted Slip Strength (kips)	Measured Slip Strength (kips)	Slip Test-to-Predicted Ratio	Predicted Shear Strength (kips)	Measured Shear Strength (kips)	Shear Test-to-Predicted Ratio
0	std	1	67.6	54.8	0.81	137.3	133.7	0.97
0	std	1	67.6	64.5	0.95	137.3	140.9	1.03
1/2	std	1	67.6	35.5	0.53	137.3	122.1	0.89
1/2	std	1	67.6	51.6	0.76	137.3	135.3	0.99
1	std	1	68.9	60.7	0.88	139.3	124.8	0.90
1	std	1	68.9	60.7	0.88	139.3	131.6	0.94
2	std	1	69.9	44.0	0.63	143.2	131.6	0.92
2	std	1	69.9	47.1	0.67	143.2	137.0	0.96
2 x 1/4 = 1/2	std	1	67.6	31.4	0.46	137.3	125.7	0.92
2 x 1/4 = 1/2	std	1	67.6	35.6	0.53	137.3	126.4	0.92
4 x 1/4 = 1	std	1	68.9	30.0	0.44	139.3	95.0	0.68
4 x 1/4 = 1	std	1	68.9	36.5	0.53	139.3	106.8	0.77
0	over	1	67.6	32.9	0.49	137.3	127.4	0.93
0	over	1	67.6	36.3	0.54	137.3	129.5	0.94
1/2	over	1	67.6	64.4	0.95	137.3	133.2	0.97
1/2	over	1	67.6	71.7	1.06	137.3	141.1	1.03
1	over	1	68.9	40.9	0.59	139.3	121.3	0.87
1	over	1	68.9	43.8	0.64	139.3	124.5	0.89
2	over	1	69.9	26.0	0.37	143.2	141.4	0.99
2	over	1	69.9	46.2	0.66	143.2	141.4	0.99
0	std	3	202.9	142.9	0.70	411.9	390.4	0.95
0	std	3	202.9	172.8	0.85	411.9	405.4	0.98
1/2	std	3	202.9	64.8	0.32	411.9	375.4	0.91
1/2	std	3	202.9	125.5	0.62	411.9	377.7	0.92
1	std	3	206.6	99.9	0.48	417.9	354.0	0.85
1	std	3	206.6	121.0	0.59	417.9	369.6	0.88
2	std	3	209.8	57.6	0.27	429.6	378.8	0.88
2	std	3	209.8	60.2	0.29	429.6	384.0	0.89
2 x 1/4 = 1/2	std	3	202.9	56.7	0.28	411.9	358.7	0.87
2 x 1/4 = 1/2	std	3	202.9	78.4	0.39	411.9	374.2	0.91
4 x 1/4 = 1	std	3	206.6	34.8	0.17	417.9	283.7	0.68
4 x 1/4 = 1	std	3	206.6	57.8	0.28	417.9	299.2	0.72
0	over	3	202.9	88.7	0.44	411.9	359.8	0.87
0	over	3	202.9	94.6	0.47	411.9	378.8	0.92
1/2	over	3	202.9	59.2	0.29	411.9	371.3	0.90
1/2	over	3	202.9	115.3	0.57	411.9	382.3	0.93
1	over	3	206.6	66.9	0.32	417.9	347.7	0.83
1	over	3	206.6	99.3	0.48	417.9	347.7	0.83
2	over	3	209.8	92.6	0.44	429.6	355.2	0.83
2	over	3	209.8	118.6	0.57	429.6	391.0	0.91

# EXPERIMENTAL SPECIMENS

## 2.1 Specimen Description

The specimens tested in this research were designed to replicate common connections. The benchmark connection was a bolted splice connection between wide-flange members of different depths, consistent with connections used in long span trusses. Sixteen specimens were tested. The specimens were designed to explore the effect of filler thickness, filler development, filler development method and bolt pretension method. The specimen test matrix is show in Table 4. In contrast to most previous studies, the specimens were tested in compression due to the fact that testing connections in tension at this scale would have been prohibitive due to cost. In addition, these types of connections are generally subjected to compression as well as tension in the field, and investigation of compression forces are warranted. Prior testing in the literature (e.g., Wallaert and Fisher, 1965; Kulak et al., 2001) on smaller-scale specimens with potentially different eccentricities and stress patterns from the specimens tested in this work has indicated that specimens tested in tension may fail approximately 10% earlier than specimens tested in compression due to prying of the lap plates in these specimens. However, eccentricities, prying forces, affects of Poisson's ratio, and possible strength reductions of these types of connections in compression versus in tension are complex, with both types of loading causing potential detrimental effects, and it is deemed that these tests in compression are appropriate for comparison with prior research on bolted connections.

The specimens were identified based on the top column nominal weight, development, and unique details. Where duplicate specimens were tested, an additional incremental number was added to the end of the name. For example, the second undeveloped specimen with a W14x159 top column was identified as 159n2. The bolt hole rows were labeled based on their geographic location in the testing machine and elevation in the top column. The bottom bolt row in the top column was bolt row 1. For example, the bolt second from the bottom in the top column in the northwest flange tip was identified as NW2.

Each specimen consisted of two wide-flange members, connected by 2 in. thick splice plates (Figure 5). Where required, filler plates were used to provide a constant connection depth (Figure 6). The bottom column for all specimens was a W14x730. The top column was a W14x159, W14x455, or W14x730. The W14x159 and W14x455 top column specimens required a filler plate of 3 3/4 in. and 1 5/8 in. respectively; the precise difference in the depths of these columns as compared to the W14x730 was 7.4 in. (3.7 in. each side) and 3.4 in. (1.7 in. each side) for the W14x159 and W14x455 respectively. All surfaces of the specimens were blasted to a Class B surface using a compressed air

nozzle and G40 (type GL) steel grit size steel shot. The resulting surface profile met SSPC SP6 and measured 3.57 mils (with a 0.43 mil standard deviation) using pressofilm tape.

**Table 4 – UIUC specimen test matrix**

<b>UIUC Specimen Name</b>	<b>Experiment Objective</b>	<b>Upper Column</b>	<b># Rows of Bolts Connecting Filler to Smaller Column</b>
730-std	No fillers TN standard holes (all others oversized)	W14x730	0 rows
730-over	No fillers TN	W14x730	0 rows
159f	3 3/4 in. fillers TN Full development	W14x159	4 rows
159h	3 3/4 in. fillers TN Half development	W14x159	2 rows
159n1	3 3/4 in. fillers TN No development #1	W14x159	0 rows
159n2	3 3/4 in. fillers TN No development #2	W14x159	0 rows
455f	1 5/8 in. fillers TN Full development	W14x455	2 rows
455h	1 5/8 in. fillers TN Half development	W14x455	1 row
455n1	1 5/8 in. fillers TN No development #1	W14x455	0 rows
455n2	1 5/8 in. fillers TN No development #2	W14x455	0 rows
159n-2ply1	3 3/4 in. fillers TN Using 3 1/2 in. and 1/4 in. fill No development #1	W14x159	0 rows
159n-2ply2	3 3/4 in. fillers TN Using 3 1/2 in. and 1/4 in. fill No development #2	W14x159	0 rows
159h-TC	3 3/4 in. fillers TC Half development	W14x159	2 rows
159n-TC	3 3/4 in. fillers TC No development	W14x159	0 rows
159f-weld	3 3/4 in. fillers welded Full development	W14x159	16 in. of 1/2" fillet weld per edge of filler
159h-weld	3 3/4 in. fillers welded Half development	W14x159	13 in. of 5/16" fillet weld per edge of filler

Two specimens (159n-2ply1 and 159-2ply2) were tested with undeveloped filler plates consisting of a 3 1/2 in. and a 1/4 in. plate, rather than a single filler plate that was 3 3/4 in. thick, as was used for the other W14x159 specimens. Two specimens (159h-TC and 159n-TC) utilized tension-controlled bolts. For two specimens (159f-weld and 159h-weld) the development was achieved by a fillet weld, instead of bolts, between the filler plate and top column at each flange tip.



**Figure 5 – Typical UIUC test specimen**

The bottom column was connected to the splice plate with sixty-four 9 in. bolts. The top column was connected to the splice plate with twenty-four 9 in. bolts, with as many as sixteen additional 7 in. development bolts. The top columns were assembled in a reverse bearing condition to provide the opportunity for as much slip as possible within the bolt holes. Specifically, the specimens were assembled such that the bolts were placed in bearing on the bottom edge of the bolt hole on the top column, the bottom edge of the bolt hole on the filler plate, and the top edge of the bolt hole on the splice plate. The bottom columns were assembled such that the bolts were placed in bearing on the bottom edge of the bolt hole on the bottom column and the top edge of the bolt hole of the splice plate so as to minimize the possibility of slip of the splice plate relative to the bottom column.

All bolts were 1 1/8 in. diameter A490X, pretensioned either by the turn-of-nut method or using tension-controlled bolts. The turn-of-nut bolts were lubricated at the fabrication shop with bees wax to achieve a consistent tension plateau. The turn-of-nut bolts were turned an additional 5/6<sup>th</sup> of a turn past snug tight to reach the bolt tension plateau. For the turn-of-nut method specimens, three bolts on one splice plate and one bolt on one filler plate (when bolted) were designated as control bolts. The elongation of the control bolts was measured and torqued further if necessary, along with the bolts neighboring the control bolt, to achieve the desired pretension. The bolt holes were oversized (the diameter of the hole was 1 7/16 in.) for 15 of the specimens; the bolt holes of the remaining specimen (730-std) were standard (the diameter of the hole was 1 3/16 in.). A 3 1/2 in. gap was provided between the top and bottom column to allow for the movement of the top column.

The filler was designated as either undeveloped, half developed, or fully developed. Development was achieved using additional 7 in. bolts or a fillet weld between the filler plate and top column. Full development was determined as the number of bolts through the filler needed to uniformly distribute the load of the connection across the fill plate and flange of the top column, rounded to a whole number of bolt rows (see Appendix A). The fillet weld was sized to have strength equal to the slip strength of the bolts required for the desired development. The means of development, percentage of bolts developed for the 24-bolt connection, as well as an effective number of bolts fully developed for all specimens is presented in Table 5. The effective number of bolts fully

**Table 5 – Effective number of bolts developed**

<b>Specimen</b>	<b>Means of Development</b>	<b>Percentage Developed for 24 Bolts</b>	<b>Effective Number of Bolts Fully Developed (percentage of 24)</b>
159n1, 159n2, 159n-2ply1, 159n-2ply2, 159n-TC	none	0%	13.6 (57%)
159h, 159h-TC	8 - 1 1/8 in. A490X bolts	43.9%	18.2 (76%)
159f	16 - 1 1/8 in. A490X bolts	87.8%	22.7 (95%)
445n1, 455n2	none	0%	18.0 (75%)
455h	4 - 1 1/8 in. A490X bolts	49.6%	21.0 (88%)
455f	8 - 1 1/8 in. A490X bolts	99.2%	24.0 (100%)
159h-weld	52 in. of 5/16 in fillet weld	50.1% for slip 0% for shear	18.8 (78%) for slip 13.6 (57%) for shear
159f-weld	64 in. of 1/2 in. fillet weld	98.3% for slip 0% for shear	23.8 (99%) for slip 13.6 (57%) for shear

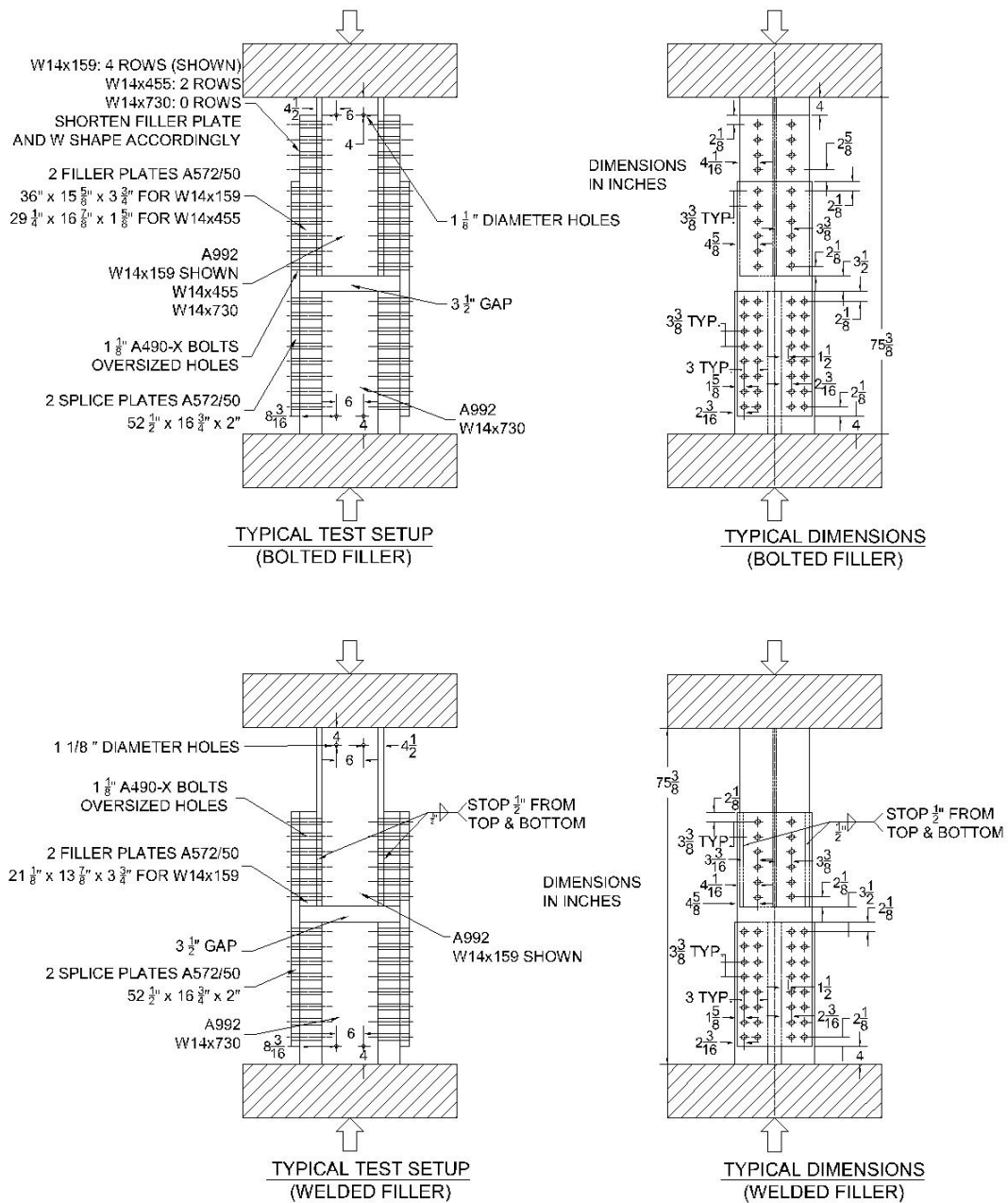


**Figure 6 – Typical UIUC test specimen configuration**

developed was determined by subtracting the number of bolts required to fully develop the connection from the total number of bolts, including the development bolts (see Section 4.5). The effectively fully developed (EFD) bolts are considered to provide the shear resistance. The remaining bolts are considered to only develop the filler and their shear strength neglected.

The specimens were fabricated and fully assembled by W&W Steel in Oklahoma City, Oklahoma and shipped to the University of Illinois at Urbana-Champaign covered under a tarp. All bolts of the same type and length were from the same lot. Mill reports were provided for the steel plates and rolled members. Material properties are reported in

Section 3. The specimens were designed to be the same total length. The top and bottom surfaces were milled to provide a flat loading surface.

## 2.2 Testing Machine and Procedure

The specimens were tested in Talbot Laboratory at the University of Illinois at Urbana-Champaign. The 3,000,000 lb. Southwark-Emery Tension/Compression testing machine (Figure 7) was used to load each specimen in compression. The top loading platen contained a spherical head which was locked into place prior to testing (Figure 8) to inhibit specimen rotation. This was done for several reasons, including to mirror the boundary condition underneath the bottom column, and because a locked condition was deemed more likely to reflect the boundary condition in the field for the column stub. For all but the first specimen tested (730-std), a steel plate was placed between the floor of the testing machine and the specimen so as to protect the steel floor (Figure 5). Similarly, for all specimens, a steel plate was placed between the top of the specimen and the spherical head (Figure 5).

The testing machine was operated manually by university personnel. Load was applied by controlling the hydraulic oil pressure and volume. The tests were generally carried out at an approximate loading rate of 1 kip per second to obtain a pseudo static loading test. After major events, such as slip, the load was held for observation of the specimen. Typically, during sudden jumps in displacement, the load briefly dropped and fluctuated as the hydraulic pressure stabilized. After bolt shear failure of the connection as a whole, the load was immediately removed by the operator.

Before the main loading sequence, the specimen was loaded with 20 kips with the spherical head unlocked so that it may adjust to the plane of the top surface of the specimen. The spherical head was then locked under load using three to four wedges (Figure 8) and the specimen was unloaded. To verify instrumentation, the specimen was then elastically loaded and unloaded. Typically, one elastic cycle to a load of 200 k was performed. Exceptions were: specimen 730-std with four elastic cycles to 50 k, 200 k, 200 k, and 400 k; specimen 455h with two elastic cycles to 200 k and 350 k; and specimen 159n-2ply1 with two elastic cycles to 300 k and 200 k. Monotonic load to failure was then applied, with periodic stops to observe the behavior. For two specimens, 159n-TC and 159h-TC, the capacity of the machine was reached before failure of the specimen. These specimens were then subjected to five elastic cycles between the approximate load at which the specimen came into bearing and the capacity of the machine. In both cases, failure did not occur and the specimen was unloaded.

A detailed study of the measured displacements and strains for each specimen has indicated that the load was successfully applied concentrically with no systematic eccentricities seen in the testing series (see Appendices B and C).



**Figure 7 – Testing area for 3,000,000 lb. testing machine**



**Figure 8 – Wedge for locking loading platen**

## **2.3 Specimen Instrumentation**

The specimens were instrumented with strain gages on the top column, filler plates, and splice plates (Figure 9). With exception of the filler plates, the strain gages were placed symmetrically about the strong and weak axes of the columns. Pairs of strain gages on each splice plate were placed below the first, fourth, and sixth row of bolts (counting from the bottom up). These monitor the introduction of strain into the splice plate. With the exception of specimens 730-std, 730-over and 159-2ply1, strain gages were also placed on the inside of the splice plate in the gap between the top and bottom columns. These were added to measure bending of the splice plates. Strain gages were applied to the filler plate if it was developed by bolts (specimens 159h, 159f, 455h, 455f, 159h-TC). These consisted of a series of seven gages distributed across the width of the filler plate, between the end of the splice plate and the first row of development bolts on the south side and two gages located in line with the bolts rows between the end of the splice plate and the first row of development bolts on the north side. For specimen 159f, four additional gages were applied in line with the bolt rows between the third and fourth rows of development bolts.

The strain gages were installed prior to placing the specimen in the testing machine. The strain gages were connected to a National Instruments SCXI-1520 interface in a SCXI data acquisition chassis. The strain gages were zeroed through balancing of the bridge prior to testing. Several strain gages were damaged during testing due to excessive strain or physical contact from breaking bolts.

After the specimen was placed in the testing machine it was instrumented with linear variable differential transformers (LVDTs) (Figure 10; see also Figure 5). The absolute displacement (with respect to the floor of the testing machine) at the middle of the top column and of the splice plates at the level of bolt row 1 of the top column were measured on both the east and west sides. The absolute displacement of the north and south filler plates at the level of bolt row 1 of the top column and of the north and south splice plates at the level of the bottom row of bolts of the bottom column were measured on the east side. LVDTs with a stroke of  $\pm 3$  in. were used to measure the absolute displacements of the top column and fill plates. LVDTs with a stroke of  $\pm 1$  in. were used to measure the absolute displacements of the splice plates at the level of bolt row 1 of the top column. LVDTs with a stroke of  $\pm 1/2$  in. were used to measure the absolute displacements of the splice plates at the level of the bottom row of bolts of the bottom column. The relative displacement (with respect to another point on the specimen) was measured between the top column and north and south filler plates on the west side of the specimen at the level of bolt row 1 of the top column. The relative displacement was also measured between the north and south filler plates and the splice plates on the west side of the specimen at the level of bolt row 2 of the top column. LVDTs with a stroke of  $\pm 1$  in. were used to measure all of the relative displacements. Figure 10 shows typical names for each LVDT.

For installing the LVDTs, 1/4 in. diameter studs were attached to the specimen using a capacitive discharge stud welder. Aluminum brackets were connected to the studs and the LVDTs were then attached to the brackets. Magnetic bases were used to secure the absolute LVDTs to the floor of the testing machine. The LVDTs were calibrated prior to testing. The normalized output was connected to a National Instruments SCXI-1102C interface in a SCXI data acquisition chassis. The applied load was measured using the machine's 3,000,000 lb. hydraulic load cell; the calibration report is available in Appendix F. The stroke of the machine crosshead was measured using the machine's internal Yo-Yo gage. For some specimens, two LVDTs with a stroke of  $\pm 3$  in. were used to measure the north and south displacement of the crosshead on the west side of the specimen to validate this crosshead measurement.

The data, including the testing machine load and stroke, was continuously sampled using National Instruments LabView software at 10 Hz. The LabView software output actual displacements and strains, which were analyzed and plotted using MATLAB.



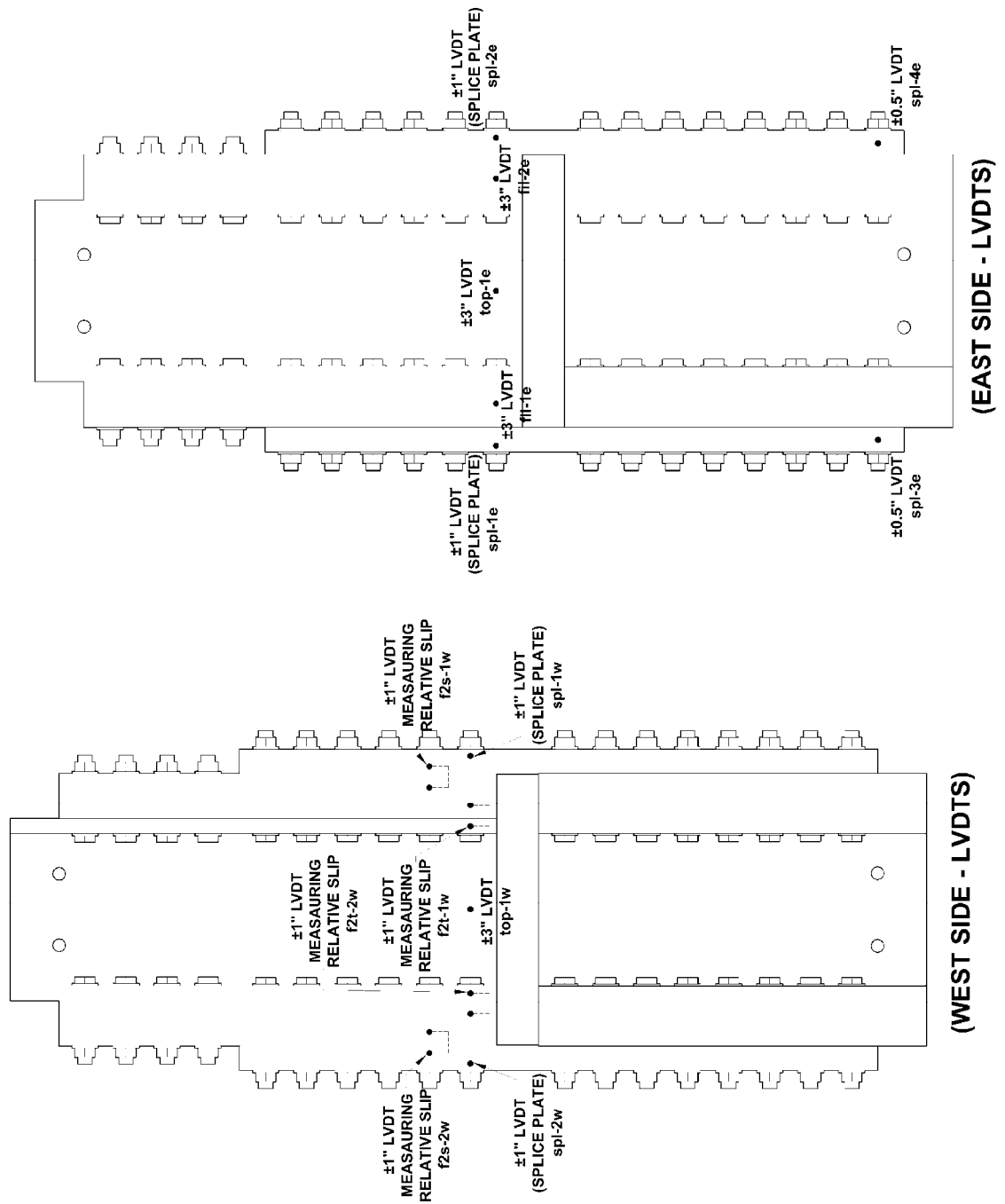


Figure 10 – LVDT Instrumentation Plan

## ANCILLARY TESTS

In order to determine the predicted strength of the specimens, ancillary tests were conducted to determine the bolt pretension, bolt shear and tensile strength, and slip coefficient. All bolts of the same type and length came from the same lot. Torqued tension tests to determine the bolt pretension were performed following standard practice at W&W Steel, Oklahoma City, Oklahoma. The bolt tension and shear strengths were determined as per ASTM F606-06 (ASTM, 2006) at the University of Cincinnati for both the turn-of-the-nut and the tension-controlled bolts. A summary of results from the bolt tests is presented in Table 6. Ancillary tests were not performed to determine the strength of the development welds. The slip coefficient was determined as per RCSC (2004) Appendix A at the University of Illinois at Urbana-Champaign.

**Table 6 – Summary of measured bolt properties**

<b>Bolt Property</b>	<b>Turn-of-nut 7 in. Length</b>	<b>Turn-of-nut 9 in. Length</b>	<b>Tension- controlled 7 in. Length</b>	<b>Tension- controlled 9 in. Length</b>
<b><math>T_b</math>, Pretension (kips)</b>	113	115	94	96
<b><math>F_v</math>, Shear Strength (ksi)</b>	102	99	104	108
<b><math>F_u</math>, Tensile Strength (ksi)</b>	160	168	172	180

### 3.1 Turn-of-Nut Bolts

Fourteen of the sixteen specimens were assembled using turn-of-nut (TN) bolts. The bolts were installed following standard practice utilizing the data presented in this section. The inspection certification provided by the bolt manufacturer is presented in Appendix E. From the inspection certification, the averaged measured tension strength for the 7 in. and 9 in. TN bolts were 119 and 130 kips, respectively.

#### 3.1.1 Pretension

The relationship between the bolt tension and bolt elongation on the TN bolts was determined using a Skidmore-Wilhelm machine at W&W Steel following standard practice (e.g., Frank and Yura, 1981) for three 7 in. and three 9 in. bolts (Figure 11). The bolts, nuts, and washers were lubricated with bees wax to achieve a consistent force plateau. Based on this data, an elongation of 0.05 in. was determined as the minimum required to reach the tension plateau. It was because of these results that the control bolts of the turn-of-nut specimens were torqued further if the elongation was less than 0.05 in. Based on a curve fit of the plateau data for the three specimens of each length, the mean value of the pretension at 0.05 in. was determined to be 113 kips and 115 kips for the 7

in. and 9 in. TN bolts, respectively (see Figure 11). All predicted calculations for the UIUC test specimens assumed these pretension values for all TN bolts.

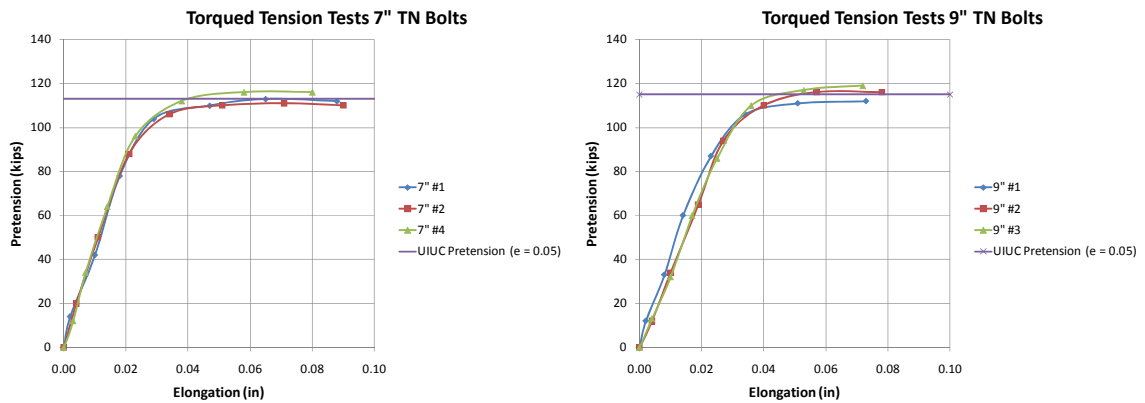


**Figure 11 – TN bolt torqued tension tests**

### 3.1.2 Tension Strength

Bolt tension tests on the TN bolts were conducted in accordance with ASTM standards (ASTM, 2006) using the testing apparatus shown in Figure 12. The failure surfaces were at approximately a 45 degree angle and through the threads (Figure 13). The relationship between the tensile load and bolt elongation from these tests is shown in Figure 14. The average tensile strength was 122 and 128 kips with a standard deviation of 0.78 and 1.9 kips for the 7 in. and 9 in. TN bolts, respectively. The tensile strength was calculated based on the stressed area (Kulak et al., 2001) and determined to be 160 ksi and 168 ksi for the 7 in. and 9 in. TN bolts, respectively.



**Figure 12 – Bolt tension test apparatus [from (Rassati and Swanson, 2007)]**



**Figure 13 – Failed TN bolts due to tension [from (Rassati and Swanson, 2007)]**

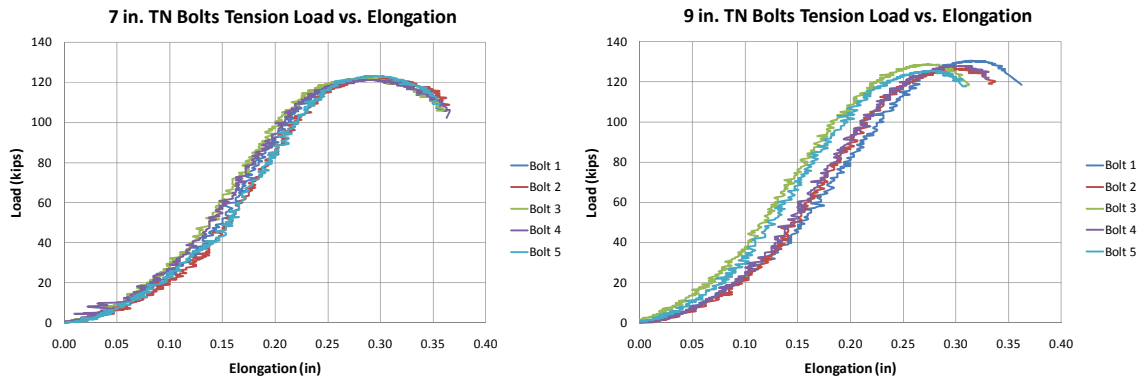


**Figure 14 – TN bolts tension test results**

### 3.1.3 Shear Strength

Bolt shear tests on the TN bolts were conducted in accordance with ASTM standards (ASTM, 2006) using the testing apparatus shown in Figure 15. The failure surfaces were relatively flat and smooth as shown in Figure 16. The relationship between shear force and bolt deformation is shown in Figure 17. The initial stiffness of bolt 1 and bolt 2 was initially influenced by accidental resistance provided by the test apparatus; the peak load was still accurate. The average shear strength was 99 and 102 kips with a standard deviation of 0.89 and 0.535 for the 7 in. and 9 in. TN bolts, respectively. Based on the area of the bolt shank, the shear strength was determined to be 99 ksi and 102 ksi for the 7 in. and 9 in. TN bolts, respectively.



Figure 15 – Bolt shear test apparatus [from (Rassati and Swanson, 2007)]



Figure 16 – Failed TN 9 in. bolts due to shear [from (Rassati and Swanson, 2007)]

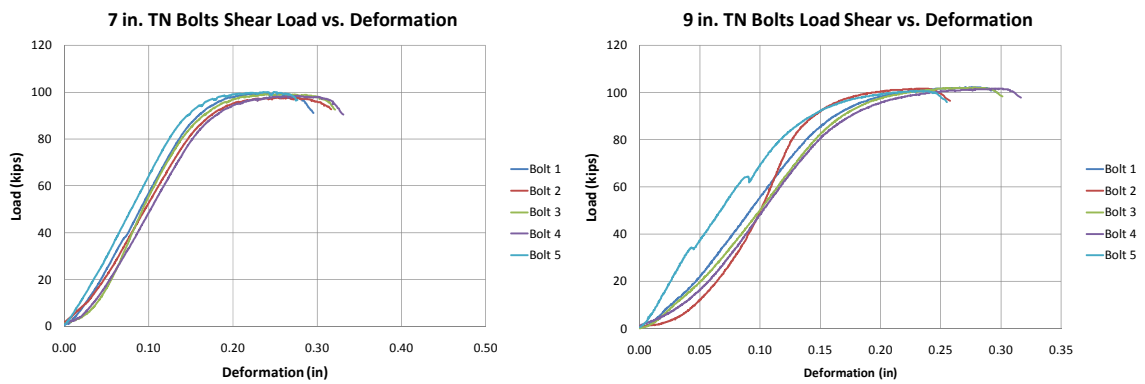


Figure 17 – TN bolt shear test results

## 3.2 Tension-Controlled Bolts

Two of the sixteen specimens were assembled using tension-controlled (TC) bolts. The bolts were installed using the manufacturer's procedures to achieve minimum pretension. The inspection certification provided by the bolt manufacturer is presented in Appendix E. From the inspection certification, the averaged measured pretension for the 7 in. and 9 in. TN bolts were 96 and 94 kips, respectively, and the averaged measured tension strength for the 7 in. and 9 in. TN bolts were 130 and 131 kips, respectively.

### 3.2.1 Pretension

It was attempted to determine the relationship between the bolt tension and bolt elongation of the TC bolts using a Skidmore-Wilhelm machine at W&W Steel following standard practice (e.g., Frank and Yura, 1981). One 7 in. bolt and four 9 in. TC bolts exceeded the 110 kip capacity of the Skidmore machine (not shown). One 7 in. bolt was tested successfully to failure of twist-off portion of the shank, yielding a torqued tension of 94 kips. Lubricant was not utilized for these six bolt tests. In the absence of sufficient data from these ancillary tests, the averaged pretension values reported in the inspection reports (96 kips for 7 in. bolts and 94 kips for 9 in. bolts) are used for the predicted calculations for the UIUC test specimens having TC bolts.

### 3.2.2 Tension Strength

The relationship between tensile load and bolt elongation for the 7 in. and 9 in. TC bolts is shown in Figure 18. The average tensile strength was 131 and 137 kips with a standard deviation of 1.2 and 0.82 kips for the 7 in. and 9 in. TC bolts, respectively (the stroke measurement of bolt 4 of the 7 in. tests was likely invalid). The tensile strength was calculated based on the stressed area (Kulak et al., 2001) and determined to be 172 ksi and 180 ksi for the 7 in. and 9 in. TC bolts, respectively.

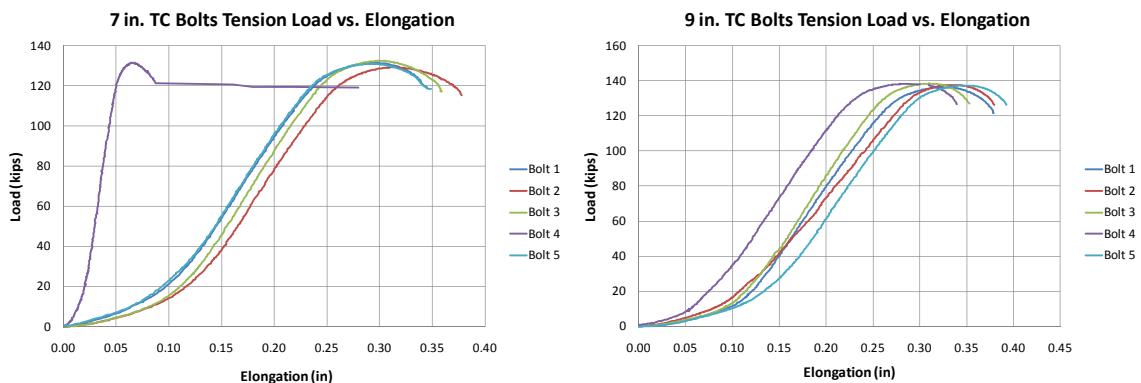
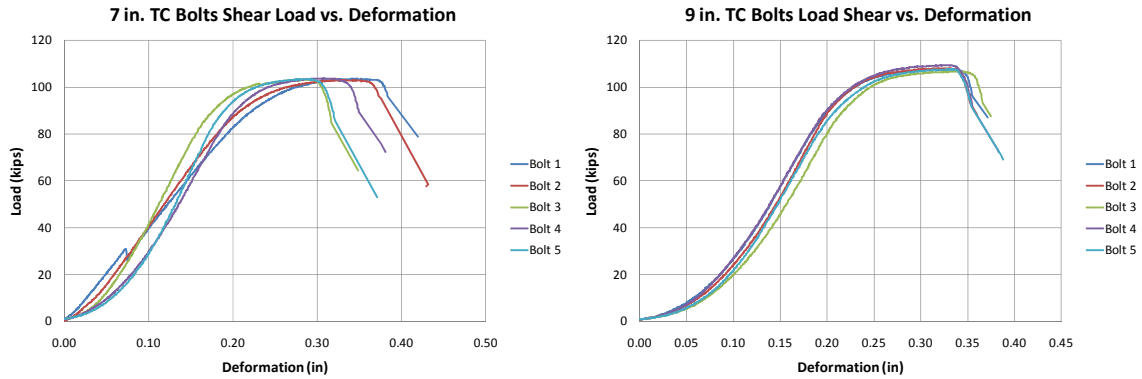


Figure 18 – TC bolt tension test results

### 3.2.3 Shear Strength

Bolt shear tests on the TC bolts were conducted in accordance with ASTM standards (ASTM, 2006) using the testing apparatus shown in Figure 15. The relationship between

shear load and bolt elongation for the 7 in. and 9 in. TC bolts is shown in Figure 19. The average shear strength was 103 and 108 kips with a standard deviation of 0.28 and 0.96 kips for the 7 in. and 9 in. TC bolts, respectively. Based on the area of the bolt shank, the shear strength was determined to be 104 ksi and 108 ksi for the 7 in. and 9 in. TC bolts, respectively.



**Figure 19 – TC bolt shear test results**

### 3.3 Slip Coefficient Tests

All surfaces of the full-scale specimens were blast-cleaned to a Class B surface. In order to determine the predicted slip strength of each specimen the coefficient of friction of the faying surfaces needed to be determined. The 2005 AISC *Specification* provides a nominal slip coefficient of 0.50. In a recent statistical study in which the results of 354 tests of blast-cleaned surfaces were compiled, the mean slip coefficient was determined to be 0.525 with a coefficient of variation of 0.193 (Grondin et al., 2008, Table 3).

#### 3.3.1 Slip Test Specimens

The slip test was designed to replicate the Appendix A guidelines in the 2004 RCSC *Specification for Structural Joints* (RCSC, 2004). Fourteen slip tests were performed, including combinations of most of the faying surfaces present in the full-scale specimens. Table 7 summarizes the components of the slip specimens tested. Square, 4 in. by 4 in., plates were cut from the W14x730's, W14x455's, W14x159's, 2 in. splice plates, 1 5/8 in. filler plates, 3 1/2 in. filler plates and 3 3/4 in. filler plates. The 1/4 in. filler plates were not tested due to excessive local buckling deformation that occurred during preliminary testing. A 1 in. diameter hole was drilled in each plate as shown in Figure 20. During construction of the specimens, handling of the faying surfaces was minimized.

To minimize testing eccentricities, the top and bottom surfaces of each specimen were milled to a flat surface. To minimize the risk of compromising the faying surface during fabrication, the plate thicknesses were not changed from the original plate thicknesses, and so the thicknesses did not conform to the 2004 RCSC Specification of having a thickness of 5/8 in. To mimic the RCSC Specification and bring the applied force closer

to the faying surface, 5/8 in. wide shims were placed between the testing machine and specimen at a location closest to each faying surface. This reduced the eccentricities induced by the larger plates.

Slip specimen 6D-2 was re-sandblasted after it was used in preliminary tests to establish the testing procedure. The reconstituted surfaces were visually similar to untested surfaces of the other specimens. Specimens 7B-1 and 7B-2 contained plates from the outside flanges of a W14x159 column. These faying surfaces were not completely flat, preventing full surface contact between the faying surfaces (Figure 21).

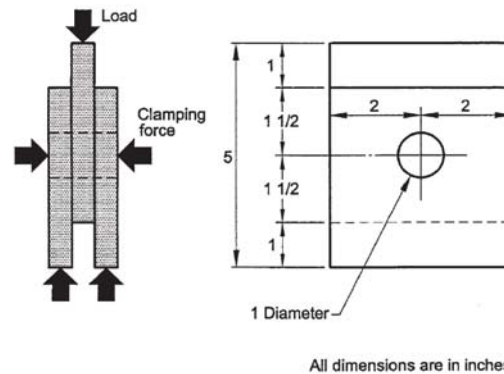


**Figure 20 – Typical slip specimen dimensions [from (RCSC, 2004)]**

### 3.3.2 Slip Test Procedure

The slip tests were performed at the University of Illinois at Urbana-Champaign in the Newmark Civil Engineering Laboratory. The slip specimens were tested in compression using a 600-kip hydraulic testing frame. Figure 22 shows a typical slip specimen prior to testing. A 50 kip clamping force was provided by a hydraulic actuator attached to a threaded rod passing through the specimen. Metal studs were welded to opposite sides of the outside plates and both sides of the inside plate using a capacitive discharge stud-welder. Aluminum brackets were attached to the studs. An extensionometer was attached to each side of the specimen, measuring the displacement between the outside plates and the inside plate on each side of the specimen. The applied load was measured using the testing machine's internal load cell.

The specimen was placed on the threaded rod and directly on the bottom platen of the testing machine. The inside plate was lifted to place the assembly in reverse bearing. The threaded rod was in contact with the bottom of the hole of the inside plate and the top of the hole of the outside plates, to provide adequate clearance for slip and to minimize the risk of damage to the threaded rod. In this position, the inside plate was placed on two wooden wedges, after which the inside plate was leveled using a bubble level. The full 50 kip clamping force was then applied to the specimen. The wooden wedges were then removed. The specimen was lifted and 5/8 in. steel shims were placed under the outside plates closest to the faying surfaces. Similarly, 5/8 in. shims were placed near each faying surfaces on top of the inner plate. A spherical head apparatus was placed on top of these shims to ensure even loading (Figure 22). The height of the threaded rod was

then adjusted to ensure that the specimen was resting squarely on the bottom shims. The crosshead was brought into contact with the spherical head and load was applied.

The test was carried out under displacement control. The rate of crosshead movement was 0.01 in. per minute, which did not exceed the slip rate 0.003 in. per minute recommended by RCSC (2004). The clamping force was maintained at 50 kips  $\pm$ 0.5 kips. The load-slip relationship was plotted in real time, and the test was stopped when sufficient deformation had occurred as per RCSC Section A3.4 (RCSC, 2004). The machine stroke, applied load, clamping load, and extensionometer displacements were recorded at 4 Hz using Instron controllers and National Instruments LabView software.

**Table 7 – Ancillary slip test matrix**

Specimen Number	Outside Plates		Inside Plates		Test Results	
	Type	Thickness	Type	Thickness	Slip Load (kips)	$\mu$
6B-3	Splice	2"	Fill	1 5/8"	43.5	0.435
6C-1	Splice	2"	Fill	3 3/4"	58	0.58
6C-2					55	0.55
6C-3					44.5	0.445
6D-2	W14x730	4 15/16"	Splice	2"	44.5	0.445
7B-1	W14x159	1 3/16"	Fill	3 1/2"	33	0.33
7B-2					50	0.5
7B-3					36.5	0.365
7C-1	W14x159	1 3/16"	Fill	3 3/4"	49	0.49
7C-2					52	0.52
7C-3					45	0.45
7D-1	W14x455	3 3/16"	Fill	1 5/8"	43	0.43
7D-2					40.5	0.405
7D-3					45	0.45
<b>Mean Value</b>						
With 7B-1 and 7B-3					45.68	0.46
Without 7B-1 and 7B-3					47.50	0.48
<b>Standard Deviation</b>						
With 7B-1 and 7B-3					6.77	0.07
Without 7B-1 and 7B-3					5.32	0.05
<b>Coefficient of Variation</b>						
With 7B-1 and 7B-3					0.15	0.15
Without 7B-1 and 7B-3					0.11	0.11

The specimen number is obtained from the fabricator piece mark on the shop drawings.

Specimen 6D-2 was re-sandblasted after an initial testing and was then retested. Specimens 7B-1 and 7B-3 consisted of outside flange plates whose faying surfaces were not completely flat. These surface irregularities prevented full surface contact between the faying surfaces.



**Figure 21 – Slip specimens cut from W14x159 flange**

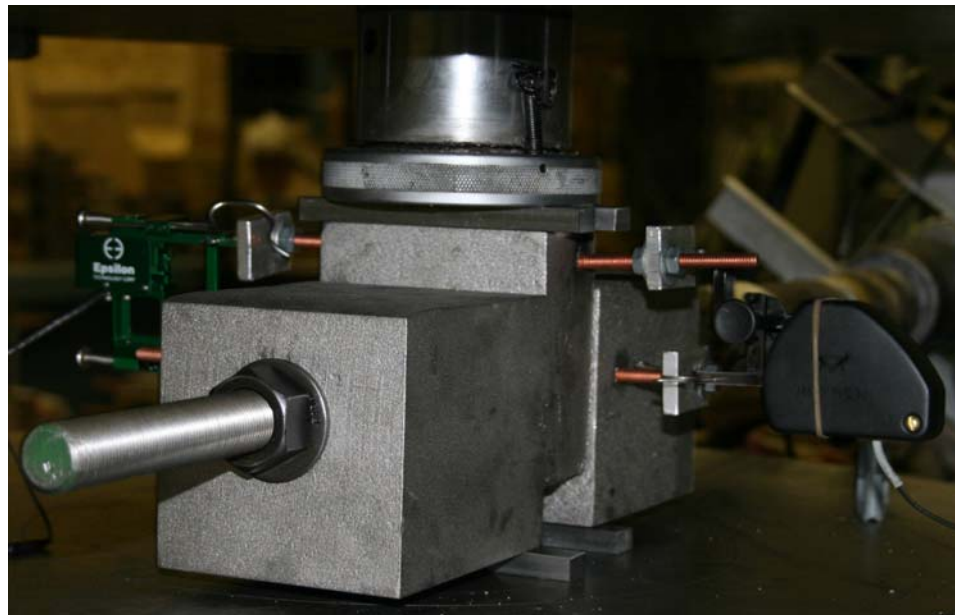


**Figure 22 – Typical slip test specimen**

### 3.3.3 Slip Test Results

The slip load was determined according to RCSC (2004) Section A3.4 (Figure 23). The slip coefficient was determined using Equation (2).

$$k_s = \frac{\text{slip load}}{2(\text{clamping force})} \quad (2)$$

The clamping force was nominally 50 kips for all of the tests and did not vary more than  $\pm 0.5$  kips. The slip loads and slip coefficients for the 14 slip tests are tabulated in Table 7. The mean and standard deviation are calculated including and excluding specimens 7B-1 and 7B-3 due to the aforementioned faying surface irregularities. However, the tests of specimens 7B-1 and 7B-3 are deemed legitimate, and the resulting slip coefficient of 0.46 is used throughout this work to calculate the predicted slip strength of the sixteen connection test specimens (see Appendix A). This value of 0.46 may be compared with the average value of the slip coefficient for blast-cleaned surfaces 0.525 (Grondin et al. 2008).

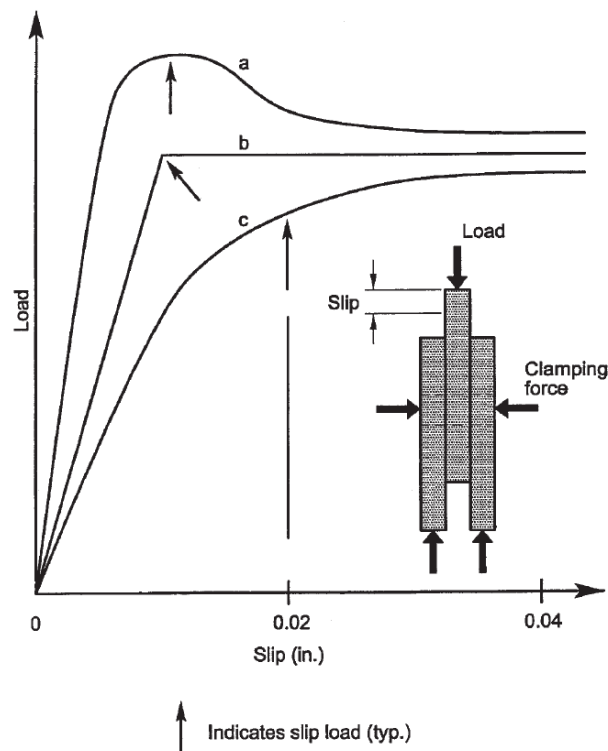


Figure 23 – RCSC definition of slip load [from (RCSC, 2004)]

### 3.4 Material Properties

The column wide-flange shapes were specified as ASTM A992 steel. The filler and splice plates were specified as ASTM A572 Grade 50 steel. Table 8 and Table 9 present the yield strength and ultimate strength from the mill reports for each component. The 2 in. plates came from two heats, and the W14x730 shapes used as the bottom columns on the fifteen specimens having oversized holes on the top column came from four heats. The strengths from each heat were averaged when needed for calculations. These values were utilized in the limit state calculations detailed in Appendix A. However, the strength of the specimens was generally governed by the bolt properties; therefore these plate and shape values were not used to calculate the predicted slip or shear loads of the specimens. It was noted during the specimen design that the W14x159 column would likely yield prior to achieving the bolt shear strength (see Appendix A). However, after consultation with the Technical Advisory Panel, it was deemed both acceptable and desirable to use a W14x159 as an extreme case for connections with very thick filler plates.

**Table 8 – Specimen plate properties**

Plate Thickness (in)	Heat ID	Yield Strength (ksi)	Ultimate Strength (ksi)
1/4	533713	53	75
1-5/8	3105972	58	84
2	7102887	59	82
	7102892	53	82
3-1/2	307461	50	71
3-3/4	S07446	51	74

**Table 9 – Specimen column properties**

Column	Hole Size	Heat Number	Yield Strength (ksi)	Ultimate Strength (ksi)
Top Columns				
W14x730	Standard	40694	71	91
W14x730	Oversize	27725	60	82
W14x455	Oversize	24788	65	82
W14x159	Oversize	287830	56	73
Bottom Columns				
W14x730	Standard	40694	71	91
W14x730	Oversize	27723	60	82
		27725	60	82
		27726	61	81
		41099	70	89

---

## EXPERIMENTAL RESULTS

### 4.1 Summary of Experimental Results

Table 10 and Table 11 summarize the nominal, design, predicted (based on measured values from ancillary tests), and actual experimental slip and bolt shear failure loads, respectively, for each test specimen. Nominal and design values are obtained from the specifications shown, including AISC (1989) and AISC (2005). The values of predicted slip strength were calculated as the product of the pretension force obtained from the ancillary tests as described in Section 3.1.1 for TN bolts and Section 3.2.1 for TC bolts, the slip coefficient of 0.46 obtained from the ancillary slip tests described in Section 3.3.3, the number of slip planes (equal to 2, independent of the number of filler plates), and the number of bolts per side of the connection. The values of predicted shear were calculated as the product of the measured bolt shear strength for the bolt from ancillary bolt shear tests of Section 3.1.3 for TN bolts and Section 3.2.3 for TC bolts, and the number of bolts. Appendix A reports detailed calculations for the nominal, design, and predicted strengths.

Section 4.2 summarizes the typical response seen in the specimens. Slip was characterized as the load at which relative displacement between any two surfaces initiated. Slip was accompanied by a loud noise and a violent vibration. There were often several slip events. Shear was determined as the maximum load the specimen achieved. Both values are readily obtained from recorded data and were obvious during testing.

Appendices B and C present the test results in detail, and include discussions of the response seen in the instrumentation, including comparative response between different groups of specimens. The data was analyzed for the effects of unusual or systematic loading eccentricities based on the trends seen in the data. While some eccentricities could be seen in each test (e.g., looking at strains or displacements on the north versus south sides, or the east versus west sides), no systematic effects of standard testing eccentricities were seen to influence the results. Also, as discussed in Section 3.4, the W14x159 column typically yielded as anticipated prior to final bolt shear failure. Disassembly and forensic investigation of several of the specimens confirmed that hole ovalization occurred in the column due to yielding in compression in the specimens with a W14x159 top column. Bolt bearing deformations were also seen in all flanges and plates, with more deformation occurring in the thinner pieces. As with any connections of this scale, eccentricities could occur, such as slight local buckling of the top column flanges creating added tension to the top row of bolts. The strain gage data also indicated that the specimens with a W14x159 top column generally had more significant bending in the splice plates in the gap between the top and bottom columns as compared to the

specimens with the W14x455 top column. This may have added stress to the bolts going through the splice plate and highlights potential eccentricities that may occur with very thick fillers. However, other than for the premature buckling of the 159f-weld specimen discussed in the next paragraph, there is no direct evidence that the yielding in the top column or bending in the splice plates caused premature shear failure in the bolts.

The shear strength of specimens 159h-TC and 159n-TC exceeded the capacity of the testing machine, yielding a lower bound for the shear strength of 3,000 kips for these specimens. The nominal yield strength of the top column of specimen 159f-weld was exceeded and subsequently suffered severe inelastic local buckling prior to shear failure of the connection, providing a lower bound for the shear strength of 2,720 kips. Three specimens, 159f, 455h, and 159n-2ply1 slipped below the predicted load, with a test-to-predicted ratio of 0.96, 0.93 and 0.52 respectively. The four 455 specimens, 455f, 455h, 455n1, and 455n2, experienced shear failure below the predicted load, with test-to-predicted ratios of 0.99, 0.90, 0.90 and 0.92, respectively. See Appendices B and C for detailed specimen results.

**Table 10 – Slip strength experimental test results**

Name	UIUC Slip Strength Experimental Test Results						
	Test (kips)	Nominal and Design Values <sup>a</sup>				Predicted Values (Measured Properties)	
		$P_n$ (kips)	$\phi P_n$ (kips)	$P_n/\Omega$ (kips)	$P_{allow,1989}$ (kips)	Predicted (kips)	Test-to-Predicted Ratio
730-std	1,697	1,085	922	616	692	1,270	1.34
730-over	1,634	1,085	922	616	692	1,270	1.29
159f	1,224	1,085	922	616	692	1,270	<b>0.96</b>
159h	1,697	1,085	922	616	692	1,270	1.34
159n1	1,879	1,085	922	616	692	1,270	1.48
159n2	1,704	1,085	922	616	692	1,270	1.34
455f	1,369	1,085	922	616	692	1,270	1.08
455h	1,175	1,085	922	616	692	1,270	<b>0.93</b>
455n1	1,388	1,085	922	616	692	1,270	1.09
455n2	1,433	1,085	922	616	692	1,270	1.13
159n-2ply1	658	1,085	922	616	692	1,270	<b>0.52</b>
159n-2ply2	1,348	1,085	922	616	692	1,270	1.06
159h-TC	1,626	1,085	922	616	692	1,060	1.53
159n-TC	1,290	1,085	922	616	692	1,060	1.22
159f-weld	1,685	1,085	922	616	692	1,270	1.33
159h-weld	1,616	1,085	922	616	692	1,270	1.27
<b>AVERAGE</b>	1464						1.19
<b>STD. DEV.</b>	296						0.25

<sup>a</sup>Nominal and design values are from AISC (2005) unless indicated as being from AISC (1989).

**Table 11 – Shear strength experimental test results**

Name	<b>UIUC Shear Strength Experimental Test Results</b>						
	Test (kips)	Nominal and Design Values <sup>a</sup>				Predicted Values (Measured Properties)	
		$P_n$ (kips)	$\phi P_n$ (kips)	$P_n/\Omega$ (kips)	$P_{allow,1989}$ (kips)	Predicted (kips)	Test-to-Predicted Ratio
730-std	2,542	1,789	1,342	895	954	2,444	1.04
730-over	2,459	1,789	1,342	895	954	2,444	1.01
159f	2,644	1,789	1,342	895	954	2,444	1.08
159h	2,907	1,789	1,342	895	954	2,444	1.19
159n1	2,548	1,789	1,342	895	954	2,444	1.04
159n2	2,616	1,789	1,342	895	954	2,444	1.07
455f	2,428	1,789	1,342	895	954	2,444	<b>0.99</b>
455h	2,197	1,789	1,342	895	954	2,444	<b>0.90</b>
455n1	2,189	1,789	1,342	895	954	2,444	<b>0.90</b>
455n2	2,248	1,789	1,342	895	954	2,444	<b>0.92</b>
159n-2ply1	2,813	1,789	1,342	895	954	2,444	1.15
159n-2ply2	2,931	1,789	1,342	895	954	2,444	1.20
159h-TC	>3,000 <sup>b</sup>	1,789	1,342	895	954	2,586	>1.16
159n-TC	>3,000 <sup>b</sup>	1,789	1,342	895	954	2,586	>1.16
159f-weld	>2,720 <sup>c</sup>	1,789	1,342	895	954	2,444	>1.10
159h-weld	2,754	1,789	1,342	895	954	2,444	1.13
<b>AVERAGE</b>	2560						>1.07
<b>STD. DEV.</b>	252						>0.10

<sup>a</sup>Nominal and design values are from AISC (2005) unless indicated as being from AISC (1989).

<sup>b</sup>The shear strength of the TC specimens exceeded the capacity of the testing machine.

<sup>c</sup>The top column of specimen 159f-weld experienced detrimental local buckling prior to the shear load.

The predicted strength values presented in this report make no attempt to account for the filler and hence represent expected strength for an equivalent connection without fillers. They thus provide for a consistent comparison among results in this study and between results from other studies in the literature. Comparable predicted strengths were developed for tests from prior work (i.e., Lee and Fisher, 1968; Frank and Yura, 1981; Dusicka and Lewis, 2007). A description of how the predicted strengths were calculated for tests from the literature is presented in Section 1.3 and summarized in Table 12. An experimental database of 81 bolted filler connection tests was thus compiled with measured and predicted values.

**Table 12 – Predicted values of test series from literature**

Researcher	Predicted Slip Strength	Predicted Shear Strength
<b>Lee and Fisher (1968)</b>	$C N_s N_b \mu$ $C$ = reported clamping force $N_s$ = number of surfaces $N_b$ = number of bolts $\mu$ = assumed slip coefficient, 0.525	N/A
<b>Frank and Yura (1981)</b>	$C N_s N_b \mu$ $C$ = reported clamping force $N_s$ = number of surfaces $N_b$ = number of bolts $\mu$ = assumed slip coefficient, 0.338	$N_b A_b F_v$ $N_b$ = number of bolts $A_b$ = area of bolt $F_b$ = reported bolt shear strength
<b>Dusicka and Lewis (2007)</b>	$C N_s N_b \mu$ $C$ = clamping force from torque tension test $N_s$ = number of surfaces $N_b$ = number of bolts $\mu$ = assumed slip coefficient, 0.525	$N_b A_b F_v$ $N_b$ = number of bolts $A_b$ = area of bolt $F_b$ = approximated bolt shear strength
<b>Borello, Denavit and Hajjar (2008) (this report)</b>	$C N_s N_b \mu$ $C$ = measured clamping force from torqued tension test $N_s$ = number of surfaces $N_b$ = number of bolts $\mu$ = measured slip coefficient, 0.46	$N_b A_b F_v$ $N_b$ = number of bolts $A_b$ = area of bolt $F_b$ = measured bolt shear strength

## 4.2 Typical Behavior

### 4.2.1 Force-Displacement Results

The absolute displacement of the top column was indicative of the overall behavior of the connection. Figure 24 illustrates the typical response of a specimen, including both load versus time and load versus the displacement of the bottom of the top column (see Figure 9 and Figure 10 for instrumentation nomenclature). Prior to slip, the load-displacement relation exhibited elastic behavior, indicated by the stiff linear response. Upon reaching the slip load, there was a sudden increase in displacement, corresponding to the slip of at least one of the faying surfaces. Since the machine could not maintain force during this dynamic action (because the hydraulic oil volume requires time to restabilize), the load decreased after slip. As the load was stabilized, slip continued. The specimens often experienced additional slip events over a period of several or tens of seconds following the initial event, whereas the load stabilization typically took approximately 30 seconds. After stabilizing, the load was often held constant for a period of time while observation and photographs were taken of the specimen (Figure 24(a)). The expected total slip was twice the difference between hole diameter and bolt shank diameter ( $2 \times 1/16$  in. = 0.125 in. for standard holes,  $2 \times 5/16 = 0.625$  in. for oversize holes). After approximately that amount of displacement, the bolts began bearing on the plates, indicated by a noticeable increase in stiffness of the connection (Figure 24(b)). As the load was further applied, the bearing surfaces and bolts begin to yield, lowering the stiffness. Ultimately, all of the

bolts on one side of the specimen failed in shear, indicating the shear strength of the connection had been reached. The bolt failures occurred in quick succession.

After slip, prior to shear, several bolts prematurely failed (see Appendix B) through the threads at the face of the nut (Figure 25); no correlation was found with overall specimen performance and these premature bolt failures, as the shank of the bolt often stayed in the hole. For example, specimen 455n1 suffered from three premature bolt failures during slip, for all of which the shank remained in the bolt hole. Compared to specimen 455n2, in which no bolts failed prematurely, the shear strength of specimen 455n1 was only 2% lower instead of the 12.5% predicted reduction associated with the premature failure of three bolts.

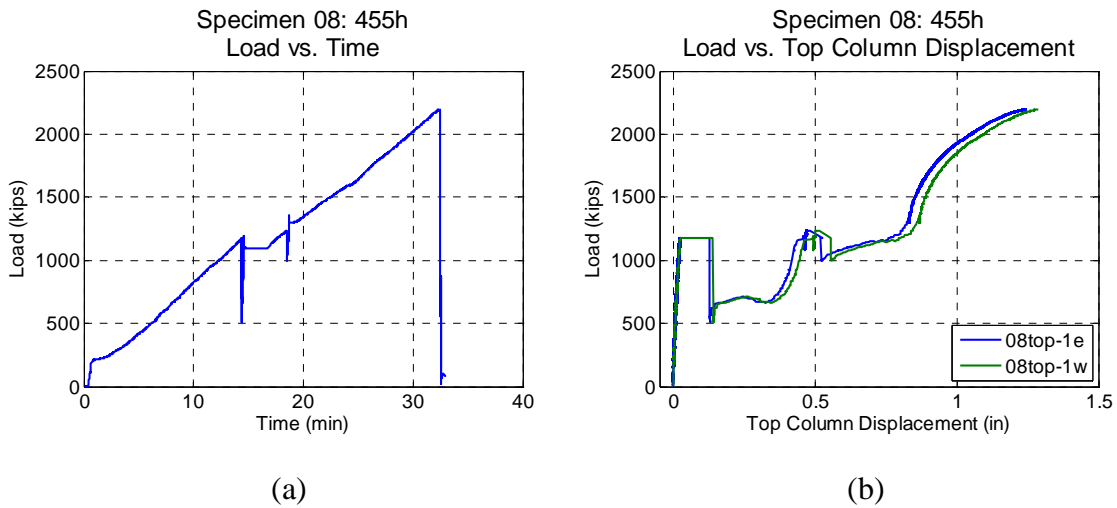


**Figure 24 – Typical specimen response: (a) load versus time; (b) load versus top column displacement**



**Figure 25 – Premature bolt failure through threads**

## 4.2.2 Specimen Slip

Table 13 shows the order in which the various surfaces of each specimen slipped. The order of slip was determined by examining the measured displacements. In frequent cases, the slip of multiple surfaces occurred in the time between the recording of two successive data points (0.1 seconds, with data being collected at 10 Hz); in these cases the surfaces were denoted to have slipped at the same time (e.g., specimen 730-std). In other cases (e.g., specimen 159h), two surfaces slipped at the same load, but the LVDT data clarifies which of the two surfaces slipped first.

With exception of 159n-2ply1, the specimens always slipped on the north and south side simultaneously (Figure 26(a)). This indicates that the specimen did not slip until the minimum slip load on each side was exceeded, indicating the connection slip coefficient equals the *average* of the two *minimum* slip coefficients of each side [i.e., slip load = slip load of side 1 + slip load of side 2 = (slip coefficient side 1 + slip coefficient side 2) \* clamping force of 12 bolts; and slip coefficient = slip load / (2 sides \* clamping force of 12 bolts); therefore slip coefficient = (slip coefficient side 1 + slip coefficient side 2) / 2 \* (clamping force of 12 bolts / clamping force of 12 bolts) = (slip coefficient side 1 + slip coefficient side 2) / 2]. Specimen 159n-2ply1 experienced early slip between the two plies of the filler plate on the south side (Figure 26(d) and Table 13).

At the initial slip load for specimens 159h (Figure 26(c)), 159n1, 159n2, 455f (Figure 26(e)), 455n1, and 455n2 all four faying surfaces slipped. This is logical for the undeveloped specimens since the predicted slip load is the same between all four surfaces. The developed specimens, however, have additional development bolts between the filler and top column, potentially increasing the predicted slip load (see Appendix D). Specimen 159h did not slip until the predicted slip load for the developed faying surfaces was exceeded. Specimen 455f (Figure 26(e)) slipped in between the slip load for twenty-four bolts on the undeveloped faying surface between the filler and the splice plate and the slip load for the developed faying surface between the filler and the top column, which has thirty-two bolts.

At the initial slip load, specimens 159f (Figure 26(b)), 455h, 159h-TC, 159f-weld, and 159h-weld (Figure 26(f)) slipped between the splice plate and the filler plate. Since all of these specimens were at least partially developed, this was the faying surface with the lowest clamping force and therefore lowest slip resistance. The slip load of specimens 159f and 455h was just below the predicted value for this faying surface, while the slip load for the other three specimens was well above the predicted value. The effect of development is explored further in Section 4.5.

Specimen 159n-2ply2 initially slipped between the filler plate and top column, but only 33 kips prior to slipping between the splice plate and filler plate. Since there was no development and the slip coefficient is a random variable, all slip planes are equally likely to slip first. Specimen 159n-TC slipped between the filler plate and top column on one side and between the splice plate and filler plate on the other side (Figure 26(d)).

**Table 13 – Slip load and sequence of slip per faying surface**

Specimen	Top Column/Filler Plate Slip Load and Sequence		Filler Plate/Splice Plate Slip Load and Sequence	
	North (kips)	South (kips)	North (kips)	South (kips)
730-std	1697 <sup>1</sup> (1)	1697 <sup>1</sup> (1)	-	-
730-over	1634 <sup>1</sup> (1)	1634 <sup>1</sup> (1)	-	-
159f	2424 (3)	2424 (3)	1224 (1)	1224 (1)
159h	1697 (1)	1697 (3)	1697(4)	1697 (1)
159n1	1879 (1)	1879 (1)	1879 (3)	1879 (3)
159n2	1704 (1)	1704 (1)	1704 (4)	1704 (1)
455f	1369 (4)	1369 (3)	1369 (1)	1369 (1)
455h	1175 (3)	1236 (4)	1175 (1)	1175 (1)
455n1	1388 (4)	1388 (3)	1388 (1)	1388 (1)
455n2	1433 (1)	1433 (3)	1433 (4)	1433 (1)
159n-2ply1	1025 (3)	1025 (2)	1199 (4)	658 (1)
159n-2ply2	1348 (1)	1348 (1)	1381 (3)	1381 (3)
159h-TC	2043 (3)	2043 (3)	1626 (1)	1626 (1)
159n-TC	1556 (3)	1290 (1)	1290 (1)	1556 (3)
159f-weld	- <sup>2</sup>	- <sup>2</sup>	1685 (1)	1685 (1)
159h-weld	2510 (3)	2510 (3)	1616 (1)	1616 (1)

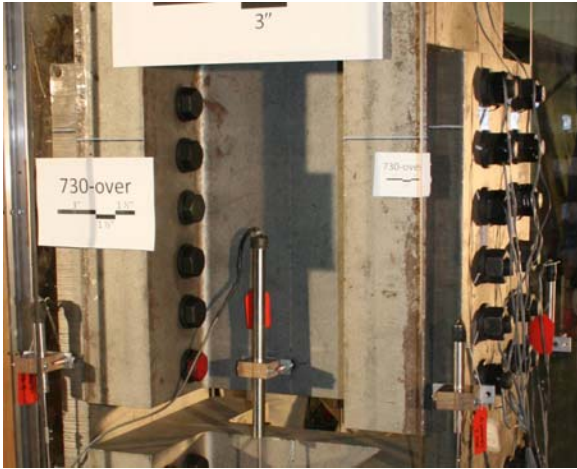
(x) Denotes x-th surface to slip

<sup>1</sup> Slip between top column and splice plate

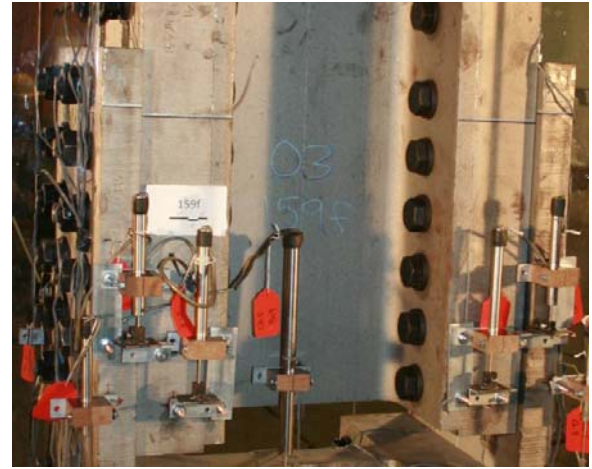
<sup>2</sup> Slip was not achieved

### 4.2.3 Specimen Shear

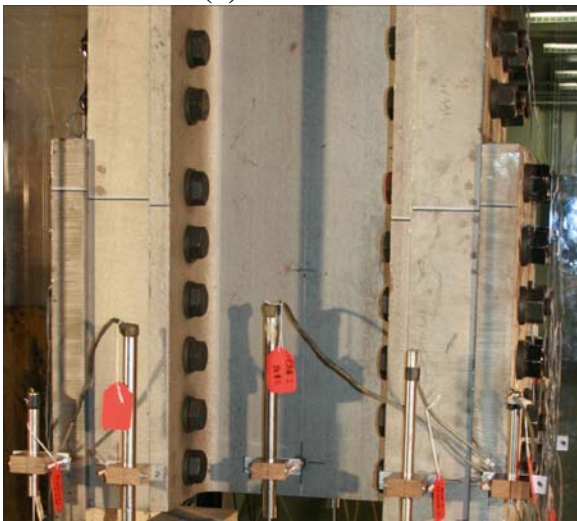
At failure, all bolts on one side of the specimen were suddenly sheared into two pieces (Figure 27(a)). The bolts often exited the specimen with significant velocity. After one side failed, the load was removed from the specimen. If the load were to remain, the other side would also fail, as was the case in 455h (Figure 27(b)). Thirteen of the specimens reached shear failure; eleven failed on the south side, two failed on the north side. The more frequent failure on the south side could not be attributed to any specific measured loading bias and was thus thought to be statistically valid. The top column of specimen 159f-weld experienced detrimental local buckling after it yielded but prior to the shear strength of the connection (Figure 27(c)).



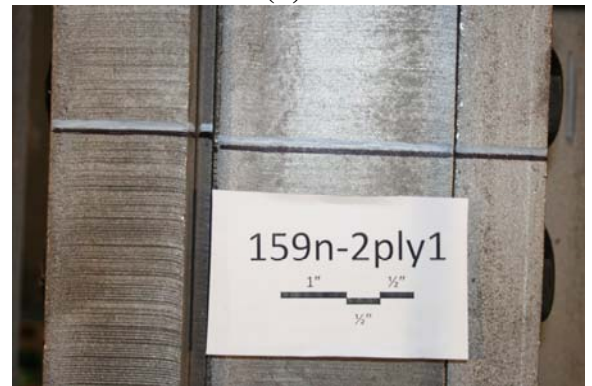
(a) 730-over



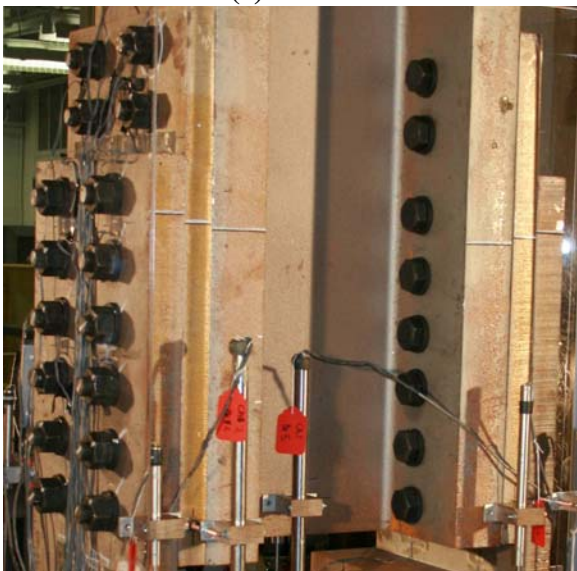
(b) 159f



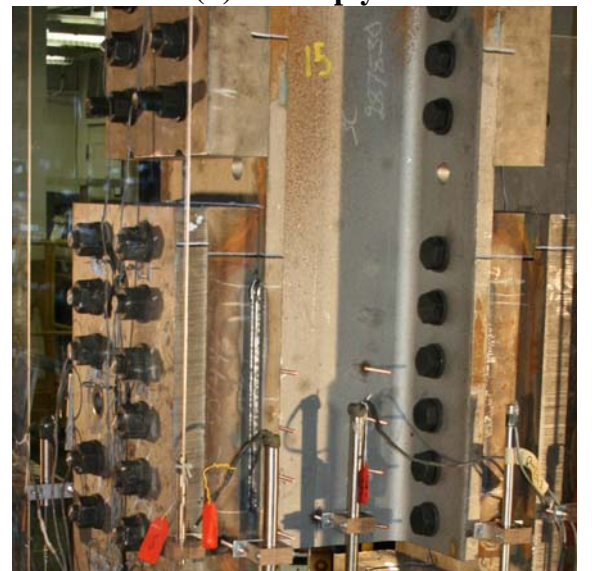
(c) 159h



(d) 159n-2ply1



(e) 455f



(f) 159h-weld

Figure 26 – Specimens after slip

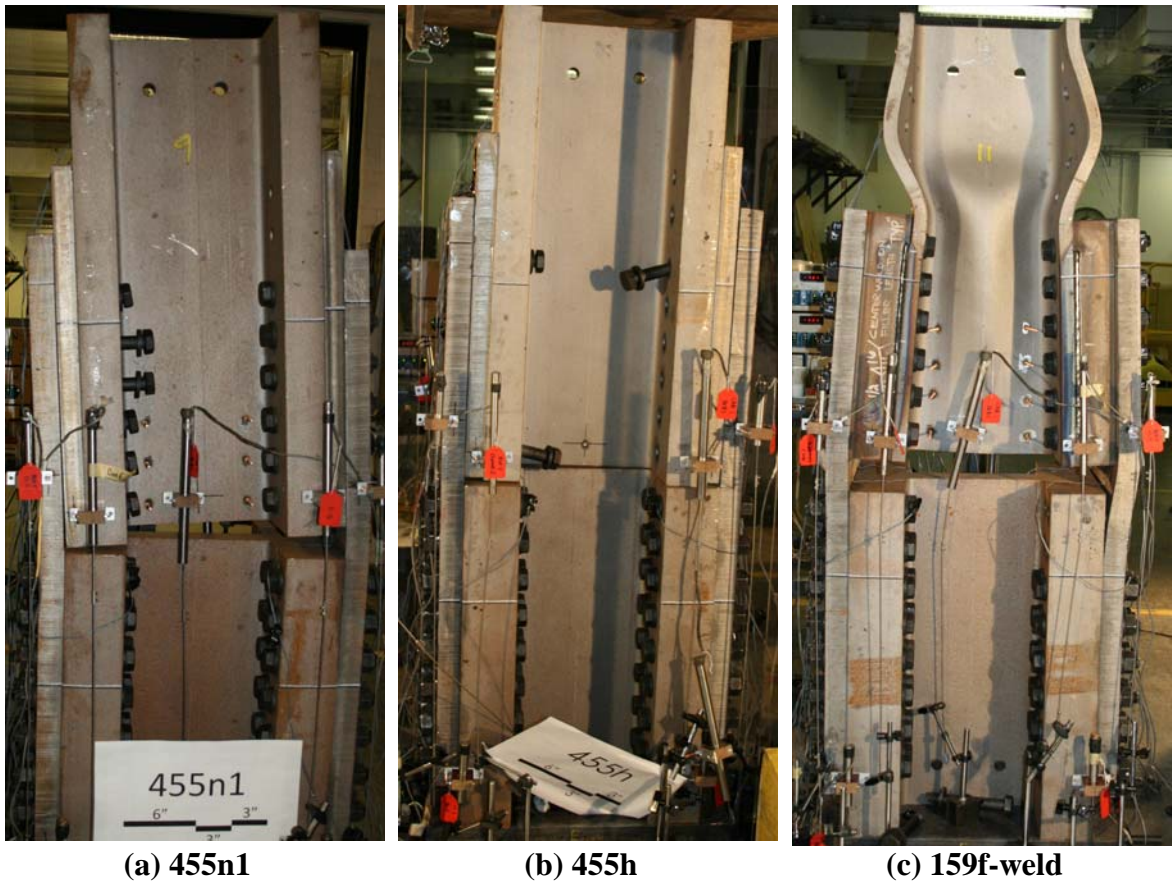


**Figure 27 – Specimens after shear**

#### 4.2.4 Comparative Results

Load versus top column displacement for specimens 159f, 159h, 159n1 and 159n2 is presented in Figure 28(a). The behavior prior to slip is due to elastic deformation and is similar for all specimens. At the slip load each specimen experienced a drop in load and a large displacement. At the slip load all faying surfaces slipped for specimens 159h, 159n1 and 159n2 (Table 13), displacing approximately 1 in. before the load increased, indicating that the bolts had begun to carry load. At the initial slip load of specimen 159f the faying surfaces between the filler plates and top column did not experience slip (Figure 28(e)); this was the only one of these four specimens that slipped below the predicted value (by 4%). The specimen stiffness began to increase after a displacement of approximately 0.5 in. At approximately 2,400 kips the remaining surfaces slipped and the specimen total displacement becomes consistent with the other specimens. The delayed slip of some of the faying surfaces did not noticeably influence the ultimate behavior of the specimen. The undeveloped specimens experienced larger displacement between the top column and filler plate (e.g., Figure 28(e) and Figure 28(f)), resulting in larger top column displacement (Figure 28(a)). The decreased displacement for

developed specimens can be attributed to the additional stiffness provided by the development bolts between the filler plate and top column. The displacement between the filler plate and splice plate was unaffected by development (Appendix C). All four of these specimens exceeded the predicted shear load.

Load verses top column displacement for specimens 455f, 455h, 455n1 and 455n2 is presented in Figure 28(b). All 455 specimens exhibited typical load verses displacement as described above. All faying surfaces slipped at the initial slip load for each specimen (Table 13), with only specimen 455h slipping below the predicted value (by 7%). The undeveloped specimens achieved approximately 0.15 in. greater displacement at ultimate failure as compared to the developed specimens. Specimen 455n2 had a greater displacement than the developed specimens during slip; specimen 455n1 displaced similarly to the developed specimens up to the shear design value, where it briefly softened and began to trace the displacement of 455n2. The additional displacement of the undeveloped specimens was between the filler plate and top column (Figure 28(f)). Of these four, only specimen 455f achieved the predicted shear load.

Load verses top column displacement for the undeveloped two-ply specimens are presented with the single-ply undeveloped specimens in Figure 28(c). These specimens exhibited typical load verses displacement as described above. Specimen 159n-2ply1 slipped at 52% of the expected load between the two south filler plates (Table 13). During slip, the two-ply specimens displaced approximately 0.10 in. further between the splice plate and filler plate than the single-ply specimens, which remained constant throughout the remainder of the test. This can be attributed to additional bolt deformation within the 1/4 in. filler plate. The bolt is essentially unrestrained within the 1/4 in. filler plate since the bolt hole oversize is significant compared to the filler thickness, requiring a large rotation to mobilize restraint from the filler. Another factor is the reduced bolt restraint provided by the 3 1/2 in. ply filler plate compared to the 3 3/4 in. filler plate in the single-ply specimens. The additional deformation is less than 8% of the ultimate connection deformation is not believed to significantly influence connection strength (see also the discussion in Sections 4.4 and 4.5). All specimens achieved the predicted shear load.

Load verses top column displacement for the welded development specimens are presented with specimens 159f, 159n1 and 159n2 for comparison in Figure 28(d). The initial slip for the welded specimens characterizes slip between the splice plates and filler plates, resulting in approximately 0.50 in. of top column displacement. The welded specimens and specimen 159f trace a path parallel to the undeveloped specimens, but since only half as many faying surfaces have slipped, the displacement is approximately half. Specimens 159h-weld and 159f experience slip of the filler plate and top column faying surfaces near the predicted shear load, resulting in approximately an addition 0.50 in. of displacement, bringing the relationship in line with the undeveloped specimens. Specimen 159f-weld experienced local buckling in the top column and the test was halted prior to failure of the development welds or bolt shear failure.

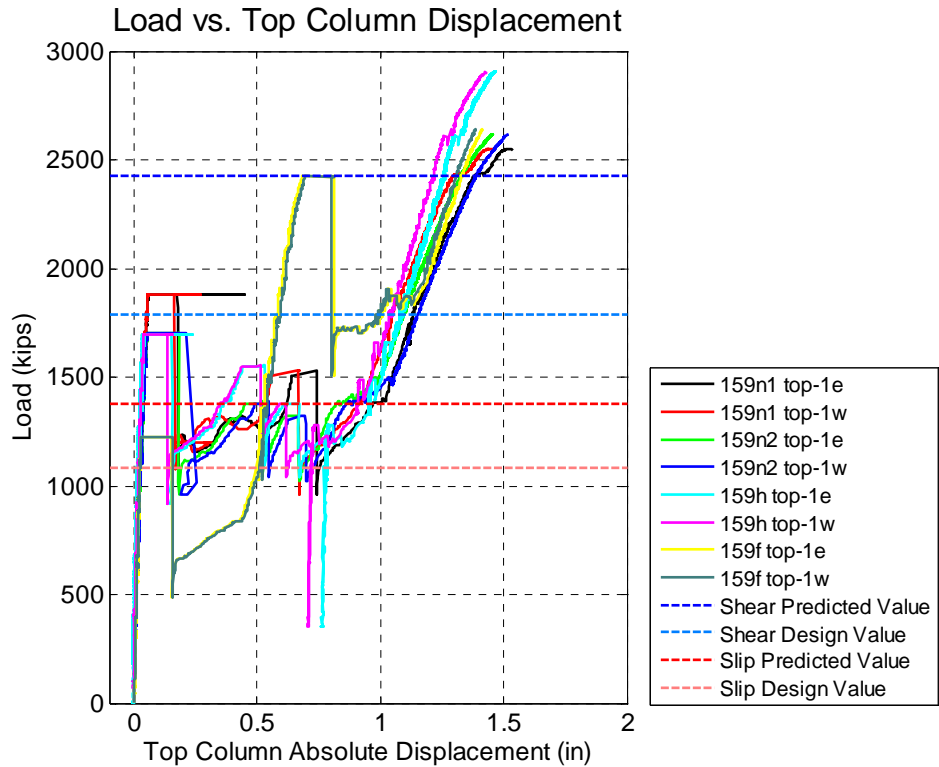


**Figure 28(a) – Top column displacement of 159 specimens**

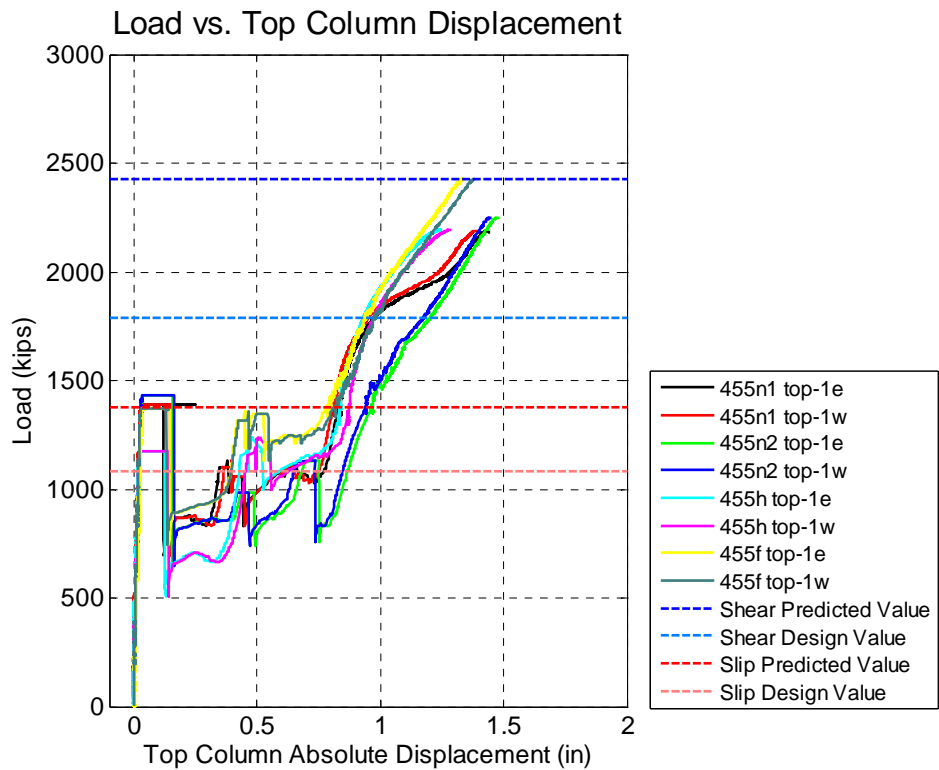


**Figure 28(b) – Top column displacement of 455 specimens**

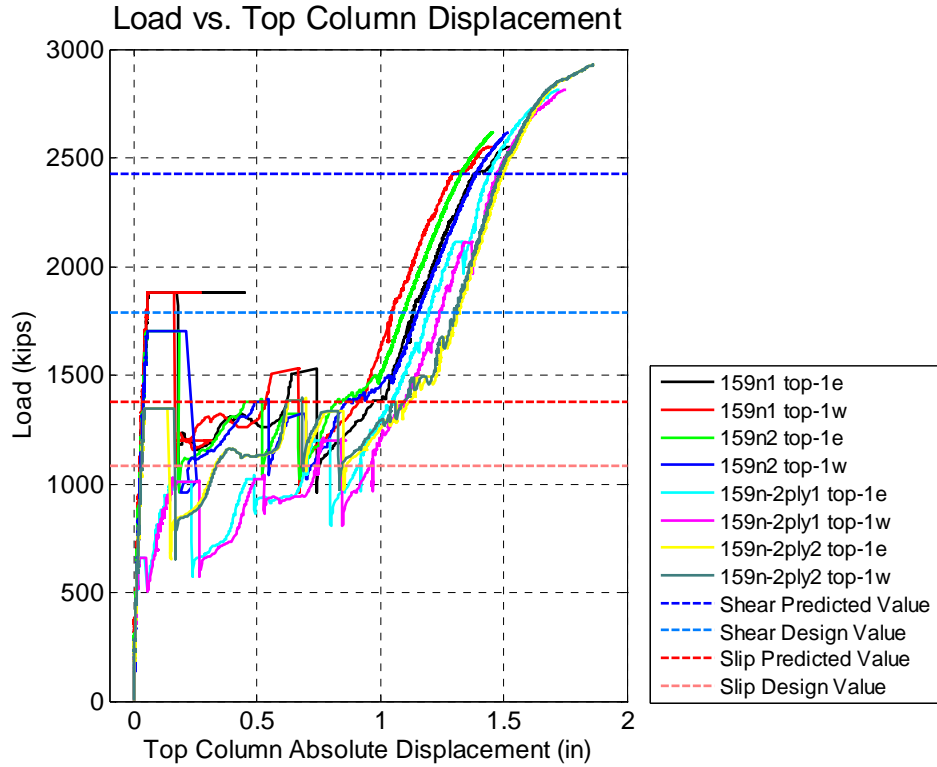


**Figure 28(c) – Top column displacement of undeveloped 159 specimens**

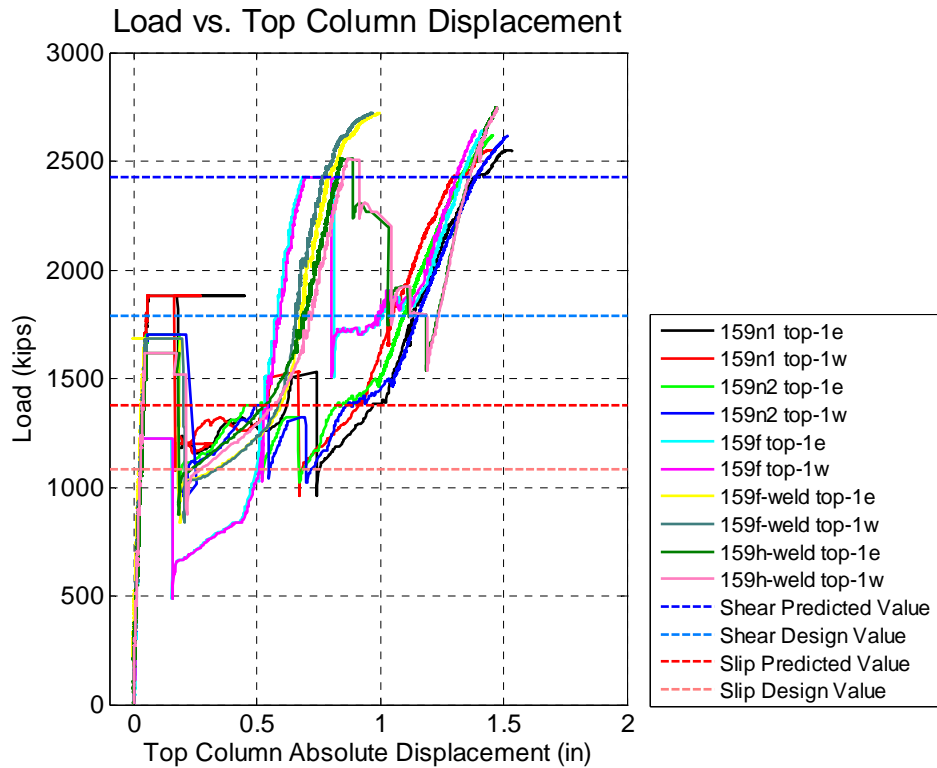


**Figure 28(d) – Top column displacement of welded 159 specimens**

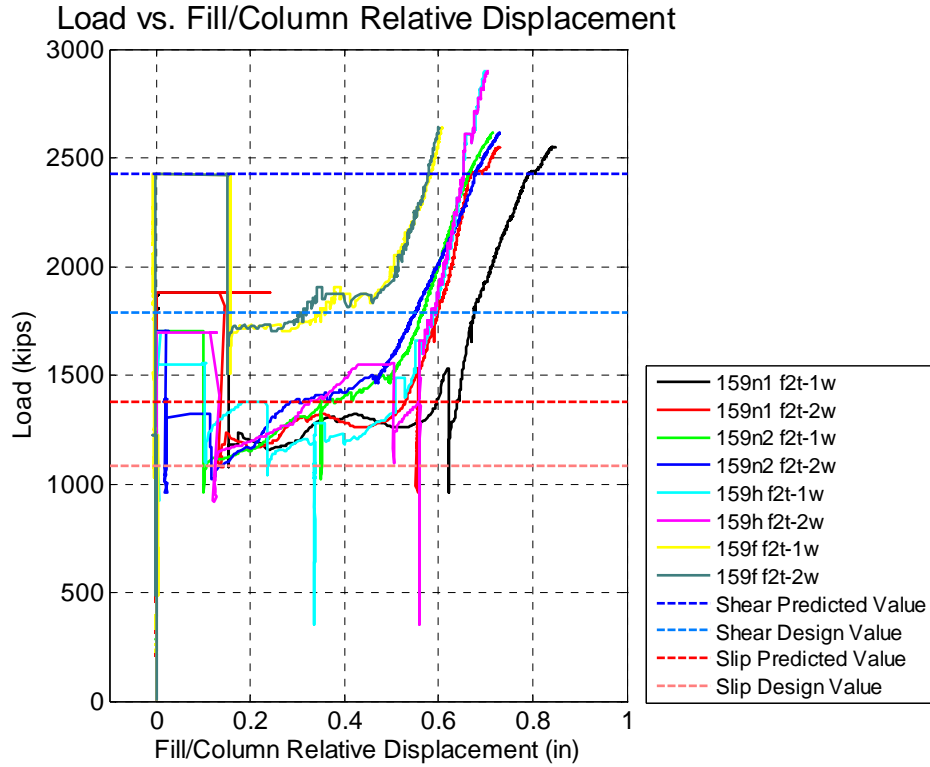


**Figure 28(e) – Top column and filler plate relative displacement of 159 specimens**

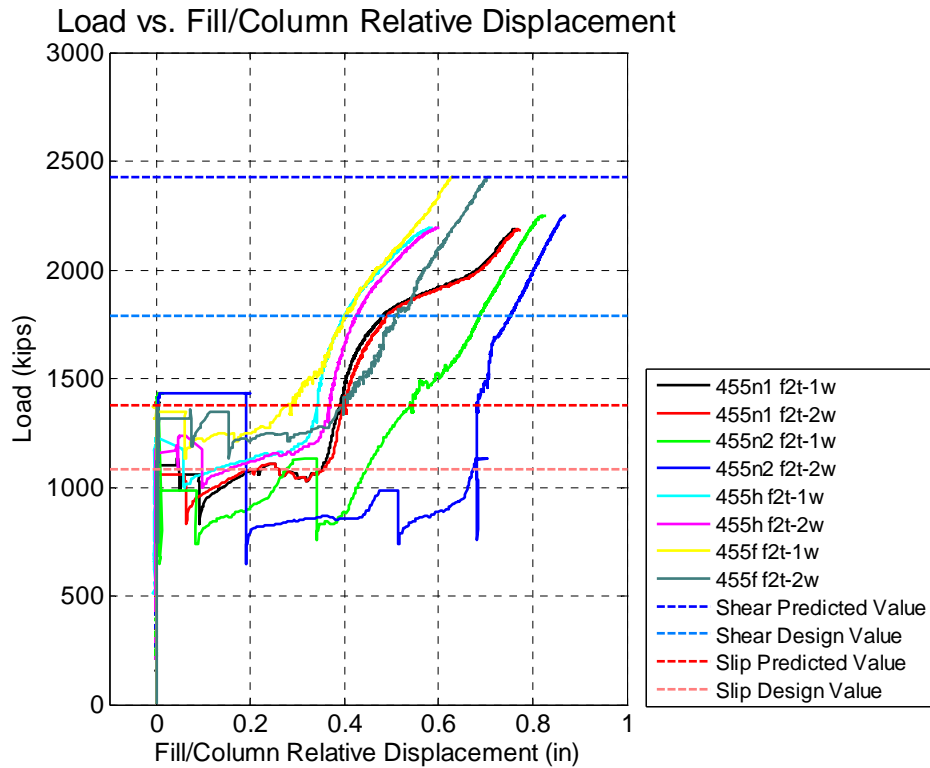


**Figure 28(f) – Top column and filler plate relative displacement of 455 specimens**

The typical behavior of the 159 and 455 specimens can be compared in Figure 28(a) and Figure 28(b). The stiffness of the 455 specimens after the bolts have slipped into bearing tends to be lower. This is likely associated with additional yielding of the bolt holes on the top column and splice plates due to the thinner filler thickness (this is discussed in Section 4.2.5).

The strain gages were placed between bolt rows in line with each column of bolts (see Figure 9 for the instrumentation plan). In the splice and filler plates the distance between the bolt holes and the strain gages was likely insufficient to develop a uniform strain distribution. In addition, prior to slip, the load is transferred to the splice plate solely by friction on the inside face, resulting in strain variation through the thickness of the plate. Although the absolute magnitude of the strain measurements is thus influenced by these effects, relative comparisons between different gages are still useful. The gages on the top and bottom column were necessarily placed near the loading platen, which also likely influenced these measurements. Detailed strain measurements are presented in Appendix B.

The curvature in the splice plates in the gap between the top and bottom column for specimens 159f, 159h, 159n1 and 159n2 for the load below 1000 kips are shown in Figure 29(a). The curvature was calculated first by dividing the difference between the average of the east and west strain gages on the inside and outside of the splice plate by the thickness for the north and south splice plate, respectively, and then those resulting values were averaged. The curvature was approximately proportional to the applied load. It is evident that the curvature in the undeveloped specimens was larger than for the developed specimens for a given load.

The curvature in the splice plates for specimens 455f, 455h, 455n1 and 455n2 are shown in Figure 29(b). There is not a discernable relationship between curvature and development. The undeveloped 159 and 455 specimens are shown in Figure 29(c). The curvature in the splice plates is much lower for the 455 specimens compared to the 159 specimens. The curvature in the splice plates for the 159 specimens including the welded specimens are shown in Figure 29(d). Although the welded specimens are developed, their response is closer to the undeveloped specimens than the bolted developed specimens; this indicates that the extended, bolted length of the filler plate in the bolted developed specimens likely stiffened the restraint offered to the splice plate in the gap region and lowered the eccentricity with which the force was introduced from the top column into the splice plate, and thus mitigated some of the curvature in the splice plate. The welded specimen, on the other hand, did not engage the filler plates above the top of the splice plate, and so responded more like the undeveloped specimens.

One possible mechanism for the resistance of the moment in the splice plate is shown in Figure 30. The moment observed in the splice plate,  $M_{SPLICE}$ , is resisted by a couple on the surface between the splice plate and filler plate. The moment in the splice plate causes an increased clamping force at the bottom of the splice plate and a lower clamping force at the top. Therefore the moment in the splice plate causes the centroid of the clamping force to move towards the bottom of the splice plate. It is then expected that a

greater proportion of the force will be transferred between the filler plate and splice plate lower in the splice plate.

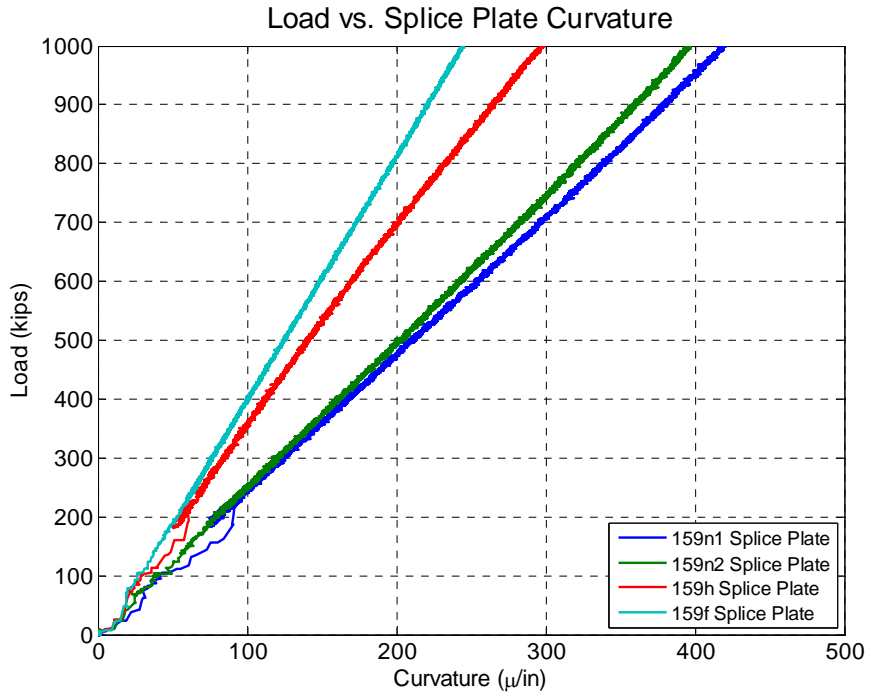


**Figure 29(a) – Curvature in splice plate at column cap vs. load for 159 specimens**

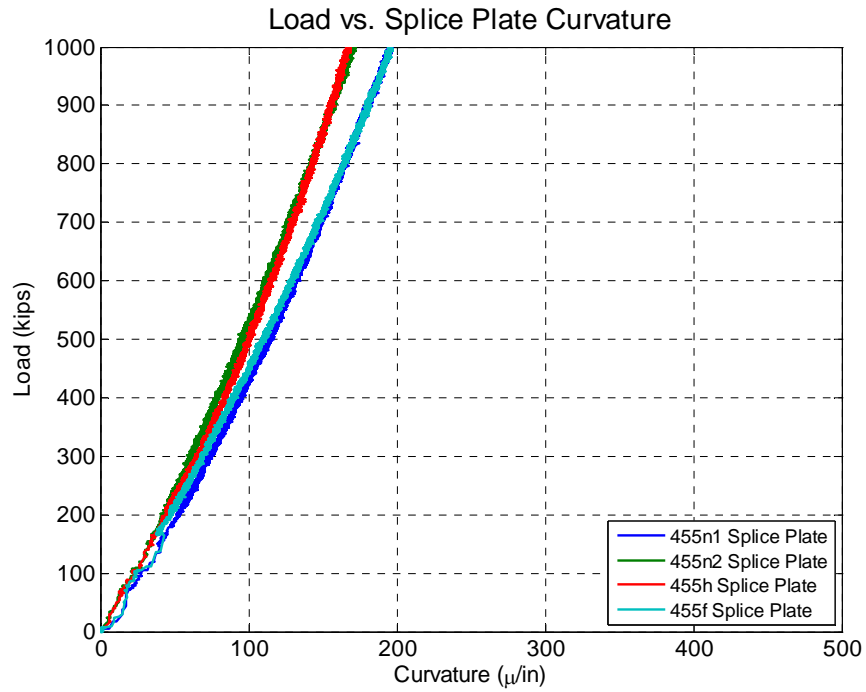


**Figure 29(b) – Curvature in splice plate at column cap vs. load for 455 specimens**

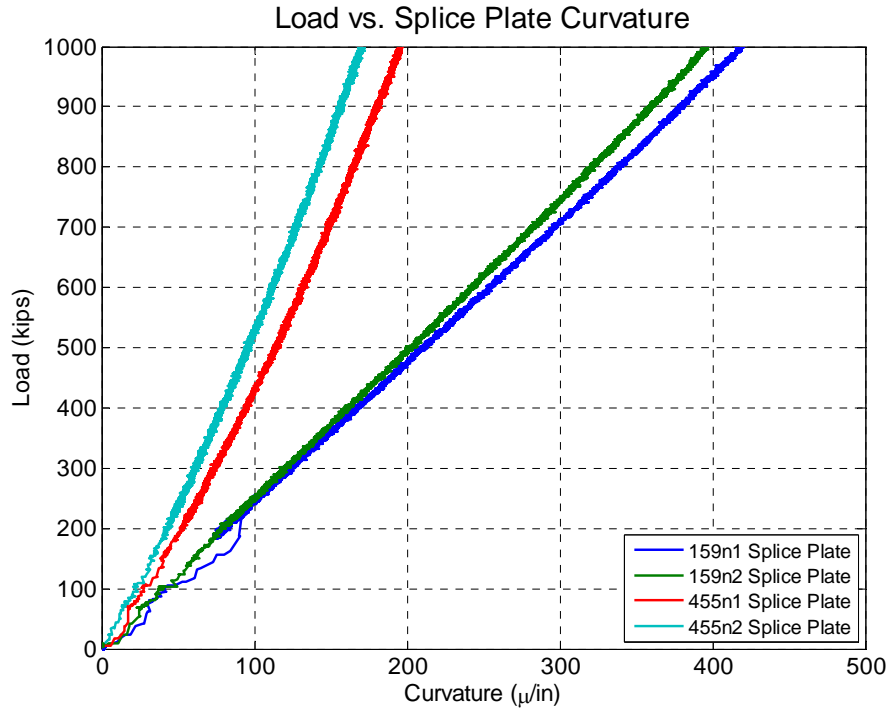


**Figure 29(c) – Curvature in splice plate at column cap vs. load for undeveloped specimens**

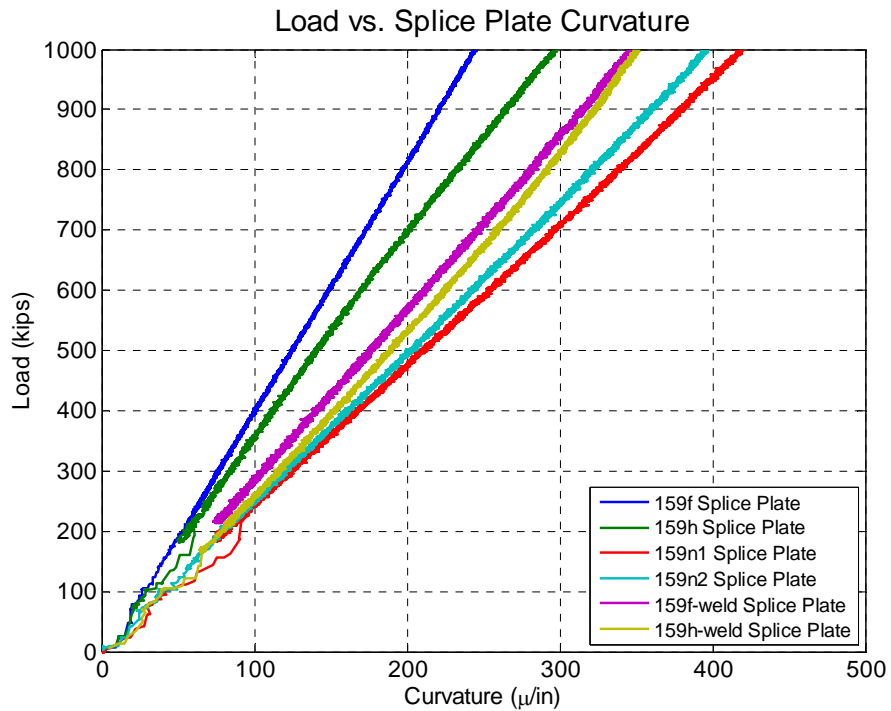


**Figure 29(d) – Curvature in splice plate at column gap vs. load for 159 welded specimens**

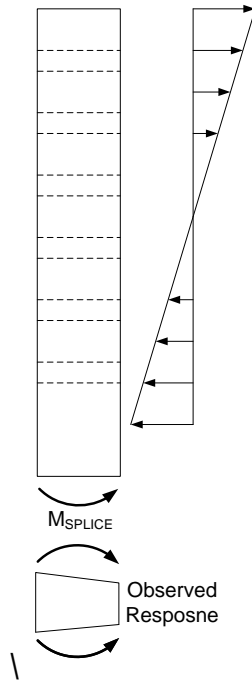


**Figure 30 – Mechanism of splice plate bending**

The distribution of strain in the splice plate for specimens 159f, 159h, 159n1 and 159n2 prior to slip (1000 kips) are presented in Figure 31(a). Although only presented for a specific load level, the trends are similar for any load level up to slip. To account for slight eccentricities, the measurements represent the average of the strain gages at each bolt row. The gages on the inside of the splice plate below bolt row 1 are also included in the average calculation at that row to account for bending in the splice plate in the gap between the columns. The black dashed line represents the expected strain assuming an elastic uniform strain distribution, with the load transferred linearly between the top of the splice plate and the bottom of the filler plate. All strain measurements are less than predicted based on elastic theory, possibly due to the effects discussed above. The four specimens have approximately the same average strain below bolt row 1 corresponding to the location of full transfer of the force into the splice plate. However, the developed specimens introduce the force into the splice plates earlier (higher on the splice plate). Therefore, a greater proportion of the force is transferred at the top of the splice plates, which is consistent with the observed splice plate bending and the mechanism discussed above, whereby the developed specimens are seen to have lower curvature in the splice plate than the undeveloped specimens.

The distribution of strain in the splice plates for specimens 455f, 455h, 455n1 and 455n2 at the same load are presented in Figure 31(b). Although there is a trend towards increased force introduction near the top of the splice plate due to development, as present in the 159 specimens, it is not as pronounced. Undeveloped specimens 159n1, 159n2, 455n1 and 455n2 are shown in Figure 31(c). The undeveloped 455 specimens transferred more force at the further up the splice plates than the undeveloped 159 specimens. This is expected since the bending in the splice plate was lower for the 455

specimens. The welded specimens are shown for comparison with the previously discussed 159 specimens in Figure 31(d). The influence of development on the introduction of force into the splice plate is not as apparent for the welded specimens, as they behave similarly to the undeveloped specimens. As discussed above, the shorter filler plate in the welded specimen leads to larger eccentricities for the introduction of force through the filler and leads to bending in the splice plate comparable to an undeveloped specimen.

The 159 specimens exhibited increased bending in the splice plate than the 455 specimens. Typically, bending is not predicted in spliced connections. The bending is likely a consequence of the use of filler plates. Therefore it is logical that the thinner filler plates of the 455 specimens have a smaller influence than the thicker filler plates of the 159 specimens. Development of the filler plate may reduce the effect of the filler plates, distributing the force in the section, simulating a single connected member. Since the welded development is not introduced before the connection, the beneficial effect is less pronounced. However, in these tests, the welded specimens failed at a large load both for slip and shear, indicating that the added continuity provided by welding helped to mitigate some of the damage to the bolts that otherwise occurred between the column and the filler plate in the bolted filler connections.

More detailed discussion of the slip and bolt shear response of these specimens, along with the effects of development, are presented in Sections 4.3., 4.4, and 4.5.

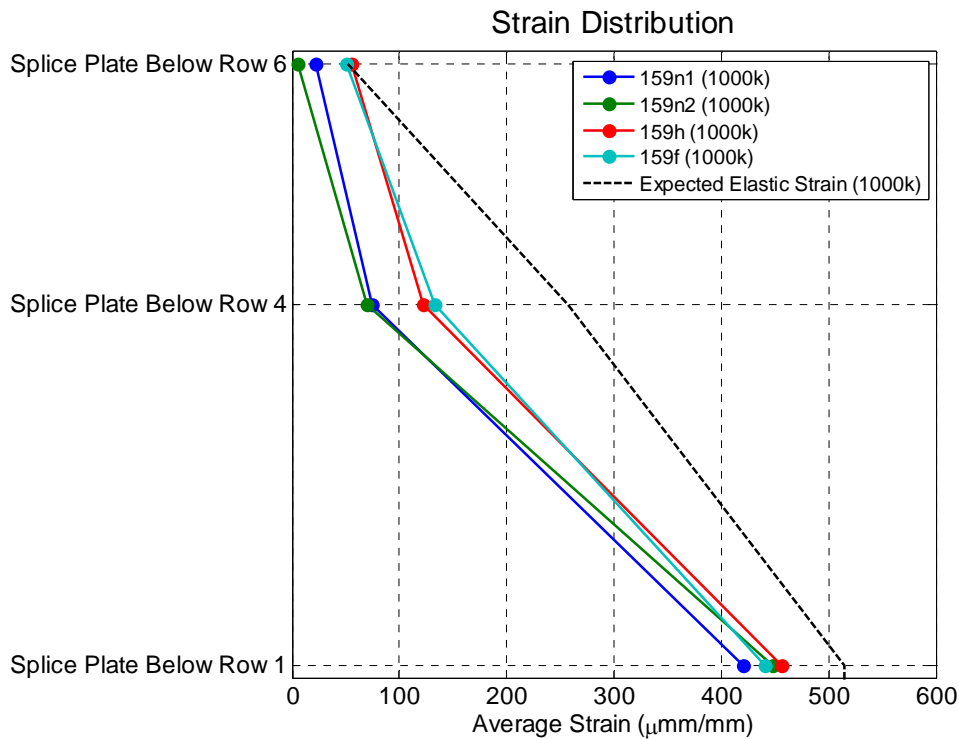


**Figure 31(a) – Distribution of strain in splice plate of 159 specimens**

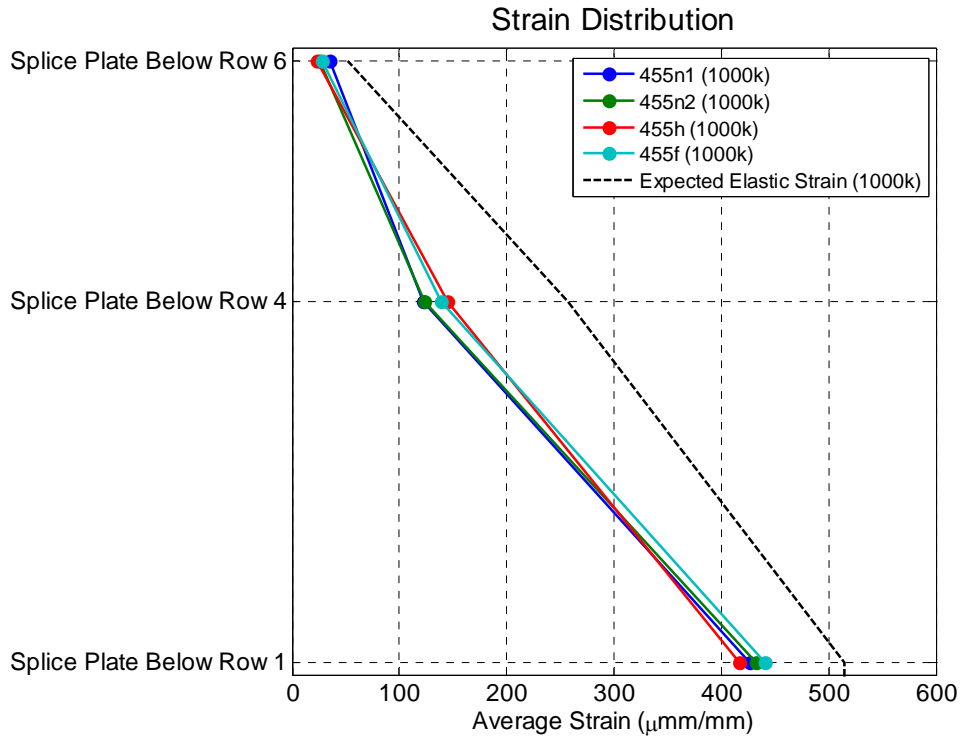


**Figure 31(b) – Distribution of strain in splice plates of 455 specimens**

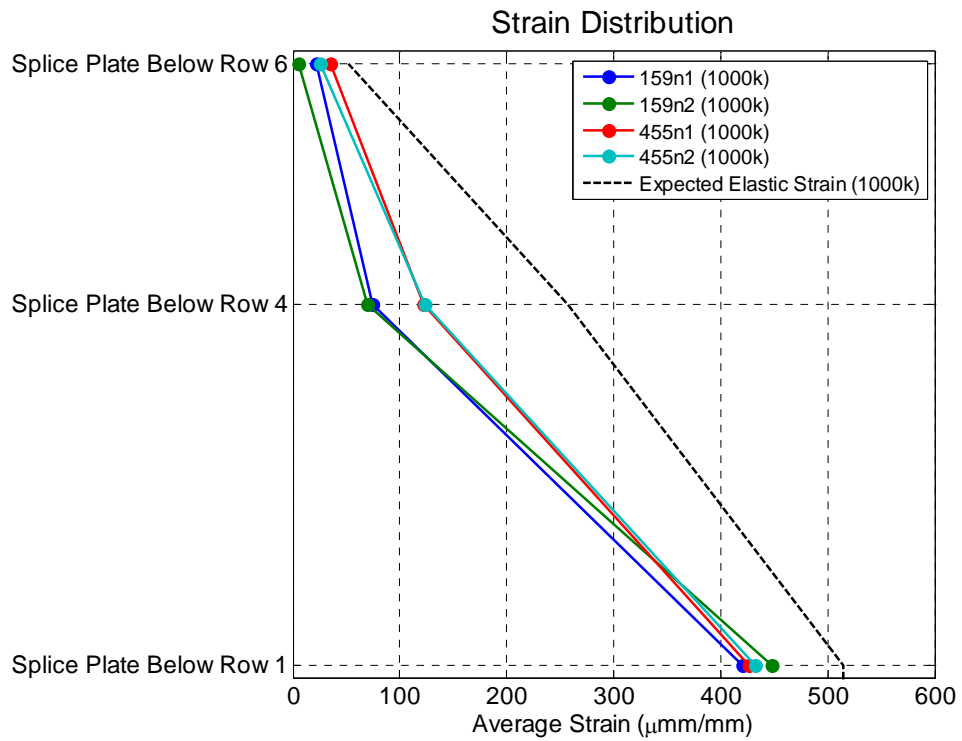


**Figure 31(c) – Distribution of strain in splice plates of undeveloped specimens**

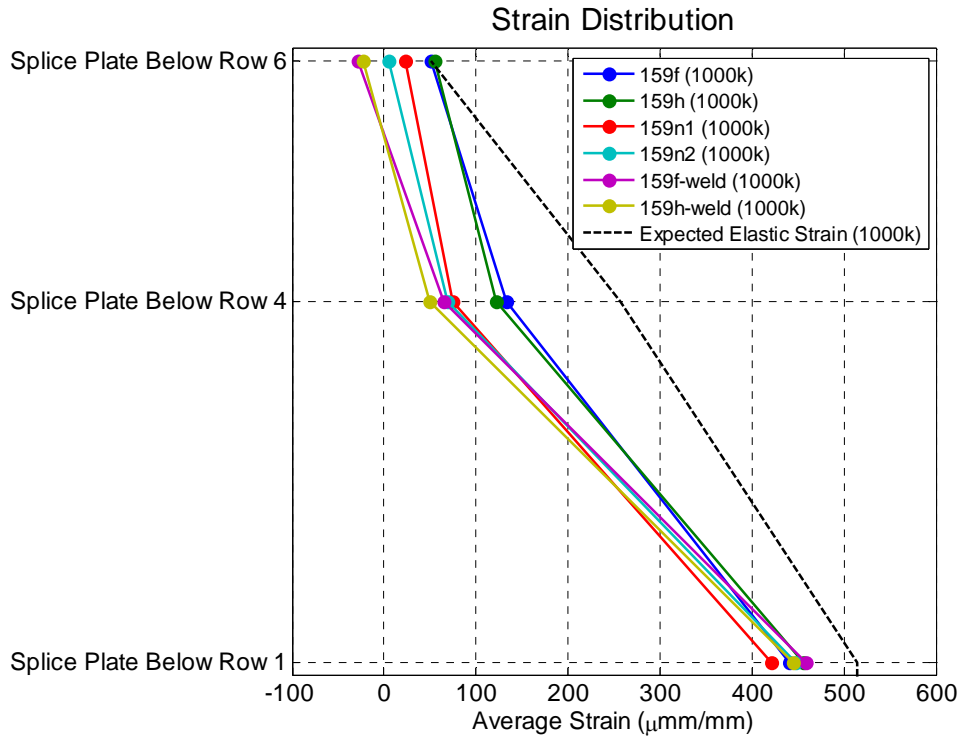


**Figure 31(d) – Distribution of strain in splice plates of 159 welded specimens**

#### 4.2.5 Forensic Analysis

To examine typical faying surfaces and bolt hole deformations, three specimens were disassembled for forensic analysis. The remaining bolts were removed from these specimens and the plates were then separated. The components were placed onto a pallet separated by wood and transported to Newmark Civil Engineering Laboratory under a tarp for examination. Specimen 455n2 was selected because it had the highest slip load of the 455 specimens. Specimen 159h was selected because it had the highest shear load of all specimens that failed. Specimen 159n-2ply1 was selected because it had an unusually low initial slip load.

Elongation of the bolt holes at the faying surface was determined by measuring the maximum diameter of each hole and subtracting the original diameter (1 7/16 in. for the oversized holes), averaged over three holes per surface; these values are presented in Table 14. The top column and splice plate exhibited similar deformation, which is expected since the load was the same at both locations. For undeveloped specimens the inside and outside of the filler plate had similar deformation and thus likely carried the same load. For developed specimens the inside hole tended to have noticeably lower deformation than the outside hole (Table 14). For developed specimens, the transfer of load from the top column into the filler plate is distributed between the 24 connection bolts combined with the development bolts. The load is transferred from the filler plate to the splice plate through only the 24 connection bolts. Therefore, the load transferred

into the filler plate per bolt on the splice plate side is greater than the load transferred per bolt on the column side of the filler plate for developed specimens.

**Table 14 – Average bolt hole elongation**

<b>Specimen</b>	<b>455n2</b>	<b>159h</b>	<b>159n-2ply1</b>	
<b>Ultimate Load (kips)</b>	2,248	2,907	2,813	
<b>Top Column (in.)<sup>a</sup></b>	0.13	0.07	0.10	
<b>Filler Plate Inside (in.)<sup>a</sup></b>	0.09	0.06	0.04 <sup>1</sup>	0.11 <sup>2</sup>
<b>Filler Plate Outside (in.)<sup>a</sup></b>	0.08	0.10	0.06 <sup>1</sup>	0.13 <sup>2</sup>
<b>Splice Plate (in.)<sup>a</sup></b>	0.15	0.07	0.10	
<sup>1</sup> 1/4 in. filler plate <sup>2</sup> 3 1/2 in. filler plate <sup>a</sup> Measurements were determined to the closest 1/32 in.				

Even though specimen 455n2 had the lowest ultimate load, it had the largest bolt hole deformation on the each surface. Since the 455 specimens had the thinnest filler, the bolt was allowed to rotate more without restraint from the filler plate. This caused the bolt to bear on the plates directly at the edge, providing a smaller bearing surface for the bolt. This increased the stress on the plates and they subsequently suffered further deformation, possibly responsible for the softening behavior prior to shear failure. The bolts in the 159 specimens on the other hand were restrained from rotating due to the thick filler, allowing for a large bearing surface. Figure 32 shows bolts from 159h and 455n2 that were removed during disassembly. The highlighted regions are the part of the bolt within the filler plate. It is clearly seen that the 455n2 bolt had greater rotation inside the filler plate than the 159h bolt. If the filler plate were constructed of lower strength steel, the bearing deformation would have been larger, reducing the bolt rotation restraint



**Figure 32 – Intact bolts from 455n2 (left) and 159h(right)**

Specimen 159h had significant gouging around the bolt holes on the top column (Figure 33(a)) and inside face of the filler plate (Figure 33(b)). The outside face of the filler plate and inside face of the splice plate had gouging between the bolt holes (Figure 33(c) and (d)). There was significant gouging between the bottom of the filler plate and splice plate (Figure 33(d)), consistent with the additional frictional resistance mechanism analysis presented in Section 4.4. The effect of the gouging between the plates is a possible cause of the observed 34% increase in slip resistance. It is also likely that the gouging still provided resistance after the bolt pretension was relaxed, contributing to the shear strength of the connection, which was 19% higher than expected.

Specimen 455n2 exhibited significantly less surface scarring than specimen 159h. The top column and inside face of the filler plate were smooth with slight damage around the bolt holes (Figure 34(a) and (b)). The north filler and splice plate surface was smooth, with minimal scarring (Figure 34(c) and (d)). The south filler and splice plate surface also was smooth but exhibited numerous polished regions that were more reflective and smoother than the surrounding area (Figure 34(e) and (f)) on both plates. The surfaces contained significantly less gouging than specimen 159h, which may contribute to the reduced slip and shear strengths.

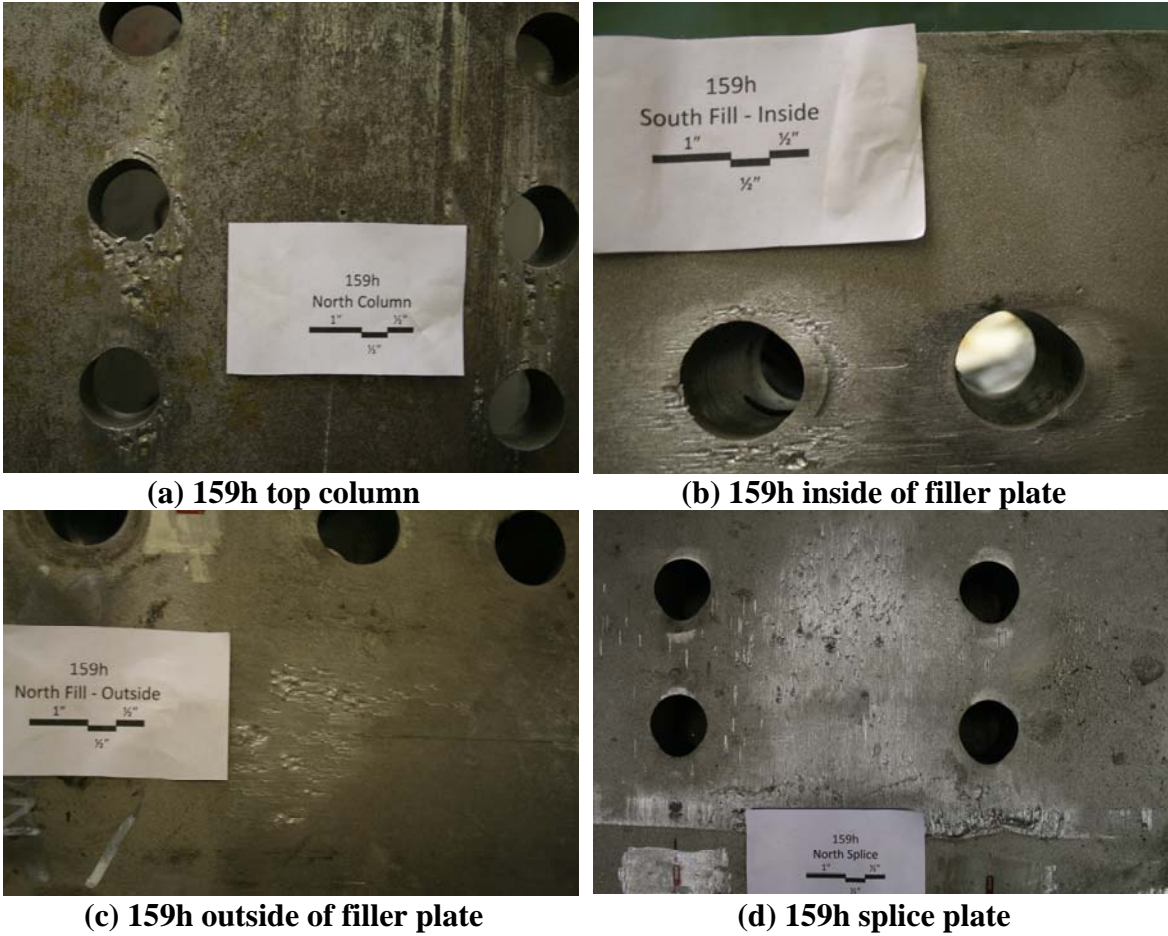


**Figure 33 – Specimen 159h faying surfaces**

Specimen 159n-2ply1 experienced more surface damage on the north side than the south side. The north side of the top column and inside surface of the 3 1/2 in. filler experienced significant gouging between the bolt holes and on the flange tips (Figure 35(a) and (b)). The respective surfaces on the south side of the specimen were smooth, with minimal gouging (Figure 35(c) and (d)). The interface between the two filler plates on the north side also experienced some gouging (Figure 35(e) and (f)). However, there was little damage to the surfaces of the two south filler plates (Figure 35(g) and (h)). This was the faying surface that slipped at approximately 50% of the predicted load and had the smoothest surface of all disassembled plates. The interface between the north splice plate and 1/4 in. plate was polished with gouging at the base of the filler plate (Figure 35(i) and (j)). The south splice plate and 1/4 in. filler plate had significant gouging (Figure 35(k) and (l)), with a 1/6 in. lip across the splice plate at the bottom of the filler plate. This may have contributed to the relatively high bolt shear strength seen in this specimen.



**(a) 455n2 top column**



**(b) 455n2 inside of filler plate**



**(c) 455n2 north outside filler plate**



**(d) 455n2 north splice plate**



**(e) 455n2 south outside filler plate**



**(f) 455n2 south splice plate**

**Figure 34 – Specimen 455n2 faying surfaces**



**(a) 159n-2ply1 north face of top column**



**(b) 159n-2ply1 inside face of north 3 1/2 in. filler plate**



**(c) 159n-2ply1 south face of top column**



**(d) 159n-2ply1 inside face of south 3 1/2 in. filler plate**



**(e) 159n-2ply1 outside face of north 3 1/2 in. filler plate**



**(f) 159n-2ply1 inside face of north 1/4 in. filler plate**



**(g) 159n-2ply1 outside face of south 3 1/2 in. filler plate**



**(h) 159n-2ply1 inside face of south 1/4 in. filler plate**



(i) 159n-2ply1 outside face of north 1/4 in. filler plate



(j) 159n-2ply1 north splice plate



(k) 159n-2ply1 outside face of south 1/4 in. filler plate



(l) 159n-2ply1 south splice plate

**Figure 35 – Specimen 159n-2ply1 faying surfaces**

## 4.3 Slip Strength

The connection slip strength, determined as described in Section 4.1, is plotted versus filler plate thickness in Figure 36. The slip strength normalized by its respective predicted strength is plotted versus filler plate thickness in Figure 37. The design and predicted values for the TN bolt specimens are represented by the horizontal lines for reference in both figures. The TC bolt specimens have a different predicted strength of 1,060 kips (as discussed in Sections 3.2.1 and 4.1), which is not shown. Table 15 shows various subsets of the data with corresponding mean and standard deviation values.

The average of all the test-to-predicted ratios is greater than unity. This could be because of the inherently uncertain nature of slip, the randomness of bolt pretension despite the use of some control bolts on one side of each connection, because of small eccentricities in the test specimens that may cause mechanisms other than pure friction to resist some of the loading, or possibly because of the large contact areas of these connections as compared to typical ancillary tests such as those in Section 3.3 and the literature.

From Table 10, Figure 36 and Figure 37, it may be seen that both specimens without a filler plate (specimens 730-std and 730-over) achieved greater slip strengths than their predicted values. Also, consistent with previous work demonstrating that there is no consistent relationship between hole oversize and slip resistance (Frank and Yura, 1981), only a slight difference was noted between the slip strengths of 730-std and 730-over.

Table 15 shows a potential trend in the slip strength as a function of number of plies. Section 4.3.1 also discusses trends seen in Table 10 and Table 15 regarding the effect of developing the connection on the slip strength. One of the specimens with two plies, 159n-2ply1, experienced very early slip between the two plies of the filler plate on one side of the connection, at 52% of the predicted load. The specimen was disassembled and there were no noticeable irregularities on the surfaces that failed early (see Section 4.2.5). The duplicate of that specimen, 159n-2ply2, experienced slip at 106% of the predicted load, resulting in an average slip strength for the two specimen of 79% of the predicted value. Specimen 159f-weld did not exhibit slip between the top column and the filler plate. Specimen 159h-weld did exhibit slip between the top column and the filler plate, at a high load, after exhibiting fractures of the welds.

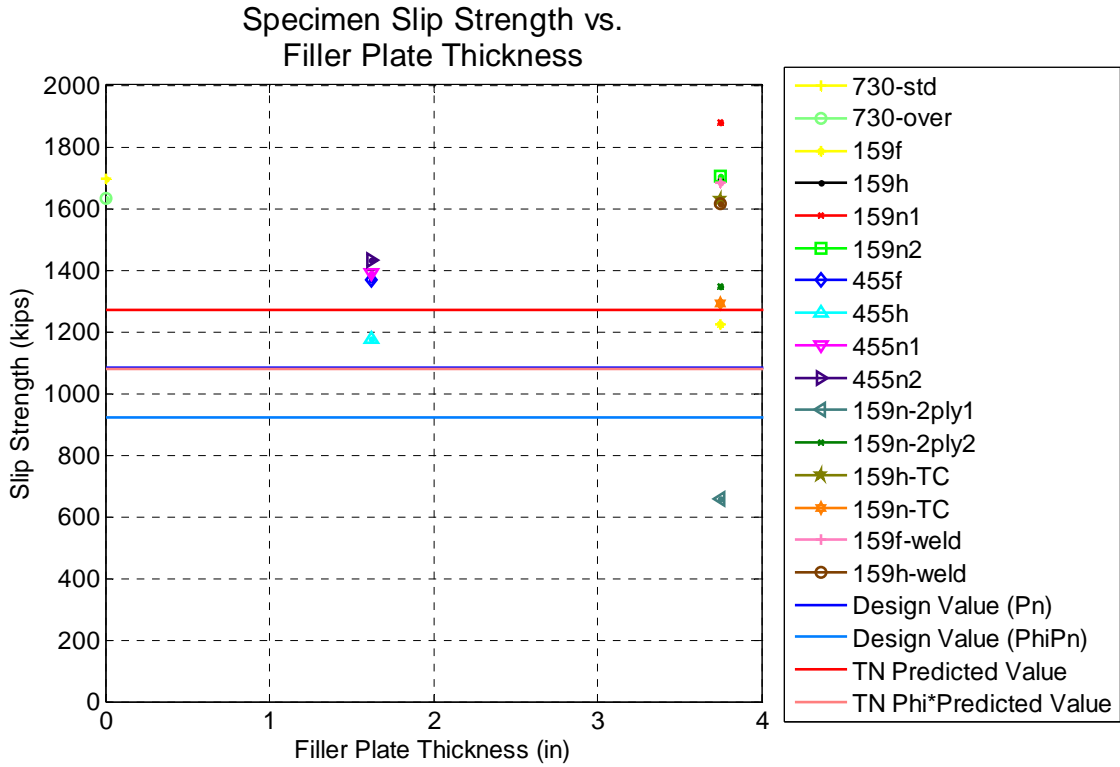


**Figure 36 – Slip strength vs. filler plate thickness**

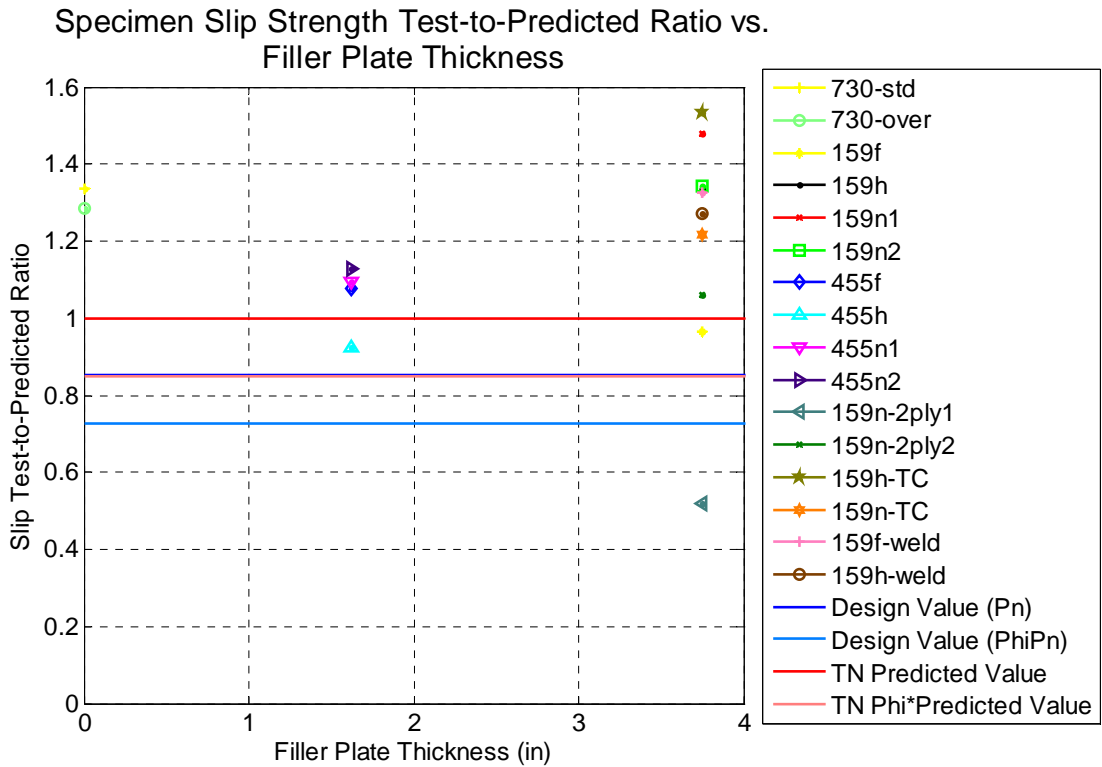


**Figure 37 – Slip strength test-to-predicted ratio vs. filler plate thickness**

**Table 15 – Slip strength tested-to-predicted ratio by specimen type**

Specimen Type	Number of Specimens	Slip Strength Test-to-Predicted Ratio	
		Mean Value	Standard Deviation
All	16	1.18	0.25
No filler	2	1.31	0.04
1 ply filler	12	1.22	0.19
2 ply filler	2	0.79	0.38
No development	7	1.12	0.30
1 ply filler, no development	5	1.25	0.16
1 ply filler, half and full development	7	1.21	0.22
1 ply filler, full development	3	1.12	0.19
TN bolts	14	1.15	0.25
TC bolts	2	1.38	0.22

#### 4.3.1 Statistical Variation of Slip Strength

The slip coefficient is a randomly varying quantity. In connections with more than one faying surface, failure may thus occur at a load less than would be indicated by a deterministic analysis assuming a single faying surface. In other words, the more slip surfaces there are, the more likely a lower value of the slip coefficient will be present for one of the slip surfaces, and therefore the more likely that initial slip of the connection will be at a lower load than in similar connections with fewer slip surfaces. As one example of how to address the detrimental effect of additional slip surfaces, the AASHTO *Specification* limits the number of plies to at most two (AASHTO, 1994).

Statistical data of the coefficient of friction is obtained from measured values from experimental tests. These tests are, in general, conducted with two slip surfaces, such as the tests in Section 3.3 and such as many of the tests reported by Grondin et al. (2008). It is reasonable for these tests to assume that the measured slip coefficient from the test is actually the *average* of the slip coefficients of the two surfaces, rather than the *lowest* value of slip coefficient from the two surfaces. This was consistently observed in the ancillary tests of Section 3.3, for example, where the extensometers and observations clearly showed that one surface did not typically fail prior to the other. For the case of the measured slip coefficient being presumed to be the average of the slip coefficient of the two surfaces of the ancillary test, it may be shown that the slip coefficient mean and standard deviation of one surface is (to avoid confusion with the slip coefficient, the mean of a random variable is designated by the symbol  $m$ , rather than the typical  $\mu$ ):

$$\begin{aligned}
 m_{\mu,one\ surface} &= m_{\mu,two\ surfaces} \\
 \sigma_{\mu,one\ surface} &= \sqrt{2}\sigma_{\mu,two\ surfaces}
 \end{aligned}
 \tag{3}$$

For blast-cleaned surfaces the mean slip coefficient is 0.525 with a standard deviation of 0.101 (Grondin et al., 2008). These values are based predominantly on experiments in

which the slip strength is the average of the slip strength of the two surfaces being tested. Thus, the mean and standard deviation of any one slip surface is given by Equation (4).

$$\begin{aligned} m_{\mu,one\ surface} &= 0.525 \\ \sigma_{\mu,one\ surface} &= 0.101\sqrt{2} = 0.143 \end{aligned} \quad (4)$$

The slip coefficient, as a random variable, may be assumed to follow a normal distribution. If one further assumes that the clamping force is deterministic, the slip strength will also follow a normal distribution. Equation (5) is the CDF of a normal random variable.

$$F_x(x) = \frac{1}{2} \left( 1 + \operatorname{erf} \left( \frac{x - m_x}{\sigma_x \sqrt{2}} \right) \right) \quad (5)$$

The concept of order statistics (David, 1970; Song and DerKiureghian, 2003) can be used to determine the statistical properties of the lowest value of a set of randomly varying quantities (see Appendix D). The cumulative distribution function (CDF) of the lowest slip strength of multiple slip surfaces with the same statistical data such as seen in undeveloped fillers is written in terms of the cumulative distribution function  $F_{S,one\ surface}(x)$  of a single slip surface and the number of slip surfaces,  $n$ , Equation (6).

$$F_{S,one\ side}(x) = 1 - \left\{ 1 - F_{S,one\ surface}(x) \right\}^n \quad (6)$$

For example, with a single-ply filler, the number of slip surfaces,  $n$ , per side is 2. Equation (6) is used to find the CDF of lowest of the two slip strengths on one side, based on using the values obtained from Equations (3) and (4). From the CDF, the probability distribution, mean ( $m_{S,one\ side}$ ), and standard deviation ( $\sigma_{S,one\ side}$ ) of the lowest slip strength on each side can then be determined using standard statistical approaches.

For the purposes of this study, failure of the primary connection test specimens is also defined as the sum of the lowest slip strengths from each side of the connection (recognizing that each side may have multiple slip surfaces). This implies that both sides of the connection fail at approximately the same load. This definition is consistent with observed behavior for most of the specimens (Table 13) (For the one exception, 159n-2ply1, slip first occurred only on one surface, not on both sides).

The average and standard deviation of the sum of the lowest slip strengths from each side is thus computed using Equation (7):

$$\begin{aligned} m_{S,connection} &= 2m_{S,one\ side} \\ \sigma_{S,connection} &= \sqrt{2}\sigma_{S,one\ side} \end{aligned} \quad (7)$$

This resulting mean is considered to be the expected connection slip strength. The expected slip strength can be determined for any number of plies in an undeveloped connection by changing  $n$  in Equation (6). The results of this process are shown in Table 16, where the reduction in the slip strength is indicated with respect to a deterministic analysis using the published value for the slip coefficient from Grondin et al. (2008). This table is based on the data for Class B surfaces presented above. The addition of fillers reduces the expected slip strength, depending of the number of slip surfaces. These results are overlaid on experimental data from this study and others (81 tests, as noted at the beginning of Section 4) in Figure 38. As may be seen in the figure, the statistical model identifies the trends in the data well, and if anything the percentage reductions in Table 16 may be conservative. Appendix D highlights other possible assumptions that may be made in the calculations above, leading to other options for statistical strength reductions, but the assumptions above were deemed to be closest to what was measured and observed in the ancillary slip tests of Section 3.3 and the connection tests. Appendix D also contains a similar analysis for developed fillers, the results of which showed that development helps lessen the reduction due to presence of fillers. However, the benefit of development is shown to be dependent on the additional pretension provided by the development bolts which depends on the thickness of the filler.

**Table 16 – Statistical multi-ply slip strength reduction**

# Plies	# Surfaces per Side	expected strength = $m_{S,connection}$	$\sigma_{S,connection}$	$\mu_{effective} =$ expected strength/ clamping force	% Reduction
0	1	1449	280	0.525	0.0%
1	2	1226	231	0.444	15.4%
2	3	1114	209	0.404	23.1%
3	4	1042	196	0.377	28.1%
4	5	989	187	0.358	31.7%
5	6	948	180	0.343	34.6%
6	7	914	175	0.331	36.9%
7	8	886	171	0.321	38.9%
8	9	862	167	0.312	40.5%

The data from Table 10 and Table 15 provide mixed results for supporting the fact that developing the connection should help minimize the possibility of slip on the developed slip surface, and thus that developed connections should (for a statistical sample) slip at higher loads than undeveloped connections due to the added clamping force of the development bolts. The data from Table 15 do not support this theory, but looking at mean values alone in that table is not adequate. From Table 13, data in support of this theory are that 1) both sides of specimen 159f slipped between the top column and the filler plate at a much higher load than between the filler plate and the splice plate; 2) one

side of specimen 455f slipped between the top column and the filler plate at a higher load than between the filler plate and the splice plate; and 3) the six developed specimens (159f, 159h, 455f, 455h, 159f-weld, 159h-weld) consistently failed first along the slip surface between the filler plate and the splice plate, whereas specimens with no development sometimes failed first along the slip surfaces between the filler plate and top column (e.g., specimen 159n1). In addition, as the number of bolts developing the fill decreases, the evidence that these bolts mitigate slip on the surface between the filler and the top column decreases, such as comparing the slip order and loads for specimens 159f versus 159h, 455f, and 455h. This indicates that if one is developing a thin filler, the few additional bolts may help very little to mitigate slip along the surface between the filler and the top column. It is also likely that once there is slip in the bolts on the surface between the filler and the splice plate, the bolt pretension is diminished and thus slip along the other slip surfaces is more likely to follow immediately. However, Table 13 shows: 1) specimens 159n1 and 159n2 slipped at higher loads than specimen 159h and than the first slip occurrence in specimens 159f, 159f-weld, and 159h-weld; and 2) specimens 455n1 and 455n2 slipped at higher loads than specimens 455h and 455f. Nevertheless, these results comparing the slip loads between developed and undeveloped specimens could be due to the inherently uncertain nature of slip, such as due to some randomness in the bolt pretension despite the use of control bolts on one side of each connection. In addition, no connections with two or more plies were tested that had developed connections – this additional information may be appropriate to obtain in future research.

A linear regression analysis conducted on the slip strengths of undeveloped fillers from all authors is presented in Figure 38. In order to have an vertical axis intercept value (reduction for zero plies) of 1.0 for the regression analysis, the best fit was obtained by not including the data for zero plies in the linear fit. The values from this regression analysis are tabulated in Table 17 along with the corresponding mean value of the associated experiments for each number of plies. This resulting empirical relationship shows that the slip resistance is reduced by 20% for each additional ply. As shown in Table 17 and Figure 38, if the regression analysis is calculated without the results from Dusicka and Lewis (2007), the reduction is reduced to approximately 10% per ply, as the data from Dusicka and Lewis (2007) tends to have low test-to-predicted ratios. Based on empirical results and the statistical analysis, it is recommended that the slip strength be reduced depending on the number of plies, independent of filler thickness. For one ply there is a large amount of scatter. Based on the fact that the mean value of the slip strength of specimens with one ply was 0.96, it is reasonable to consider having no reduction in slip strength for one ply.

Figure 39 shows the test-to-predicted ratios of slip strength plotted versus filler thickness. No discernable trend can be identified, indicating that filler thickness does not significantly affect the slip strength.

When the test-to-predicted ratios for of all 81 tests considered are separated by hole oversize in Figure 40, no significant difference in strength is seen. This implies that, with respect to filler connections, it is not necessary to have both a hole factor,  $h_{sc}$ , and simultaneously design connections with oversized holes at the required strength level

(e.g.,  $\phi = 0.85$ ,  $\Omega = 1.76$ ), versus designing the connection at a serviceability limit state (e.g.,  $\phi = 1.0$ ,  $\Omega = 1.50$ ). Since no significant difference in strength is seen, the two provisions are likely redundant. Only one provision reflecting the increased consequences of slip with oversize holes should be necessary. Grondin et al. (2008) provides guidance as to what the resistance factor should be for a given desired levels of reliability. For example, the data in this study justifies adopting resistance factors corresponding to two different desired levels of reliability and then eliminating the hole factor, or vice versa by retaining the hole factor and then having only one resistance and safety factor regardless of the type of hole. It is also noted that slotted holes are not included in this study.

**Table 17 – Recommended slip strength reduction values for multi-ply connections**

Number of Plies on One Side of Connection	All Studies		L&F, F&Y, BD&H	
	Experimental Mean Test-to- Predicted Ratio	Reduction Factor	Experimental Mean Test-to- Predicted Ratio	Reduction Factor
<b>0</b>	0.90	1.0	1.18	1.0
<b>1</b>	0.81	0.8	1.0	0.9 (1.0) <sup>a</sup>
<b>2</b>	0.54	0.6	0.79	0.8
<b>3</b>	0.51	0.4	0.51	0.7

<sup>a</sup>A reduction factor of 1.0 may be adequate for design.

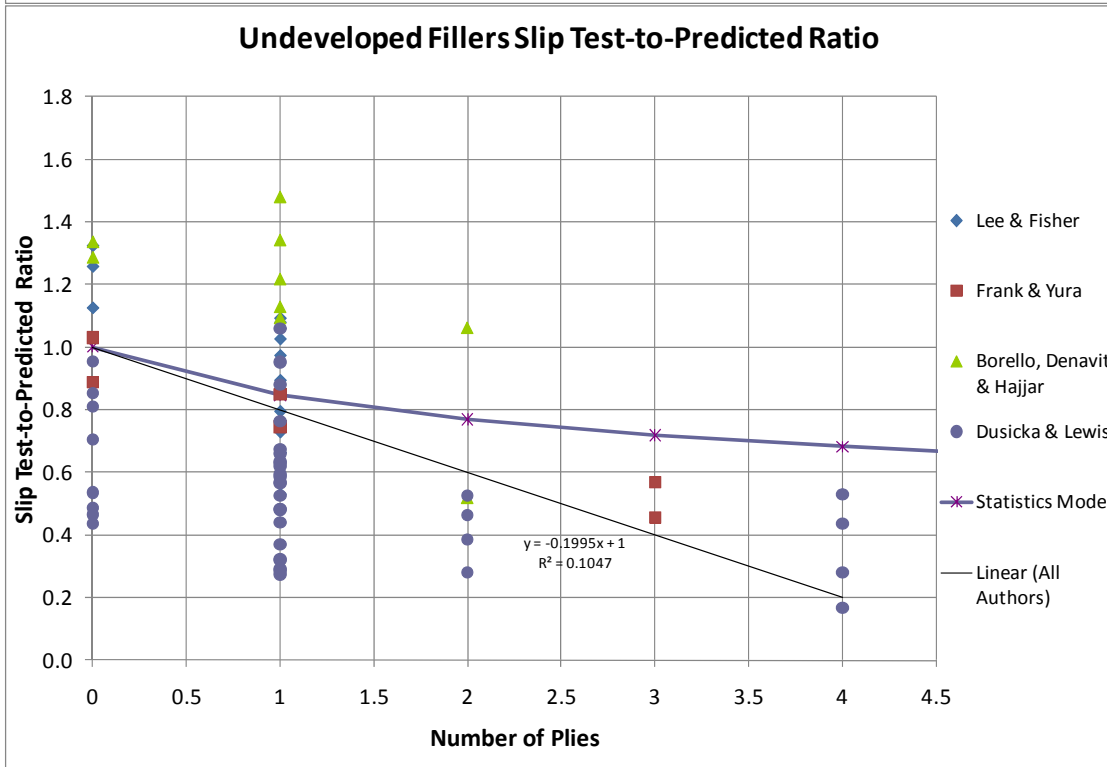
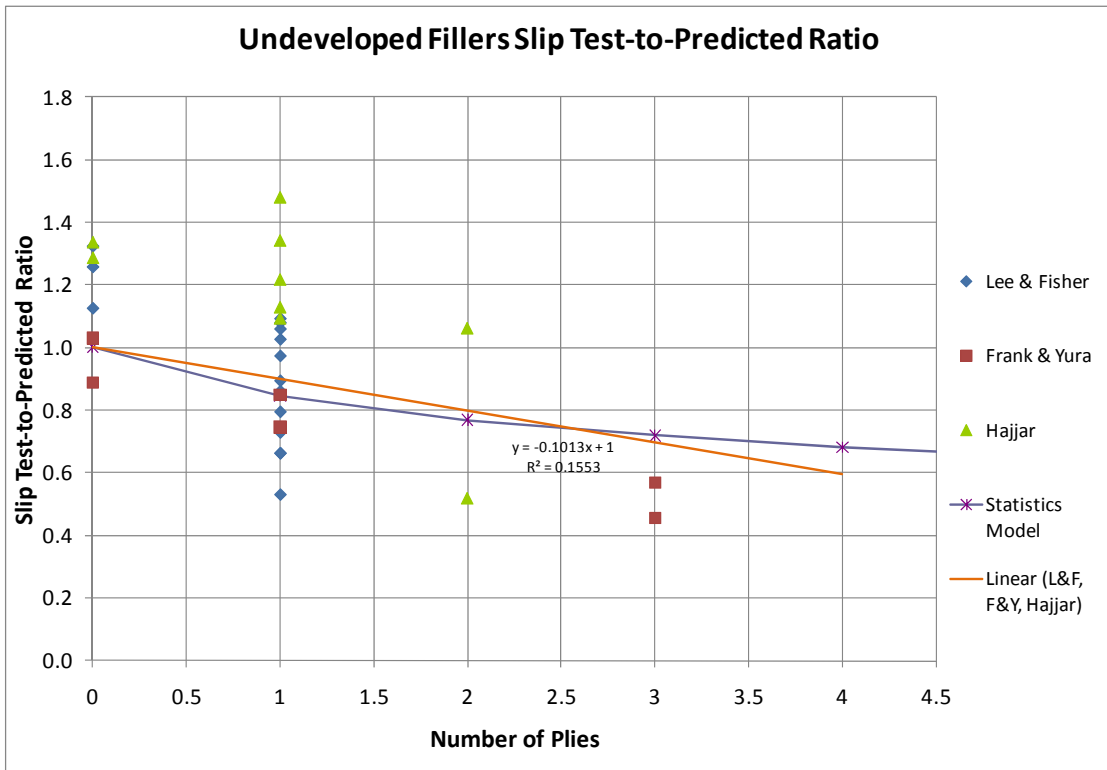


**Figure 38 – Undeveloped fillers slip strength test-to-predicted ratio vs. number of plies. a) Lee & Fisher, Frank & Yura, and Borello, Denavit & Hajjar. b) Lee & Fisher, Frank & Yura, Borello, Denavit & Hajjar, and Dusicka & Lewis**

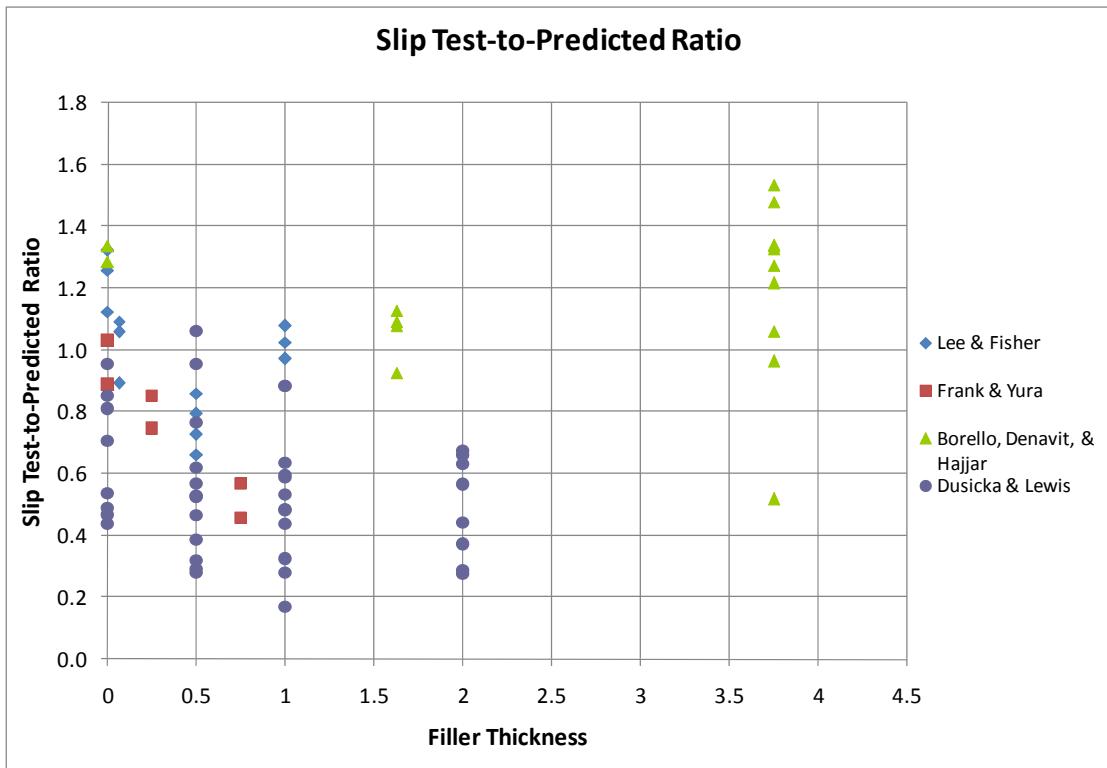
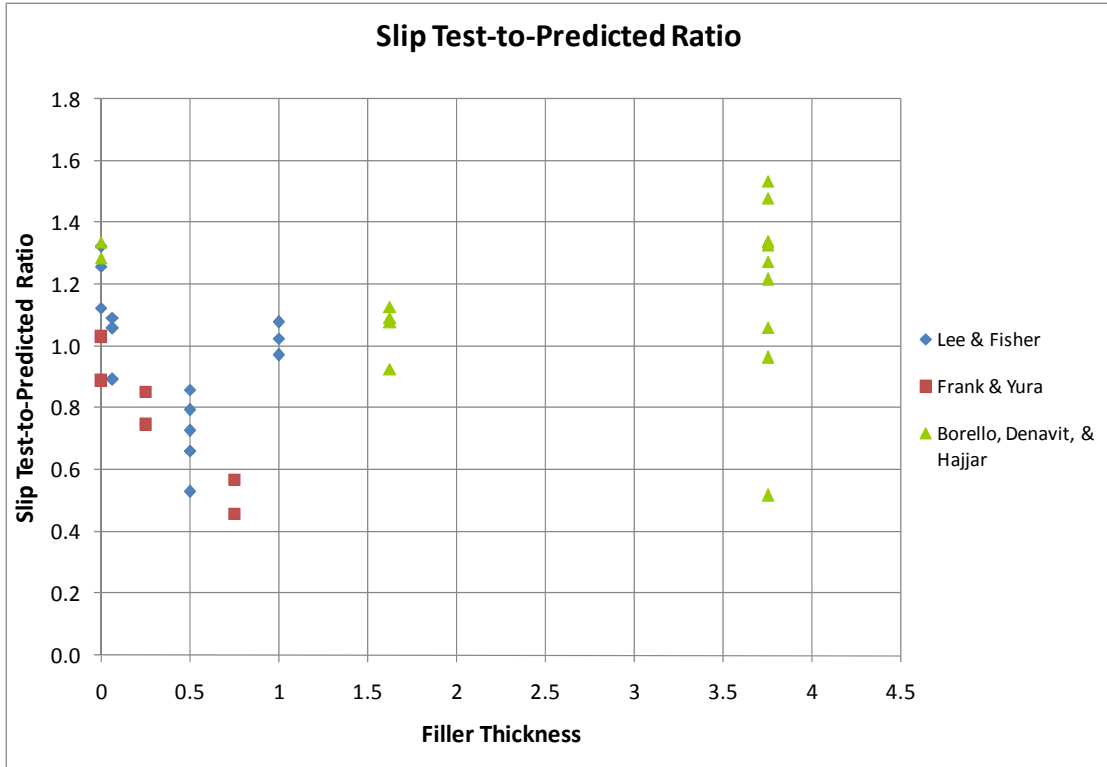


**Figure 39 – Slip strength test-to-predicted ratio vs. filler thickness. a) Lee & Fisher, and Borello, Denavit & Hajjar. b) Lee & Fisher, Borello, Denavit & Hajjar, and Dusicka & Lewis**

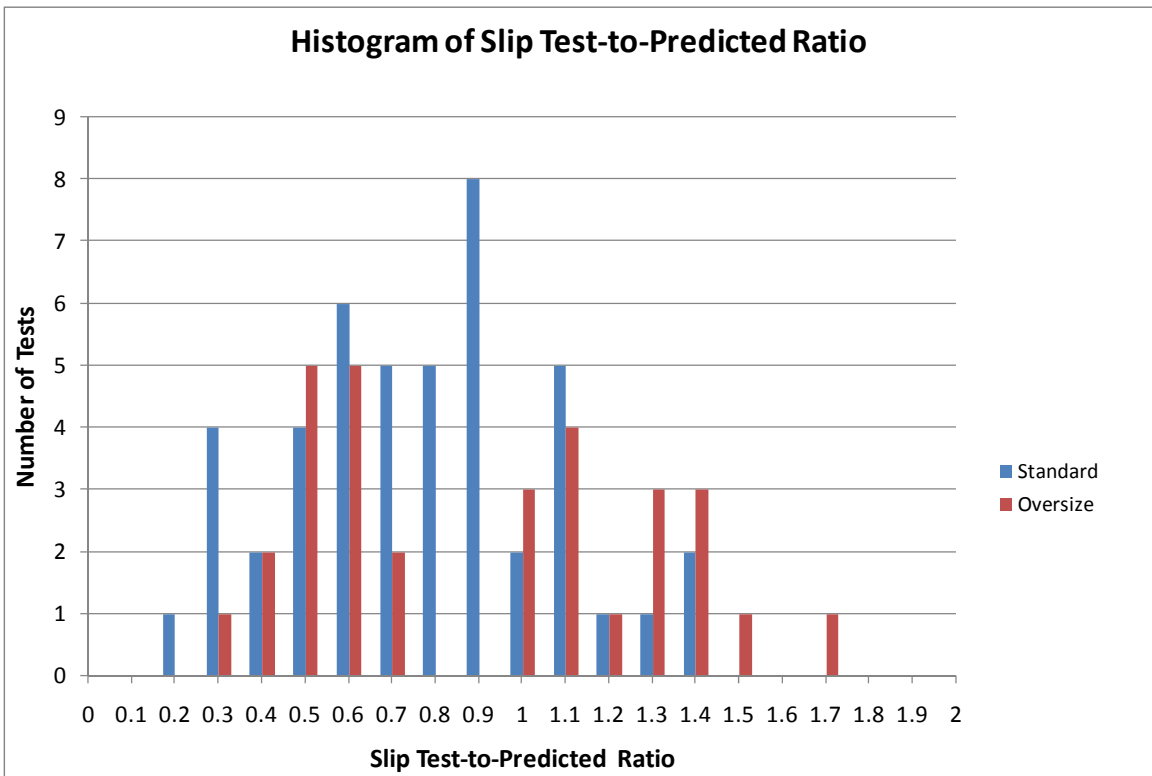
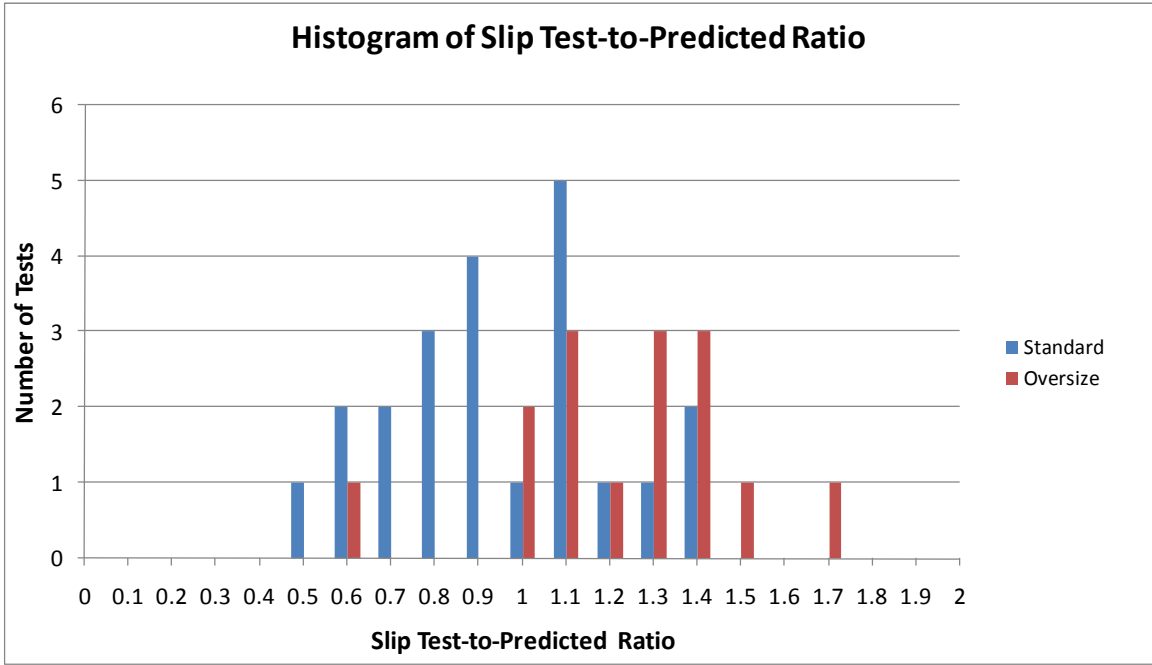


**Figure 40 – Slip strength test-to-predicted ratio results by hole size. a) Lee & Fisher, Frank & Yura, and Borello, Denavit & Hajjar. b) Lee & Fisher, Frank & Yura, Borello, Denavit & Hajjar, and Dusicka & Lewis**

## 4.4 Shear Strength

The connection shear strength of each specimen, determined as described in Section 4.1, is plotted versus the filler plate thickness in Figure 41. The shear strength normalized by the predicted shear strength plotted versus the filler plate thickness is shown in Figure 42. The design and predicted values for the TN bolt specimens are represented by the horizontal lines for reference in both figures. The TC bolt specimens have a different predicted strength of 2,586 kips, which is not shown. Figure 41 and Figure 42 also show the bolt shear strength reduction formula of Section J5 of AISC (2005); the range of applicability of this formula from 1/4 in. to 3/4 in. is also identified in these figures with vertical dashed lines.

The shear strength of specimens 159h-TC and 159n-TC exceeded the capacity of the testing machine. The shear strength of specimen 159f-weld was not achieved due to local buckling of the top column prior to shear failure, but after the predicted yield strength. For these three specimens, the lower bound of shear strength was plotted but was neglected for statistical calculations.

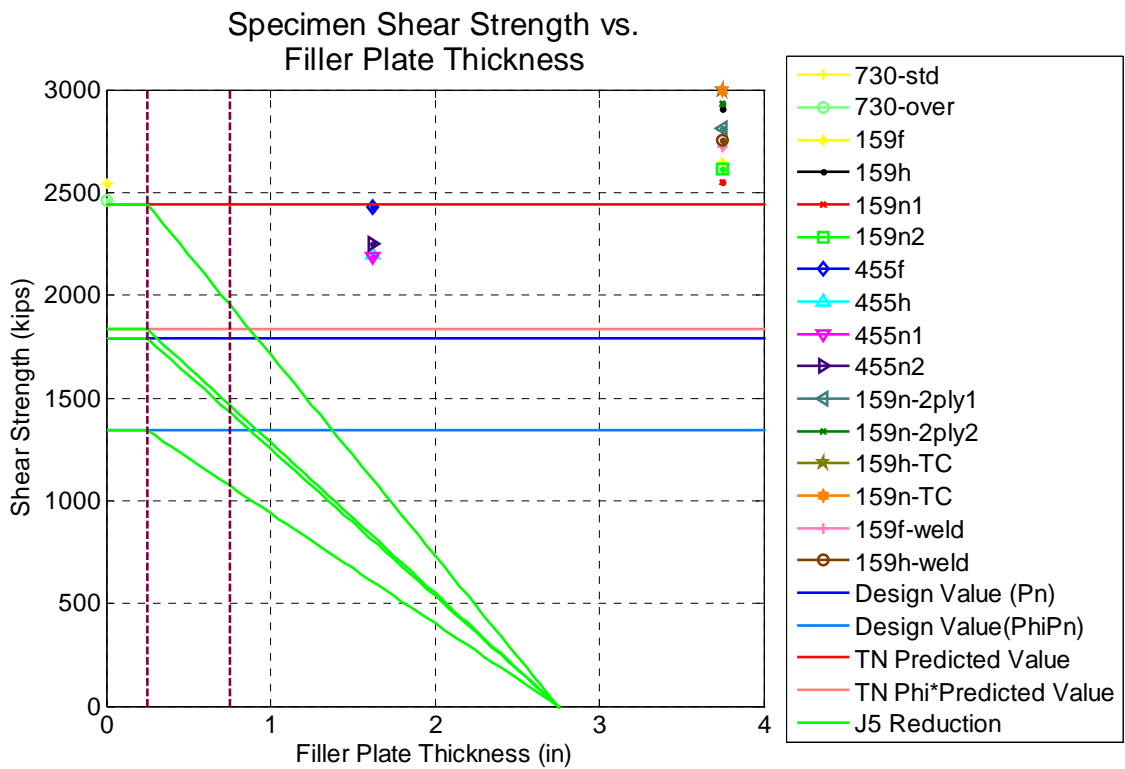


**Figure 41 – Shear strength vs. filler plate thickness**

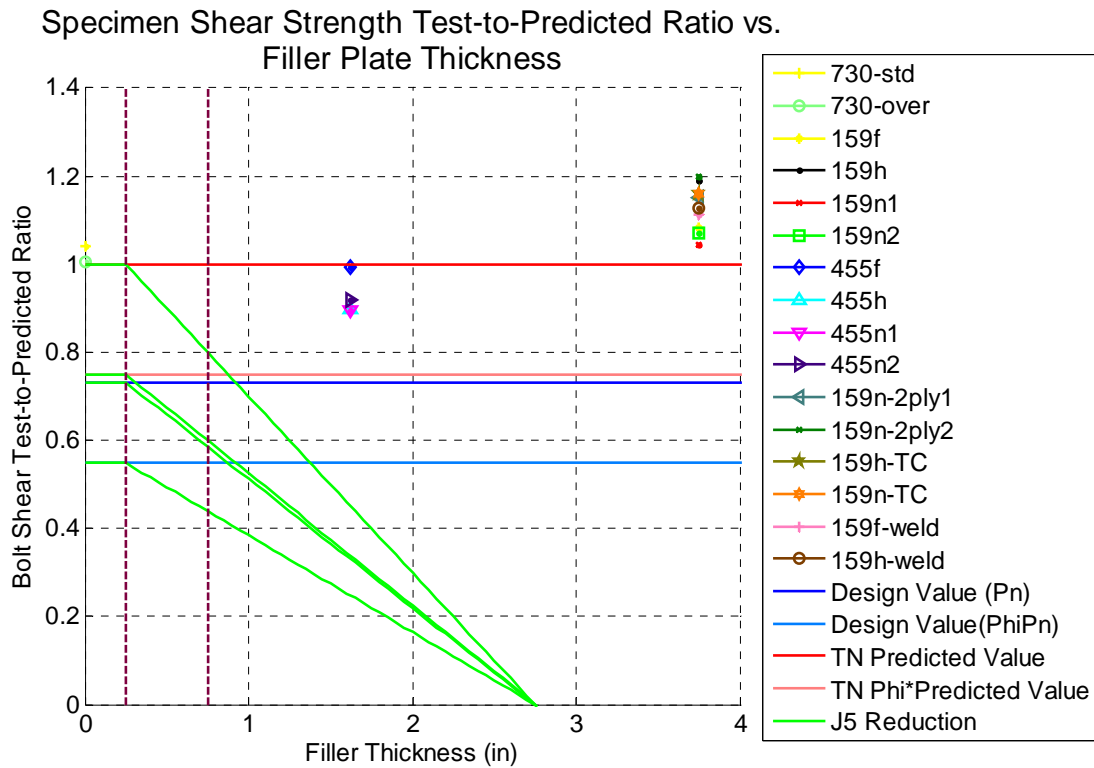


**Figure 42 – Shear strength test-to-predicted vs. filler plate thickness**

Specimens 730-std and 730-over achieved shear strengths close to predicted values, with a test-to-predicted ratio of 1.04 and 1.01 respectively. All specimens with a W14x159 top column achieved a shear strength at least 4% higher than predicted value, with an average test-to-predicted ratio of 1.13 with a standard deviation of 0.05. There are several possible reasons for the test-to-predicted ratios greater than unity, as discussed later in this section.

All specimens with a W14x455 top column failed to achieve the predicted shear strength, with the lowest specimen reaching 90% of the predicted strength. The mean and standard deviation of the test-to-predicted ratios for these four columns were 0.93 and 0.05 respectively. They did however meet the predicted strength multiplied by the shear resistance factor ( $\phi = 0.75$ ) and the design strength. Specimen 455f achieved the highest shear strength of the group with a test-to-predicted ratio of 0.99.

Table 18 shows various subsets of the data with corresponding mean and standard deviation of the shear strength. The 159 specimens with one-ply fillers (159f, 159h, 159n1 and 159n2) demonstrated similar strength to 159 specimens with two-ply fillers (159n-2ply1 and 159n-2ply2). The two-ply filler consisted of a thick ply and a relatively thin ply, the influence of the thin plate was minimal. It is expected that multiple plies of similar size would further reduce the shear strength of the connection, since the bending restraint of the bolt within the bolt hole of the thick filler would be reduced; these effects are investigated further in the mechanistic analysis presented in this section. The use of TC bolts over TN bolts resulted in the shear strength exceeding 3,000 kips, providing a

lower bound test-to-predicted ratio of 1.16. Although the mean lower bound shear test-to-predicted ratio of the TC bolt specimens was higher than the TN bolt specimens, it is within one standard deviation of the mean of all tests.

Overall, there are slight trends for the 159 specimens and clearer trends for the 455 specimens that developing the connection increases the shear resistance of the connection. This is investigated further in Section 4.5. Development of the filler by additional bolts or an equivalent fillet weld produced similar strengths.

**Table 18 – Shear strength test-to-predicted ratio by specimen type**

Specimen Type	Shear Strength Test-to-Predicted Ratio	
	Mean Value	Standard Deviation
All	1.07	0.10
No filler	1.02	0.02
1 ply filler	1.05	0.10
159 1 ply filler	1.10	0.06
159 2 ply filler	1.18	0.03
No development	1.06	0.12
1 ply filler, no development	1.02	0.11
1 ply filler, some development	1.08	0.10
1 ply filler, full development	1.06	0.06
159 1 ply filler, some development using bolts	1.14	0.08
159 1 ply filler, some development using welds	>1.12	>0.02
TN bolts	1.05	0.10
TC bolts	>1.16	0.00

The results from this study for the shear strength test-to-predicted ratio verses filler thickness are combined with the results from previous studies in Figure 43, including specimens without fillers and specimens with undeveloped single-ply fillers. The bolt shear strength decreases as a function of filler thickness for relatively thin fillers, but this reduction is mitigated by having sufficiently large fillers, approximately 1 in. or greater.

The bolt shear strength reduction formula of Section J5 of AISC (2005) and two proposed reduction equations (representing rounded values obtained from regression analyses based on single ply fillers) are superimposed with the data from all of the studies in Figure 43. The two proposed equations are identified as Reduction Equations A and B. Reduction Equations A and B are given by Equations (8) and (9), respectively, where  $t$  is the thickness of the filler. To account for the presence of single-ply fillers the bolt shear strength of the connection is then multiplied by the reduction factor  $\kappa$ :

$$\kappa = 1 - 0.13t \geq 0.87 \quad (8)$$

$$\kappa = \begin{cases} 1 - 0.13t & t \leq 1 \text{ in.} \\ 0.87 + 0.08(t - 1) & 1 \text{ in.} < t \leq 2.625 \text{ in.} \end{cases} \quad (9)$$

Both equations presume that the shear strength is influenced by the thickness of the fillers but is independent of the number of plies, a further reduction for the number of plies is proposed below. Reduction Equation A does not account the reduction mitigation provided by thick fillers. The maximum and minimum values are 1.0 and 0.87, respectively, for both equations. The 2005 AISC filler reduction equation is calibrated for 0.25 in. maximum connection deformation, based on the results from Frank and Yura (1981). The proposed reduction equations are calibrated based on ultimate shear strength, which requires significant connection deformation to achieve. Calibration based on 0.25 in. deformation is unreasonable for oversize holes due to the large initial slip. For design, the proposed reduction equations: a) use rounded coefficients: for Equation (8),  $\kappa = 1 - 0.15t \geq 0.85$ ; and for Equation (9)  $\kappa = 1 - 0.15t$  for  $t \leq 1$  in. and  $0.85 + 0.10(t - 1)$  for  $1 \text{ in.} \leq t \leq 2.5 \text{ in.}$ ; and b) could be shifted by 0.25 in. to avoid a reduction for fillers thinner than 0.25 in., similar to the AISC (2005) equation. A further alternative would be to retain the AISC (2005) equation, which is presently applicable for fillers 0.25 in. to 0.75 in. thick, expand its applicability to all filler thicknesses and limit the reduction to 0.85 (which would occur at a filler thickness of 0.625 in.). Because of the small number of developed tests and small scatter, the addition of developed fillers in the regression are not statistically significant and do not alter the reduction equations significantly.

The shear strength test-to-predicted ratio verses the number of plies is summarized for previous studies in Figure 44 and the shear strength test-to-predicted ratio verses the filler thickness by hole size and number of plies is summarized for all studies in Figure 45. The reduction for the addition of a one-ply filler is modest, however, the reduction increases with the number of plies. Specifically, for fillers thinner than 1 in., multi-ply fillers have a lower strength than single-ply fillers of the same total thickness. This can be attributed to the reduced bolt restraint provided by multi-ply fillers, thus enabling more bolt bending within multi-ply fillers. For fillers thinner than 1 in. the mean test-to-predicted ratio for multi-ply and respective single-ply fillers are presented in Table 19. The multi-ply reduction factor is the reduction required to further reduce reduction Equation A to the mean test-to-predicted ratio for the multi-ply tests for a given thickness. The multi-ply reduction factor is derived using Dusicka and Lewis (2007) for 2 and 4 plies and Frank and Yura (1981) for 3 plies in Table 19. For design, it does not appear that a reduction in bolt shear due to multiple plies is required, as using four or more plies is uncommon in a connection, and the reduction value for 2 or 3 plies is modest. In addition, if one includes the multi-ply test results from the current study, in which one of the fillers is much thicker than in the earlier studies in the literature, the result is that no reduction is needed (i.e., the reduction factor in the last column of the table for 2 or 3 plies would be larger than 1.0).

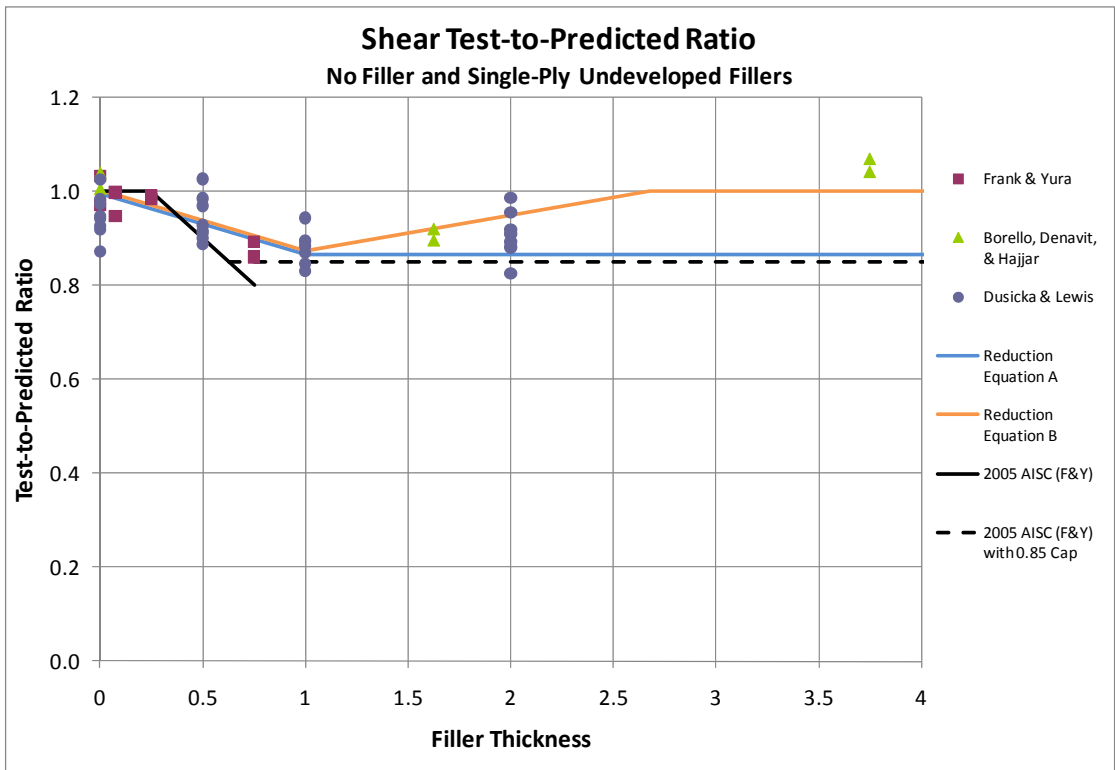
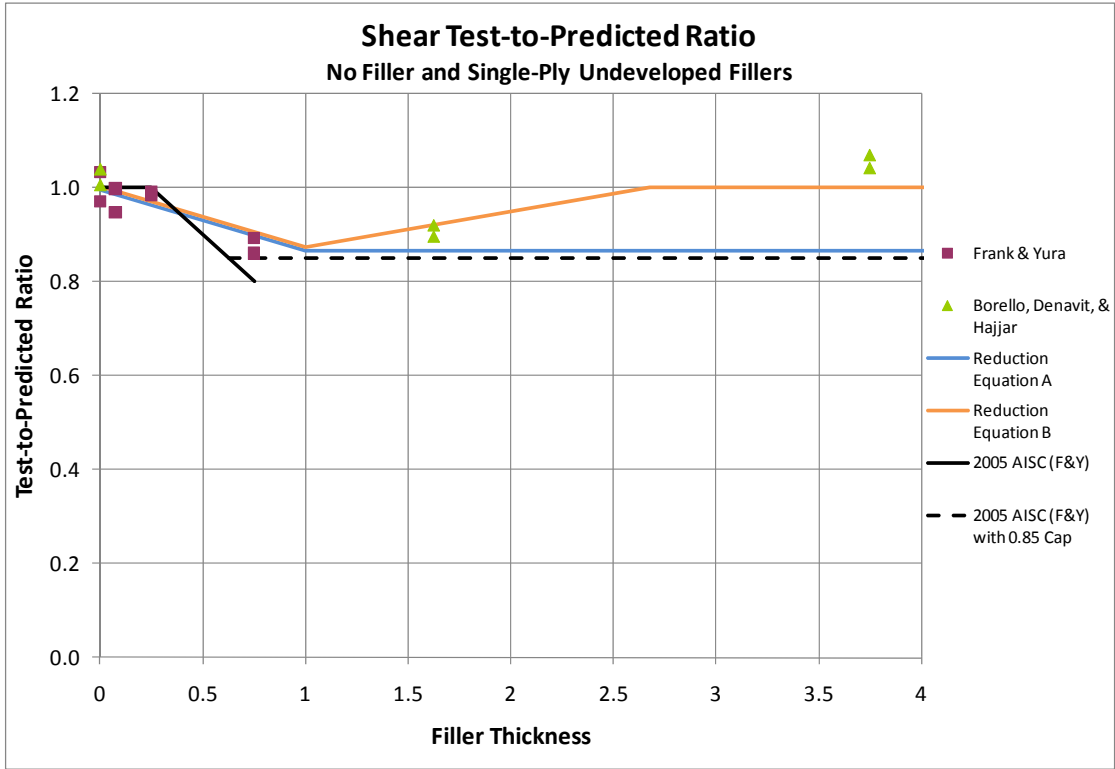


**Figure 43 – Shear test-to-predicted ratio vs. filler thickness. a) Frank & Yura, and Borello, Denavit & Hajjar. b) Frank & Yura, Borello, Denavit & Hajjar, and Dusicka & Lewis**

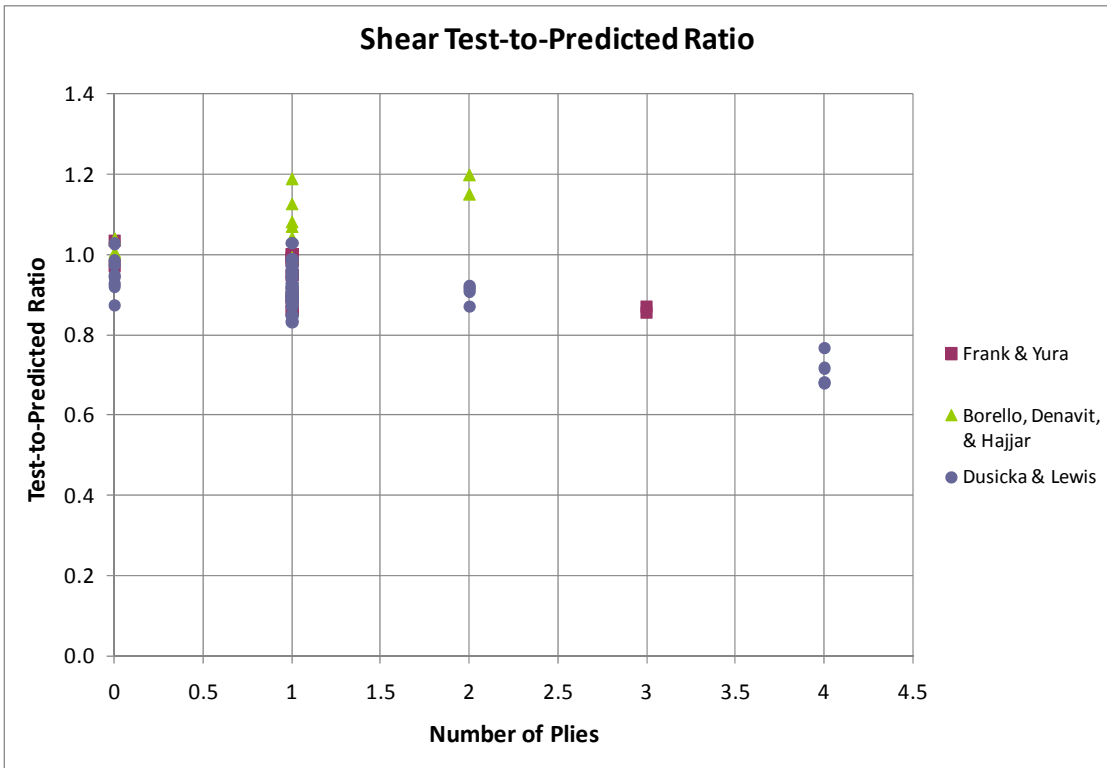
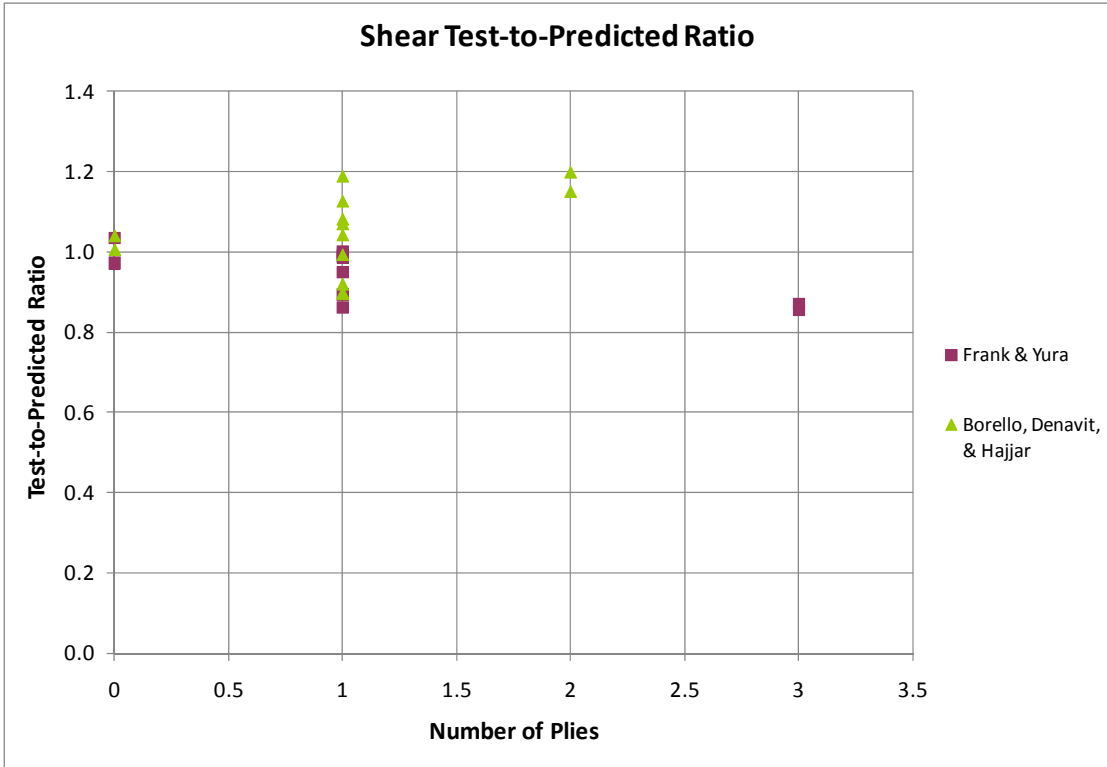


**Figure 44 – Shear strength test-to-predicted ratio vs. number of plies. a) Frank & Yura, and Borello, Denavit & Hajjar. b) Frank & Yura, Borello, Denavit & Hajjar, and Dusicka & Lewis**

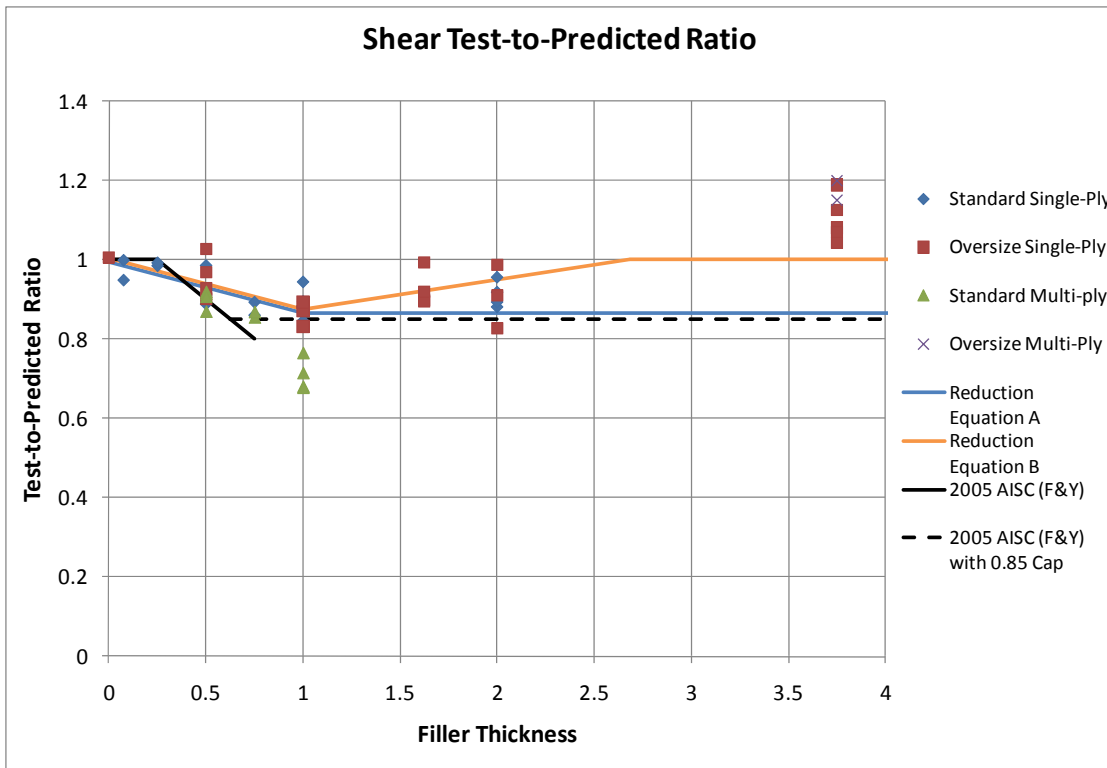
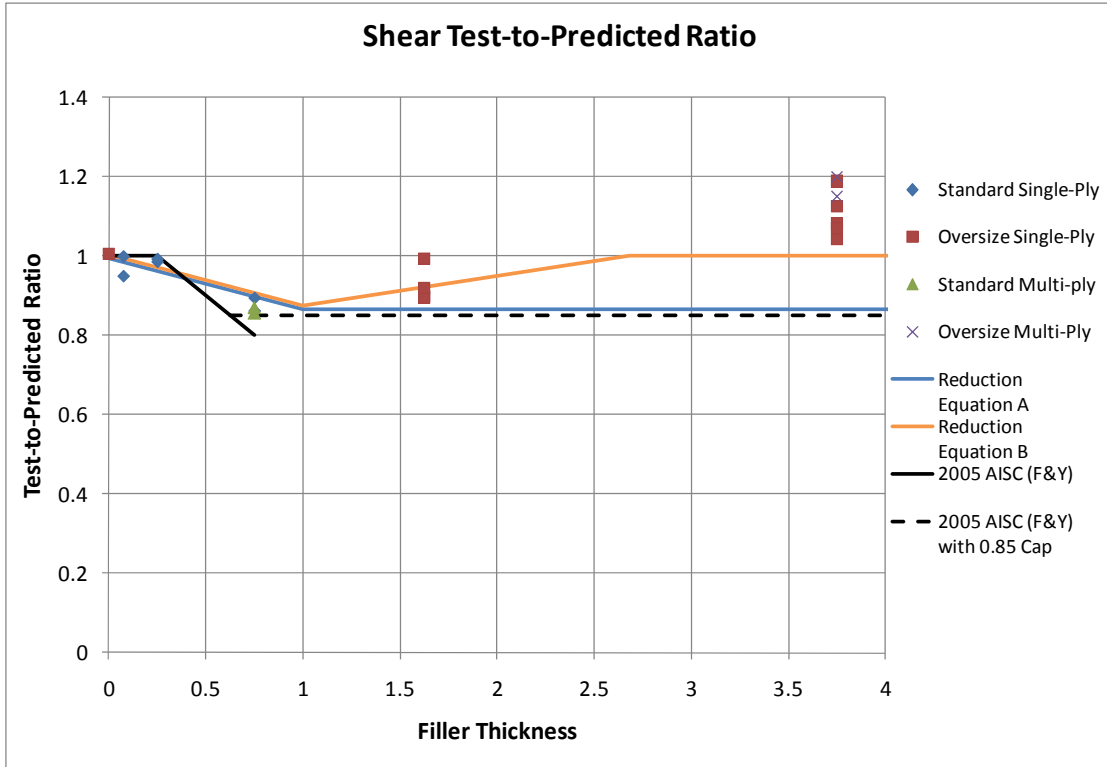


**Figure 45 – Shear strength test-to-predicted vs. fill thickness separated by bolt size and quantity of fillers. a) Frank & Yura, and Borello, Denavit & Hajjar. b) Frank & Yura, Borello, Denavit & Hajjar, and Dusicka & Lewis**

**Table 19 – Thin multi-ply filler data**

<b>Number of Plies on One Side of Connection</b>	<b>Total Filler Thickness</b>	<b>Single Ply Experimental Mean Test-to-Predicted Ratio</b>	<b>Reduction Equation A</b>	<b>Multi Ply Experimental Mean Test-to-Predicted Ratio</b>	<b>Multi Ply Reduction Factor</b>
<b>2</b>	0.5 in.	0.94	0.94	0.90	0.95
<b>3</b>	0.75 in.	0.88	0.90	0.86	0.95
<b>4</b>	1.0 in.	0.87	0.87	0.71	0.8

The shear behavior of bolted filler connection can be characterized in more depth by studying two phenomena further. The first phenomenon is the bending in the bolt due to the relative movement of the shear planes. In an idealized connection without fillers, there is no bending the bolts, simply pure shear at the shear plane between the faying surfaces (see the deformation at the end of specimen 730-over in Figure 46). With fillers, the original faying surfaces are separated, which has the effect of preventing a clear definition of the shear plane and adding bending to the bolt (Figure 46, which shows the difference in bending in the 159 versus the 455 specimens). An appropriate parameter to capture this behavior is the thickness of the filler. This phenomenon is documented in prior filler research, notably Frank and Yura (1981), who developed a strength reduction formula for bolted connections with undeveloped fillers based on filler thickness, as discussed above. As the thickness of the filler is increased, the applied couple likely becomes further apart, increasing the bolt bending.

The second phenomenon is the resistance to bending provided by the filler plate as the bolt jams in the hole. Two situations illustrate the extremes of this behavior (Figure 47(a)). The first situation is a filler plate with a very large hole, such that no part of the bolt is in contact with filler plate. In this case, the effect of the filler plate is to maintain separation between the other plates (e.g., splice plate and column). In addition to not being as stiff as a connection without fillers, the bending in the bolt will result in a lower strength due to the interaction of shear and bending. The second situation is a rigid filler plate with the hole precisely the same size as the bolt, leaving no tolerance. In this case, the bolt will be completely restrained from bending and the behavior will be essentially the same as two uncoupled shear connections without fillers and no reduction in strength will be observed. The bolt hole tolerance (hole diameter minus bolt shank diameter) in relation to the thickness of the filler plate would seem like an appropriate parameter to capture this behavior, however, experimental evidence shows little variation between specimens with different hole oversize. Figure 45 shows a plot of the test-to-predicted ratios of available tests versus filler thickness, separated into single-ply standard hole, single-ply oversize hole, multi-ply standard hole and multi-ply oversize hole. This shows experimental evidence of little difference between standard and oversize holes, and so the data does not exhibit a discernible trend for this factor. It is possible that the two common tolerances, standard and oversize holes, do not differ sufficiently to affect the strength as compared to the wide range of filler thicknesses that are being investigated. The strength and stiffness of the filler plate may also affect the resistance to bolt bending.

These two phenomena may be extended to the behavior of multiple ply fillers. Consider two filler connections with the same total filler thickness. The first is made of a thick filler and a thin filler, and the second is made of several thin fillers. For the first connection, the portion of the bolt inside of the thick filler will be restrained against bending while the portion of the bolt inside the thin filler will not. The behavior of such a connection would likely be much like two uncoupled shear connections (one with a filler). For the second connection, since the filler plates are able to move relative to each other, no part of the bolt will be restrained against bolt bending and it will behave as though there were one filler with a larger hole. As a result, if a small filler needs to be added for fit up in the field, this model does not predict a large reduction in shear strength since this situation would likely be more like the case of thick filler and thin filler. Figure 45 shows more significant differences between single ply and multiple ply fillers. The multiple ply tests shown at filler thickness of 3.75 in. consisted of a 3.5 in. plate and 0.25 in. plate, as opposed to the other multiple ply tests, which had equal plate thicknesses.

Many of the specimens achieved shear strengths greater than predicted from simple shear tests of the individual bolts (i.e., a test-to-predicted ratio greater than unity); this indicates that additional mechanisms are in effect. One possible mechanism is additional resistance provided by friction when the filler plate is jammed between the splice plate and top column due to moments applied by the bolts. Figure 47(b) shows a free body diagram of the filler plate. Each bolt applies a pair of equal (for undeveloped fillers) and opposite forces to the filler. To maintain equilibrium, an equivalent couple is generated by the filler plate bearing on the top column and splice plate. This bearing pressure causes a frictional resistance that would be additive to the shear resistance of the bolts. To gain a sense of the magnitude of this effect, several approximations are made. The applied force is assumed to transfer through the filler plate by a couple applied by each bolt with a lever arm 90% of the thickness of the filler. The bolts are assumed to have lost all pretension at shear failure. The bearing pressure is only compressive and varies linearly along the height of the specimen (Figure 47). The additional frictional resistance is then computed in Equation (10), where  $P_{shear}$  is sum of the bolt shear strengths,  $t_{filler}$  is the thickness of the filler and  $h_{filler}$  is the height of the filler.

$$P_{slip,max} = \mu N = \mu \frac{(2sides) \left( \frac{(12bolts / side) P_{shear}}{24bolts} \right) (0.9t_{filler})}{\frac{2}{3} h_{filler}}$$

$$P_{slip,max} = 1.35 \mu \frac{t_{filler}}{h_{filler}} P_{shear} \quad (10)$$

$$P_{total} = P_{slip,max} + P_{shear} = (1 + 1.35 \mu \frac{t_{filler}}{h_{filler}}) P_{shear}$$

The additional strength for the 159 and 455 specimens using these approximations are presented in Table 20. The 159 TN single-ply specimens achieved an average ultimate strength 10% higher than the predicted shear strength (see Table 10), whereas this additional friction mechanism predicts an ultimate strength 7% greater than predicted the

shear strength. The additional strength is predicted to be 3% for the 455 specimens. Disassembly of the specimens revealed increased plate damage near the top and bottom of the filler plates, often with large ridges where the edge of the filler plate met the plate, which was greater for the 159 specimens compared to the 455 specimen.

**Table 20 – Induced slip resistance at ultimate failure**

Specimen	$t_{filler}$	$h_{filler}$	$P_{total}$
159f, 159h, 159n1, 159n2, 159n-1ply1, 159n-2ply2	3 3/4 in.	36 in.	1.07 $P_{shear}$
159f-weld, 159h-weld	3 3/4 in.	21 in.	1.11 $P_{shear}$
455f, 455h, 455n1, 455n2	1 5/8 in.	29 in.	1.03 $P_{shear}$
<sup>1</sup> Excluding TC bolt specimens			

Due to the complex, indeterminate nature of this problem and the simple parameters used to capture this behavior, it is difficult to characterize these mechanisms further through simple equations. However, this research provides available experimental data such as in Figure 45, where a clear trend in the data is seen, with the bolt shear strength first reducing with thickness, and then increasing. To capture this behavior most comprehensively through a parametric study, nonlinear finite element analyses are recommended.



**Figure 46 – Specimen bolt deformation (730-over, 159n1, and 455n1)**

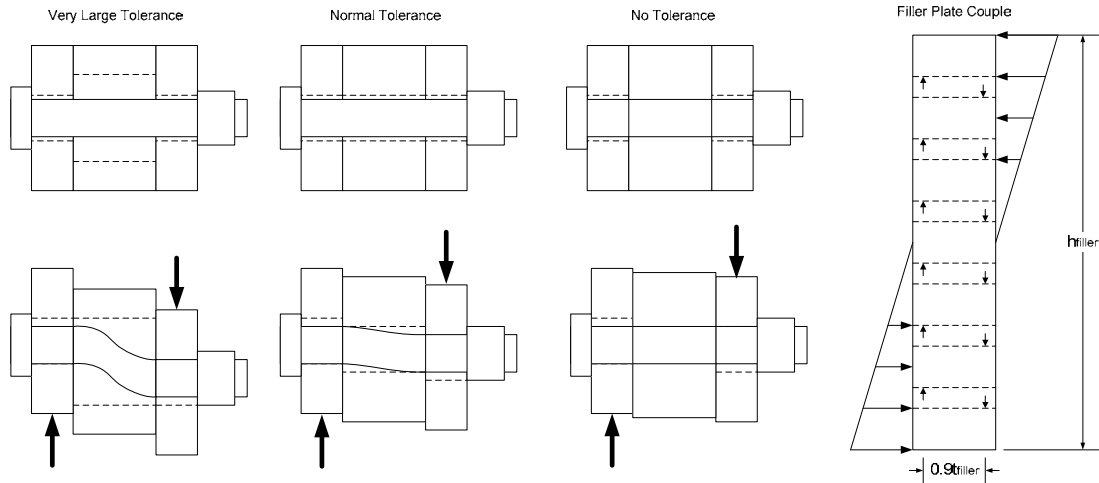


**Figure 47 – Shear mechanism: (a) deformation modes; (b) filler free body diagram**

## 4.5 Development

A direct comparison between different levels of development in bolted connections is seen in the specimens with a W14x455 top column. In this series of specimens, the effect of development on the bolt shear strength is clear. The fully developed specimen, 455f, achieved 99% of its predicted shear strength while the less than fully developed specimens, 455n1, 455n2, and 455h, achieved 90%, 92% and 90% of their predicted shear strengths. This data indicates that a connection with developed fillers may not suffer the same detrimental effects in shear as one with undeveloped fillers. The similar series of tests with a W14x159 top column all achieved higher than predicted shear strengths, limiting the applicability of a comparison based on development. It is seen in Table 11 that specimens 159f, 159h, 159f-weld, and 159h-weld achieved slightly higher shear strengths than specimens 159n1 and 159n2. However, specimens 159n-2ply1 and 159n-2ply2 achieved higher shear strengths than specimen 159f and comparable strengths to specimen 159h. The specimens with TC bolts did not fail in shear, as noted earlier. The beneficial effects of development are thus modest for the 159 specimens.

To examine the effect of development further, one can consider an undeveloped or partially developed filler connection as fully developed for a fewer number of bolts. For this analysis, the bolts are considered to be separated into those that resist shear and those that develop the filler. The total number of bolts remains the same; however, using common terminology, there are fewer bolts in the connection (those that resist shear). The number of bolts that are assumed to resist shear (those “in the connection” or “effectively fully developed”) are less than the total number of bolts by the number of bolts required to fully develop the bolts that resist shear. This is analogous to the third option provided to designers in Section J5 of AISC (2005), where the size of the joint may be extended to accommodate the number of bolts required to develop the filler. The number of bolts effectively fully developed can be calculated as follows: full development is achieved when the strength of the connection of the filler extension to the

connected element is sufficient to uniformly distribute the total force across the combined cross section, satisfying Equation (11).

$$R_{u,development} = \frac{A_{fill}}{A_{fill} + A_{connected\ element}} R_{u,connection} \quad (11)$$

If the width of the fill and connected element are the same, as they are for all tests considered, then thicknesses may be used:

$$R_{u,development,effective} = \frac{t_{fill}}{t_{fill} + t_{connected\ element}} R_{u,connection} \quad (12)$$

Defining  $\rho = \frac{t_{fill}}{t_{connected\ element}}$  (13)

$$R_{u,development,effective} = \frac{\rho}{1 + \rho} R_{u,connection} \quad (14)$$

Defining %EFD as the percentage of bolts in the undeveloped, partially developed, or fully developed filler connection that are considered to resist shear when the connection is considered fully developed, i.e., effectively fully developed, we obtain:

$$(1 - \%EFD) R_{u,connection} + R_{u,development,provided} = \frac{\rho}{1 + \rho} \%EFD R_{u,connection} \quad (15)$$

The first term on the left side of Equation (15) represents the portion of total number of bolts assumed to be development bolts. The second term on the left side represents the strength of the bolts provided to explicitly develop the filler; this term is for specimens with bolts, or other means of development, between the filler extension and connected element. Together, the two terms on the left side provide an alternative representation of the left side of Equation (14). The term on the right side of Equation (15) follows from the right side of Equation (14), but now with only the effectively fully developed bolts (%EFD  $R_{u,connection}$ ) contributing to the connection strength. Solving for %EFD,

$$\%EFD = \frac{1 + \rho}{1 + 2\rho} \left( 1 + \frac{R_{u,development,provided}}{R_{u,connection}} \right) \quad (16)$$

The limits of this equation are logical: when  $\rho$  approaches zero, i.e., very thin fillers, nearly no bolts are required to develop the filler, i.e., %EFD approaches 1 for undeveloped fillers. When  $\rho$  approaches infinity, i.e., very thick fillers, the same number of bolts are required to develop the filler as in the joint, i.e., %EFD approaches 0.5 for undeveloped fillers. Table 5 provides the effective number of developed bolts for the sixteen specimens based on the specimen dimensions. For the fully developed connections (Table 5), %EFD approaches unity.

This analysis has been formulated such that multiplying the predicted slip and shear strengths of the undeveloped, partially developed, or fully developed filler connections by  $\%EFD$  would result in predicted values of the effectively fully developed connection. The strength is reduced due to the allocation of some of the connection strength towards connection development. Test-to-predicted ratios using predictions based on effectively fully developed strengths are plotted in Figure 48 , Figure 49 and Figure 50.

The shear strength test-to-predicted ratios based on the effectively fully developed prediction, shown in Figure 48, indicate that if the connection is fully developed by extending the joint, the test-to-predicted ratio is always greater than unity. This indicates that the detrimental effects of fillers on shear strength are mitigated by developing the filler and extending the connection to include the development bolts. The shear strength test-to-predicted ratios increase with filler thickness in Figure 48 because as the filler thickness is increased, the number development bolts increases. These bolts likely offer shear resistance that is conservatively neglected in the predicted strength.

The slip strength test-to-predicted ratios based on the effectively fully developed prediction, shown in Figure 49, indicate that if the specimen is fully developed by extending the joint, the test-to-predicted ratio is larger than if the specimen is assumed to be undeveloped (e.g., with values calculated as in Figure 38), but still with significant scatter and many values less than unity. This indicates that the detrimental effects of fillers on slip strength are not entirely mitigated by developing the filler and extending the connection to include the development bolts.

Following the statistical argument presented in Section 4.3 and Appendix D, there is evidence that development of the filler should reduce the likelihood of slip of the faying surface between the filler and connecting element because of the additional pretension from the development bolts and thus increase the statistically expected slip strength of the connection above that of an undeveloped connection. However, since the possibility still exists, although less likely, that slip may occur between the filler and connecting element, the statistically expected slip strength of the connection is less than that of a equivalent connection without fills.

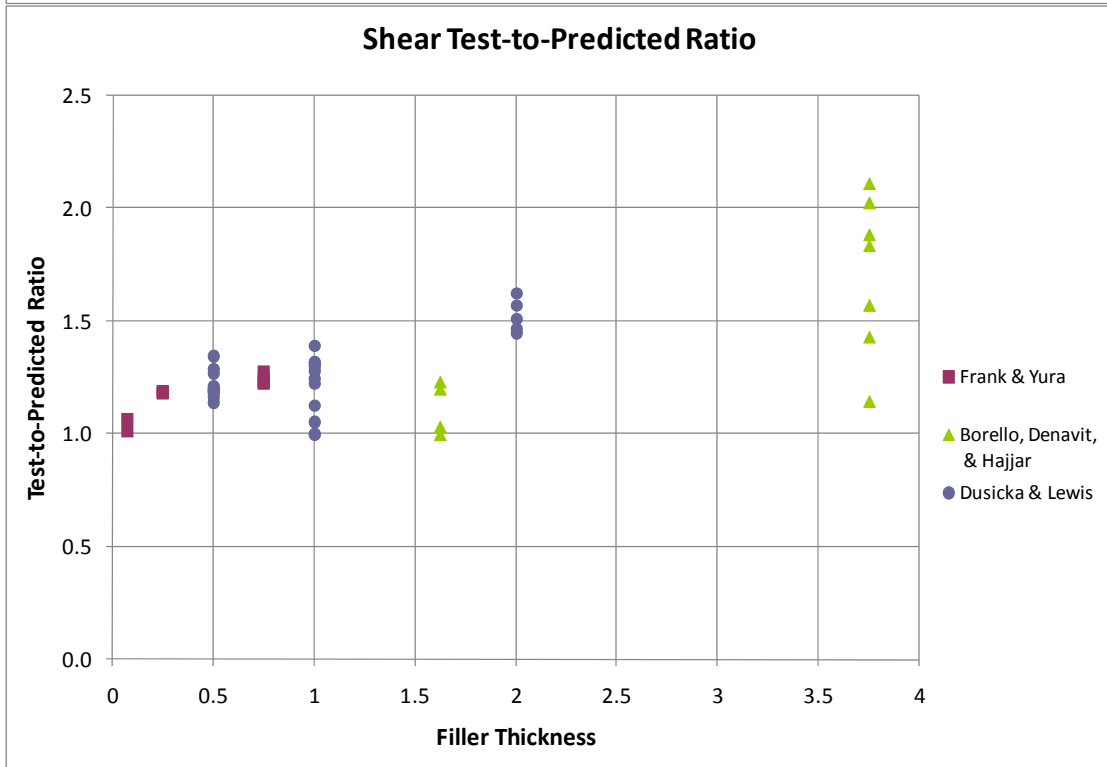
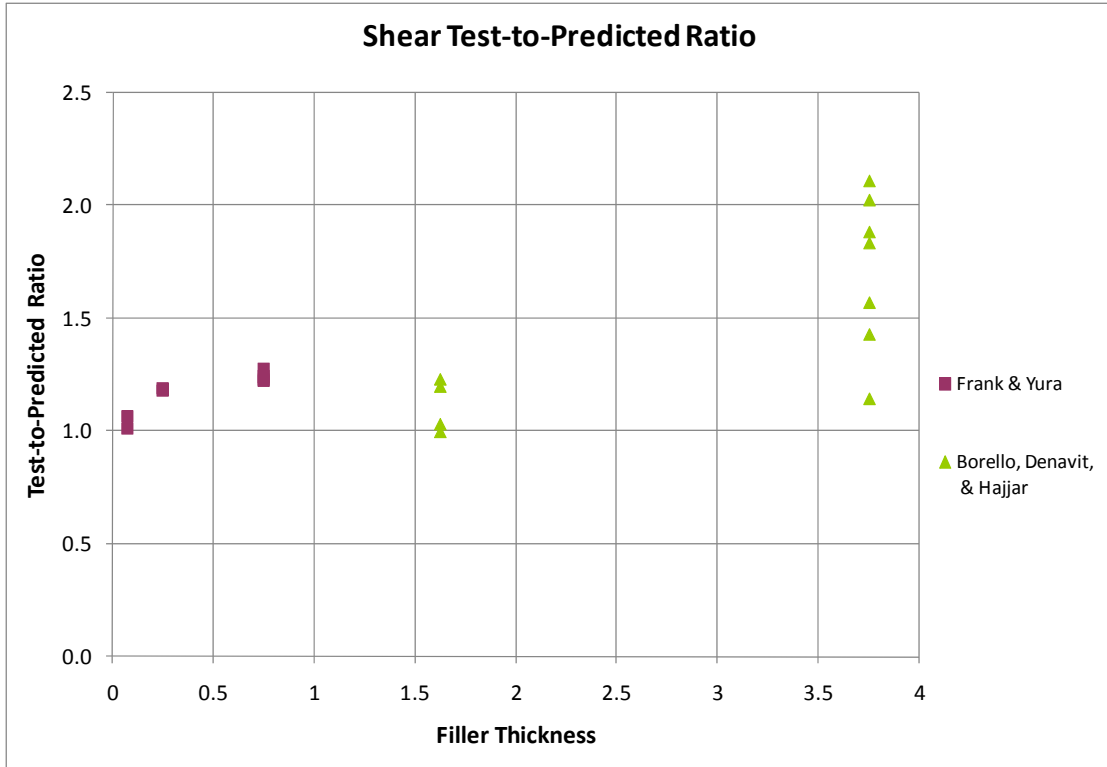


**Figure 48 – Shear strength test-to-predicted ratio vs. fill thickness for effectively developed bolts. a) Frank & Yura, and Borello, Denavit & Hajjar. b) Frank & Yura, Borello, Denavit & Hajjar, and Dusicka & Lewis**

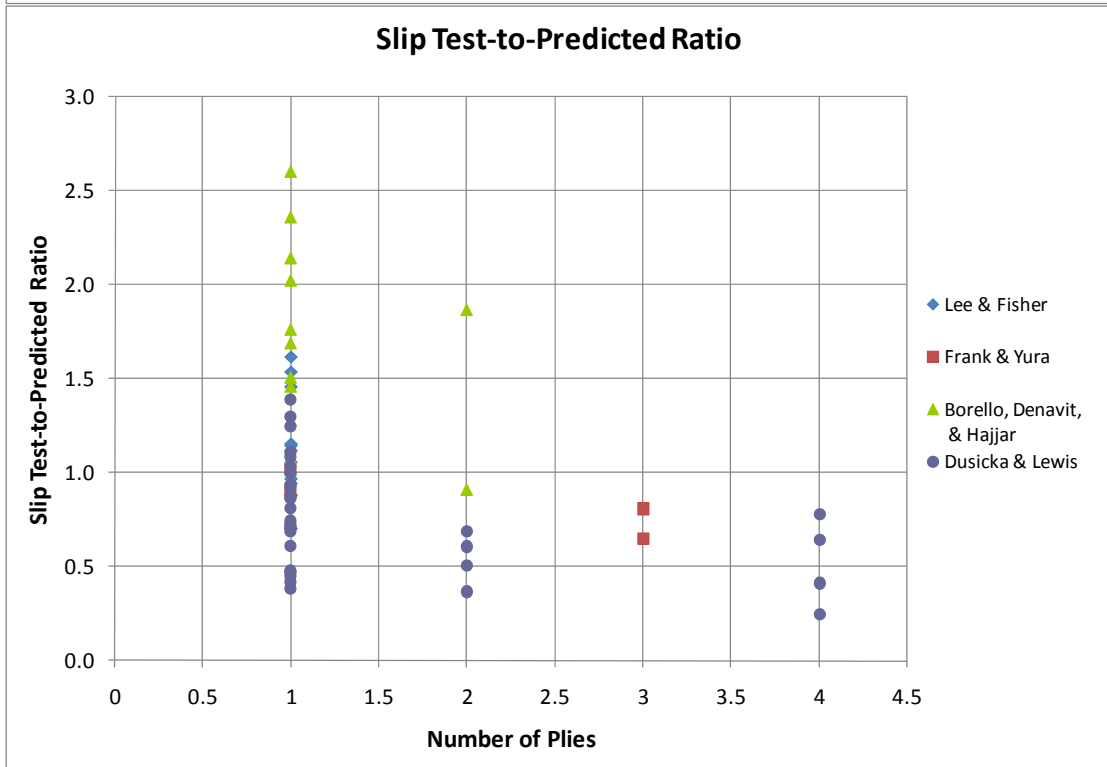
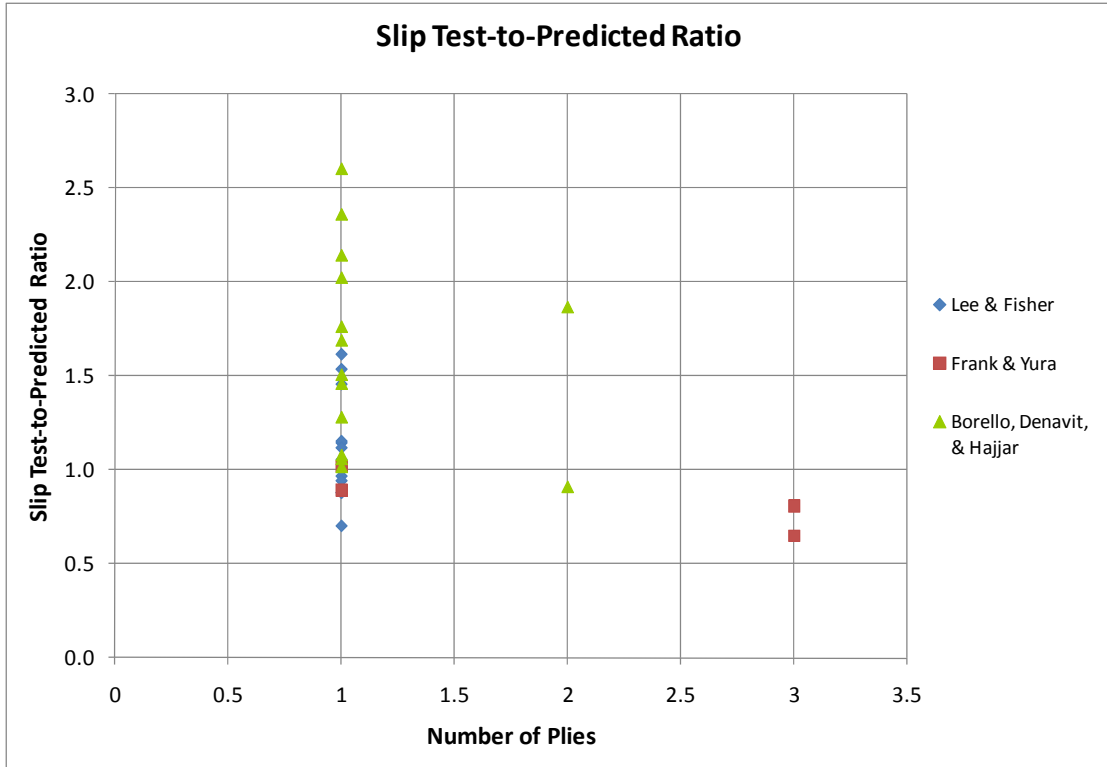


**Figure 49 – Slip strength test-to-predicted ratio vs. number of plies for effectively developed bolts. a) Lee & Fisher, Frank & Yura, and Borello, Denavit & Hajjar. b) Lee & Fisher, Frank & Yura, Borello, Denavit & Hajjar, and Dusicka & Lewis.**

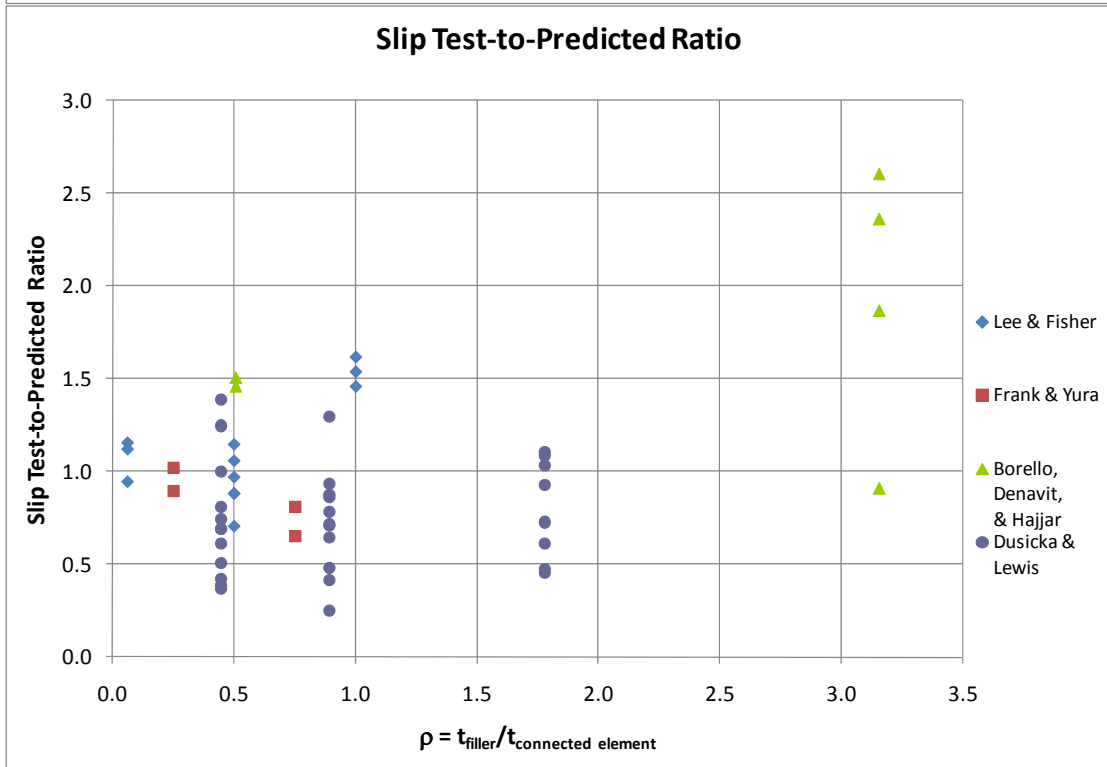
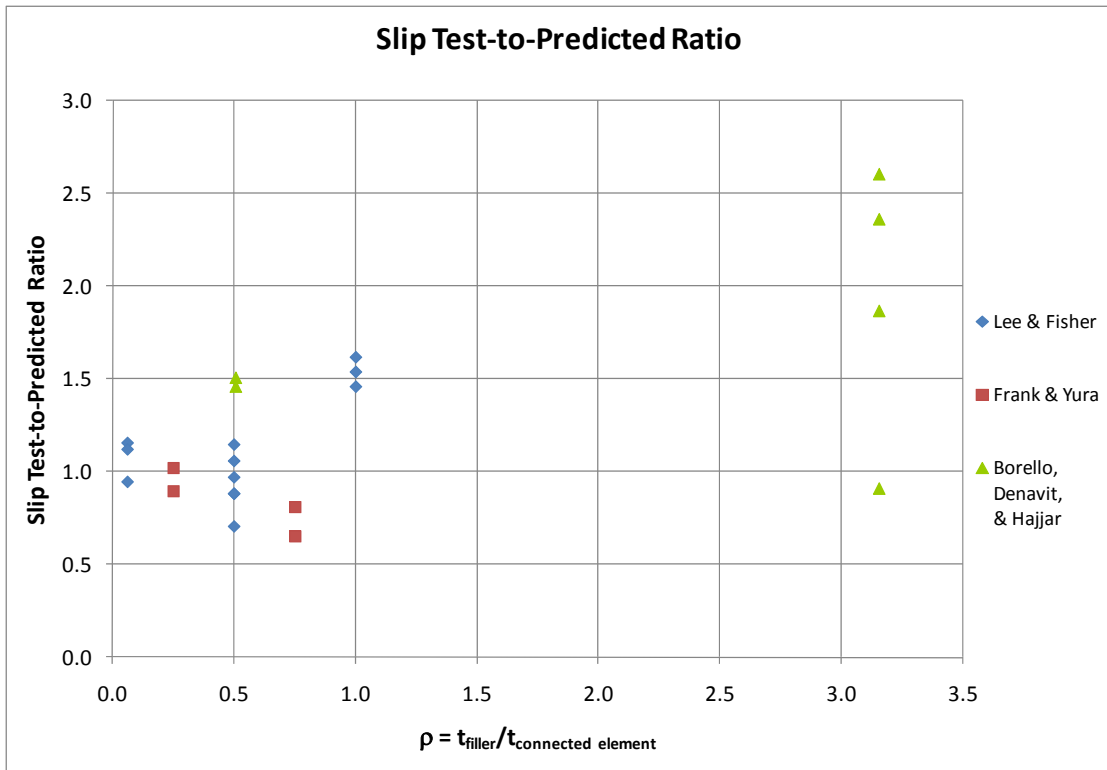


**Figure 50 – Slip strength test-to-predicted ratio vs. ratio of thickness of fill to thickness of connected element for effectively developed bolts. a) Lee & Fisher, Frank & Yura, and Borello, Denavit & Hajjar. b) Lee & Fisher, Frank & Yura, Borello, Denavit & Hajjar, and Dusicka & Lewis**

Alternately, extending the connection to accommodate the development bolts reduces the likelihood of slip on all surfaces, making it possible to entirely mitigate the detrimental effects of multiple possible slip surfaces. However, the increase in expected slip strength is primarily dependent on the number of additional bolts. The number of additional bolts required to develop a connection is dependent on the thickness of the filler. The reduction of slip strength appears to be dependent on the number of plies and not the thickness of the filler. Therefore, the number of additional bolts needed to entirely mitigate the detrimental effects of multiple possible slip surfaces may exceed the number of additional bolts needed to develop the filler. This topic is discussed further in Appendix D. It is important to note that the slip strength is most detrimentally affected by multiple-ply fillers, for which there are no studies involving multiple-ply developed fillers.

# CONCLUSIONS

The research presented in this report, augmented by previous studies from the literature, demonstrate definitive trends regarding the influence of filler plates on the slip and shear strengths of bolted connections. The research presented in this report explores the influence of developing the connection for a variety of configurations. A summary of the results and conclusions are included below.

## 5.1 Slip

The connections tested in this work generally provided excellent resistance to slip, with only three failing below the predicted value, and with two of those having test-to-predicted ratios above 0.93. When combined with assessment of experiments reported in the literature on the behavior of connections with fillers, the slip strength is seen to generally be reduced by the introduction of filler plates, independent of filler thickness and hole size. According to a statistical analysis of the data, the slip strength reduction is related to the number of plies (assuming the fabrication adequately pretensions the bolts). Possible reduction factors are proposed that account for these trends in the data. The reduction for single ply filler plates is modest and may possibly be neglected. There is also some evidence that developing the filler increases the slip strength on the developed faying surface, thus reducing the effects of having one or more plies (Appendix D).

For connections with filler plates, the bolt hole oversize does not affect the slip strength of the connection. Therefore there is no evidence to support the reduction for oversize holes based on experimental data. However, the detrimental effect to the stability of the structure caused by slip with oversize holes may warrant a more cautious treatment in design than for connections with standard holes (e.g., by designing slip-critical connections to have a lower reliability against slip than for connections with standard holes).

## 5.2 Shear

The shear strength exhibited in these connections was consistently larger than the slip strength, and was larger than the predicted value for all but four of the specimens. Those four specimens all had test-to-predicted ratios larger than 0.90. The specimens never failed in bolt shear immediately after bolt slip (other than an occasional premature bolt failure), despite potentially large dynamic effects during slip; rather, the specimens took on significant additional load prior to bolt shear failure. Bolt shear failure was dynamic and accompanied by several of the bolts exiting the holes with significant velocity.

The shear strength of a connection is influenced by the introduction of filler plates. The filler plate separates the splice plate and column shear planes and introduces bending into the bolt. The interaction of shear and bending reduces the shear strength of the bolt. The

bolt bending increases with the thickness of the filler. Additional clamping force is also induced by the reaction of the bolt onto the filler, proportional to the filler thickness, which tends to increase the bolt shear strength of the connection. These two mechanisms offset each other and the shear strength is initially reduced with increasing thickness in relatively thin fillers, and then increases in strength for thicker fillers. Reduction formulas are proposed to account for these trends in the data.

Multiple ply fillers also introduce more bolt bending than single ply fillers, although a thick and thin ply filler will behave similar to a single ply thick filler. Additional reductions for multiple plies are presented in this work, although the values are such that they become significant only for connections with four fillers or more per side of the connection, which are rare.

### **5.3 Development**

In this work, a developed filler plate is seen to act quite integrally with the member to which it is connected. Developing or extending the connection helps to mitigate reductions both in slip strength due to multiple plies or in shear strength due to thick fillers or multiple plies. However, for assessment of slip in particular, the evidence is a less definitive, because an inadequate number of tests have been completed, for example for investigation of slip strength with multi-ply specimens that are developed and also since the number additional bolts provided by developing the connection depends on the size of the filler. Specimens with filler plates welded to the columns also performed well.

This research also shows that undeveloped connections generally perform well both for bolt slip and for bolt shear. Reduction formulas and associated statistical assessment are presented to account for the effect of the number of plies on the slip strength and the filler thickness on the shear strength for cases where the connection is not developed. Assessment of the undeveloped connections as effectively developing a reduced number of bolts also shows that extending the connection works well to ensure the predicted slip and shear strengths are reached in the connection.

### **5.4 Recommended Design Provisions**

In light of the findings of this study, the following recommendations are made for the design of bolted connections with fillers, based on current provisions in Section J5 AISC (2005).

When a bolt that carries load passes through fillers, one of the following requirements shall apply for a slip-critical connection. The connection shall also be checked in bearing as per the provisions below for bearing-type connections.

- 1) The joint shall be designed to prevent slip in accordance with Section J3.8, using the slip strength reduction values listed below for connections with one or more filler plates (plies).

<b>Number of Plies on One Side of Connection</b>	<b>Reduction Factor</b>
<b>0</b>	1.0
<b>1</b>	0.90 <sup>a</sup>
<b>2</b>	0.80
<b>3</b>	0.70

<sup>a</sup> A reduction factor of 1.0 may be adequate for design.

*Note: As the mean value of the test-to-predicted ratios for specimens with one ply on each side was approximately 1.0 for the data of Lee and Fisher (1968), Frank and Yura (1981), and this work, the reduction factor for connections with one filler on each side may be taken as 1.0. Inclusion of the data from Dusicka and Lewis (2007) suggests a reduction factor instead of 0.90.*

- 2) The fillers shall be extended beyond the *joint* and the filler extension shall be secured with enough bolts to uniformly distribute the total *force* in the connected element over the combined cross section of the connected element and the fillers;
- 3) The size of the joint shall be increased to accommodate a number of bolts that is equivalent to the total number required in (2) above.

When a bolt that carries load passes through fillers that are equal to or less than ¼ in. (6 mm) thick, the shear strength shall be used without reduction. When a bolt that carries load passes through fillers that are greater than ¼ in. (6 mm) thick, one of the following requirements shall apply for a bearing-type connection:

- 1) For a bearing type connection, the shear strength of the bolts shall be multiplied by

$$\kappa = 1 - 0.13t \geq 0.87$$

*Note: Rounded values for this equation may be used with little loss of accuracy:*

$$\kappa = 1 - 0.15t \geq 0.85$$

*The formula may also be adjusted such that it is applicable only for fillers greater than or equal to 0.25 in. As an alternative, this research has shown that the bolt shear strength reduction formulation in AISC (2005) may be extended to fillers great than 0.75 in. thick and may be capped at a minimum value of 0.85 with little loss of accuracy.*

*These proposed provisions are based on results of bolt shear strength failures, in which significant connection deformation with oversized holes occurred prior to deformation. The current AISC (2005) equation is*

*based on achieving a maximum connection deformation of 0.25 in.; however, this limit is not pragmatic for connections with oversized holes.*

*An additional reduction may also be considered if the filler is comprised of more than four plies. Reduction values obtained in this research are listed below.*

<b>Number of Plies</b>	<b>Reduction Factor</b>
<b>2</b>	0.95 <sup>a</sup>
<b>3</b>	0.95 <sup>a</sup>
<b>4</b>	0.80

<sup>a</sup> A reduction factor of 1.0 may be adequate for design.

*However, as a reduction factor of 1.0 may be adequate for design with 2 and 3 plies, and using 4 plies is rare, this reduction is probably not needed in design provisions.*

- 2) The fillers shall be extended beyond the *joint* and the filler extension shall be secured with enough bolts to uniformly distribute the total *force* in the connected element over the combined cross section of the connected element and the fillers;
- 3) The size of the joint shall be increased to accommodate a number of bolts that is equivalent to the total number required in (2) above.

Using the ASD approach, the slip-critical strength for connections with single-ply fillers based on these design recommendations is approximately 11% lower than the 1989 *Specification* for standard and oversized holes (assuming no reduction for single-ply fillers). The 2005 *Specification* slip-critical strength was 24% lower for oversized holes than the 1989 *Specification*. The increase in slip-critical strength in these recommended provisions is due to the elimination of the hole factor (assuming no filler reduction for single-ply fillers). For connections with multiple-ply fillers, additional reduction is recommended.

## **5.5 Recommendations for Future Work**

Two directions are recommended for future research. First, it is recommended that additional full-scale testing be conducted. High priority specimens are those with standard holes and those with fully-developed connections with multiple plies. In particular, the following specimens are suggested: 455n-std, 159n-std, 159f-2ply1 and 159f-2ply2, (following the same naming convention as the completed tests). The first two specimens would allow a direct comparison to the behavior of the specimens already tested and provide unique experimental data on full-scale bolted filler connections with standard holes. The last two specimens would be show the effect of development on multi-ply fillers, which has not been explored in previous studies. Since bearing-type connections are allowed only with standard holes, these tests would explore predicted

behavior based on the first three options in section J5 of AISC (2005). In addition, research on long-slotted holes should be conducted, as should snug-tight bearing connections with oversized holes to ensure that residual effects of bolt pretension did not contribute extensively to the high test-to-predicted ratios of the 159 specimens in bolt shear. Second is conducting a parametric study of connection behavior using nonlinear continuum finite element analysis of bolted connections with fillers. This would allow for modeling of connections with various filler thicknesses, material strengths, hole diameters, numbers of plies, and levels of development. It would also enable investigation of the failure mechanisms in these connections without the simplifying assumptions that are needed for simpler mechanism analyses such as those presented in this study.

## REFERENCES

- American Association of State Highway and Transportation Officials (AASHTO) (1994). *AASHTO LRFD Bridge Design Specifications*, 1st edition, AASHTO, Washington, D.C.
- American Institute of Steel Construction (AISC) (1989). *Specification for Structural Steel Buildings: Allowable Stress Design and Plastic Design*, AISC, Chicago, Illinois.
- American Institute of Steel Construction (AISC) (2005). *ANSI/AISC360-05: Specification for Structural Steel Buildings*, AISC, Chicago, Illinois.
- American Society of Testing Materials (ASTM) (2006). “Designation F606–06: Standard Test Methods for Determining the Mechanical Properties of Externally and Internally Threaded Fasteners, Washers, Direct Tension Indicators, and Rivets,” ASTM International, West Conshohocken, Pennsylvania.
- Cook, R. D., Malkus, D. S., Plesha, M. E., & Witt, R. J. (2002). *Concepts and Applications of Finite Element Analysis*, 4th ed., John Wiley & Sons, New York, New York.
- Cowper, G. R. (1966). “The Shear Coefficient in Timoshenko's Beam Theory,” *Journal of Applied Mechanics*, ASME, Vol. 33, pp. 335-340.
- David, H. A. (1970). *Order Statistics*, Wiley, New York, New York.
- Dusicka, P. and Lewis, G. (2007). “Effect of Fillers on Steel Girder Field Splice Performance Year 1 Progress Report,” *Research Council on Structural Connection*, Department of Civil and Environmental Engineering, Portland State University, Portland, Oregon, October.
- Frank, K. H. and Yura, J. A. (1981). *An Experimental Study of Bolted Shear Connections*, Report No. FHWA/RD-81/148, Federal Highway Administration, U.S. Department of Transportation, Washington, D.C., December.
- Grondin, G., Jin, M., and Josi, G. (2008). “Slip Critical Bolted Connection – A Reliability Analysis for Design at the Ultimate Limit State,” *The American Institute of Steel Construction*, Department of Civil and Environmental Engineering, University of Alberta, Edmonton, Alberta, Canada, April.
- Kanda, K., Uemura, A., and Mori, T. (2006). “Slip Resistance of High Strength Bolted Single Friction Joints with Filler Plates,” *Journal of Construction Steel*, Vol. 14, pp. 639-646. (in Japanese)
- Kulak, G. L., Fisher, J. W., and Struik, J. H. A. (2001). *Guide to Design Criteria for Bolted and Riveted Joints*, 2nd edition, John Wiley & Sons, New York, New York.

Lee, J. H. and Fisher, J. W. (1968). *Bolted Joints with Rectangular or Circular Fillers*, Report No. 318.6, Fritz Engineering Laboratory, Department of Civil Engineering, Lehigh University, Bethlehem, Pennsylvania, June.

Miyachi, S. and Koeda, Y. (1999). "Slip-Behavior Characteristics of Bolted Joint with a Filler Plate," *Kawada Technical Report*, Vol. 18, pp. 68-69. (in Japanese)

Rassati, G. A. and Swanson, J. A. (2007). "Ancillary Bolt Shear and Tension Tests," Internal Report, Department of Civil and Environmental Engineering, University of Cincinnati, Cincinnati, Ohio

Research Council on Structural Connections (RCSC) (1989). *Specification for Structural Joints Using ASTM A325 or A490 Bolts*, RCSC, Chicago, Illinois.

Research Council on Structural Connections (RCSC) (2004). *Specification for Structural Joints Using ASTM A325 or A490 Bolts*, RCSC, Chicago, Illinois, June.

Song, J., and Der Kiureghian, A. (2003). "Bounds on System Reliability by Linear Programming," *Journal of Engineering Mechanics*, ASCE, Vol. 129 No. 6, pp. 627-636.

Sugiyama, N., Kubo, M., Kondou, A., Ito, I., and Oda, H. (2001). "Slip Test on High-Strength Bolted Friction Joints with Filler Plate," *Reports of the Faculty of Science and Technology*, Vol. No. 41, pp. 50-56. (in Japanese)

Takizawa, S., Sawada, H., Kuroda, I., and Abe, Y. (1999). "Slip Test of Friction Type High Tension Bolted Joints According to 'Guideline of Steel Road Bridges,'" *Bridge and Foundation Engineering*, Vol. 33, No. 9, pp 25-28. (in Japanese)

Wallaert, J. J. and Fisher, J. W. (1965). "Shear Strength of High-Strength Bolts," *Journal of the Structural Division*, ASCE. Vol. 91, No. ST3, pp. 99-125.

---

# CALCULATION OF NOMINAL, DESIGN, AND PREDICTED STRENGTHS

## A.1 General Information

This appendix presents the calculations for the test specimens investigated in this research. Calculations are shown in detail for specimen 159h unless otherwise specified. Tabular results are then presented for all specimens based on similar calculations to those shown. Pertinent information about these calculations includes:

- Each limit state is calculated as if it were the first limit state. For example, bolt slip is calculated both for the interface between the splice plate and a developed filler and between a developed filler and the top column, both calculations assuming the same bolt pretension. However, it is recognized that after the initial slip occurs, the bolt pretension may change and thus influence the slip strength of the second slip surface. These sequential effects are not included in the calculations.
- All rolled shapes were specified as ASTM A992 steel.
  - Nominal and measured strengths based on mill reports are summarized in Table A.1.
- All plates were ASTM A572/50 steel.
  - Nominal and measured strengths based on mill reports are summarized in Table A.2.
- All welds were 70 ksi. Ancillary tests of the weld material were not conducted.
- All bolts were 1 1/8 in. A490-X.
  - Nominal and measured strengths based on ancillary reports are summarized in Table A.3.
- Specimen 730-std had standard size bolt holes. All other specimens had oversize bolt holes.
- The measured slip coefficient was 0.46 based on ancillary tests.
- Diameter of bolt:  $d_{bolt} = 1\frac{1}{8} in$

- Diameter of standard bolt hole:

$$d_{hole} = d_{bolt} + \frac{1}{16}in = 1\frac{1}{8}in + \frac{1}{16}in = 1\frac{3}{16}in$$

- Diameter of oversize bolt hole:

$$d_{hole} = d_{bolt} + \frac{5}{16}in = 1\frac{1}{8}in + \frac{5}{16}in = 1\frac{7}{16}in$$

- Area of bolt:  $A_b = \frac{\pi}{4}d_b^2 = \frac{\pi}{4}(1.125in)^2 = 0.994in^2$
- Minimum edge distance to sheared edge:  $e = 2in + \frac{1}{8}in = 2\frac{1}{8}in$
- Minimum edge distance to rolled edge:  $e' = 1\frac{1}{2}in + \frac{1}{8}in = 1\frac{5}{8}in$

**Table A.1 – Specimen column properties**

Column	Hole Size	Heat Number	Yield Strength (ksi)	Ultimate Strength (ksi)
Top Columns				
W14x730	Standard	40694	71	91
W14x730	Oversize	27725	60	82
W14x455	Oversize	24788	65	82
W14x159	Oversize	287830	56	73
Bottom Columns				
W14x730	Standard	40694	71	91
W14x730	Oversize	27723	60	82
		27725	60	82
		27726	61	81
		41099	70	89

**Table A.2 – Specimen plate properties**

Plate Thickness (in)	Heat ID	Yield Strength (ksi)	Ultimate Strength (ksi)
1/4	533713	53	75
1-5/8	3105972	58	84
2	7102887	59	82
	7102892	53	82
3-1/2	307461	50	71
3-3/4	S07446	51	74

**Table A.3 – Summary of measured bolt properties**

<b>Bolt Property</b>	<b>Turn-of-nut 7 in. Length</b>	<b>Turn-of-nut 9 in. Length</b>	<b>Tension- controlled 7 in. Length</b>	<b>Tension- controlled 9 in. Length</b>
<b><math>T_b</math>, Pretension (kips)</b>	113	115	94	96
<b><math>F_v</math>, Shear Strength (ksi)</b>	102	99	104	108
<b><math>F_u</math>, Tensile Strength (ksi)</b>	160	168	172	180

## A.2 Design Criteria

There are currently two design methodologies in the 2005 AISC *Specification*; Allowable Strength Design (ASD) and Load and Resistance Factor Design (LRFD). The strength of connections in the 2005 AISC *Specification* compared to the 1989 AISC ASD *Specification* differs, as discussed in Section 1 of this report.

The hole factor present in slip strength calculations for AISC (2005) is a reduction due to the increased repercussions associated with slip of an oversize hole compared to a standard hole. It is not representative of an expected strength reduction. Therefore a value of 1.0 is used for the hole factor in all of the AISC (2005) calculations (expected slip strength with the hole factor may be obtained by multiplying all AISC (2005) values by 0.85). However, the allowable slip stress for oversized holes in the calculations for the 1989 ASD *Specification* is what was used historically from those provisions and is thus used in the calculations below. That value,  $F_v = 29$  ksi, is approximately equal to 0.85 times the allowable slip stress for standard holes.

For each limit state, the design strength is calculated using 2005 AISC LRFD and 2005 AISC ASD provisions assuming nominal material properties. For key limit states (i.e., slip and shear strengths) 1989 AISC ASD strengths are also calculated assuming nominal material properties. The predicted strengths are determined using measured material properties and 2005 AISC design equations without a resistance factor or safety factor reduction.

## A.3 Design Slip Strength

### Design slip strength between filler plate and splice plate

Six rows of 2 bolts for each flange, total of 24 bolts for slip resistance.

$$\text{AISC 2005 Equation J3-4: } R_{ni} = \mu D_u h_{sc} T_b N_s$$

$$\mu = 0.50 \qquad \qquad \qquad \text{(Class B Surface)}$$

$$D_u = 1.13$$

$$h_{sc} = 1 \text{ (0.85 neglected)}$$

$$T_b = 80k$$

$$N_s = 1$$

Resistance of a single bolt:  $R_{ni} = (0.50)(1.13)(1)(80k)(1) = 45.2k$

Resistance of all bolts:  $R_n = 24R_{ni} = 24(45.2k) = 1084.8k$

2005 LRFD Strength:  $\phi R_n = 0.85R_n = 0.85(1084.8k) = 922k$

2005 ASD Strength:  $R_n/\Omega = 1084.8k/1.76 = 616k$

AISC 1989 ASD Section J3.4:  $R_{ni} = F_v A_b$

RCSC 1989 Table 3:  $F_v = 29.0ksi$  (Oversize holes)

Resistance of a single bolt:  $R_{ni} = (29ksi)(0.994in^2) = 28.8k$

1989 ASD Strength:  $R_n = 24R_{ni} = 24(28.8k) = 692k$

### Design slip strength between filler plate and top column

Eight rows of 2 bolts for each flange, total of 32 bolts for slip resistance.

AISC 2005 Equation J3-4:  $R_{ni} = \mu D_u h_{sc} T_b N_s$

$$\mu = 0.50 \quad \text{(Class B Surface)}$$

$$D_u = 1.13$$

$$h_{sc} = 1 \text{ (0.85 neglected)}$$

$$T_b = 80k$$

$$N_s = 1$$

Resistance of a single bolt:  $R_{ni} = (0.50)(1.13)(1)(80k)(1) = 45.2k$

Resistance of all bolts:  $R_n = 32R_{ni} = 32(45.2k) = 1446k$

2005 LRFD Strength:  $\phi R_n = 0.85R_n = 0.85(1446k) = 1229k$

2005 ASD Strength:  $R_n/\Omega = 1446k/1.76 = 822k$

AISC 1989 ASD Section J3.4:  $R_{ni} = F_v A_b$

RCSC 1989 Table 3:  $F_v = 29.0ksi$  (Oversize holes)

Resistance of a single bolt:  $R_{ni} = (29ksi)(0.994in^2) = 28.8k$

1989 ASD Strength:  $R_n = 32R_{ni} = 32(28.8k) = 922k$

### Design slip strength between splice plate and bottom column

Eight rows of 4 bolts for each flange, total of 64 bolts for slip resistance.

AISC 2005 Equation J3-4:  $R_{ni} = \mu D_u h_{sc} T_b N_s$

$$\mu = 0.50 \quad \text{(Class B Surface)}$$

$$D_u = 1.13$$

$$h_{sc} = 1 \text{ (0.85 neglected)}$$

$$T_b = 80k$$

$$N_s = 1$$

Resistance of a single bolt:  $R_{ni} = (0.50)(1.13)(1)(80k)(1) = 45.2k$

Resistance of all bolts:  $R_n = 64R_{ni} = 64(45.2k) = 2893k$

2005 LRFD Strength:  $\phi R_n = 0.85R_n = 0.85(2893k) = 2459k$

2005 ASD Strength:  $R_n/\Omega = 2893k/1.76 = 1644k$

AISC 1989 ASD Section J3.4:  $R_{ni} = F_v A_b$

RCSC 1989 Table 3:  $F_v = 29.0ksi$  (Oversize holes)

Resistance of a single bolt:  $R_{ni} = (29ksi)(0.994in^2) = 28.8k$

1989 ASD Strength:  $R_n = 64R_{ni} = 64(28.8k) = 1845k$

## A.4 Design Shear Strength

### Design bolt shear strength between filler plate and splice plate

Six rows of 2 bolts for each flange, total of 24 bolts for shear resistance.

Nominal shear strength:  $F_{nv} = 75ksi$

Resistance of a single bolt:  $R_{ni} = F_{nv} A_b = F_{nv} \frac{\pi}{4} d^2 = (75ksi) \frac{\pi}{4} (1 \frac{1}{8} \text{''})^2 = 74.6k$

Resistance of all bolts:  $R_n = 24R_{ni} = 24(74.6k) = 1789k$

2005 LRFD Strength:  $\phi R_n = 0.75R_n = 0.75(1789k) = 1342k$

2005 ASD Strength:  $R_n/\Omega = 1789k/2.0 = 895k$

AISC 1989 ASD Section J3.4:  $R_{ni} = F_v A_b$

AISC 1989 ASD Table J3.2:  $F_v = 40.0ksi$

Resistance of a single bolt:  $R_{ni} = (40ksi)(0.994in^2) = 39.76k$

1989 ASD Strength:  $R_n = 24R_{ni} = 24(39.76k) = 954k$

### Design bolt shear strength between filler plate and top column

Eight rows of 2 bolts for each flange, total of 32 bolts for shear resistance.

Nominal shear strength:  $F_{nv} = 75ksi$

Resistance of a single bolt:  $R_{ni} = F_{nv} A_b = F_{nv} \frac{\pi}{4} d^2 = (75ksi) \frac{\pi}{4} (1 \frac{1}{8} \text{''})^2 = 74.6k$

Resistance of all bolts:  $R_n = 32R_{ni} = 32(74.6k) = 2386k$

2005 LRFD Strength:  $\phi R_n = 0.75R_n = 0.75(2386k) = 1789k$   
 2005 ASD Strength:  $R_n/\Omega = 2386k/2.0 = 1193k$   
 AISC 1989 ASD Section J3.4:  $R_{ni} = F_v A_b$   
 AISC 1989 ASD Table J3.2:  $F_v = 40.0ksi$   
 Resistance of a single bolt:  $R_{ni} = (40ksi)(0.994in^2) = 39.76k$   
 1989 ASD Strength:  $R_n = 32R_{ni} = 32(39.76k) = 1272k$

### Design bolt shear strength between splice plate and bottom column

Eight rows of 2 bolts for each flange, total of 32 bolts for shear resistance.

Nominal shear strength:  $F_{nv} = 75ksi$   
 Resistance of a single bolt:  $R_{ni} = F_{nv} A_b = F_{nv} \frac{\pi}{4} d^2 = (75ksi) \frac{\pi}{4} (1\frac{1}{8}in)^2 = 74.6k$   
 Resistance of all bolts:  $R_n = 64R_{ni} = 64(74.6k) = 4771k$   
 2005 LRFD Strength:  $\phi R_n = 0.75R_n = 0.75(4771k) = 3578k$   
 2005 ASD Strength:  $R_n/\Omega = 4771k/2.0 = 2386k$   
 AISC 1989 ASD Section J3.4:  $R_{ni} = F_v A_b$   
 AISC 1989 ASD Table J3.2:  $F_v = 40.0ksi$   
 Resistance of a single bolt:  $R_{ni} = (40ksi)(0.994in^2) = 39.76k$   
 1989 ASD Strength:  $R_n = 64R_{ni} = 64(39.76k) = 2545k$

## A.5 Design Strength of Connected Elements

### Strength of splice plate in compression

Yield strength:  $F_y = 50ksi$   
 Ultimate strength:  $F_u = 65ksi$   
 Width of plate:  $w = 16\frac{3}{4}in$   
 Unsupported length:  $L = \text{edge dist.} + \text{gap} + \text{edge dist}$   
 $L = (2\frac{1}{8}in) + (3\frac{1}{2}in) + (2\frac{1}{8}in) = 7\frac{3}{4}in$   
 Splice plate thickness:  $t = 2in$   
 Radius of gyration:  $r = \sqrt{\frac{bt^3/12}{bt}} = t/\sqrt{12} = 0.2887t = 0.2887(2in) = 0.577in$   
 If pinned-pinned is assumed:  $KL/r = (1.0)(7\frac{3}{4}in)/(0.577in) = 13.43$   
 If fixed-fixed is assumed:  $KL/r = (0.65)(7\frac{3}{4}in)/(0.577in) = 8.73$

Either case:  $\frac{KL}{r} \leq 25 \quad \therefore \quad P_n = F_y A_g$

Gross area of one plate:  $A_g = bt = (16\frac{3}{4}")(2") = 33.50in^2$

Nominal strength of one plate:  $P_n = F_y A_g = (50ksi)(33.50in^2) = 1675k$

Nominal strength of two plates:  $P_n = 2(1675k) = 3350k$  (3306k if one uses Eq. E3-2)

2005 LRFD Strength:  $\phi P_n = 0.9(3350k) = 3015k$  (2975k if one uses Eq. E3-2)

2005 ASD Strength:  $\frac{P_n}{\Omega} = 3350k/1.67 = 2006k$  (1980k if one uses E. E3-2)

### Yield strength of splice plate

Gross area:  $A_g = bt = (16\frac{3}{4}")(2") = 33.50in^2$

Nominal strength of one plate:  $P_n = F_y A_g = (50ksi)(33.50in^2) = 1675k$

Nominal strength of two plates:  $P_n = 2(1675k) = 3350k$

2005 LRFD Strength:  $\phi P_n = 0.9(3350k) = 3015k$

2005 ASD Strength:  $\frac{P_n}{\Omega} = 3350k/1.67 = 2006k$

### Fracture of net area of splice plate (calculated as if in tension)

Two oversize holes for 1 1/8" bolts

Net area:  $A_n = t(w - 2d_{hole}) = (2")(16\frac{3}{4}" - 2(1\frac{7}{16}")) = 27.75in$

Nominal strength of one plate:  $P_n = F_u A_n = (65ksi)(27.75in^2) = 1804k$

Nominal strength of two plates:  $P_n = 2(1804k) = 3607k$

2005 LRFD Strength:  $\phi P_n = 0.75(3607k) = 2706k$

2005 ASD Strength:  $\frac{P_n}{\Omega} = 3607k/2.0 = 1804k$

### Yield strength of W14x159 cross section

Nominal strength of flange:  $P_n = F_y A_g = (50ksi)(46.7in^2) = 2335k$

2005 LRFD Strength:  $\phi P_n = 0.9(2335k) = 2101k$

2005 ASD Strength:  $\frac{P_n}{\Omega} = 2335k/1.67 = 1398k$

### Fracture on net area strength of W14x159 cross section (calculated as if in tension)

Two oversize holes for 1 1/8" bolts

Column flange thickness  $t_f = 1.19"$

Net area:  $A_n = A_g - 2(2d_{hole})t_f = (46.7in^2) - 2(2)(1\frac{7}{16}in)(1.19in) = 39.86in^2$

Nominal strength:  $P_n = F_u A_e = F_u A_n U = (65ksi)(39.86in^2)(0.85[estimate]) = 2202k$

2005 LRFD Strength:  $\phi P_n = 0.75(2202k) = 1652k$

2005 ASD Strength:  $P_n/\Omega = 2202k/2.0 = 1101k$

**Bearing strength on splice plate on W14x159 side**

4 Bolts

Large clear distance:  $L_c = big$

Resistance of a single bolt:  $R_{ni} = 1.2L_c t F_u \leq 2.4dtF_u$   
 $R_{ni} = 1.2(big)(2")(65ksi) \leq 2.4(1\frac{1}{8}")(2")(65ksi)$   
 $R_{ni} = big \leq 351.0k = 351.0k$

20 Bolts

Clear distance:  $L_c = (3\frac{3}{8} ") - d_{hole} = (3\frac{3}{8} ") - (1\frac{7}{16} ") = 1.938in$

Resistance of a single bolt  $R_{ni} = 1.2L_c t F_u \leq 2.4dtF_u$   
 $R_{ni} = 1.2(1.938")(2")(65ksi) \leq 2.4(1\frac{1}{8}")(2")(65ksi)$   
 $R_{ni} = 302.3 \leq 351.0k = 302.3k$

Total resistance:  $R_n = 4(351.0k) + 20(302.3k) = 7450k$

2005 LRFD Strength:  $\phi R_n = 0.75R_n = 0.75(7450k) = 5588k$

2005 ASD Strength:  $R_n/\Omega = 7450k/2.0 = 3725k$

**Bearing strength on W14x159 column flange**

Column flange thickness  $t_f = 1.19in$

4 Bolts

Large clear distance:  $L_c = big$

Resistance of a single bolt:  $R_{ni} = 1.2L_c t F_u \leq 2.4dtF_u$   
 $R_{ni} = 1.2(big)(1.19")(65ksi) \leq 2.4(1\frac{1}{8}")(1.19")(65ksi)$   
 $R_{ni} = big \leq 208.8k = 208.8k$

4 Bolts

Clear distance:  $L_c = (4\frac{3}{4} ") - d_{hole} = (4\frac{3}{4} ") - (1\frac{7}{16} ") = 3.1875in$

Resistance of a single bolt:  $R_{ni} = 1.2L_c t F_u \leq 2.4dtF_u$   
 $R_{ni} = 1.2(3.1875")(1.19")(65ksi) \leq 2.4(1\frac{1}{8}")(1.19")(65ksi)$   
 $R_{ni} = 295.9 \leq 208.8k = 208.8k$

24 Bolts

Clear distance:  $L_c = (3\frac{3}{8} ") - d_{hole} = (3\frac{3}{8} ") - (1\frac{7}{16} ") = 1.938in$

Resistance of a single bolt:  $R_{ni} = 1.2L_c t F_u \leq 2.4dtF_u$

$$R_{ni} = 1.2(1.938")(1.19")(65ksi) \leq 2.4(1\frac{1}{8}")(1.19")(65ksi)$$

$$R_{ni} = 179.9 \leq 208.8k = 179.9k$$

Total resistance:  $R_n = 4(208.8k) + 4(208.8k) + 24(179.9k) = 5988k$

2005 LRFD Strength:  $\phi R_n = 0.75R_n = 0.75(5988k) = 4491k$

2005 ASD Strength:  $R_n/\Omega = 5988k/2.0 = 2994k$

## A.6 Predicted Strength

The ancillary tests revealed that the nominal strengths differ from the actual properties. The predicted slip strength is based on the ancillary slip coefficient for the surfaces used in the specimens. The bolt properties also were derived from the ancillary tests. The plate and shape properties were taken from mill certificates.

### Predicted slip strength between filler plate and splice plate

Six rows of two 9 in. TN bolts for each flange, total of 24 bolts for slip resistance.

Measured bolt pretension:  $T_b = 115k$

Measured slip coefficient:  $\mu = 0.46$

Resistance of single bolt:  $R_{ni} = \mu T_b = (0.46)(115k) = 52.9k$

Predicted TN slip strength:  $R_n = 24R_{ni} = (24)(52.9k) = 1270k$

### Predicted slip strength between filler plate and top column

Six rows of two 9 in. TN bolts for each flange, twenty-four 9 in. bolts for slip resistance.

Two rows of two 7 in. TN bolts for each flange, eight 7 in. bolts for slip resistance.

32 total bolts for slip resistance

Measured bolt pretension:  $T_{b,9in} = 115k$   
 $T_{b,7in} = 113k$

Measured slip coefficient:  $\mu = 0.46$

Resistance of single bolt:  $R_{ni,9in} = \mu T_{b,9in} = (0.46)(115k) = 52.9k$   
 $R_{ni,7in} = \mu T_{b,7in} = (0.46)(113k) = 52.0k$

Predicted TN slip strength:  $R_n = 24R_{ni,9in} + 8R_{ni,7in} = (24)(52.9k) + (8)(52.0k) = 1686k$

### **Predicted slip strength between splice plate and bottom column**

Eight rows of four 9 in. TN bolts for each flange, total of 64 bolts for slip resistance.

$$\begin{aligned}\text{Measured bolt pretension: } T_b &= 115k \\ \text{Measured slip coefficient: } \mu &= 0.46 \\ \text{Resistance of single bolt: } R_{ni} &= \mu T_b = (0.46)(115k) = 52.9k \\ \text{Predicted TN slip strength: } R_n &= 64R_{ni} = (64)(52.9k) = 3386k\end{aligned}$$

### **Predicted bolt shear strength between filler plate and splice plate**

Six rows of two 9 in. TN bolts for each flange, total of 24 bolts for shear resistance.

$$\begin{aligned}\text{Nominal shear strength: } F_{nv} &= 102.5ksi \\ \text{Resistance of a single bolt: } R_{ni} &= F_{nv} A_b = F_{nv} \frac{\pi}{4} d^2 = (102.5ksi) \frac{\pi}{4} (1 \frac{1}{8} in)^2 = 101.8k \\ \text{Predicted TN shear strength: } R_n &= 24R_{ni} = 24(101.8k) = 2444k\end{aligned}$$

### **Predicted bolt shear strength between filler plate and splice plate**

Six rows of two 9 in. TN bolts for each flange, twenty-four 9 in. bolts for shear resistance.

Two rows of two 7 in. TN bolts for each flange, eight 7 in. bolts for shear resistance.

Total of 32 bolts for shear resistance

$$\begin{aligned}\text{Nominal shear strength: } F_{nv,9in} &= 102.5ksi \\ &F_{nv,7in} = 99.5ksi \\ \text{Resistance of a single bolt: } \\ R_{ni,9in} &= F_{nv,9in} A_b = F_{nv,9in} \frac{\pi}{4} d^2 = (102.5ksi) \frac{\pi}{4} (1 \frac{1}{8} in)^2 = 101.8k \\ R_{ni,7in} &= F_{nv,7in} A_b = F_{nv,7in} \frac{\pi}{4} d^2 = (99.5ksi) \frac{\pi}{4} (1 \frac{1}{8} in)^2 = 98.9k \\ \text{Predicted TN shear strength: } R_n &= 24R_{ni,9in} + 8R_{ni,7in} = 24(101.8k) + 8(98.9k) = 3234k\end{aligned}$$

### **Predicted bolt shear strength between filler plate and splice plate**

Eight rows of four 9 in. TN bolts for each flange, total of 64 bolts for shear resistance.

$$\begin{aligned}\text{Nominal shear strength: } F_{nv} &= 102.5ksi \\ \text{Resistance of a single bolt: } R_{ni} &= F_{nv} A_b = F_{nv} \frac{\pi}{4} d^2 = (102.5ksi) \frac{\pi}{4} (1 \frac{1}{8} in)^2 = 101.8k \\ \text{Predicted TN shear strength: } R_n &= 64R_{ni} = 64(101.8k) = 6515k\end{aligned}$$

### Strength of splice plate in compression

Yield strength:  $F_y = 56ksi$

Ultimate strength:  $F_u = 82ksi$

Width of plate:  $w = 16\frac{3}{4}in$

Unsupported length:  $L = \text{edge dist.} + \text{gap} + \text{edge dist}$   
 $L = (2\frac{1}{8}in) + (3\frac{1}{2}in) + (2\frac{1}{8}in) = 7\frac{3}{4}in$

Splice plate thickness:  $t = 2in$

Radius of gyration:  $r = \sqrt{\frac{bt^3/12}{bt}} = \frac{t}{\sqrt{12}} = 0.2887t = 0.2887(2in) = 0.577in$

If pinned-pinned is assumed:  $\frac{KL}{r} = \frac{(1.0)(7\frac{3}{4}in)}{(0.577in)} = 13.43$

If fixed-fixed is assumed:  $\frac{KL}{r} = \frac{(0.65)(7\frac{3}{4}in)}{(0.577in)} = 8.73$

Either case:  $\frac{KL}{r} \leq 25 \quad \therefore \quad P_n = F_y A_g$

Gross area of one plate:  $A_g = bt = (16\frac{3}{4}in)(2in) = 33.50in^2$

Nominal strength of one plate:  $P_n = F_y A_g = (56ksi)(33.50in^2) = 1876k$

Nominal strength of two plates:  $P_n = 2(1876k) = 3752k$  (3697k if one uses Eq. E3-2)

2005 LRFD Strength:  $\phi P_n = 0.9(3752k) = 3377k$  (3327k if one uses Eq. E3-2)

2005 ASD Strength:  $\frac{P_n}{\Omega} = \frac{3752k}{1.67} = 2247k$  (2214k if one uses Eq. E3-2)

### Yield strength of splice plate

Gross area:  $A_g = bt = (16\frac{3}{4}in)(2in) = 33.50in^2$

Nominal strength of one plate:  $P_n = F_y A_g = (56ksi)(33.50in^2) = 1876k$

Nominal strength of two plates:  $P_n = 2(1876k) = 3752k$

2005 LRFD Strength:  $\phi P_n = 0.9(3752k) = 3377k$

2005 ASD Strength:  $\frac{P_n}{\Omega} = \frac{3752k}{1.67} = 2247k$

### Fracture of net area of splice plate (calculated as if in tension)

Two oversize holes for 1 1/8" bolts

Net area:  $A_n = t(w - 2d_{hole}) = (2in)(16\frac{3}{4}in - 2(1\frac{7}{16}in)) = 27.75in$

Nominal strength of one plate:  $P_n = F_u A_n = (82ksi)(27.75in^2) = 2275k$

Nominal strength of two plates:  $P_n = 2(2275k) = 4551k$

2005 LRFD Strength:  $\phi P_n = 0.75(4551k) = 3413k$

2005 ASD Strength:  $\frac{P_n}{\Omega} = \frac{4551k}{2.0} = 2275k$

### Yield strength of W14x159 cross section

Nominal strength of flange:  $P_n = F_y A_g = (56 \text{ksi})(46.7 \text{in}^2) = 2615 \text{k}$

2005 LRFD Strength:  $\phi P_n = 0.9(2615 \text{k}) = 2353 \text{k}$

2005 ASD Strength:  $P_n / \Omega = 2615 \text{k} / 1.67 = 1566 \text{k}$

### Fracture on net area strength of W14x159 cross section (calculated as if in tension)

Two oversize holes for 1 1/8" bolts

Column flange thickness  $t_f = 1.19 \text{''}$

Net area:  $A_n = A_g - 2(2d_{hole})t_f = (46.7 \text{in}^2) - 2(2)(1\frac{7}{16} \text{in})(1.19 \text{in}) = 39.86 \text{in}^2$

Nominal strength:  $P_n = F_u A_e = F_u A_n U = (73 \text{ksi})(39.86 \text{in}^2)(0.85[\text{estimate}]) = 2473 \text{k}$

2005 LRFD Strength:  $\phi P_n = 0.75(2473 \text{k}) = 1855 \text{k}$

2005 ASD Strength:  $P_n / \Omega = 2473 \text{k} / 2.0 = 1237 \text{k}$

### Bearing strength on splice plate on W14x159 side

4 Bolts

Large clear distance:  $L_c = \text{big}$

Resistance of a single bolt:  $R_{ni} = 1.2L_c t F_u \leq 2.4dt F_u$

$$R_{ni} = 1.2(\text{big})(2'')(82 \text{ksi}) \leq 2.4(1\frac{1}{8}')(2'')(82 \text{ksi})$$

$$R_{ni} = \text{big} \leq 442.8 \text{k} = 442.8 \text{k}$$

20 Bolts

Clear distance:  $L_c = (3\frac{3}{8}') - d_{hole} = (3\frac{3}{8}') - (1\frac{7}{16}') = 1.938 \text{in}$

Resistance of a single bolt  $R_{ni} = 1.2L_c t F_u \leq 2.4dt F_u$

$$R_{ni} = 1.2(1.938'')(2'')(82 \text{ksi}) \leq 2.4(1\frac{1}{8}')(2'')(82 \text{ksi})$$

$$R_{ni} = 381.4 \leq 442.8 \text{k} = 381.4 \text{k}$$

Total resistance:  $R_n = 4(442.8 \text{k}) + 20(381.4 \text{k}) = 9399 \text{k}$

2005 LRFD Strength:  $\phi R_n = 0.75R_n = 0.75(9399 \text{k}) = 7049 \text{k}$

2005 ASD Strength:  $R_n / \Omega = 9399 \text{k} / 2.0 = 4700 \text{k}$

### Bearing strength on W14x159 column flange

Column flange thickness  $t_f = 1.19 \text{in}$

4 Bolts

Large clear distance:  $L_c = big$

$$\begin{aligned} \text{Resistance of a single bolt: } R_{ni} &= 1.2L_c t F_u \leq 2.4dtF_u \\ R_{ni} &= 1.2(big)(1.19")(73ksi) \leq 2.4(1\frac{1}{8}")(1.19")(73ksi) \\ R_{ni} &= big \leq 234.5k = 234.5k \end{aligned}$$

4 Bolts

Clear distance:  $L_c = (4\frac{3}{4} ") - d_{hole} = (4\frac{3}{4} ") - (1\frac{7}{16} ") = 3.1875in$

$$\begin{aligned} \text{Resistance of a single bolt: } R_{ni} &= 1.2L_c t F_u \leq 2.4dtF_u \\ R_{ni} &= 1.2(3.1875")(1.19")(73ksi) \leq 2.4(1\frac{1}{8}")(1.19")(73ksi) \\ R_{ni} &= 332.3 \leq 234.5k = 234.5k \end{aligned}$$

24 Bolts

Clear distance:  $L_c = (3\frac{3}{8} ") - d_{hole} = (3\frac{3}{8} ") - (1\frac{7}{16} ") = 1.938in$

$$\begin{aligned} \text{Resistance of a single bolt: } R_{ni} &= 1.2L_c t F_u \leq 2.4dtF_u \\ R_{ni} &= 1.2(1.938")(1.19")(73ksi) \leq 2.4(1\frac{1}{8}")(1.19")(73ksi) \\ R_{ni} &= 202.0 \leq 234.5k = 202.0k \end{aligned}$$

Total resistance:  $R_n = 4(234.5k) + 4(234.5k) + 24(202.0k) = 6724k$

2005 LRFD Strength:  $\phi R_n = 0.75R_n = 0.75(6724k) = 5043k$

2005 ASD Strength:  $R_n / \Omega = 6724k / 2.0 = 3362k$

## A.7 Development of the Filler Plates

According to 2005 AISC *Specification* Section J5 a filler is developed by securing the filler to the connected element to uniformly distribute the total force over the combined cross section.

### Percent Developed of the Filler Plate

Strength of developing filler:  $R_{u,development,provided} = 8 \text{ bolts}$

Strength of connection:  $R_{u,connection} = 24 \text{ bolts}$

Thickness ratio:  $\rho = \frac{t_{fill}}{t_{connected \ element}} = \frac{3.75in}{1.19in} = 3.15$

Percent developed: 
$$\% dev = \frac{R_{u,development,provided}}{\frac{\rho}{1+\rho} R_{u,connection}} = \frac{8 \text{ bolts}}{\frac{3.15}{1+3.15} 24 \text{ bolts}} = 43.9\%$$

### Percent Developed of the Filler Plate (159f-weld)

Development achieved with 64 in. total of 1/2 in. fillet weld

Strength developing filler:

$$R_{u,development,provided} = L \frac{size}{\sqrt{2}} 0.6 F_{EXX} = (64in) \frac{0.5in}{\sqrt{2}} 0.6(70ksi) = 950k$$

Strength of connection:  $R_{u,connection} = 24 \text{ bolts}$

At slip:  $1 \text{ bolt} = 52.9k$  (see above)

$$R_{u,development,provided} = 950k \frac{1 \text{ bolt}}{52.9k} = 17.9 \text{ bolts}$$

$$\% dev = \frac{R_{u,development,provided}}{\frac{\rho}{1+\rho} R_{u,connection}} = \frac{17.9 \text{ bolts}}{\frac{3.15}{1+3.15} 24 \text{ bolts}} = 98.3\%$$

At shear: Weld would have fractured and provide negligible resistance.

$$R_{u,development,provided} = 0 \text{ bolts}$$

$$\% dev = \frac{R_{u,development,provided}}{\frac{\rho}{1+\rho} R_{u,connection}} = \frac{0 \text{ bolts}}{\frac{3.15}{1+3.15} 24 \text{ bolts}} = 0.0\%$$

### Percent Effectively Fully Developed

Strength developing filler:  $R_{u,development,provided} = 8 \text{ bolts}$

Strength of connection:  $R_{u,connection} = 24 \text{ bolts}$

Thickness ratio: 
$$\rho = \frac{t_{fill}}{t_{connected \ element}} = \frac{3.75in}{1.19in} = 3.15$$

Percent effectively fully developed (derivation of formula similar to that presented in the section 4.5):

$$\% EFD = \frac{1 + \rho}{1 + 2\rho} \left( 1 + \frac{R_{u,development,provided}}{R_{u,connection}} \right) = \frac{1 + 3.15}{1 + 2(3.15)} \left( 1 + \frac{8 \text{ bolts}}{24 \text{ bolts}} \right) = 75.8\%$$

<b>Calculations for Specimen(s) 730-std &amp; 730-over</b>					
	Nominal and Design Values				Predicted
	$P_n$	$\phi P_n$	$P_n/\Omega$	$P_{allow,1989}$	$P_n$
<b>slip between:</b>					
splice and top column	1,085	922	616	692	1,270
splice and bot. column	2,893	2,459	1,644	1,845	3,386
<b>shear between:</b>					
splice and top column	1,789	1,342	895	954	2,445
splice and bot. column	4,771	3,578	2,386	2,545	6,521
<b>splice in compression:</b>					
Eq. E3-2	3,306	2,975	1,980	N/C	3,697
yield strength	3,350	3,015	2,006	N/C	3,752
fracture of net area	3,608	2,706	1,804	N/C	4,551
<b>top column in compression:</b>					
yield strength	10,750	9,675	6,437	N/C	12,900
fracture of net area	10,319	7,739	5,159	N/C	13,018
<b>bearing:</b>					
on splice	7,449	5,587	3,725	N/C	9,397
on top column flange	18,287	13,715	9,144	N/C	23,070
N/C = not calculated					

<b>Calculations for Specimen(s) 159f</b>					
	Nominal and Design Values				Predicted
	$P_n$	$\phi P_n$	$P_n/\Omega$	$P_{allow,1989}$	$P_n$
<b>slip between:</b>					
filler and splice	1,085	922	616	692	1,270
filler and top column	1,808	1,537	1,027	1,153	2,101
splice and bot. column	2,893	2,459	1,644	1,845	3,386
<b>shear between:</b>					
filler and splice	1,789	1,342	895	954	2,445
filler and top column	2,982	2,237	1,491	1,590	4,028
splice and bot. column	4,771	3,578	2,386	2,545	6,521
<b>splice in compression:</b>					
Eq. E3-2	3,306	2,975	1,980	N/C	3,697
yield strength	3,350	3,015	2,006	N/C	3,752
fracture of net area	3,608	2,706	1,804	N/C	4,551
<b>top column in compression:</b>					
yield strength	2,335	2,102	1,398	N/C	2,615
fracture of net area	2,202	1,652	1,101	N/C	2,473
<b>bearing:</b>					
on splice	7,449	5,587	3,725	N/C	9,397
on top column flange	7,426	5,569	3,713	N/C	8,340
<b>effectively fully developed:</b>					
slip strength	1,028	874	584	655	1,203
shear strength	1,695	1,271	848	904	2,317
percent developed		87.8%			
percent effectively fully developed		94.7%			
N/C = not calculated					

<b>Calculations for Specimen(s) 159h</b>					
	Nominal and Design Values				Predicted
	$P_n$	$\phi P_n$	$P_n/\Omega$	$P_{allow,1989}$	$P_n$
<b>slip between:</b>					
filler and splice	1,085	922	616	692	1,270
filler and top column	1,446	1,229	822	922	1,685
splice and bot. column	2,893	2,459	1,644	1,845	3,386
<b>shear between:</b>					
filler and splice	1,789	1,342	895	954	2,445
filler and top column	2,386	1,789	1,193	1,272	3,237
splice and bot. column	4,771	3,578	2,386	2,545	6,521
<b>splice in compression:</b>					
Eq. E3-2	3,306	2,975	1,980	N/C	3,697
yield strength	3,350	3,015	2,006	N/C	3,752
fracture of net area	3,608	2,706	1,804	N/C	4,551
<b>top column in compression:</b>					
yield strength	2,335	2,102	1,398	N/C	2,615
fracture of net area	2,202	1,652	1,101	N/C	2,473
<b>bearing:</b>					
on splice	7,449	5,587	3,725	N/C	9,397
on top column flange	5,987	4,490	2,993	N/C	6,724
<b>effectively fully developed:</b>					
slip strength	822	699	467	524	962
shear strength	1,356	1,017	678	723	1,853
percent developed		43.9%			
percent effectively fully developed		75.8%			
N/C = not calculated					

<b>Calculations for Specimen(s) 159n1, 159n2, 159n-2ply1, 159n-2ply2</b>					
	Nominal and Design Values				Predicted
	$P_n$	$\phi P_n$	$P_n/\Omega$	$P_{allow,1989}$	$P_n$
<b>slip between:</b>					
filler and splice	1,085	922	616	692	1,270
filler and top column	1,085	922	616	692	1,270
splice and bot. column	2,893	2,459	1,644	1,845	3,386
<b>shear between:</b>					
filler and splice	1,789	1,342	895	954	2,445
filler and top column	1,789	1,342	895	954	2,445
splice and bot. column	4,771	3,578	2,386	2,545	6,521
<b>splice in compression:</b>					
Eq. E3-2	3,306	2,975	1,980	N/C	3,697
yield strength	3,350	3,015	2,006	N/C	3,752
fracture of net area	3,608	2,706	1,804	N/C	4,551
<b>top column in compression:</b>					
yield strength	2,335	2,102	1,398	N/C	2,615
fracture of net area	2,202	1,652	1,101	N/C	2,473
<b>bearing:</b>					
on splice	7,449	5,587	3,725	N/C	9,397
on top column flange	4,432	3,324	2,216	N/C	4,978
<b>effectively fully developed:</b>					
slip strength	617	524	350	393	722
shear strength	1,017	763	509	542	1,390
percent developed		0.0%			
percent effectively fully developed		56.8%			
N/C = not calculated					

<b>Calculations for Specimen(s) 455f</b>					
	Nominal and Design Values				Predicted
	$P_n$	$\phi P_n$	$P_n/\Omega$	$P_{allow,1989}$	$P_n$
<b>slip between:</b>					
filler and splice	1,085	922	616	692	1,270
filler and top column	1,446	1,229	822	922	1,685
splice and bot. column	2,893	2,459	1,644	1,845	3,386
<b>shear between:</b>					
filler and splice	1,789	1,342	895	954	2,445
filler and top column	2,386	1,789	1,193	1,272	3,237
splice and bot. column	4,771	3,578	2,386	2,545	6,521
<b>splice in compression:</b>					
Eq. E3-2	3,306	2,975	1,980	N/C	3,697
yield strength	3,350	3,015	2,006	N/C	3,752
fracture of net area	3,608	2,706	1,804	N/C	4,551
<b>top column in compression:</b>					
yield strength	6,700	6,030	4,012	N/C	8,710
fracture of net area	6,384	4,788	3,192	N/C	8,053
<b>bearing:</b>					
on splice	7,449	5,587	3,725	N/C	9,397
on top column flange	16,150	12,112	8,075	N/C	20,373
<b>effectively fully developed:</b>					
slip strength	1,083	920	615	690	1,267
shear strength	1,786	1,339	893	952	2,440
percent developed		99.2%			
percent effectively fully developed		99.8%			
N/C = not calculated					

<b>Calculations for Specimen(s) 455h</b>					
	Nominal and Design Values				Predicted
	$P_n$	$\phi P_n$	$P_n/\Omega$	$P_{allow,1989}$	$P_n$
<b>slip between:</b>					
filler and splice	1,085	922	616	692	1,270
filler and top column	1,266	1,076	719	807	1,478
splice and bot. column	2,893	2,459	1,644	1,845	3,386
<b>shear between:</b>					
filler and splice	1,789	1,342	895	954	2,445
filler and top column	2,087	1,566	1,044	1,113	2,841
splice and bot. column	4,771	3,578	2,386	2,545	6,521
<b>splice in compression:</b>					
Eq. E3-2	3,306	2,975	1,980	N/C	3,697
yield strength	3,350	3,015	2,006	N/C	3,752
fracture of net area	3,608	2,706	1,804	N/C	4,551
<b>top column in compression:</b>					
yield strength	6,700	6,030	4,012	N/C	8,710
fracture of net area	6,384	4,788	3,192	N/C	8,053
<b>bearing:</b>					
on splice	7,449	5,587	3,725	N/C	9,397
on top column flange	14,209	10,657	7,105	N/C	17,925
<b>effectively fully developed:</b>					
slip strength	947	805	538	604	1,109
shear strength	1,562	1,172	781	833	2,135
percent developed		49.6%			
percent effectively fully developed		87.3%			
N/C = not calculated					

<b>Calculations for Specimen(s) 455n1 &amp; 455n2</b>					
	Nominal and Design Values				Predicted
	$P_n$	$\phi P_n$	$P_n/\Omega$	$P_{allow,1989}$	$P_n$
<b>slip between:</b>					
filler and splice	1,085	922	616	692	1,270
filler and top column	1,085	922	616	692	1,270
splice and bot. column	2,893	2,459	1,644	1,845	3,386
<b>shear between:</b>					
filler and splice	1,789	1,342	895	954	2,445
filler and top column	1,789	1,342	895	954	2,445
splice and bot. column	4,771	3,578	2,386	2,545	6,521
<b>splice in compression:</b>					
Eq. E3-2	3,306	2,975	1,980	N/C	3,697
yield strength	3,350	3,015	2,006	N/C	3,752
fracture of net area	3,608	2,706	1,804	N/C	4,551
<b>top column in compression:</b>					
yield strength	6,700	6,030	4,012	N/C	8,710
fracture of net area	6,384	4,788	3,192	N/C	8,053
<b>bearing:</b>					
on splice	7,449	5,587	3,725	N/C	9,397
on top column flange	11,956	8,967	5,978	N/C	15,083
<b>effectively fully developed:</b>					
slip strength	812	690	461	518	950
shear strength	1,339	1,004	670	714	1,830
percent developed		0.0%			
percent effectively fully developed		74.8%			
N/C = not calculated					

<b>Calculations for Specimen(s) 159h-TC</b>					
	Nominal and Design Values				Predicted
	$P_n$	$\phi P_n$	$P_n/\Omega$	$P_{allow,1989}$	$P_n$
<b>slip between:</b>					
filler and splice	1,085	922	616	692	1,060
filler and top column	1,446	1,229	822	922	1,406
splice and bot. column	2,893	2,459	1,644	1,845	2,826
<b>shear between:</b>					
filler and splice	1,789	1,342	895	954	2,576
filler and top column	2,386	1,789	1,193	1,272	3,404
splice and bot. column	4,771	3,578	2,386	2,545	6,871
<b>splice in compression:</b>					
Eq. E3-2	3,306	2,975	1,980	N/C	3,697
yield strength	3,350	3,015	2,006	N/C	3,752
fracture of net area	3,608	2,706	1,804	N/C	4,551
<b>top column in compression:</b>					
yield strength	2,335	2,102	1,398	N/C	2,615
fracture of net area	2,202	1,652	1,101	N/C	2,473
<b>bearing:</b>					
on splice	7,449	5,587	3,725	N/C	9,397
on top column flange	5,987	4,490	2,993	N/C	6,724
<b>effectively fully developed:</b>					
slip strength	822	699	467	524	770
shear strength	1,356	1,017	678	723	1,953
percent developed		43.9%			
percent effectively fully developed		75.8%			
N/C = not calculated					

<b>Calculations for Specimen(s) 159n-TC</b>					
	Nominal and Design Values				Predicted
	$P_n$	$\phi P_n$	$P_n/\Omega$	$P_{allow,1989}$	$P_n$
<b>slip between:</b>					
filler and splice	1,085	922	616	692	1,060
filler and top column	1,085	922	616	692	1,060
splice and bot. column	2,893	2,459	1,644	1,845	2,826
<b>shear between:</b>					
filler and splice	1,789	1,342	895	954	2,576
filler and top column	1,789	1,342	895	954	2,576
splice and bot. column	4,771	3,578	2,386	2,545	6,871
<b>splice in compression:</b>					
Eq. E3-2	3,306	2,975	1,980	N/C	3,697
yield strength	3,350	3,015	2,006	N/C	3,752
fracture of net area	3,608	2,706	1,804	N/C	4,551
<b>top column in compression:</b>					
yield strength	2,335	2,102	1,398	N/C	2,615
fracture of net area	2,202	1,652	1,101	N/C	2,473
<b>bearing:</b>					
on splice	7,449	5,587	3,725	N/C	9,397
on top column flange	4,432	3,324	2,216	N/C	4,978
<b>effectively fully developed:</b>					
slip strength	617	524	350	393	577
shear strength	1,017	763	509	542	1,465
percent developed		0.0%			
percent effectively fully developed		56.8%			
N/C = not calculated					

<b>Calculations for Specimen(s) 159f-weld</b>					
	Nominal and Design Values				Predicted
	$P_n$	$\phi P_n$	$P_n/\Omega$	$P_{allow,1989}$	$P_n$
<b>slip between:</b>					
filler and splice	1,085	922	616	692	1,270
filler and top column	2,035	2,443	1,632	1,167	2,220
splice and bot. column	2,893	2,459	1,644	1,845	3,386
<b>shear between:</b>					
filler and splice	1,789	1,342	895	954	2,445
filler and top column	1,789	1,342	895	954	2,445
splice and bot. column	4,771	3,578	2,386	2,545	6,521
<b>splice in compression:</b>					
Eq. E3-2	3,306	2,975	1,980	N/C	3,697
yield strength	3,350	3,015	2,006	N/C	3,752
fracture of net area	3,608	2,706	1,804	N/C	4,551
<b>top column in compression:</b>					
yield strength	2,335	2,102	1,398	N/C	2,615
fracture of net area	2,202	1,652	1,101	N/C	2,473
<b>bearing:</b>					
on splice	7,449	5,587	3,725	N/C	9,397
on top column flange	4,432	3,324	2,216	N/C	4,978
<b>effectively fully developed at slip:</b>					
slip strength	1,078	917	613	688	1,262
shear strength	1,778	1,334	889	949	2,431
<b>effectively fully developed at shear:</b>					
slip strength	617	524	350	393	722
shear strength	1,017	763	509	542	1,390
percent developed at slip			98.6%		
percent developed at shear			0.0%		
percent effectively fully developed at slip			99.4%		
percent effectively fully developed at shear			56.8%		
N/C = not calculated					
weld strength assumed only to act in conjunction with slip strength, not shear strength					

<b>Calculations for Specimen(s) 159h-weld</b>					
	Nominal and Design Values				Predicted
	$P_n$	$\phi P_n$	$P_n/\Omega$	$P_{allow,1989}$	$P_n$
<b>slip between:</b>					
filler and splice	1,085	922	616	692	1,270
filler and top column	1,567	1,694	1,132	933	1,752
splice and bot. column	2,893	2,459	1,644	1,845	3,386
<b>shear between:</b>					
filler and splice	1,789	1,342	895	954	2,445
filler and top column	1,789	1,342	895	954	2,445
splice and bot. column	4,771	3,578	2,386	2,545	6,521
<b>splice in compression:</b>					
Eq. E3-2	3,306	2,975	1,980	N/C	3,697
yield strength	3,350	3,015	2,006	N/C	3,752
fracture of net area	3,608	2,706	1,804	N/C	4,551
<b>top column in compression:</b>					
yield strength	2,335	2,102	1,398	N/C	2,615
fracture of net area	2,202	1,652	1,101	N/C	2,473
<b>bearing:</b>					
on splice	7,449	5,587	3,725	N/C	9,397
on top column flange	4,432	3,324	2,216	N/C	4,978
<b>effectively fully developed at slip:</b>					
slip strength	851	723	484	543	996
shear strength	1,404	1,053	702	749	1,918
<b>effectively fully developed at shear:</b>					
slip strength	617	524	350	393	722
shear strength	1,017	763	509	542	1,390
percent developed at slip			50.1%		
percent developed at shear			0.0%		
percent effectively fully developed at slip			78.5%		
percent effectively fully developed at shear			56.8%		
N/C = not calculated					
weld strength assumed only to act in conjunction with slip strength, not shear strength					

---

## INDIVIDUAL SPECIMEN RESULTS

### B.1 General Information

This appendix presents the results of the sixteen experiments of bolted slip-critical connections with fillers. The results include a complete set of both the LVDT and the strain data that was collected, along with observations about the response of the specimen, including documentation of any unusual events during the test (such as premature bolt failures) or any unusual eccentricities that were seen in the results. The gage names are identified in Figures 9 and 10 of the main report, including identifying north, south, east, and west. The bolt hole rows were labeled based on their geographic location in the testing machine and elevation in the top column. The bottom bolt row in the top column was bolt row 1. For example, the bolt second from the bottom in the top column in the northwest flange tip was identified as NW2.

For the turn-of-nut method specimens, three bolts on one splice plate (in the first, third, and sixth rows) and one bolt on one filler plate (in the first or second row, when bolted) were designated as control bolts. The elongation of the control bolts was measured and torqued further if necessary, along with the bolts neighboring the control bolt, to achieve the desired pretension. The specimen test matrix (Table B.1) indicates the geographical location of the control bolts, and Table B.2 indicates which control bolts (and their neighboring bolts) were retorqued. Appendix E includes drawings showing the locations and numbering scheme of the torquing sequence used by W&W Steel. The bolts on the splice plate that were typically retorqued were SE1, SW3, and SW6 if the control bolts are on the south side, or NW1, NE3, and NE6 if the control bolts are on the north side.

Overall, while normal eccentricities are exhibited that may be seen in tests of this scale, the measured displacements and strains of all specimens do not demonstrate a specific or sustained loading bias. Although there are some loading biases for each specimen, these are attributed to slight loading surface irregularities unique to each specimen rather than significant imperfections in the testing machine or procedure. As discussed in the main report, wedges were inserted above the top loading platen to lock the top spherical head into place. During this process it was noted that several of the specimens were not milled precisely square. Such eccentricities thus can propagate into the loading for the specimen, although the loading procedure used, including centering of the specimen, minimizes these eccentricities. When the total slip was not the same on the north and south side of the specimen, the consequent strain was larger on the higher side. The variance in slip between the two sides was likely due to small variations of the bolts in the bolt holes during fabrication. Although 11 specimens experienced shear failure on the south side compared to 2 specimens on the north side (3 specimens did not fail in shear), the data does not show a clear bias that the south side was consistently loaded unevenly as compared to the north side, and thus this can constitute an unusual but not inappropriate randomness in the results. As part of the evaluation of eccentricities, this

appendix documents biases seen in the gages attached to the top column and bottom column. However, these gages in particular were only each 2 inches away from the loading surfaces on the top and bottom of the specimen and were thus subjected to boundary condition effects that likely make their results not indicative of the overall force distributions seen in the specimens. The strains seen in the gap region of the splice plate are typically more uniform and more indicative of the force flow through the connection.

Prior to slip, the load is transferred into the splice plates by friction. The data shows that the load is gradually introduced into the splice plates from the top to the middle of the plate. After slip the load is transferred by friction and the bolts bearing on the splice plate, the load distribution through the splice plate remains relatively uniform. The strain gage data provides little evidence that development of the filler plate significantly influences the introduction of force into the splice plate before or after slip. However, as documented in the main report, the added clamping force and bolt strength of the development bolts does affect the slip and shear strength of the specimens.

Table B.3 lists bolts that failed prior to the ultimate strength of the specimen. All bolt failures were through the threads, indicating a likely tension failure in the bolt. The majority of these bolt failures were during slip, likely due to the pretension combined with additional tension from catenary action caused by the bolt deformation. The remaining bolt failures were at the bolt shear strength failure load.

In the plots shown, a positive displacement is oriented downwards. A positive load or strain value is compressive.

**Table B.1 – UIUC specimen test matrix**

<b>UIUC Specimen Name</b>	<b>Experiment Objective</b>	<b>Upper Column</b>	<b># Rows of Bolts Connecting Filler to Smaller Column</b>	<b>Location of Control Bolts</b>
730-std	No fillers TN standard holes (all others oversized)	W14x730	0 rows	South
730-over	No fillers TN	W14x730	0 rows	South
159f	3 3/4 in. fillers TN Full development	W14x159	4 rows	North
159h	3 3/4 in. fillers TN Half development	W14x159	2 rows	North
159n1	3 3/4 in. fillers TN No development #1	W14x159	0 rows	South
159n2	3 3/4 in. fillers TN No development #2	W14x159	0 rows	South
455f	1 5/8 in. fillers TN Full development	W14x455	2 rows	South
455h	1 5/8 in. fillers TN Half development	W14x455	1 row	South
455n1	1 5/8 in. fillers TN No development #1	W14x455	0 rows	South
455n2	1 5/8 in. fillers TN No development #2	W14x455	0 rows	South
159n-2ply1	3 3/4 in. fillers TN Using 3 1/2 in. and 1/4 in. fill No development #1	W14x159	0 rows	South
159n-2ply2	3 3/4 in. fillers TN Using 3 1/2 in. and 1/4 in. fill No development #2	W14x159	0 rows	South
159h-TC	3 3/4 in. fillers TC Half development	W14x159	2 rows	N/A
159n-TC	3 3/4 in. fillers TC No development	W14x159	0 rows	N/A
159f-weld	3 3/4 in. fillers welded Full development	W14x159	16 in. of 1/2” fillet weld per edge of filler	South
159h-weld	3 3/4 in. fillers welded Half development	W14x159	13 in. of 5/16” fillet weld per edge of filler	South

**Table B.2 – Retorqued control bolts**

<b>Specimen</b>	<b>Bolt</b>	<b>Initial Elongation (in)<sup>a</sup></b>
159h	NW1	0.048
159n1	SW6	0.031
	SE1	0.042
159n2	SW6	0.036
455h	SE1	0.045
455n1	SW6	0.039
159n-2ply1	SW6	0.038
	SW3	0.015
	SE1	0.045
159n-2ply2	SW6	0.010
159h-weld	SW6	0.046
	SW3	0.023
	SE1	0.057

<sup>a</sup> The target elongation to reach the plateau of the torque-elongation curve was 0.05 in. for both 9 in. and 7 in. bolts; these bolts and their neighboring bolts were all retorqued to achieve the target elongation.

**Table B.3 – Premature bolt failures**

Specimen	Bolt	Load (kips)	Bolt shank remained in specimen?	Comments
<b>730-std</b>	-			
<b>730-over</b>	SW6	1,634	N	Failed during slip
<b>159f</b>	-			
<b>159h</b>	-			
<b>159n1</b>	SE1	1,879	N	Failed during slip
	SW2	1,879	Y	Failed during slip
	SW5	1,879	N	Failed during slip
	SE5	1,930	Y	Bolt nut observed not to be flush after slip
	NW1	2,465	Y	
	NE1	2,548	Y	Failed during shear failure of the south side
	NE3	2,548	Y	Failed during shear failure of the south side
	NW5	2,548	Y	Failed during shear failure of the south side
<b>159n2</b>	SE5	1,704	N	Failed during slip
	SW5	1,704	N	Failed during slip
<b>455f</b>	-			
<b>455h</b>	-			
<b>455n1</b>	-			
<b>455n2</b>	NE2	1,433	Y	Failed during slip
	NE3	1,433	Y	Failed during slip
	NW6	1,433	Y	Immediately upon commencing reloading after slip
<b>159n-2ply1</b>	NE5	658	Y	Failed during slip
<b>159n-2ply2</b>	SW2	1,348	Y	Failed during slip
<b>159h-TC</b>	-			
<b>159n-TC</b>	-			
<b>159f-weld</b>	-			
<b>159h-weld</b>	SW3	1,616	N	Failed during slip
	SW2	2,033	Y	Failed during slip
	SE4	2,508	Y	Failed during failure of welds
<p>Note: All bolts failed through the threads, indicating a tension failure.</p>				

## B.2 Specimen 730-std

Specimen 730-std (Figure B.1 to Figure B.21) displaced approximately linearly with applied load (Figure B.5 and Figure B.7) until the observed slip load (1,697 kips). At the slip load, the relative displacement between the splice plates and top column increased suddenly by approximately 0.1 in. over a period of approximately 4 seconds; both sides of the specimen (i.e., north and south) slipped approximately the same amount (Figure B.12). This is most clearly seen in the relative LVDTs between the top column and splice plates (Figure B.10). The maximum expected clearance in the holes based on the assembly procedure and standard holes was  $2*(1/16 \text{ inches}) = 0.125 \text{ inches}$ . During the slip event the load dropped to 1,331 kips as the machine stabilized, settling around 1,800 kips, where it was held for observation (Figure B.6).

Once loading was resumed, the stiffness was initially high, indicating the bolts began bearing (Figure B.7). As the load was increased, the stiffness began to decrease, indicating softening of the bolts and bolt hole bearing surfaces due to yielding. The twelve bolts on the south side of the specimen failed simultaneously at an observed load of 2,542 kip (Figure B.2, Figure B.3 and Figure B.4). The twelve bolts on the north side of the specimen remained intact. The load was immediately removed from the specimen upon failure.

Prior to slip, the specimen produced several noises between 700 and 800 kips. After slip, the specimen was relatively quiet, producing noises at approximately 2000, 2150 and 2300 kips. Noises believed to be produced by the testing machine were neglected. The noises are likely associated with additional small slip events, bolts coming into bearing with the bolt holes, or possibly initiation of fractures within the bolts.

Figure B.11 compares the LVDTs directly measuring relative slip between the top column and the splice plate (Figure B.10) with the difference between the average of the two LVDTs at the bottom center of the top column (Figure B.7) and the average of the two LVDTs on either splice plate at that same cross section as the LVDTs on the top column (Figure B.8). The measurements of the relative LVDTs correspond well to the difference between the corresponding absolute LVDTs.

The splice plate LVDTs (Figure B.8 and Figure B.9) showed a dynamic increase or decrease in displacement during the slip events. This may be due to a number of reasons, including stress relief in the splice plates after slip, very small slips relative to the column flanges, or small dynamic vibrations (with resulting small permanent offsets) of the LVDT holders, but the displacements are an order of magnitude smaller than the primary slip displacements (Figure B.10) and are not likely to indicate significant behavior.

The top column strain gages show that the localized introduction of load had a bias to the east side (Figure B.13), with the northeast side lightly loaded. The bottom column strain gages show that the localized reaction exhibited fairly uniform loading, with the northeast side the most heavily loaded (Figure B.17).

The splice plate strain gages below the top row of bolts also shows a small bias towards the northeast after slip (Figure B.14). The strain gages further down the splice plate, below the fourth row of bolts, indicate a stronger bias to the south after slip (Figure B.15). However, the strain gages below the first row of bolts show that the load has been relatively evenly redistributed (Figure B.16). Near ultimate shear failure, the south splice plate experienced larger strain than the north splice plate (Figure B.15 and Figure B.16). Snapshots of the specimen strain at 1000 kips, immediately prior to slip, 2000 kips and immediately prior to shear are visually presented in Figure B.18, Figure B.19, Figure B.20 and Figure B.21, respectively. These graphs show that the strain enters into the splice plate gradually and relatively uniformly from bolt row 6 to bolt row 1 throughout the experiment.

The experiment was executed in load control. The loading rate for the experiment was approximately 5 kips per second up to a load of 1200 kips. The loading rate was approximately 1 kip per second thereafter (Figure B.6). Four elastic cycles were executed prior to the test, going up to loads of 50 kips, 200 kips, 200 kips, and 400 kips, respectively, returning to zero load each time, to verify instrumentation and machine characteristics. The data collection rate for the experiment was held constant at 10 Hertz (10 sets of readings per second).



**Figure B.1 – 730-std: Before test (southeast corner)**

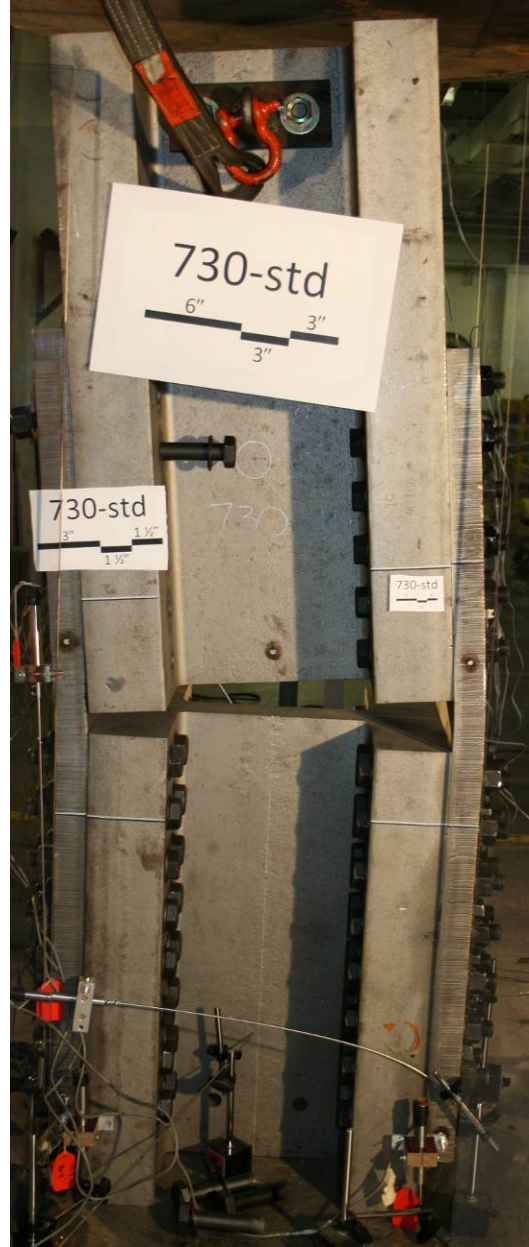


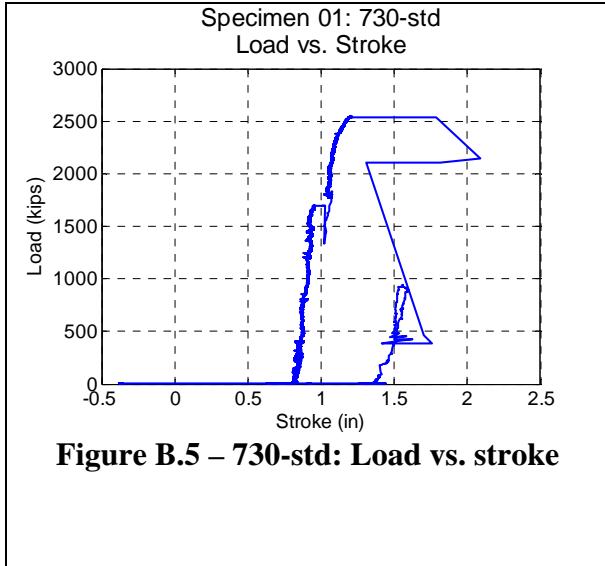
**Figure B.2 – 730-std: After test (east side)**



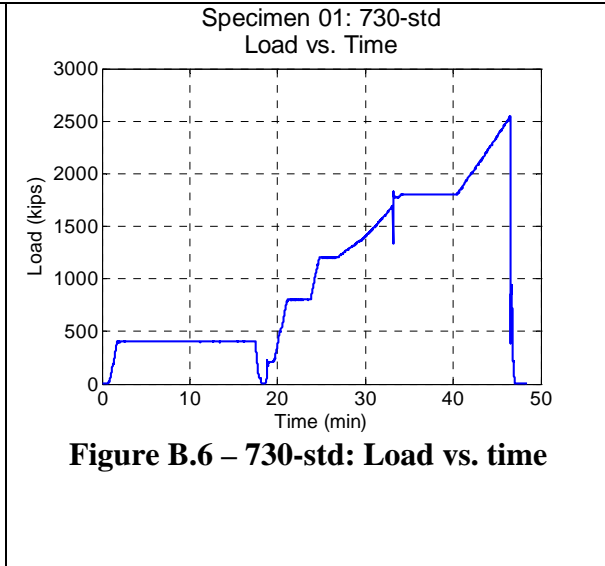
**Figure B.3 – 730-std: After test (southeast corner)**



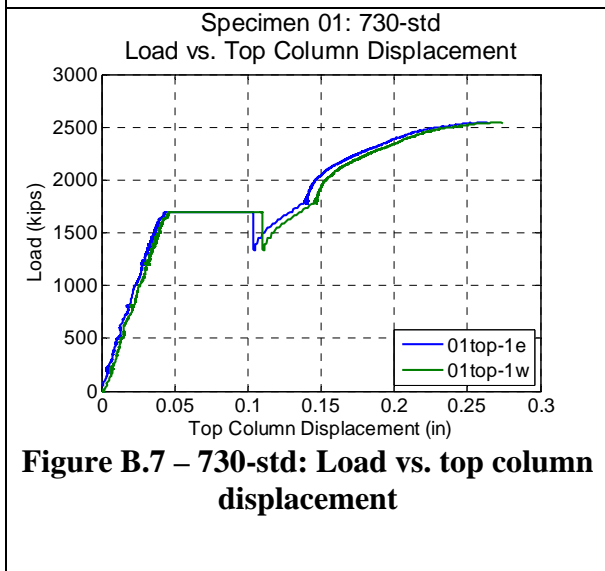
**Figure B.4 – 730-std: After test (south side)**



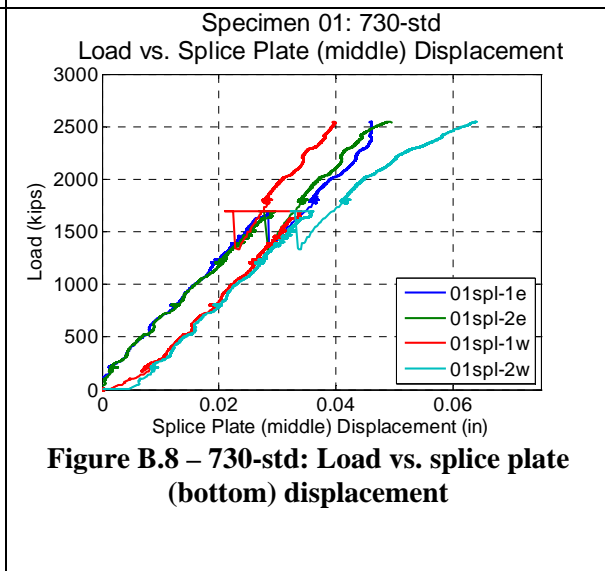
**Figure B.5 – 730-std: Load vs. stroke**



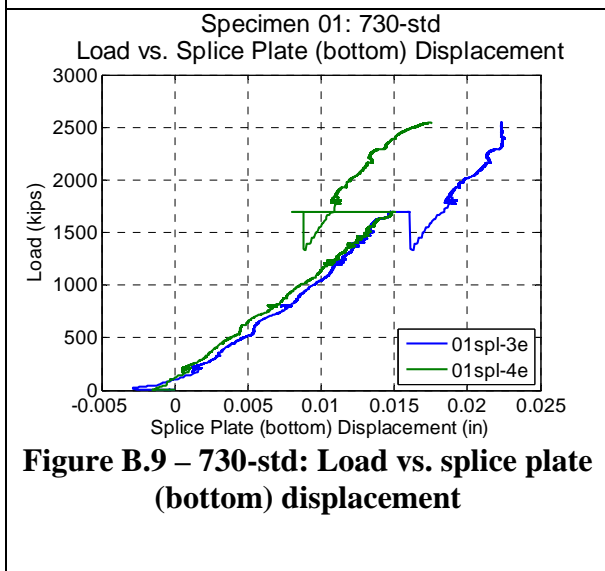
**Figure B.6 – 730-std: Load vs. time**



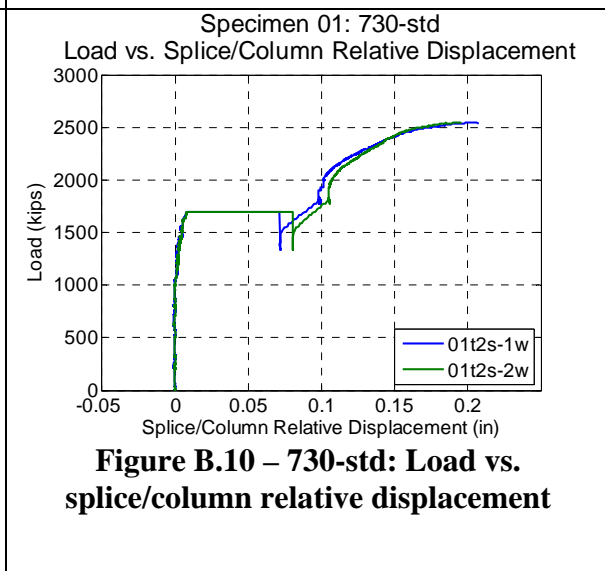
**Figure B.7 – 730-std: Load vs. top column displacement**



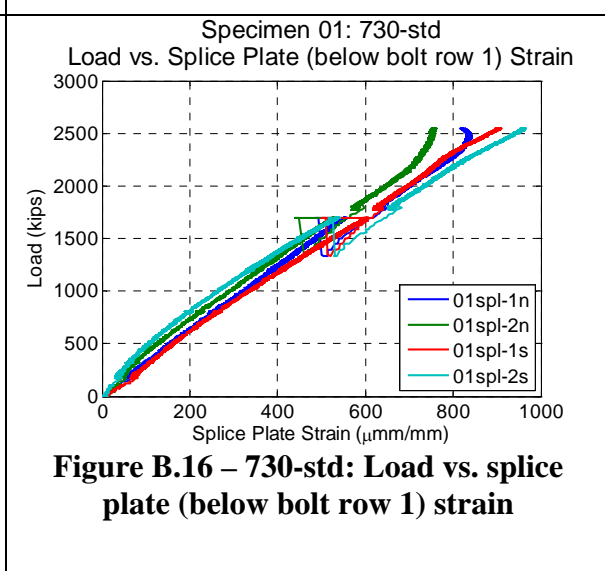
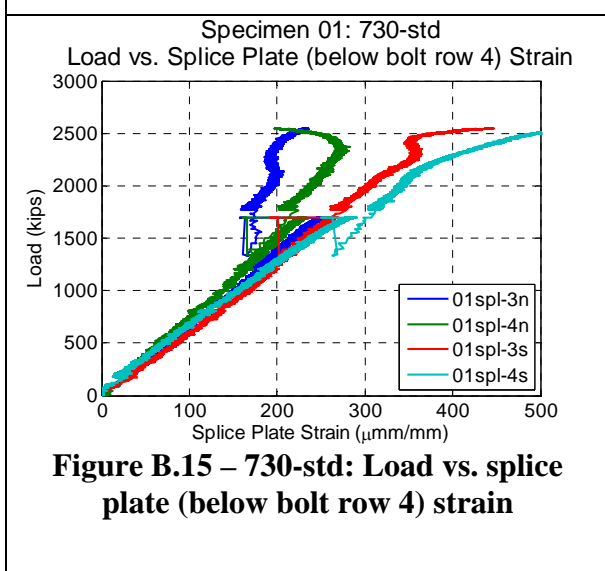
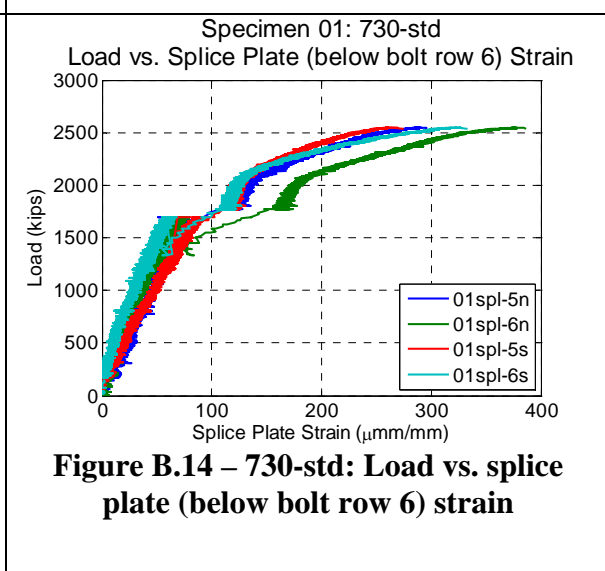
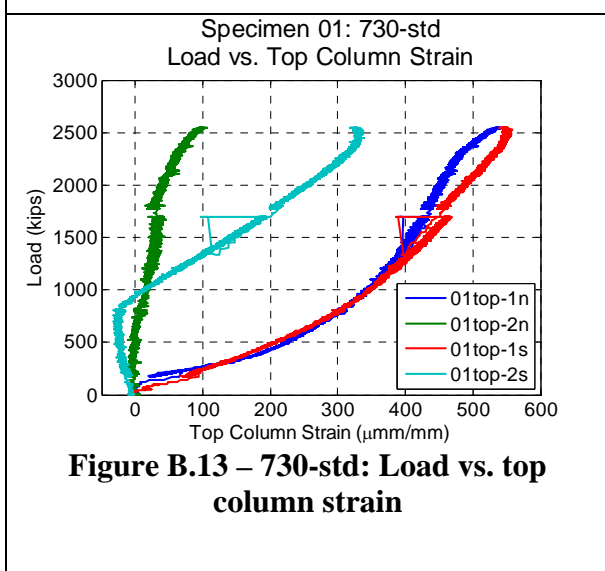
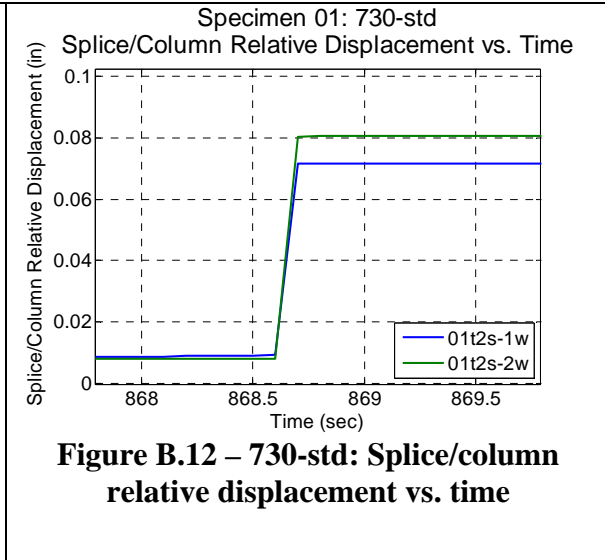
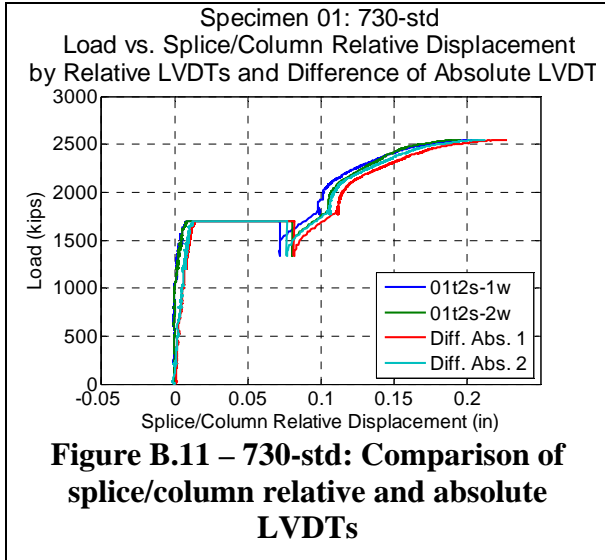
**Figure B.8 – 730-std: Load vs. splice plate (bottom) displacement**

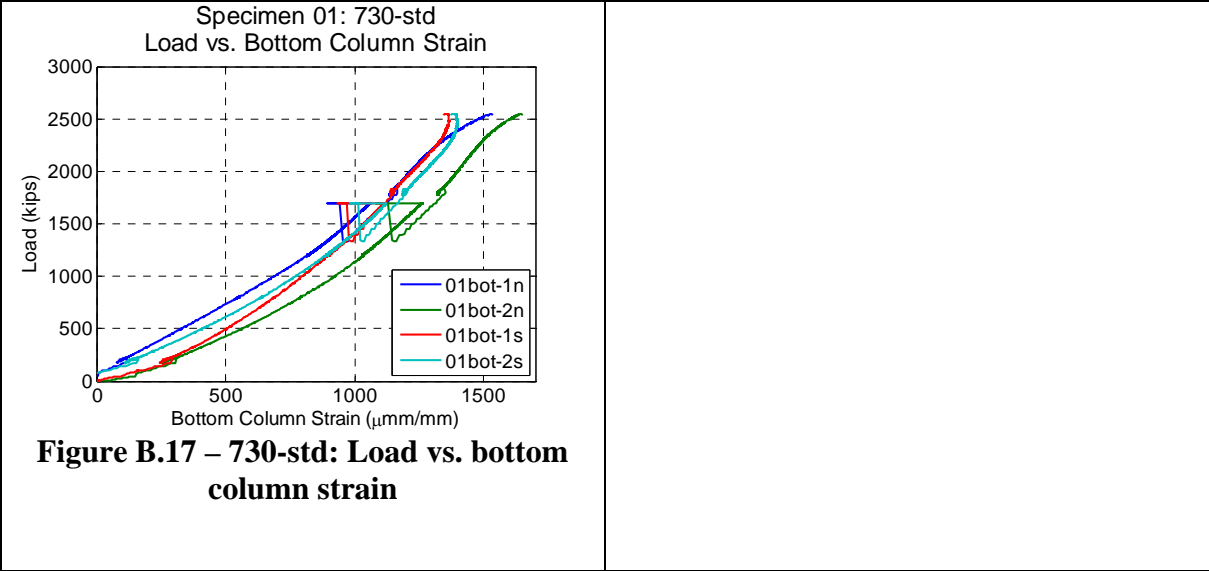


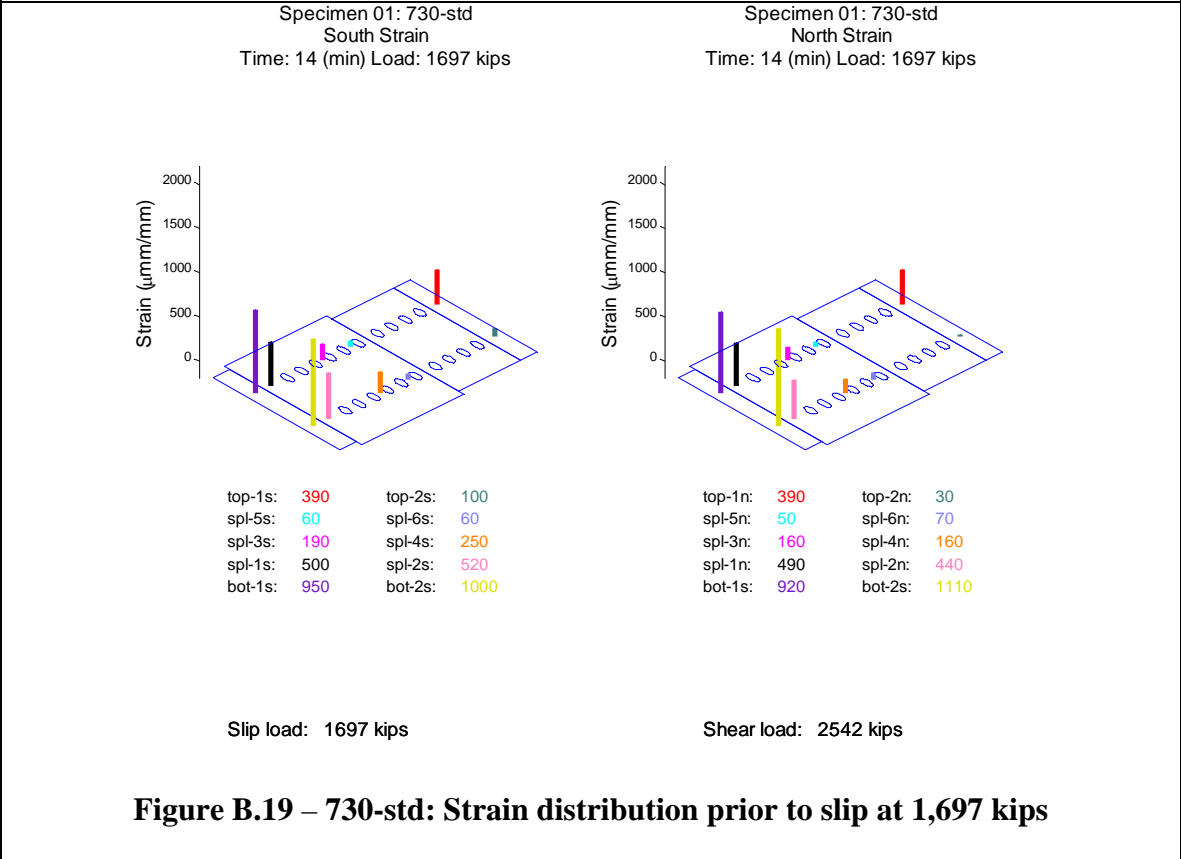
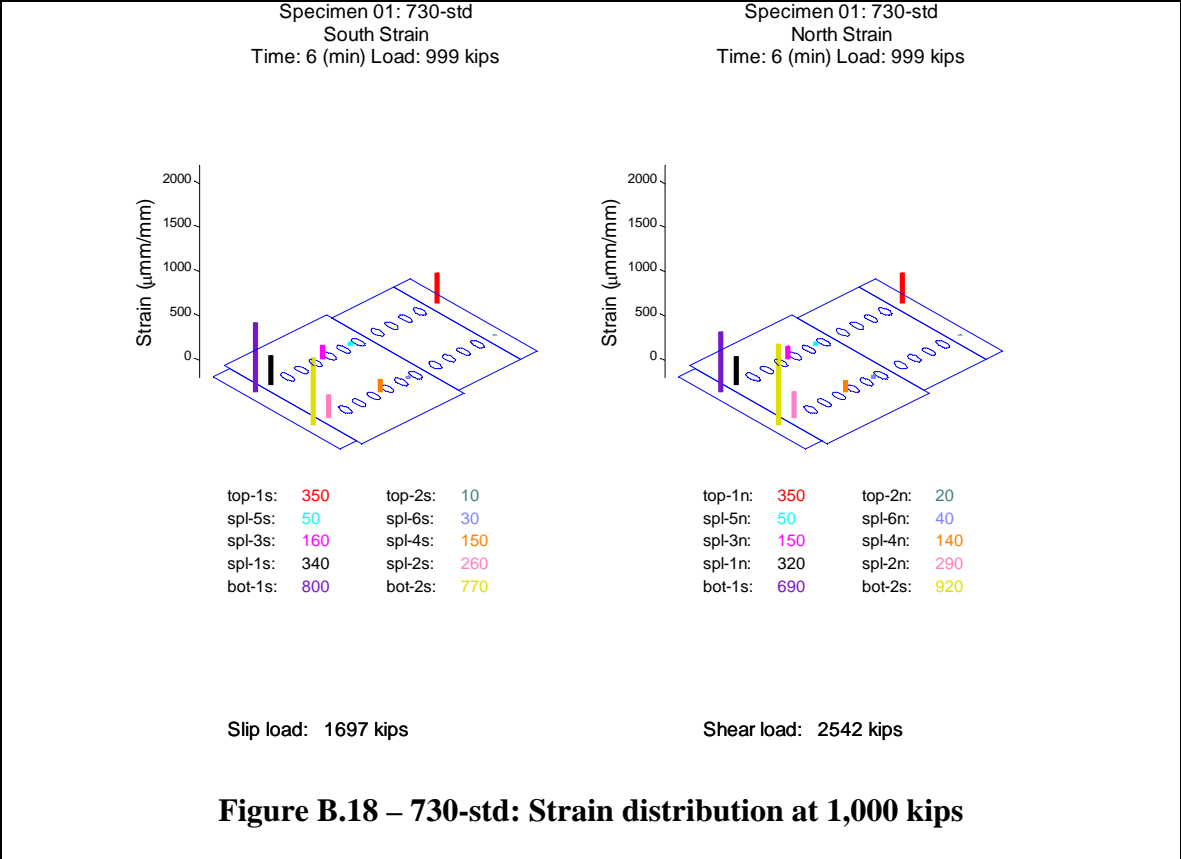
**Figure B.9 – 730-std: Load vs. splice plate (bottom) displacement**

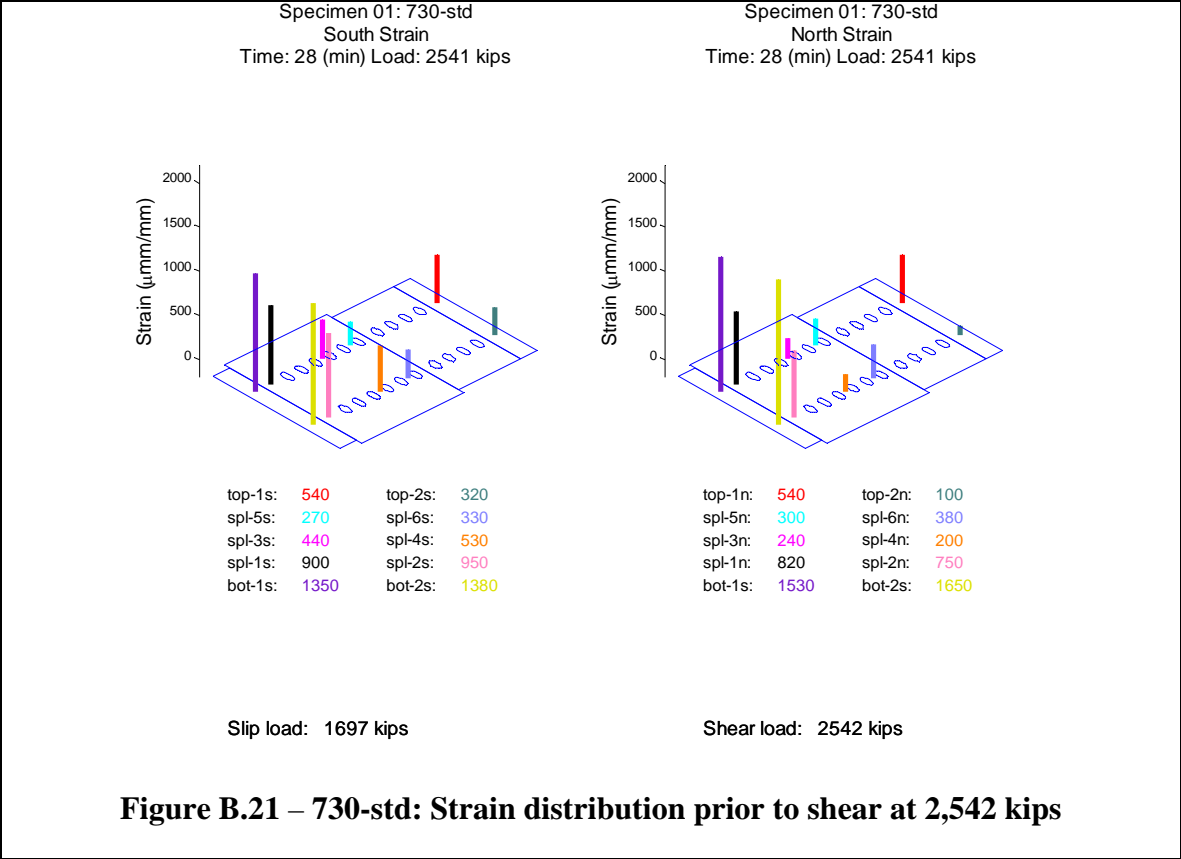
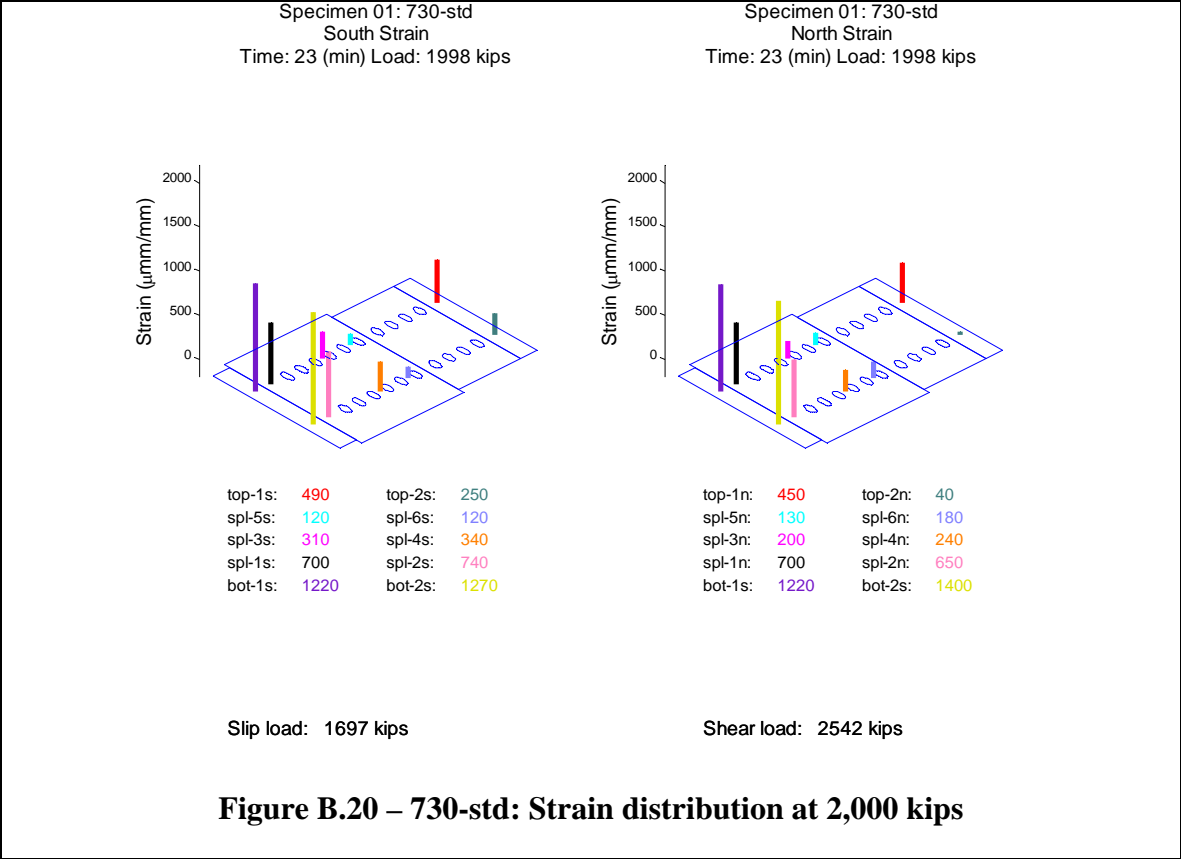


**Figure B.10 – 730-std: Load vs. splice/column relative displacement**









## B.3 Specimen 730-over

Specimen 730-over (Figure B.22 to Figure B.44) displaced approximately linearly with applied load (Figure B.28 and Figure B.30) until the observed slip load (1,634 kips). At the slip load, the relative displacement between the splice plates and the top column increased suddenly by approximately 0.57 inches over a period of approximately 20 seconds (Figure B.35) (as compared to 0.09 in. for a similar event for 730-std). This is most clearly seen in the relative LVDTs between the top column and splice plates (Figure B.33) and the movement of the top column (Figure B.30). The maximum expected clearance in the holes based on the assembly procedure and standard holes was  $2 \times (5/16 \text{ inches}) = 0.625 \text{ in.}$  During this dynamic event, the load dropped immediately to 665 kips and then increased to approximately 1,300 kips (reaching 1475 kips briefly first), where the load was held for observation of the specimen (Figure B.29). It is also likely that the bolts slipped into bearing during this slip event, as no appreciable change in stiffness occurred in the initial phases of loading after testing was resumed.

As the load was recovering from 665 kips to 1,475 kips the west top bolt on the south splice plate (bolt SW6) failed through the threads at 1,048 kips (Figure B.27, typical of all premature bolt failures), indicating a tension failure. The failure occurred as the machine was stabilizing, at a load of 1,048 kips. The bolt was a control bolt, elongated during assembly by 0.081 inches. It was not retorqued after the initial tightening. The failed bolt contacted the west top column LVDT (02top-1w) as seen in the jolt in displacement in Figure B.30, further data collection was unaffected. It also removed the southwest splice strain gage (02spl-5s) below the top row of bolts (bolt row 6), rendering it useless for the rest of the test (Figure B.37).

Once loading was resumed, the stiffness was approximately linear (Figure B.30), but lower than prior to slip, indicating elastic deformation of the bolts and bearing surfaces of the bolt holes. Further loading reveals periods of near zero stiffness in Figure B.30 and Figure B.33. As discussed below, noises heard at 2198 kips could possibly be associated with some of these events. These changes in stiffness could be associated with yielding of the bolts, bearing of the bolts with the bolt holes, or possibly initiation of fractures within the bolts. The remaining 11 bolts on the south side of the specimen failed simultaneously at an observed bolt shear load (2,459 kips) (Figure B.23, Figure B.24 and Figure B.25). The failure on the south side can be attributed to the fewer number of intact bolts. The bolts on the north side of the specimen remained intact. The load was immediately removed from the specimen upon failure.

After slip, the specimen produced pinging noises at the following loads; 1482, 1504, 1525, 1560, 1604, 1615, 1640, 1658, 1684, 1695, 1740, 1774, 1805, 1814, 1840, 1855, 1880, 1899, 1960, 2003 and 2198 kips. Noises believed to be produced by the testing machine were neglected. The noises are likely associated with additional small slip events, bolts coming into bearing with the bolt holes, or possibly initiation of fractures within the bolts.

Figure B.34 compares the LVDTs directly measuring relative slip between the top column and the splice plate (Figure B.33) with the difference between the average of the

two LVDTs at the bottom center of the top column (Figure B.30) and the average of the two LVDTs on either splice plate at that same cross section as the LVDTs on the top column (Figure B.31). The measurements of the relative LVDTs correspond well to the difference between the corresponding absolute LVDTs.

The splice plate LVDTs (Figure B.31 and Figure B.32) showed a dynamic increase or decrease in displacement during the slip event at 1634 kips. This may be due to a number of reasons, including stress relief in the splice plates after slip, very small slips relative to the column flanges, or small dynamic vibrations (with resulting small permanent offsets) of the LVDT holders, but the displacements are an order of magnitude smaller than the primary slip displacements (Figure B.33) and are not likely to indicate significant behavior.

The top column strain gages show that the localized introduction of load had a significant bias towards the west side of the specimen (Figure B.36). Through the duration of the test, the northeast corner of the top column was negligibly loaded. The southeast corner of the top column was not loaded until approximately 700 kips, and remained lower than both of the west gages. The bottom column strain gages show that the localized reaction exhibited a bias towards the east side of the specimen, with the northeast side the heaviest loaded (Figure B.40).

However, prior to slip, the splice plates are not significantly biased. The premature failure of the bolt causes the remaining south strain gage to detect decreasing strain with increasing load (Figure B.37). Bolt row 4 introduced more load into the splice plate on the south side compared to the north side (Figure B.38). However, the strain gages below bolt row 1 seem unaffected by the premature failure of the bolt, and they show a bias more towards the east side of the specimen (Figure B.39), most likely due to standard connection eccentricities due to the loading. Snapshots of the specimen strain at 1000 kips, immediately prior to slip, 2000 kips and immediately prior to shear are visually presented in Figure B.41, Figure B.42, Figure B.43 and Figure B.44, respectively. These graphs show that the strain enters into the splice plate gradually and relatively uniformly from bolt row 6 to bolt row 1 throughout the experiment.

The experiment was executed in load control. The loading rate for the experiment was approximately 1 kip per second. One elastic cycle was executed prior to the test, going up to a load of 200 kips and returning to zero load, to verify instrumentation. The data collection rate for the experiment was held constant at 10 Hertz (10 sets of readings per second).

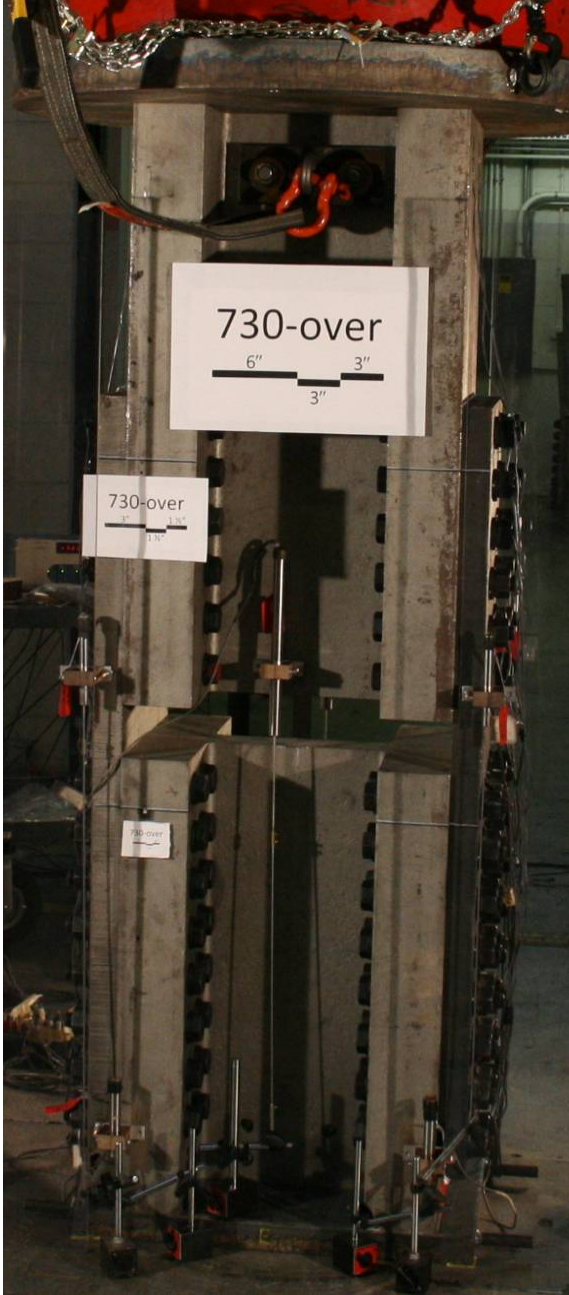


Figure B.22 – 730-over: Before test (east side)



Figure B.23 – 730-over: After test (east side)

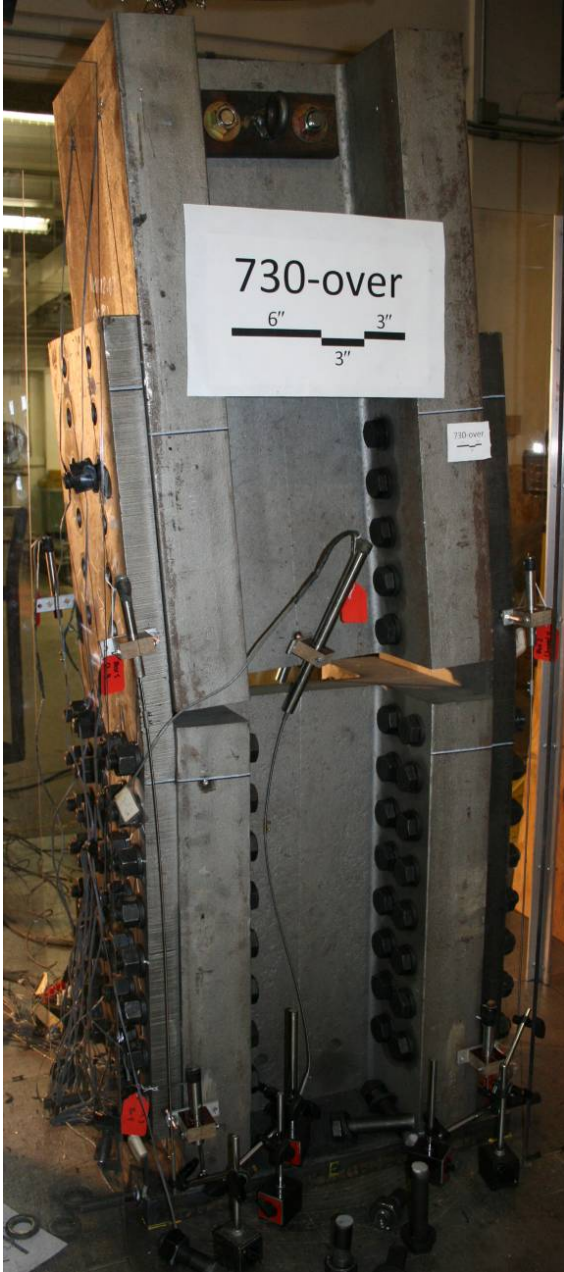


Figure B.24 – 730-over: After test (east side)

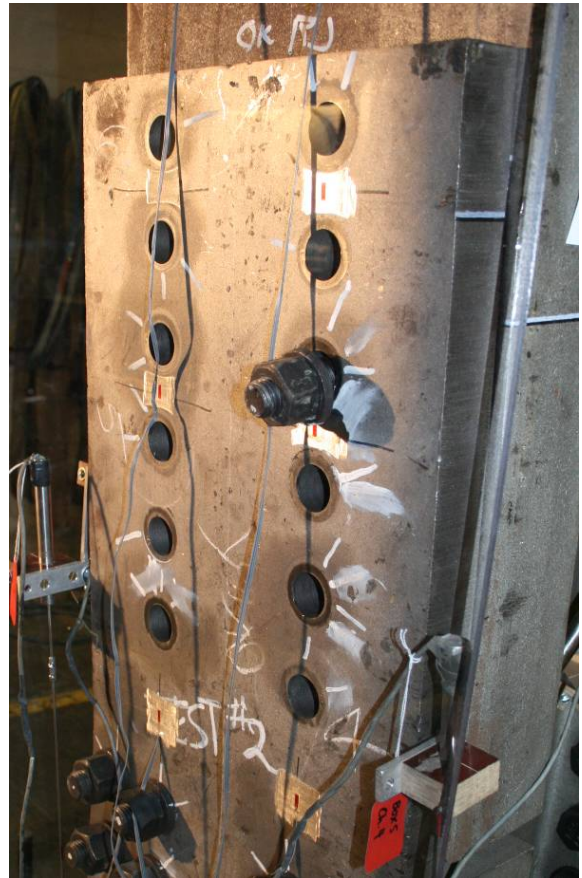


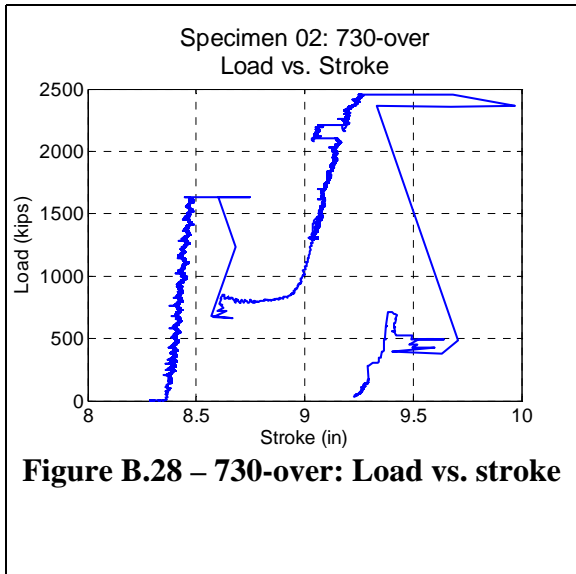
Figure B.25 – 730-over: After test (south side)



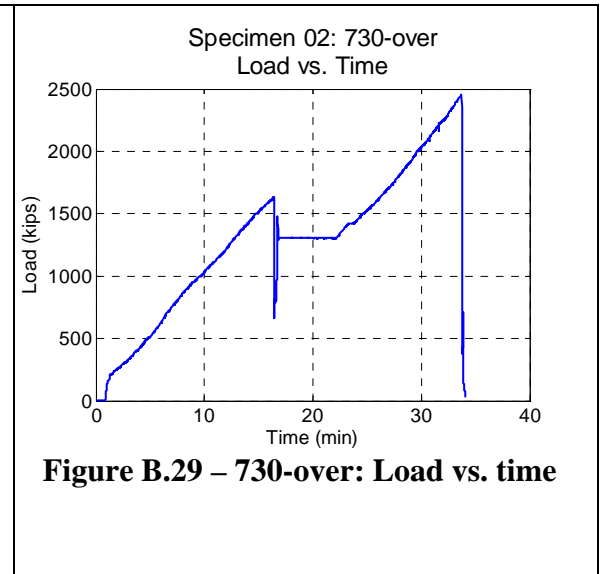
**Figure B.26 – 730-over: Early bolt failure (south side)**



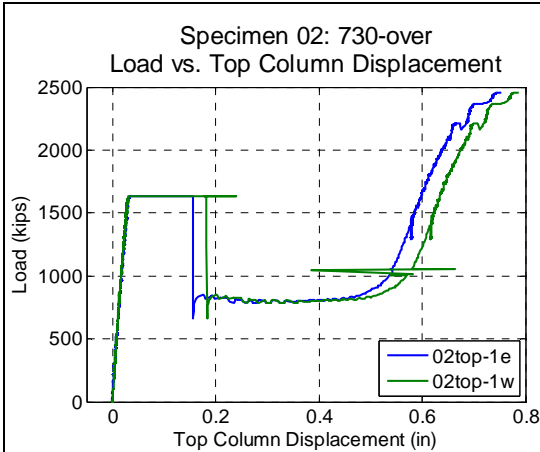
**Figure B.27 – 730-over: Early Bolt Failure**



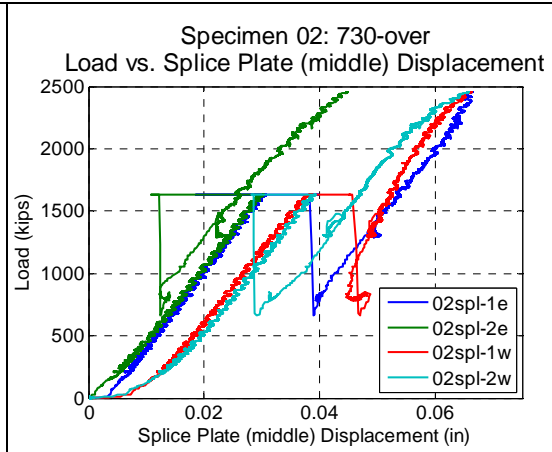
**Figure B.28 – 730-over: Load vs. stroke**



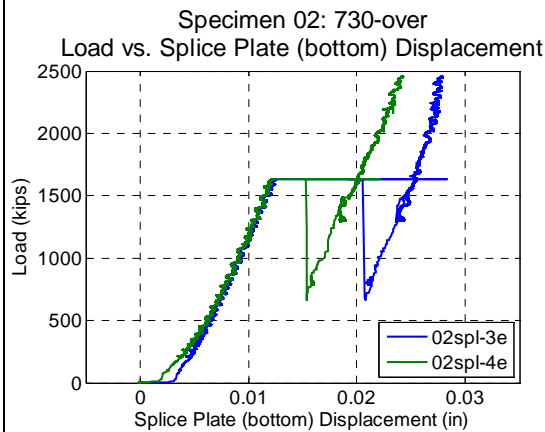
**Figure B.29 – 730-over: Load vs. time**



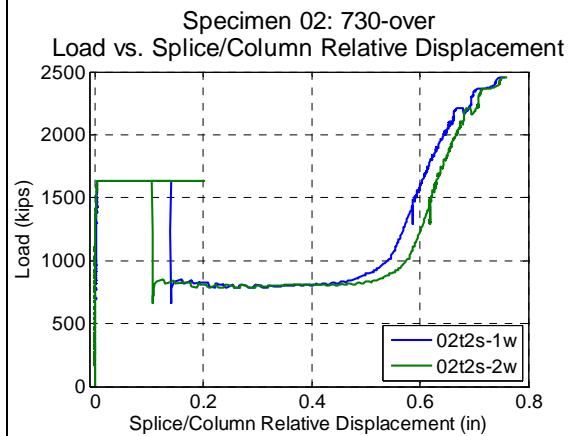
**Figure B.30 – 730-over: Load vs. top column displacement**



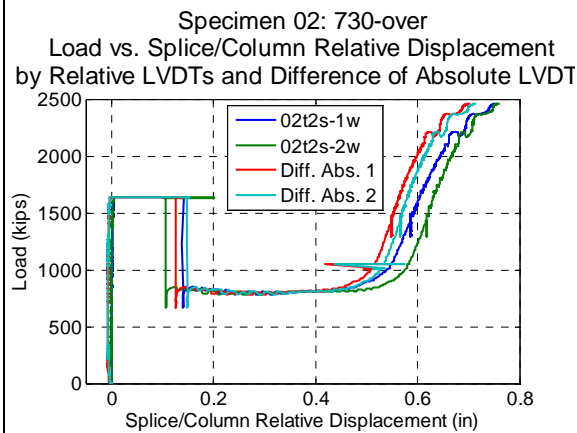
**Figure B.31 – 730-over: Load vs. splice plate (middle) displacement**



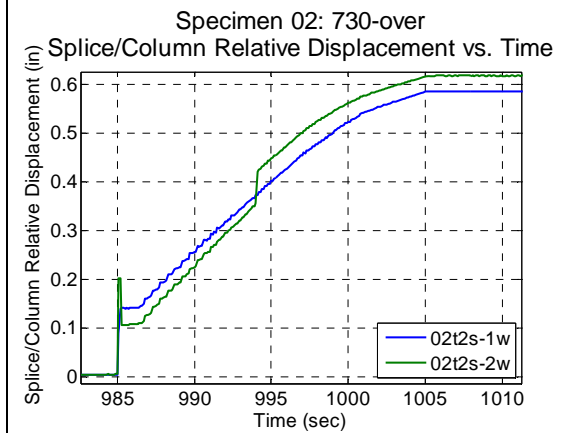
**Figure B.32 – 730-over: Load vs. splice plate (bottom) displacement**



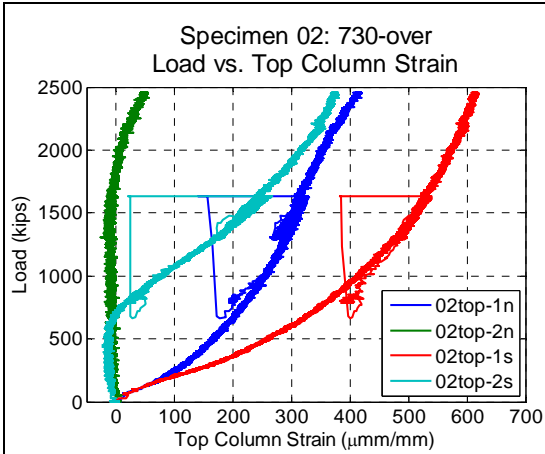
**Figure B.33 – 730-over: Load vs. splice/column relative displacement**



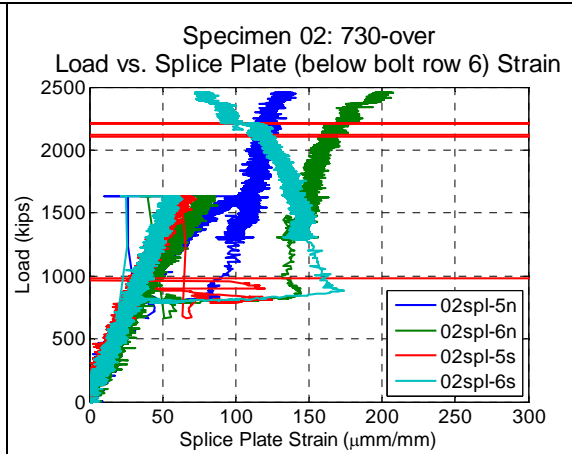
**Figure B.34 – 730-over: Comparison of splice/column relative and absolute LVDTs**



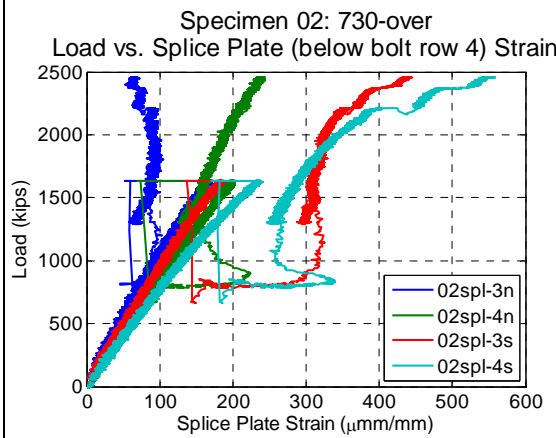
**Figure B.35 – 730-over: Splice/column relative displacement vs. time**



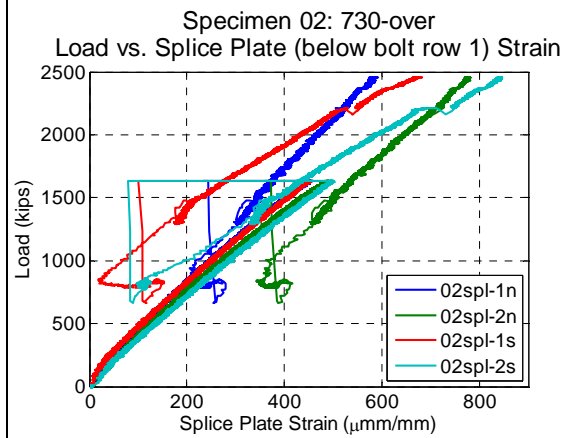
**Figure B.36 – 730-over: Load vs. top column strain**



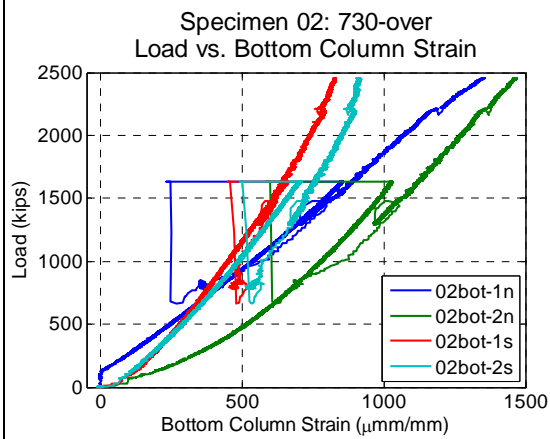
**Figure B.37 – 730-over: Load vs. splice plate (below bolt row 6) strain**



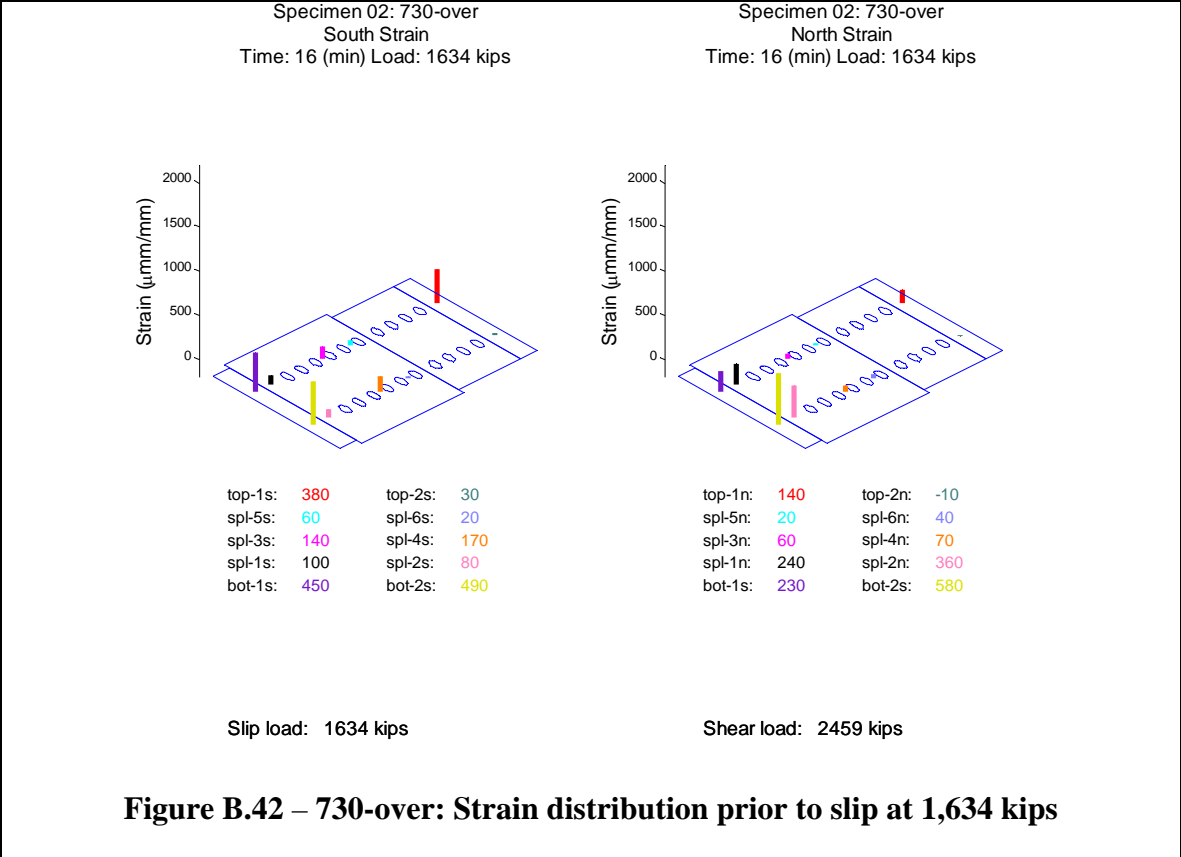
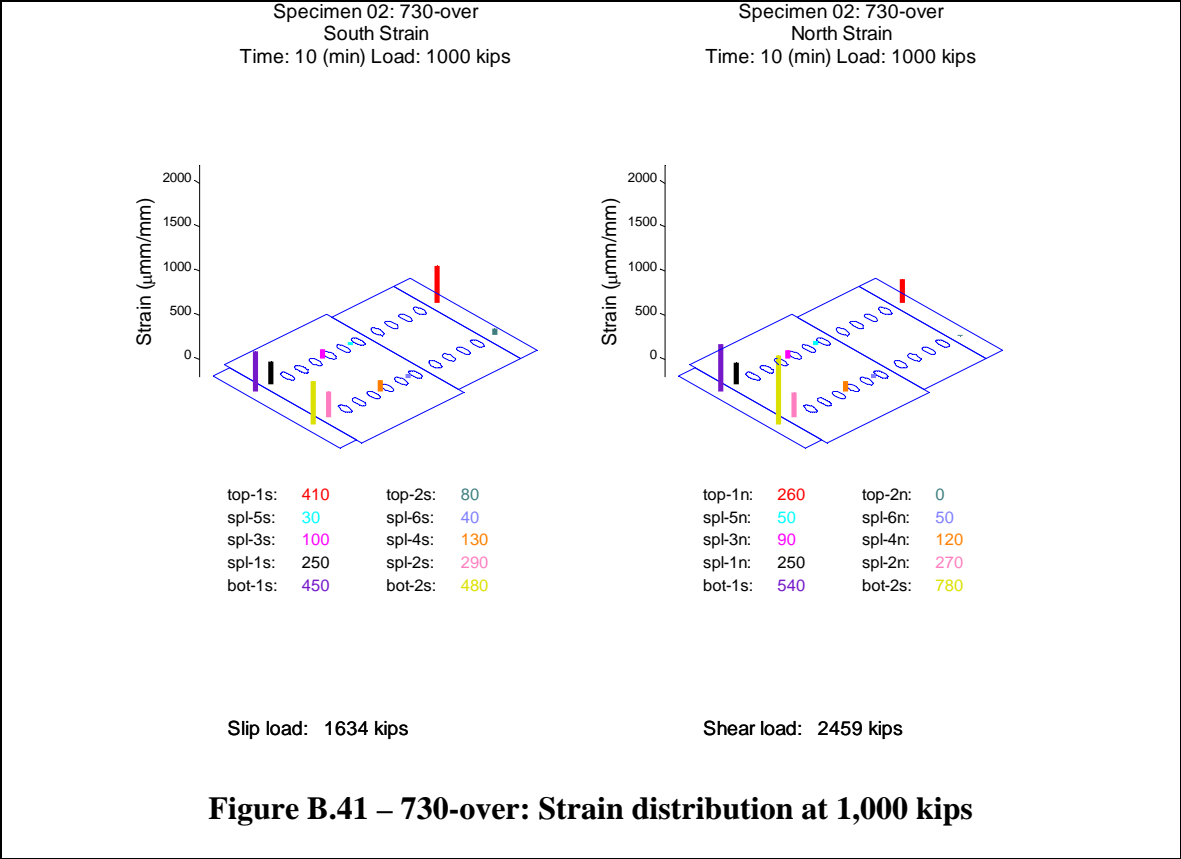
**Figure B.38 – 730-over: Load vs. splice plate (below bolt row 4) strain**

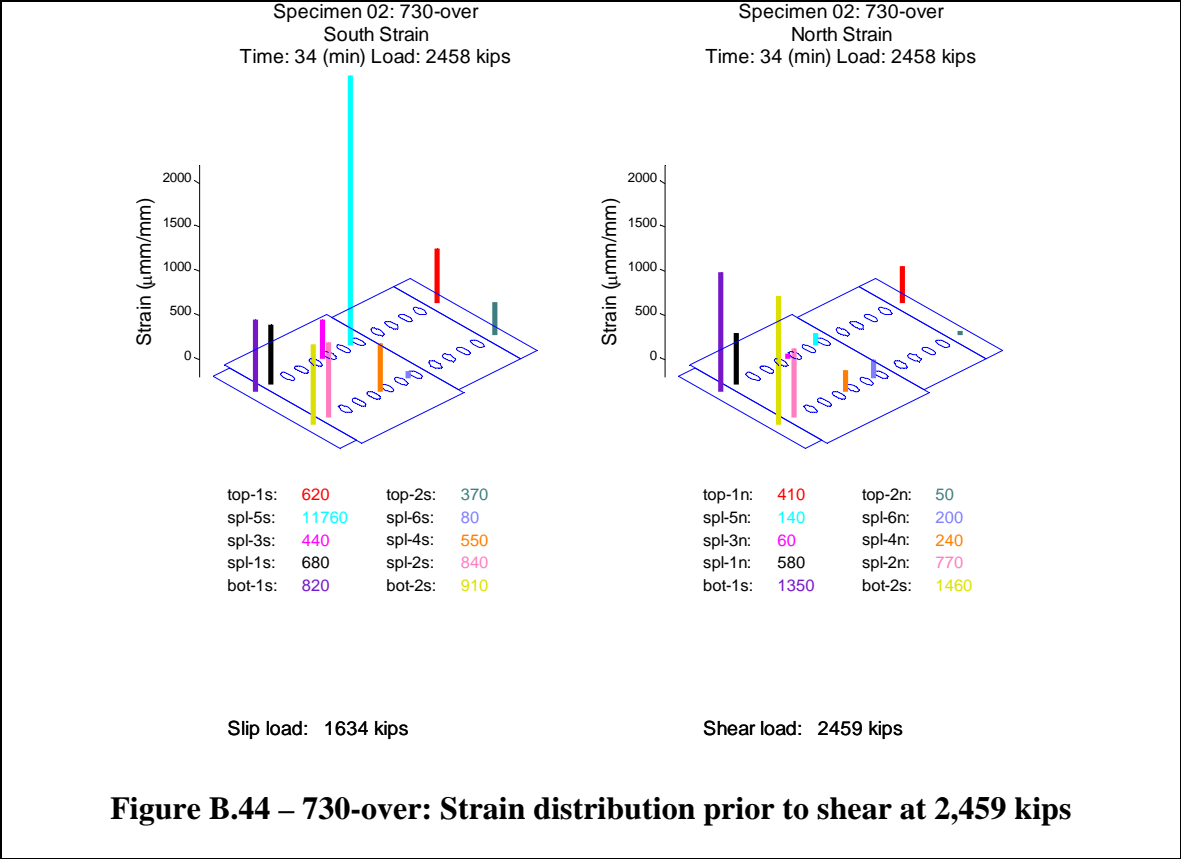
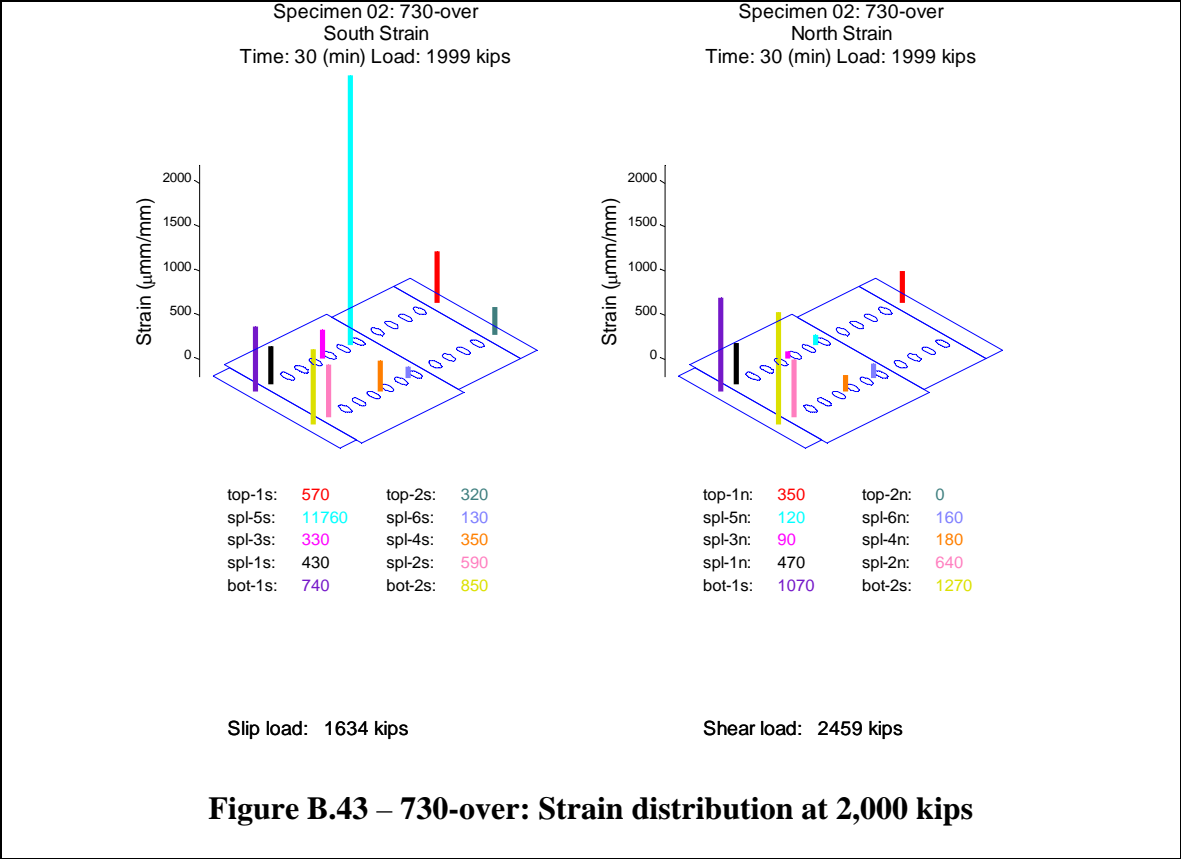


**Figure B.39 – 730-over: Load vs. splice plate (below bolt row 1) strain**



**Figure B.40 – 730-over: Load vs. bottom column strain**





## B.4 Specimen 159f

The response of specimen 159f (Figure B.45) was approximately linear (Figure B.50) until the observed slip load (1,224 kips). At the observed slip load the relative displacement between the splice plate and the filler plate increased suddenly by approximately 0.39 inches and 0.45 inches over a period of 13 seconds on the north and south sides of the specimen, respectively (Figure B.57 and Figure B.61). During this dynamic event, the load dropped immediately to 485 kips and increased to approximately 1,074 kips (reaching 1212 kips briefly first), where the load was held for observation of the specimen (Figure B.51). A second major slip event was recorded at a load of 2,423 kips. At the observed slip load the relative displacement between the filler plate and the top column increased suddenly by approximately 0.31 in. over a period of approximately 6 seconds, with the two sides (i.e., both column flanges) slipping approximately the same amount. This is seen most clearly in Figure B.56 and Figure B.60. During this dynamic event, the load dropped immediately to 1506 kips and increased to 1732 kips (reaching 1753 kips briefly first), where the load was held for observation. During subsequent loading, slip continued for approximately 0.2 in. (Figure B.56) before the bolts likely slipped into bearing on the top column, as the increase in stiffness in Figure B.56 shows at approximately a load of 2000 kips and a relative slip of 0.5 inches. The maximum expected clearance in the holes based on the assembly was nominally  $2 * (5/16 \text{ inches}) = 0.625 \text{ inches}$ . The relative slip between each surface is summarized in Table B.4.

**Table B.4 – 159f: Relative slip**

<b>Location</b>	<b>North</b>	<b>South</b>
<b>Between Splice and Filler</b>	0.46 in	0.50 in
<b>Between Filler and Top Column</b>	0.30 in	0.34 in
<b>Sum</b>	0.76 in	0.84 in

After each slip event, the bolts slipped into bearing and began deforming elastically (Figure B.57 and Figure B.56), demonstrated by the approximately linear stiffness. The top column began to yield at approximately 2,400 kips (Figure B.62). The bolts then began to yield, causing a decrease in stiffness. By the end of the test there was slight local buckling seen in the flanges of the top column.

Upon further loading, the bolts, now experiencing shear, yielded and eventually failed at the observed bolt shear load (2,644 kips) (Figure B.45 through Figure B.49). The twelve bolts through the splice plate on the south side of the specimen failed simultaneously, leaving the twelve bolts through the splice plate on the north side of the specimen intact. Once the twelve bolts on the south flange failed, the relative movement of the splice plate to the filler plate caused the failure of two additional bolts through the filler plate (Figure B.48 and Figure B.49).

After slip, the specimen produced pinging noises at the following loads; 1358, 1513, 1592 1670, 1774, 1907, 2096, 2421 (slip between top column and filler plates), 1775, 1788, 1806, 1857, 1903, 1994, 2050, 2070, 2090, 2153, 2253, 2274, 2292, 2303, 2320, 2360, 2370, 2390, 2542, 2567, 2613 and 2642 kips. Noises believed to be produced by the testing machine were neglected. The noises are likely associated with additional small slip events, bolts coming into bearing with the bolt holes, or possibly initiation of fractures within the bolts.

The LVDT measuring the absolute displacement of the north side filler plate (03fil-2e) was improperly set and the measurement went out of range early in the test. The initial measurements are valid and are shown in Figure B.53, Figure B.58 and Figure B.59. The east strain gage on the south splice plate under bolt row 4 (03spl-4s) also failed after slip (Figure B.64). Near the end of the test the middle strain gage on the south side of the filler plate (03fil-7s) failed (Figure B.69). Data for these gages and LVDT are valid prior to failure.

The splice plate LVDTs showed a dynamic increase or decrease in displacement during the slip events. This may be due to a number of reasons, including stress relief in the splice plates after slip, very small slips relative to the column flanges, or small dynamic vibrations (with resulting small permanent offsets) of the LVDT holders, but the displacements are an order of magnitude smaller than the primary slip displacements (Figure B.57 and Figure B.56) and are not likely to indicate significant behavior.

Figure B.58 and Figure B.59 compare the LVDTs directly measuring relative slip between the filler plate and either the top column (Figure B.56) or the splice plate (Figure B.57) with the difference between the average of the two LVDTs on either filler plate at that same cross section as the LVDTs on the top column (Figure B.53) and either the average of the two LVDTs at the bottom center of the top column (Figure B.52) or the average of the two LVDTs on either splice plate at that same cross section as the LVDTs on the top column (Figure B.54). The measurements of the relative LVDTs correspond well to the difference between the corresponding absolute LVDTs.

For this specimen, strain gages were attached to the inside face of the splice plate in the gap between the top and bottom columns. These measurements (Figure B.66), when compared to the measurements from the outside face of the splice plate (Figure B.65), indicate significant bending in the splice plates. Yielding was recorded on the inside of the splice plate on the north side.

The top column strain gages show that the localized introduction of load was reasonably uniform throughout the duration of the test (Figure B.62). The bottom strain gages also exhibited relatively uniform distribution, with a small bias to the north side (Figure B.67).

Prior to the initial observed slip, the splice plate was also uniformly loaded (Figure B.63, through Figure B.66). After slip, the specimen rotated towards the south side, introducing eccentricities into the splice plates. The rotation causes increased bending in the north splice plate, indicated by the sudden drop in strain, in certain cases into tension, on the outside of the north splice plate (Figure B.63, Figure B.64, and Figure B.65). The

inside of the north splice plate exhibits an increase in compression (Figure B.66). The bending in the north splice plate continues increasing as the specimen was loaded (Figure B.66). The south splice plate undergoes minimal bending (Figure B.66). Snapshots of the specimen strain at 1000 kips, immediately prior to slip, 2000 kips and immediately prior to shear are visually presented in Figure B.70, Figure B.72, Figure B.73 and Figure B.74, respectively. These graphs show that the strain enters into the filler plate (Figure B.68, Figure B.69 and Figure B.70) and then into the splice plate gradually and relatively uniformly from bolt row 6 to bolt row 1 throughout the experiment. After slip, the north splice plate shows some increased strain in the west gages relative to the east gages, and the bias of the south gages relative to the north may be seen, as described above.

The induced north-south eccentricities cause the south splice plate to be more heavily loaded (Figure B.63, Figure B.64 and Figure B.65), likely causing the failure of the bolts through the splice plate on the south side. The uneven slip between the filler plates and splice plate was likely due to uneven assembly. The bolts on the north side may also have not been able to be placed into full reverse bearing during assembly.

The experiment was executed in load control. The loading rate for the experiment was approximately 1 kip per second. One elastic cycle was executed prior to the test, going up to a load of 200 kips and returning to zero load, to verify instrumentation. The data collection rate for the experiment was held constant at 10 Hertz (10 sets of readings per second).

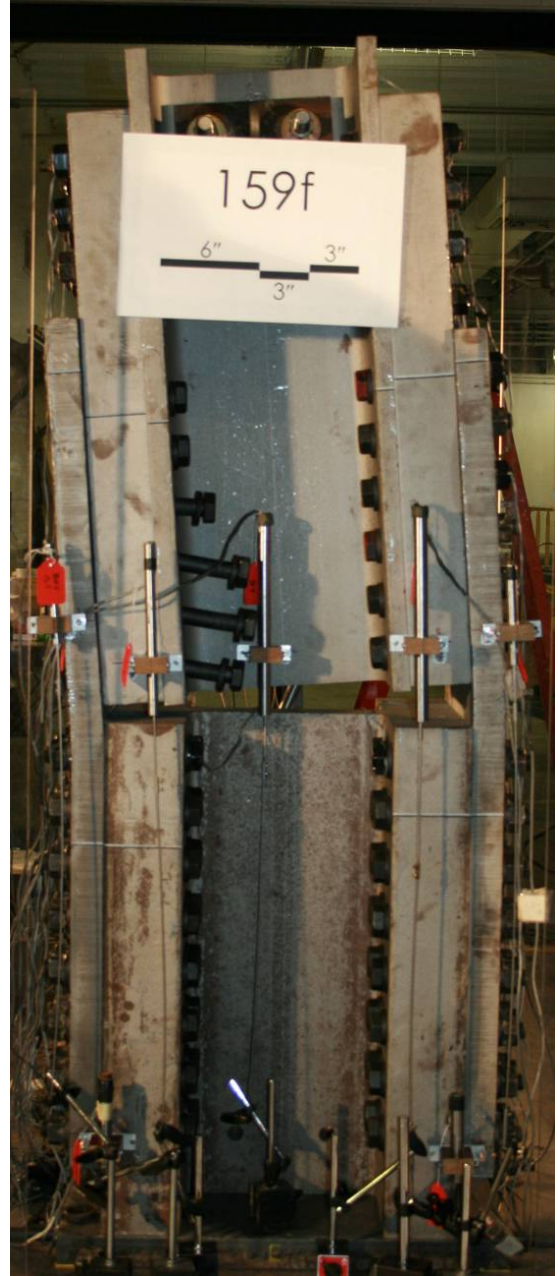


**Figure B.45 – 159f: Before test (east side)    Figure B.46 – 159f: After test (east side)**



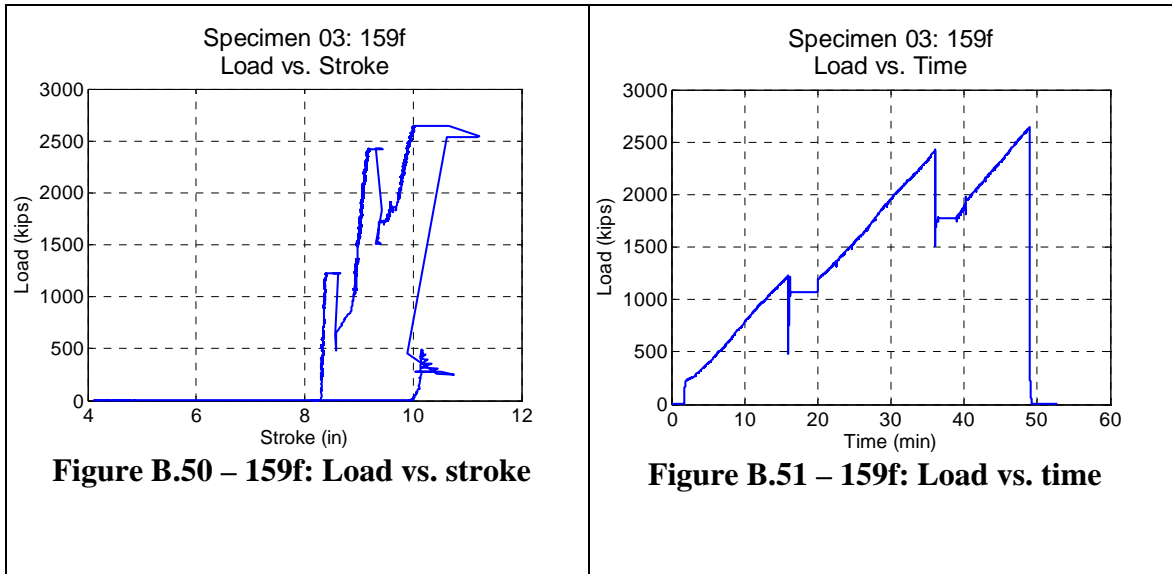
Figure B.47 – 159f: After test (east side)

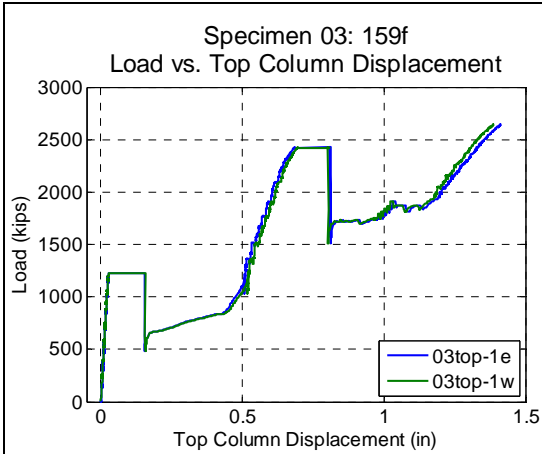


Figure B.48 – 159f: After test (south side)

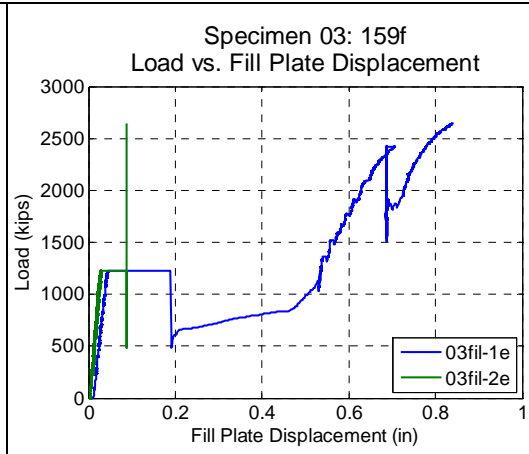


**Figure B.49 – 159f: After test (top of splice plate)**

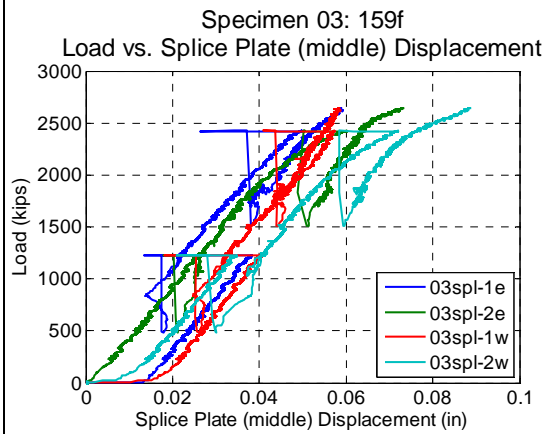




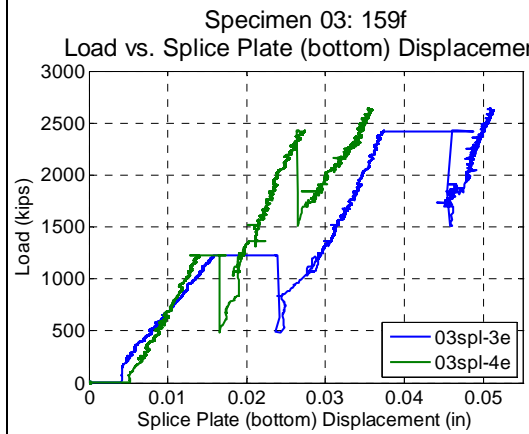
**Figure B.52 – 159f: Load vs. top column displacement**



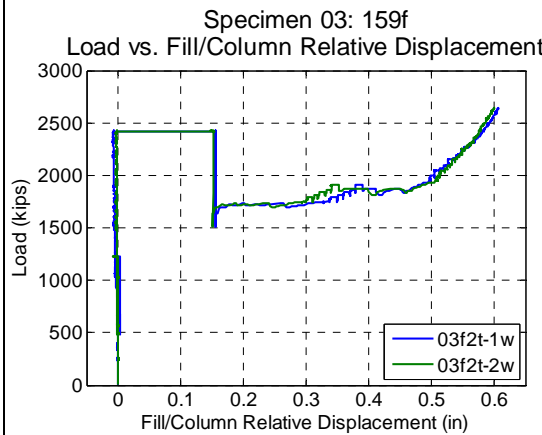
**Figure B.53 – 159f: Load vs. filler plate displacement**



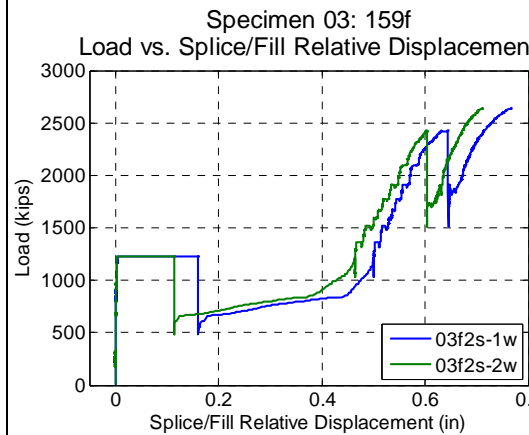
**Figure B.54 – 159f: Load vs. splice plate (middle) displacement**



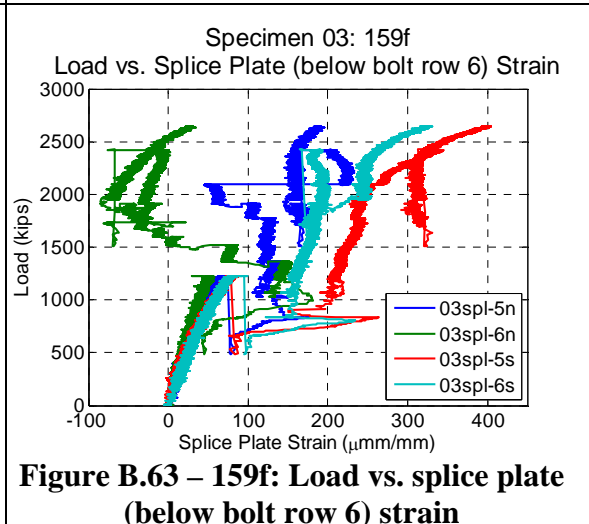
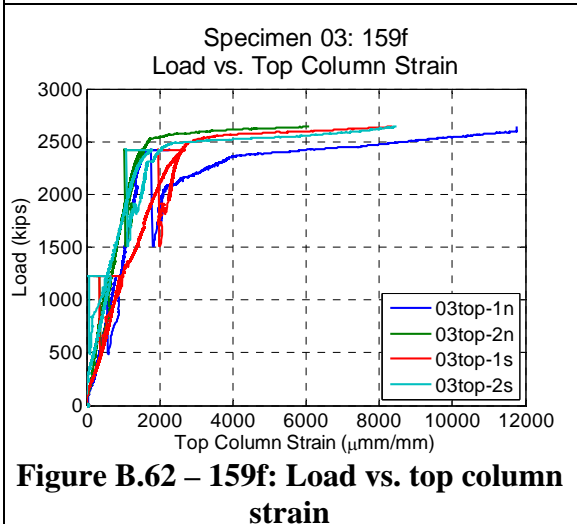
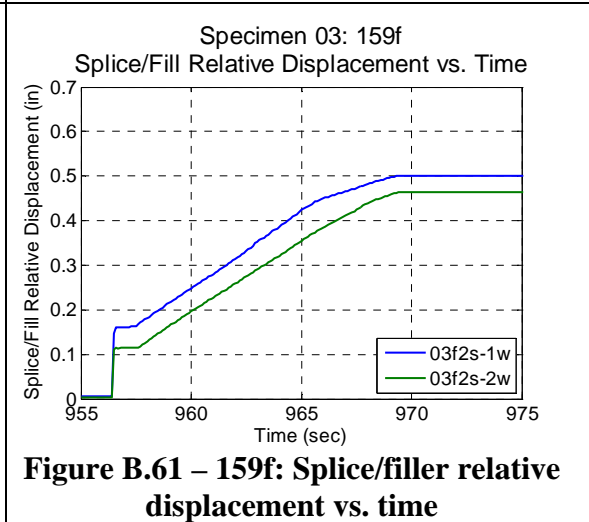
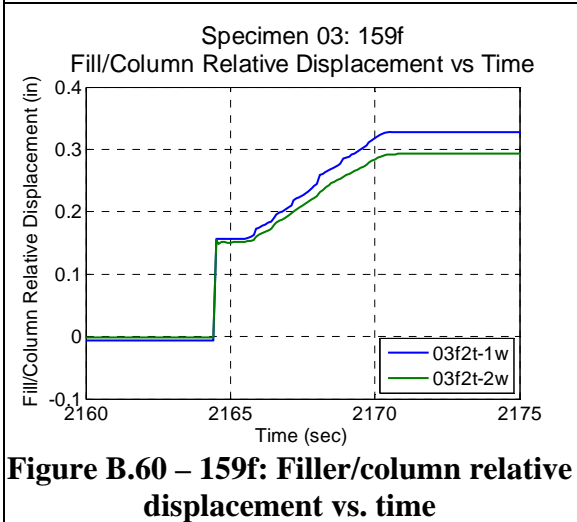
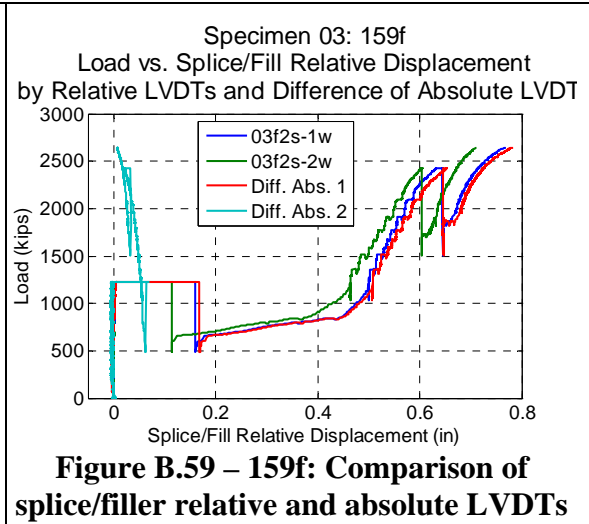
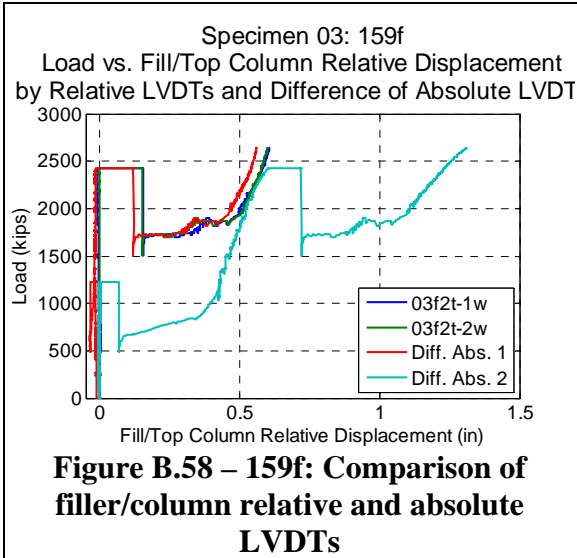
**Figure B.55 – 159f: Load vs. splice plate (bottom) displacement**

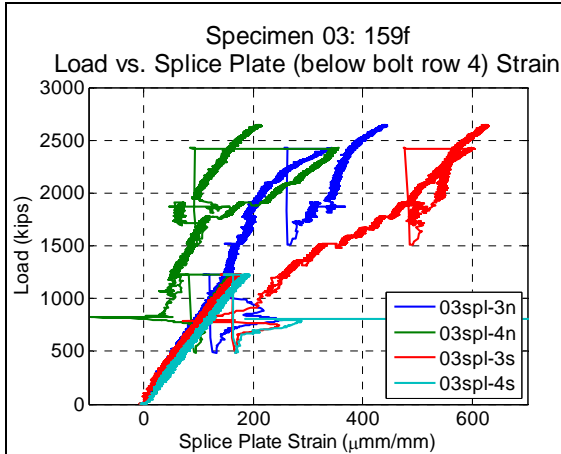


**Figure B.56 – 159f: Load vs. filler/column relative displacement**

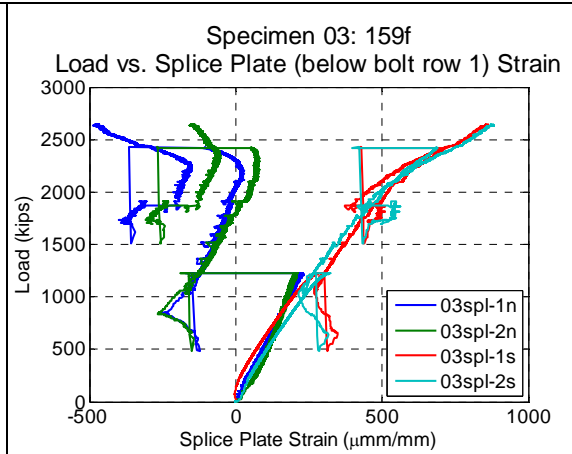


**Figure B.57 – 159f: Load vs. splice/filler relative displacement**

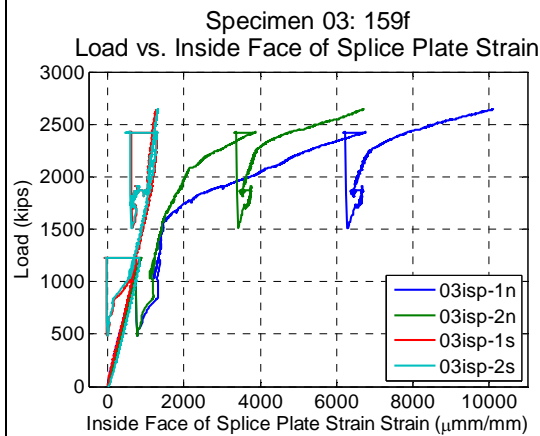




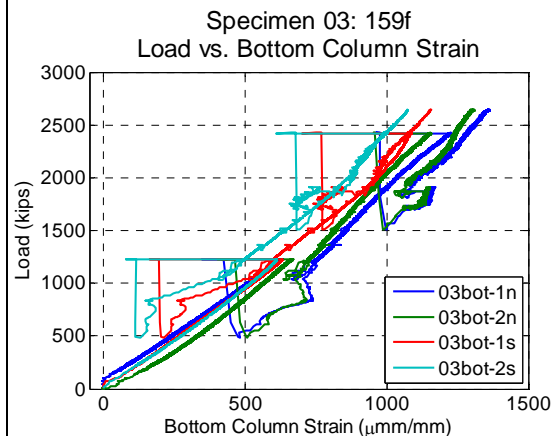
**Figure B.64 – 159f: Load vs. splice plate (below bolt row 4) strain**



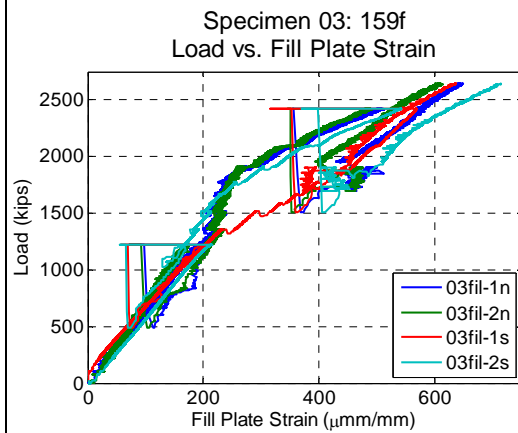
**Figure B.65 – 159f: Load vs. splice plate (below bolt row 1) strain**



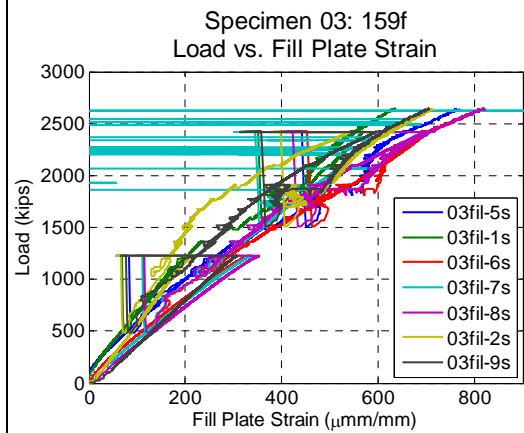
**Figure B.66 – 159f: Load vs. inside face of splice plate (below bolt row 1) strain**



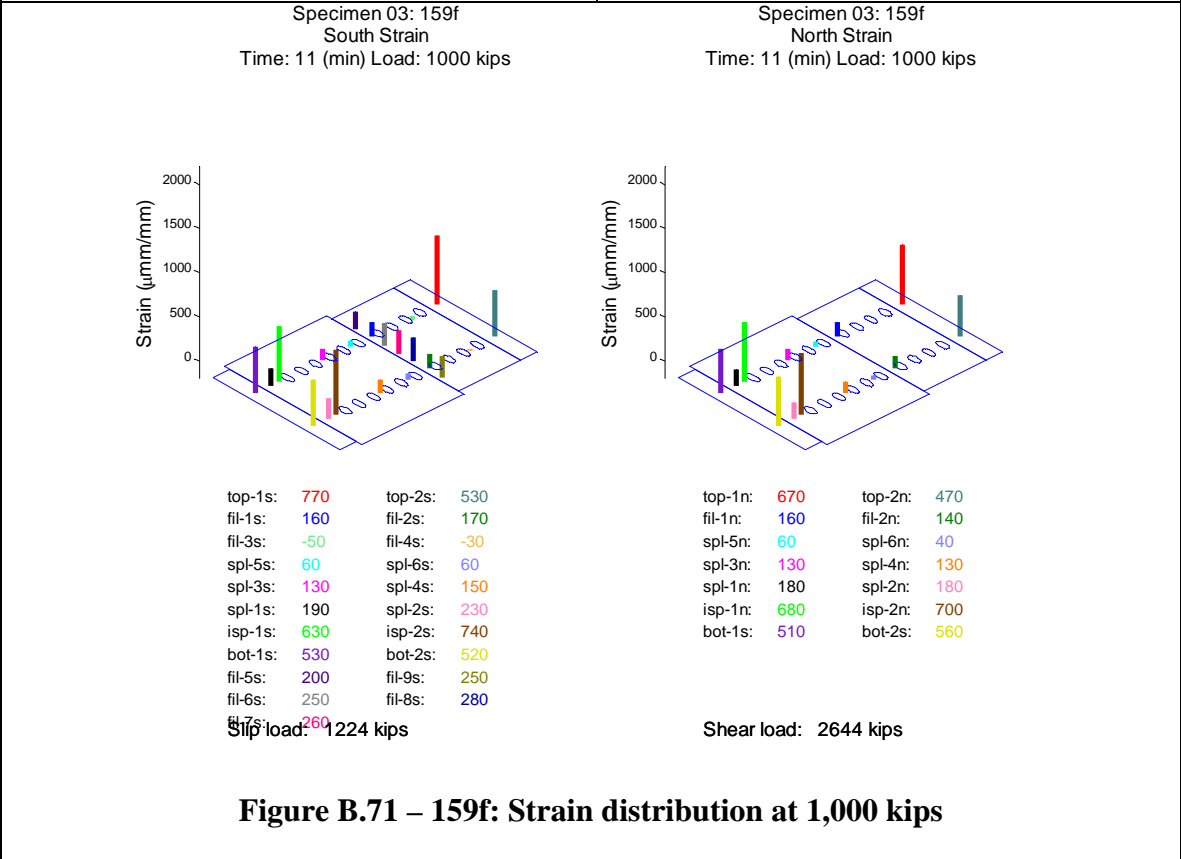
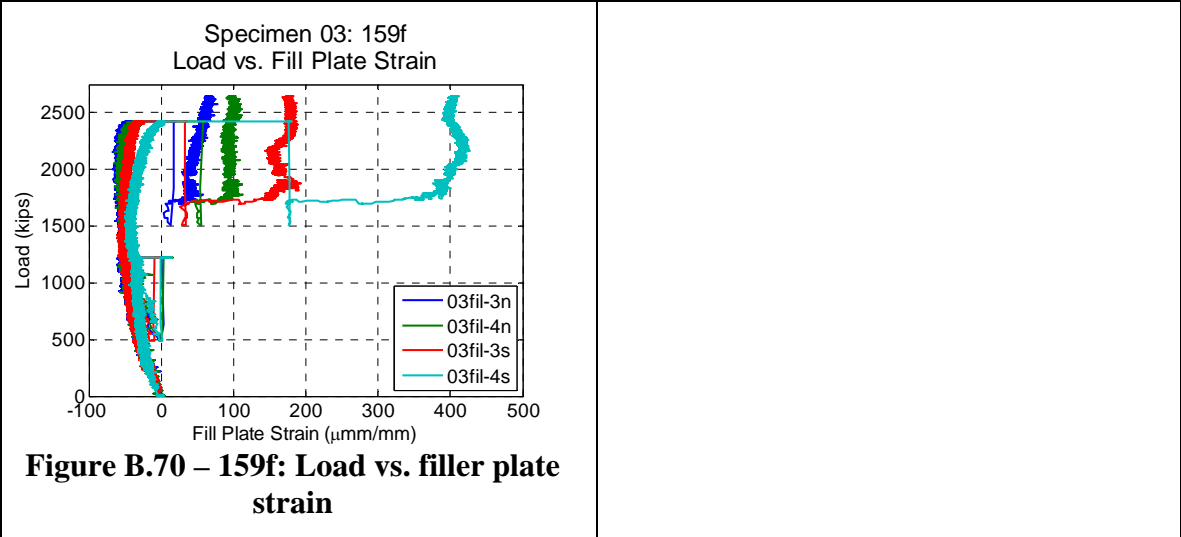
**Figure B.67 – 159f: Load vs. bottom column strain**



**Figure B.68 – 159f: Load vs. filler plate strain**



**Figure B.69 – 159f: Load vs. filler plate strain**



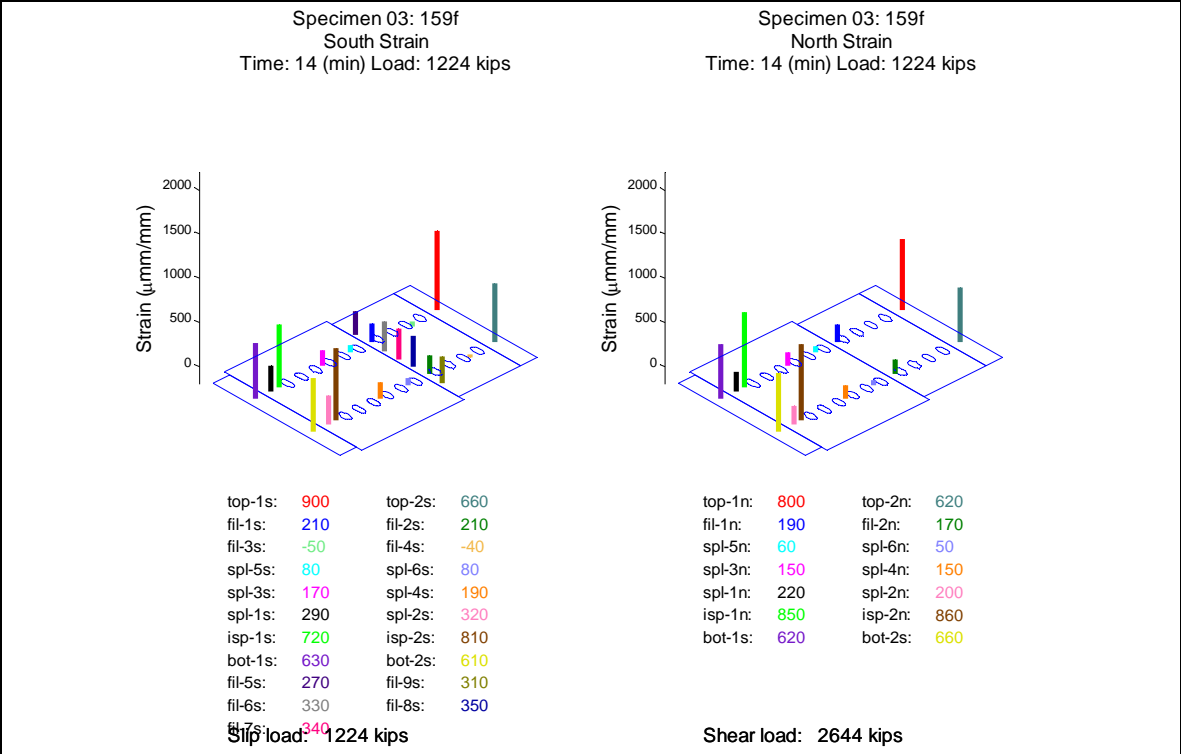


**Figure B.72 – 159f: Strain distribution prior to slip at 1,224 kips**

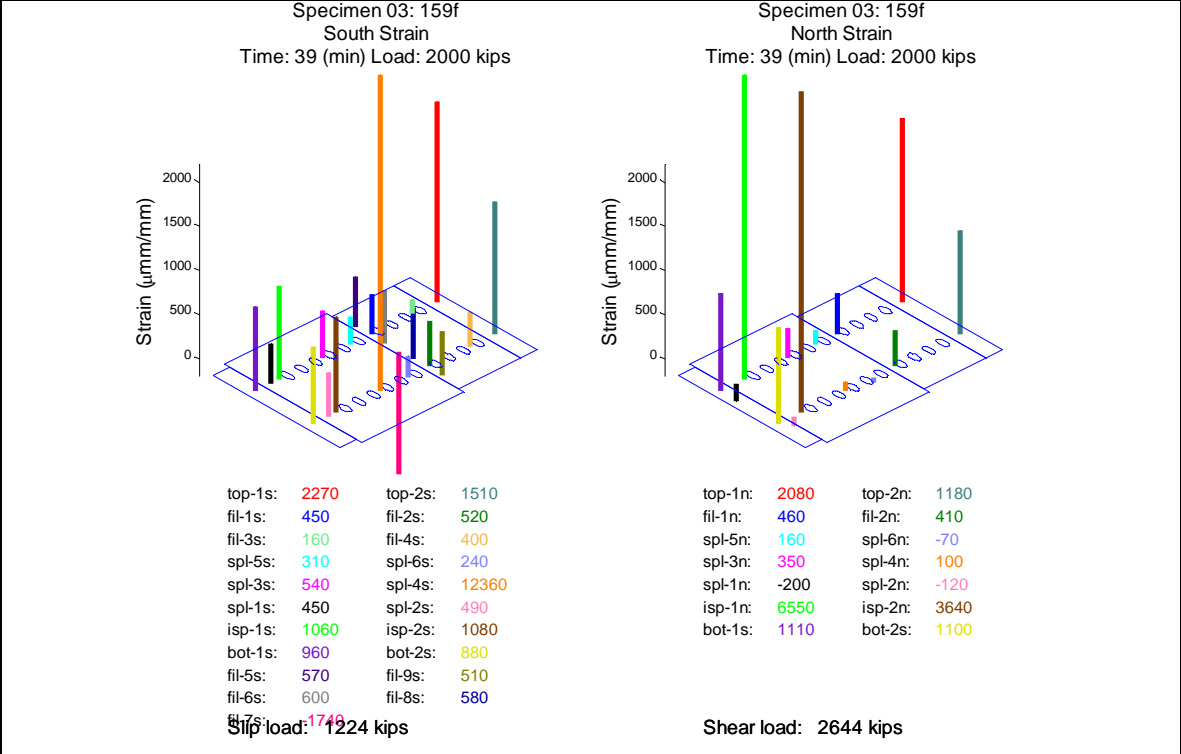


**Figure B.73 – 159f: Strain distribution prior to slip at 2,000 kips**

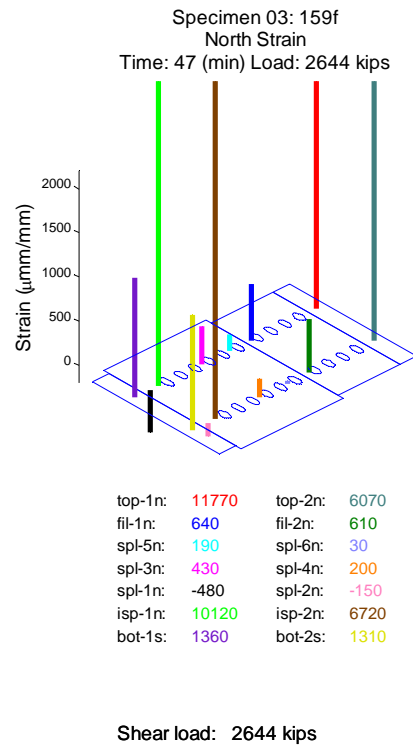
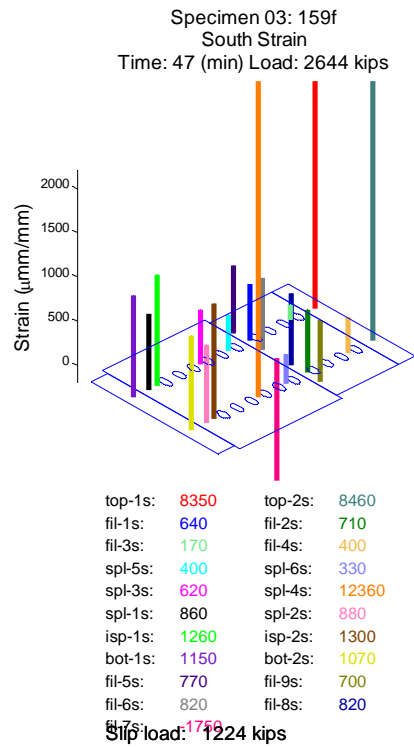


**Figure B.74 – 159f: Strain distribution prior to shear at 2,644 kips**

## B.5 Specimen 159h

Specimen 159h (Figure B.75 to Figure B.102) behaved approximately linearly until the observed slip load (1,697 kips). At the observed slip load the relative displacement between the splice plate and the filler plate, as well as the filler plate and the top column increased suddenly. Slip initiated between the filler plate and the splice plate on the south side and between the filler plate and the top column on the north side. Over a period of 22 seconds, the relative displacements increased by the amounts shown in Table B.5. This is seen most clearly in the relative LVDTs (Figure B.85 and Figure B.86). During this dynamic event, the load dropped and increased several times. The lowest load measured was 350 kips (Figure B.79). The machine and specimen stabilized at 1,030 kips and the load was held for observation of the specimen (Figure B.80). During the slip event the top southwest bolt through the south splice plate (SW6) failed through the threads, indicating a tension failure. This does not correlate with any bolts that were retorqued during assembly (in this specimen, bolt NW1 and its neighboring bolts were retorqued as per Table B.2).

**Table B.5 – 159h: Relative slip**

<b>Location</b>	<b>North</b>	<b>South</b>
<b>Between Splice and Filler</b>	0.20 in	0.40 in
<b>Between Filler and Top Column</b>	0.56 in	0.33 in
<b>Sum</b>	0.76 in	0.73 in

Three smaller slip events were recorded at loads of 1,280 kips, 1,485 kips, and 1,660 kips (Figure B.81). During each of these events, there was a slip on both the north and south sides of approximately 0.02 inches. After these three events, the bolts likely slipped into bearing on the top column, as the increase in stiffness in Figure B.85 shows at approximately a load of 1,500 kips and a relative slip of 0.55 inches. The maximum expected clearance in the holes based on the assembly was nominally  $2 * (5/16 \text{ inches}) = 0.625 \text{ inches}$ . During subsequent loading, approximately every 50 kips there was a small (approximately 0.005 inches) increase in the relative displacement measurements, which corresponded to a small and momentary decrease in load, as well as an audible noise. The main body of the report highlights a forensic investigation of this specimen that shows gouging on the faying surfaces, whose creation may have contributed to the creation of these noises.

The top column began to yield at approximately 2,400 kips (Figure B.91). The filler plate likely restrained the column yielding and began to pickup additional load demonstrated by the decreased slope in Figure B.98. By the end of the test, there was also slight local buckling seen in the flanges. Upon further loading, the bolts, now experiencing shear, yielded and eventually failed at the observed bolt shear load (2,904 kips) (Figure B.76,

Figure B.77 and Figure B.78). The twelve bolts through the splice plate on the south flange of the top column failed simultaneously, leaving the twelve bolts through the splice plate on the north flange of the top column intact on the specimen. Once the twelve bolts on the south flange failed, the relative movement of the splice plate to the filler plate caused the failure of two additional bolts through the filler plate, knocking these nuts and bolt shanks off through the bolt threads (Figure B.78). The LVDTs at the middle of the splice plate (Figure B.83) demonstrated nonlinear behavior near the end of the test, likely resulting from yielding of the splice plate due to bending. The LVDTs comparing the relative displacement between the splice plate and filler plate (Figure B.86) suffered a stiffness reduction near shear failure, demonstrated by the nonlinear response. This is likely due to the bolts yielding prior to shear failure in this plane. By comparison, the LVDTs comparing the relative displacement between the splice plate and top column (Figure B.85) remained linear up to the shear load. The additional development bolts in this shear plane reduced the force in each bolt; therefore they remained elastic when the specimen failed.

After slip, the specimen produced pinging noises at the following loads; 1483, 1660, 1705, 1748, 1807, 1828, 1877, 1943, 2011, 2051, 2106, 2127, 2200, 2250, 2314, 2355, 2713 and 2821 kips. Noises believed to be produced by the testing machine were neglected. The noises are likely associated with additional small slip events as noted above, bolts coming into bearing with the bolt holes, or possibly initiation of fractures within the bolts.

During slip the west strain gage at bolt row 6 on the south splice plate (04spl-5s) was damaged, reporting spurious data (Figure B.92). After slip, prior to shear failure, both strain gages on the north filler plate (04fil-1n and 04fil-2n) were damaged (Figure B.97).

The splice plate LVDTs (Figure B.83 and Figure B.84) showed a dynamic increase or decrease in displacement during the slip events. This may be due to a number of reasons, including stress relief in the splice plates after slip, very small slips relative to the column flanges, or small dynamic vibrations (with resulting small permanent offsets) of the LVDT holders, but the displacements are an order of magnitude smaller than the primary slip displacements (Figure B.85 and Figure B.86) and are not likely to indicate significant behavior.

Figure B.87 and Figure B.88 compare the LVDTs directly measuring relative slip between the filler plate and either the top column (Figure B.85) or the splice plate (Figure B.86) with the difference between the average of the two LVDTs on either filler plate at that same cross section as the LVDTs on the top column (Figure B.82) and either the average of the two LVDTs at the bottom center of the top column (Figure B.81) or the average of the two LVDTs on either splice plate at that same cross section as the LVDTs on the top column (Figure B.83). The measurements of the relative LVDTs correspond well to the difference between the corresponding absolute LVDTs.

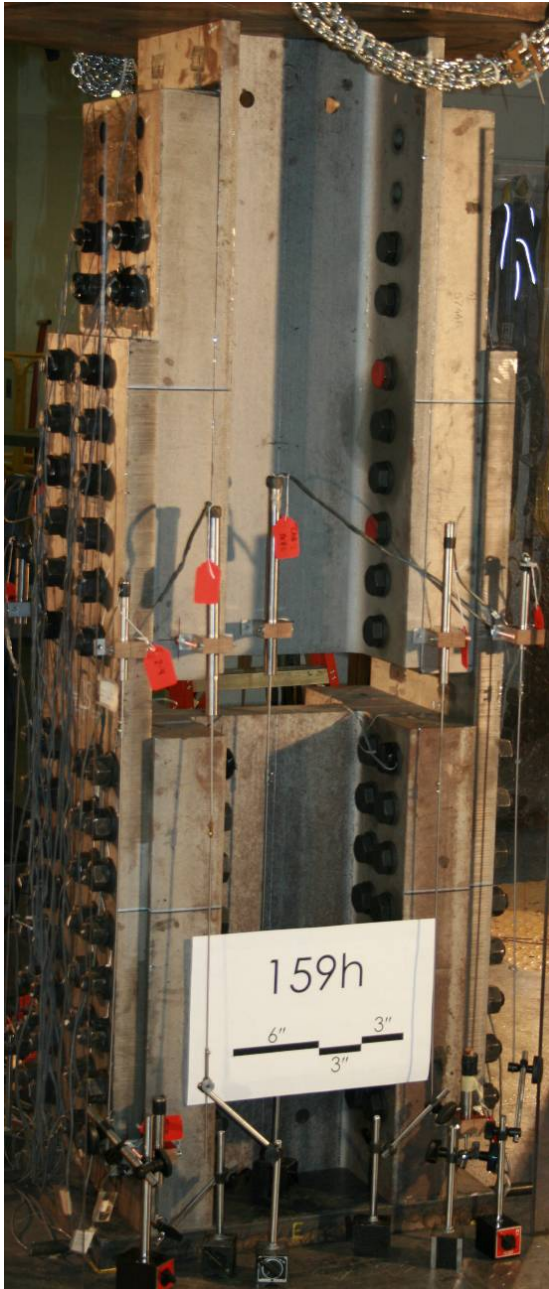
For this specimen, strain gages were attached to the inside face of the splice plate in the gap between the top and bottom columns (Figure B.95). These measurements, when

compared to the measurements from the outside face of the splice plate (Figure B.94), indicate significant bending in the splice plates, with the gages on the outside face of both splice plates below the first row of bolts going into tension in the later stages of the test. Yielding was recorded on the inside of the splice plate on both the north and south sides. After slip, the inside splice plate gages demonstrate nonlinear behavior, likely associated with bending. After slip the bolts were bearing on the inside edge of the splice plate (confirmed by disassembly of the specimens) which induced additional eccentricity into the splice plate.

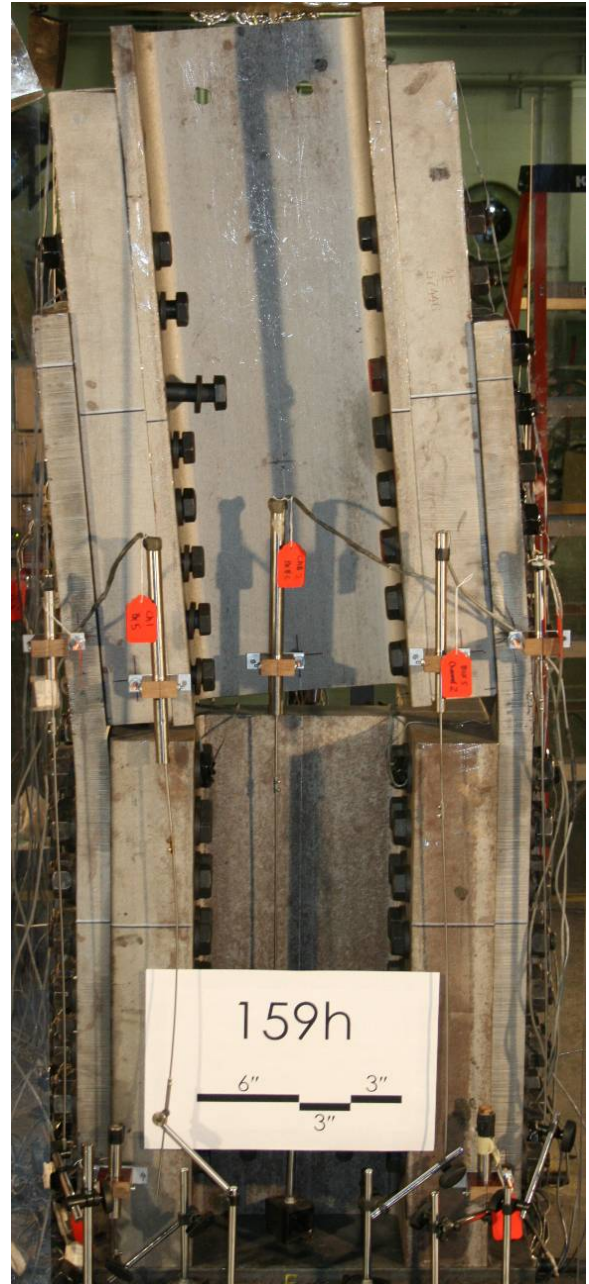
The top column strain gages show that the localized introduction of load was slightly biased to the southwest side (Figure B.91), likely due to variations of the loading surface. The bottom column strain gages showed a bias to the north side (Figure B.96).

The load was relatively uniformly distributed in the splice plates (Figure B.92, Figure B.93, and Figure B.94), filler plate (Figure B.87 and Figure B.88). Snapshots of the specimen strain at 1000 kips, immediately prior to slip, 2000 kips and immediately prior to shear are visually presented in Figure B.99, Figure B.100, Figure B.101 and Figure B.102, respectively. These graphs show that the strain enters into the filler plate and then into the splice plate gradually and relatively uniformly from bolt row 6 to bolt row 1 throughout the experiment.

The experiment was executed in load control. The loading rate for the experiment was approximately 1 kip per second. One elastic cycle was executed prior to the test, going up to a load of 200 kips and returning to zero load, to verify instrumentation. The data collection rate for the experiment was held constant at 10 Hertz (10 sets of readings per second).



**Figure B.75 – 159h: Before test (east side)**



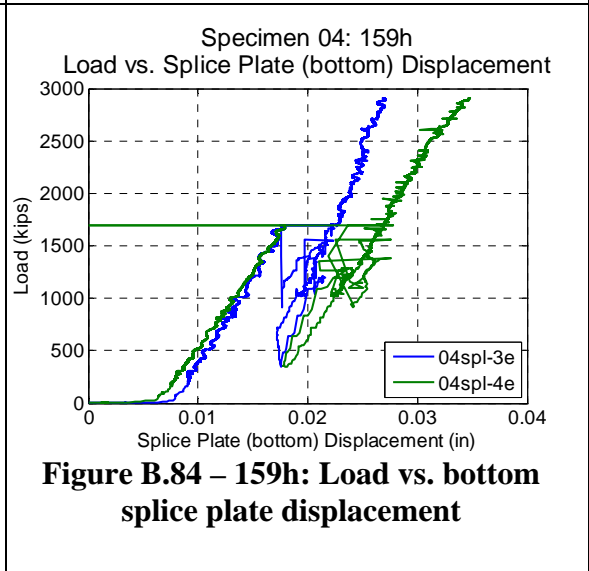
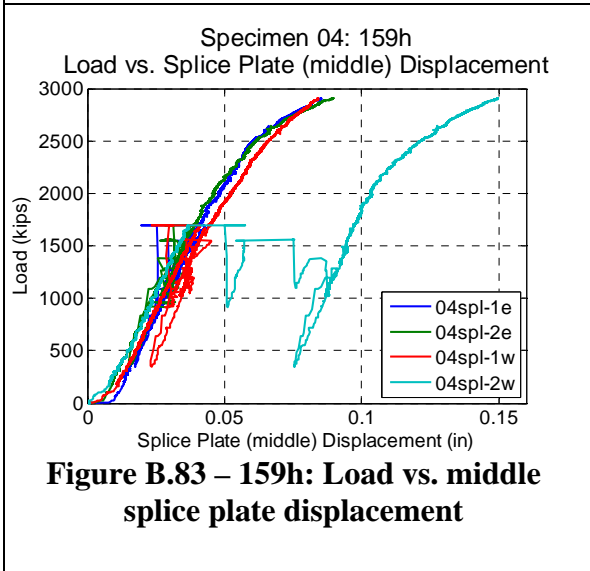
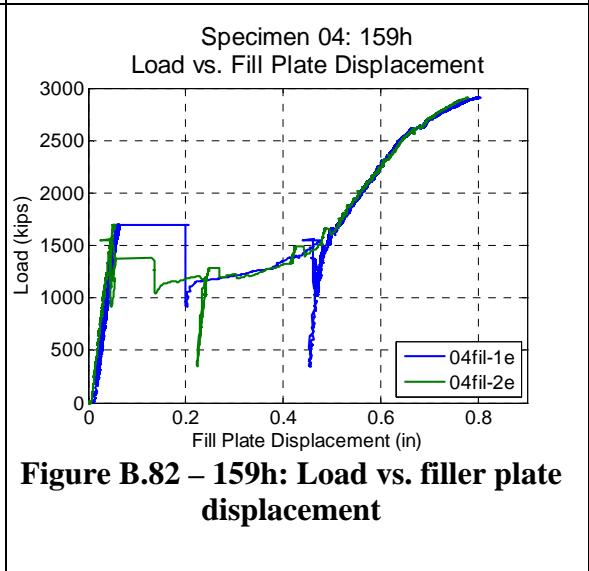
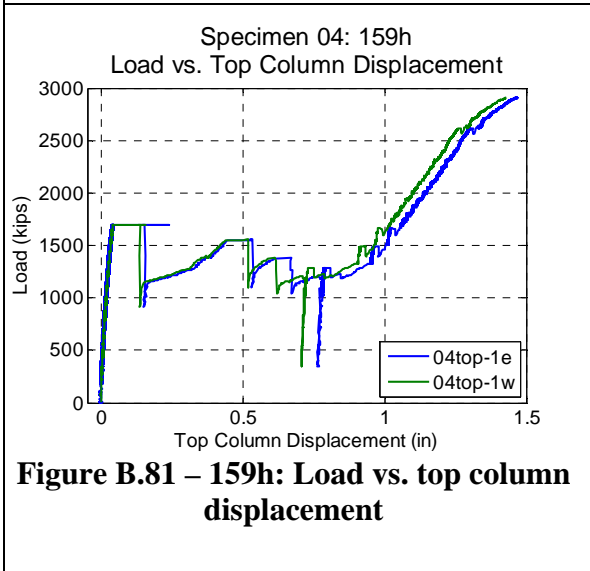
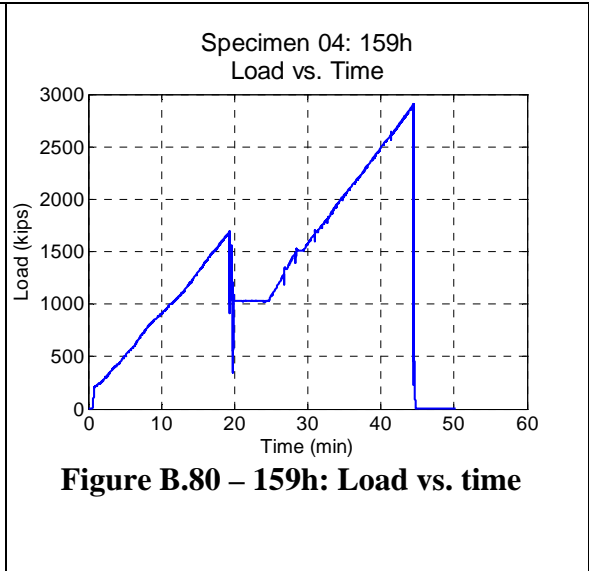
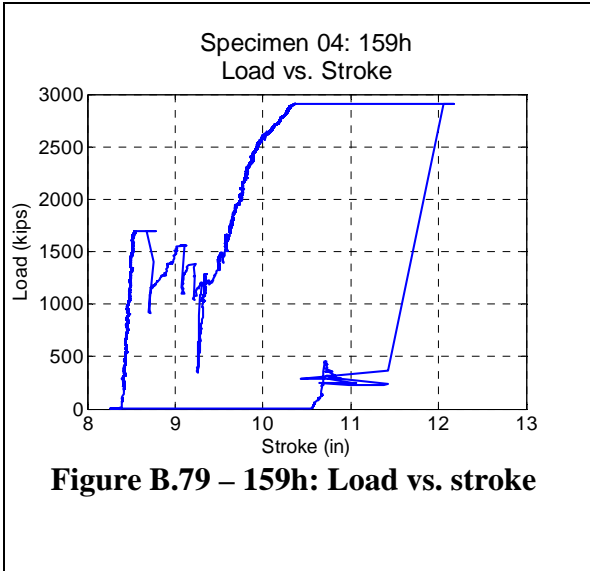
**Figure B.76 – 159h: After test (east side)**

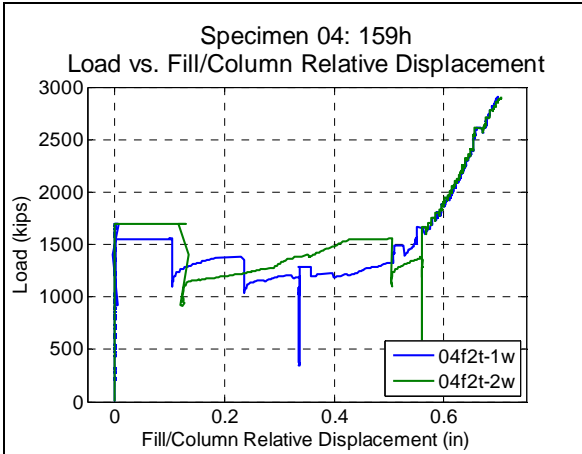


Figure B.77 – 159h: After test (east side)

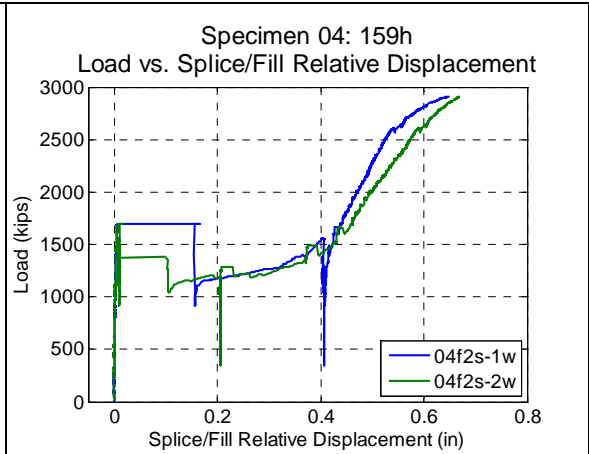


Figure B.78 – 159h: After test (south side)

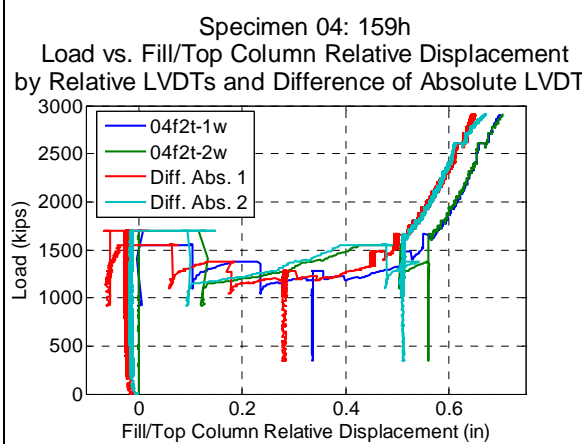




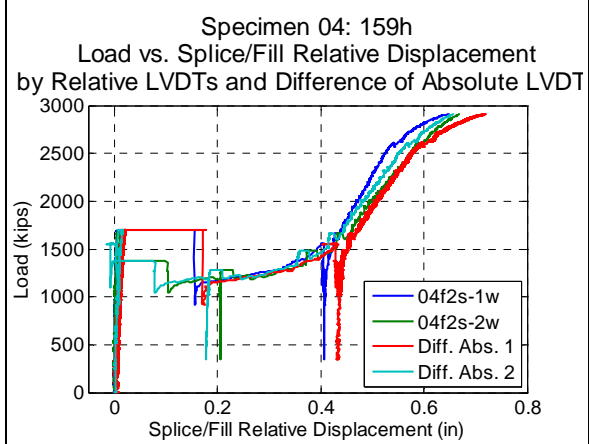
**Figure B.85 – 159h: Load vs. filler/column relative displacement**



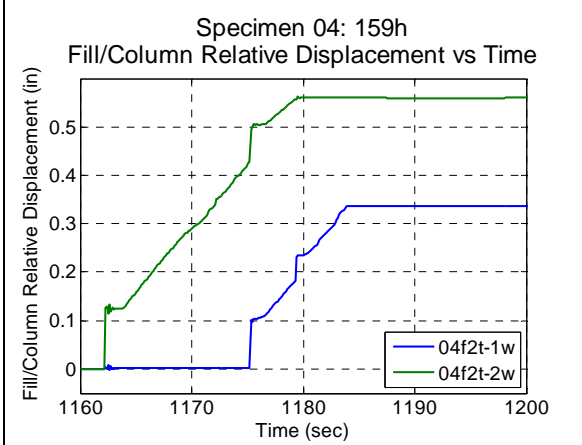
**Figure B.86 – 159h: Load vs. splice/filler relative displacement**



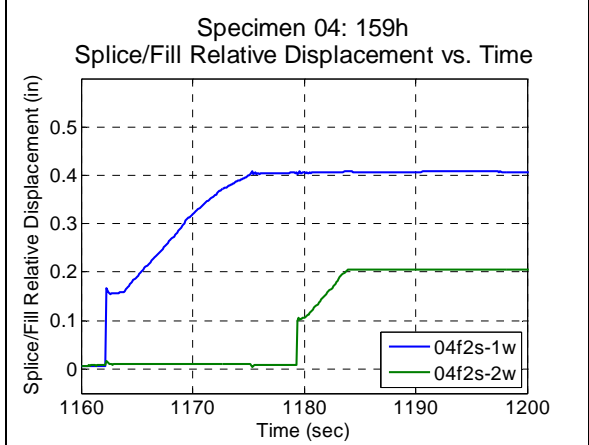
**Figure B.87 – 159h: Comparison of filler/column relative and absolute LVDTs**



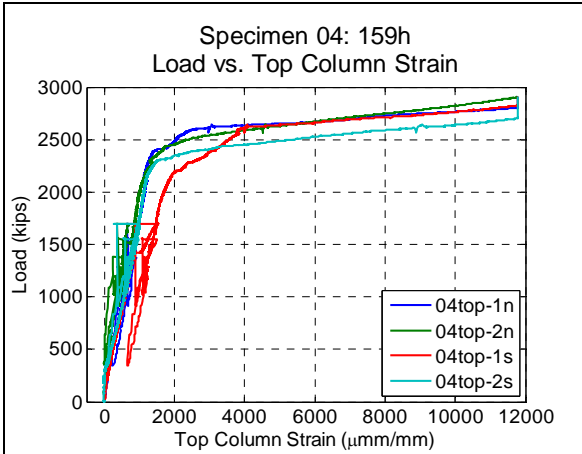
**Figure B.88 – 159h: Comparison of splice/filler relative and absolute LVDTs**



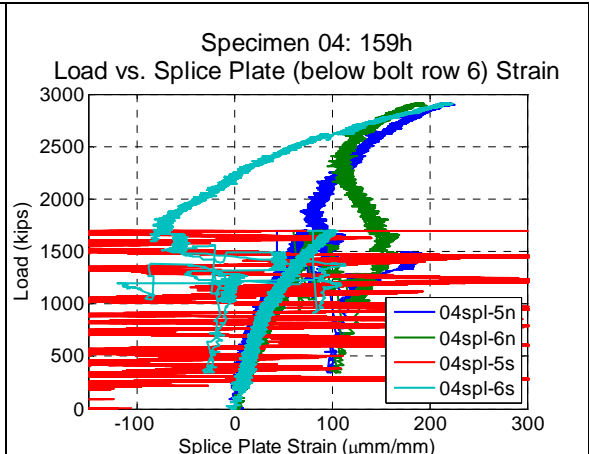
**Figure B.89 – 159h: Filler/column relative displacement vs. time**



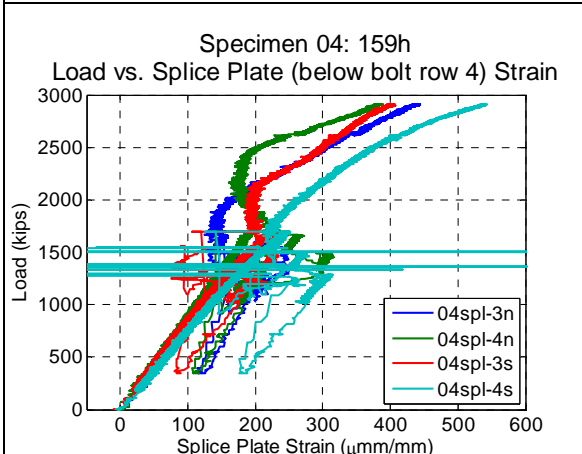
**Figure B.90 – 159h: Splice/filler relative displacement vs. time**



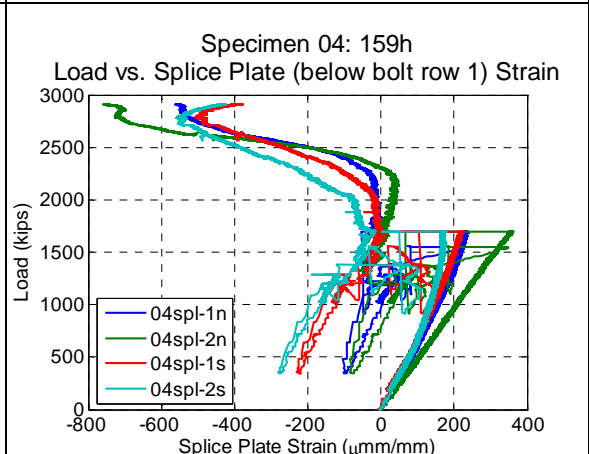
**Figure B.91 – 159h: Load vs. top column strain**



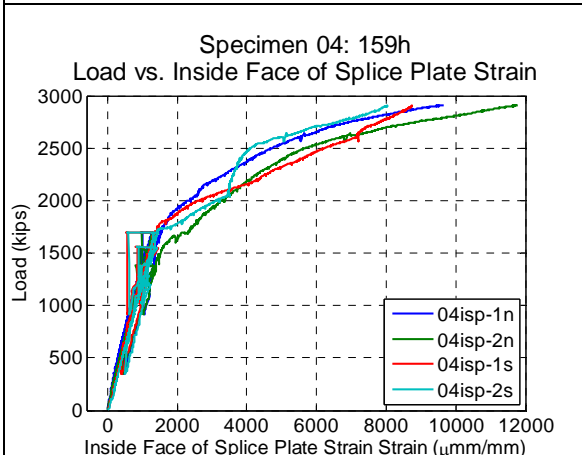
**Figure B.92 – 159h: Load vs. splice plate (below bolt row 6) strain**



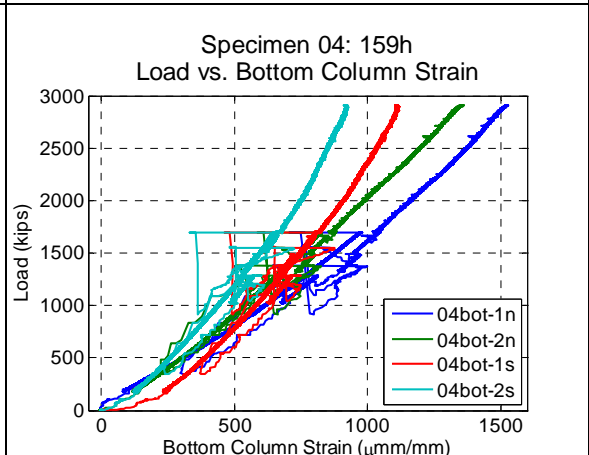
**Figure B.93 – 159h: Load vs. splice plate (below bolt row 4) strain**



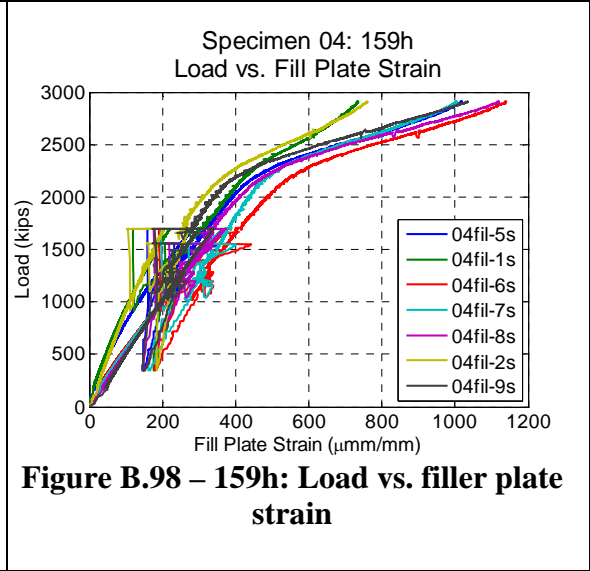
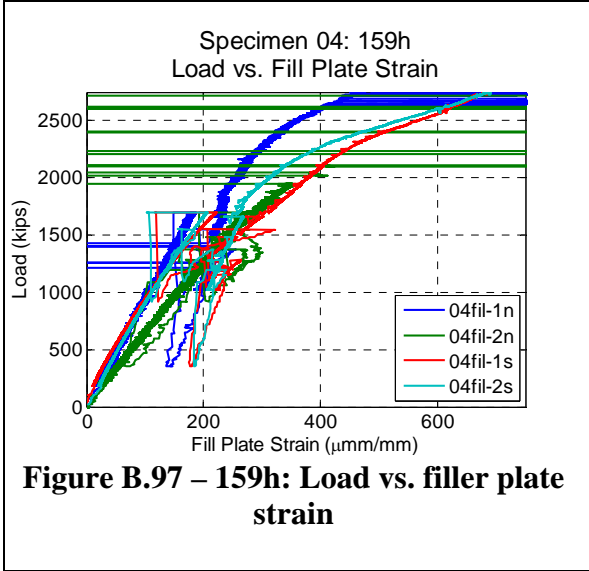
**Figure B.94 – 159h: Load vs. splice plate (below bolt row 1) strain**

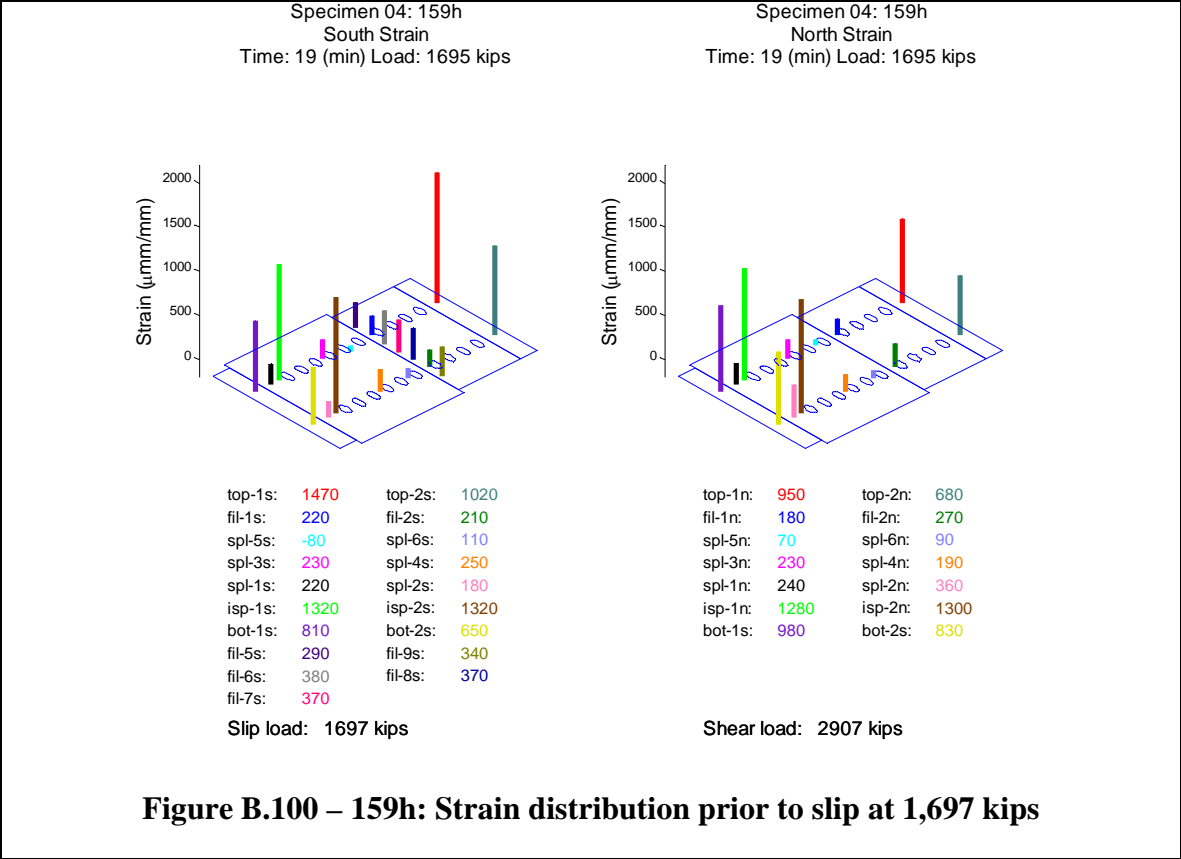
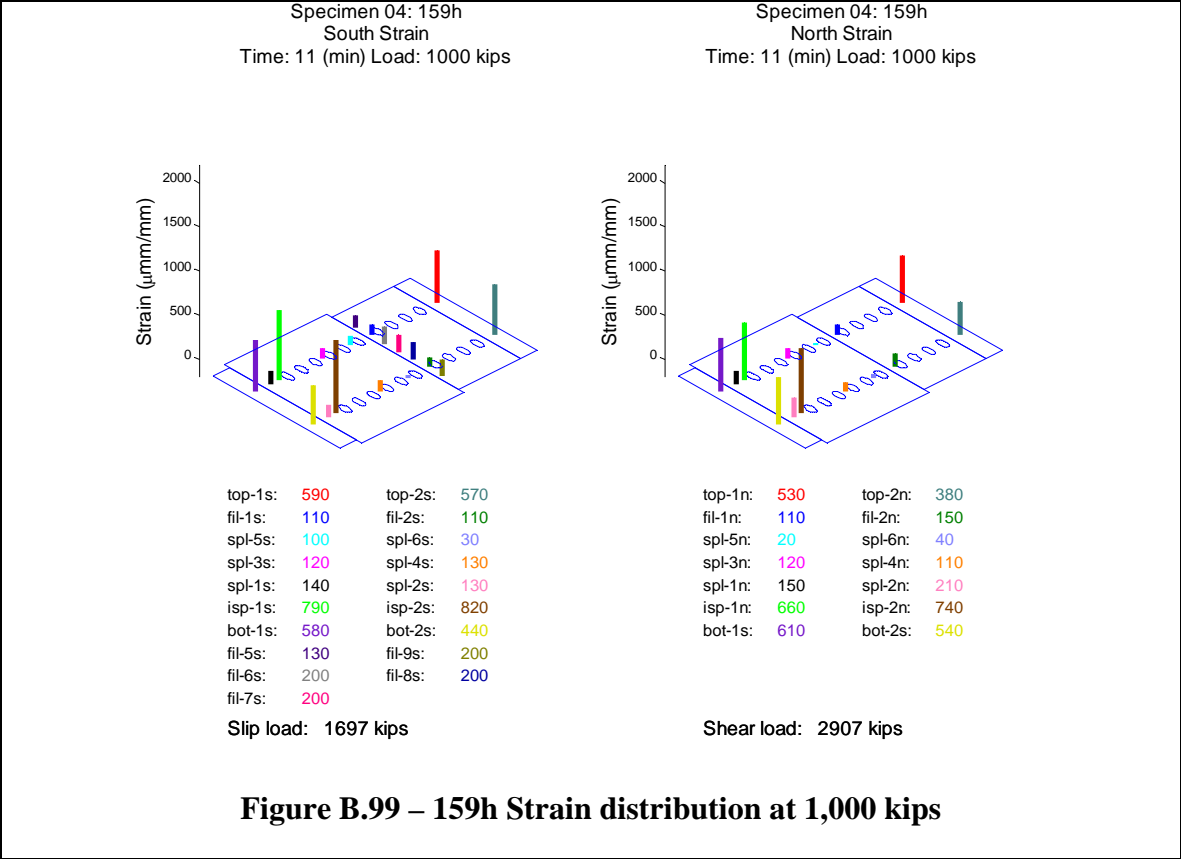


**Figure B.95 – 159h: Load vs. inside face of splice plate strain**



**Figure B.96 – 159h: Load vs. bottom column strain**





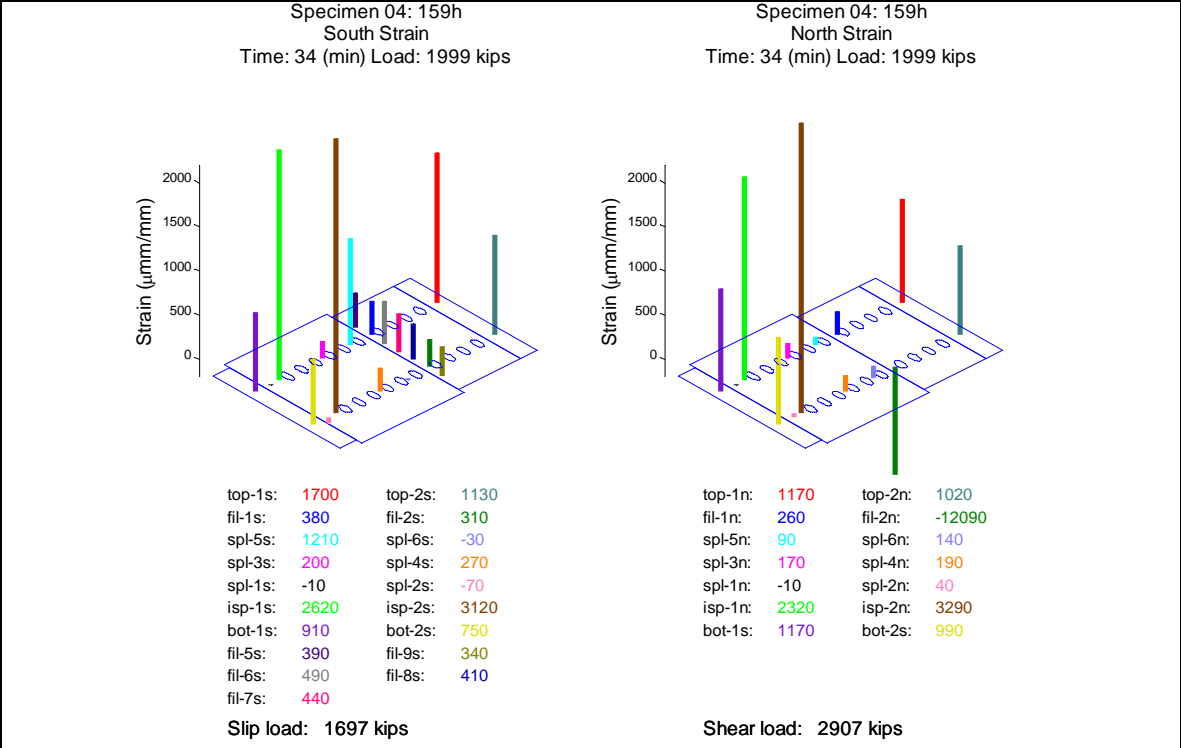


**Figure B.101 – 159h: Strain distribution at 2,000 kips**

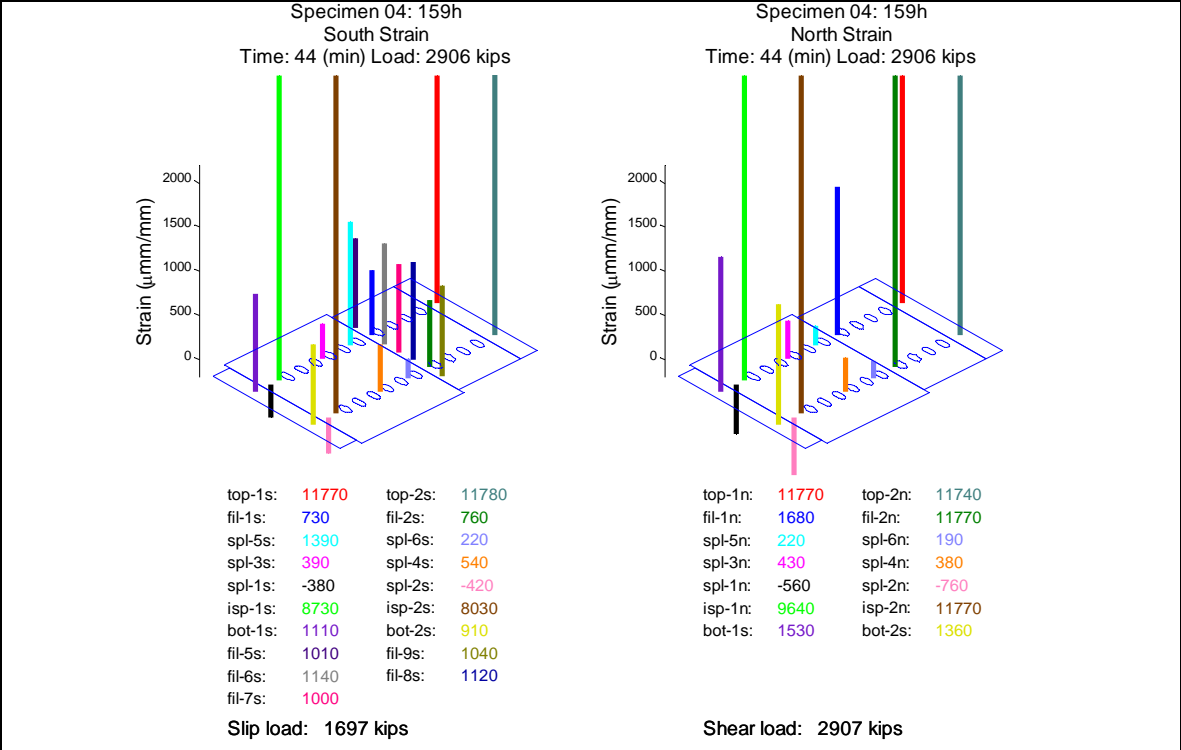


**Figure B.102 – 159h: Strain distribution prior to shear at 2,907 kips**

## B.6 Specimen 159n1

Specimen 159n1 (Figure B.103 to Figure B.131) behaved approximately linearly until the observed slip load (1,879 kips). During the slip event, the relative displacement between the filler plate and the top column increased suddenly. Slip initiated between the filler plate and the top column on both the north and south sides of the specimen (Figure B.112). During this dynamic event, the load dropped and increased several times, and at a load of approximately 1500 kips, slip initiated between the splice plate and the filler plate (Figure B.113). Over a period of 27 seconds total, the relative displacements increased by the amounts shown in Table B.6. This is seen most clearly in the relative LVDTs (Figure B.120 and Figure B.121). The lowest load measured was 960 kips (Figure B.110) during this dynamic event. The machine and specimen stabilized at 1,670 kips and the load was held for observation of the specimen (Figure B.111).

**Table B.6 – 159n1: Relative Slip**

<b>Location</b>	<b>North</b>	<b>South</b>
<b>Between Splice and Filler</b>	0.43 in	0.41 in
<b>Between Filler and Top Column</b>	0.59 in	0.67 in
<b>Sum</b>	1.12 in	1.08 in

During this event the bolts likely slipped into bearing on the top column, as the seen by the increase in stiffness in Figure B.116 at approximately a load of 1,300 kips and a relative slip of 0.55 inches. The maximum expected clearance in the holes based on the assembly was nominally  $2 * (5/16 \text{ inches}) = 0.625 \text{ inches}$ .

Also during the slip event, three bolts on the south side failed (SE1, SW2 and SW5). All three of the bolts failed through the threads, indicating a pretension failure. The bolt head and shank of SW2 remained in the specimen, while the other two shot out of the specimen. The bolt which remained in the specimen provided some doweling action and failed a second time in shear at the ultimate load of the specimen. The east bolt at bolt row 5 on the south side (SE5) was observed to not be flush with the flange when observations were made after the major slip event (Figure B.107). The west strain gage at bolt row 6 on the south splice plate (05spl-5s) was also damaged during this event, but earlier readings are valid (Figure B.123).

Bolt SE5, previously observed not flush, failed through the threads on the south side of the specimen at 1,930 kips. The bolt head and shank remained in the specimen. Bolt NW1 failed through the threads on the north side of the specimen at 2,465 kips. The shank remained in the specimen. During fabrication, bolts SE1, SW6, and their neighboring bolts were retorqued as per Table B.2.

The top column began to yield at approximately 2,200 kips (Figure B.122), damaging the top column strain gages (top-1n, top-1s, top-2n and top-2s) (Figure B.122). Upon further loading, the bolts, now experiencing shear, yielded and eventually failed at the observed bolt shear load (2,548 kips) (Figure B.104, Figure B.105, Figure B.106 and Figure B.108). The eight intact bolts and two bolt shanks through the splice plate on the south flange of the top column failed nearly simultaneously. From the video recording of the specimen failure it is clear three bolts failed first then a fraction of a second later, the remaining bolts failed. One bolt through the splice plate on the north flange of the top column failed through the threads at some time during the loading between slip and shear. Three additional bolts on the north splice plate failed through the threads during the shear failure of the specimen. All four of these failures left the bolt head and shank in the specimen.

After slip, the specimen produced pinging noises at the following loads; 1734, 1743, 1758, 1792, 1798, 1810, 1816, 1830, 1840 (cracking noise), 1846, 1847, 1850, 1856, 1865, 1881, 1885, 1890, 1902, 1909, 1917, 1930 (bolt SE5 failed), 1945, 1953, 2000, and 2003. Clicking sounds were heard twice a second above 2365 kips. A noise was observed at 2465 kips, during the failure of bolt NW1. Noises believed to be produced by the testing machine were neglected. The noises are likely associated with additional small slip events, bolts coming into bearing with the bolt holes, or possibly initiation of fractures within the bolts.

The splice plate LVDTs (Figure B.114 and Figure B.115) showed a dynamic increase or decrease in displacement during the slip events. This may be due to a number of reasons, including stress relief in the splice plates after slip, very small slips relative to the column flanges, or small dynamic vibrations (with resulting small permanent offsets) of the LVDT holders, but the displacements are an order of magnitude smaller than the primary slip displacements (Figure B.116 and Figure B.117) and are not likely to indicate significant behavior.

Figure B.118 and Figure B.119 compare the LVDTs directly measuring relative slip between the filler plate and either the top column (Figure B.116) or the splice plate (Figure B.117) with the difference between the average of the two LVDTs on either filler plate at that same cross section as the LVDTs on the top column (Figure B.113) and either the average of the two LVDTs at the bottom center of the top column (Figure B.112) or the average of the two LVDTs on either splice plate at that same cross section as the LVDTs on the top column (Figure B.114). The measurements of the relative LVDTs correspond well to the difference between the corresponding absolute LVDTs.

For this specimen, strain gages were attached to the inside face of the splice plate in the gap between the top and bottom columns (Figure B.126). These measurements, when compared to the measurements from the outside face of the splice plate (Figure B.125), indicate significant bending in the splice plates. Yielding was recorded on the inside of the splice plate.

The top column strain gages show that the localized introduction of load had a small bias to the northwest (Figure B.122). The bottom column strain gages show that the localized reaction had a slight bias to the south (Figure B.127).

Throughout the splice plate the bias is minimal (Figure B.123, Figure B.124 and Figure B.125) prior to slip. After the bolts have slipped into bearing the south side of the specimen had a larger displacement between the top column and filler plate than the north side (Figure B.116) with the relative displacement between the filler and splice plate similar. This resulted in significant bending in the splice plates, particularly the north splice plate, where the outer gages had significant tension and the inner gages significant compression. Snapshots of the specimen strain at 1000 kips, immediately prior to slip, 2000 kips and immediately prior to shear are visually presented in Figure B.128, Figure B.129, Figure B.130 and Figure B.131, respectively. These graphs show that the strain enters into the splice plate gradually and relatively uniformly from bolt row 6 to bolt row 1 throughout the experiment.

The experiment was executed in load control. The loading rate for the experiment was approximately 1 kip per second. One elastic cycle was executed prior to the test, going up to a load of 200 kips and returning to zero load, to verify instrumentation. The data collection rate for the experiment was held constant at 10 Hertz (10 sets of readings per second).

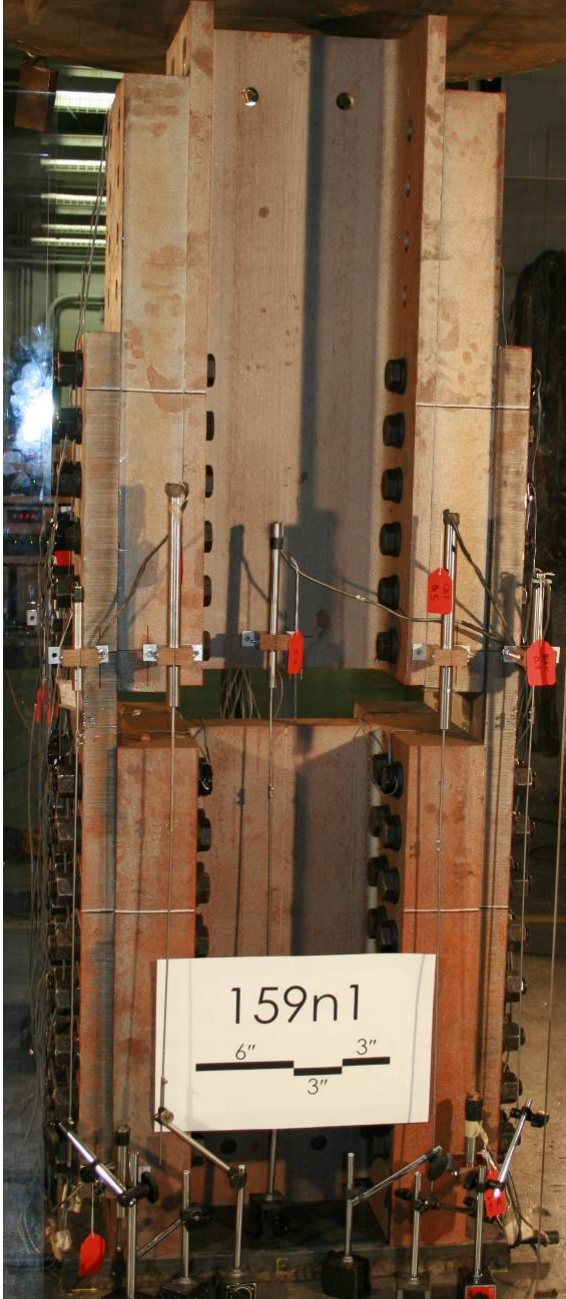


Figure B.103 – 159n1: Before test (east side)

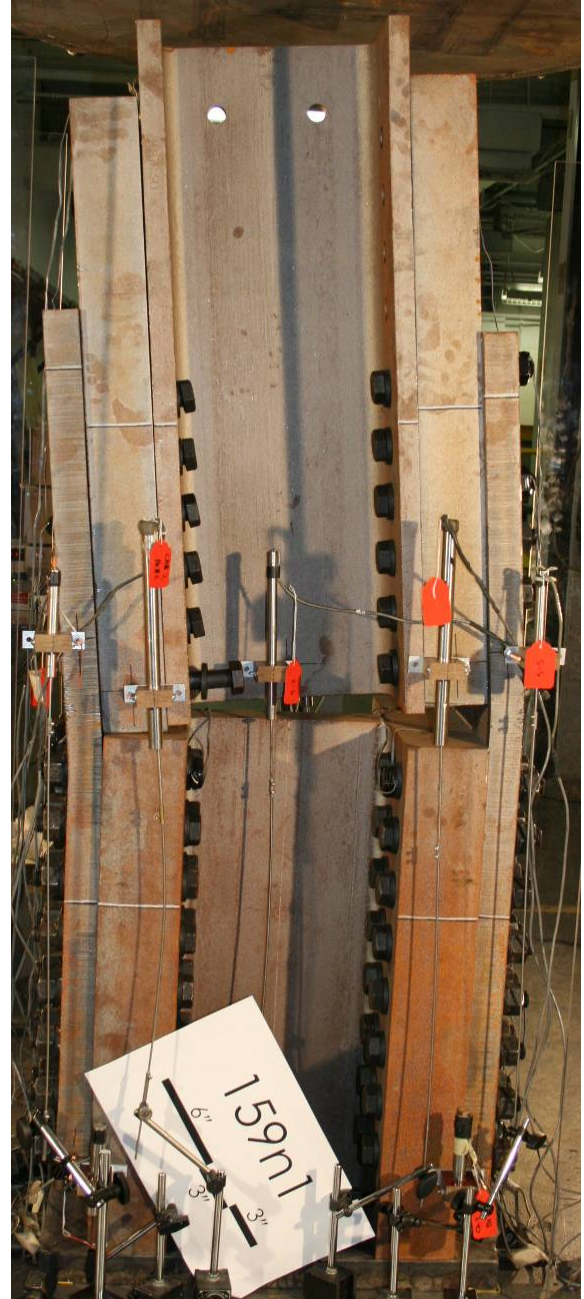


Figure B.104 – 159n1: After test (east side)



**Figure B.105 – 159n1: After test (east side)**



**Figure B.106 – 159n1: After test (south side)**

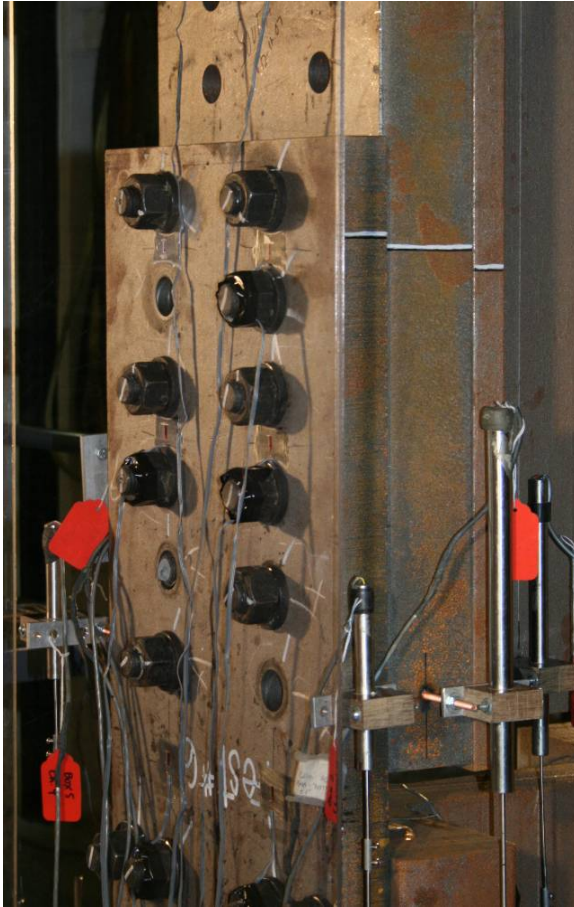


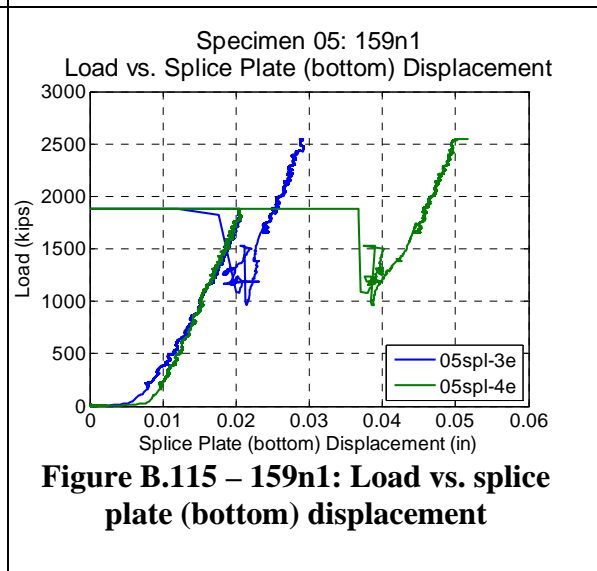
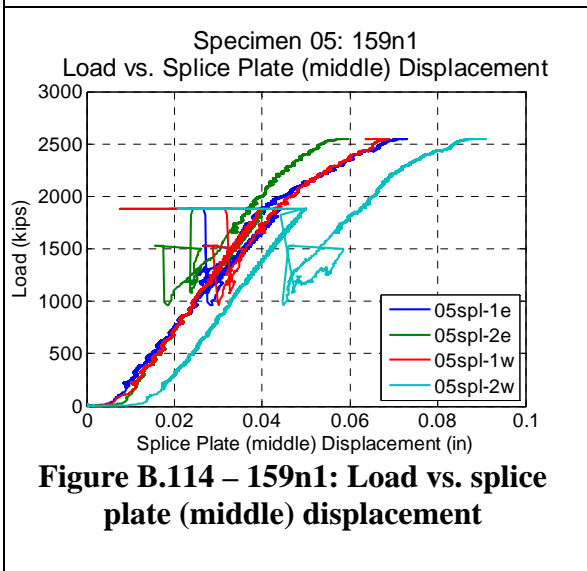
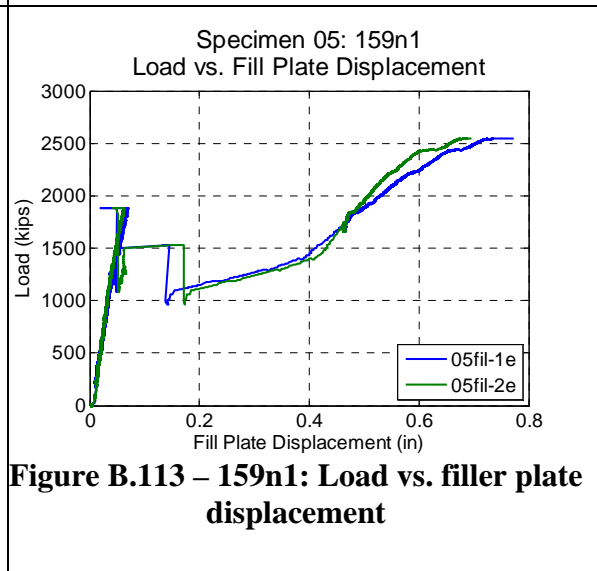
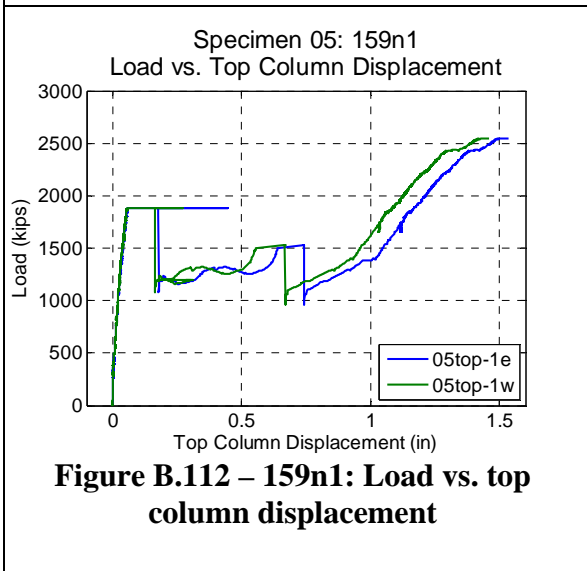
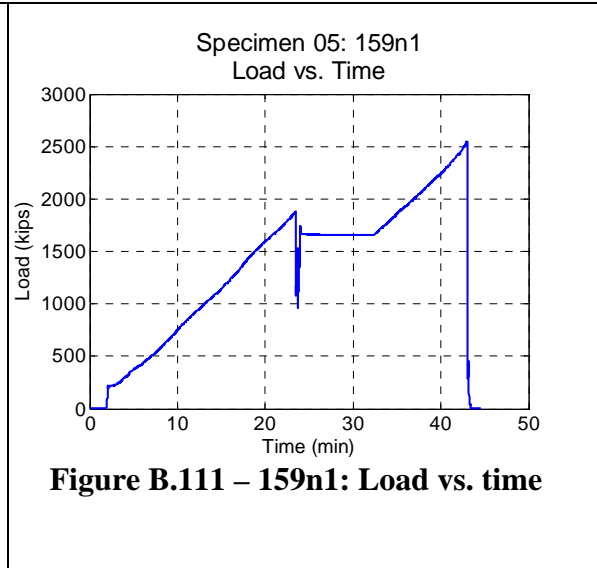
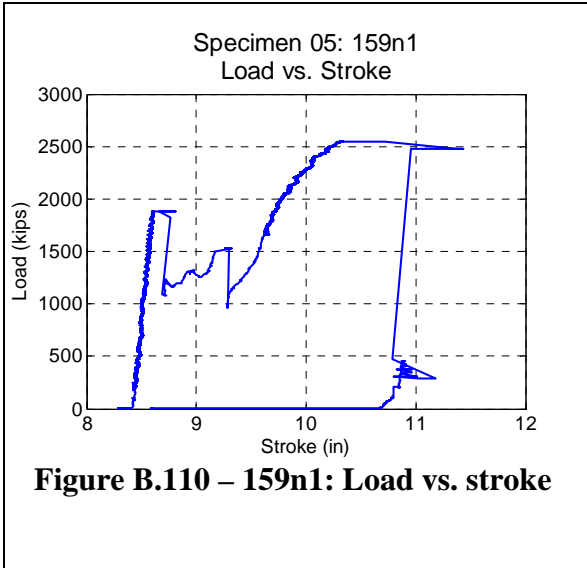
**Figure B.107 – 159n1: After slip (south side)**

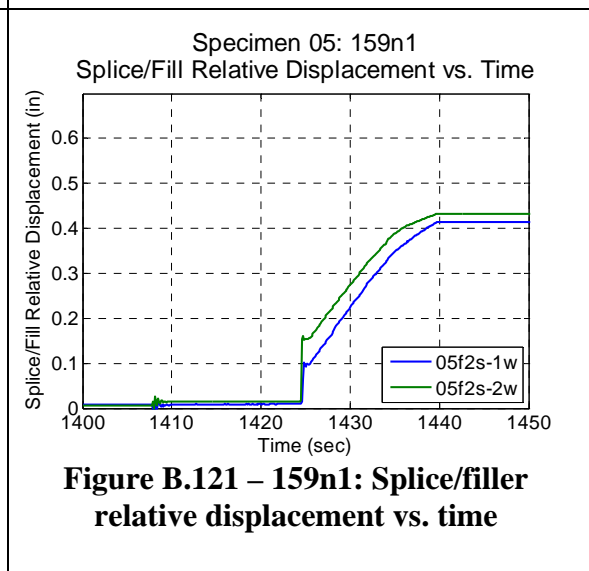
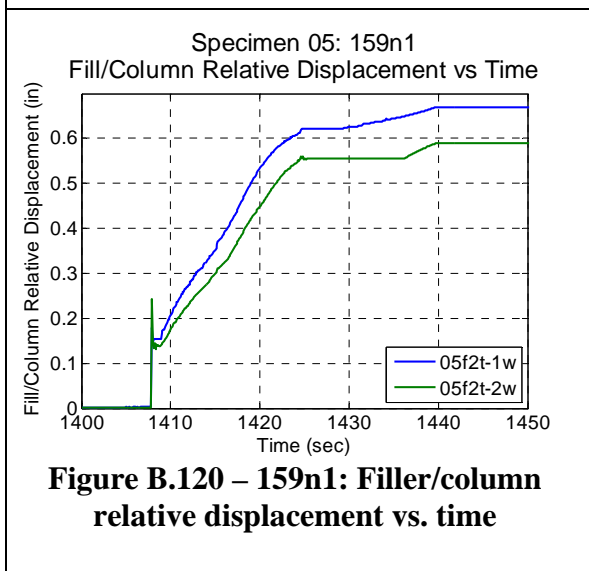
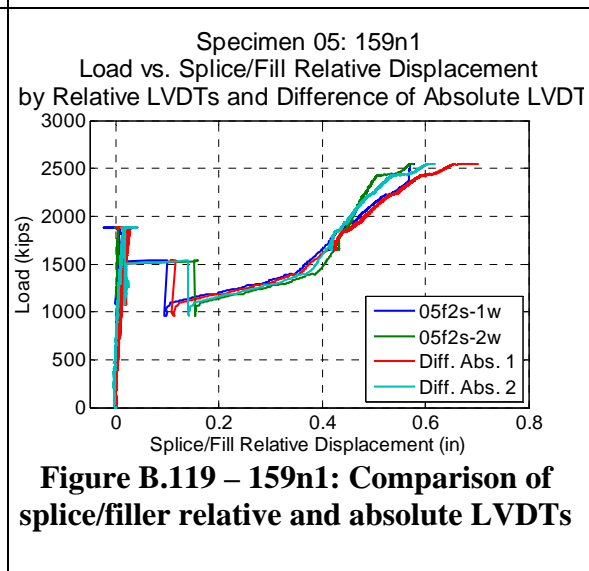
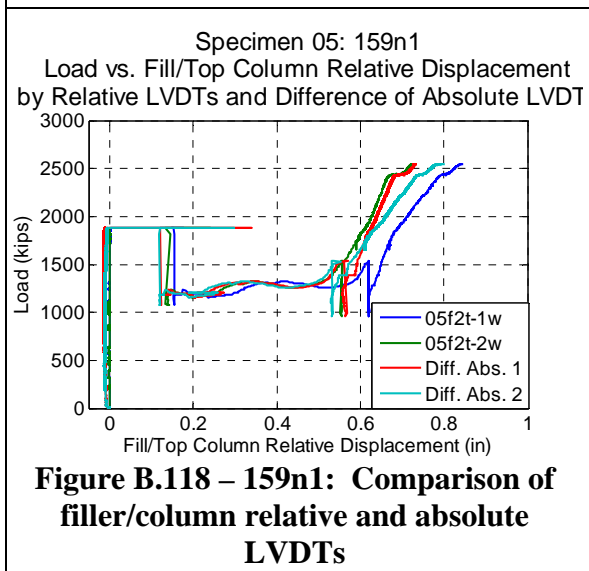
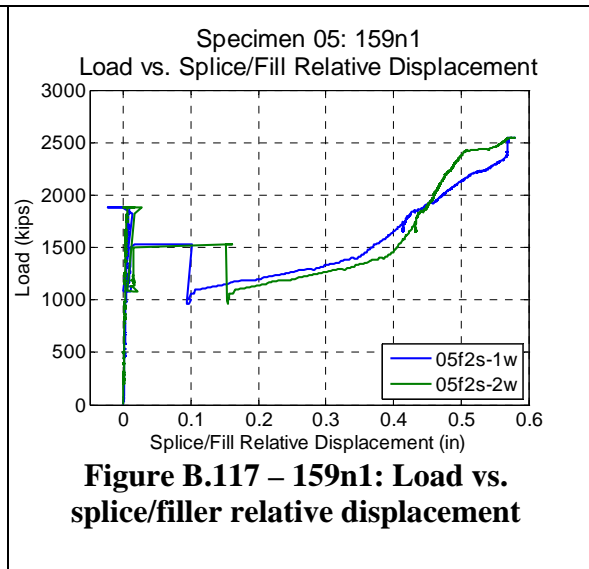
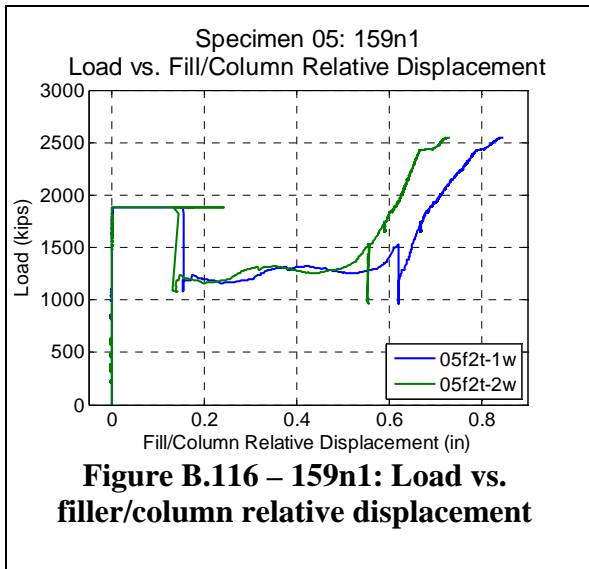


**Figure B.108 – 159n1: After test (north side)**



**Figure B.109 – 159n1: Bolt SE5 after slip (south side)**





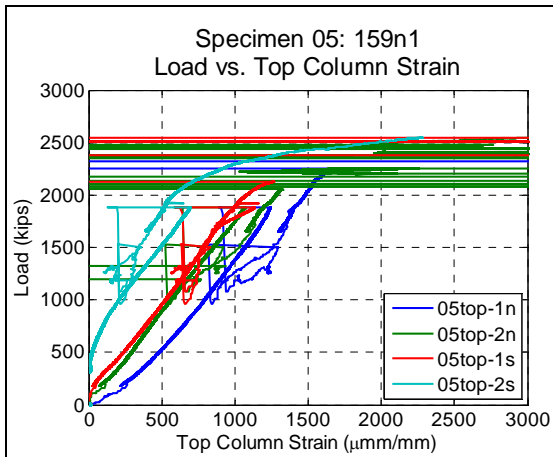


**Figure B.122 – 159n1: Load vs. top column strain**

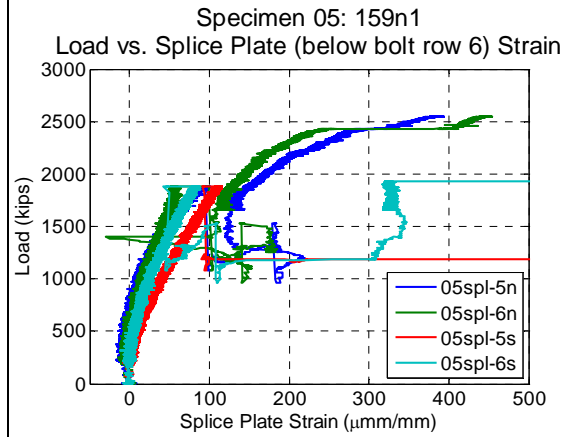


**Figure B.123 – 159n1: Load vs. splice plate (below bolt row 6) strain**

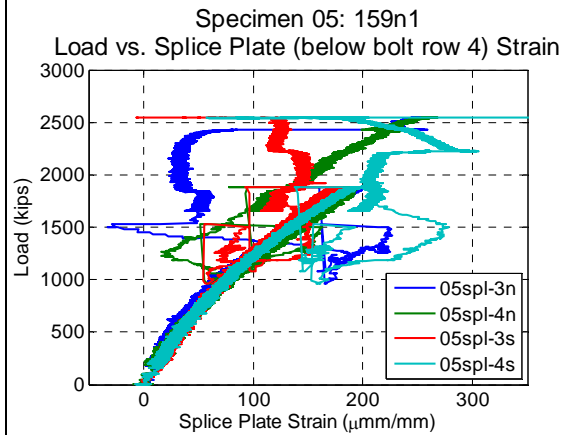


**Figure B.124 – 159n1: Load vs. splice plate (below bolt row 4) strain**

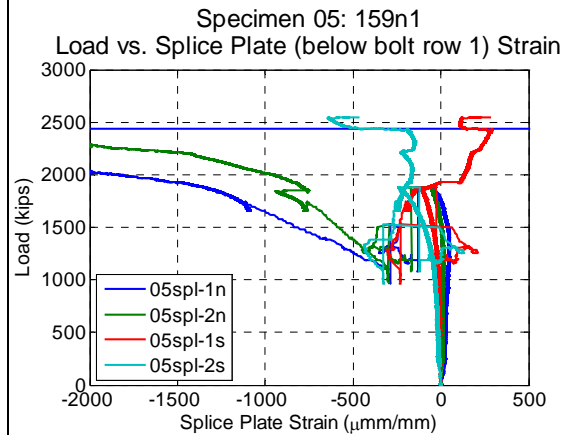


**Figure B.125 – 159n1: Load vs. splice plate (below bolt row 1) strain**

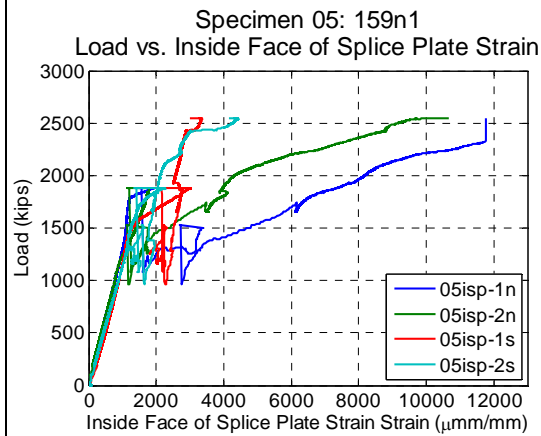


**Figure B.126 – 159n1: Load vs. inside face of splice plate strain**

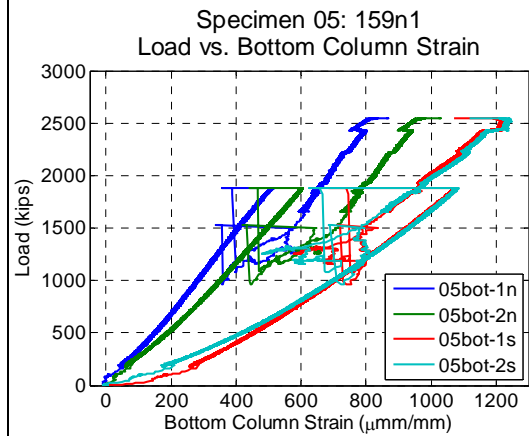


**Figure B.127 – 159n1: Load vs. bottom column strain**

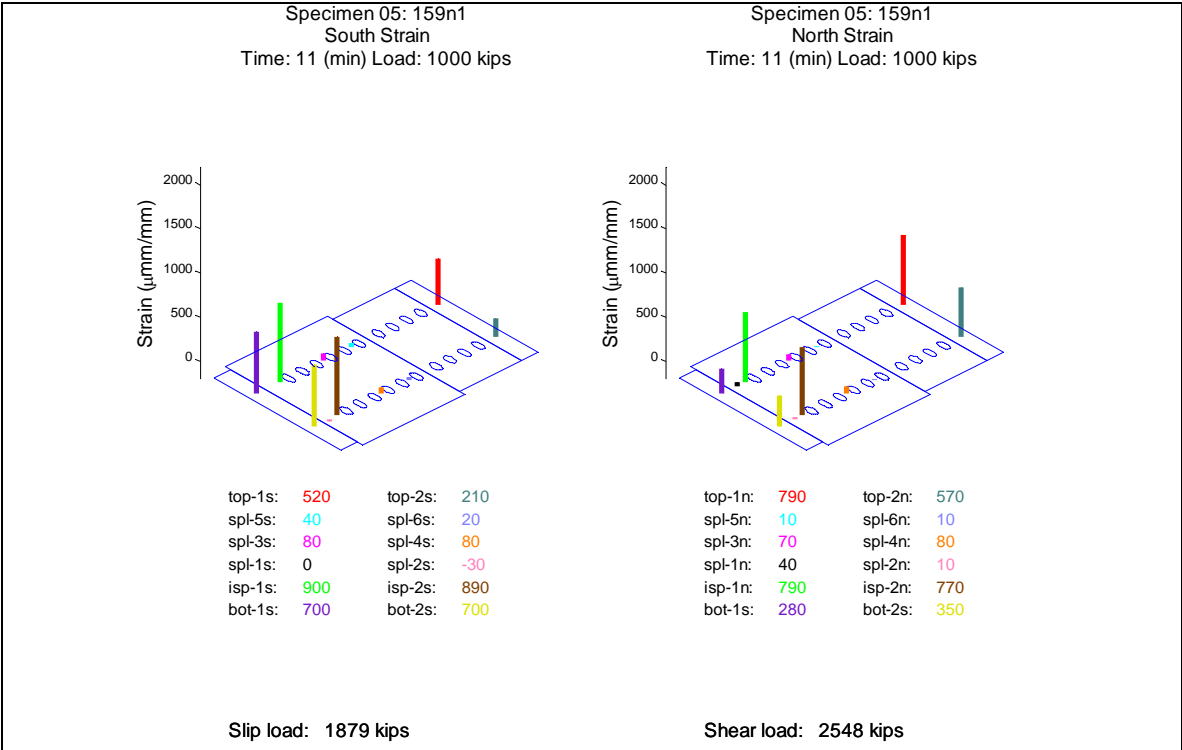


**Figure B.128 – 159n1: Strain distribution at 1,000 kips**

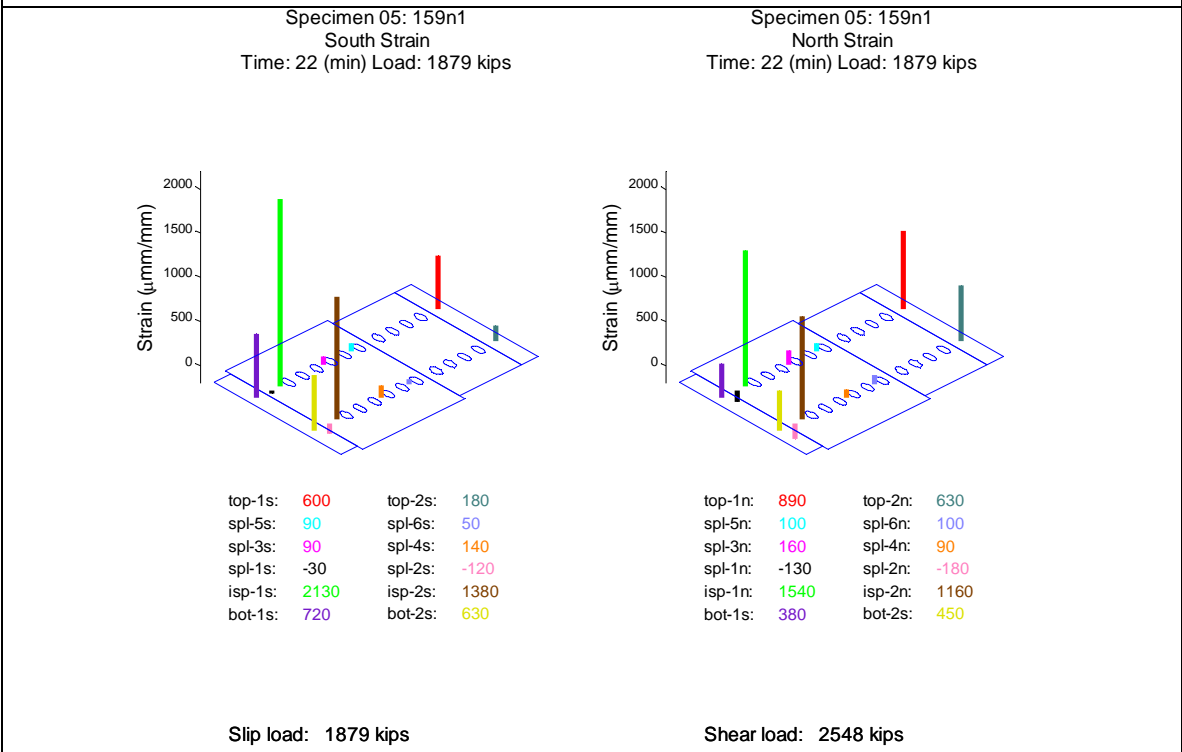


**Figure B.129 – 159n1: Strain distribution prior to slip at 1,879 kips**

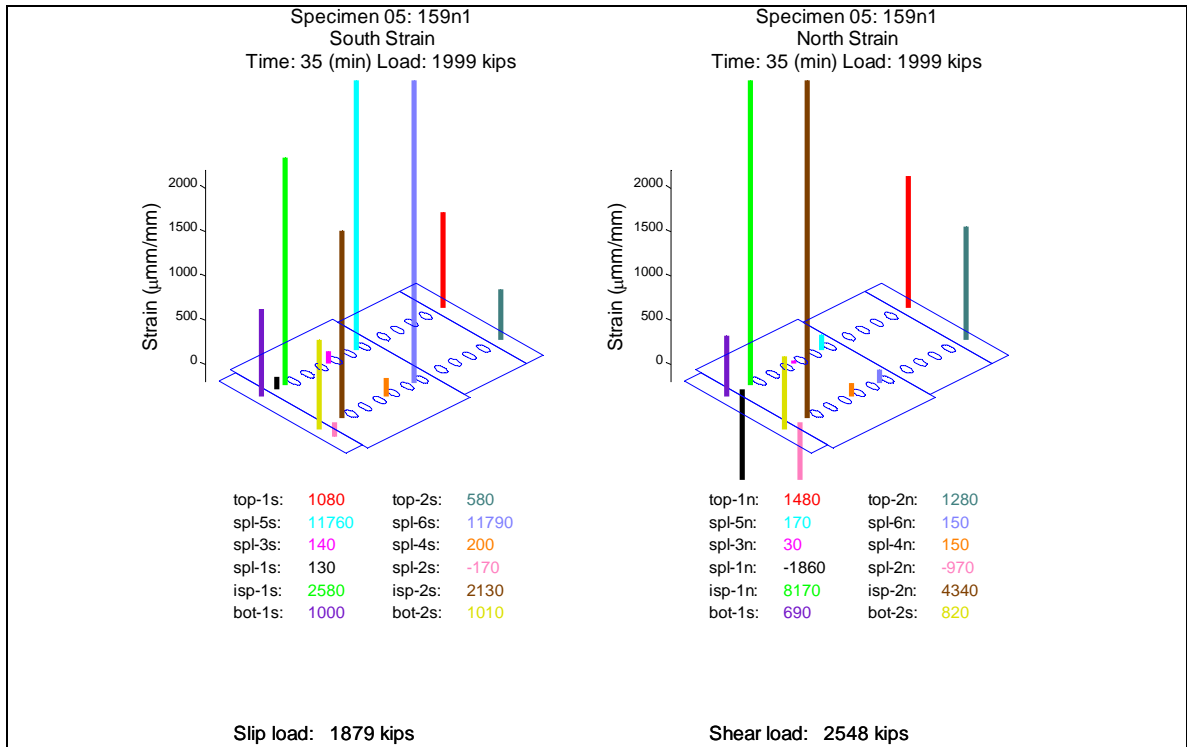


**Figure B.130 – 159n1: Strain distribution at 2,000 kips**

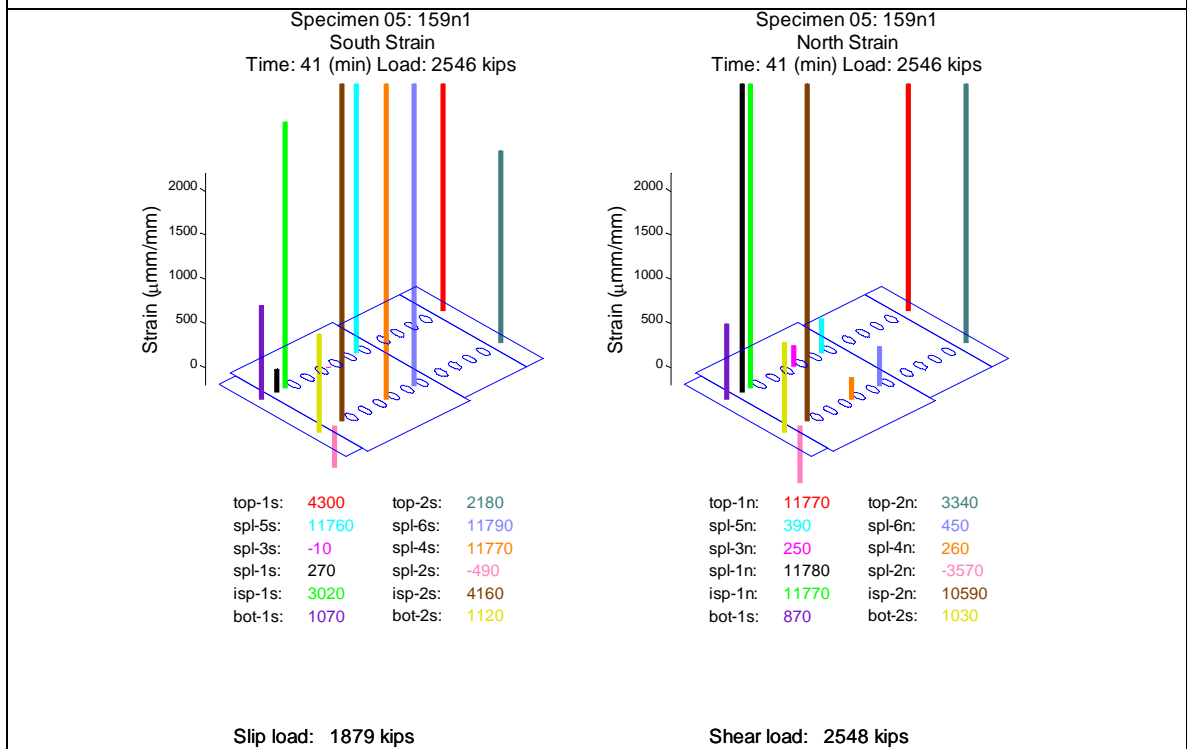


**Figure B.131 – 159n1: Strain distribution prior to shear at 2,548 kips**

## B.7 Specimen 159n2

Specimen 159n2 (Figure B.132 to Figure B.158) behaved approximately linearly until the observed slip load (1,704 kips). During the slip event, the relative displacement between the splice plate and the filler plate, as well as the filler plate and the top column increased suddenly. Slip initiated between the splice plate and the filler plate on the north side and between the filler plate and the top column on both the north and south sides of the specimen (Figure B.144). However, slip between the filler plate and the top column on the north side halted after 0.02 in. only to begin again later in the slip event. Over a period of 28 seconds, the relative displacements increased by the amounts shown in Table B.7. This is seen most clearly in the relative LVDTs (Figure B.147 and Figure B.148). During this dynamic event, the load dropped and increased several times. The lowest load measured was 962 kips (Figure B.137). The machine and specimen stabilized at 1,469 kips and the load was held for observation of the specimen (Figure B.138).

**Table B.7 – 159n2: Relative slip**

<b>Location</b>	<b>North</b>	<b>South</b>
<b>Between Splice and Filler</b>	0.50 in	0.40 in
<b>Between Filler and Top Column</b>	0.47 in	0.49 in
<b>Sum</b>	0.97 in	0.89 in

During this slip event, two bolts on the south side (SE5 and SW5) failed through the threads, indicating a pretension failure (Figure B.136). The bolt heads and shanks shot out of the specimen, leaving the south side with only 10 bolts. During fabrication, bolts SE5, SW5, and their neighboring bolts were retorqued as per Table B.2; these correlate with the bolts that failed prematurely.

Also during the slip event, it is likely that the bolts slipped into bearing on the top column, as the increase in stiffness in Figure B.139 shows at approximately a load of 1500 kips and a displacement of 1.0 inches. The maximum expected clearance in the holes based on the assembly was nominally  $2 * (5/16 \text{ inches}) = 0.625 \text{ inches}$ . During the slip event, the west strain gage at bolt row 4 on the south splice plate (06spl-3s) and the east strain gage inside of the north splice plate (06isp-2n) were damaged (Figure B.151 and Figure B.153).

The top column began to yield at approximately 2,400 kips (Figure B.149), damaging the southwest strain gage on the top column (top-1s) (Figure B.149). Upon further loading, the bolts, now experiencing shear, yielded and eventually failed at the observed bolt shear load (2,616 kips) (Figure B.133, Figure B.134 and Figure B.135). The ten remaining bolts through the splice plate on the south flange of the top column failed simultaneously, leaving the twelve bolts through the splice plate on the north flange of the top column intact on the specimen.

After slip, the specimen produced clanging noises every 5 kips. At 1900 kips the clanging noises were produced every 2 kips. Noises believed to be produced by the testing machine were neglected. The noises are likely associated with additional small slip events, bolts coming into bearing with the bolt holes, or possibly initiation of fractures within the bolts.

The signal box for the actuator stroke measurement was not turned on at the start of the test. It was turned on at a load of approximately 600k, consequently any actuator stroke data before this load is invalid.

The splice plate LVDTs (Figure B.141 and Figure B.142) showed a dynamic increase or decrease in displacement during the slip events. This may be due to a number of reasons, including stress relief in the splice plates after slip, very small slips relative to the column flanges, or small dynamic vibrations (with resulting small permanent offsets) of the LVDT holders, but the displacements are an order of magnitude smaller than the primary slip displacements (Figure B.143 and Figure B.144) and are not likely to indicate significant behavior.

Figure B.145 and Figure B.146 compare the LVDTs directly measuring relative slip between the filler plate and either the top column (Figure B.143) or the splice plate (Figure B.144) with the difference between the average of the two LVDTs on either filler plate at that same cross section as the LVDTs on the top column (Figure B.140) and either the average of the two LVDTs at the bottom center of the top column (Figure B.139) or the average of the two LVDTs on either splice plate at that same cross section as the LVDTs on the top column (Figure B.141). The measurements of the relative LVDTs correspond well to the difference between the corresponding absolute LVDTs.

For this specimen, strain gages were attached to the inside face of the splice plate in the gap between the top and bottom columns (Figure B.153). These measurements, when compared to the measurements from the outside face of the splice plate (Figure B.152), indicate significant bending in the splice plates, particularly on the south side. Yielding was recorded on the inside of the splice plate.

The top column strain gages (Figure B.149) indicate that the localized introduction of load had a small loading bias towards the west. The bottom column strain gages (Figure B.154) show that the localized reaction on the south side was more heavily loaded.

The splice plate strain gages (Figure B.150, Figure B.151, Figure B.152 and Figure B.153) indicate the south side of the specimen is more heavily loaded. This is consistent with the decreased displacement present on the south side (Figure B.144). This caused the specimen to ultimately fail on the south side. Snapshots of the specimen strain at 1000 kips, immediately prior to slip, 2000 kips and immediately prior to shear are visually presented in Figure B.155, Figure B.156, Figure B.157 and Figure B.158, respectively. These graphs show that the strain enters into the splice plate gradually and relatively uniformly from bolt row 6 to bolt row 1 throughout the experiment.

The experiment was executed in load control. The loading rate for the experiment was approximately 1 kip per second. One elastic cycle was executed prior to the test, going up to a load of 200 kips and returning to zero load, to verify instrumentation. During this elastic cycle and during the start of the main test, the load was stopped at several predetermined load values to record the deformation of the crosshead. The data collection rate for the experiment was held constant at 10 Hertz (10 sets of readings per second).



**Figure B.132 – 159n2: Before test (east side)**

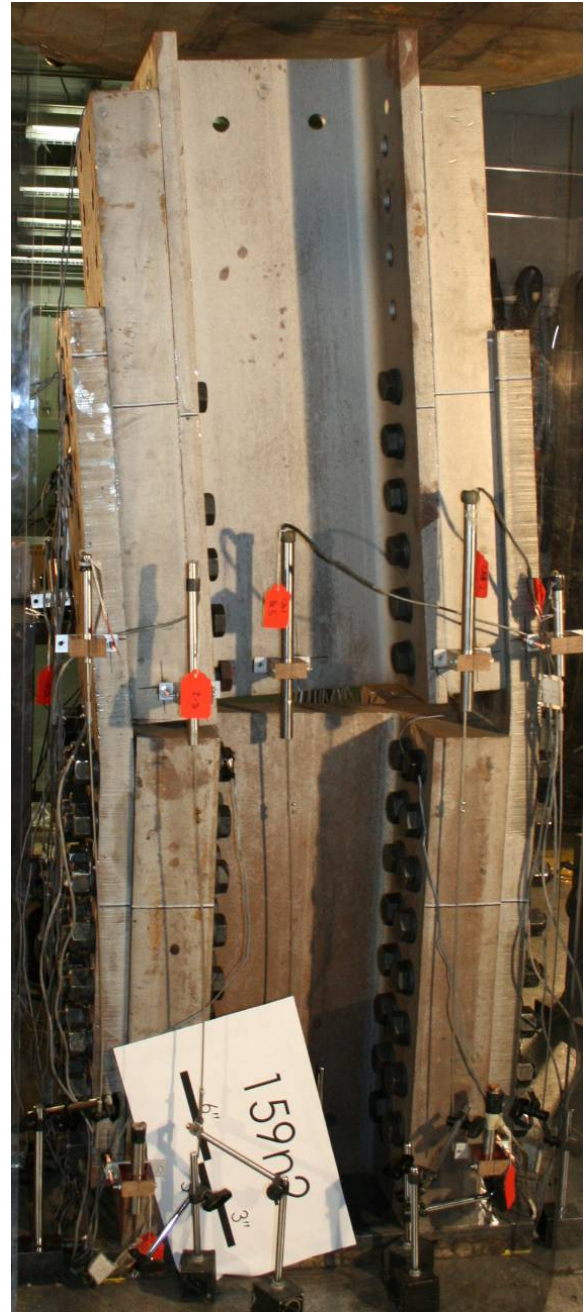


**Figure B.133 – 159n2: After test (east side)**

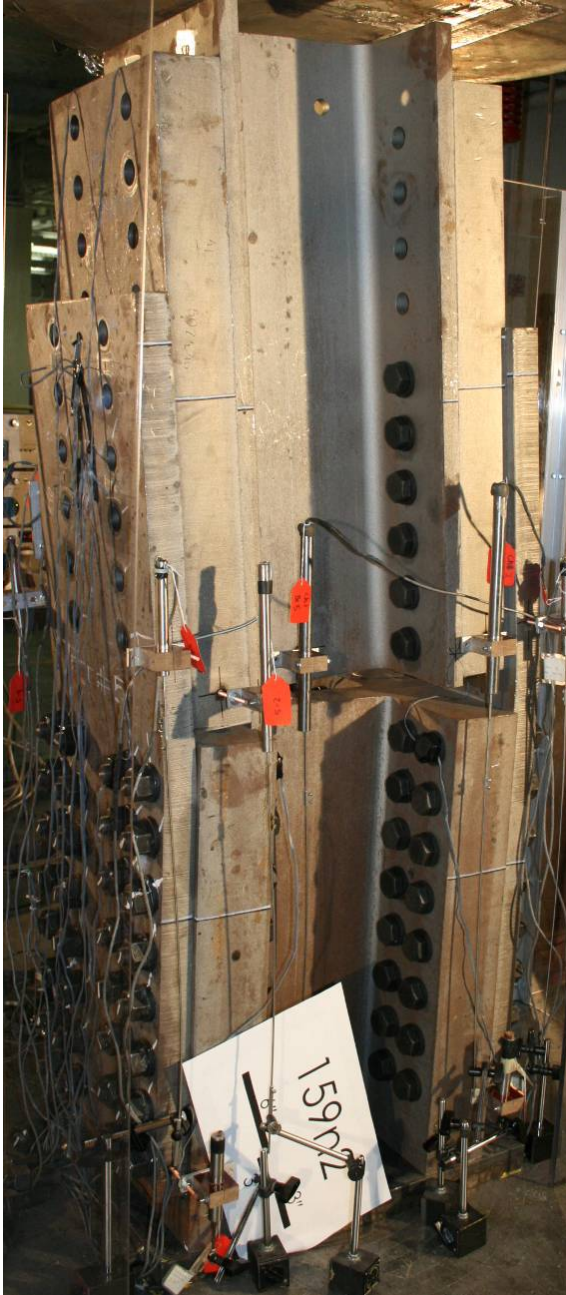


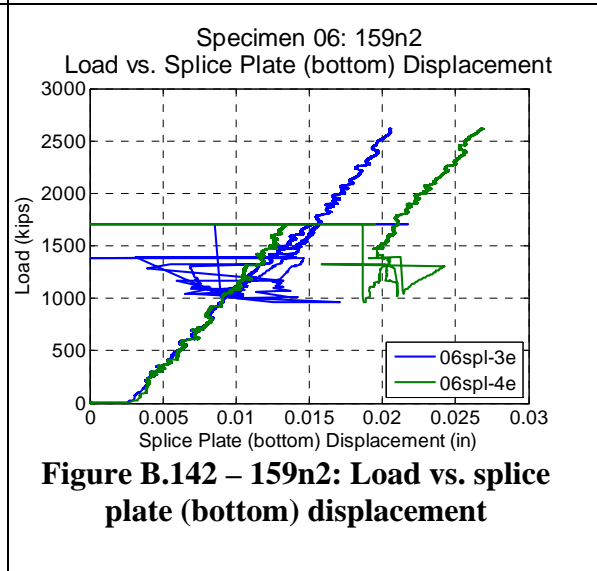
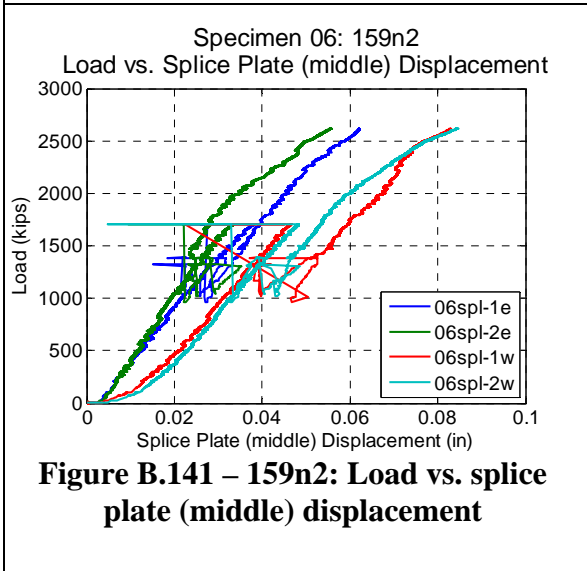
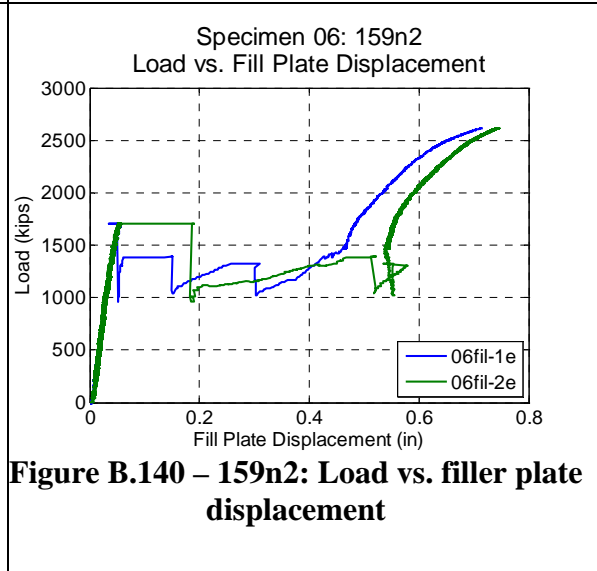
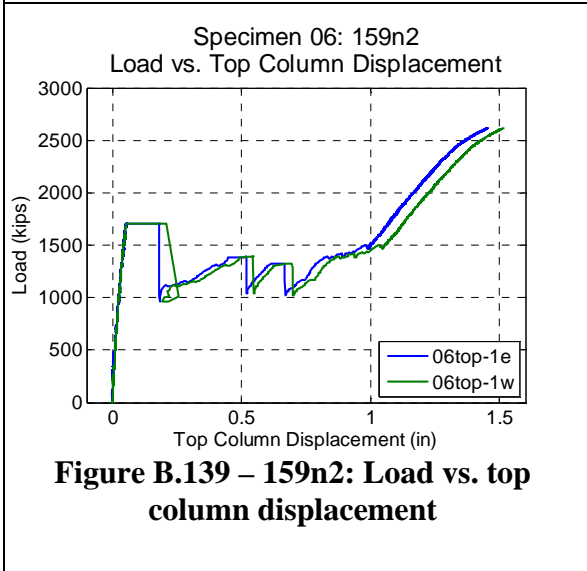
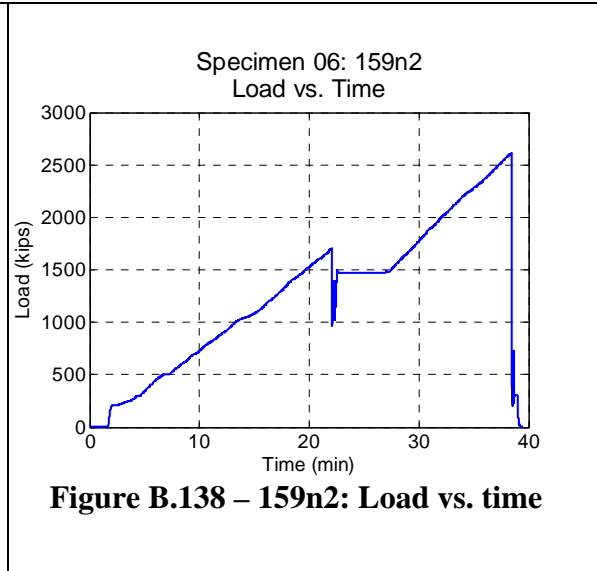
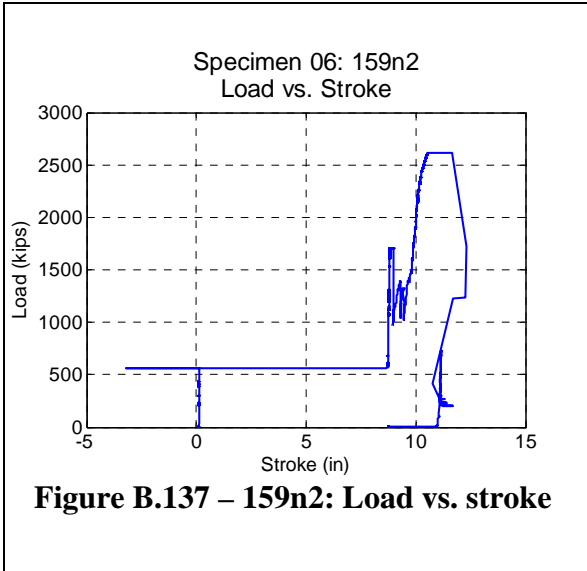
**Figure B.134 – 159n2: After test (east side)**

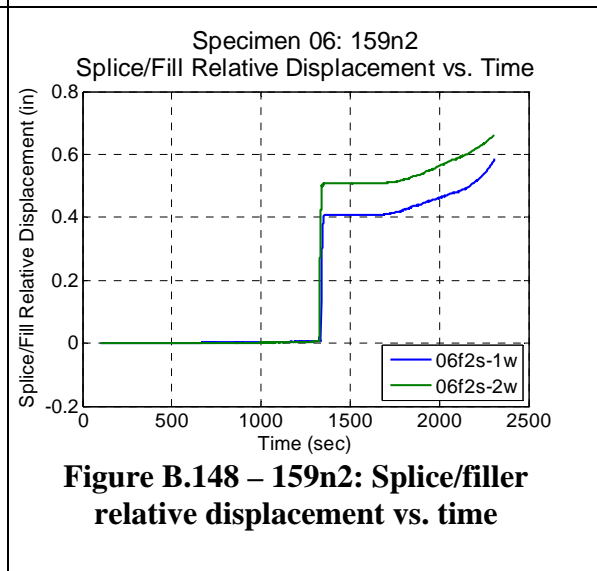
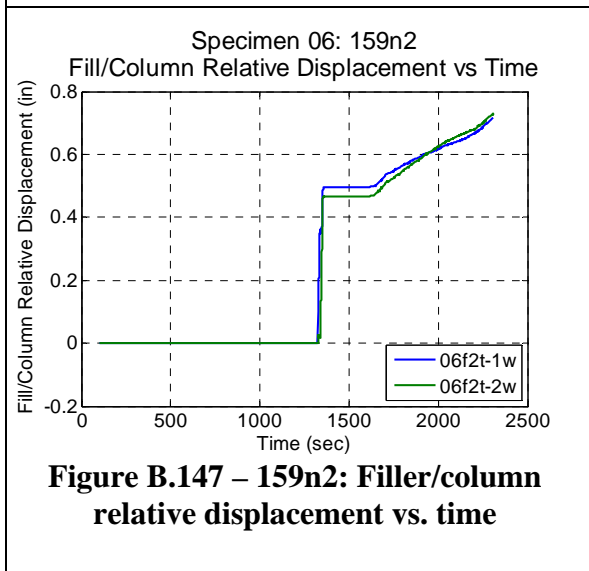
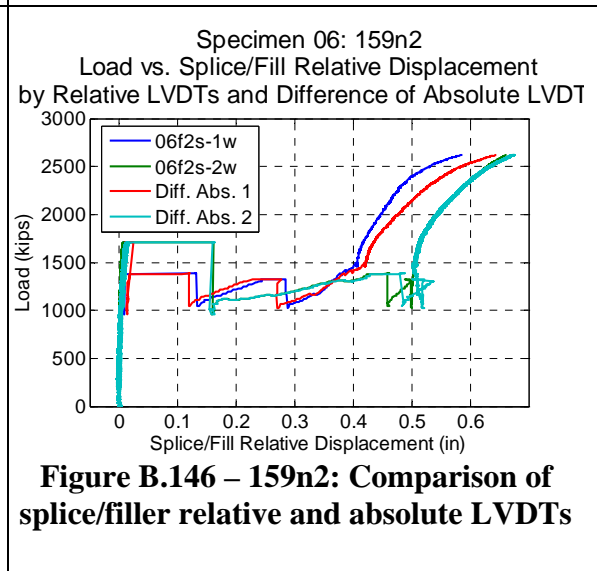
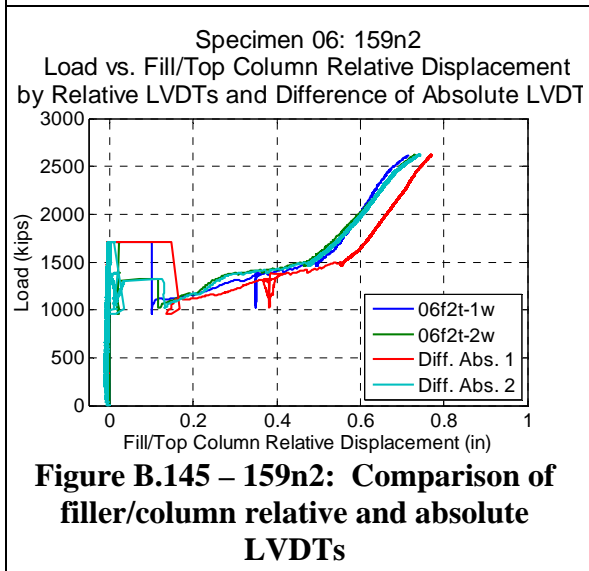
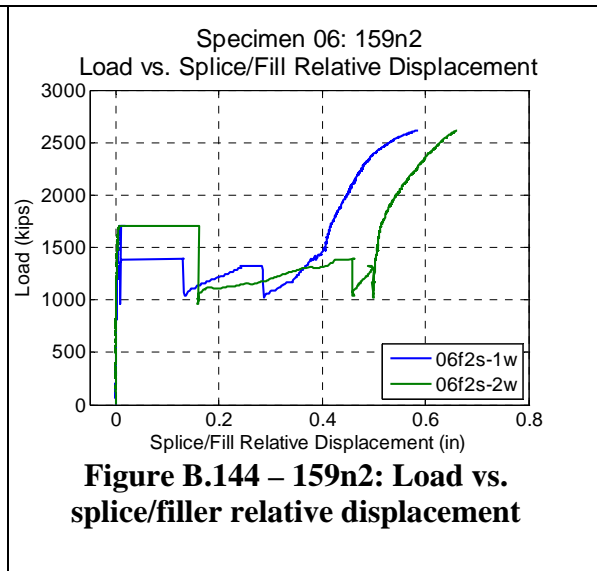
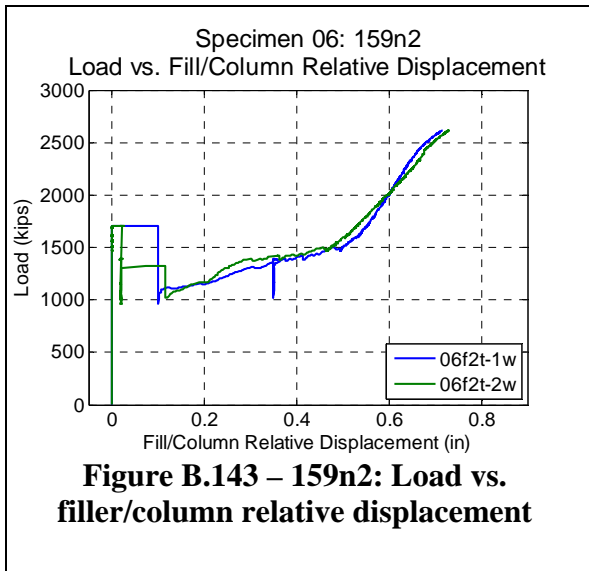


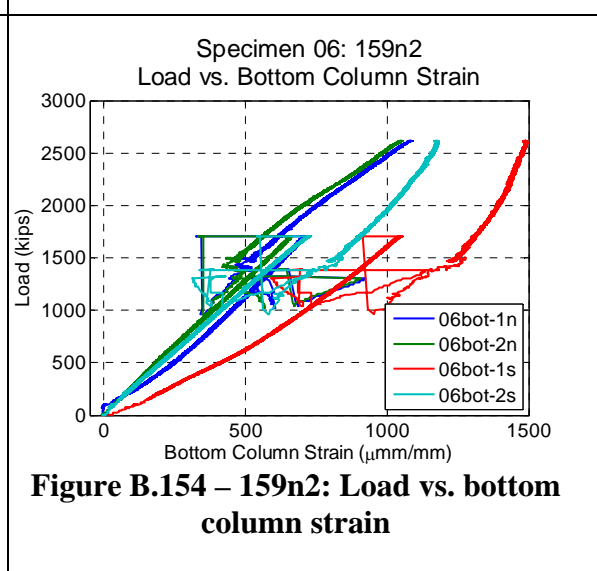
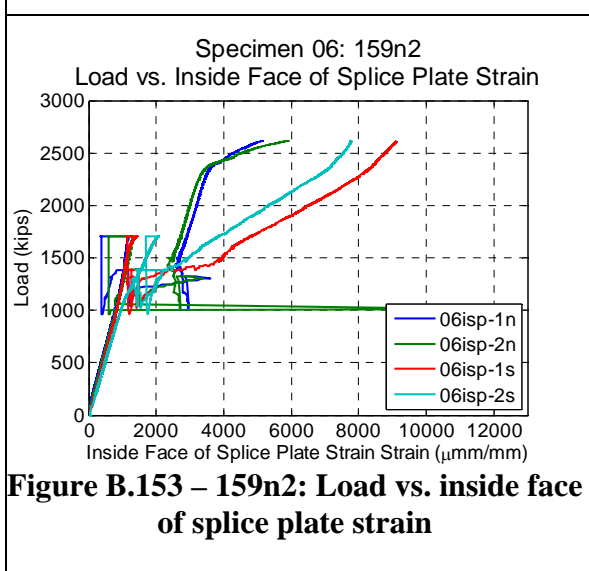
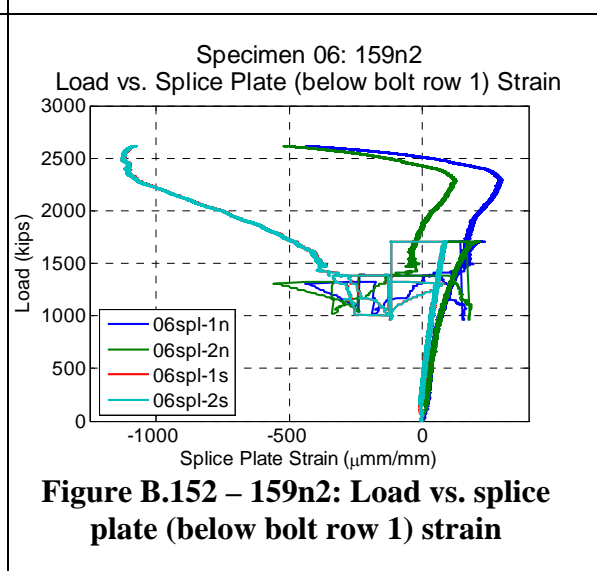
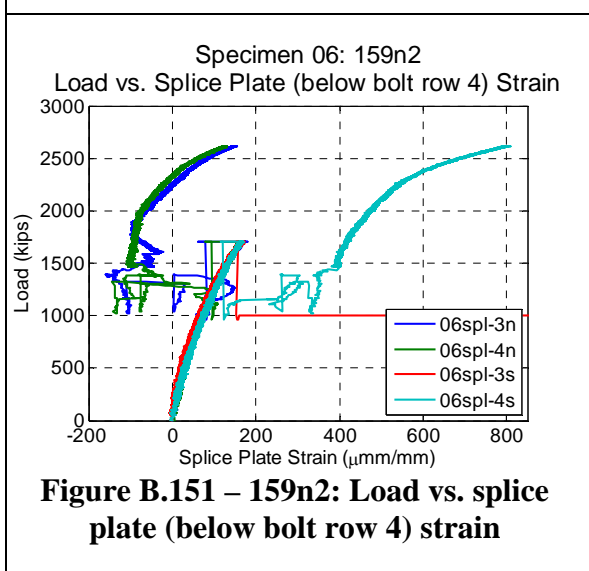
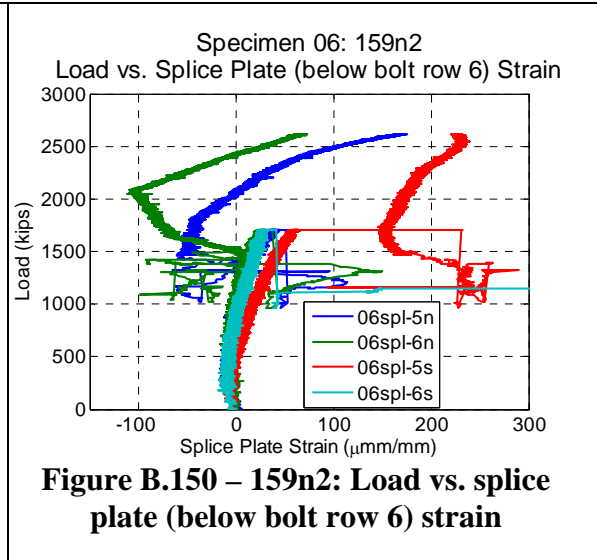
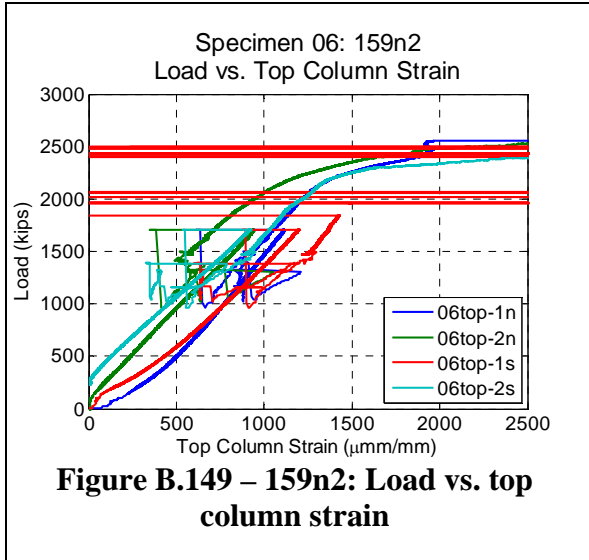
**Figure B.135 – 159n2: After test (south side)**

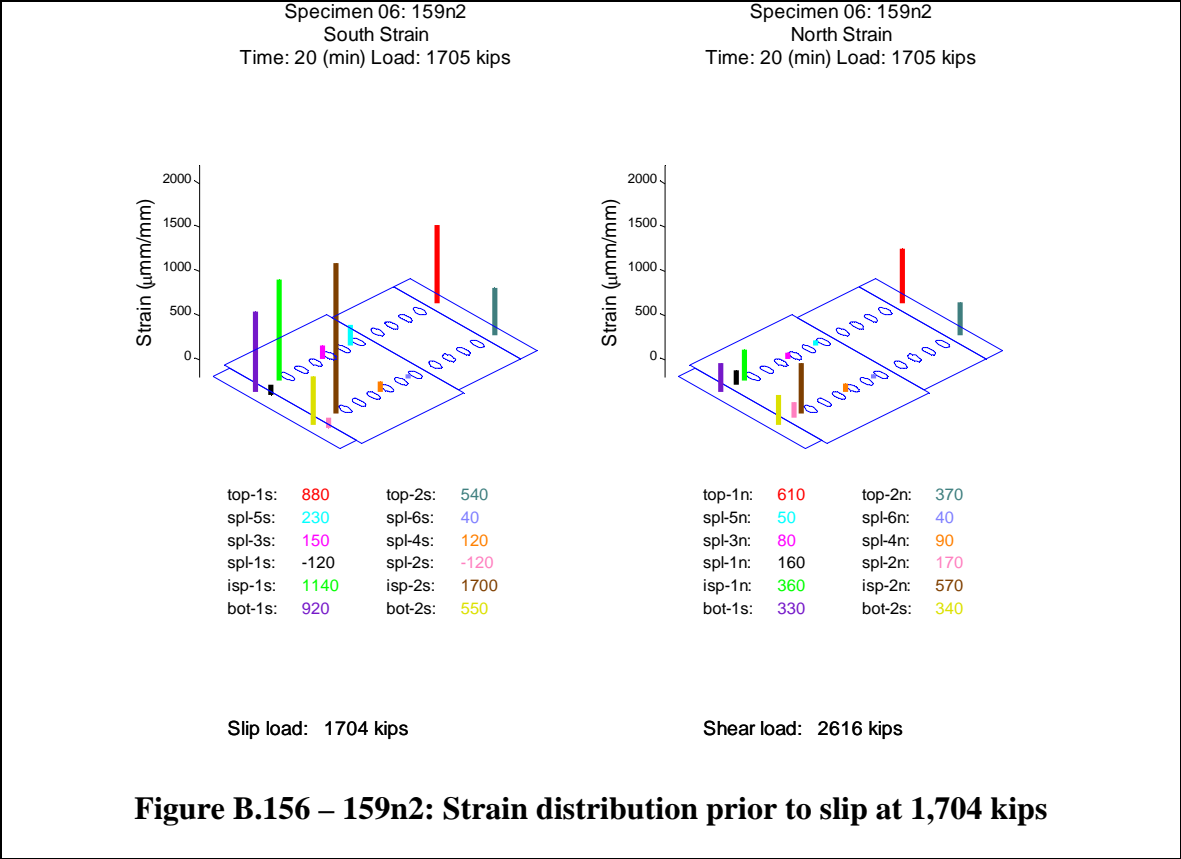
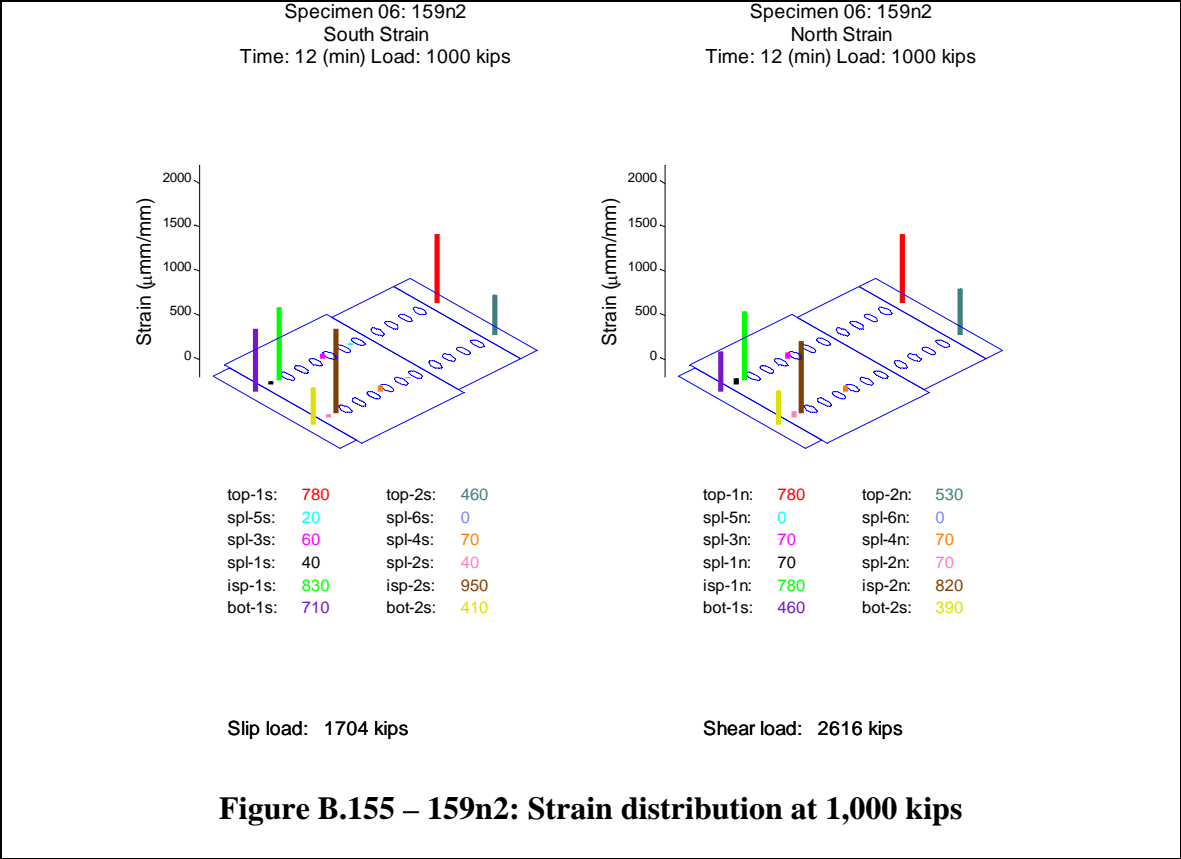


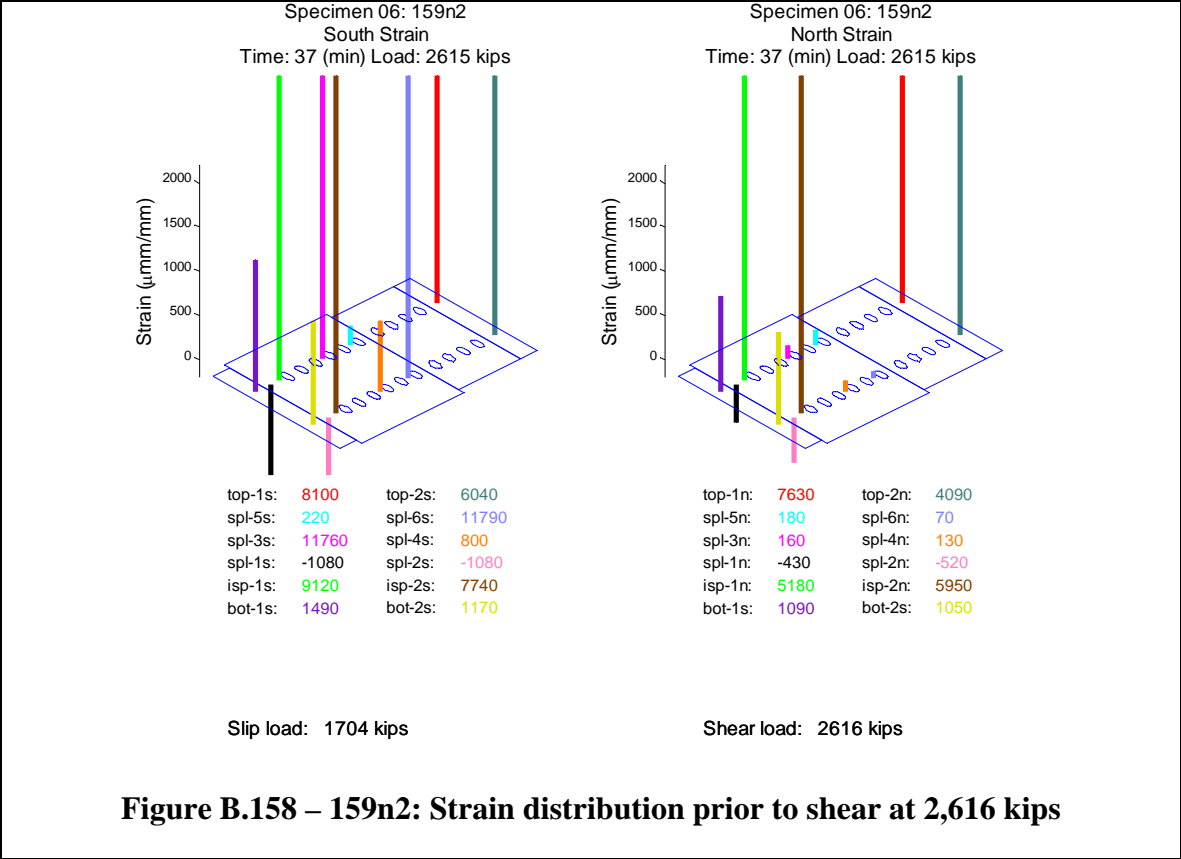
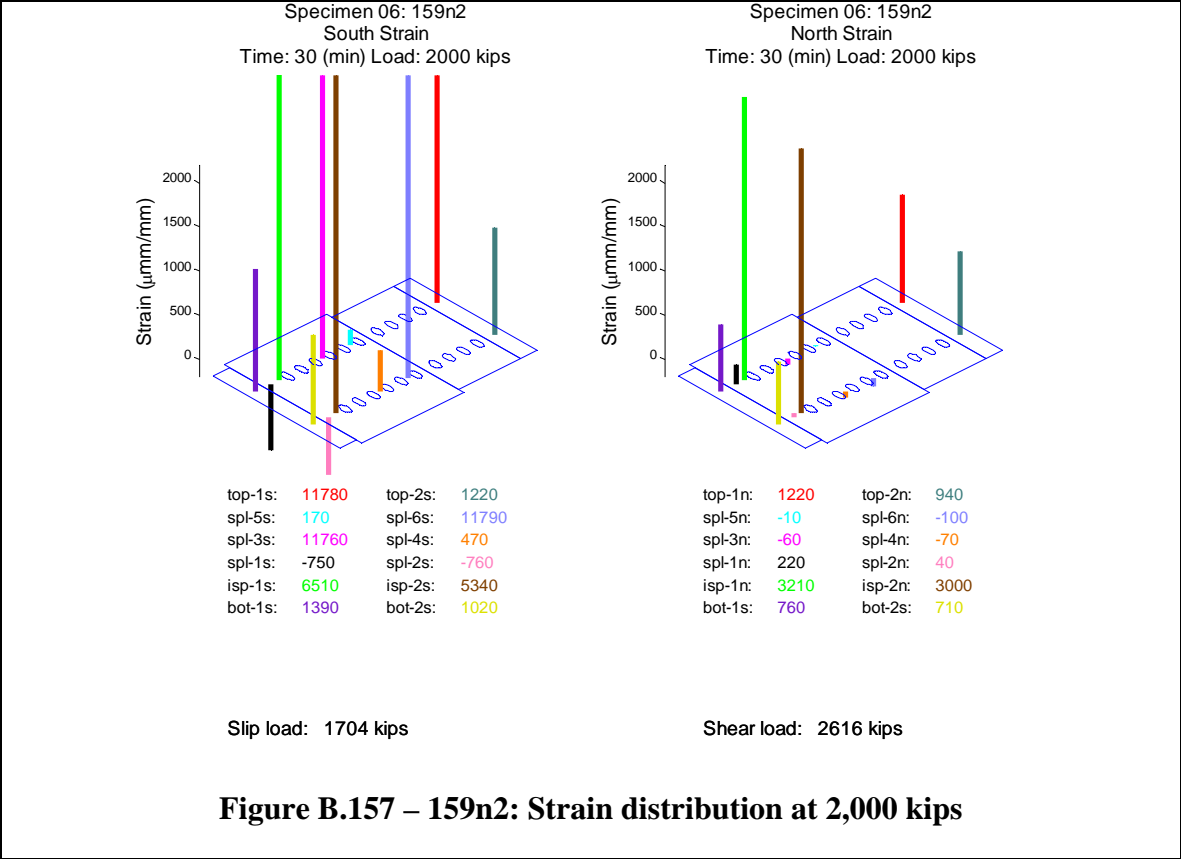
**Figure B.136 – 159n2: After slip (south side)**











## B.8 Specimen 455f

Specimen 455f (Figure B.159) behaved approximately linearly until the observed slip load (1,369 kips). During the slip event, the relative displacement between the splice plate and the filler plate, as well as the filler plate and the top column increased suddenly. Slip initiated between the splice plate and the filler plate on the both the north and south sides of the specimen. Over a period of 23 seconds, the relative displacements increased by the amounts shown in Table B.8. This is seen most clearly in the relative LVDTs (Figure B.173 and Figure B.174). During this dynamic event, the load dropped and increased several times. The lowest load measured was 743 kips (Figure B.163). The machine and specimen stabilized at 1,337 kips and the load was held for observation of the specimen (Figure B.164).

**Table B.8 – 455f: Relative slip**

<b>Location</b>	<b>North</b>	<b>South</b>
<b>Between Splice and Filler</b>	0.36 in	0.47 in
<b>Between Filler and Top Column</b>	0.39 in	0.28 in
<b>Sum</b>	0.75 in	0.75 in

During the slip event, it is likely that the bolts slipped into bearing on the top column, as the increase in stiffness in Figure B.165 shows at approximately a load of 1,250 kips and a displacement of 0.75 inches. The maximum expected clearance in the holes based on the assembly was nominally  $2 * (5/16 \text{ inches}) = 0.625 \text{ inches}$ .

Upon further loading, the bolts, now experiencing shear, yielded and eventually failed at the observed bolt shear load (2,428 kips) (Figure B.160, Figure B.161 and Figure B.162). The twelve bolts through the splice plate on the south flange of the top column failed simultaneously, leaving the twelve bolts through the splice plate on the north flange of the top column intact on the specimen. Noises from the specimen, which had started after the slip event, dramatically increased in frequency immediately before shear failure. Once the twelve bolts on the south flange failed, the relative movement of the splice plate to the filler plate caused the failure of two additional bolts through the filler plate, knocking these nuts and bolt shanks off through the bolt threads (Figure B.162).

After slip, the specimen produced pinging noises at the following loads; 1412, 1424, 1440, 1456, 1482, 1487, 1503, 1528, 1542, 1574, 1600, 1613, 1655, 1704, 1730, 1736, 1750, 1820, 1823, 1840, 1857, 1884, 1977, 1987, 2000, 2008, 2017, 2026, 2036, 2050, 2052, 2061, 2073, 2080, 2086, 2097, 2104 (higher pitched), 2111, 2123, 2132, 2150, 2168, 2174, 2185, 2191, 2197, 2205, 2207, 2213, 2219, and 2220 (higher pitched) kips. Noises continued occurring every 3 to 4 kips. Noises believed to be produced by the testing machine were neglected. The noises are likely associated with additional small

slip events, bolts coming into bearing with the bolt holes, or possibly initiation of fractures within the bolts.

The splice plate LVDTs (Figure B.167 and Figure B.168) showed a dynamic increase or decrease in displacement during the slip events. This may be due to a number of reasons, including stress relief in the splice plates after slip, very small slips relative to the column flanges, or small dynamic vibrations (with resulting small permanent offsets) of the LVDT holders, but the displacements are an order of magnitude smaller than the primary slip displacements (Figure B.170 and Figure B.171) and are not likely to indicate significant behavior.

Figure B.171 and Figure B.172 compare the LVDTs directly measuring relative slip between the filler plate and either the top column (Figure B.169) or the splice plate (Figure B.170) with the difference between the average of the two LVDTs on either filler plate at that same cross section as the LVDTs on the top column (Figure B.166) and either the average of the two LVDTs at the bottom center of the top column (Figure B.165) or the average of the two LVDTs on either splice plate at that same cross section as the LVDTs on the top column (Figure B.167). The measurements of the relative LVDTs correspond well to the difference between the corresponding absolute LVDTs.

For this specimen, strain gages were attached to the inside face of the splice plate in the gap between the top and bottom columns (Figure B.179). These measurements, when compared to the measurements from the outside face of the splice plate (Figure B.178), indicate slight bending in the splice plates. Minor yielding was recorded on the inside of the splice plate.

The top column strain gages show that the localized introduction of load was more heavily loaded on the northwest side (Figure B.175). The bottom column strain gages indicate that the localized reaction was more heavily loaded on the south side (Figure B.182).

The splice plate was slightly biased toward the west side (Figure B.176, Figure B.177, Figure B.178 and Figure B.179). Nevertheless, this eccentricity had largely dissipated within the splice plate below the first row of bolts (Figure B.178 and Figure B.179). The filler plate was relatively uniformly loaded (Figure B.180 and Figure B.181). Snapshots of the specimen strain at 1000 kips, immediately prior to slip, 2000 kips and immediately prior to shear are visually presented in Figure B.183, Figure B.184, Figure B.185 and Figure B.186, respectively. These graphs show that the strain enters into the filler plate and then into the splice plate gradually and relatively uniformly from bolt row 6 to bolt row 1 throughout the experiment.

The experiment was executed in load control. The loading rate for the experiment was approximately 1 kip per second. One elastic cycle was executed prior to the test, going up to a load of 200 kips and returning to zero load, to verify instrumentation. The data collection rate for the experiment was held constant at 10 Hertz (10 sets of readings per second).

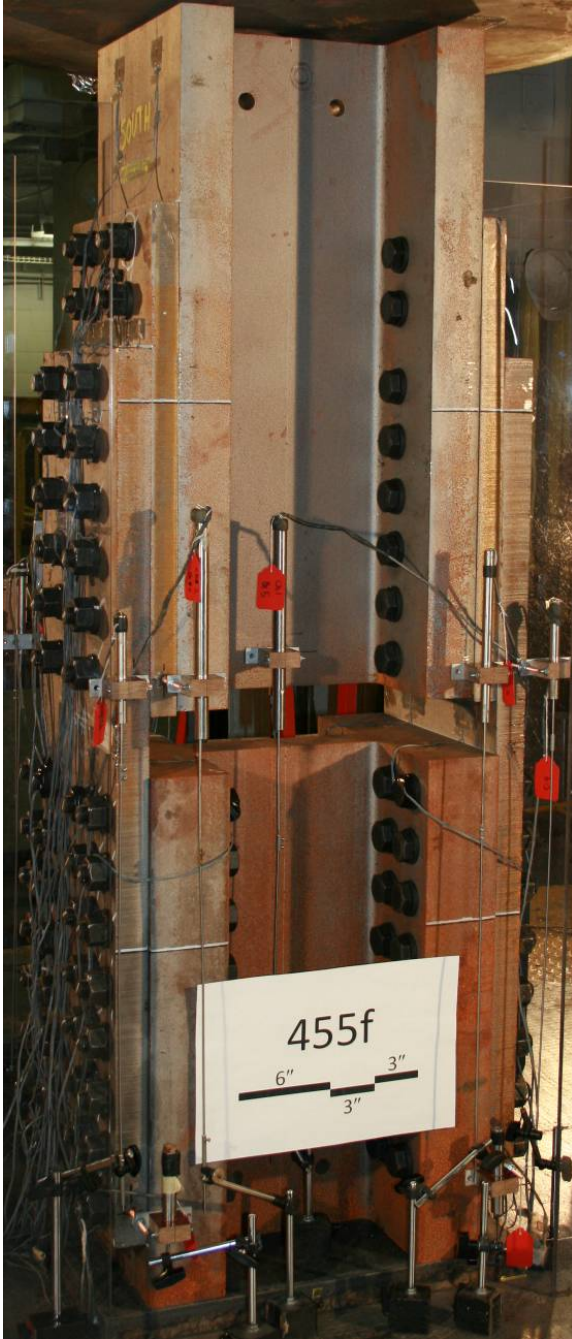


**Figure B.159 – 455f: Before test (east side)**



**Figure B.160 – 455f: After test (east side)**



Figure B.161 – 455f: After test (east side)

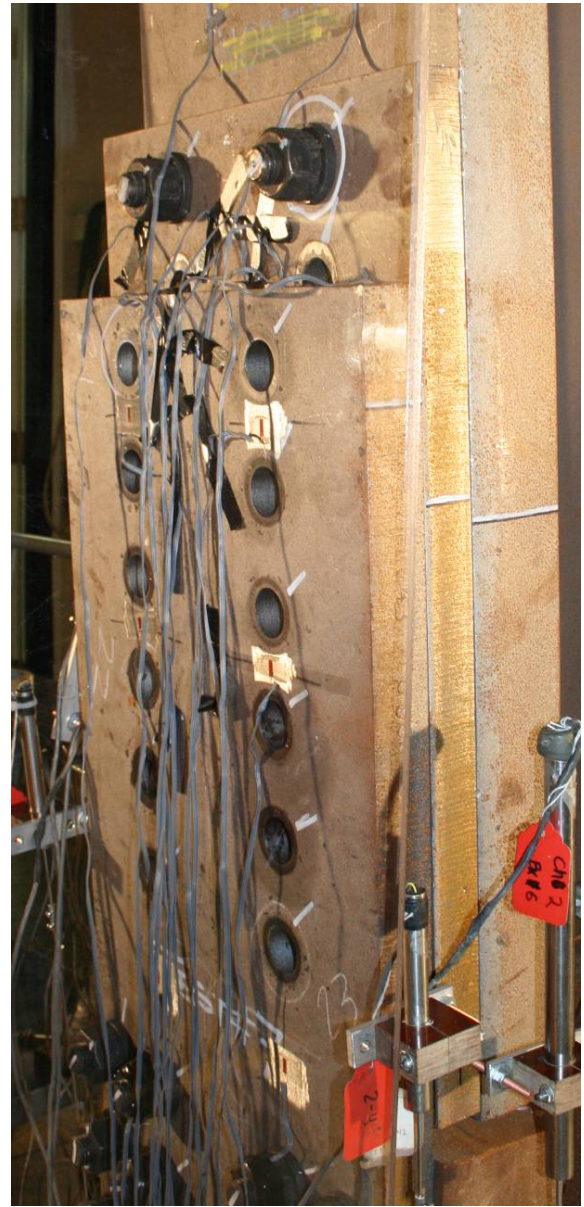
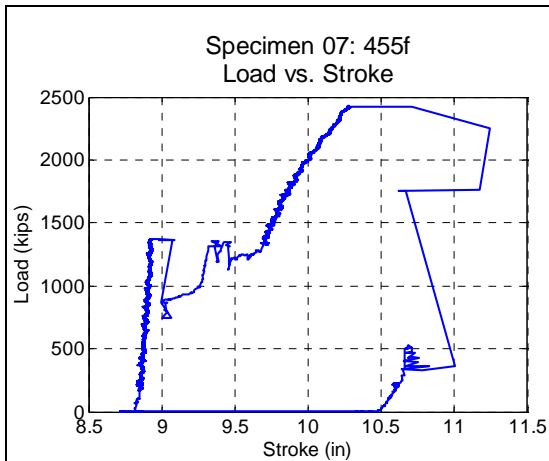
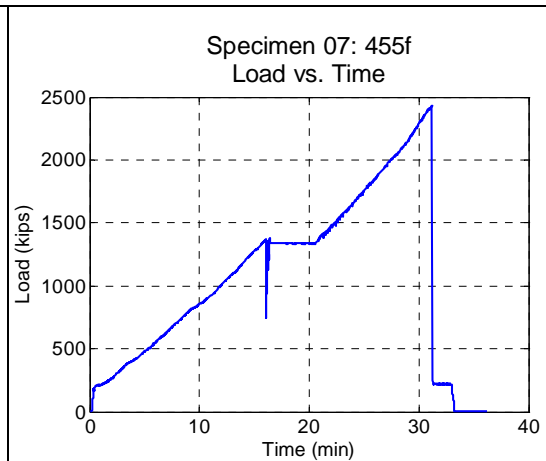


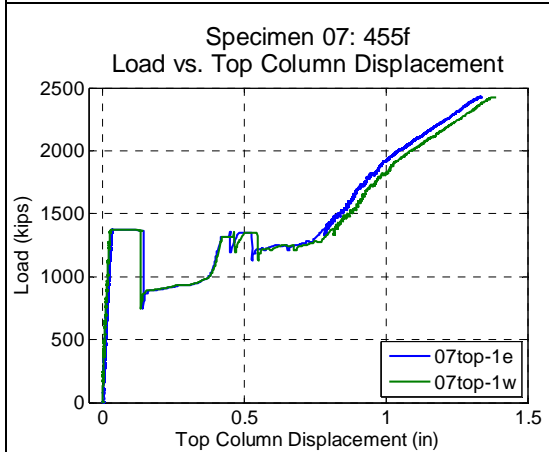
Figure B.162 – 455f: After test (south side)



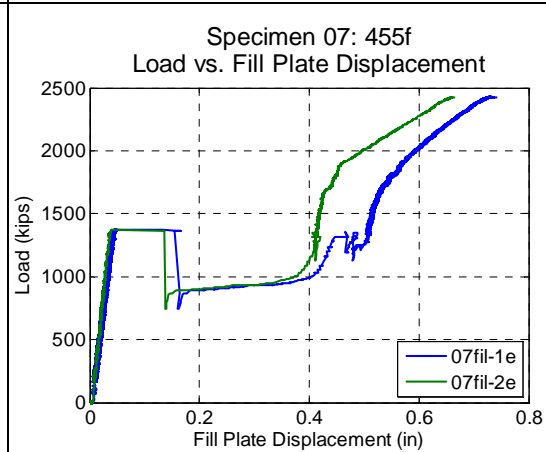
**Figure B.163 – 455f: Load vs. stroke**



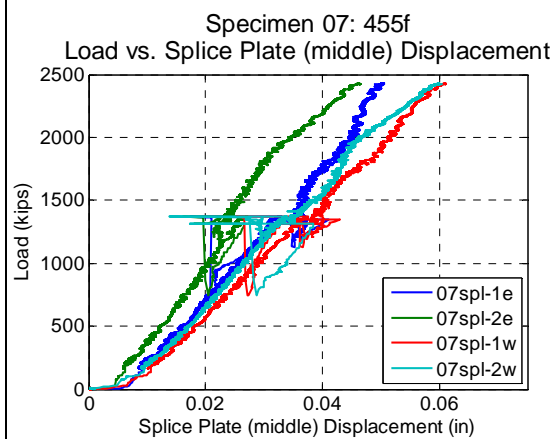
**Figure B.164 – 455f: Load vs. time**



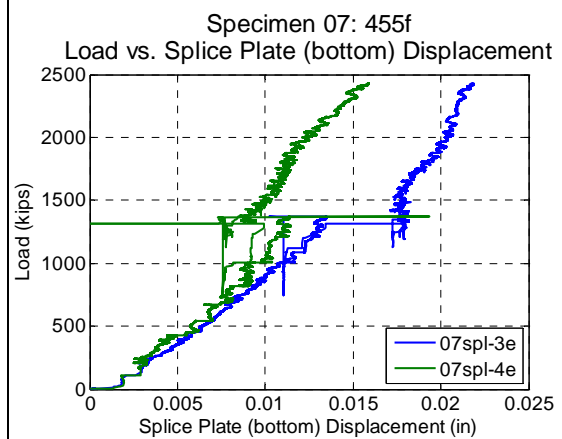
**Figure B.165 – 455f: Load vs. top column displacement**



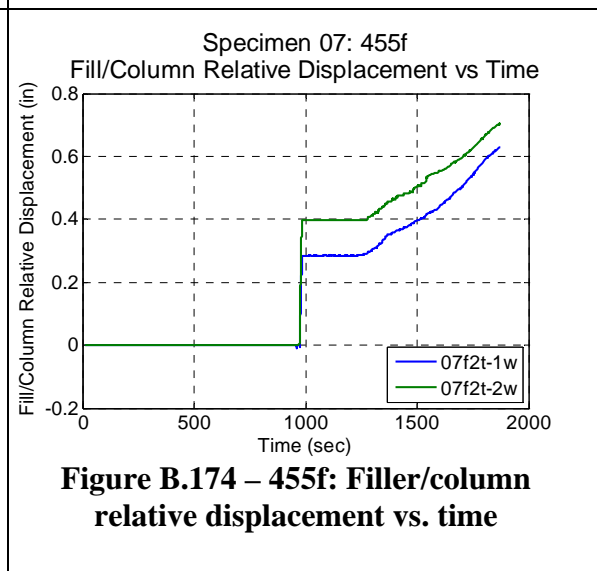
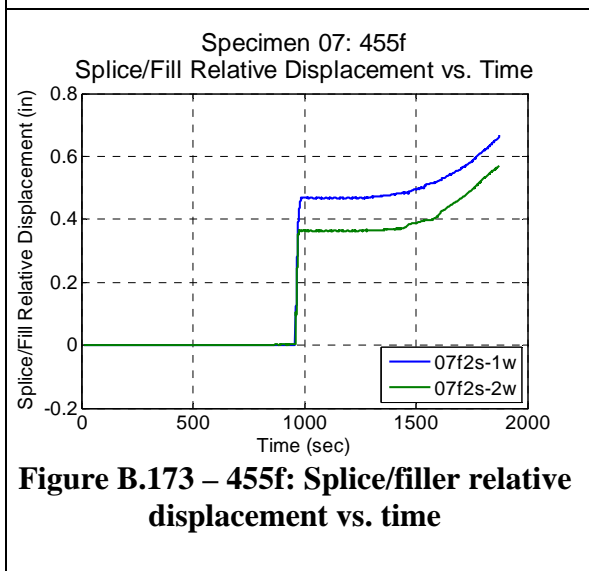
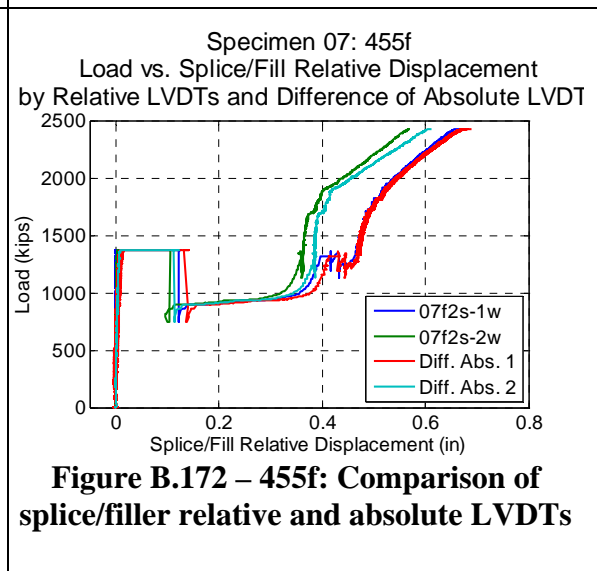
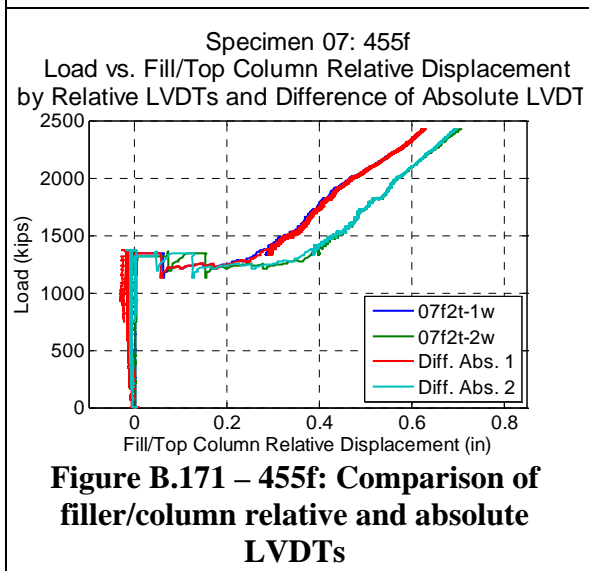
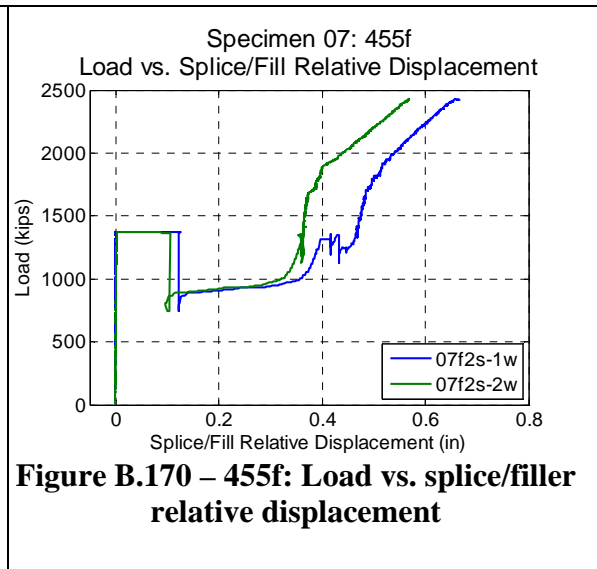
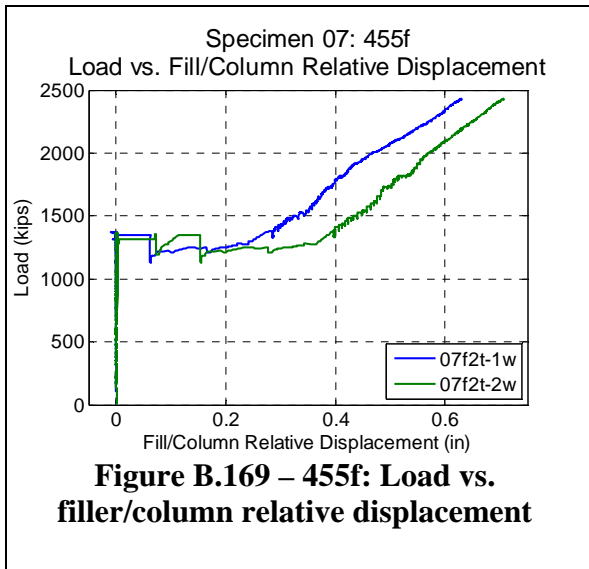
**Figure B.166 – 455f: Load vs. Filler plate displacement**

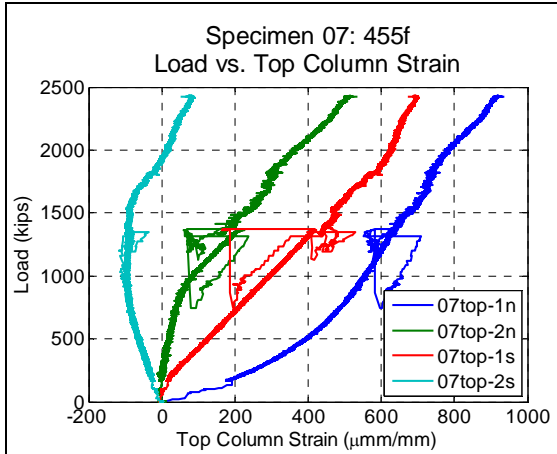


**Figure B.167 – 455f: Load vs. splice plate (middle) displacement**

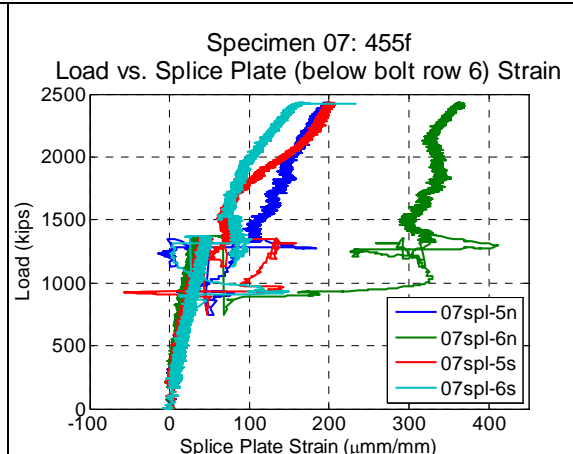


**Figure B.168 – 455f: Load vs. splice plate (bottom) displacement**

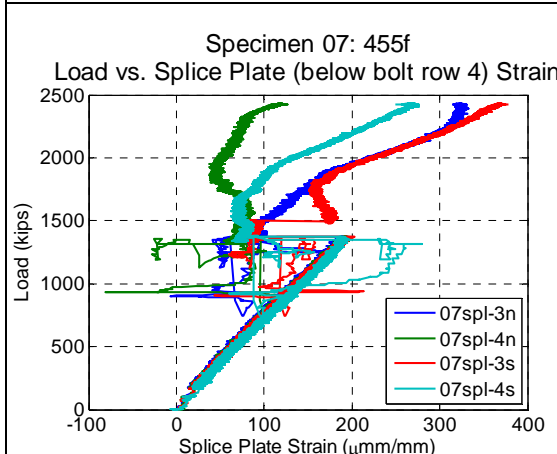




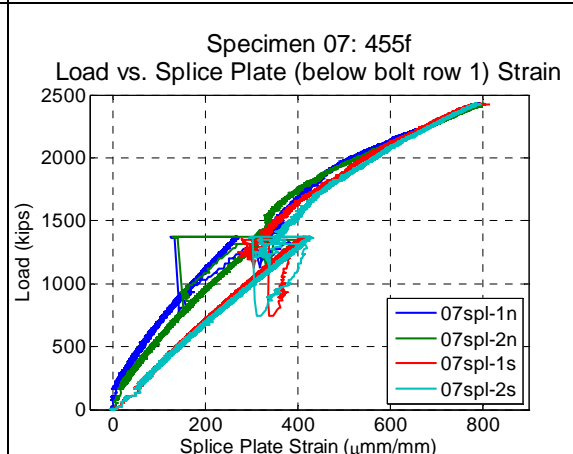
**Figure B.175 – 455f: Load vs. top column strain**



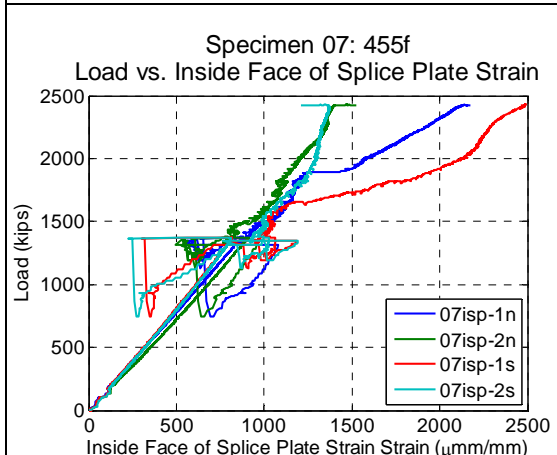
**Figure B.176 – 455f: Load vs. splice plate (below bolt row 6) strain**



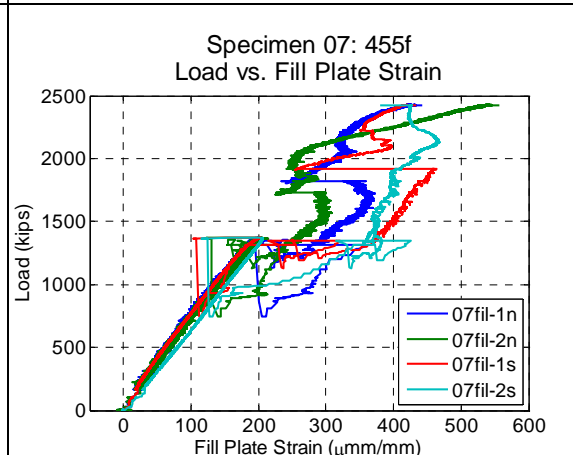
**Figure B.177 – 455f: Load vs. splice plate (below bolt row 4) strain**



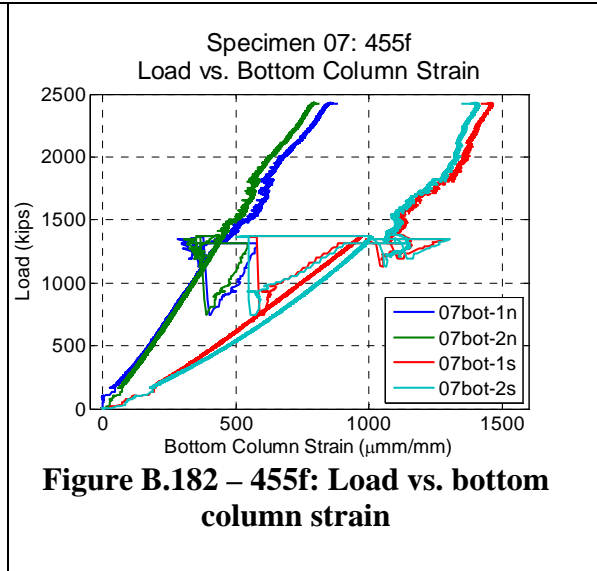
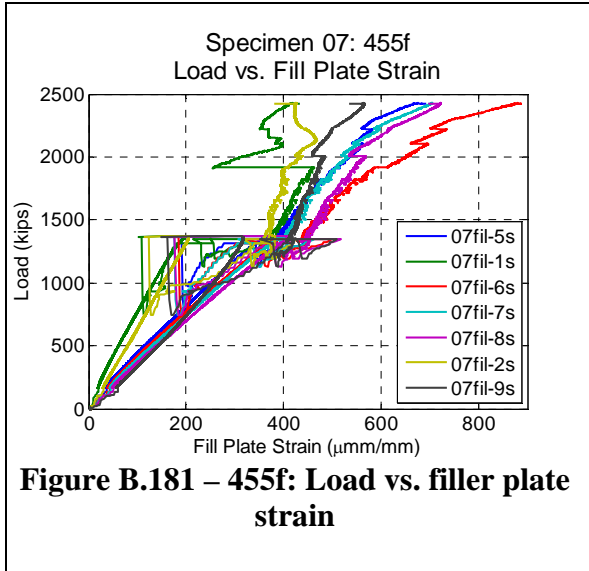
**Figure B.178 – 455f: Load vs. splice plate (below bolt row 1) strain**

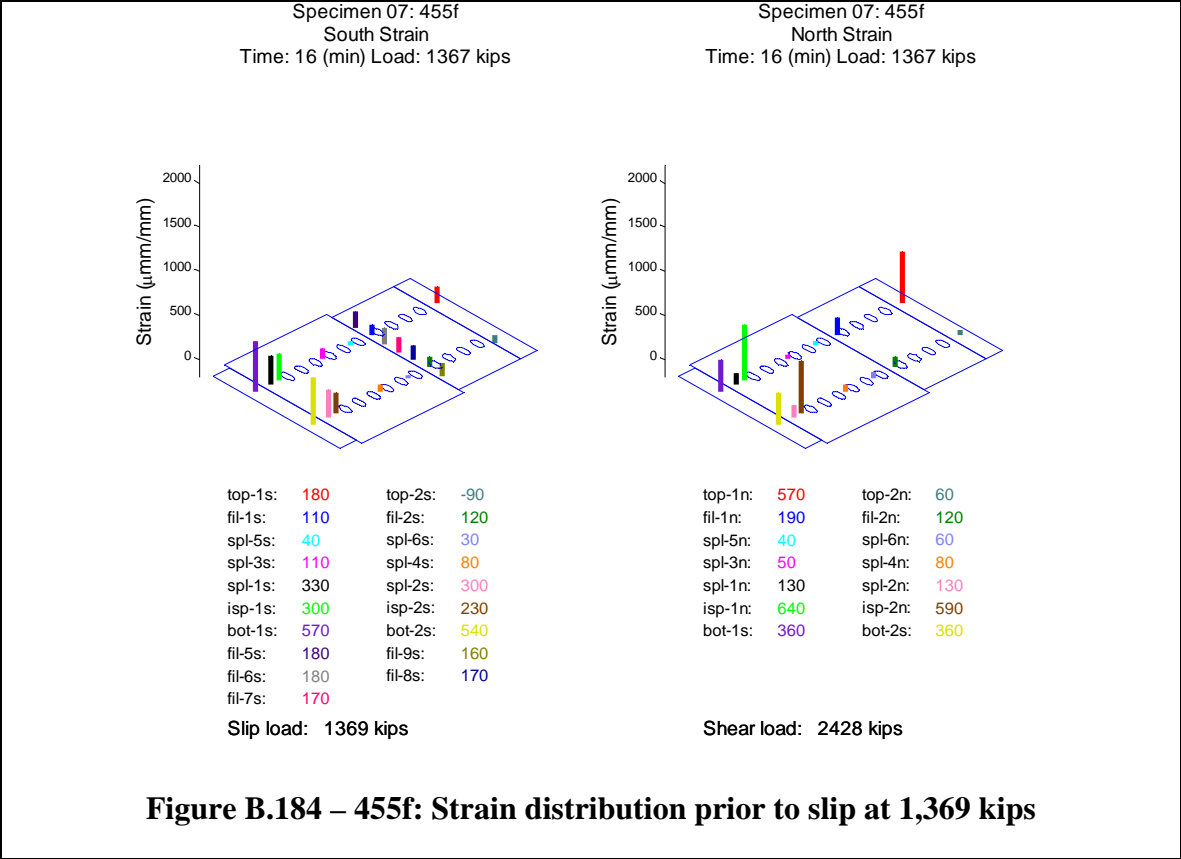
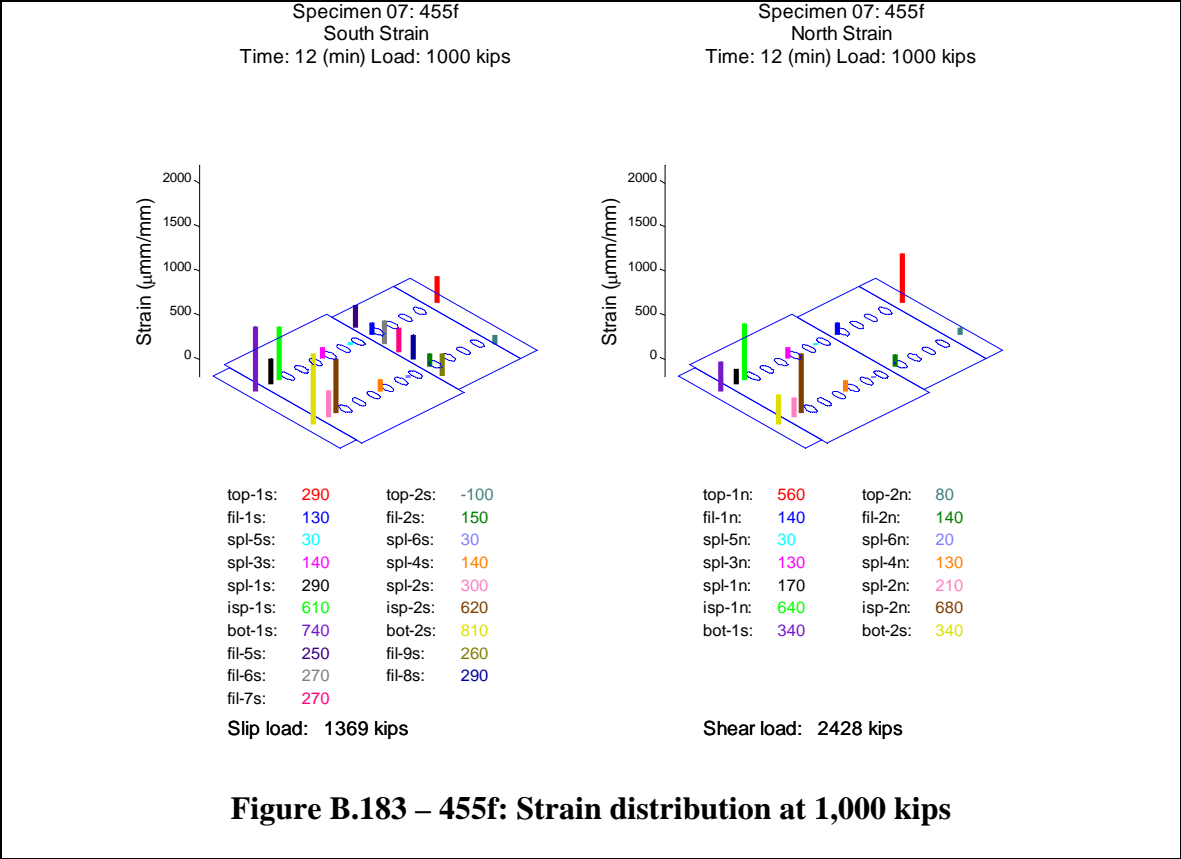


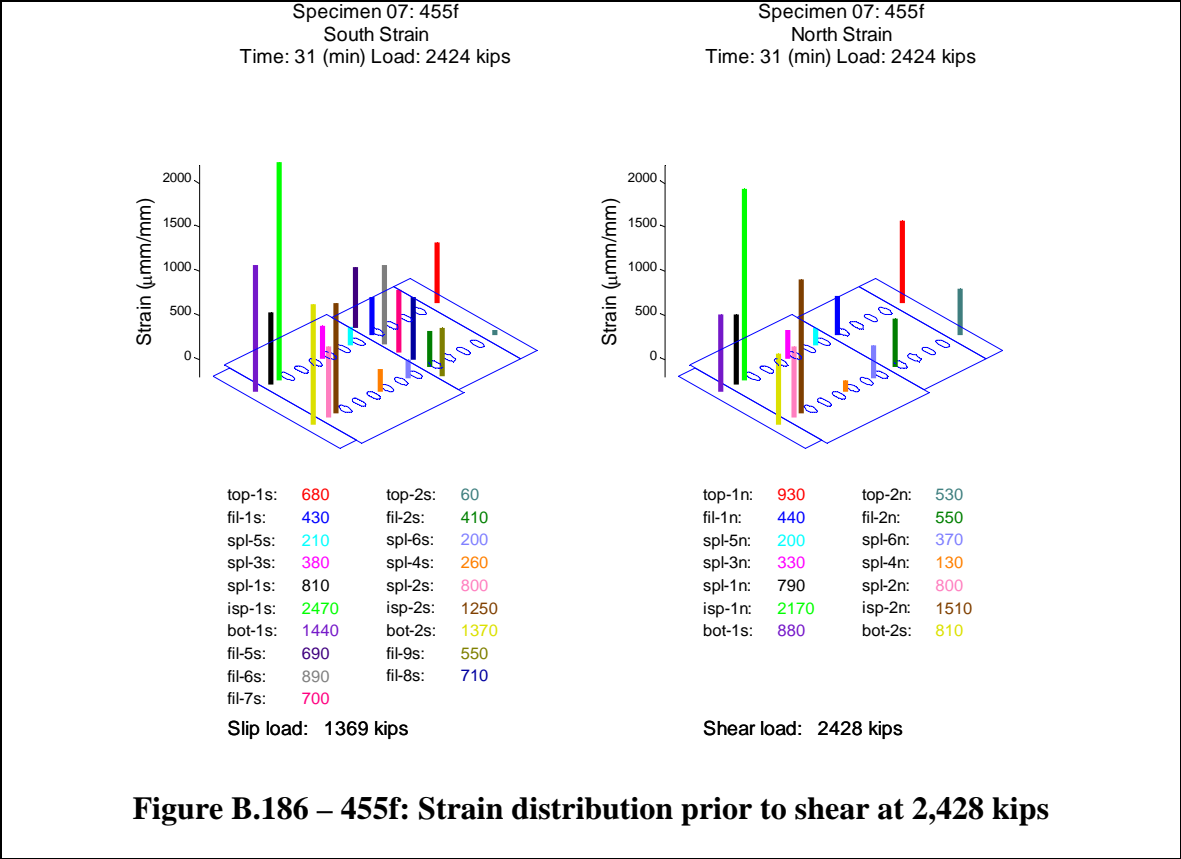
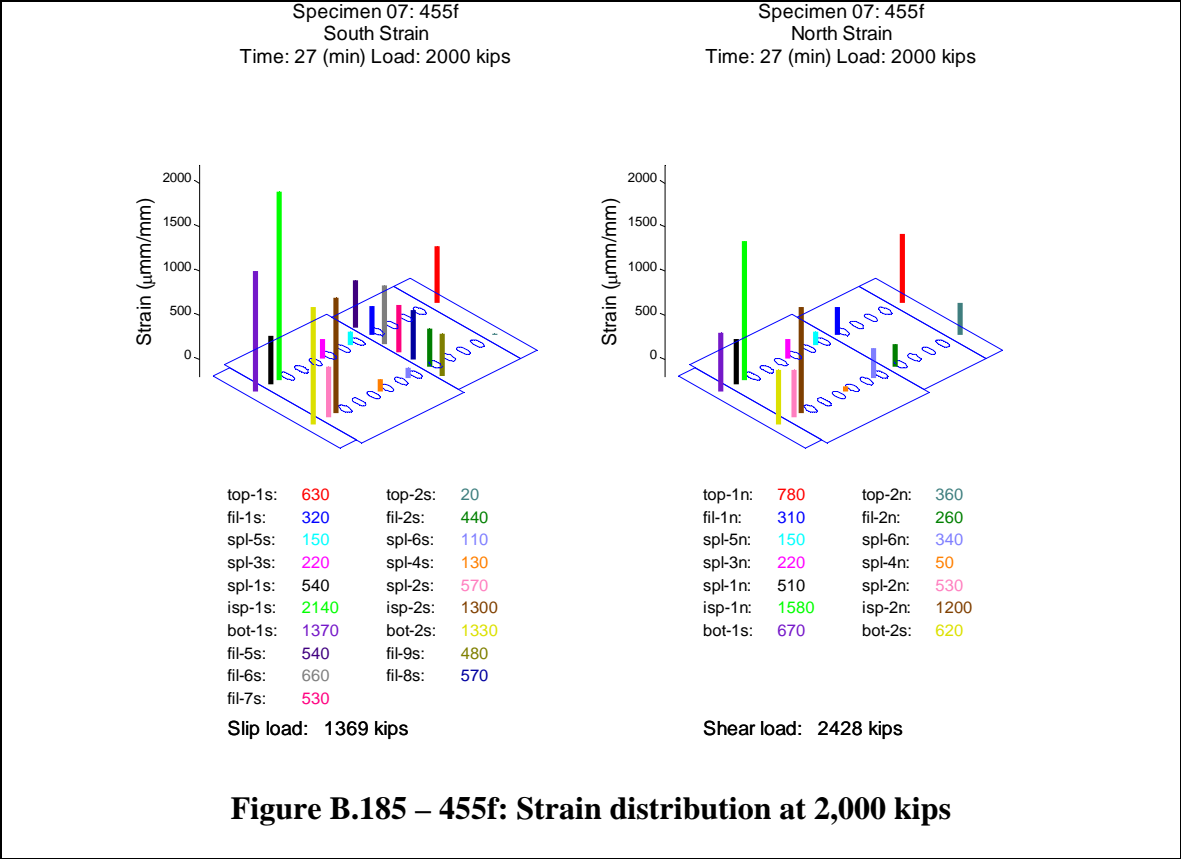
**Figure B.179 – 455f: Load vs. inside face of splice plate strain**



**Figure B.180 – 455f: Load vs. filler plate strain**







## B.9 Specimen 455h

Specimen 455h (Figure B.187 to Figure B.215) behaved approximately linearly until the observed slip load (1,175 kips). During the slip event, the relative displacement between the splice plate and the filler plate, as well as the filler plate and the top column increased suddenly. Slip initiated between the filler plate and the splice plate on both the north and south sides of the specimen as well as between the filler plate and top column on the north side and then the south side of the specimen (Figure B.198 and Figure B.199). Over a period of 12 seconds, the relative displacements increased by the amounts shown in Table B.9. This is seen most clearly in the relative LVDTs (Figure B.202 and Figure B.203). During this dynamic event, the load dropped and increased several times. The lowest load measured was 509 kips (Figure B.192). The machine and specimen stabilized at 1,098 kips and the load was held for observation of the specimen (Figure B.193).

**Table B.9 – 455h: Relative slip**

<b>Location</b>	<b>North</b>	<b>South</b>
<b>Between Splice and Filler</b>	0.41 in	0.45 in
<b>Between Filler and Top Column</b>	0.36 in	0.34 in
<b>Sum</b>	0.77 in	0.79 in

Around 1,250 kips the bolts likely slipped into bearing on the top column, as the seen by the increase in stiffness in Figure B.198 at approximately a load of 1,250 kips and a relative slip of 0.34 inches. The maximum expected clearance in the holes based on the assembly was nominally  $2 * (5/16 \text{ inches}) = 0.625 \text{ inches}$ .

All bolts remained intact prior to shear failure. Upon further loading, the bolts, now experiencing shear, yielded and eventually failed at the observed bolt shear load (2,197 kips) (Figure B.188 through Figure B.191). Initially one bolt failed on each side, followed by the remaining bolts on the north side and 3 additional bolts on the south side. A few seconds later the remaining bolts failed on the south side.

After slip, the specimen produced pinging noises at the following loads; 1350, 1377, 1390, 1403, 1411, 1421, 1434, 1440, 1451, 1459, 1465, 1475, 1480, 1490, 1495, 1503, 1507, 1522, 1528, 1533, 1538, 1544, 1549, 1556, 1560, 1564, 1571, 1575, 1579 and 1583 kips. The noises continued every few kips, increasing in frequency until failure. The noises are likely associated with additional small slip events, bolts coming into bearing with the bolt holes, or possibly initiation of fractures within the bolts.

The splice plate LVDTs (Figure B.196 and Figure B.197) showed a dynamic increase or decrease in displacement during the slip events. This may be due to a number of reasons, including stress relief in the splice plates after slip, very small slips relative to the column flanges, or small dynamic vibrations (with resulting small permanent offsets) of the LVDT holders, but the displacements are an order of magnitude smaller than the primary

slip displacements (Figure B.198 and Figure B.199) and are not likely to indicate significant behavior.

Figure B.200 and Figure B.201 compare the LVDTs directly measuring relative slip between the filler plate and either the top column (Figure B.198) or the splice plate (Figure B.199) with the difference between the average of the two LVDTs on either filler plate at that same cross section as the LVDTs on the top column (Figure B.195) and either the average of the two LVDTs at the bottom center of the top column (Figure B.194) or the average of the two LVDTs on either splice plate at that same cross section as the LVDTs on the top column (Figure B.196). The measurements of the relative LVDTs correspond well to the difference between the corresponding absolute LVDTs.

For this specimen, strain gages were attached to the inside face of the splice plate in the gap between the top and bottom columns (Figure B.208). These measurements, when compared to the measurements from the outside face of the splice plate (Figure B.207), indicate slight bending in the splice plates.

The top column strain gages exhibit that the localized introduction of load had a small bias to the south side, particularly the southwest corner (Figure B.204). The bottom column strain gages show that the localized reaction was relatively uniformly loaded, with the northwest corner loaded the least (Figure B.209).

The filler plate on the south side displaced further than the north filler plate during slip (Figure B.195), leading to a larger overall displacement on the south side. Therefore, additional load was possibly applied to the north side after slip, leading to the shear failure on the north side of the specimen. The splice plates were relatively uniformly loaded once the load had distributed into the plate in the bottom row of bolts (Figure B.205, Figure B.206, Figure B.207 and Figure B.208). The upper rows of bolts experienced some biases, but in no clear pattern. The south filler plate experienced a slight bias toward the west (Figure B.210 and Figure B.211). Snapshots of the specimen strain at 1000 kips, immediately prior to slip, 2000 kips and immediately prior to shear are visually presented in Figure B.212, Figure B.213, Figure B.214 and Figure B.215, respectively. These graphs show that the strain enters into the filler plate and then into the splice plate gradually and relatively uniformly from bolt row 6 to bolt row 1 throughout the experiment.

The experiment was executed in load control. The loading rate for the experiment was approximately 1 kip per second. One elastic cycle was executed prior to the test, going up to a load of 200 kips and returning to zero load, to verify instrumentation. An additional elastic cycle was executed prior to the test, going up to a load of 350 kips and returning to zero load, to fix the instrumentation. The data collection rate for the experiment was held constant at 10 Hertz (10 sets of readings per second).

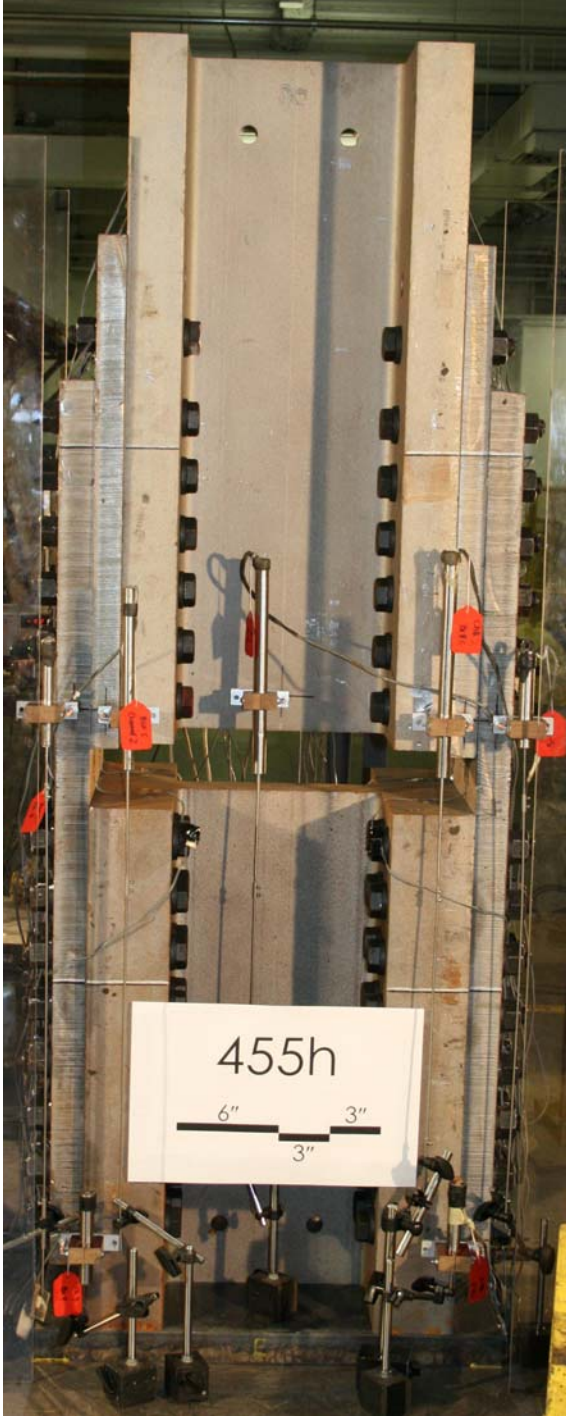


**Figure B.187 – 455h: Before test (east side)**

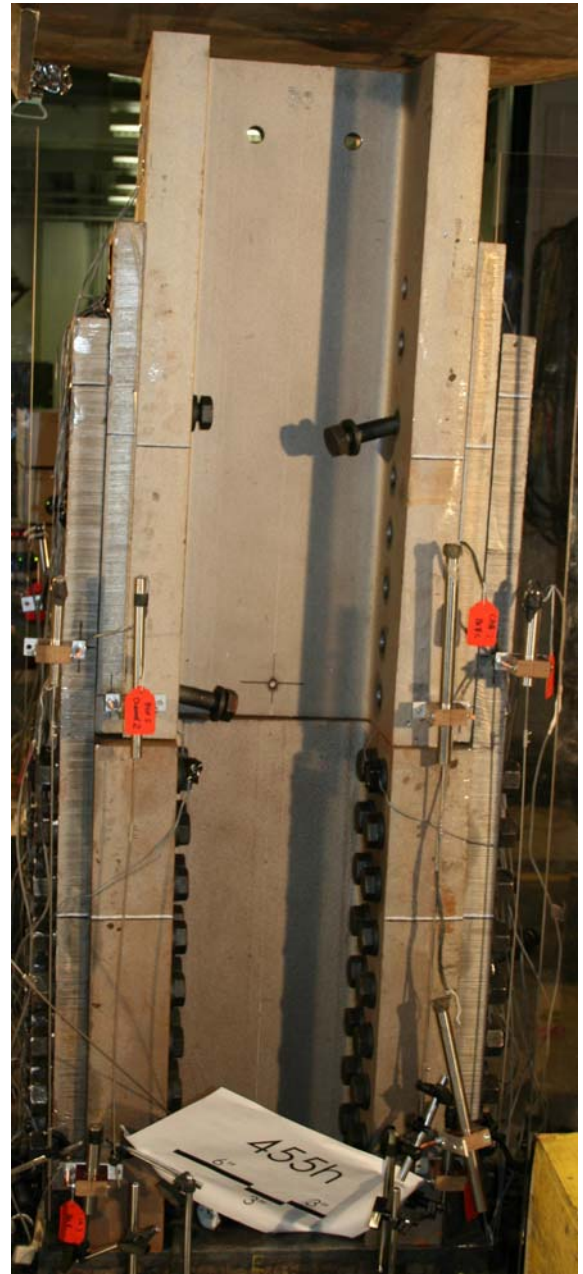


**Figure B.188 – 455h: After test (east side)**



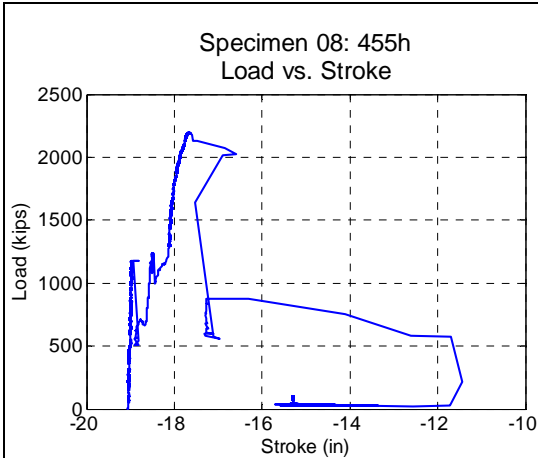
**Figure B.189 – 455h: After test (west side)**



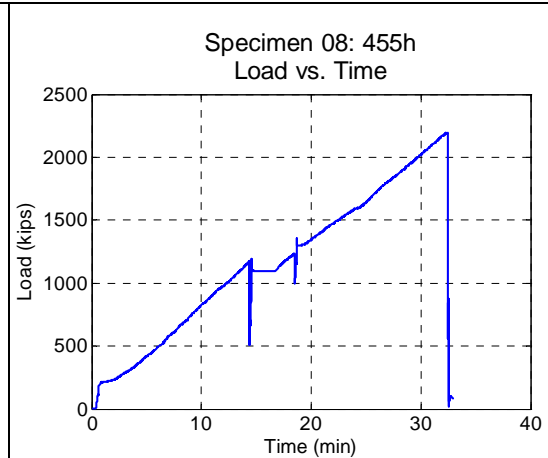
**Figure B.190 – 455h: After test (south side)**



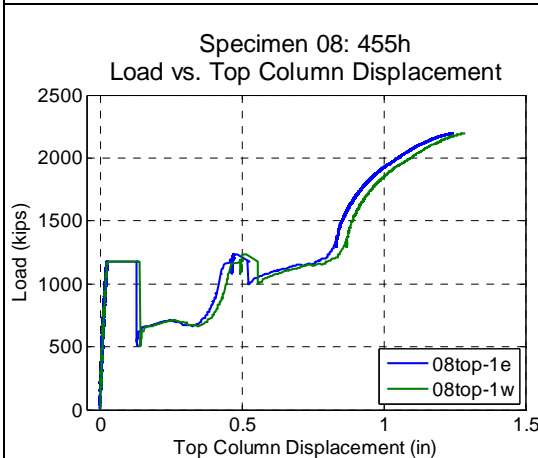
**Figure B.191 – 455h: After test (north side)**



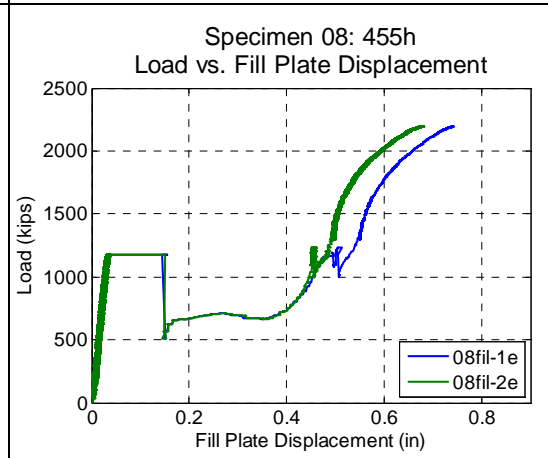
**Figure B.192 – 455h: Load vs. stroke**



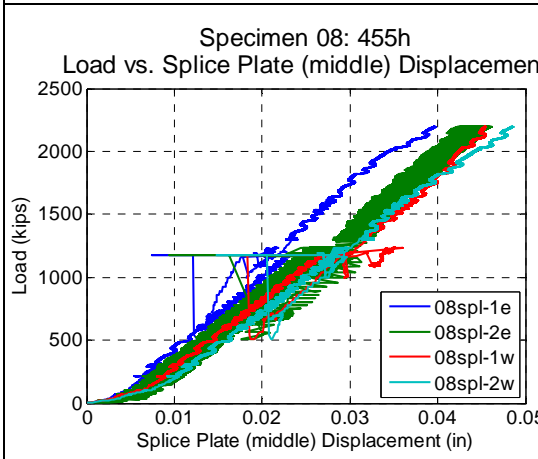
**Figure B.193 – 455h: Load vs. time**



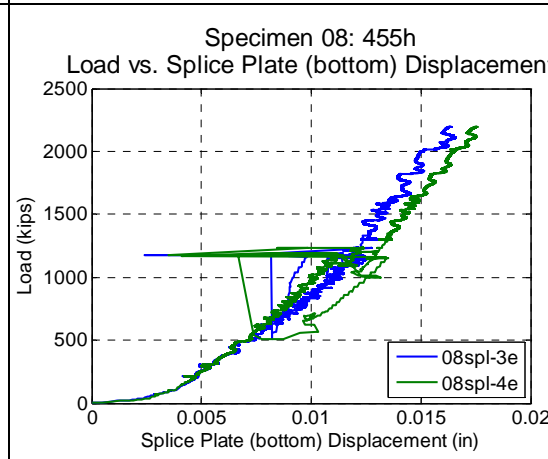
**Figure B.194 – 455h: Load vs. top column displacement**



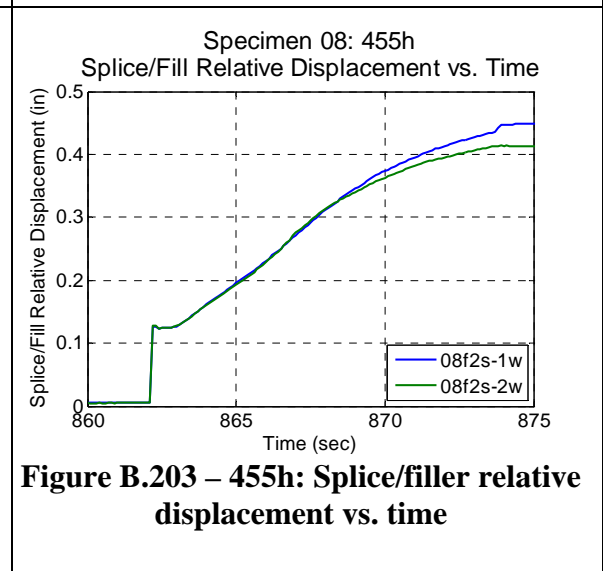
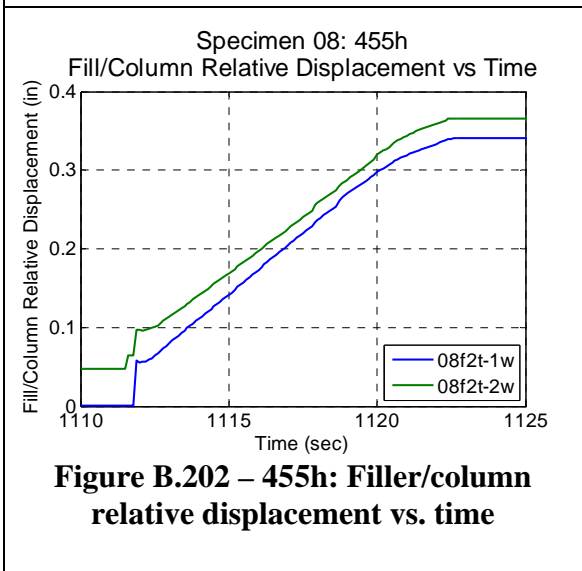
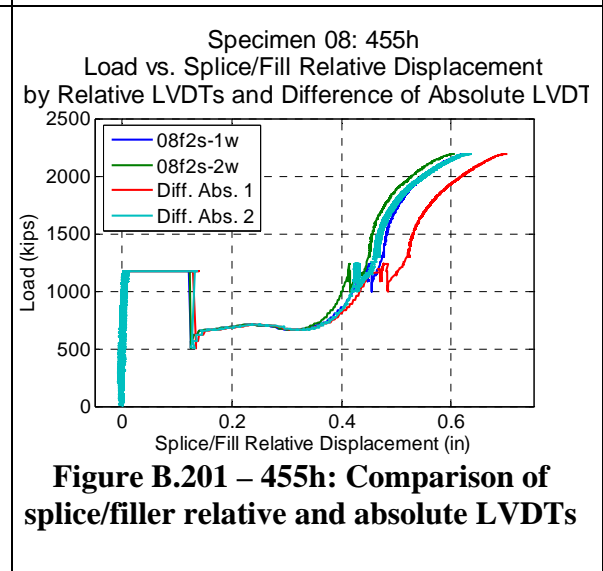
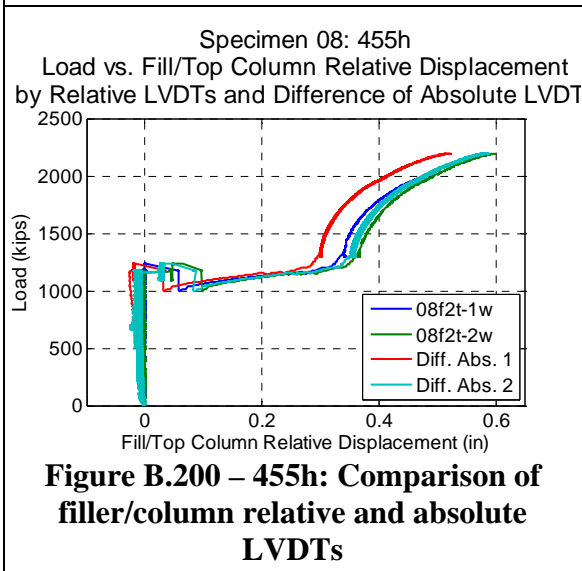
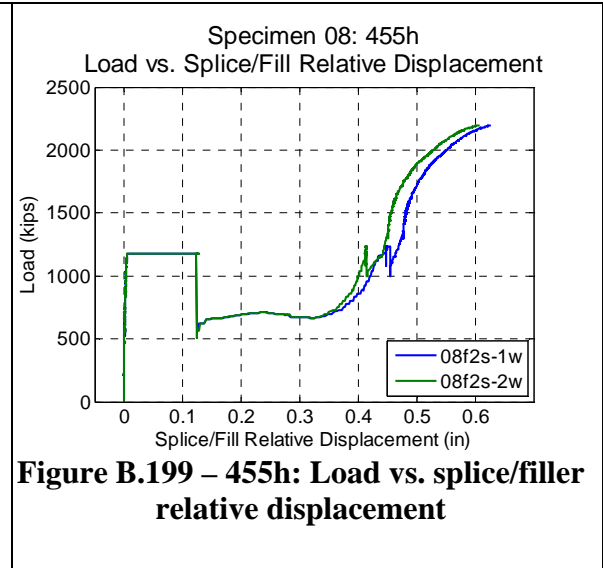
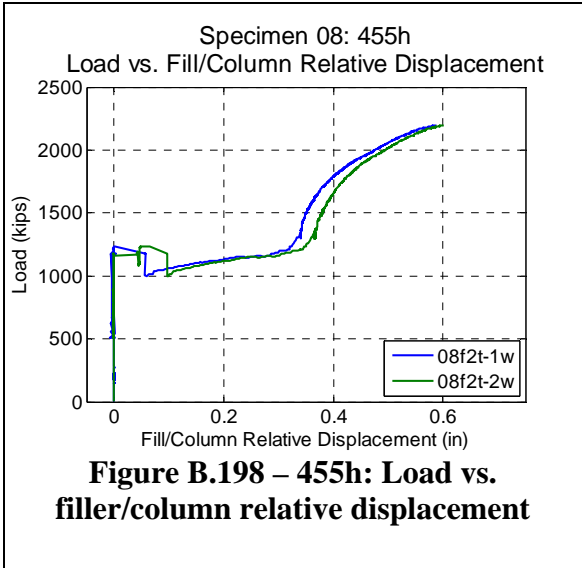
**Figure B.195 – 455h: Load vs. filler plate displacement**

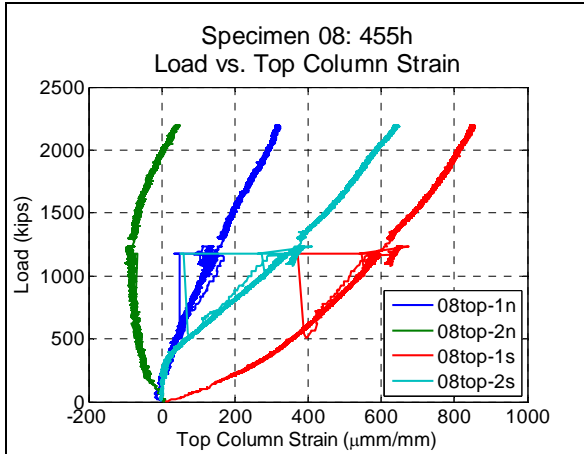


**Figure B.196 – 455h: Load vs. splice plate (middle) displacement**

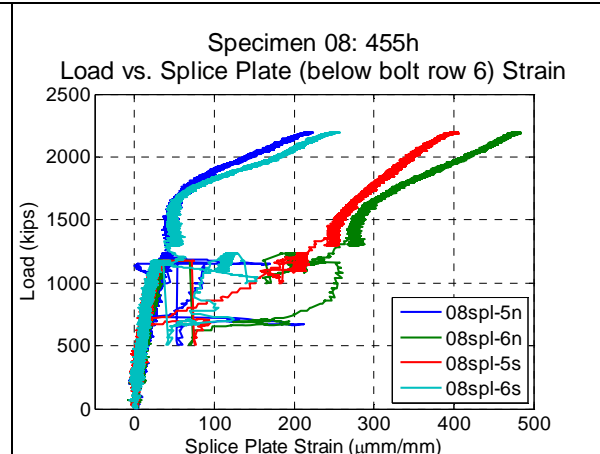


**Figure B.197 – 455h: Load vs. splice plate (bottom) displacement**

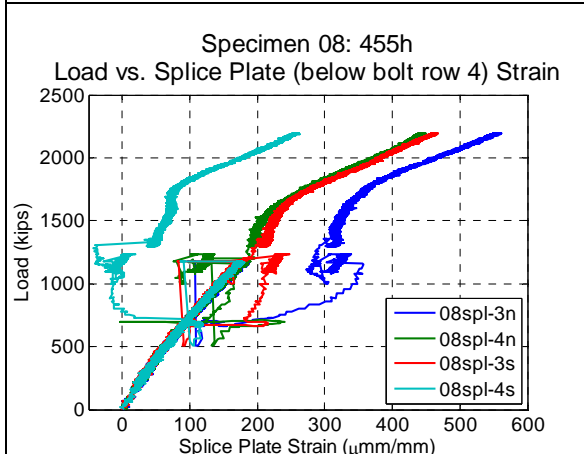




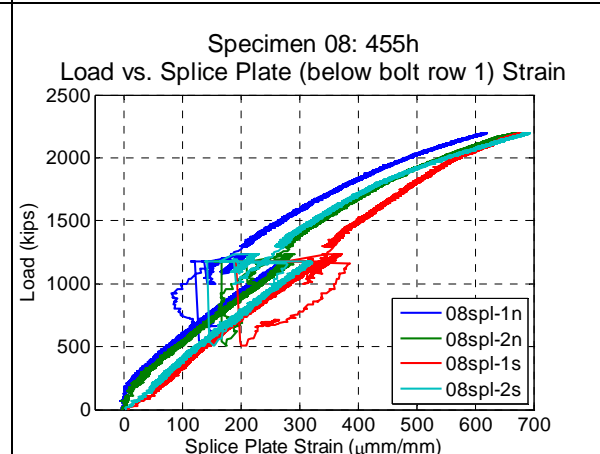
**Figure B.204 – 455h: Load vs. top column strain**



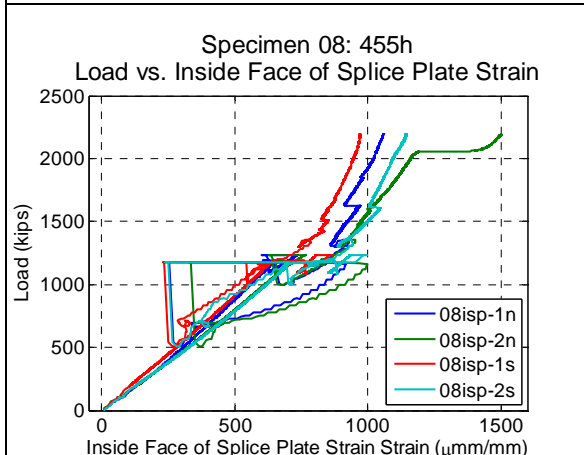
**Figure B.205 – 455h: Load vs. splice plate (below bolt row 6) strain**



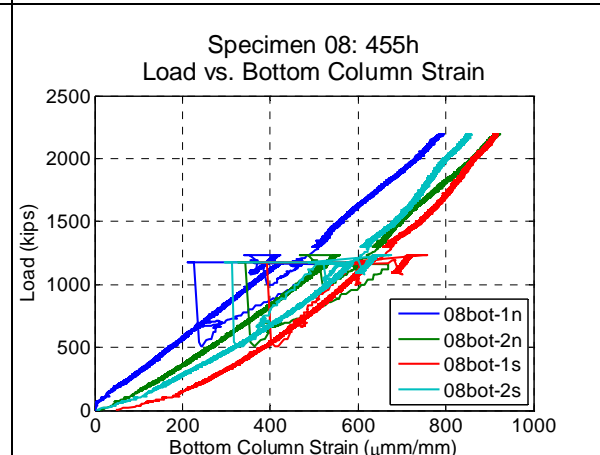
**Figure B.206 – 455h: Load vs. splice plate (below bolt row 4) strain**



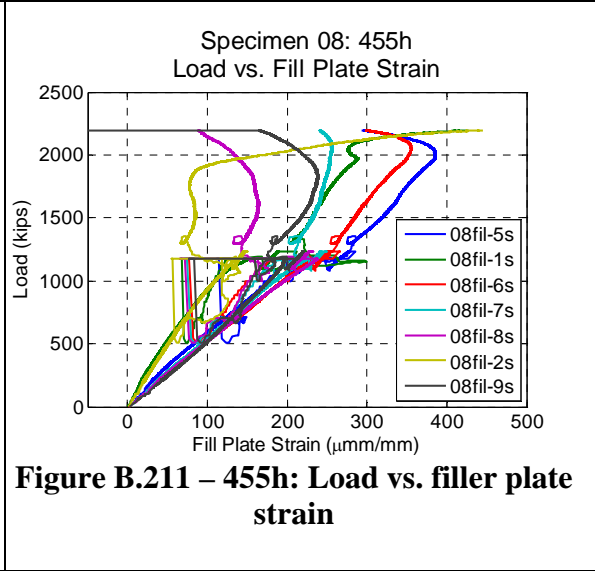
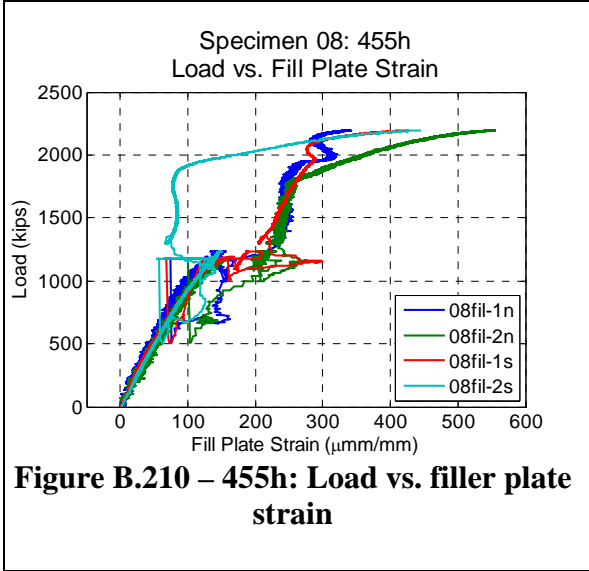
**Figure B.207 – 455h: Load vs. splice plate (below bolt row 1) strain**

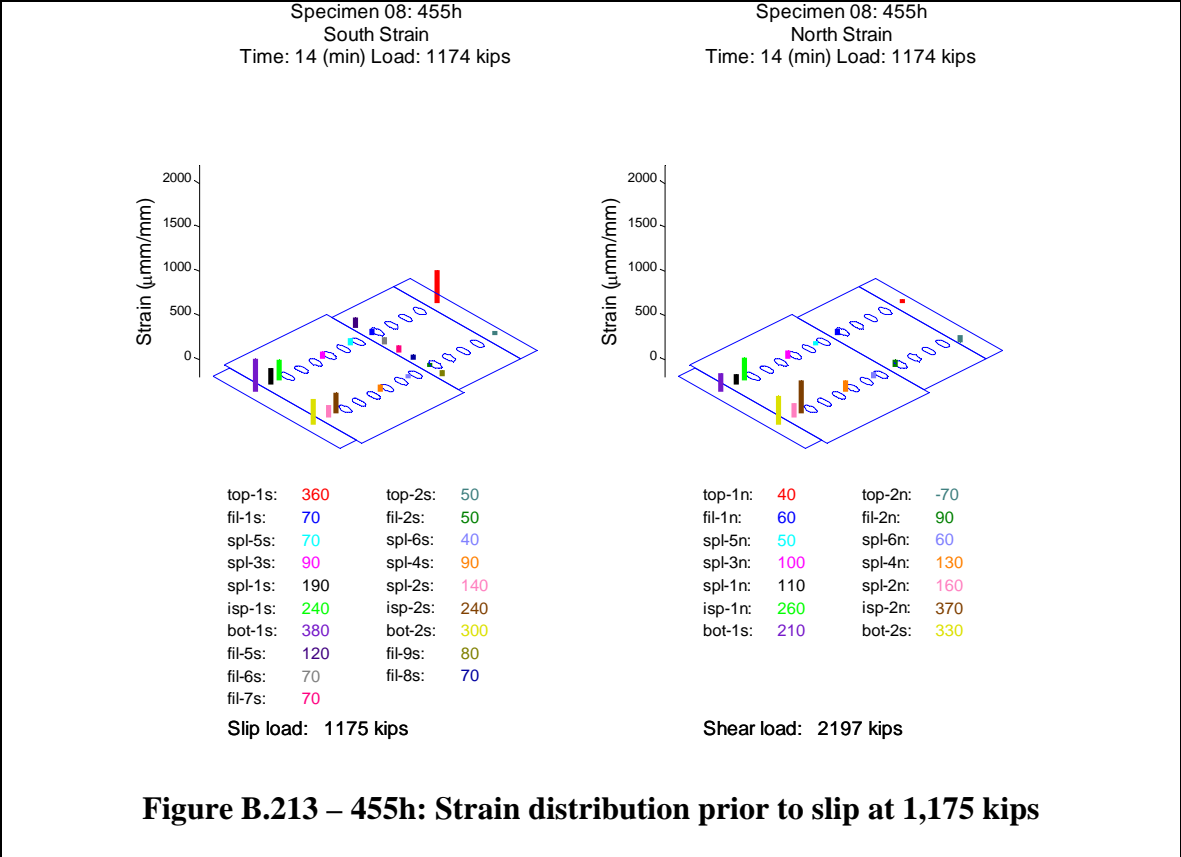
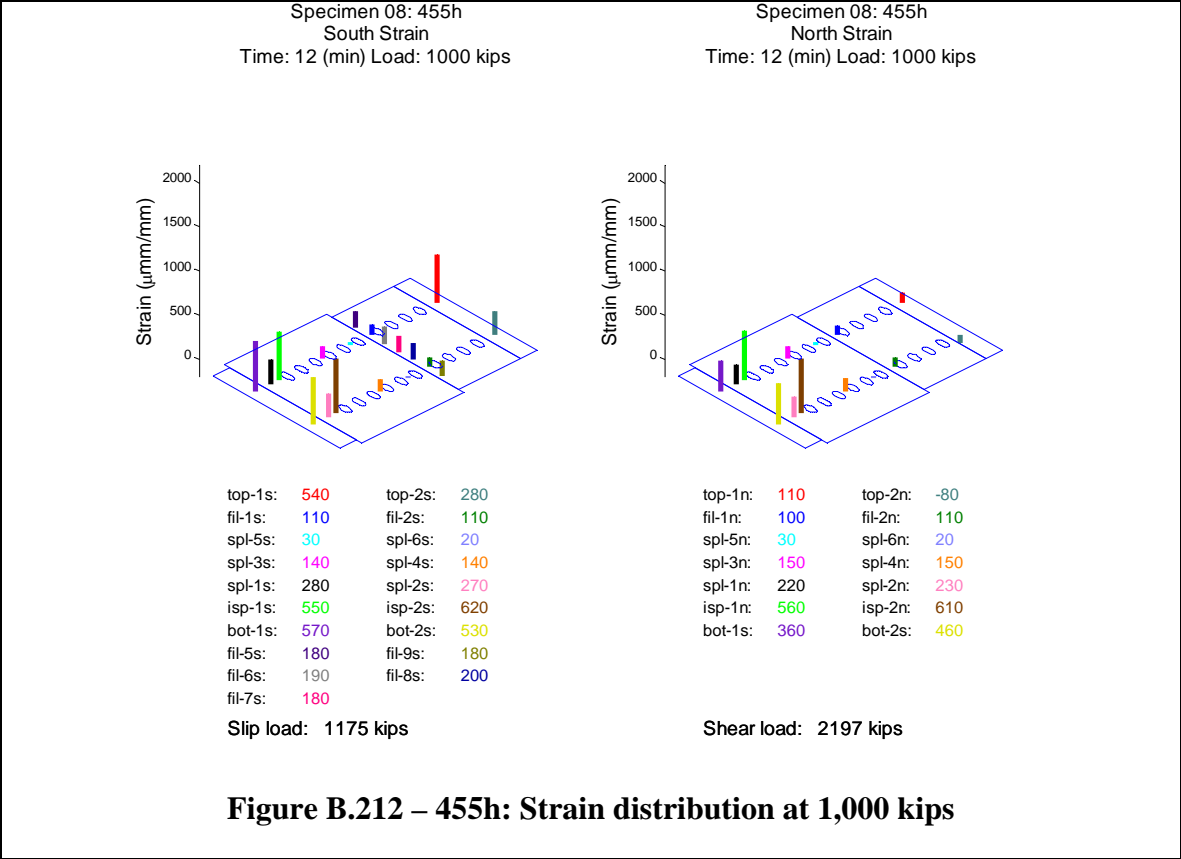


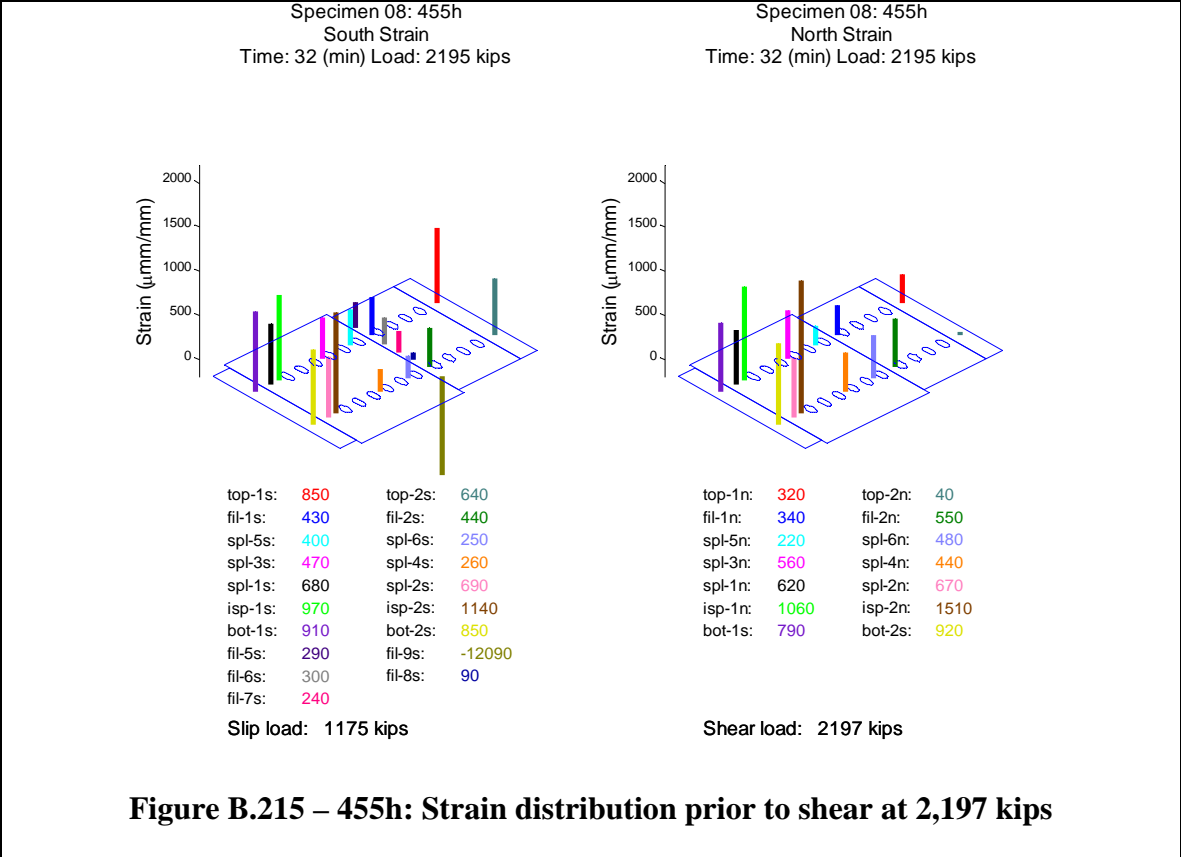
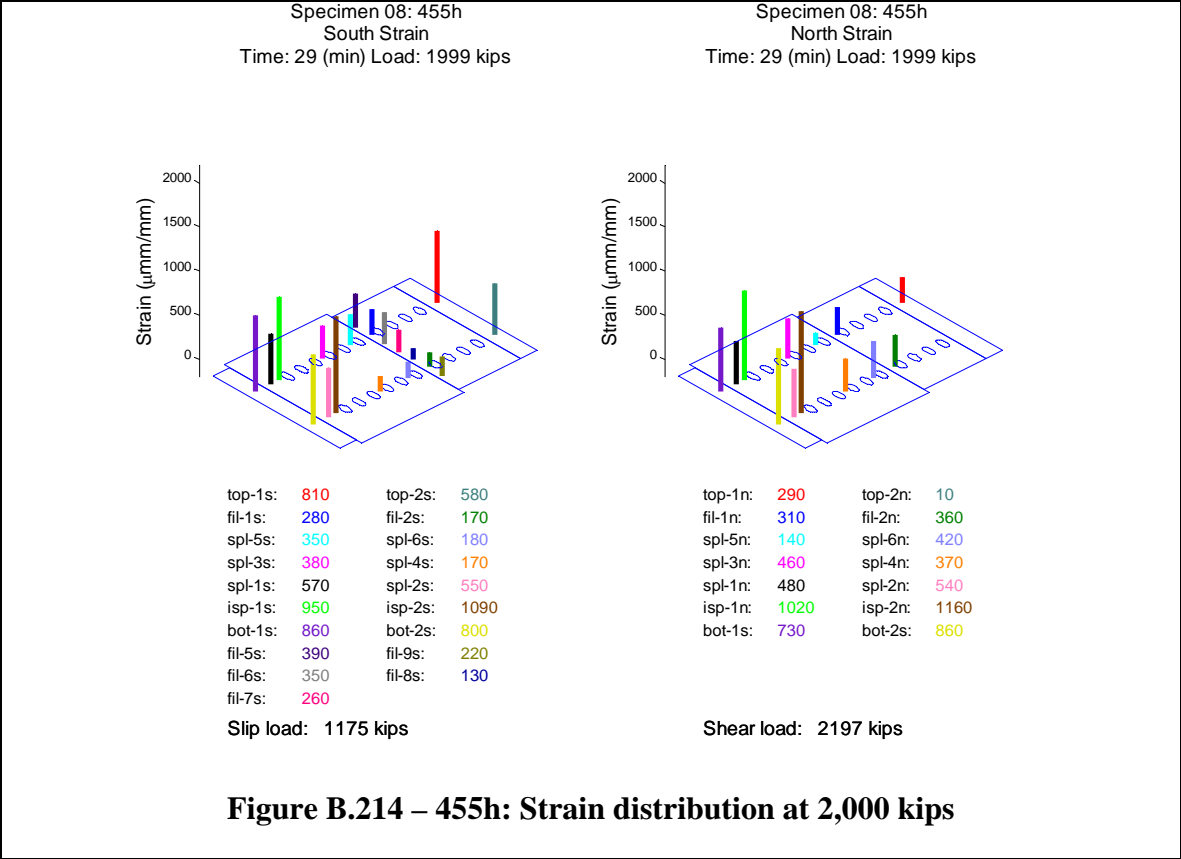
**Figure B.208 – 455h: Load vs. inside face of splice plate strain**



**Figure B.209 – 455h: Load vs. bottom column strain**







## B.10 Specimen 455n1

Specimen 455n1 (Figure B.216 to Figure B.243) behaved approximately linearly until the observed slip load (1,388 kips). During the slip event, the relative displacement between the splice plate and the filler plate, as well as the filler plate and the top column increased suddenly. Slip initiated between the filler plate and the splice plate on both the north and south sides of the specimen, followed several seconds later by the slip between the filler plate and the top column on both the north and south sides. Over a period of 17 seconds, the relative displacements increased by the amounts shown in Table B.10. This is seen most clearly in the relative LVDTs (Figure B.232 and Figure B.233). During this dynamic event, the load dropped and increased several times. The lowest load measured was 700 kips (Figure B.222). The machine and specimen stabilized at 1,340 kips and the load was held for observation of the specimen (Figure B.223).

**Table B.10 – 455n1: Relative slip**

<b>Location</b>	<b>North</b>	<b>South</b>
<b>Between Splice and Filler</b>	0.41 in	0.40 in
<b>Between Filler and Top Column</b>	0.39 in	0.40 in
<b>Sum</b>	0.80 in	0.80 in

During this event the bolts likely slipped into bearing on the top column, as seen by the increase in stiffness in Figure B.228 at approximately a load of 1,100 kips and a relative slip of 0.35 inches. The maximum expected clearance in the holes based on the assembly was nominally  $2 * (5/16 \text{ inches}) = 0.625 \text{ inches}$ .

Upon further loading, the bolts, now experiencing shear, yielded and eventually failed at the observed bolt shear load (2,189 kips) (Figure B.217 through Figure B.221). All bolts remained intact prior to shear failure. The twelve bolts through the splice plate on the south flange of the top column failed nearly simultaneously on the shear plane between the splice plate and the fill plate. The specimen exhibited an increased stiffness prior to shear failure (Figure B.224 and Figure B.225). This may be the point in which the bolts came into contact with bolt edges of the filler plate. This behavior was not observed in any other specimens.

After slip, the specimen produced pinging noises at the following loads; 1397, 1412, 1442, 1453, 1471, 1486, 1502, 1509, 1519, 1534, 1542, 1549, 1555, 1566, 1580, 1590, 1598, 1603, 1624, 1629, 1634, 1639, 1648, 1652, 1657, and 1663 kips. Noises continued occurring every few kips of increasing load, silencing at 1830 kips. At 2140 kips the specimen emitted a high pitched noise. The specimen began ticking at 2168 kips. Noises believed to be produced by the testing machine were neglected. The noises are likely associated with additional small slip events, bolts coming into bearing with the bolt holes, or possibly initiation of fractures within the bolts.

The splice plate LVDTs (Figure B.226 and Figure B.227) showed a dynamic increase or decrease in displacement during the slip events. This may be due to a number of reasons, including stress relief in the splice plates after slip, very small slips relative to the column flanges, or small dynamic vibrations (with resulting small permanent offsets) of the LVDT holders, but the displacements are an order of magnitude smaller than the primary slip displacements (Figure B.228 and Figure B.229) and are not likely to indicate significant behavior.

Figure B.230 and Figure B.231 compare the LVDTs directly measuring relative slip between the filler plate and either the top column (Figure B.228 or the splice plate (Figure B.229) with the difference between the average of the two LVDTs on either filler plate at that same cross section as the LVDTs on the top column (Figure B.225) and either the average of the two LVDTs at the bottom center of the top column (Figure B.224) or the average of the two LVDTs on either splice plate at that same cross section as the LVDTs on the top column (Figure B.226). The measurements of the relative LVDTs correspond well to the difference between the corresponding absolute LVDTs.

For this specimen, strain gages were attached to the inside face of the splice plate in the gap between the top and bottom columns (Figure B.238). These measurements, when compared to the measurements from the outside face of the splice plate (Figure B.237), indicate slight bending in the splice plates.

The loading of the top column strain gages showed that the localized introduction of load was slightly biased towards the west side (Figure B.234). The bottom column was biased towards the south side (Figure B.239).

The splice plates (Figure B.235, Figure B.236, Figure B.237 and Figure B.238) exhibited relatively uniform loading. Snapshots of the specimen strain at 1000 kips, immediately prior to slip, 2000 kips and immediately prior to shear are visually presented in Figure B.240, Figure B.241, Figure B.242 and Figure B.243, respectively. These graphs show that the strain enters into the splice plate gradually and relatively uniformly from bolt row 6 to bolt row 1 throughout the experiment.

The experiment was executed in load control. The loading rate for the experiment was approximately 1 kip per second. One elastic cycle was executed prior to the test, going up to a load of 200 kips and returning to zero load, to verify instrumentation. The data collection rate for the experiment was held constant at 10 Hertz (10 sets of readings per second).

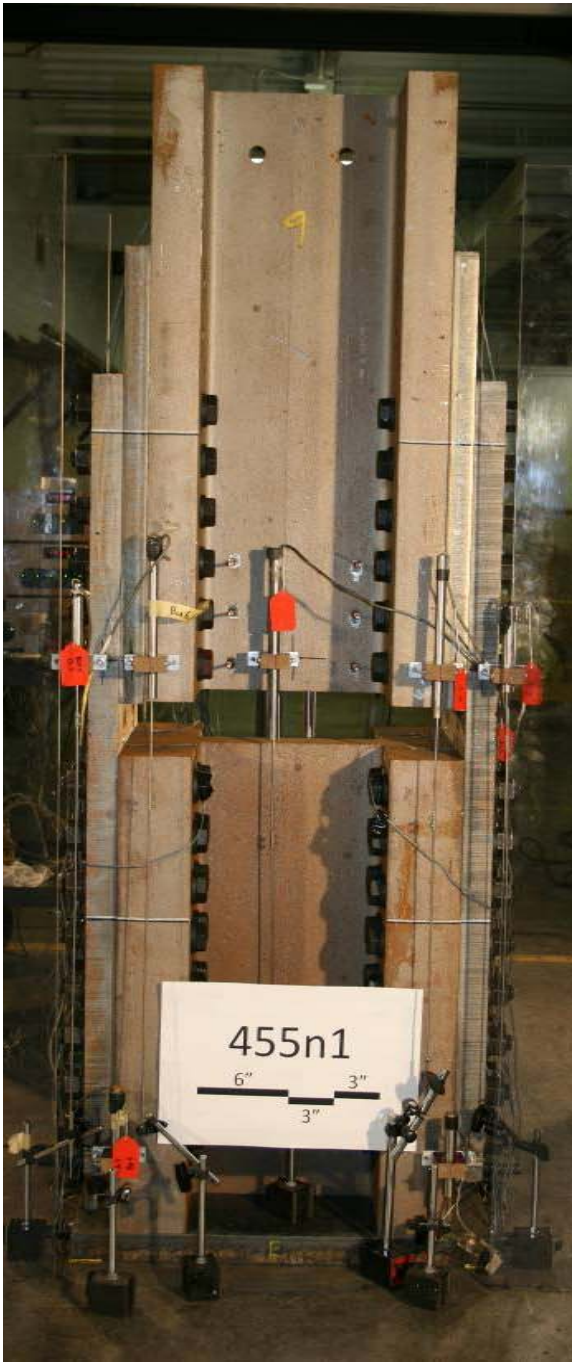


Figure B.216 – 455n1: Before test (east side)

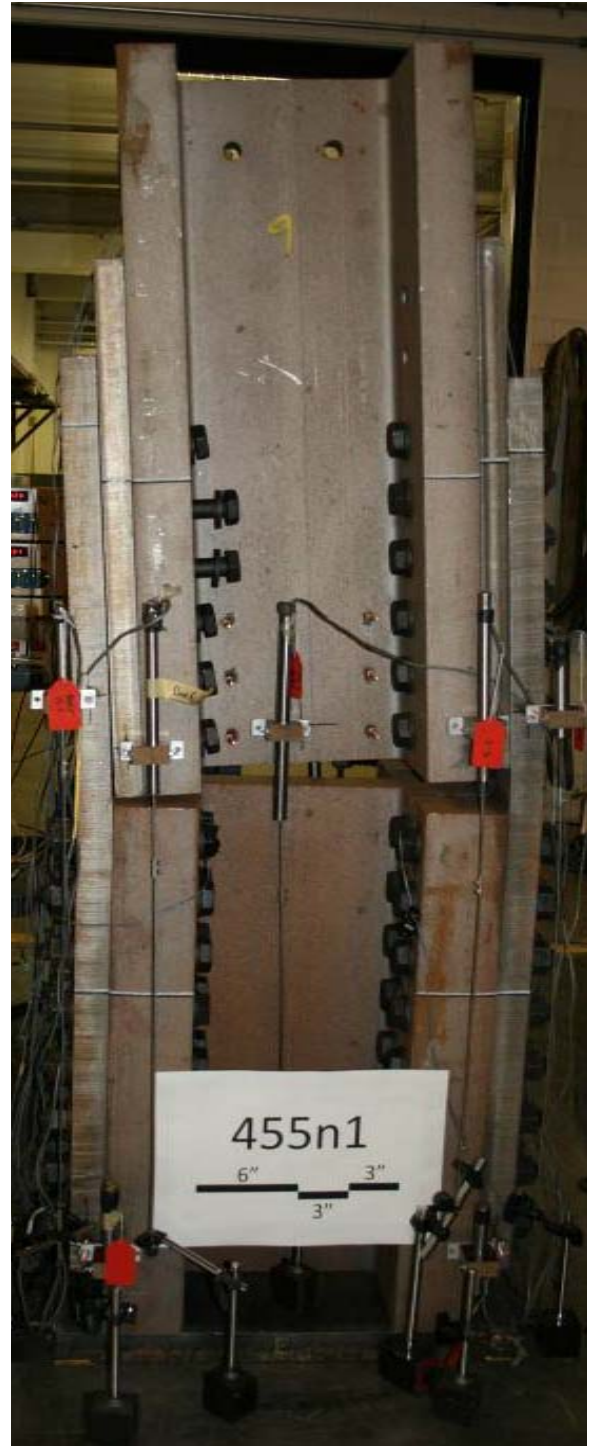


Figure B.217 – 455n1: After test (east side)



**Figure B.218 – 455n1: After test (east side)**



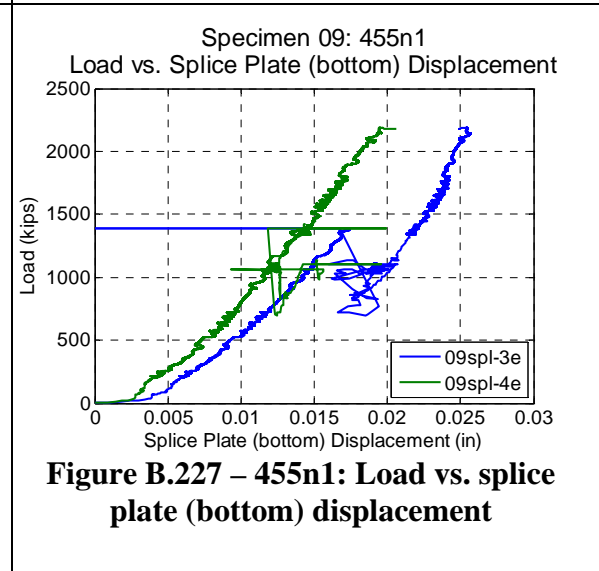
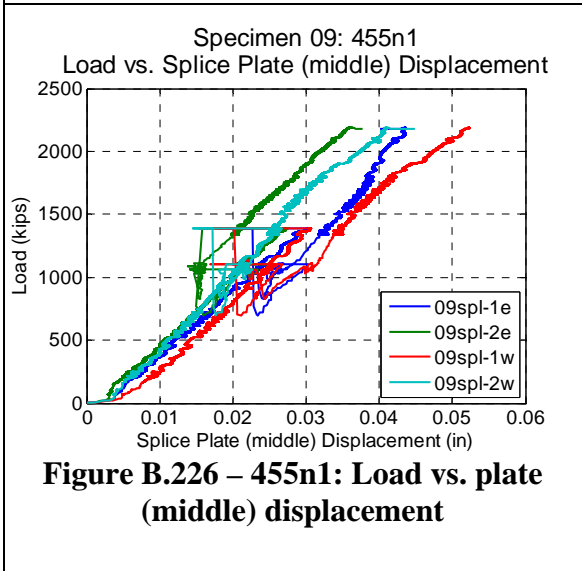
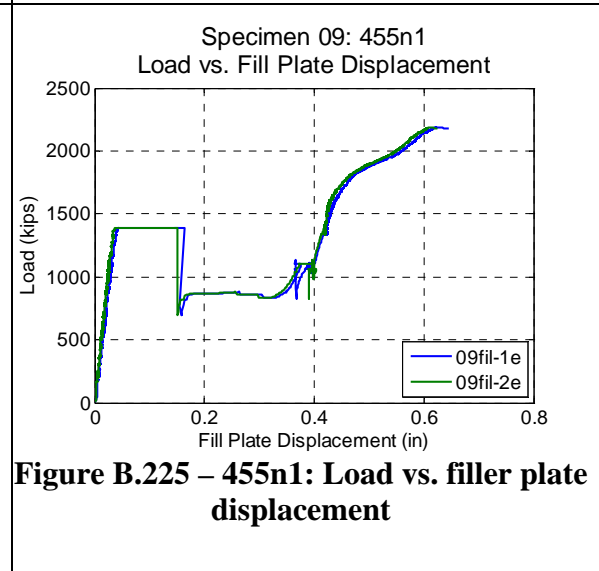
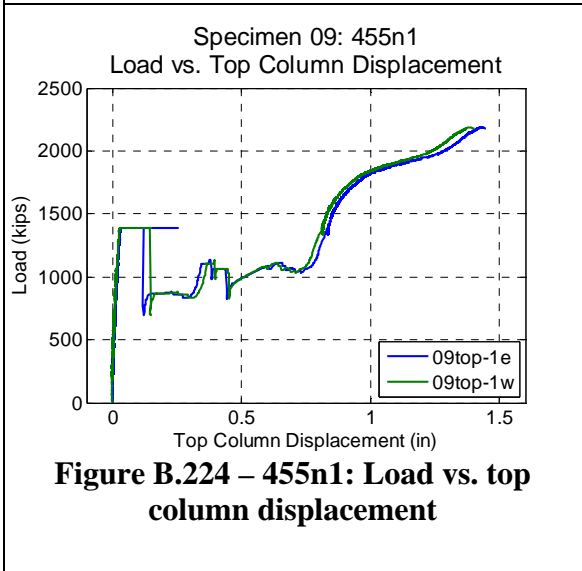
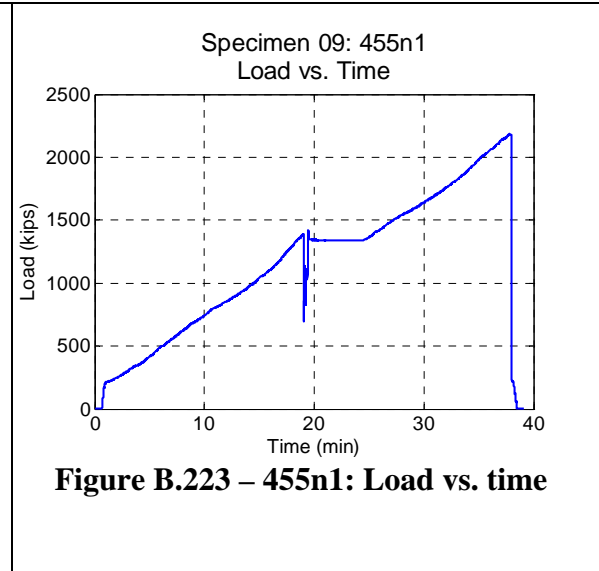
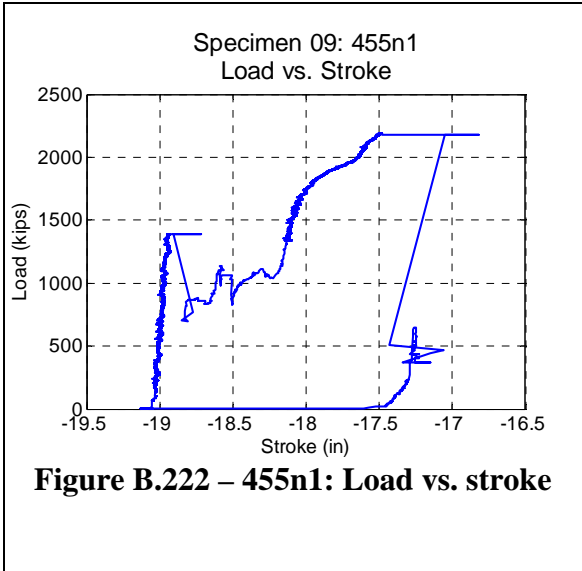
**Figure B.219 – 455n1: After test (west side)**

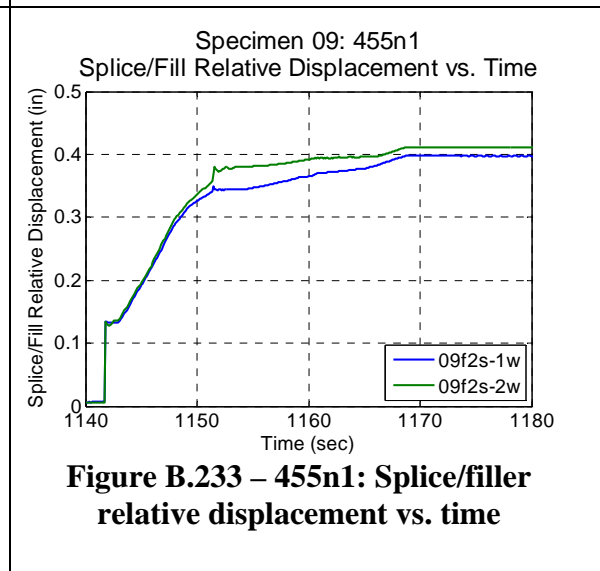
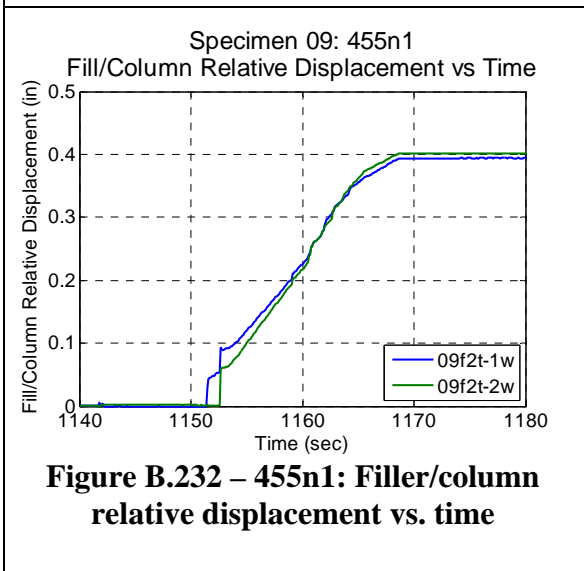
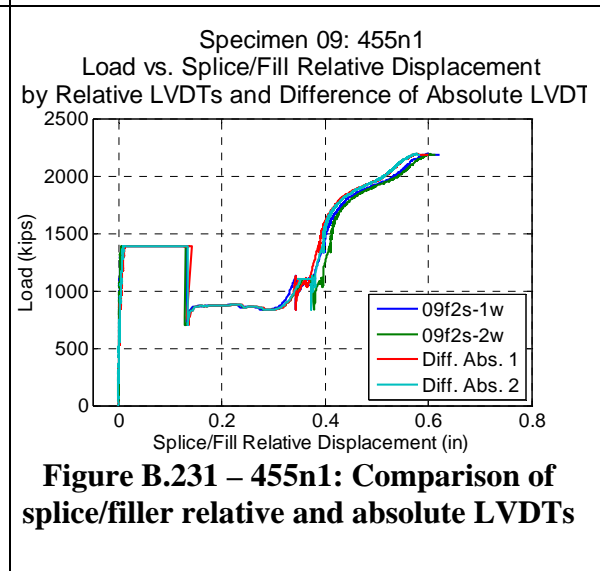
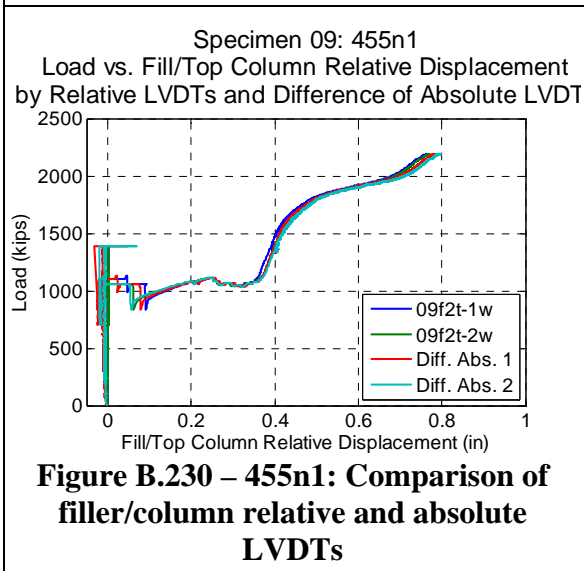
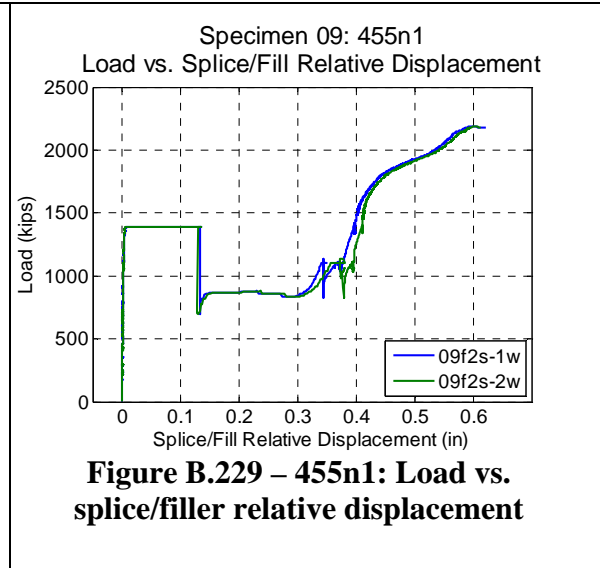
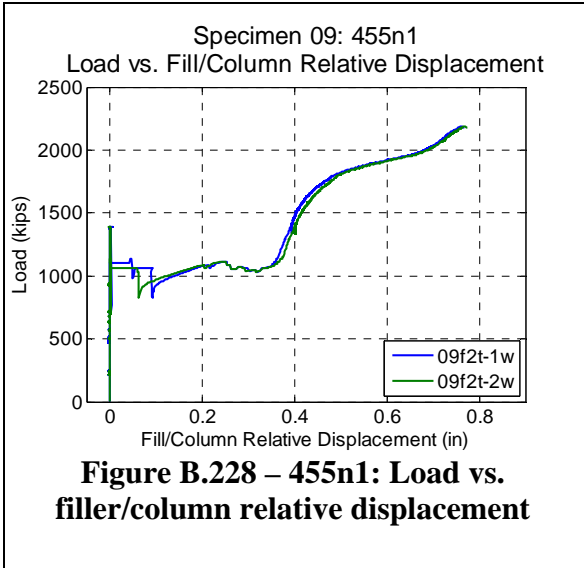


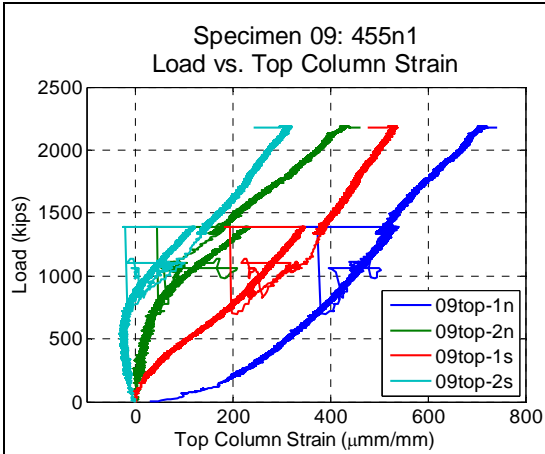
**Figure B.220 – 455n1: After test (south side)**



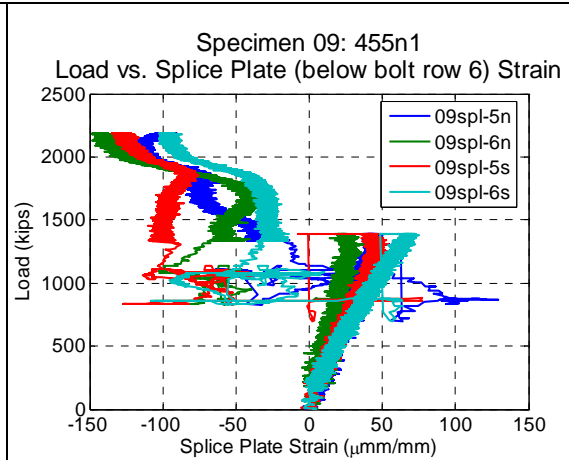
**Figure B.221 – 455n1: After test (north side)**



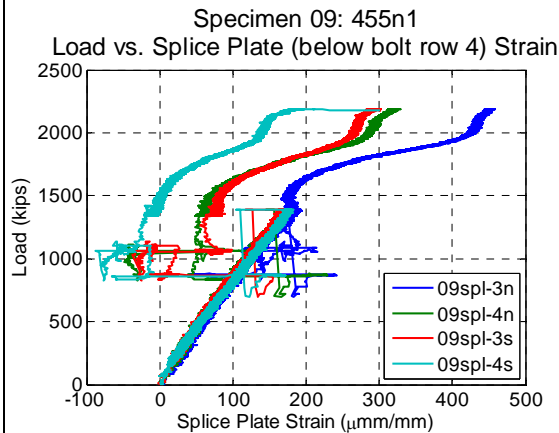




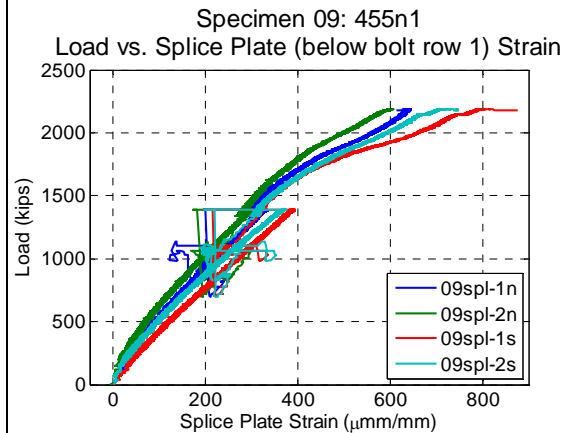
**Figure B.234 – 455n1: Load vs. top column strain**



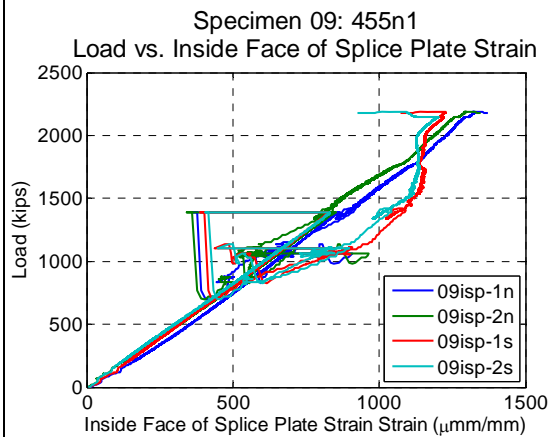
**Figure B.235 – 455n1: Load vs. splice plate (below bolt row 6) strain**



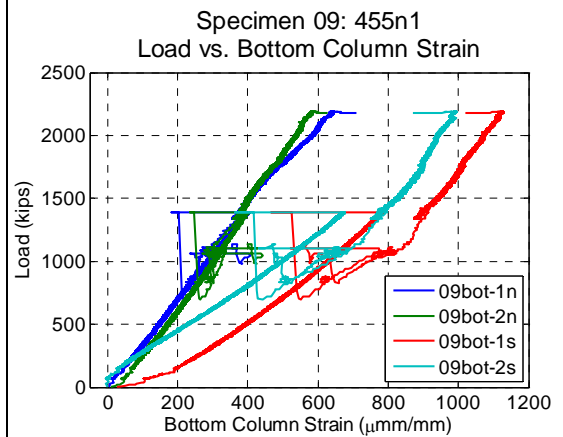
**Figure B.236 – 455n1: Load vs. splice plate (below bolt row 4) strain**



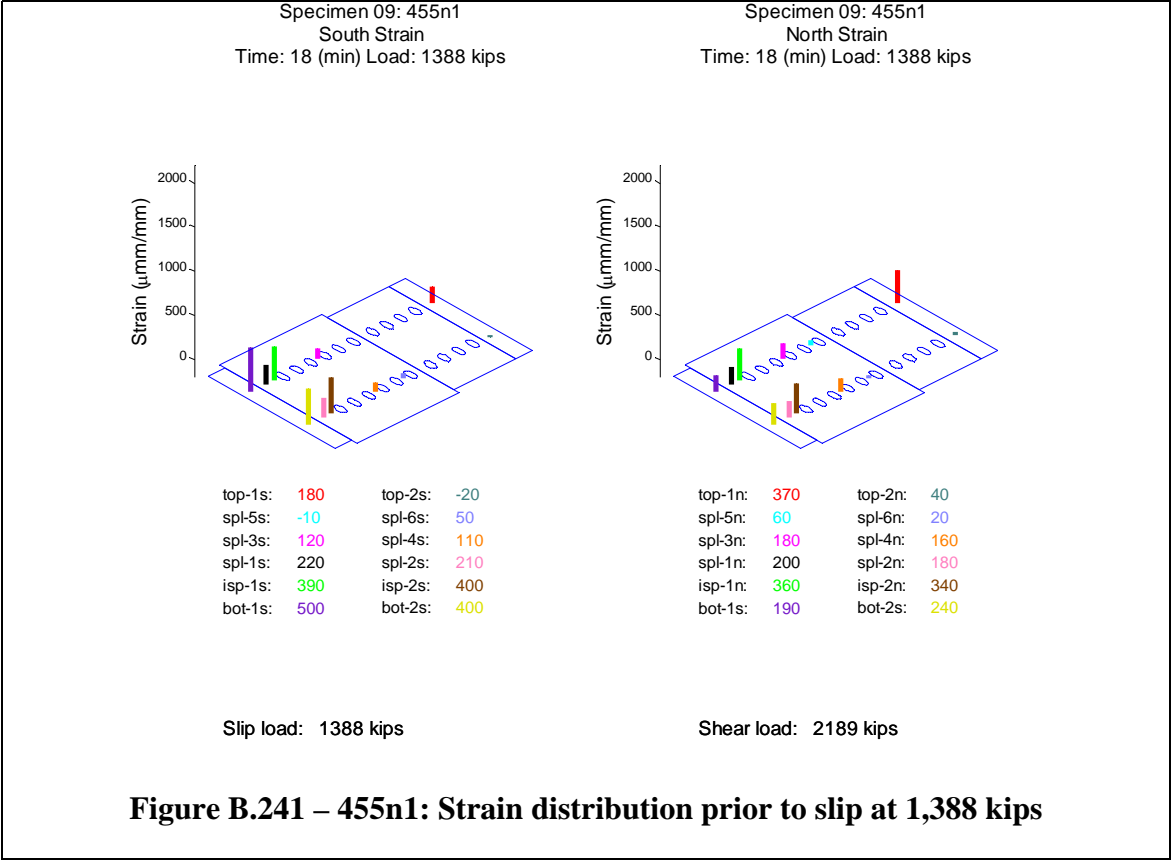
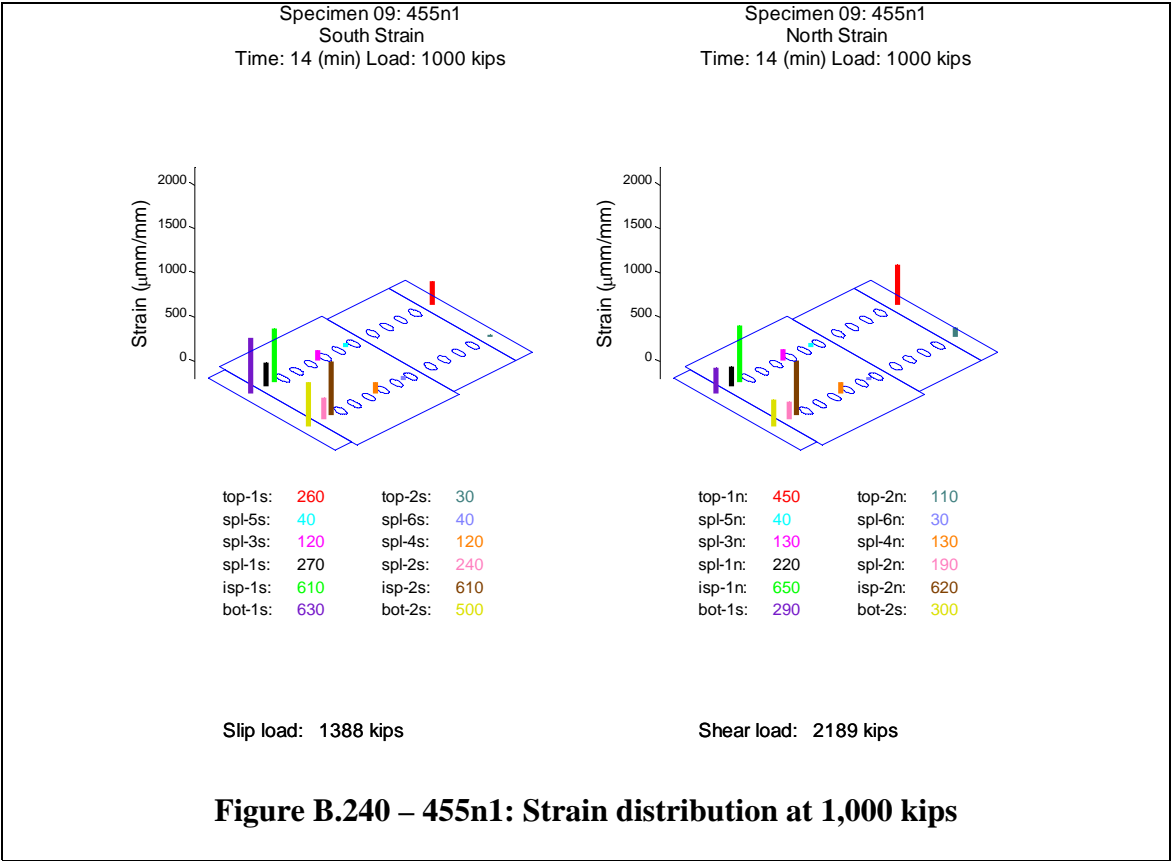
**Figure B.237 – 455n1: Load vs. splice plate (below bolt row 1) strain**

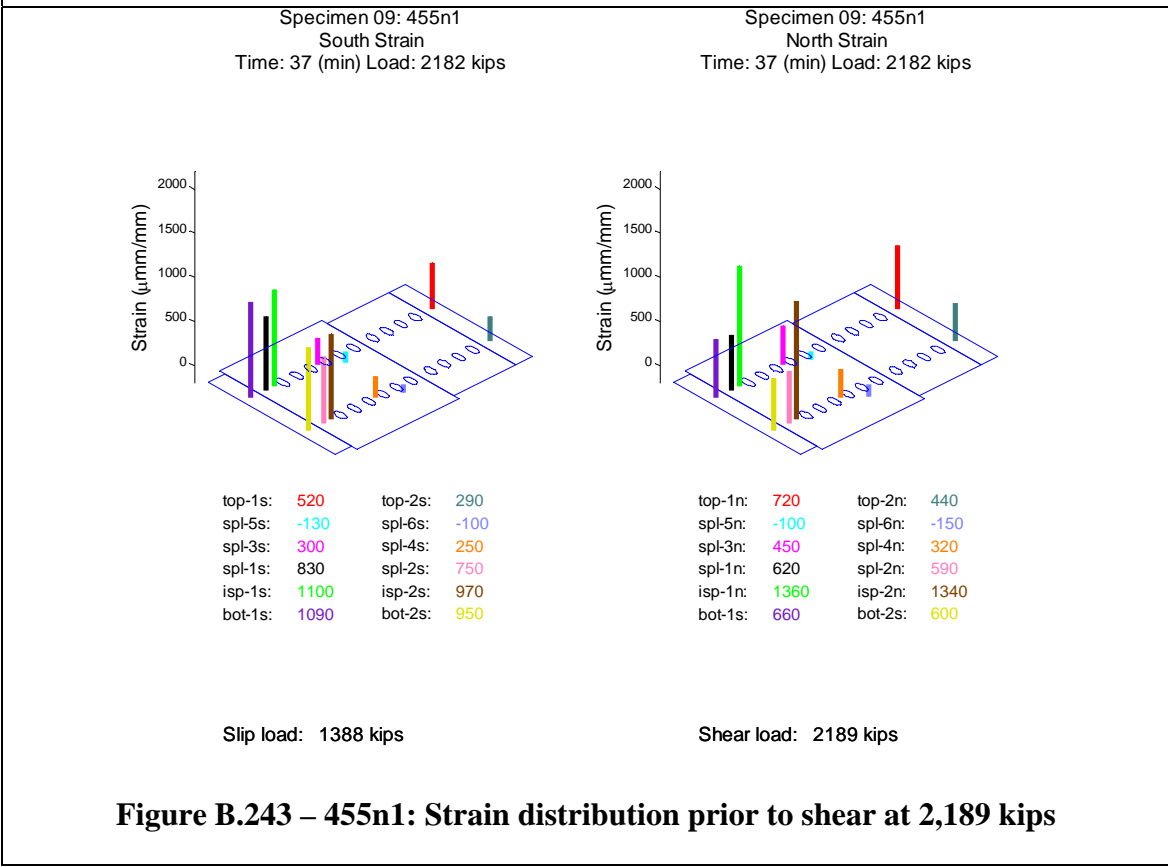
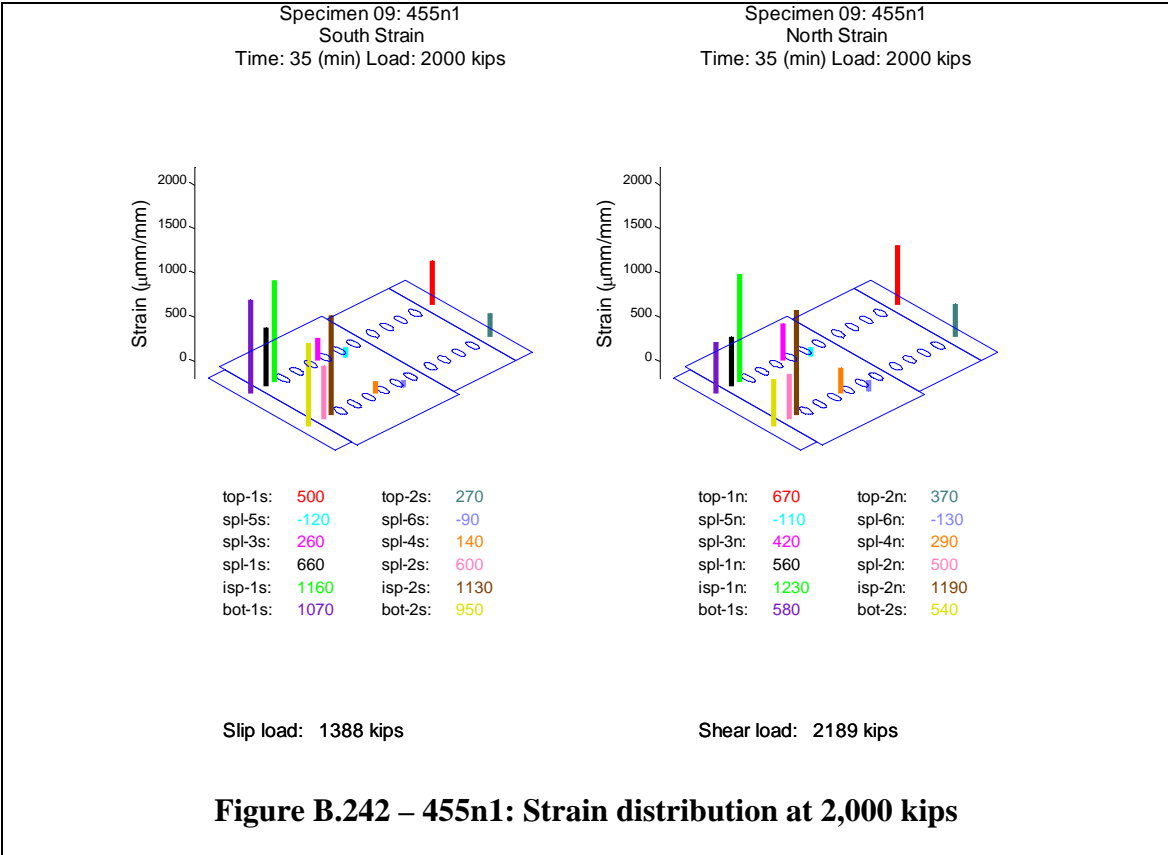


**Figure B.238 – 455n1: Load vs. inside face of splice plate strain**



**Figure B.239 – 455n1: Load vs. bottom column strain**





## B.11 Specimen 455n2

Specimen 455n2 (Figure B.244) behaved approximately linearly until the observed slip load (1,433 kips). During the slip event, the relative displacement between the splice plate and the filler plate, as well as the filler plate and the top column increased suddenly. Slip initiated between the filler plate and the splice plate on south side of the specimen as well as between the filler plate and top column on the north side of the specimen. After losing load dynamically and then starting to pick up load again, slip initiated between the filler plate and the splice plate on the north side of the specimen as well as between the filler plate and the top column on the south side of the specimen (Figure B.256 and Figure B.257). Over a period of 30 seconds, the relative displacements increased by the amounts shown in Table B.11. This is seen most clearly in the relative LVDTs (Figure B.260 and Figure B.261). During this dynamic event, the load dropped and increased several times. The lowest load measured was 645 kips (Figure B.250). The machine and specimen stabilized at 1,360 kips and the load was held for observation of the specimen (Figure B.251).

**Table B.11 – 455n2: Relative slip**

<b>Location</b>	<b>North</b>	<b>South</b>
<b>Between Splice and Filler</b>	0.68 in	0.54 in
<b>Between Filler and Top Column</b>	0.33 in	0.39 in
<b>Sum</b>	1.01 in	0.93 in

During this event the bolts likely slipped into bearing on the top column, as seen by the increase in stiffness in Figure B.256 at approximately a load of 1,450 kips and a relative slip of 0.6 inches. The maximum expected clearance in the holes based on the assembly was nominally  $2 * (5/16 \text{ inches}) = 0.625 \text{ inches}$ .

After the slip event, two bolts on the northeast side of the specimen (NE2 and NE3) failed through the threads, indicating a pretension failure (Figure B.245). The bolt head and shank of both of the failed bolts remained in the specimen. The bolts which remained in the specimen provided some doweling action and failed a second time in shear at the ultimate load of the specimen. One bolt on the northwest side of the specimen (NW6) was observed to be no longer be flush. It failed, through the threads, immediately upon additional loading.

Upon further loading, the bolts, now experiencing shear, yielded and eventually failed at the observed bolt shear load (2,248 kips) (Figure B.246 through Figure B.249). The twelve bolts through the splice plate on the south flange of the top column failed nearly simultaneously on the shear plane between the splice plate and the fill plate.

After slip, the specimen produced pinging noises at the following loads; 1425 (deep noise), 1449, 1484, 1523, 1556, 1578, 1592, 1601, 1624, 1657, 1658, 1676 and 1682 kips. Noises believed to be produced by the testing machine were neglected. The noises are likely associated with additional small slip events, bolts coming into bearing with the bolt holes, or possibly initiation of fractures within the bolts.

The splice plate LVDTs (Figure B.254 and Figure B.255) showed a dynamic increase or decrease in displacement during the slip events. This may be due to a number of reasons, including stress relief in the splice plates after slip, very small slips relative to the column flanges, or small dynamic vibrations (with resulting small permanent offsets) of the LVDT holders, but the displacements are an order of magnitude smaller than the primary slip displacements (Figure B.256 and Figure B.257) and are not likely to indicate significant behavior.

Figure B.258 and Figure B.259 compare the LVDTs directly measuring relative slip between the filler plate and either the top column (Figure B.256) or the splice plate (Figure B.257) with the difference between the average of the two LVDTs on either filler plate at that same cross section as the LVDTs on the top column (Figure B.253) and either the average of the two LVDTs at the bottom center of the top column (Figure B.252) or the average of the two LVDTs on either splice plate at that same cross section as the LVDTs on the top column (Figure B.254). The measurements of the relative LVDTs correspond well to the difference between the corresponding absolute LVDTs.

For this specimen, strain gages were attached to the inside face of the splice plate in the gap between the top and bottom columns (Figure B.266). These measurements, when compared to the measurements from the outside face of the splice plate (Figure B.265), indicate slight bending in the splice plates.

The top and bottom column strain gages show that the localized introduction of load had a bias to the south (Figure B.262).

However, the south bias is not reflected in the splice plates (Figure B.263, Figure B.264, Figure B.265 and Figure B.266) and bottom column (Figure B.267). The strains are very small below the sixth row of bolts, they favor the east side below the third row of bolts, and the splice plates are relatively uniformly loaded below the first row of bolts. Snapshots of the specimen strain at 1000 kips, immediately prior to slip, 2000 kips and immediately prior to shear are visually presented in Figure B.268, Figure B.269, Figure B.270 and Figure B.271, respectively. These graphs show that the strain enters into the splice plate gradually and relatively uniformly (with some east bias below the third row of bolts as noted above) from bolt row 6 to bolt row 1 throughout the experiment.

The experiment was executed in load control. The loading rate for the experiment was approximately 1 kip per second. One elastic cycle was executed prior to the test, going up to a load of 200 kips and returning to zero load, to verify instrumentation. The data collection rate for the experiment was held constant at 10 Hertz (10 sets of readings per second).

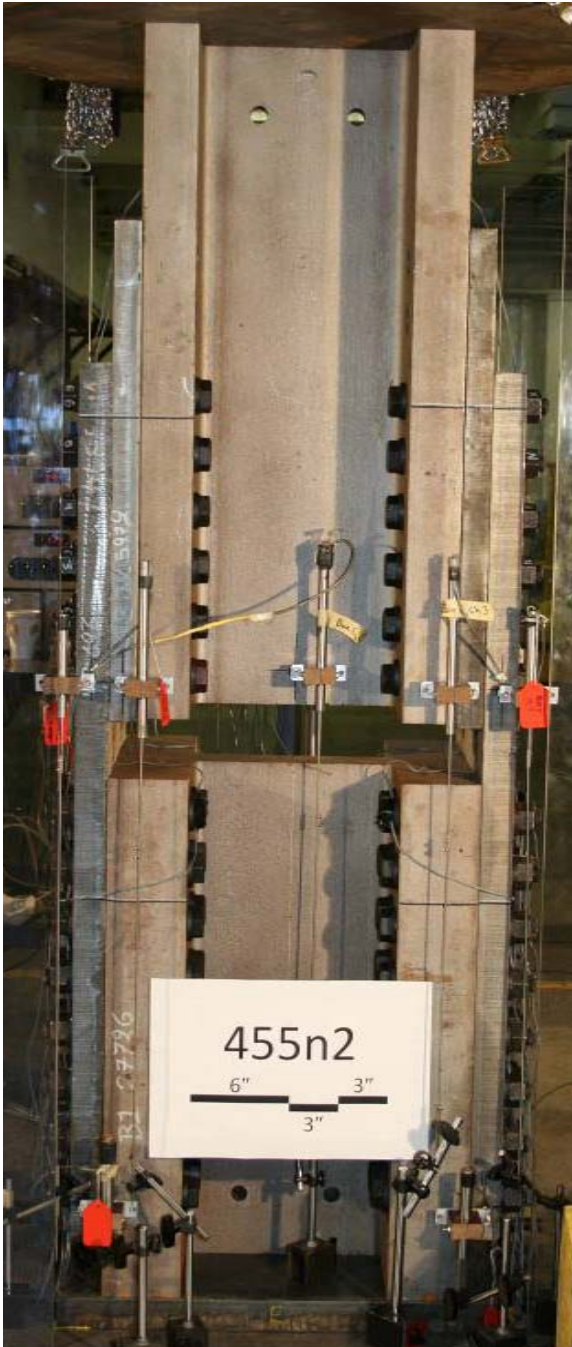


**Figure B.244 – 455n2: Before test (east side)**

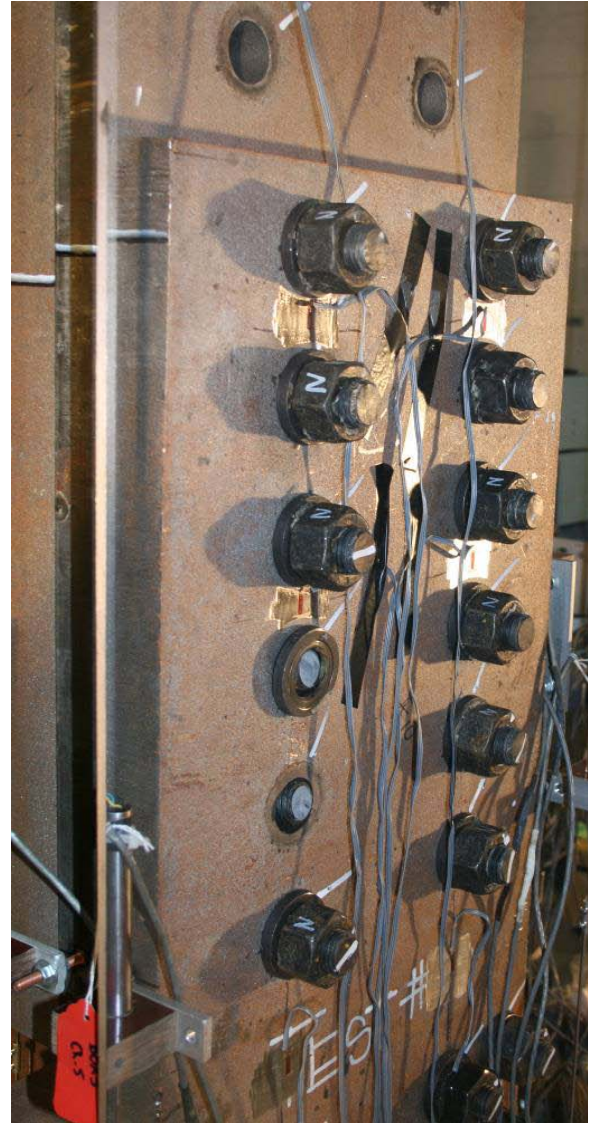


**Figure B.245 – 455n2: After slip (north side)**



Figure B.246 – 455n2: After test (east side)

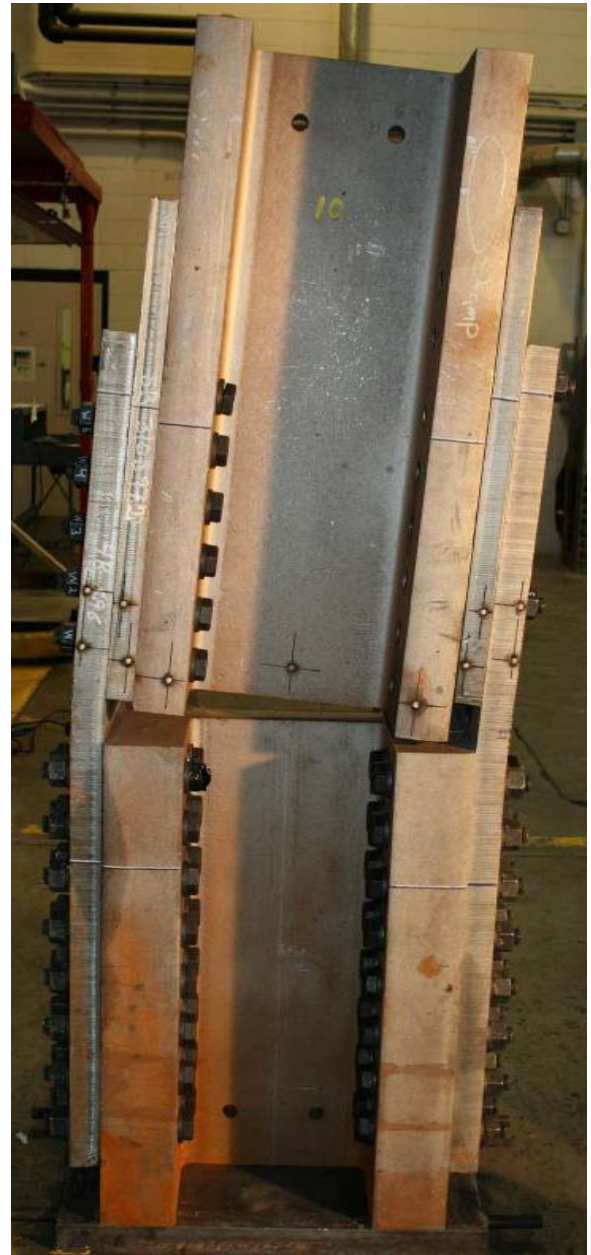


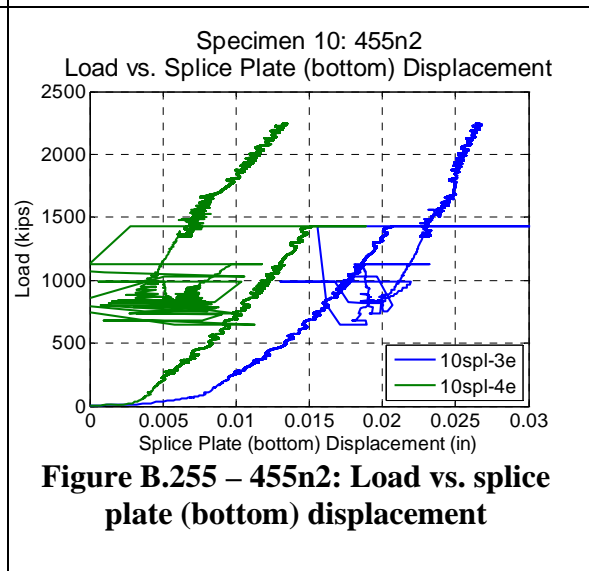
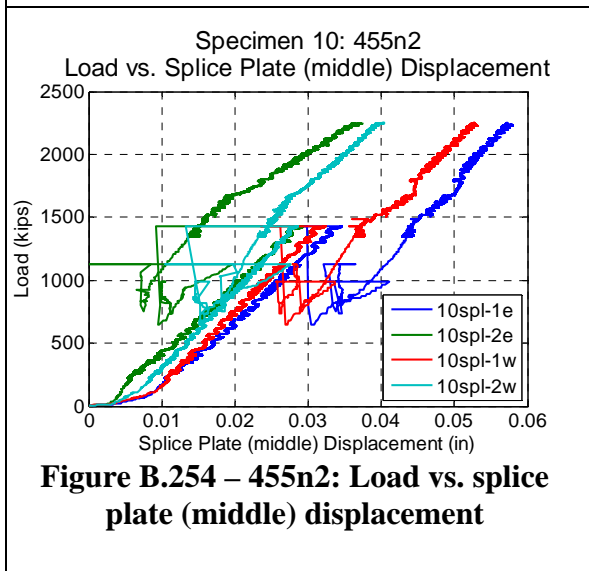
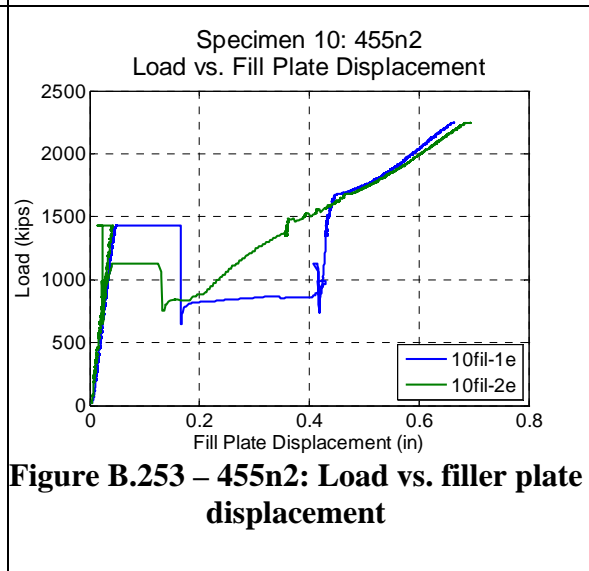
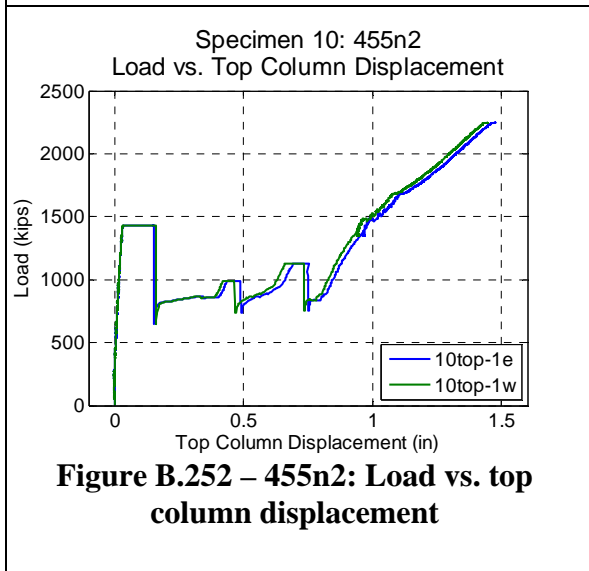
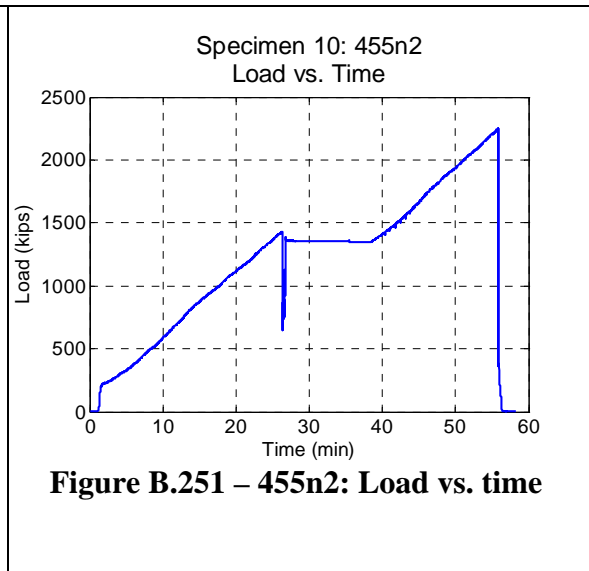
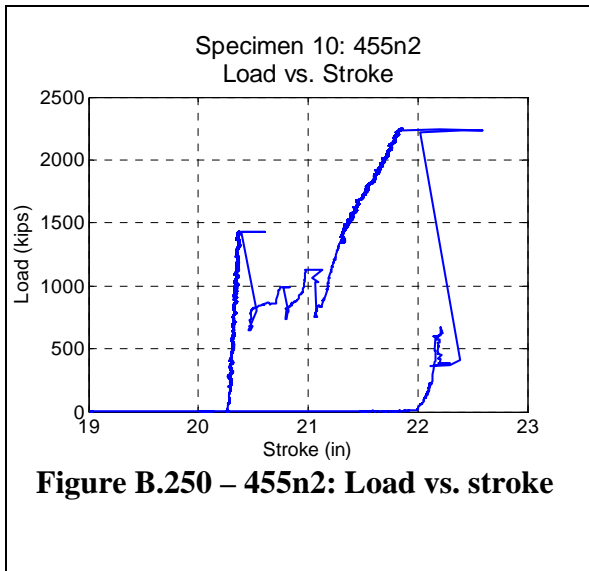
Figure B.247 – 455n2: After test (west side)

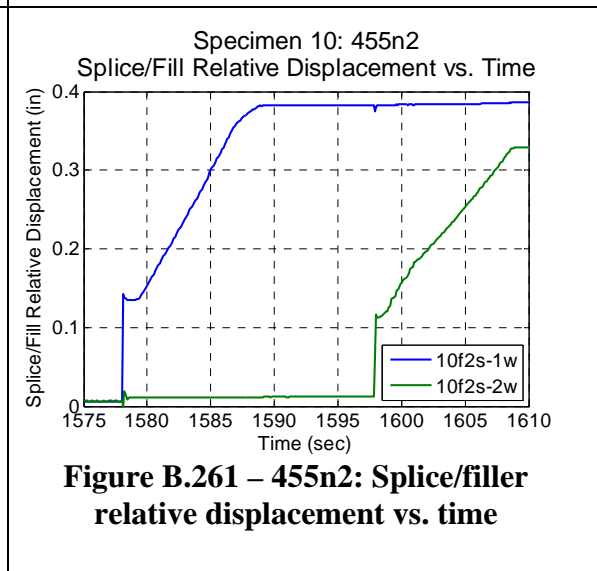
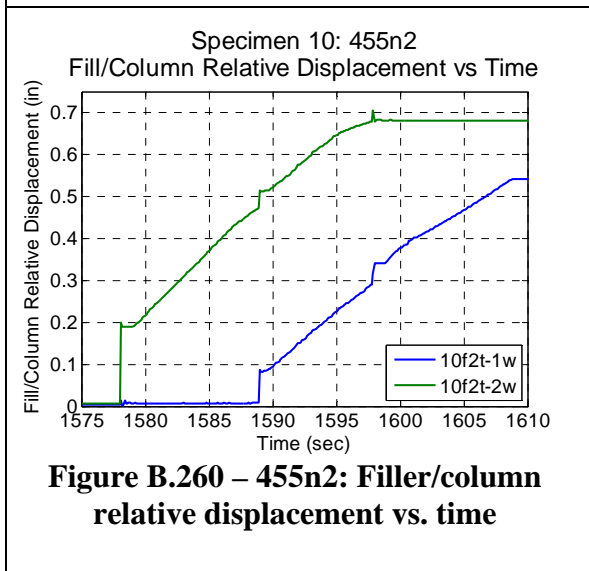
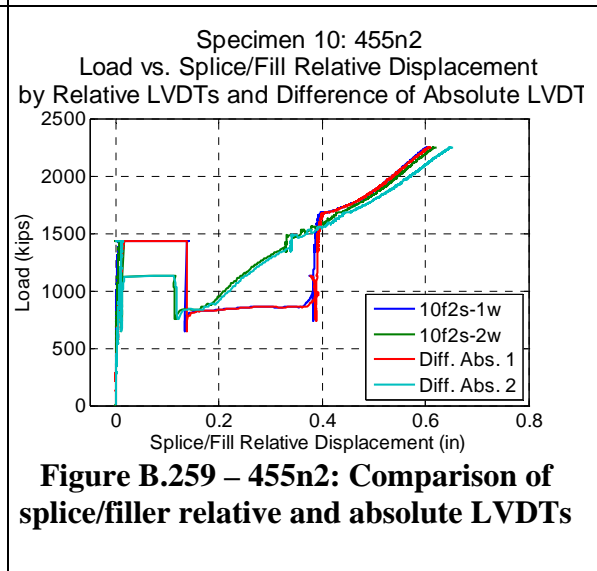
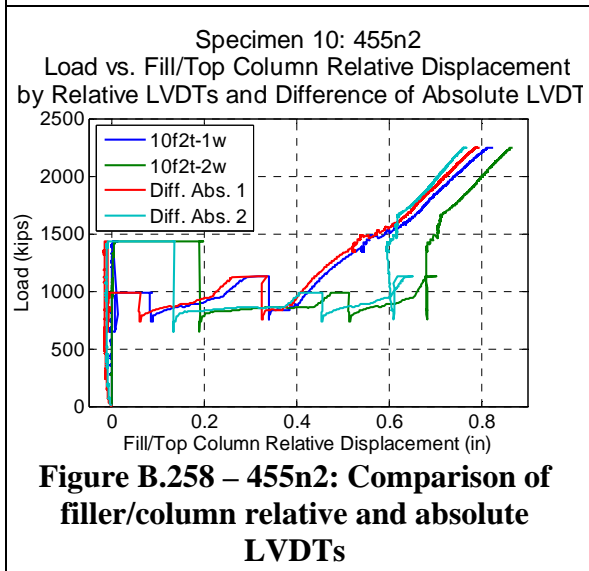
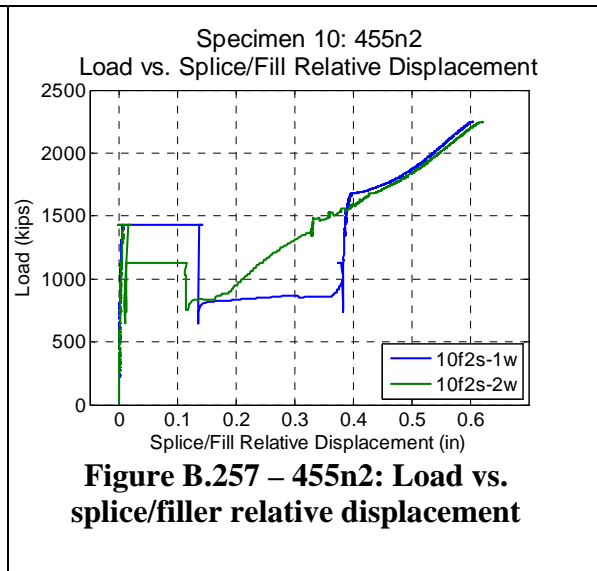
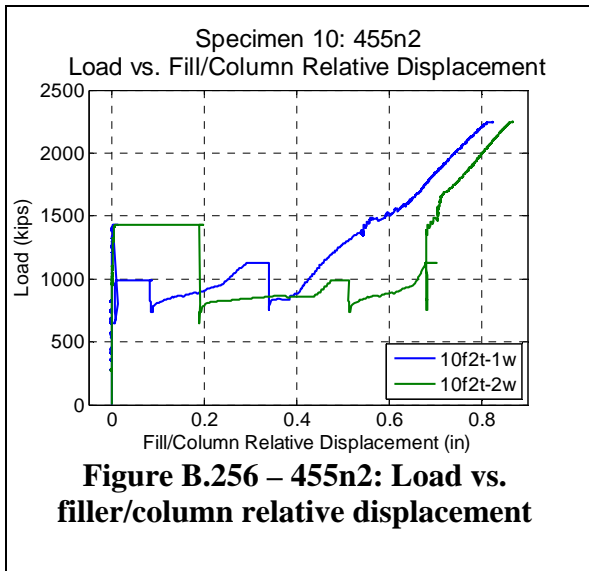


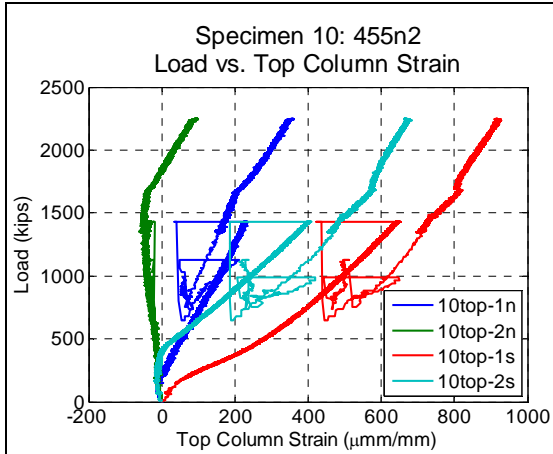
Figure B.248 – 455n2: After test (south side)



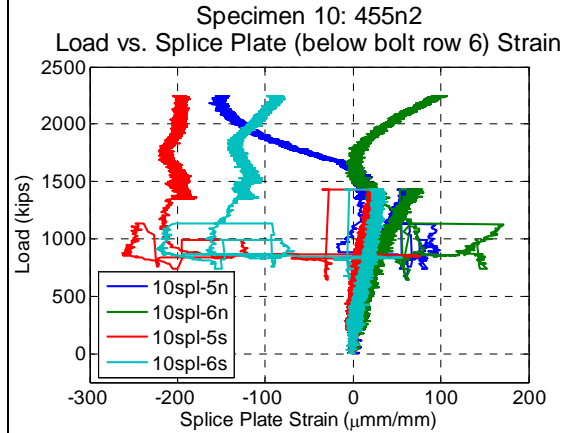
Figure B.249 – 455n2: After test (north side)



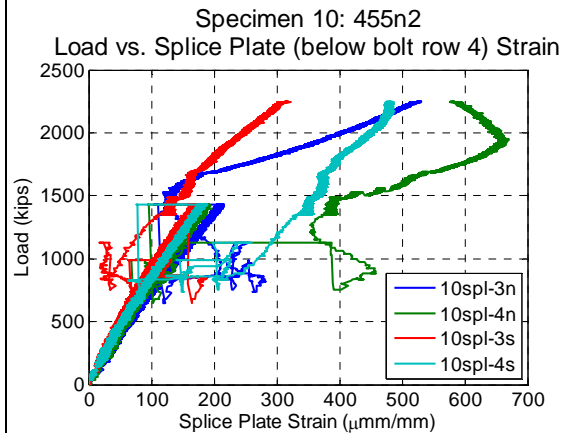




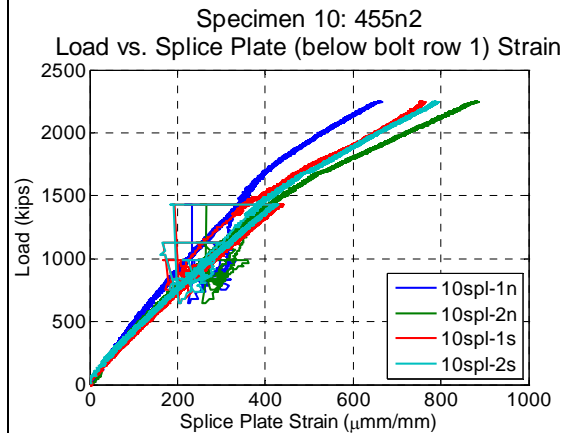
**Figure B.262 – 455n2: Load vs. top column strain**



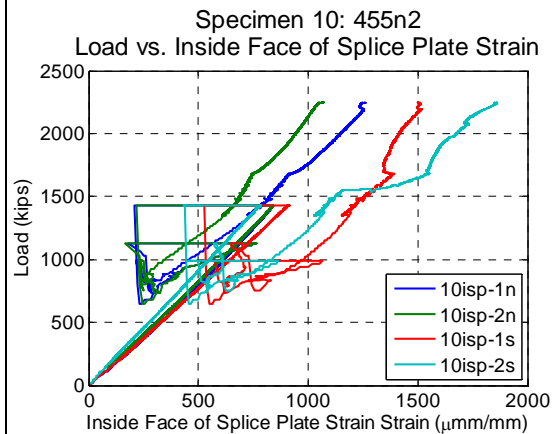
**Figure B.263 – 455n2: Load vs. splice plate (below bolt row 6) strain**



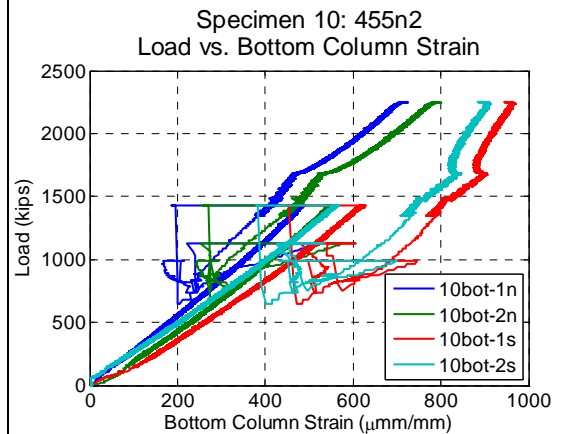
**Figure B.264 – 455n2: Load vs. splice plate (below bolt row 4) strain**



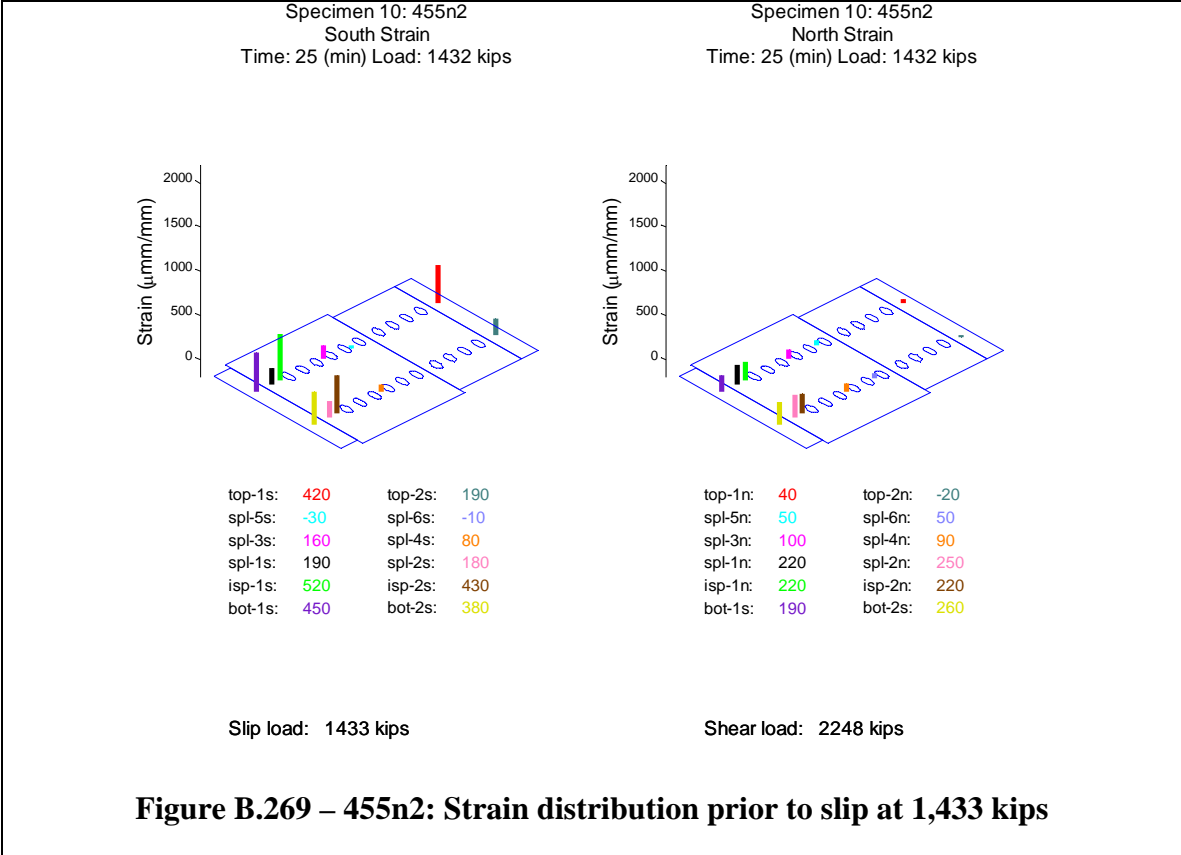
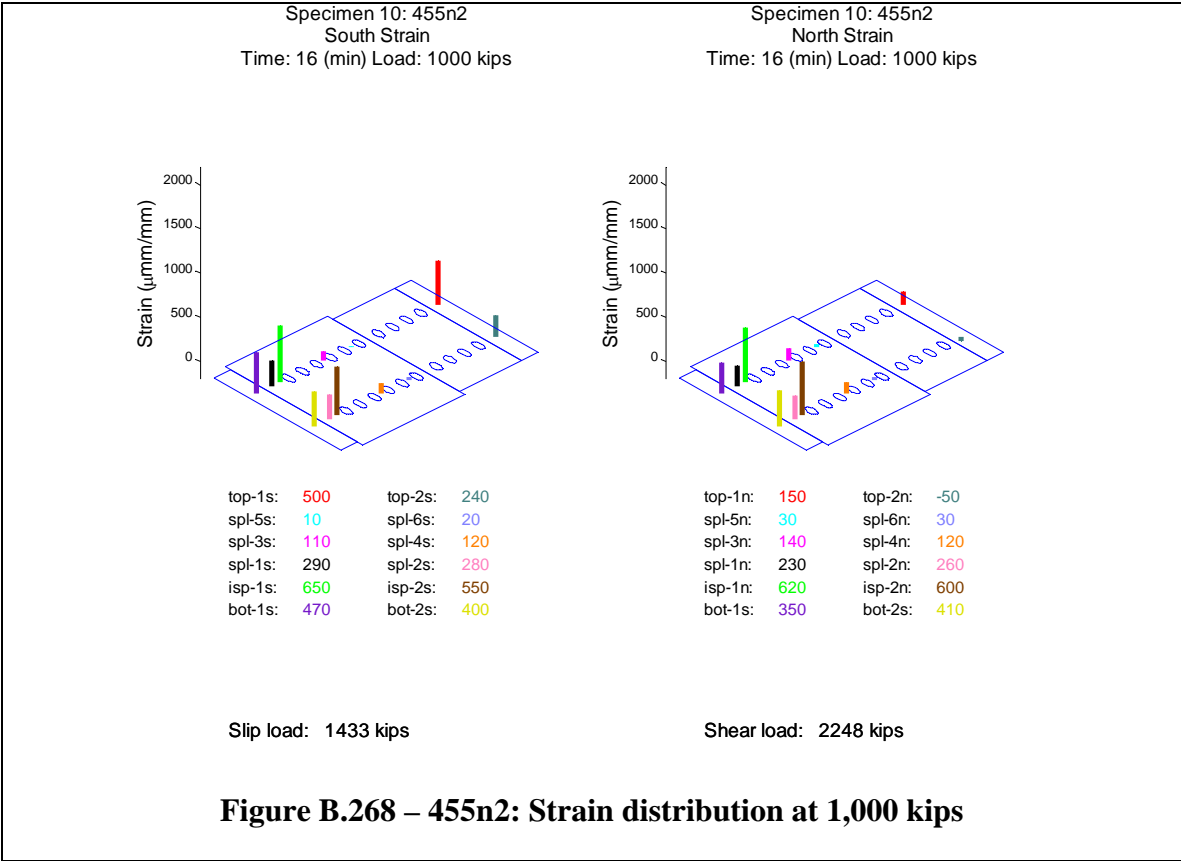
**Figure B.265 – 455n2: Load vs. splice plate (below bolt row 1) strain**



**Figure B.266 – 455n2: Load vs. inside face of splice plate strain**



**Figure B.267 – 455n2: Load vs. bottom column strain**



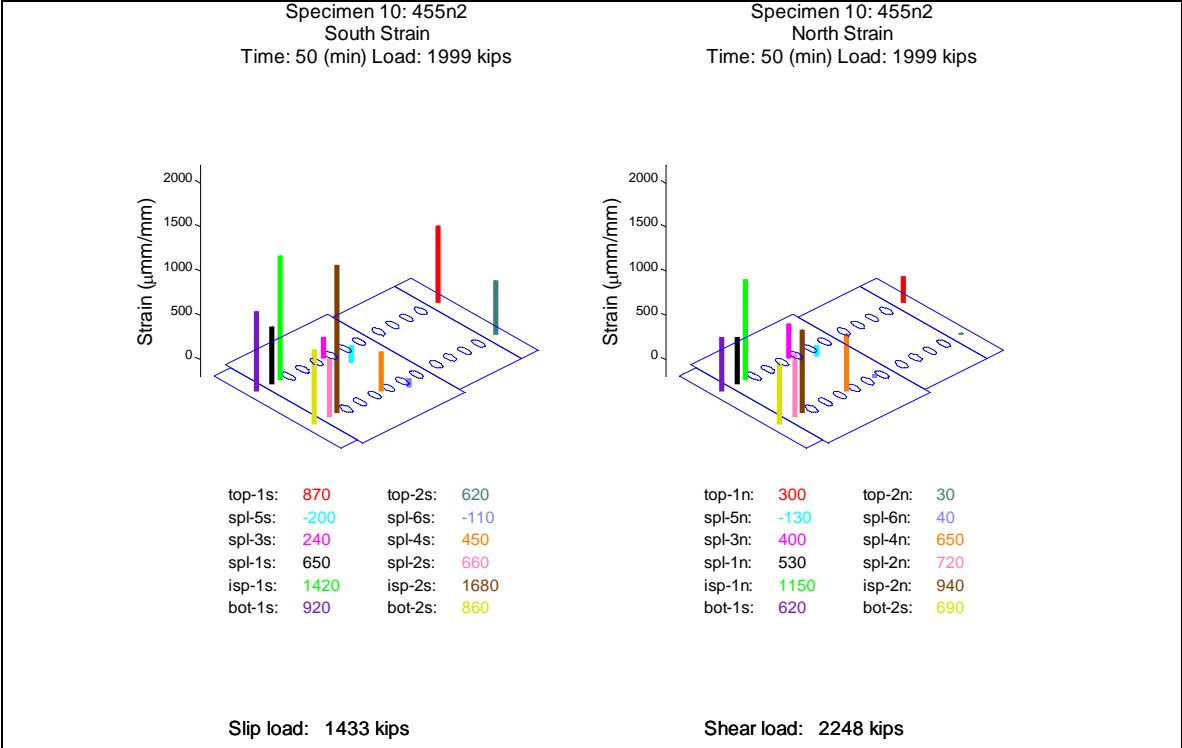


**Figure B.270 – 455n2: Strain distribution at 2,000 kips**

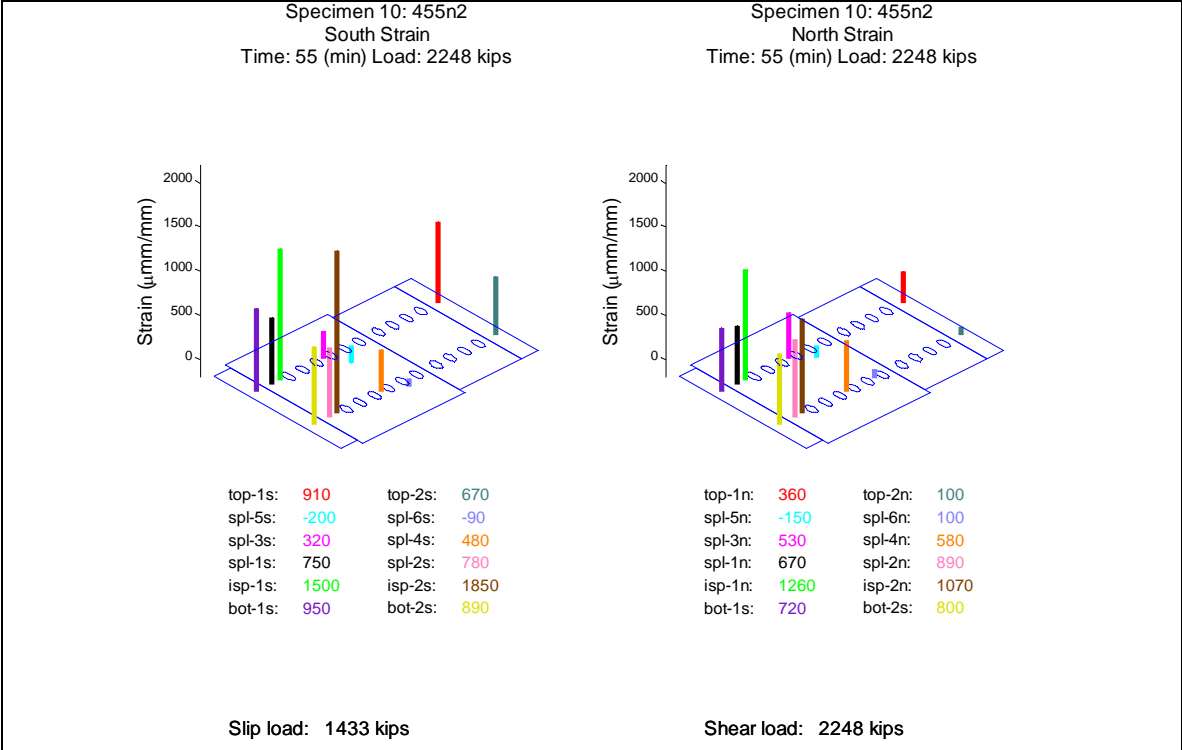


**Figure B.271 – 455n2: Strain distribution prior to shear at 2,248 kips**

## B.12 Specimen 159n-2ply1

Specimen 159n-2ply1 (Figure B.272 to Figure B.298) behaved approximately linearly until the observed slip load (658 kips). At the observed slip load the relative displacement between the two filler plates on the south side increased suddenly by approximately 0.13 in. over a period of approximately 3 seconds (Figure B.287, Figure B.288 and Figure B.289). No significant deformation was observed between the other faying surfaces at that load, and bending was clearly introduced into the specimen. The maximum expected clearance in the holes based on the assembly was nominally  $2 * (5/16 \text{ inches}) = 0.625$  inches. During this dynamic event, the load dropped immediately to 503 kips and increased to approximately 700 kips (reaching 751 kips briefly first), where the load was held for observation of the specimen (Figure B.279). As the load was increased, there were several more slip events, the most significant of which occurred at 1,005 kips, 1,020 kips, 1,200 kips (Figure B.278 and Figure B.280). Each of these events corresponded to a sudden increase in the relative deformation and a small drop in the load (Figure B.279 and Figure B.280), with slip starting appreciably on all surfaces, particularly between the top column and the fillers on both sides (Figure B.284 and Figure B.288).

After 1200 kips, the behavior exhibited some slight stiffening, but it is difficult to assess clearly if and when the bolts slipped into bearing. There is another dynamic event at a load of 2,110 kips, generally occurring on both column flanges. It is most likely due to further slip, but this is not conclusive. After recovering from this event, the specimen stiffened slightly, indicating that the bolts were in bearing at this point.

Starting at a load of approximately 2,400 kips the top column began to yield (Figure B.290). This was visually confirmed after the test by the ovalization of holes in the top of the web of the top column (these were used for lifting the specimen), as well as slight local buckling of the top column flanges.

The west bolt in bolt row 5 of the north splice plate (NE5) failed after slip and before the remaining bolts failed. The bolt failed mostly likely due more to tension, not bolt shear. This bolt was not one of the three control bolts, whose elongation was measured during assembly to ensure proper pretension.

Upon further loading, the bolts yielded and eventually failed simultaneously at the observed bolt shear load (2,813 kips) (Figure B.273, Figure B.274 and Figure B.275). Only the twelve bolts on south flange of the top column failed (one of these bolts failed earlier as noted above), leaving the twelve bolts on the north flange intact on the specimen.

After the initial slip (658 kips), the specimen produced noises approximately every 50 kips, up to 2600 kips. Noises were observed during slip of each plane. Noises believed to be produced by the testing machine were neglected. The noises are likely associated with additional small slip events, bolts coming into bearing with the bolt holes, or possibly initiation of fractures within the bolts.

The LVDTs measuring the relative displacement between the splice plate and filler plate (11f2s-1w and 11f2s-2w) were improperly set and the measurement went out of range early in the test. The initial measurements are valid and are shown in Figure B.285 and Figure B.287. After slip, prior to shear failure, the east strain gage at bolt row 6 on the north splice plate (11spl-6n) was damaged.

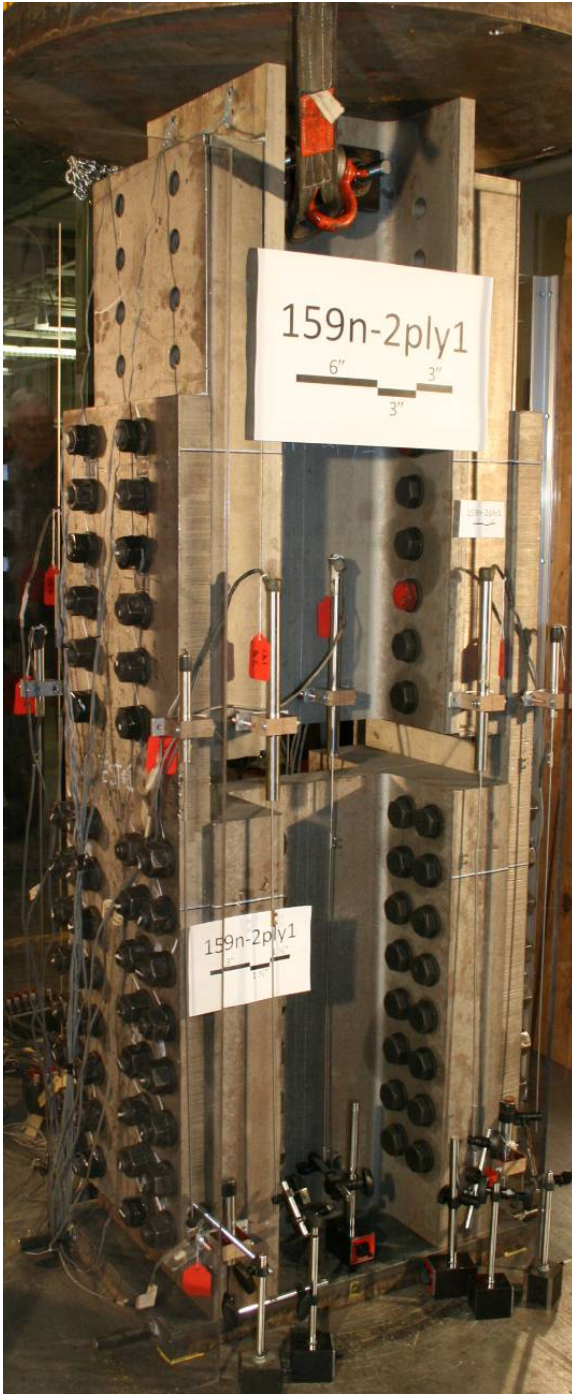
The splice plate LVDTs (Figure B.282 and Figure B.283) showed a dynamic increase or decrease in displacement during the slip event at 1634 kips. This may be due to a number of reasons, including stress relief in the splice plates after slip, very small slips relative to the column flanges, or small dynamic vibrations (with resulting small permanent offsets) of the LVDT holders, but the displacements are an order of magnitude smaller than the primary slip displacements (Figure B.284) and are not likely to indicate significant behavior.

Figure B.286 and Figure B.287 compare the LVDTs directly measuring relative slip between the 3½ thick filler plate and either the top column (Figure B.284) or the splice plate (Figure B.285) with the difference between the average of the two LVDTs on either 3½ inch thick filler plate at that same cross section as the LVDTs on the top column (Figure B.281) and either the average of the two LVDTs at the bottom center of the top column (Figure B.280) or the average of the two LVDTs on either splice plate at that same cross section as the LVDTs on the top column (Figure B.282). The measurements of the relative LVDTs correspond reasonably well to the difference between the corresponding absolute LVDTs (Figure B.286).

The top column strain gages indicate that the localized introduction of load had a small bias to the southwest (Figure B.290). The bottom column strain gages indicate that the localized reaction had a north bias (Figure B.294).

The splice plate experiences tension as well as compression during the loading due to bending due to the initial unsymmetrical slip (Figure B.291, Figure B.292 and Figure B.293). Snapshots of the specimen strain at 1000 kips, immediately prior to slip, 2000 kips and immediately prior to shear are visually presented in Figure B.295, Figure B.296, Figure B.297 and Figure B.298, respectively. These graphs show that the strain enters into the splice plate gradually and relatively uniformly from bolt row 6 to bolt row 1 throughout the experiment.

The experiment was executed in load control. The loading rate for the experiment was approximately 1 kip per second. Two elastic cycles were executed prior to the test, going up to loads of 300 kips and 200 kips, respectively, returning to zero load each time, to verify instrumentation. The data collection rate for the experiment was held constant at 10 Hertz (10 sets of readings per second).



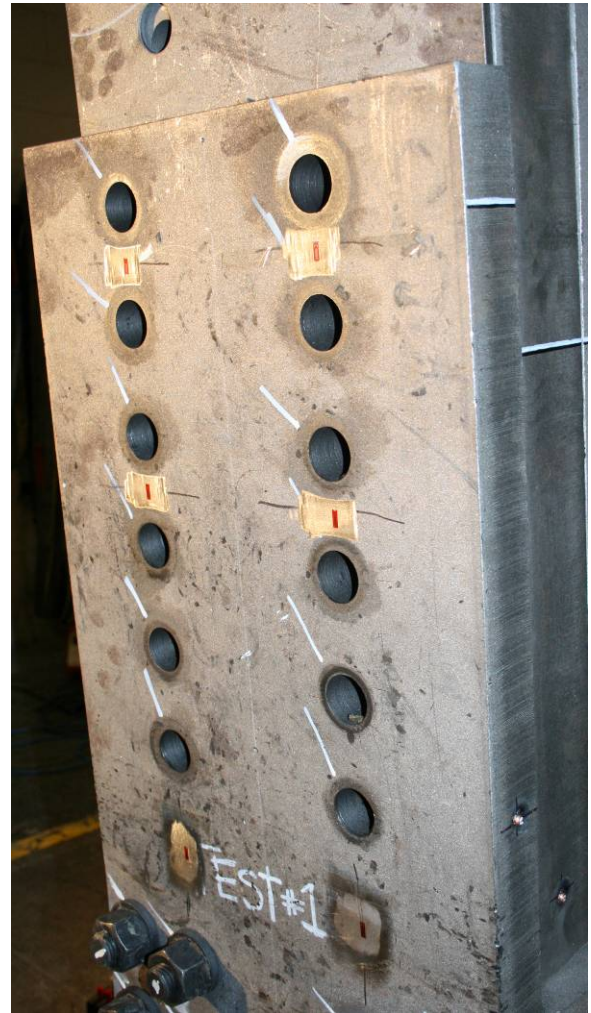
**Figure B.272 – 159n-2ply1: Before test (southeast corner)**



**Figure B.273 – 159n-2ply1: After test (east side)**



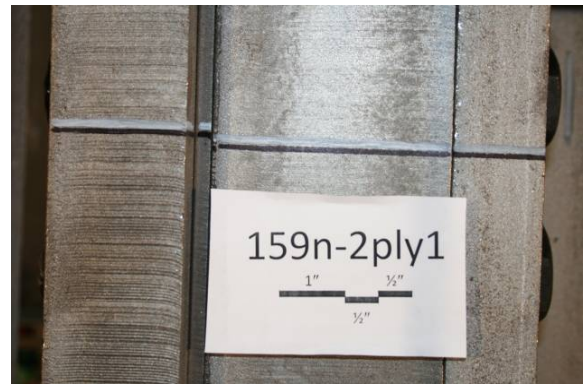
**Figure B.274 – 159n-2ply1: After test  
(southeast corner)**



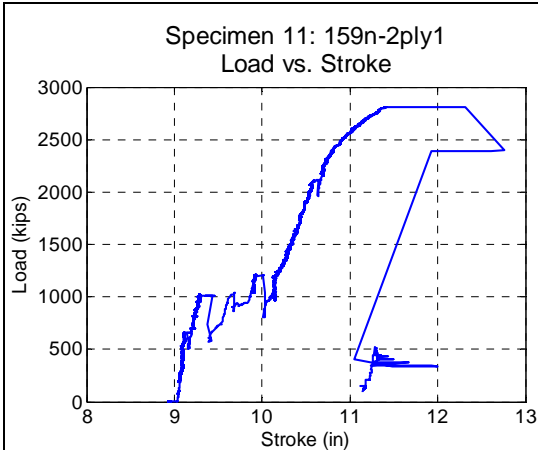
**Figure B.275 – 159n-2ply1: After test  
(south side)**



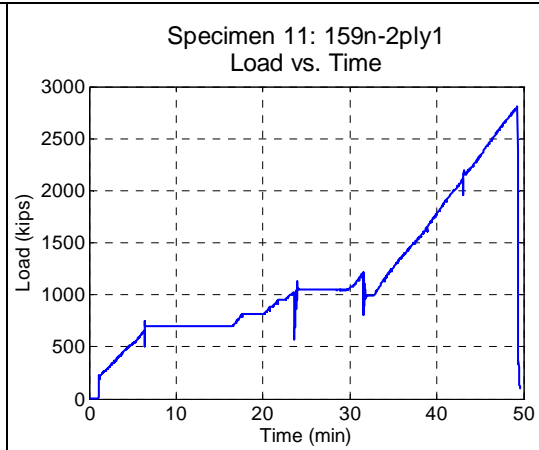
**Figure B.276 – 159n-2ply1: Initial single bolt failure (northwest corner)**



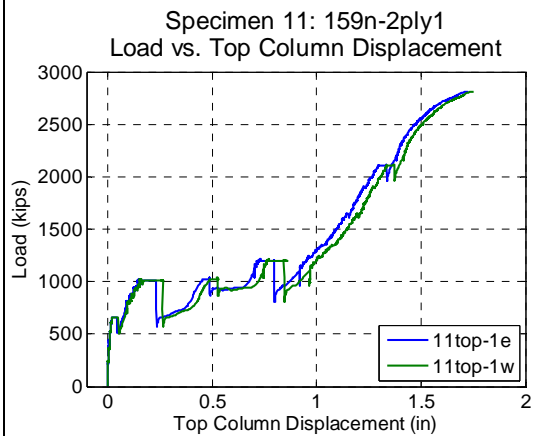
**Figure B.277 – 159n-2ply1: Initial slip at 700 kips (south side)**



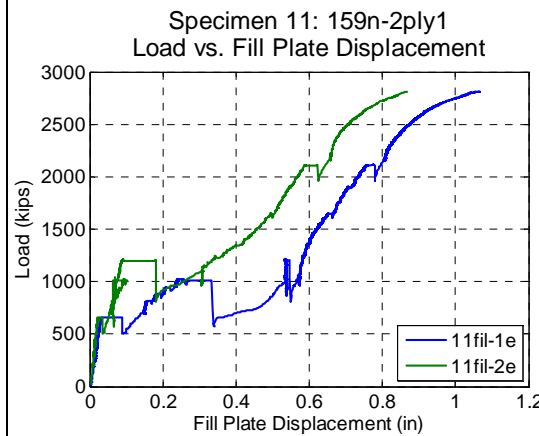
**Figure B.278 – 159n-2ply1: Load vs. stroke**



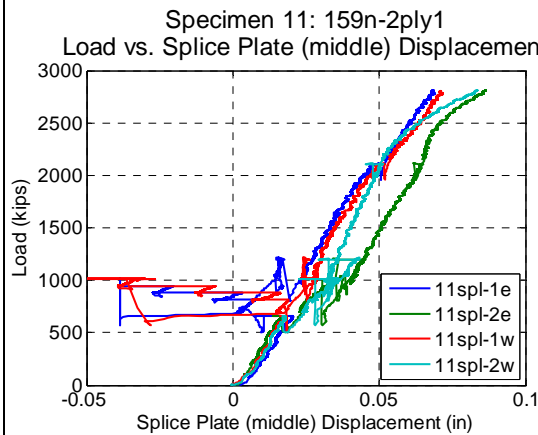
**Figure B.279 – 159n-2ply1: Load vs. time**



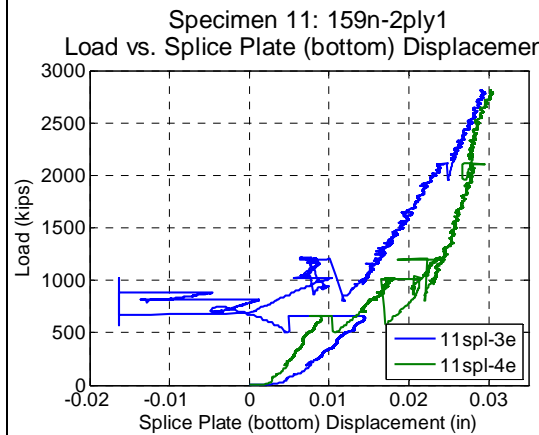
**Figure B.280 – 159n-2ply1: Load vs. top column displacement**



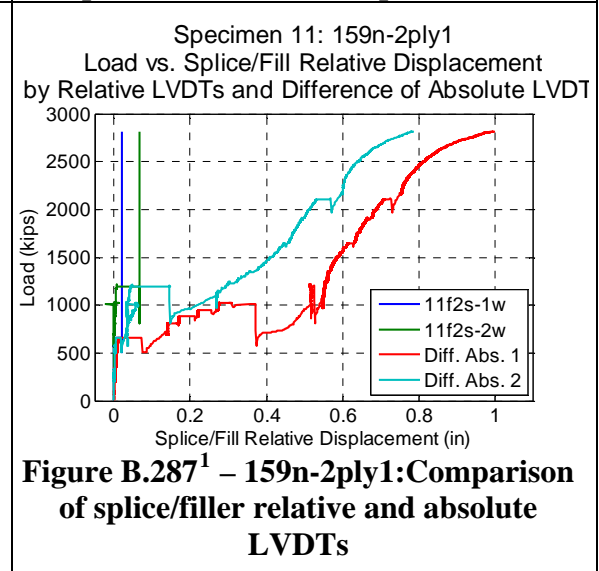
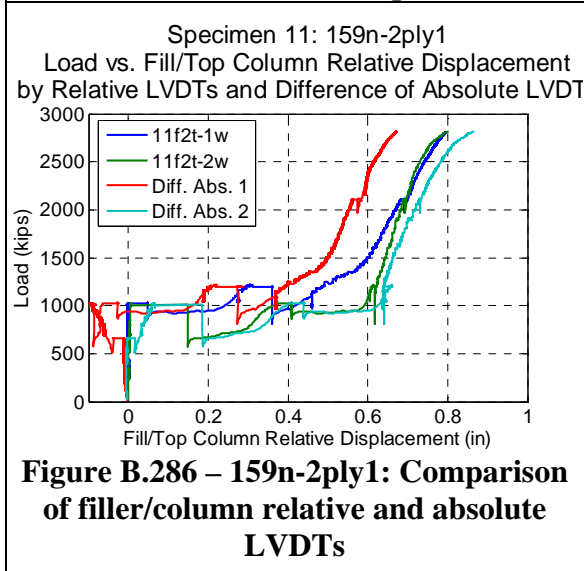
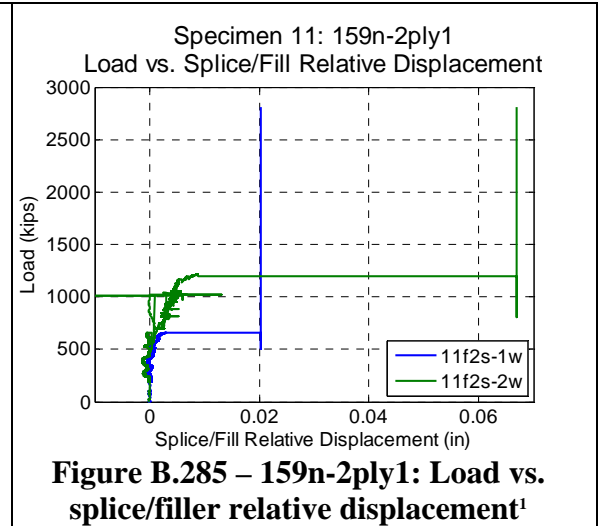
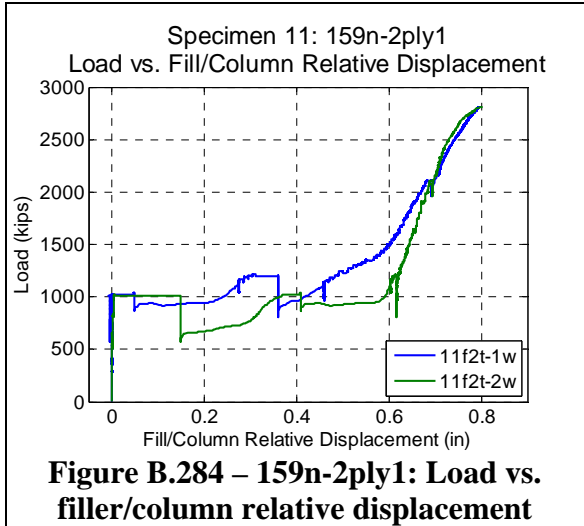
**Figure B.281 – 159n-2ply1: Load vs. filler plate displacement**



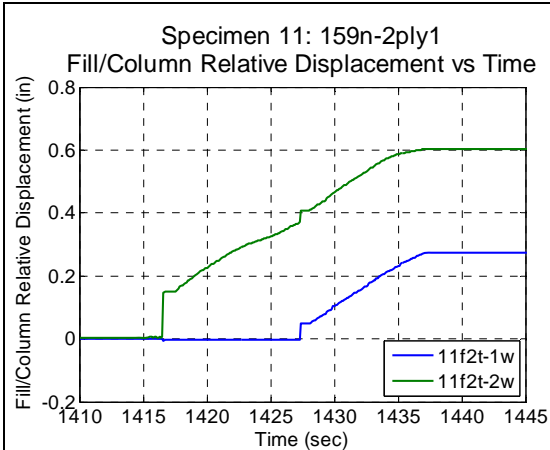
**Figure B.282 – 159n-2ply1: Load vs. splice plate (middle) displacement**



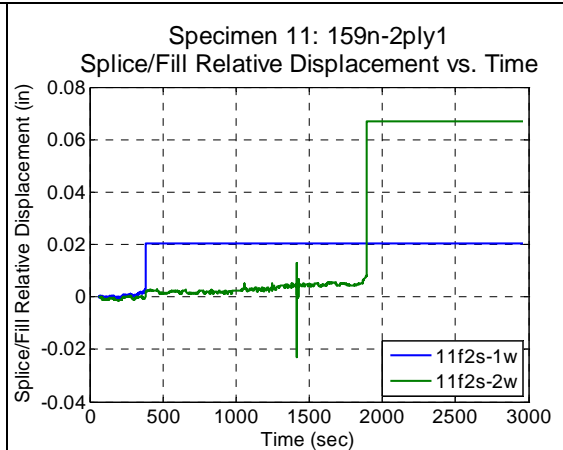
**Figure B.283 – 159n-2ply1: Load vs. splice plate (bottom) displacement**



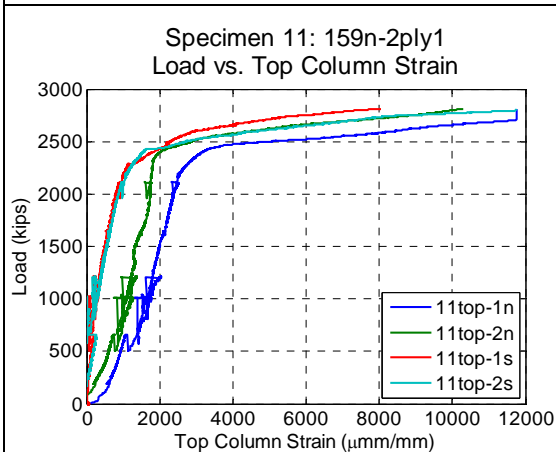
<sup>1</sup> Only measurements less than approximately 0.02 in. displacement are valid for LVDTs 11f2s-1w and 11f2s-2w.



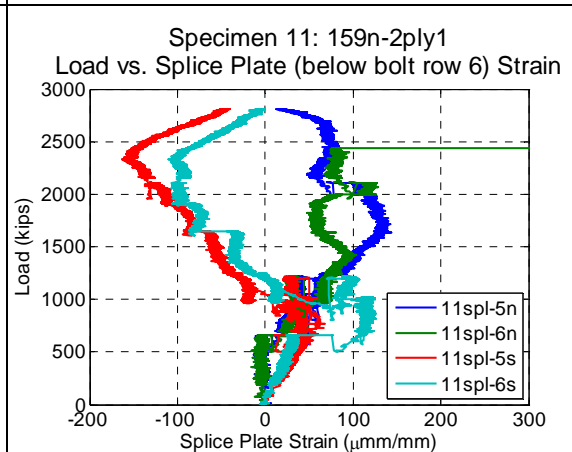
**Figure B.288 – 159n-2ply1: Filler/column relative displacement vs. time**



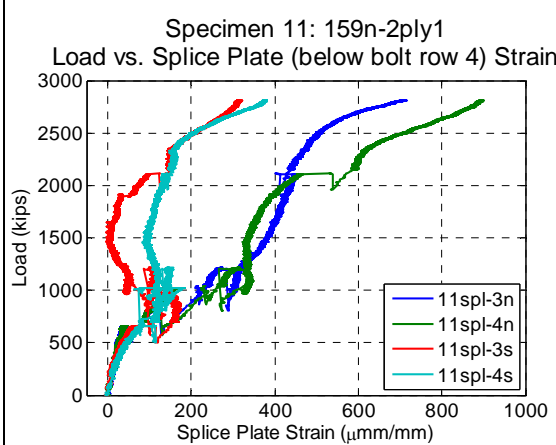
**Figure B.289 – 159n-2ply1: Splice/filler relative displacement vs. time**



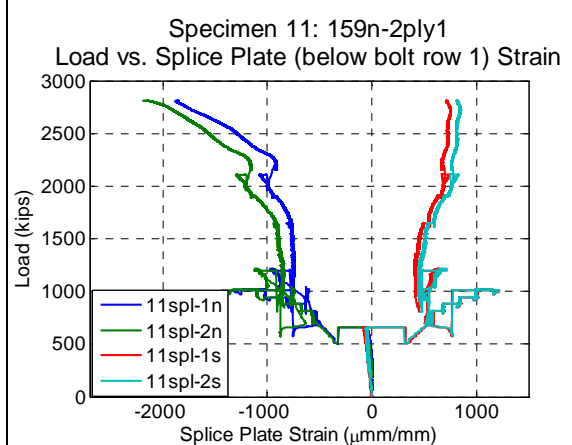
**Figure B.290 – 159n-2ply1: Load vs. top column strain**



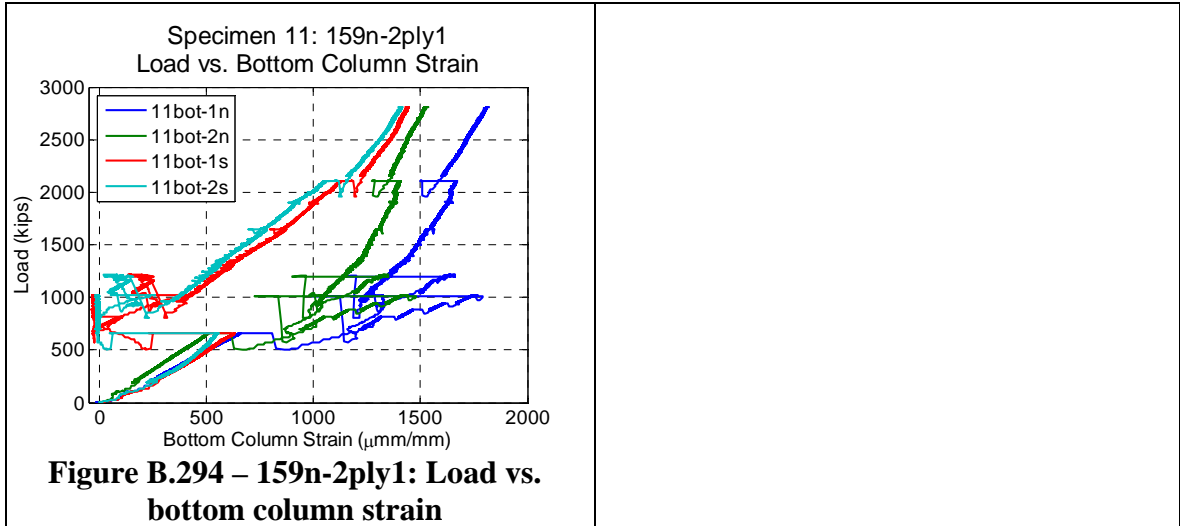
**Figure B.291 – 159n-2ply1: Load vs. splice plate (below bolt row 6) strain**

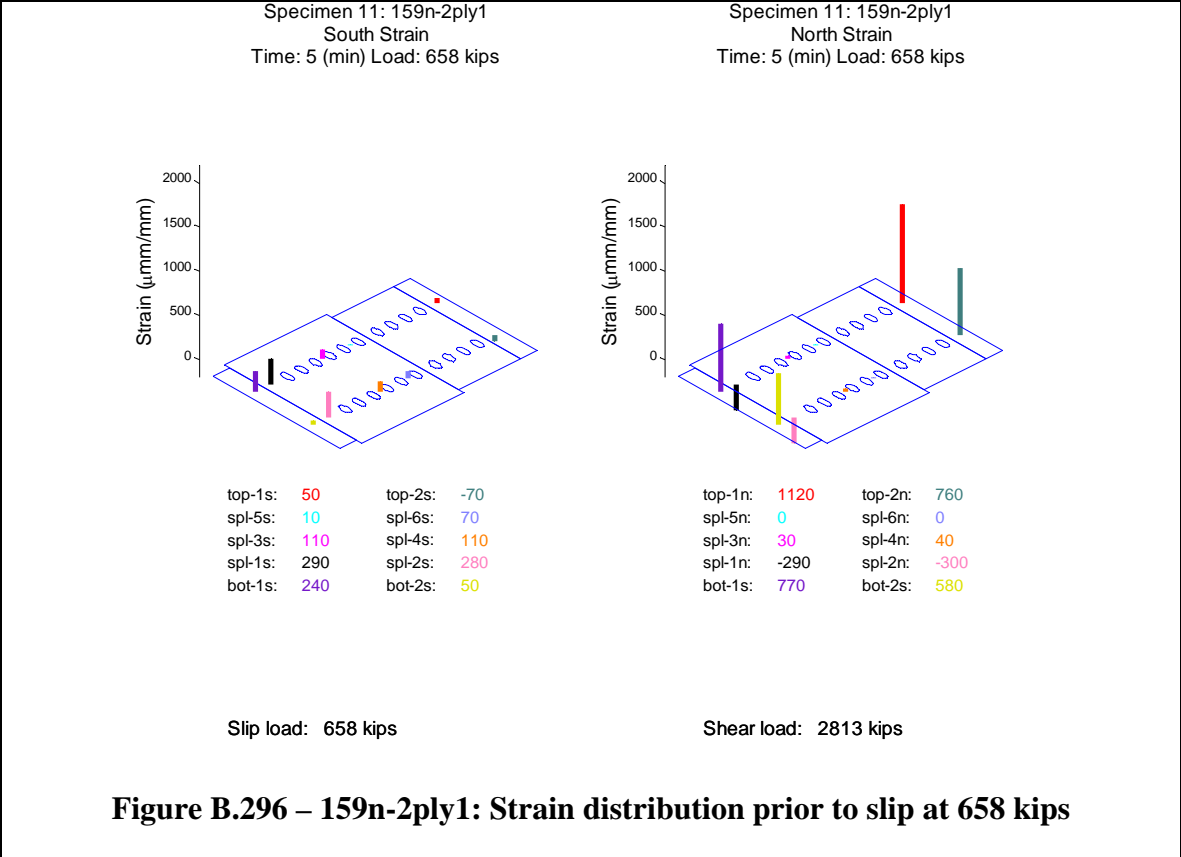
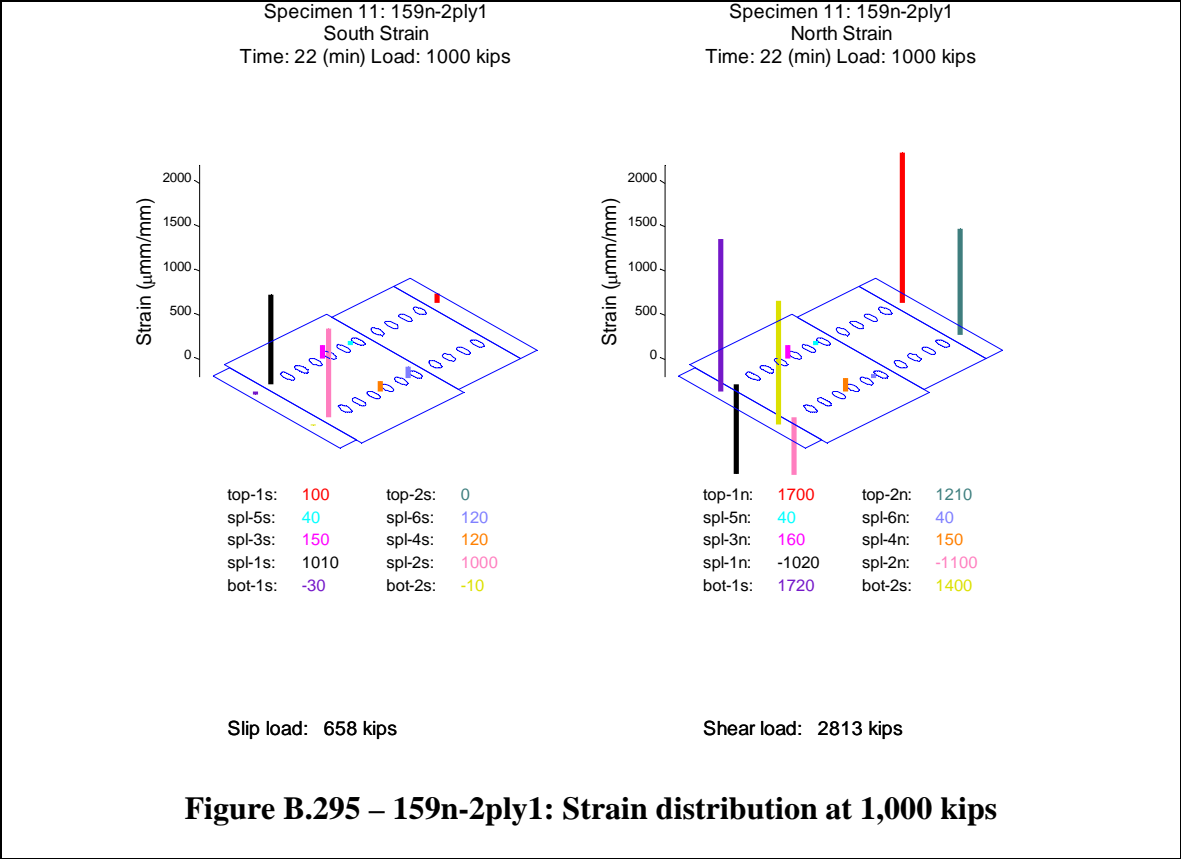


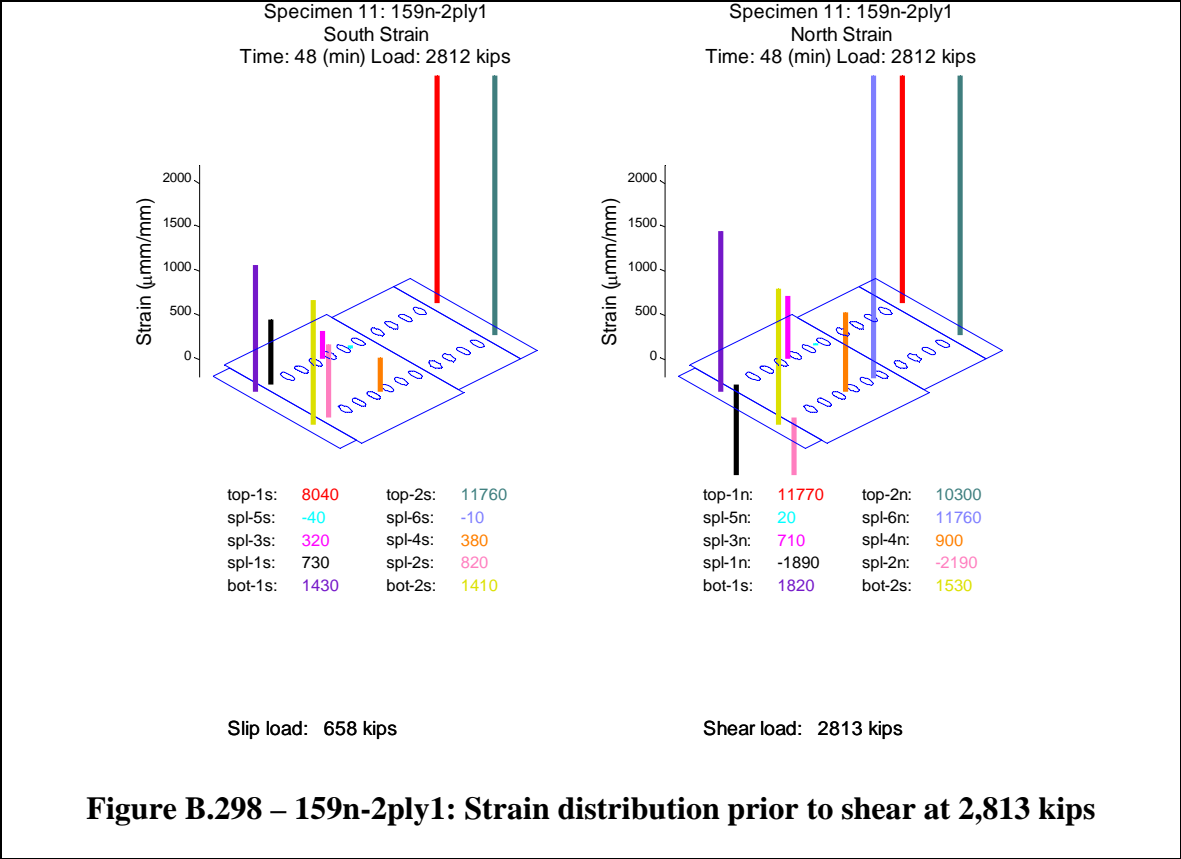
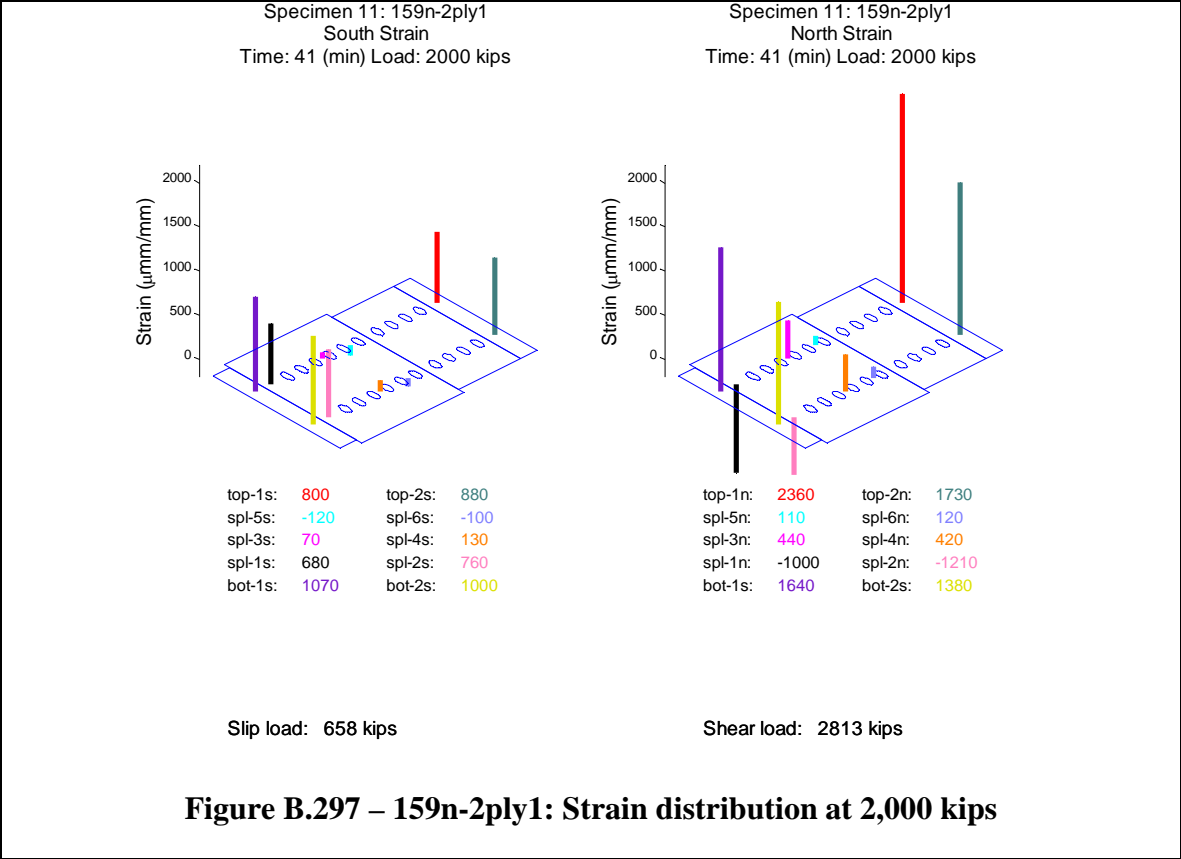
**Figure B.292 – 159n-2ply1: Load vs. splice plate (below bolt row 4) strain**



**Figure B.293 – 159n2ply1: Load vs. splice plate (below bolt row 1) strain**







## B.13 Specimen 159n-2ply2

Specimen 159n-2ply2 (Figure B.299 to Figure B.326) behaved approximately linearly until the observed slip load (1,349 kips). During the slip event, the relative displacement between the splice plate and the filler plate, as well as the filler plate and the top column increased suddenly. Slip initiated between the filler plate and the top column on north and south sides of the specimen (Figure B.311). After losing load dynamically and then starting to pick up load again, slip initiated between the filler plate and the splice plate on the north side of the specimen as well as between the filler plate and the top column on the south side of the specimen (Figure B.312). Over a period of 25 seconds, the relative displacements increased by the amounts shown in Table B.12. This is seen most clearly in the relative LVDTs (Figure B.315 and Figure B.316). During this dynamic event, the load dropped and increased several times. The lowest load measured was 652 kips (Figure B.305). The machine and specimen stabilized at 1,290 kips and the load was held for observation of the specimen (Figure B.306).

**Table B.12 – 159n-2ply2: Relative slip**

<b>Location</b>	<b>North</b>	<b>South</b>
<b>Between Splice and Filler</b>	0.44 in	0.41 in
<b>Between Filler And Top Column</b>	0.62 in	0.59 in
<b>Sum</b>	1.06 in	1.00 in

During this event the bolts likely slipped into bearing on the top column and splice plates, as seen by the increase in stiffness in Figure B.312 at approximately a load of 1,500 kips and a relative slip of 0.55 inches. The maximum expected clearance in the holes based on the assembly was nominally  $2 * (5/16 \text{ inches}) = 0.625 \text{ inches}$ .

After the slip event, one bolt on the southwest side of the specimen (SW2) failed through the threads, indicating a pretension failure (Figure B.300). The bolt head and shank remained in the specimen and provided some doweling action and failed a second time in shear at the ultimate load of the specimen. This was not near the control bolt that was retorqued (bolt SW6 as per Table B.2)

The top column began to yield at approximately 2,500 kips (Figure B.317). Upon further loading, the bolts, now experiencing shear, yielded and eventually failed at the observed bolt shear load (2,932 kips) (Figure B.301 through Figure B.304). The twelve bolts through the splice plate on the north flange of the top column failed nearly simultaneously on the shear plane between the splice plate and the fill plate.

Prior to slip, the specimen made pinging noises at 742 and 1175 kips. After slip, the specimen produced pinging noises at the following loads; 1673, 1757, 1803, 1850, 1910, 1952, 2018, 2063, 2091, 2120, 2158, 2181, 2217, 2246, 2277, 2302, 2330, 2349, 2379, 2400, 2421, 2431, 2453, 2470, 2493, 2512, 2524, 2531, 2541, 2554, 2565, 2589, 2600,

2617, 2630, 2656, 2659, 2669, 2682, 2697, 2710, 2723, 2734, 2747, 2755, 2767, 2780, 2789, 2804, 2812, 2819 and 2828 kips. The noises continued every few kips up to the failure load (2932 kips). Noises believed to be produced by the testing machine were neglected. The noises are likely associated with additional small slip events, bolts coming into bearing with the bolt holes, or possibly initiation of fractures within the bolts.

The splice plate LVDTs (Figure B.309 and Figure B.310) showed a dynamic increase or decrease in displacement during the slip events. This may be due to a number of reasons, including stress relief in the splice plates after slip, very small slips relative to the column flanges, or small dynamic vibrations (with resulting small permanent offsets) of the LVDT holders, but the displacements are an order of magnitude smaller than the primary slip displacements (Figure B.311 and Figure B.312) and are not likely to indicate significant behavior.

Figure B.313 and Figure B.314 compare the LVDTs directly measuring relative slip between the filler plate and either the top column (Figure B.311) or the splice plate (Figure B.312) with the difference between the average of the two LVDTs on either filler plate at that same cross section as the LVDTs on the top column (Figure B.308) and either the average of the two LVDTs at the bottom center of the top column (Figure B.307) or the average of the two LVDTs on either splice plate at that same cross section as the LVDTs on the top column (Figure B.309). The measurements of the relative LVDTs correspond well to the difference between the corresponding absolute LVDTs.

For this specimen, strain gages were attached to the inside face of the splice plate in the gap between the top and bottom columns (Figure B.321). These measurements, when compared to the measurements from the outside face of the splice plate (Figure B.320), indicate significant bending in the splice plates. Yielding was recorded on the inside of the splice plate.

The top column strain gages exhibit that the localized introduction of load was approximately uniform (Figure B.317). The bottom column strain gages show that the localized reaction had a small bias towards the south (Figure B.322).

The splice plate data demonstrates the north splice plate is under higher compression than the south splice plate (Figure B.318, Figure B.319, Figure B.320 and Figure B.321), likely indicated by larger force in the north bolts, consistent with the ultimate shear failure of the north bolts. Snapshots of the specimen strain at 1000 kips, immediately prior to slip, 2000 kips and immediately prior to shear are visually presented in Figure B.323, Figure B.324, Figure B.325, Figure B.326, respectively. These graphs show that the strain enters into the splice plate gradually and relatively uniformly from bolt row 6 to bolt row 1 throughout the experiment.

The experiment was executed in load control. The loading rate for the experiment was approximately 1 kip per second. One elastic cycle was executed prior to the test, going up to a load of 200 kips and returning to zero load, to verify instrumentation. The data

collection rate for the experiment was held constant at 10 Hertz (10 sets of readings per second).

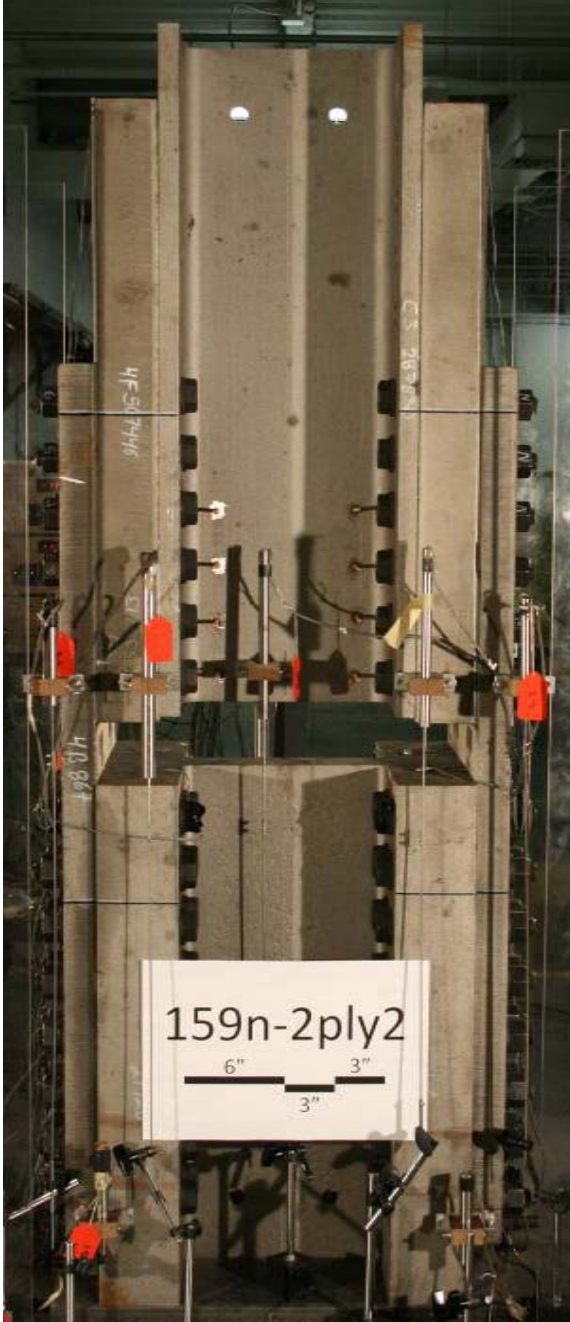


**Figure B.299 – 159n-2ply2: Before test (east side)**



**Figure B.300 – 159n-2ply2: After slip (east side)**

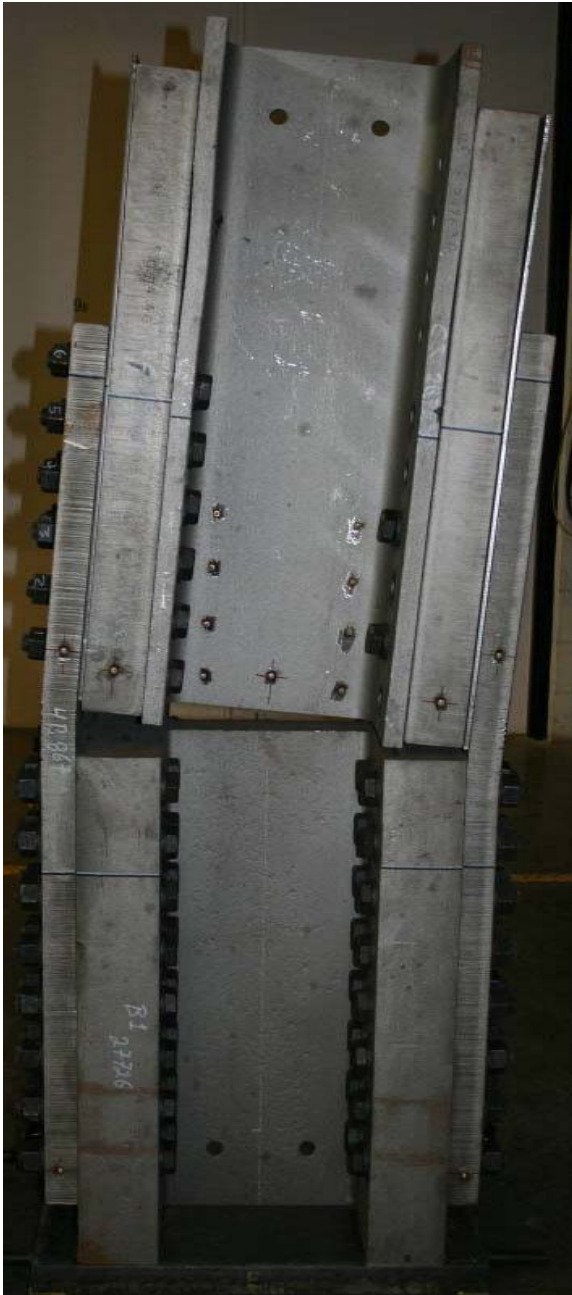


**Figure B.301 – 159n-2ply2: After test  
(east side)**



**Figure B.302 – 159n-2ply2: After test  
(west side)**

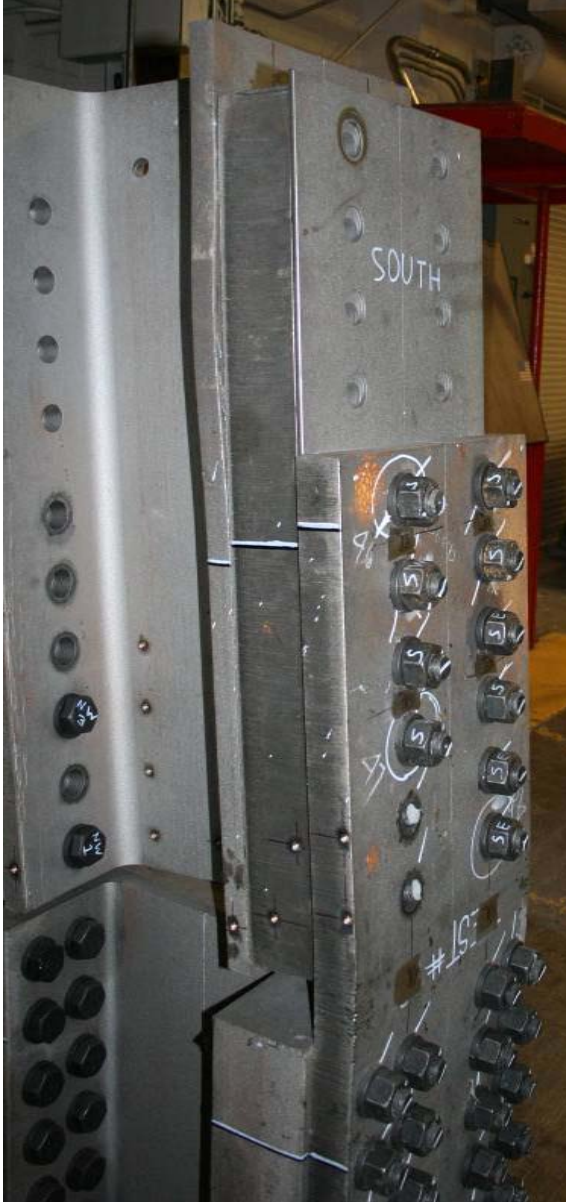
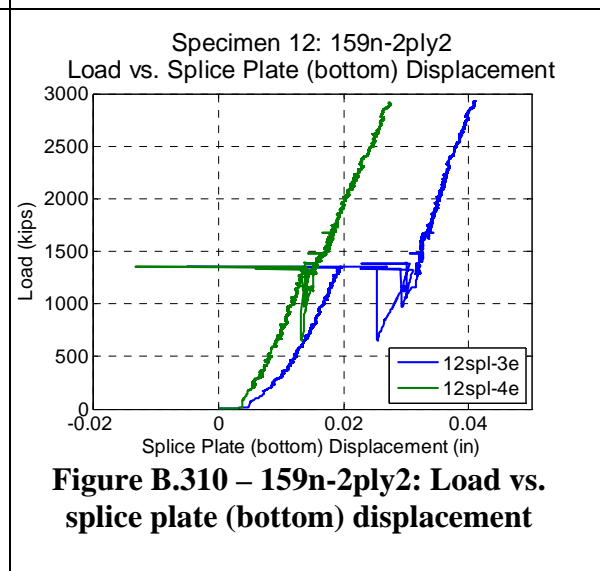
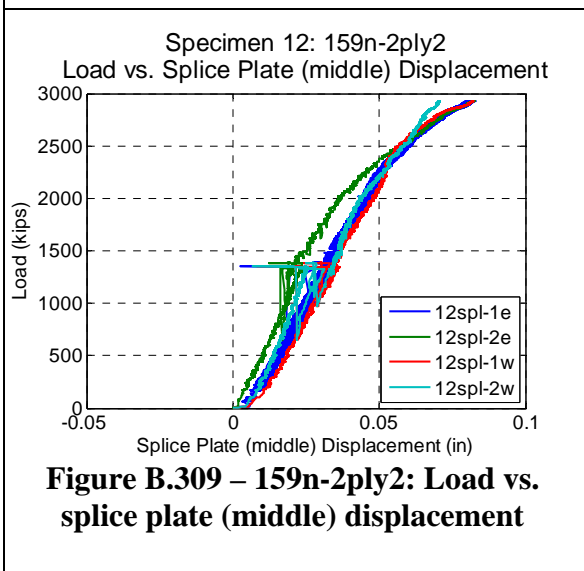
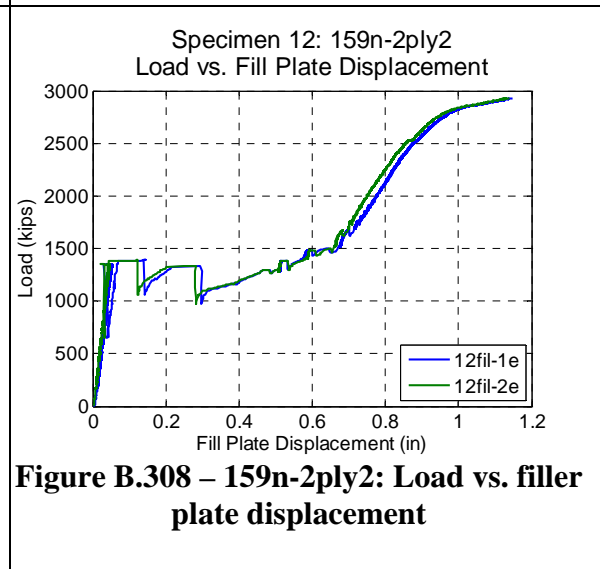
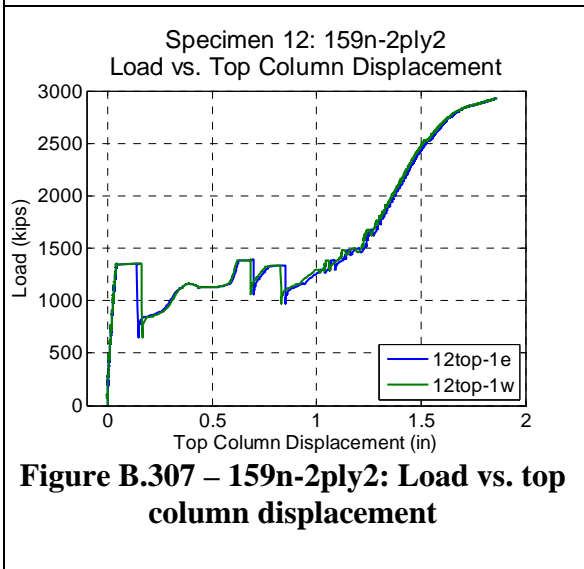
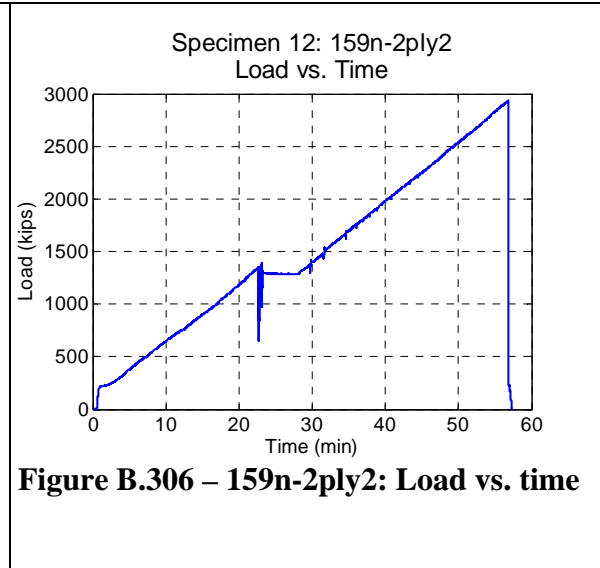
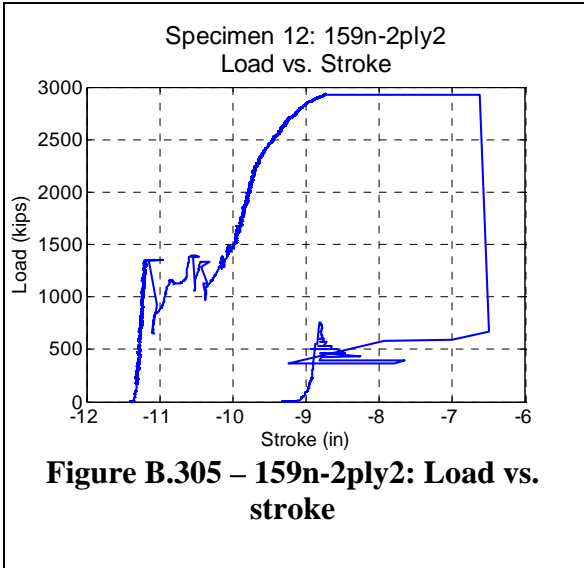
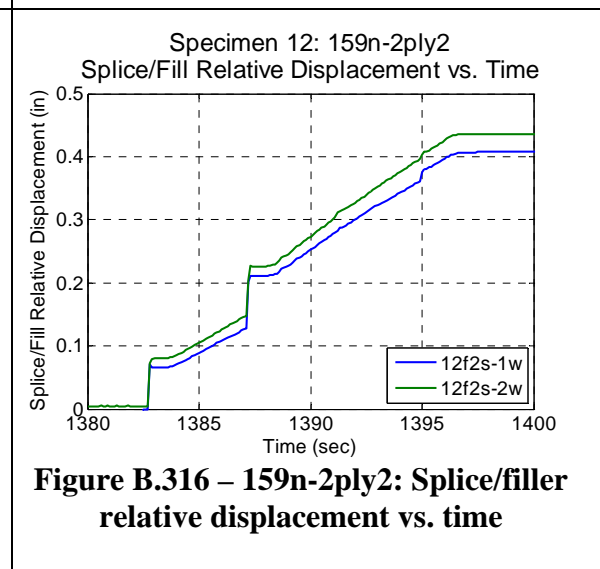
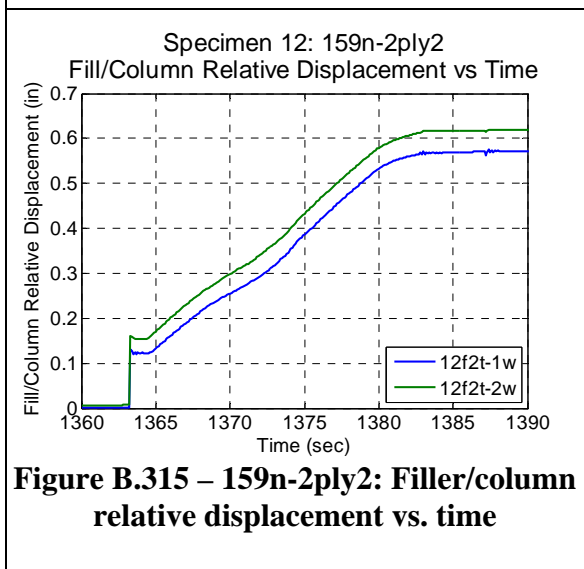
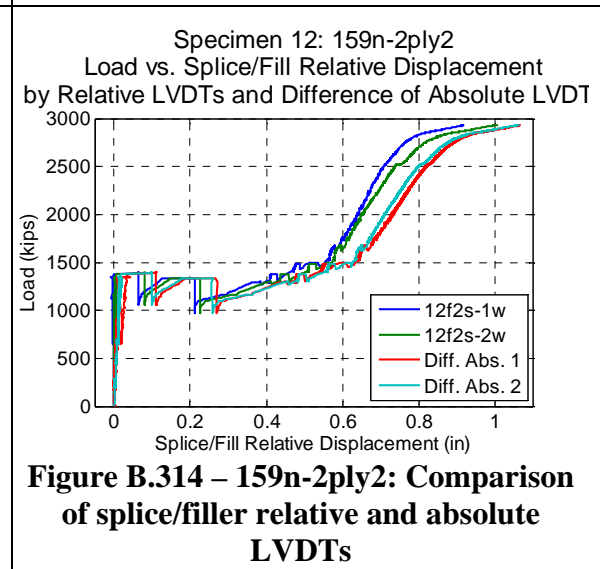
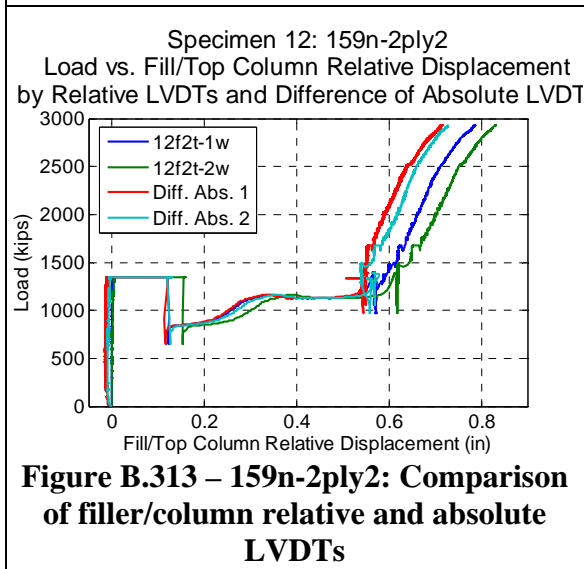
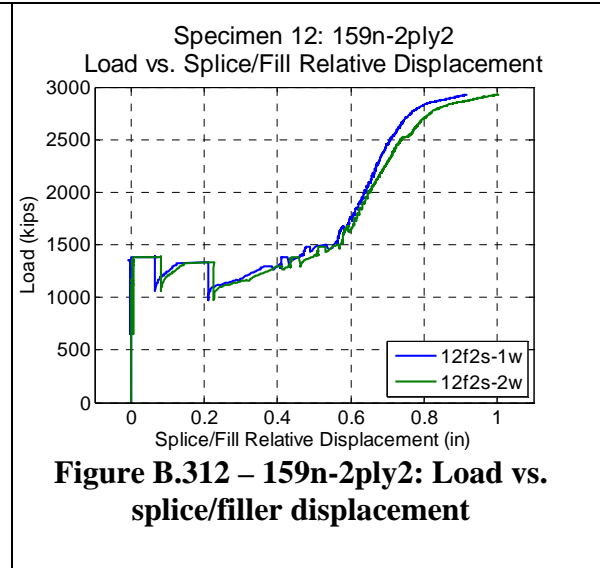
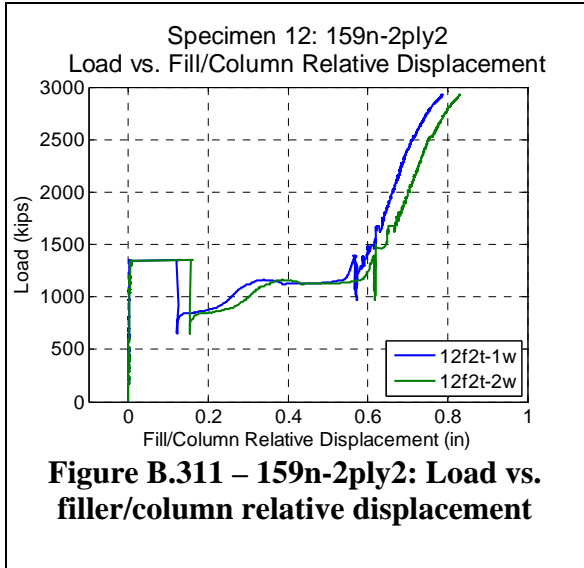


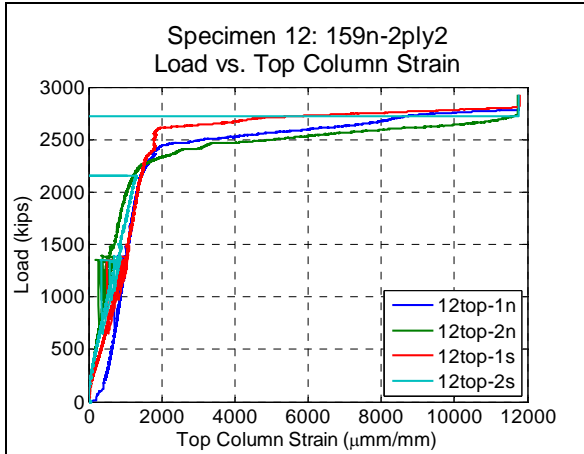
Figure B.303 – 159n-2ply2: After test (south side)



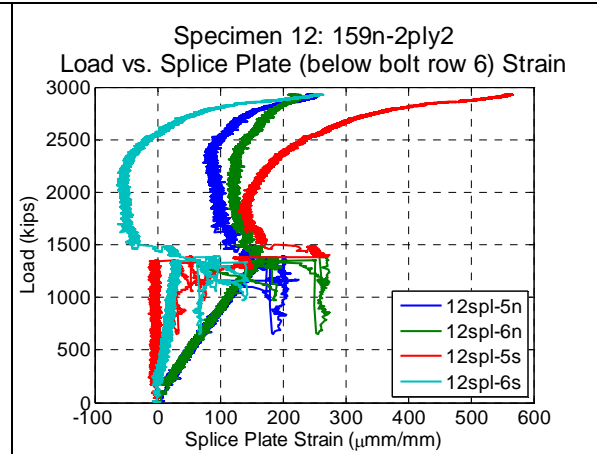
Figure B.304 – 159n-2ply2: After test (north side)



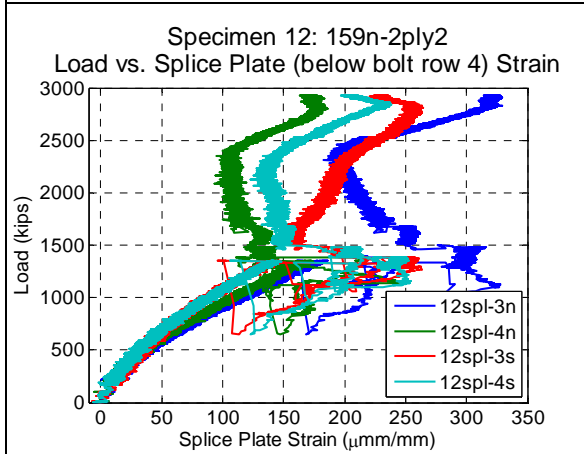




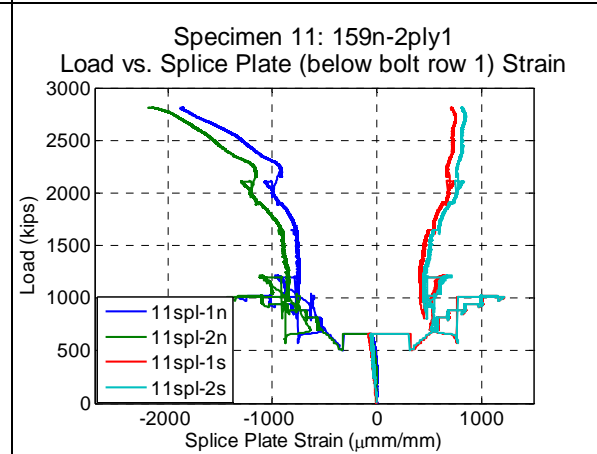
**Figure B.317 – 159n-2ply2: Load vs. top column strain**



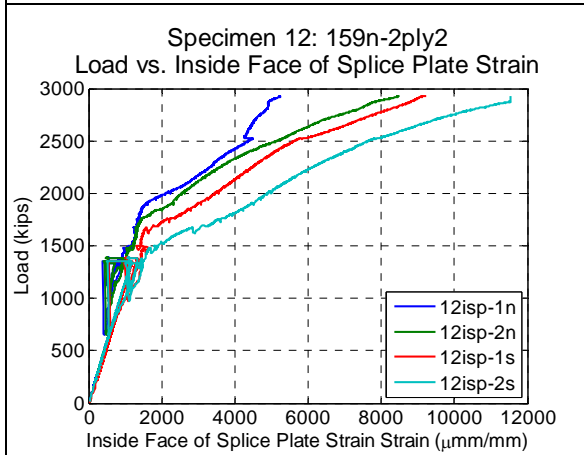
**Figure B.318 – 159n-2ply2: Load vs. splice plate (below bolt row 6) strain**



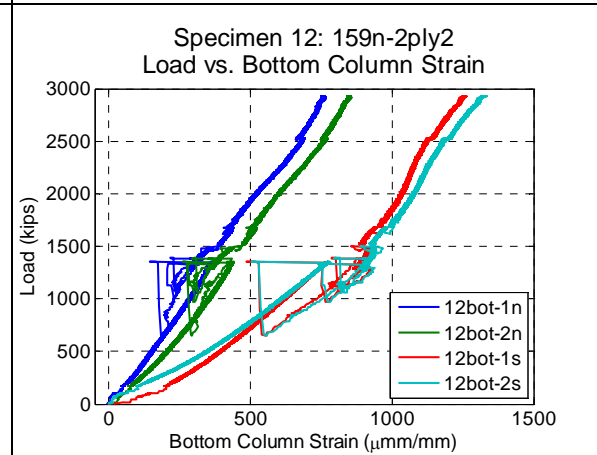
**Figure B.319 – 159n-2ply2: Load vs. splice plate (below bolt row 4) strain**



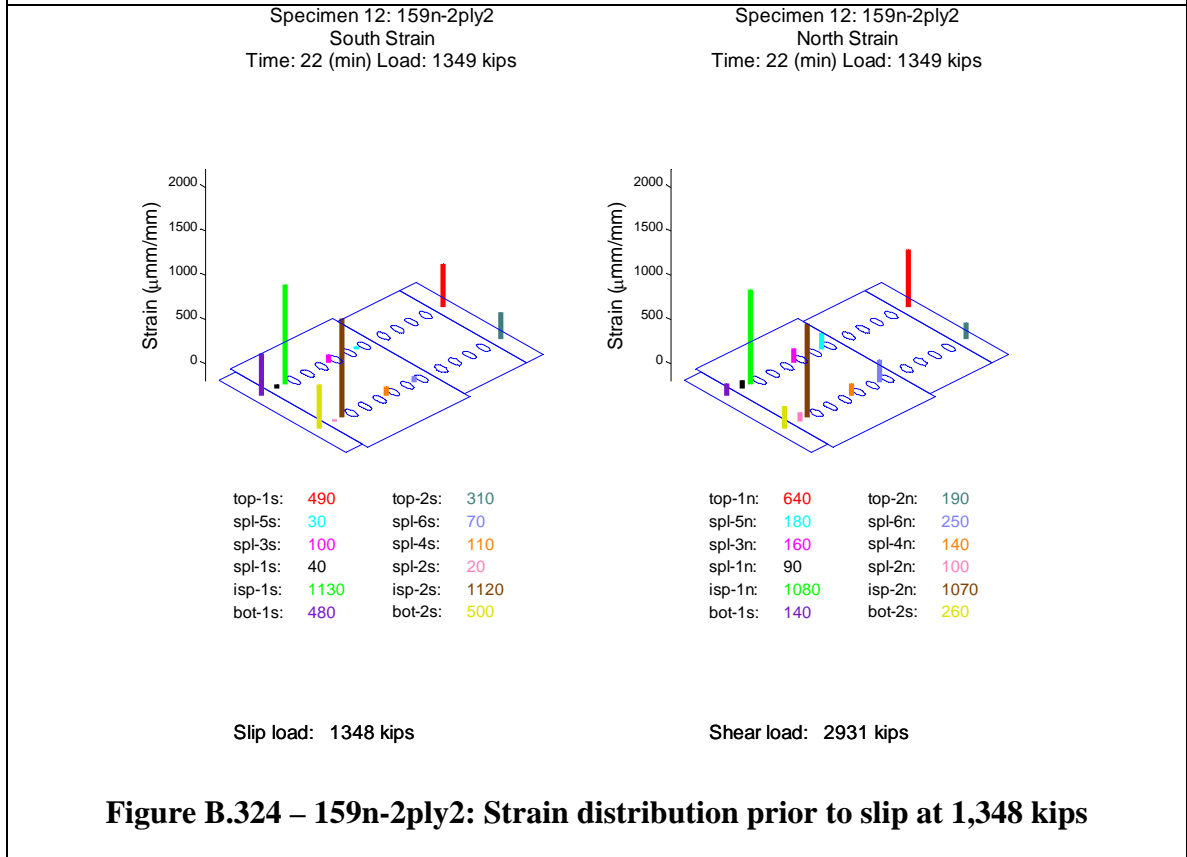
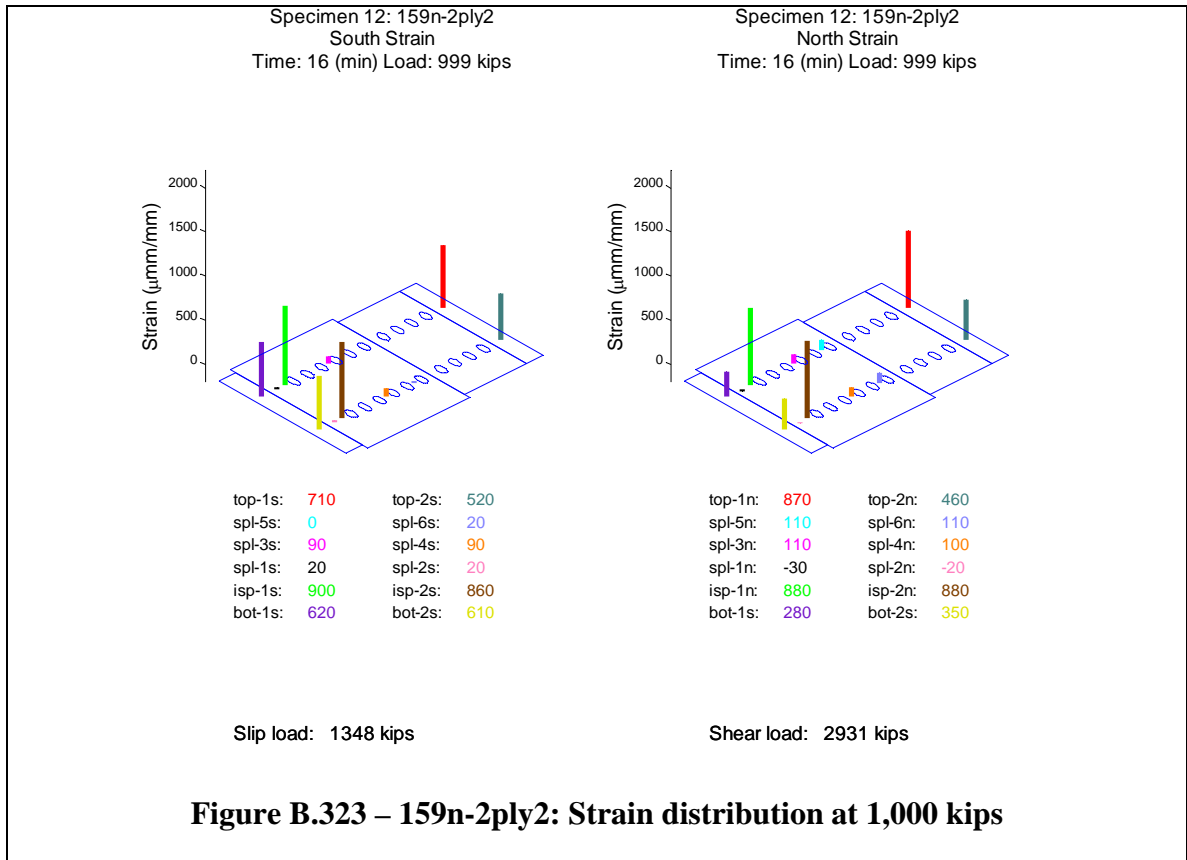
**Figure B.320 – 159n-2ply2: Load vs. splice plate (below bolt row 1) strain**

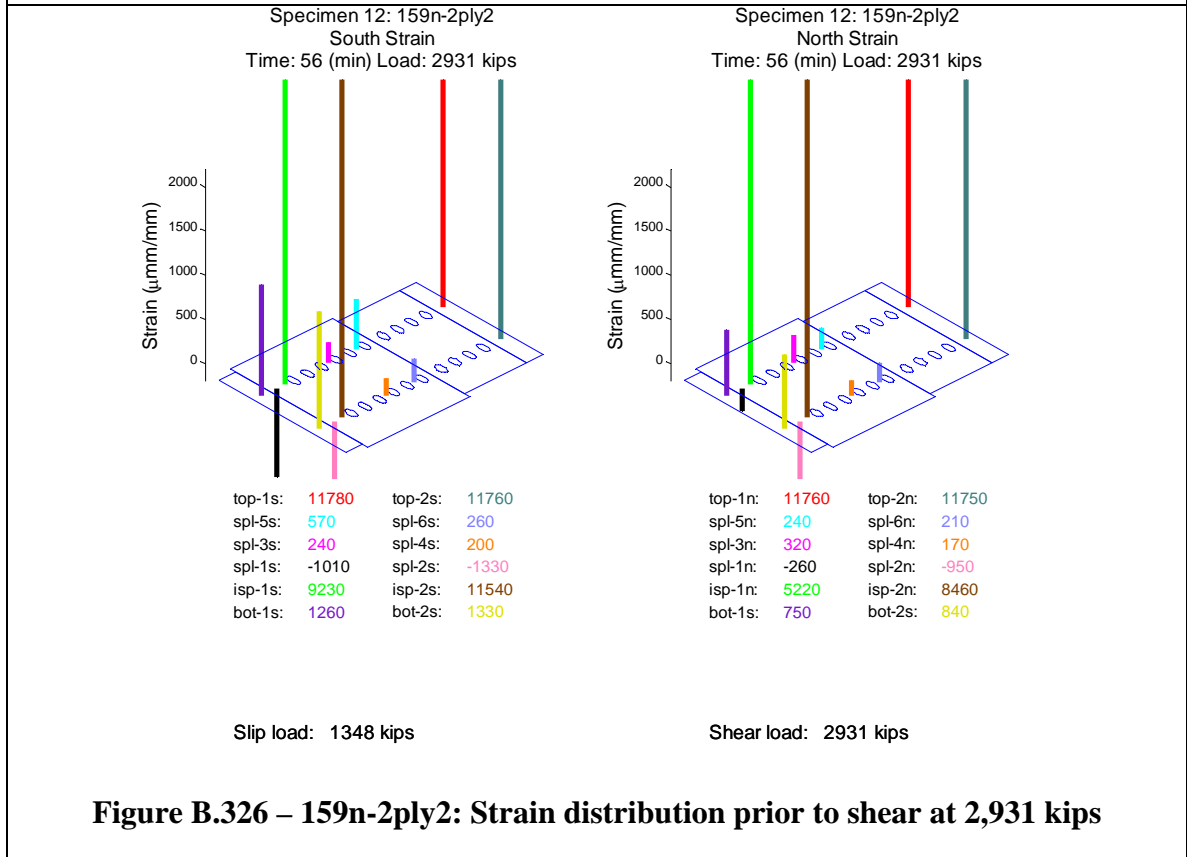
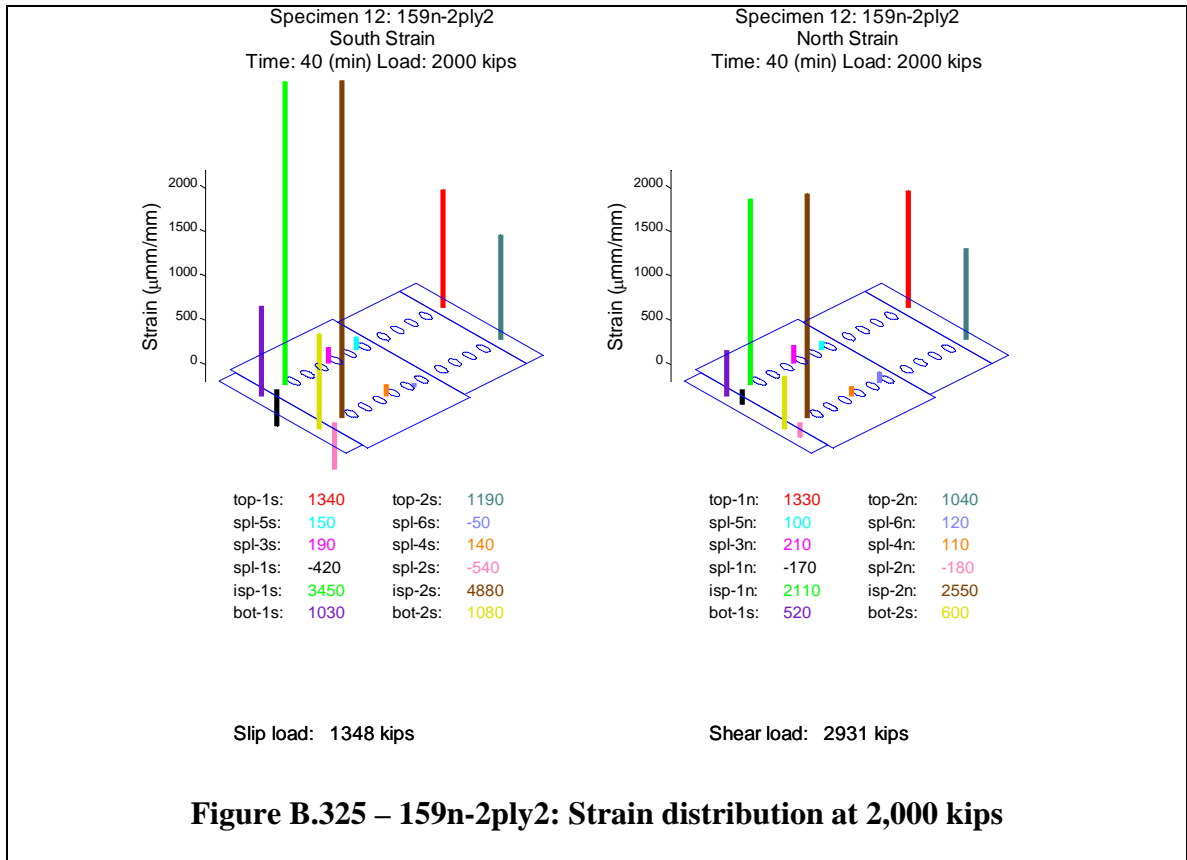


**Figure B.321 – 159n-2ply2: Load vs. inside face of splice plate strain**



**Figure B.322 – 159n-2ply2: Load vs. bottom column strain**





## B.14 Specimen 159h-TC

Specimen 159h-TC (Figure B.327 and Figure B.328) behaved approximately linearly until the observed initial slip load (1,626 kips). During the slip event, the relative displacement between the splice plate and the filler plate on the north and south side of the specimen increased suddenly and continued slipping for 10 seconds. Approximately 700 seconds later, at a load of 2,043 kips, slip was observed between the filler plate and the top column, continuing slipping for 16 seconds. Table B.13 summarizes the slip events. The slip events are seen most clearly in the relative LVDTs (Figure B.343 and Figure B.344). During each dynamic slip event, the load dropped and increased several times. For the initial slip the lowest load measured was 1,152 kips (Figure B.333). The machine and specimen stabilized at 1,490 kips and the load was held for observation of the specimen (Figure B.334). For the secondary slip, the lowest load measured was 1,472 kips (Figure B.333). The machine and specimen once again was stabilized at 1,867 kips and the load was held for observation of the specimen (Figure B.334).

**Table B.13 – 159h-TC: Relative slip**

<b>Location</b>	<b>North</b>	<b>South</b>
<b>Between Splice and Filler</b>	0.21 in	0.21 in
<b>Between Filler and Top Column</b>	0.50 in	0.46 in
<b>Sum</b>	0.71 in	0.67 in

During the final slip event the bolts likely slipped into bearing on the top column (Figure B.329 and Figure B.330), as seen by the increase in stiffness in Figure B.339 at approximately a load of 1,800 kips and a relative slip of 0.47 inches. The maximum expected clearance in the holes based on the assembly was nominally  $2 * (5/16 \text{ inches}) = 0.625 \text{ inches}$ .

The top column began to yield at approximately 2,200 kips (Figure B.345), damaging the southwest strain gage on the top column (top-1s). The specimen was loaded to the capacity of the machine (3,000 kips) without failure of the bolts. The specimen was cycled between 2,200 kips and 3,000 kips five times at approximately 2 kip per second and one time at 5 kips per second (Figure B.334). The specimen retraced an identical Load vs. Displacement (Figure B.333) path during each cycle. At the beginning of each cycle, the load cell instrumentation was reset to capture maximum load. This is indicated on Figure B.333 by a sudden spike to a lower load, and is not indicative of a load applied to the specimen. The specimen was unloaded without failure (Figure B.331 and Figure B.332). All bolts remained intact through the duration of the test.

After slip, the specimen produced pinging noises at the following loads; 1874, 1902, 2170, 2525, 2580 and 2700 kips. Above 2000 kips, ticking noises were observed from the specimen. During cycling between 2200 and 3000 kips, the specimen exerted popping noises associated with load jumps. Noises believed to be produced by the testing

machine were neglected. The noises are likely associated with additional small slip events, bolts coming into bearing with the bolt holes, or possibly initiation of fractures within the bolts.

Near the end of the test the west strain gage on the north side of the filler plate (13fil-1n) and middle strain gage on the south side of the filler plate (13fil-7s) and failed (Figure B.351 and Figure B.352).

The splice plate LVDTs (Figure B.337 and Figure B.338) showed a dynamic increase or decrease in displacement during the slip events. This may be due to a number of reasons, including stress relief in the splice plates after slip, very small slips relative to the column flanges, or small dynamic vibrations (with resulting small permanent offsets) of the LVDT holders, but the displacements are an order of magnitude smaller than the primary slip displacements (Figure B.339 and Figure B.340) and are not likely to indicate significant behavior.

Figure B.341 and Figure B.342 compare the LVDTs directly measuring relative slip between the filler plate and either the top column (Figure B.339) or the splice plate (Figure B.340) with the difference between the average of the two LVDTs on either filler plate at that same cross section as the LVDTs on the top column (Figure B.336) and either the average of the two LVDTs at the bottom center of the top column (Figure B.335) or the average of the two LVDTs on either splice plate at that same cross section as the LVDTs on the top column (Figure B.337). The measurements of the relative LVDTs correspond well to the difference between the corresponding absolute LVDTs.

For this specimen, strain gages were attached to the inside face of the splice plate in the gap between the top and bottom columns (Figure B.349). These measurements, when compared to the measurements from the outside face of the splice plate (Figure B.348), indicate significant bending in the splice plates. Yielding was recorded on the inside of the splice plate.

The top column strain gages indicate that the localized introduction of load was approximately uniform (Figure B.345). The bottom column strain gages exhibit a slight bias to the northeast for the localized reaction (Figure B.350).

The splice plate was relatively uniformly loaded (Figure B.346, Figure B.347, Figure B.348 and Figure B.349), with some bias to the south side seen below bolt row 3. Snapshots of the specimen strain at 1000 kips, immediately prior to slip, 2000 kips and 3000 kips are visually presented in Figure B.353, Figure B.354, Figure B.355 and Figure B.356, respectively. These graphs show that the strain enters into the filler plate and then into the splice plate gradually and relatively uniformly from bolt row 6 to bolt row 1 throughout the experiment.

The experiment was executed in load control. The loading rate for the experiment was approximately 1 kip per second, unless noted above. One elastic cycle was executed prior to the test, going up to a load of 200 kips and returning to zero load, to verify

instrumentation. The data collection rate for the experiment was held constant at 10 Hertz (10 sets of readings per second).



**Figure B.327 – 159h-TC: Before test  
(east side)**



**Figure B.328 – 159h-TC: Before test  
(west side)**



**Figure B.329 – 159h-TC: After initial slip (east side)**



**Figure B.330 – 159h-TC: After initial slip (west side)**



Figure B.331 – 159h-TC: After test (east side)

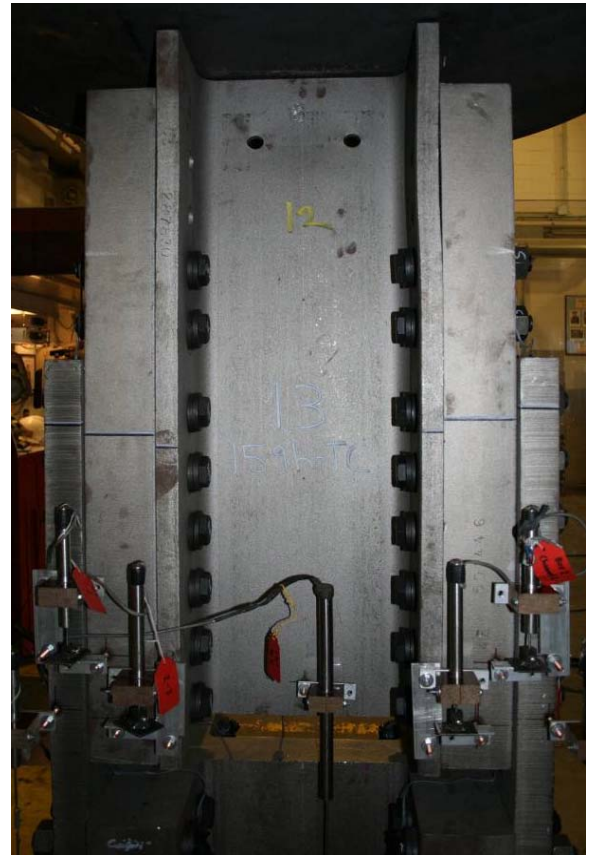
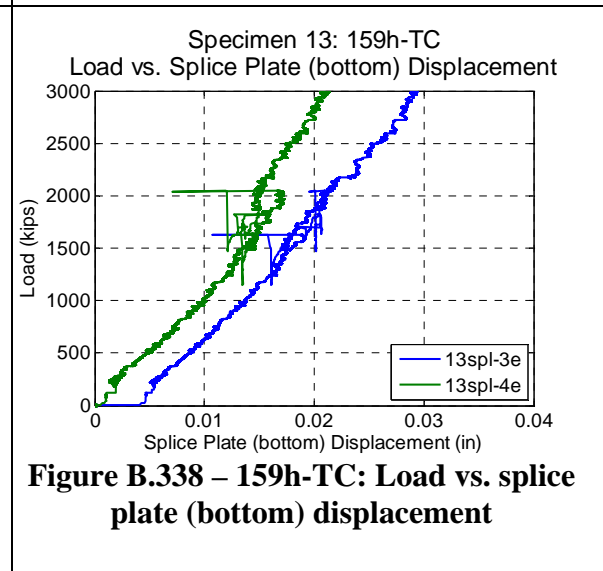
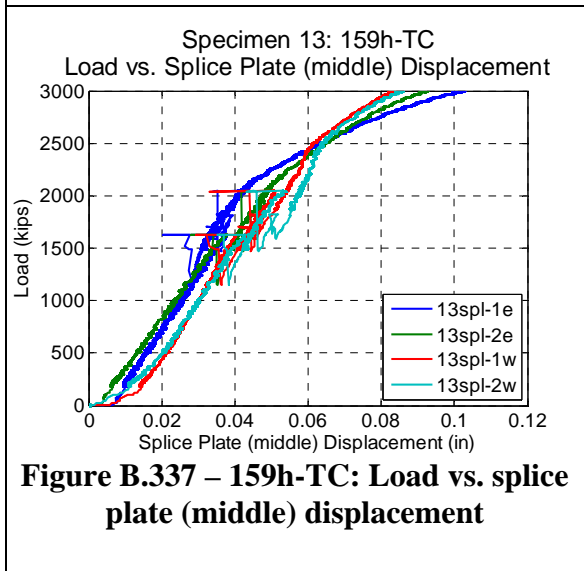
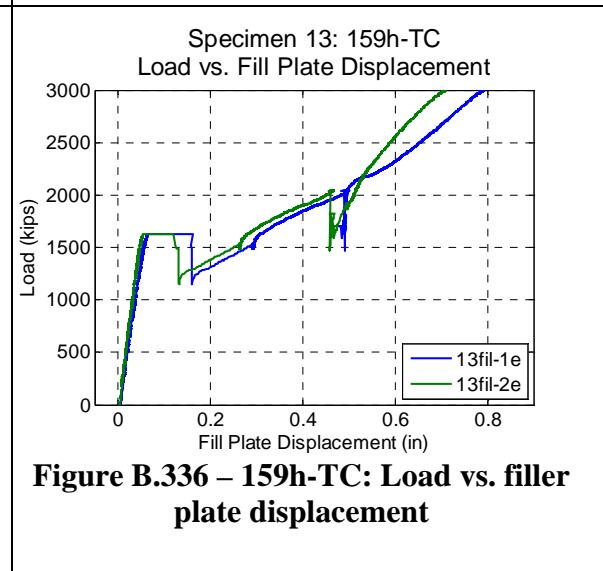
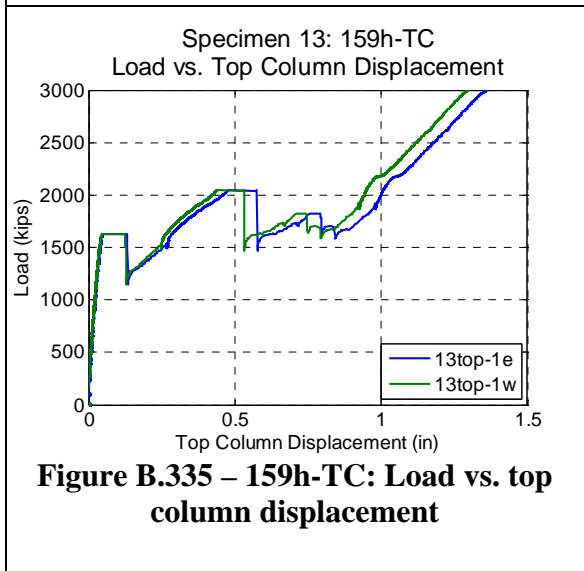
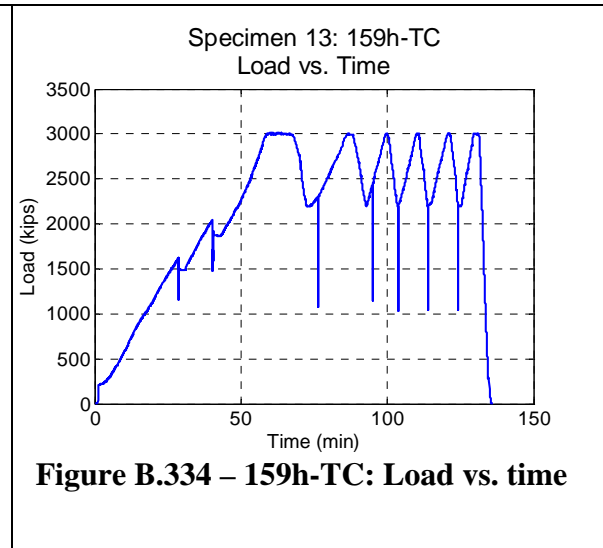
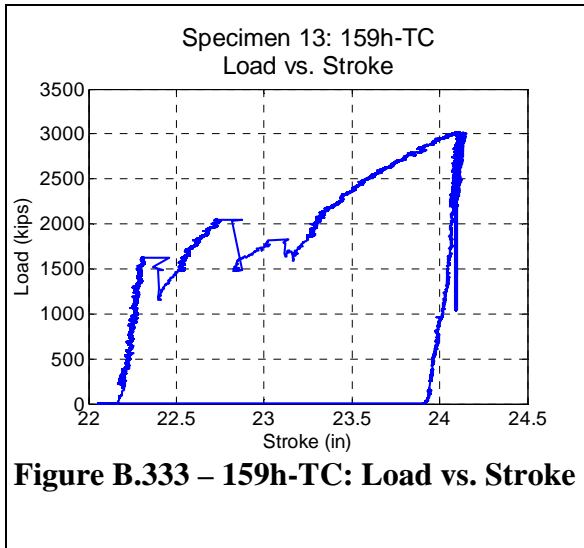
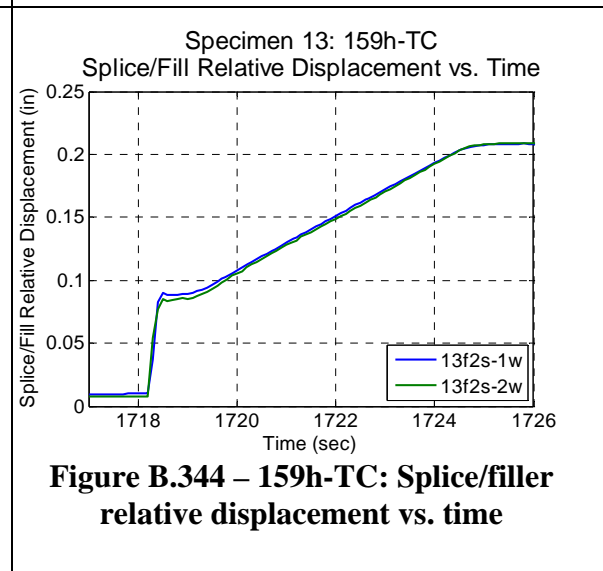
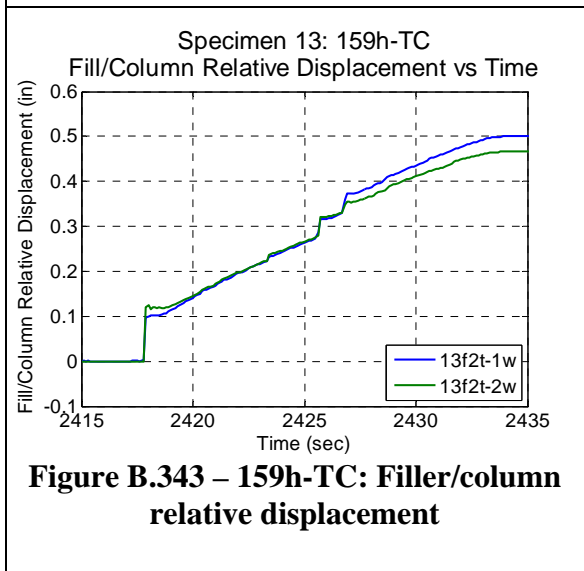
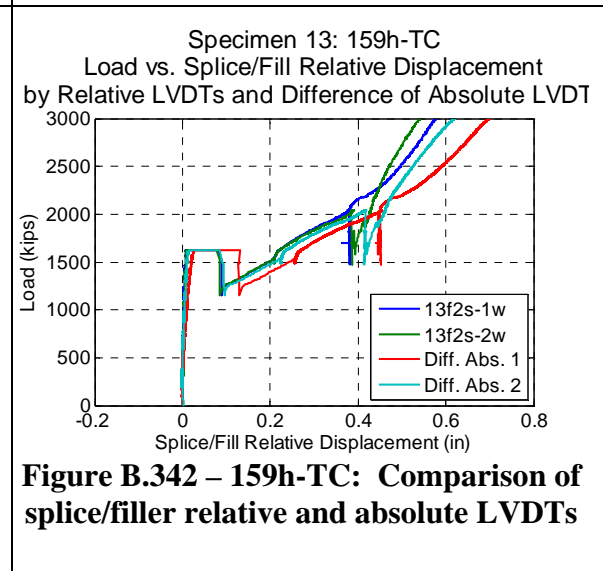
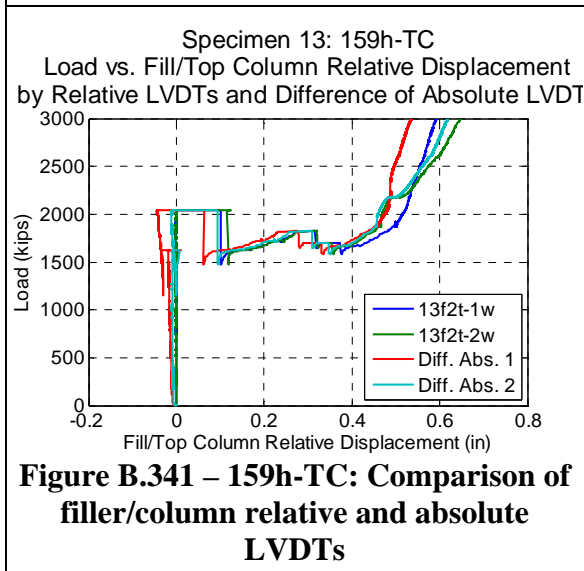
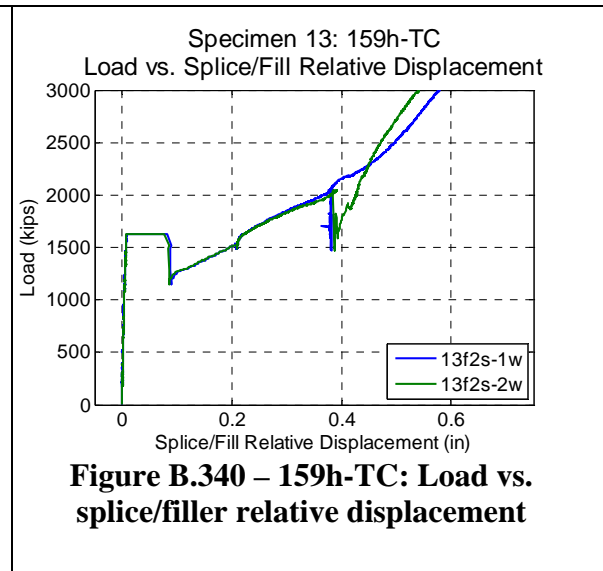
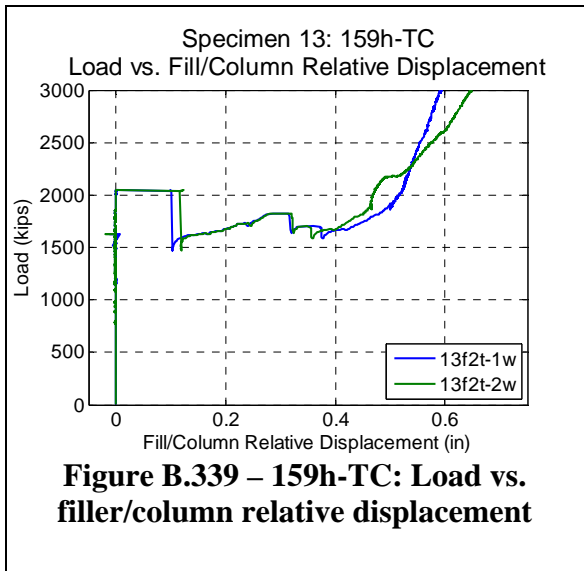
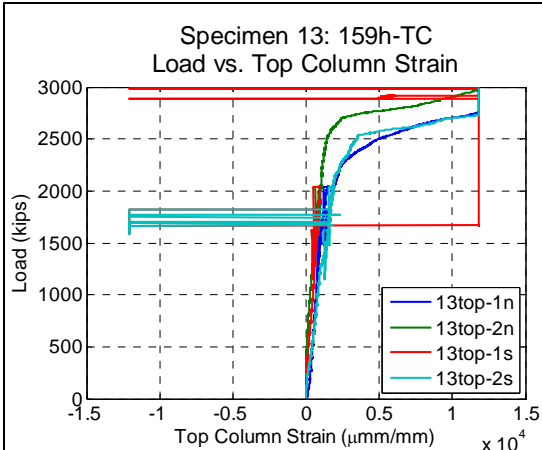


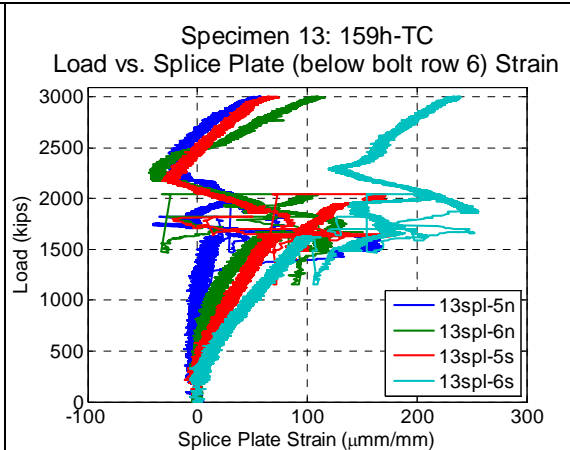
Figure B.332 – 159h-TC: After test (west side)



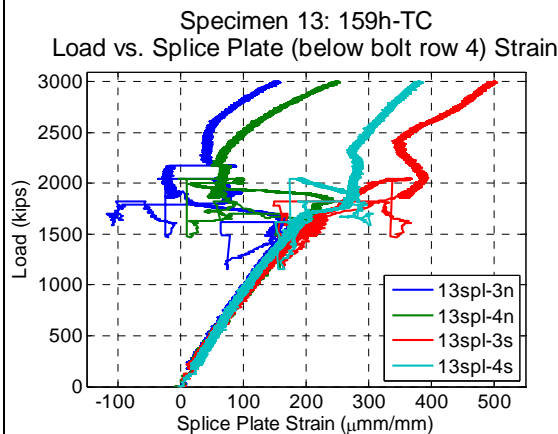




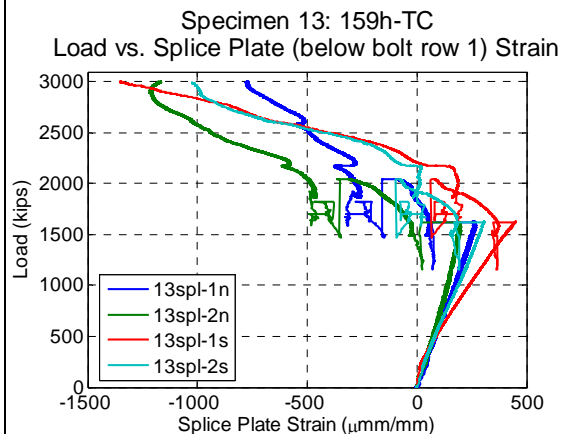
**Figure B.345 – 159h-TC: Load vs. top column strain**



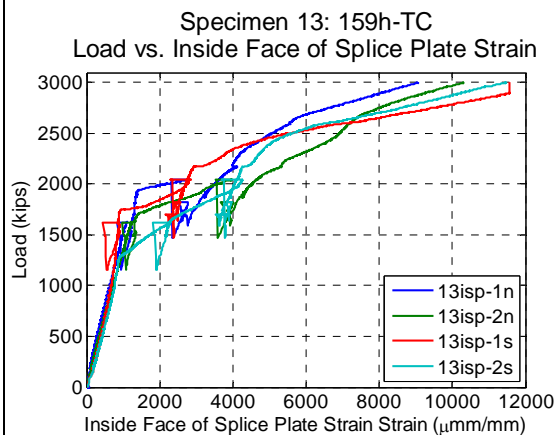
**Figure B.346 – 159h-TC: Load vs. splice plate (below bolt row 6) strain**



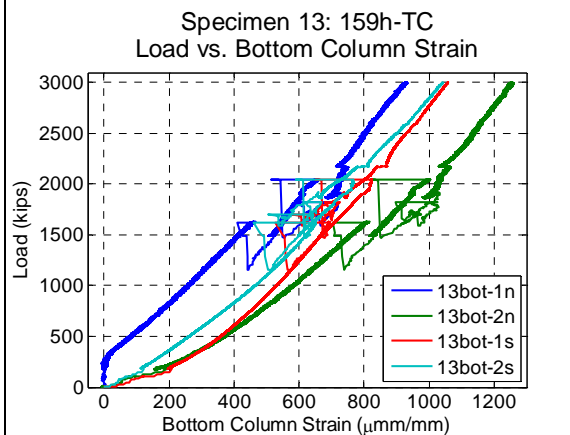
**Figure B.347 – 159h-TC: Load vs. splice plate (below bolt row 4) strain**



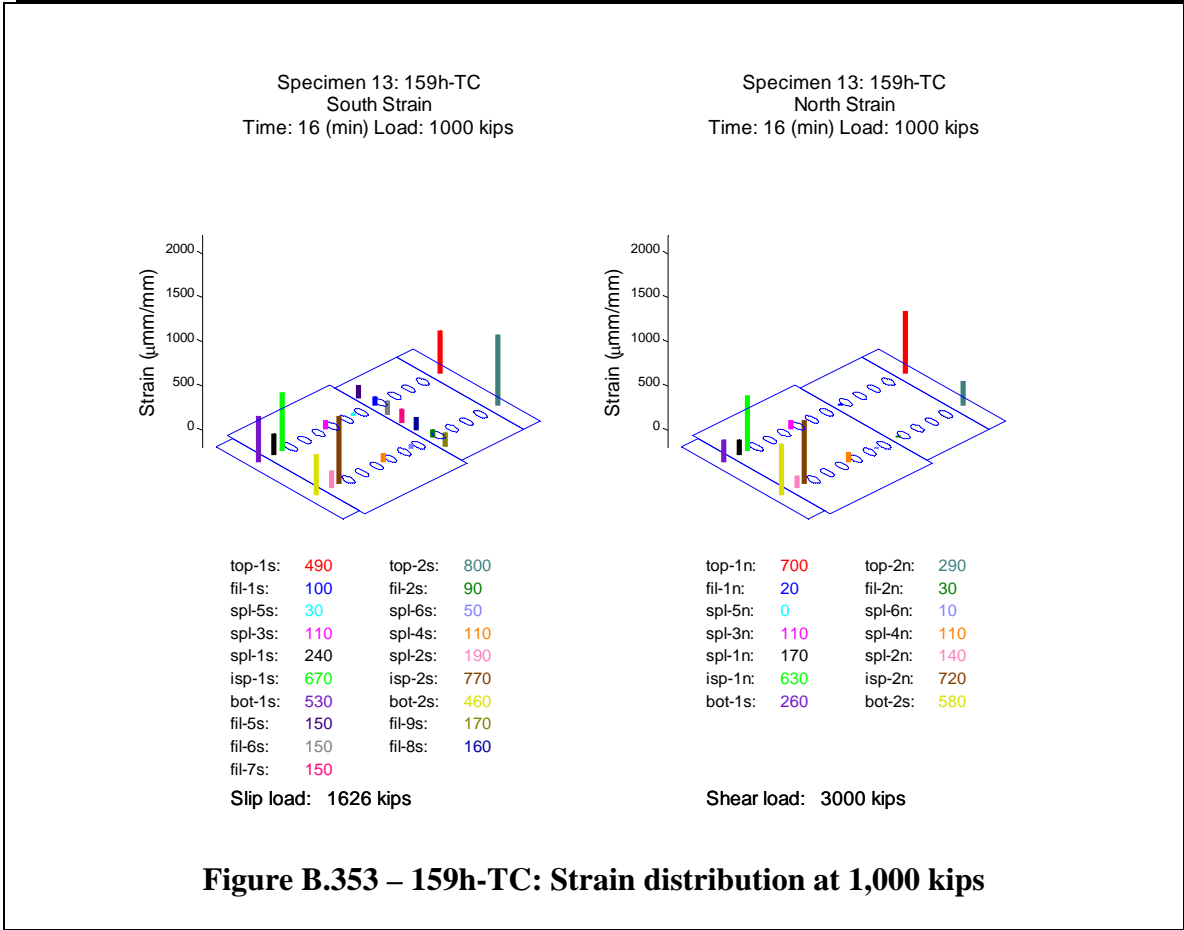
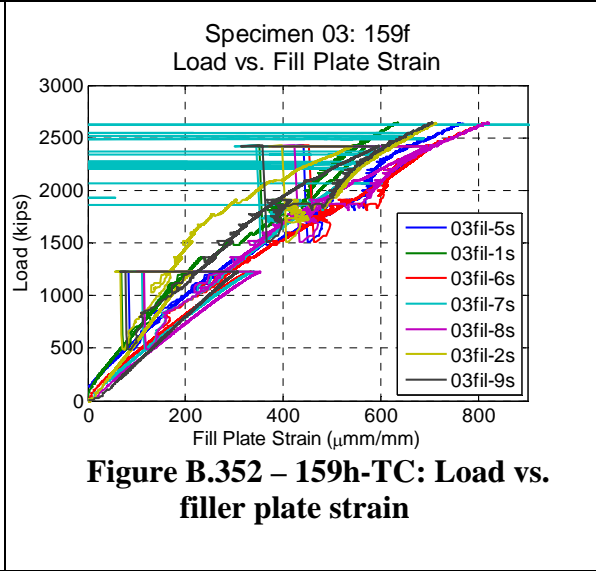
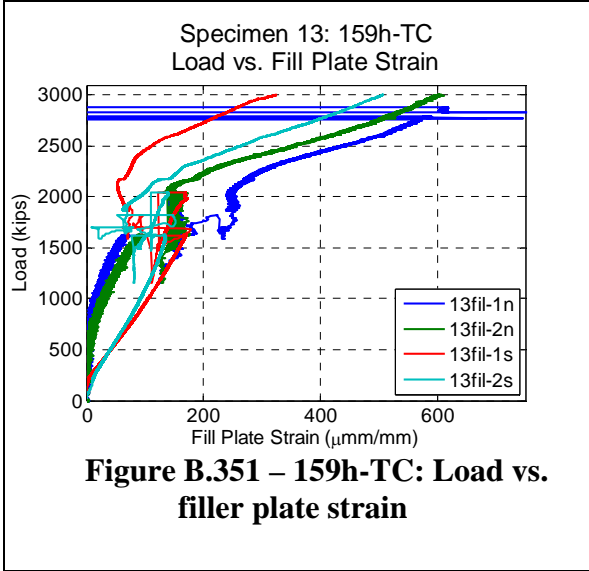
**Figure B.348 – 159h-TC: Load vs. splice plate (below bolt row 1) strain**



**Figure B.349 – 159h-TC: Load vs. inside face of splice plate strain**



**Figure B.350 – 159h-TC: Load vs. bottom column strain**



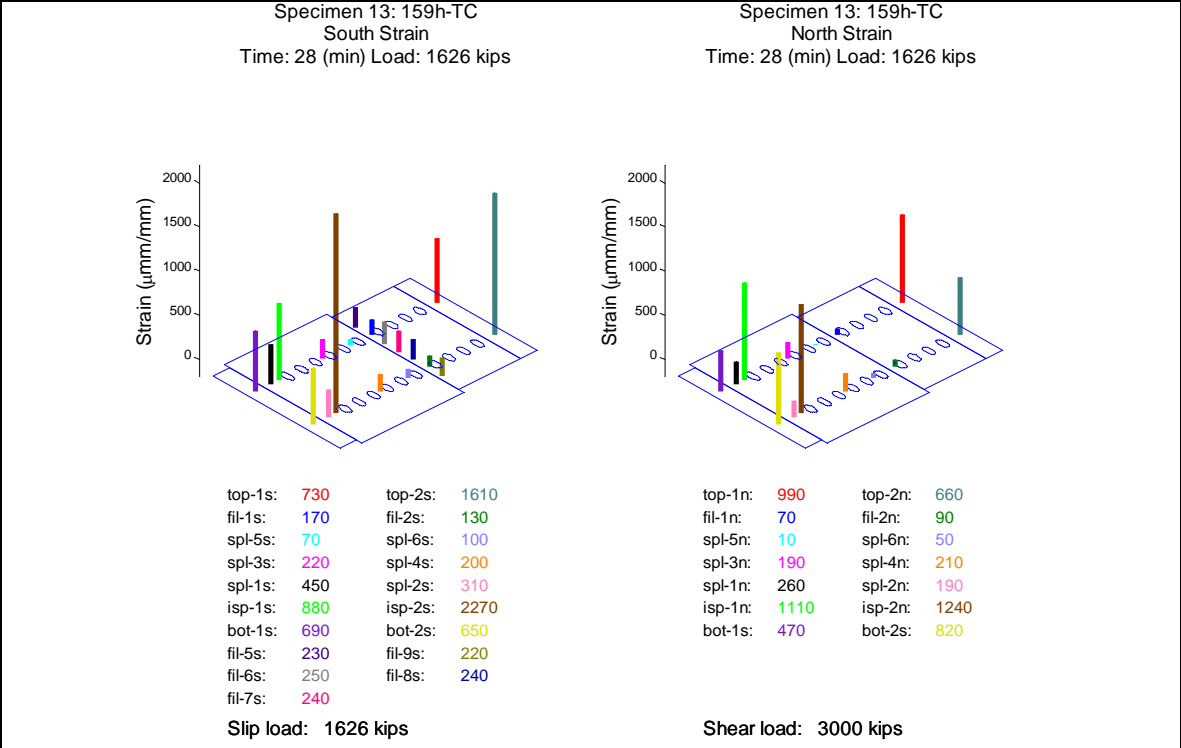


**Figure B.354 – 159h-TC: Strain distribution prior to slip at 1,626 kips**

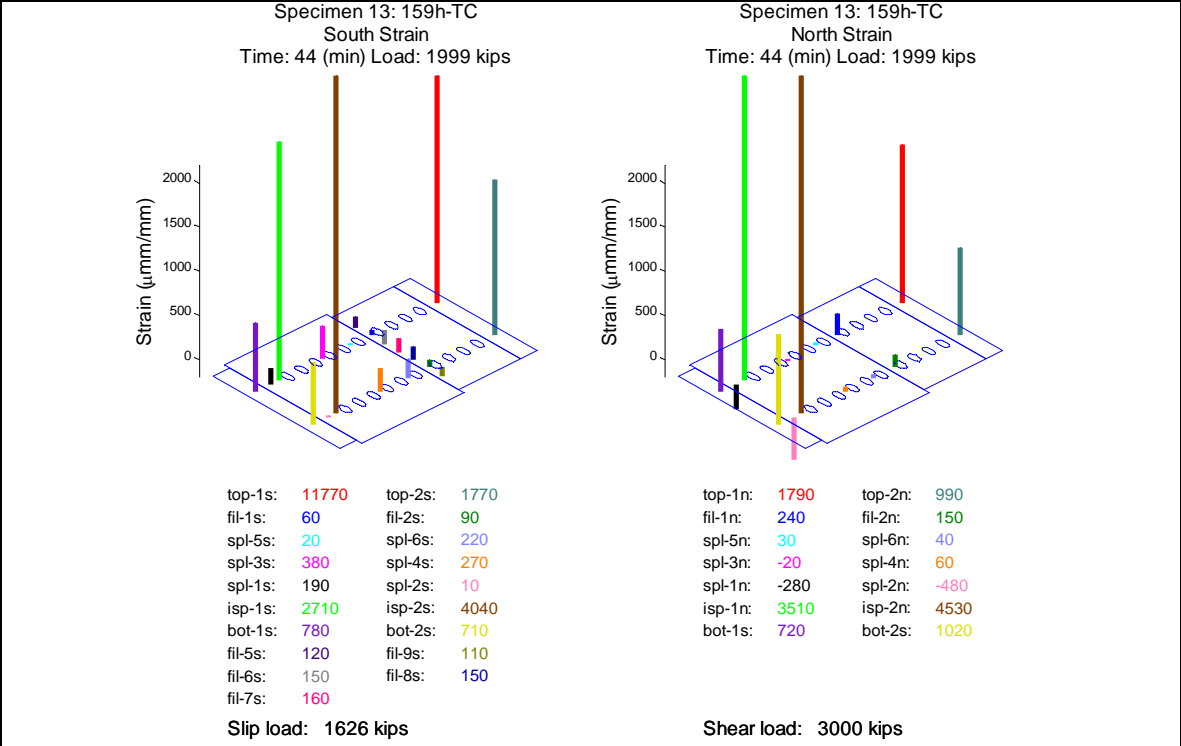


**Figure B.355 – 159h-TC: Strain distribution at 2,000 kips**

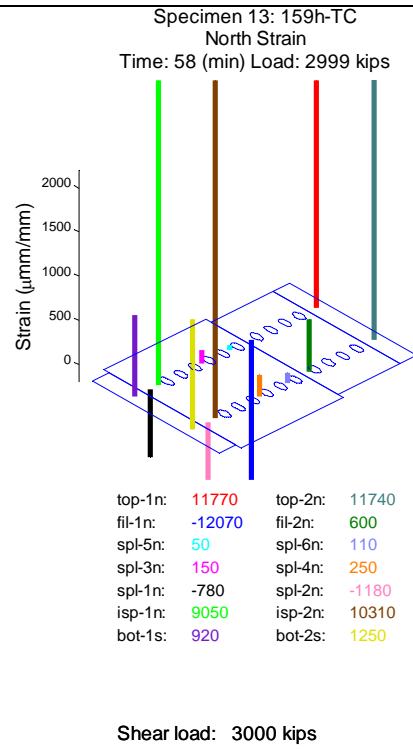
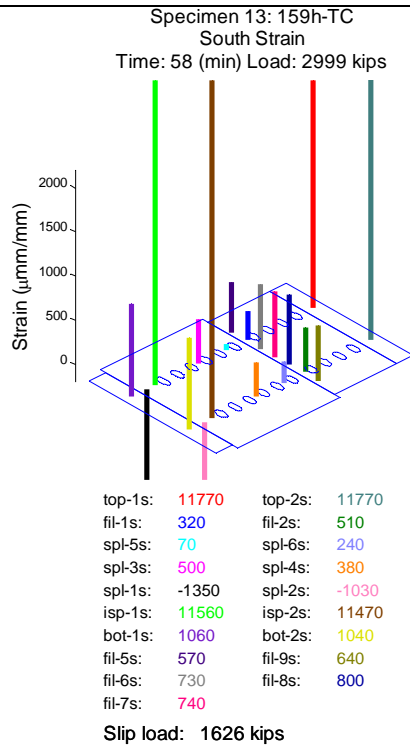


**Figure B.356 – 159h-TC: Strain distribution at 3,000 kips**

## B.15 Specimen 159n-TC

Specimen 159n-TC (Figure B.357 and Figure B.358) behaved approximately linearly until the observed slip load (1,290 kips). During the slip event, the relative displacement between the filler plate and the splice plate on the south side of the specimen increased suddenly and continued slipping for 9 seconds. The relative displacement between the filler plate and the top column on the north side of the specimen also increased suddenly and continued slipping for 10 seconds. Approximately 527 seconds later, at a load of 1,556 kips slip was observed between the filler plate and the splice plate on the north side of the specimen, continuing slipping for 25 seconds. The relative displacement between the filler plate and the top column on the south side of the specimen also slipped, continuing for 20 seconds. Table B.14 summarizes the slip events. The slip events are seen most clearly in the relative LVDTs (Figure B.373 and Figure B.374). During each dynamic slip event, the load dropped and increased several times. For the initial slip the lowest load measured was 894 kips (Figure B.363). The machine and specimen stabilized at 1,260 kips and the load was held for observation of the specimen (Figure B.364). For the secondary slip the lowest load measured was 1,127 kips (Figure B.363). The machine and specimen once again was stabilized at 1,554 kips and the load was held for observation of the specimen (Figure B.364).

**Table B.14 – 159n-TC: Relative slip**

<b>Location</b>	<b>North</b>	<b>South</b>
<b>Between Splice and Filler</b>	0.47 in	0.29 in
<b>Between Filler And Top Column</b>	0.26 in	0.54 in
<b>Sum</b>	0.73 in	0.83 in

During the final slip event the bolts likely slipped into bearing on the top column, as seen by the increase in stiffness in Figure B.369 at approximately a load of 1,500 kips and a relative slip of 0.50 inches (Figure B.359 and Figure B.360). The maximum expected clearance in the holes based on the assembly was nominally  $2 * (5/16 \text{ inches}) = 0.625$  inches.

The top column began to yield at approximately 2,300 kips (Figure B.375), damaging the north strain gages on the top column (top-1n and top-2n). The specimen was loaded to the capacity of the machine (3,000 kips) without failure of the bolts. The specimen was cycled between 1,800 kips and 3,000 kips six times at approximately 8 kips per second (Figure B.364). The specimen retraced an identical Load vs. Displacement (Figure B.363) path during each cycle. The specimen was unloaded without failure (Figure B.361 and Figure B.362). All bolts remained intact through the duration of the test.

After slip, the specimen produced pinging noises at the following loads; 1552, 1575, 1813, 1818 and 2006 kips. After slip faint ticking noises were observed. Upon unloading, the specimen emitted several low pitched noises. Noises believed to be

produced by the testing machine were neglected. The noises are likely associated with additional small slip events, bolts coming into bearing with the bolt holes, or possibly initiation of fractures within the bolts.

The splice plate LVDTs (Figure B.367 and Figure B.368) showed a dynamic increase or decrease in displacement during the slip events. This may be due to a number of reasons, including stress relief in the splice plates after slip, very small slips relative to the column flanges, or small dynamic vibrations (with resulting small permanent offsets) of the LVDT holders, but the displacements are an order of magnitude smaller than the primary slip displacements (Figure B.369 and Figure B.370) and are not likely to indicate significant behavior.

Figure B.371 and Figure B.372 compare the LVDTs directly measuring relative slip between the filler plate and either the top column (Figure B.369) or the splice plate (Figure B.370) with the difference between the average of the two LVDTs on either filler plate at that same cross section as the LVDTs on the top column (Figure B.366) and either the average of the two LVDTs at the bottom center of the top column (Figure B.365) or the average of the two LVDTs on either splice plate at that same cross section as the LVDTs on the top column (Figure B.367). The measurements of the relative LVDTs correspond well to the difference between the corresponding absolute LVDTs.

For this specimen, strain gages were attached to the inside face of the splice plate in the gap between the top and bottom columns (Figure B.379). These measurements, when compared to the measurements from the outside face of the splice plate (Figure B.378), indicate significant bending in the splice plates, with the outer portion of the splice plates exhibiting tensile strains. Yielding was recorded on the inside of the splice plate.

The top column strain gages indicate that the localized introduction of load was approximately uniform (Figure B.375). The bottom column strain gages show that the localized reaction was loaded on opposite corners, southwest and northeast (Figure B.380), likely due to surface imperfections.

The splice plates were also relatively uniformly loaded (Figure B.376, Figure B.377, Figure B.378 and Figure B.379), with some bias to the south seen below bolt rows 1 and 3. Snapshots of the specimen strain at 1000 kips, immediately prior to slip, 2000 kips and 3000 kips are visually presented in Figure B.381, Figure B.382, Figure B.383 and Figure B.384, respectively. These graphs show that the strain enters into the splice plate gradually and relatively uniformly from bolt row 6 to bolt row 1 throughout the experiment.

The experiment was executed in load control. The loading rate for the experiment was approximately 1 kip per second, unless noted above. One elastic cycle was executed prior to the test, going up to a load of 200 kips and returning to zero load, to verify instrumentation. The data collection rate for the experiment was held constant at 10 Hertz (10 sets of readings per second).

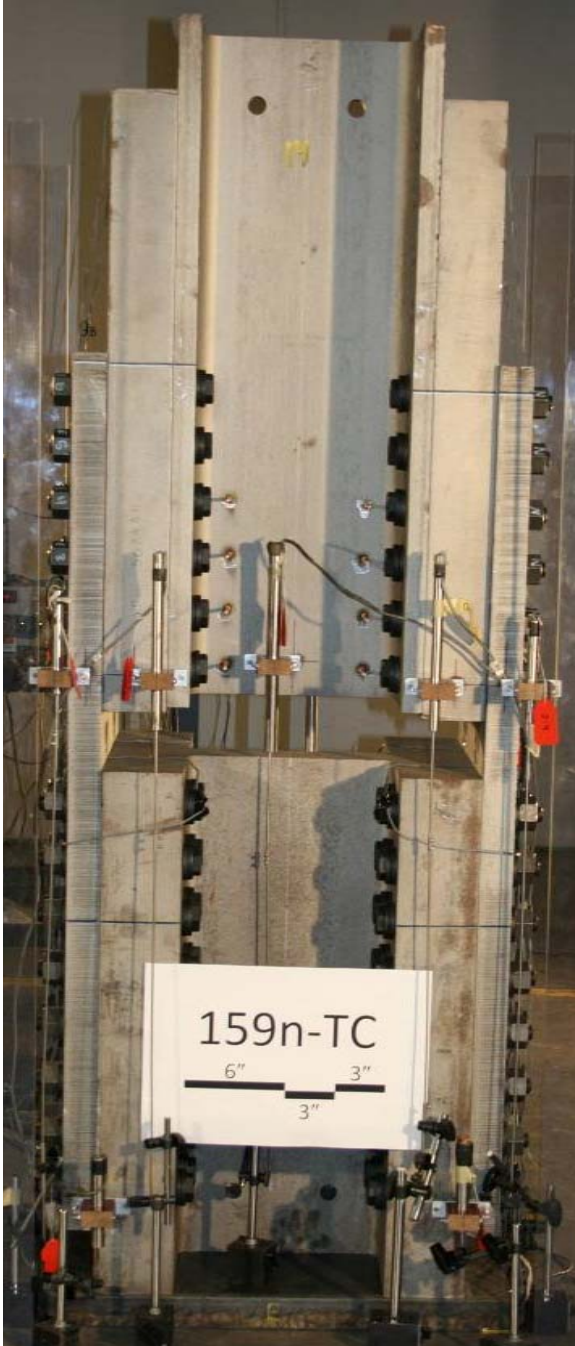


**Figure B.357 – 159n-TC: Before test  
(east side)**



**Figure B.358 – 159n-TC: Before test  
(west side)**



**Figure B.359 – 159n-TC: After initial slip (east side)**



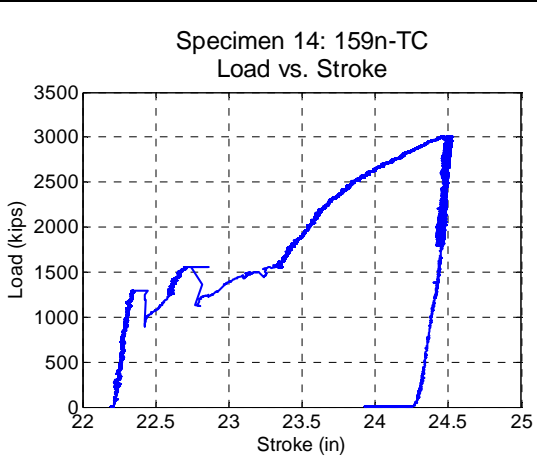
**Figure B.360 – 159n-TC: After initial slip (west side)**



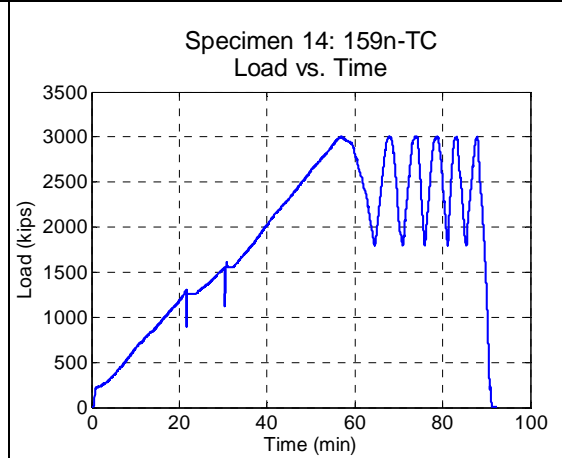
**Figure B.361 – 159n-TC: After test (east side)**



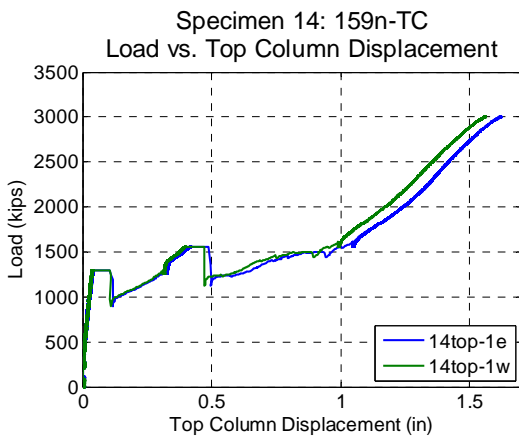
**Figure B.362 – 159n-TC: After test (west side)**



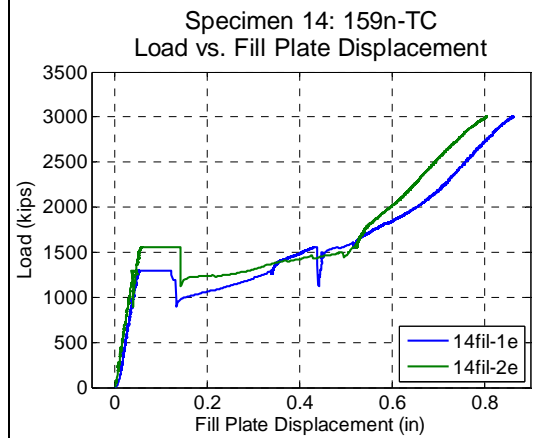
**Figure B.363 – 159n-TC: Load vs. stroke**



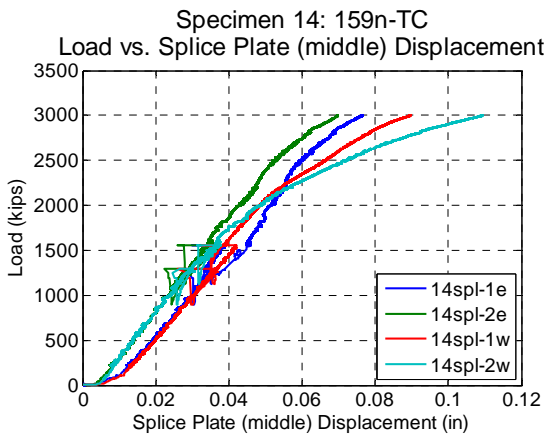
**Figure B.364 – 159n-TC: Load vs. time**



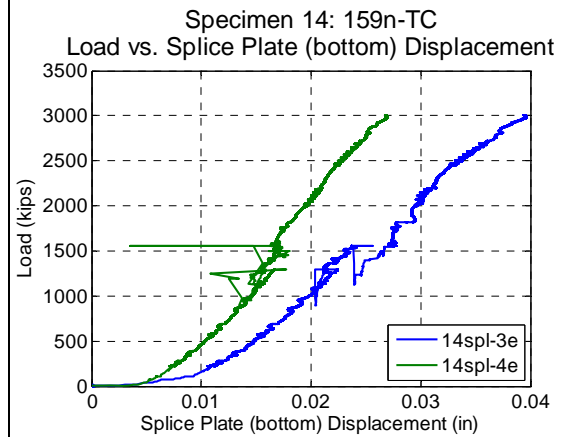
**Figure B.365 – 159n-TC: Load vs. top column displacement**



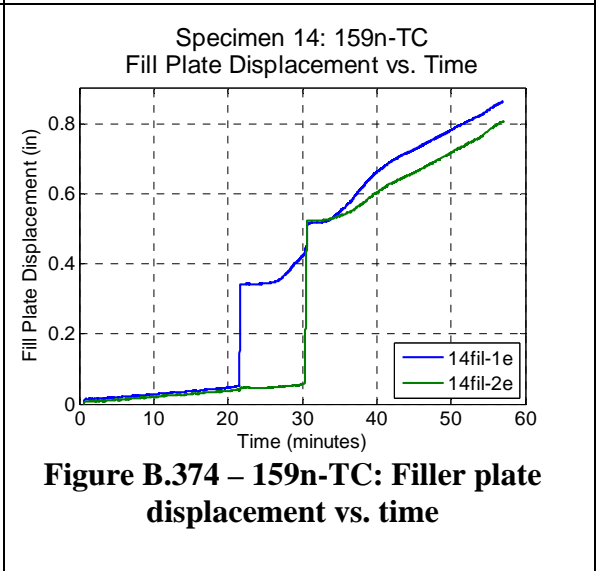
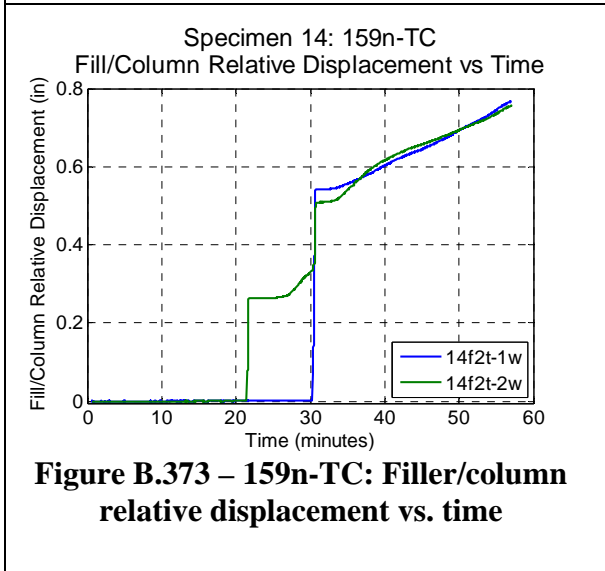
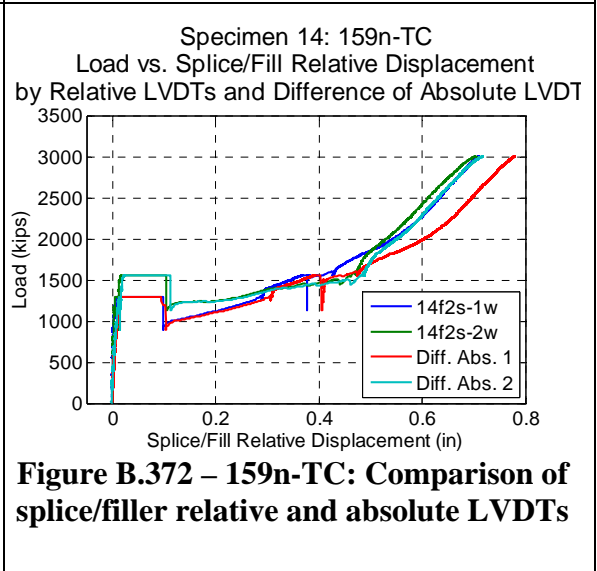
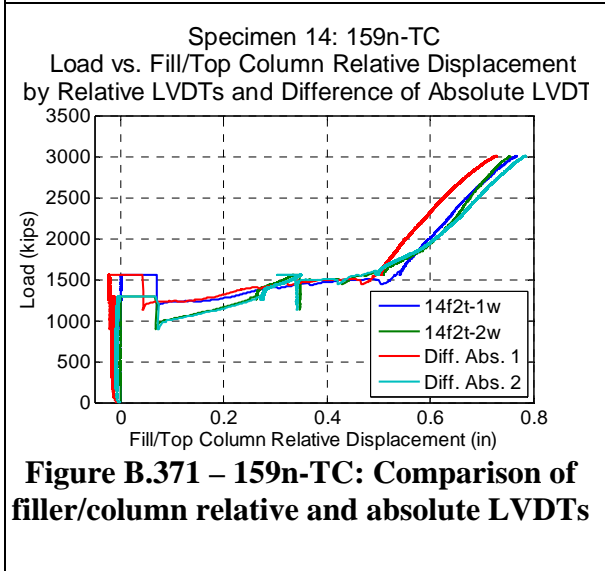
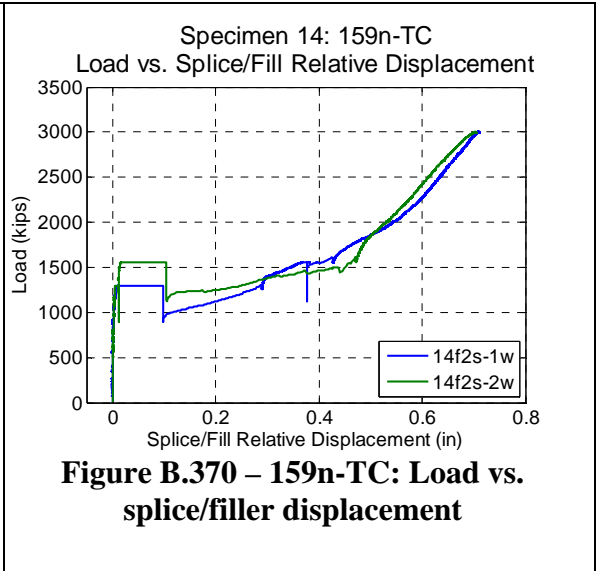
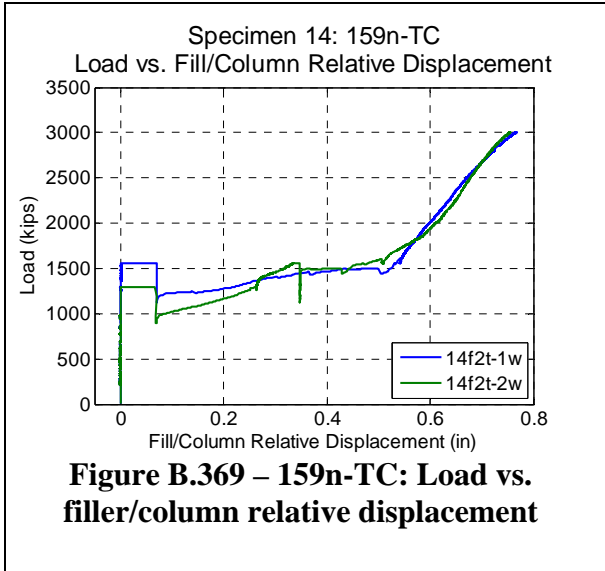
**Figure B.366 – 159n-TC: Load vs. filler plate displacement**



**Figure B.367 – 159n-TC: Load vs. splice plate (middle) displacement**



**Figure B.368 – 159n-TC: Load vs. splice plate (bottom) displacement**



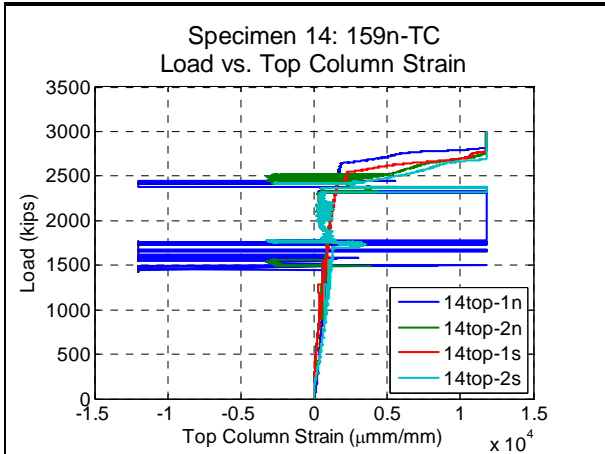


**Figure B.375 – 159n-TC: Load vs. top column strain**

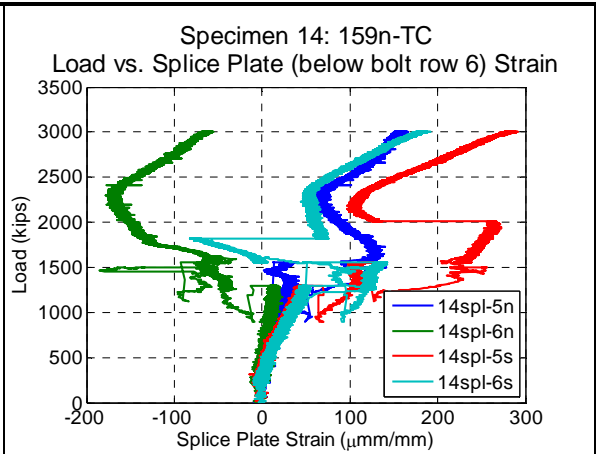


**Figure B.376 – 159n-TC: Load vs. splice plate (below bolt row 6) strain**

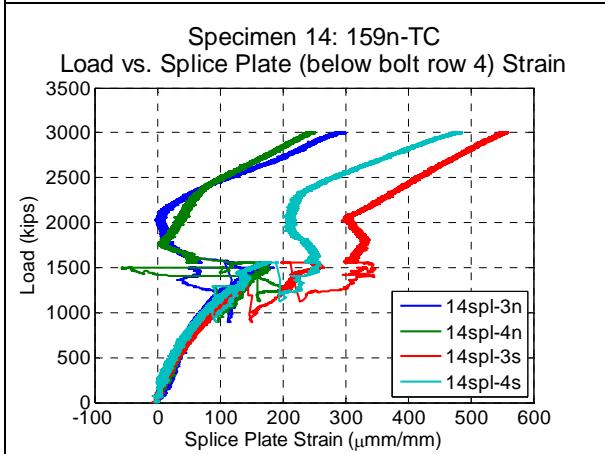


**Figure B.377 – 159n-TC: Load vs. splice plate (below bolt row 4) strain**

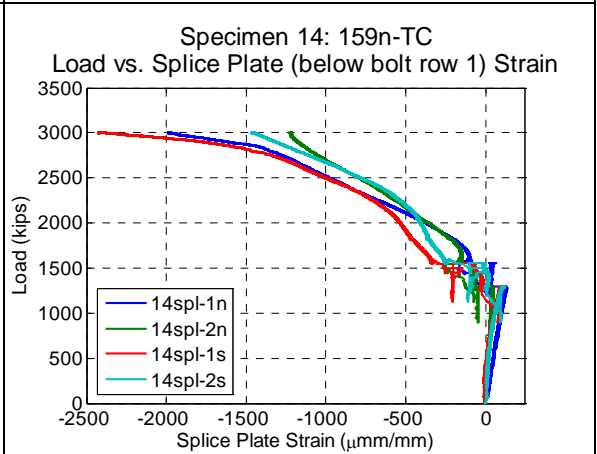


**Figure B.378 – 159n-TC: Load vs. splice plate (below bolt row 1) strain**

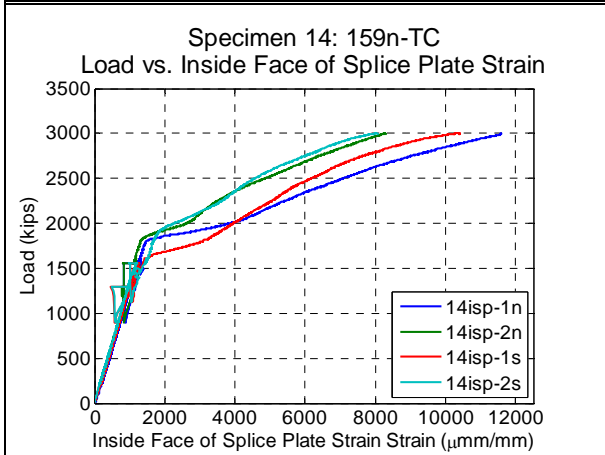


**Figure B.379 – 159n-TC: Load vs. inside face of splice plate strain**

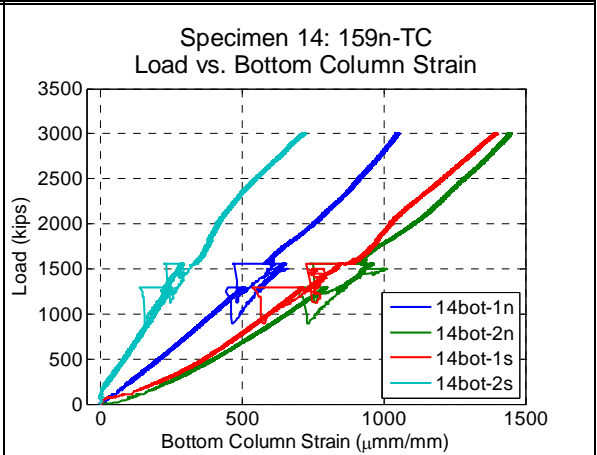


**Figure B.380 – 159n-TC: Load vs. bottom column strain**

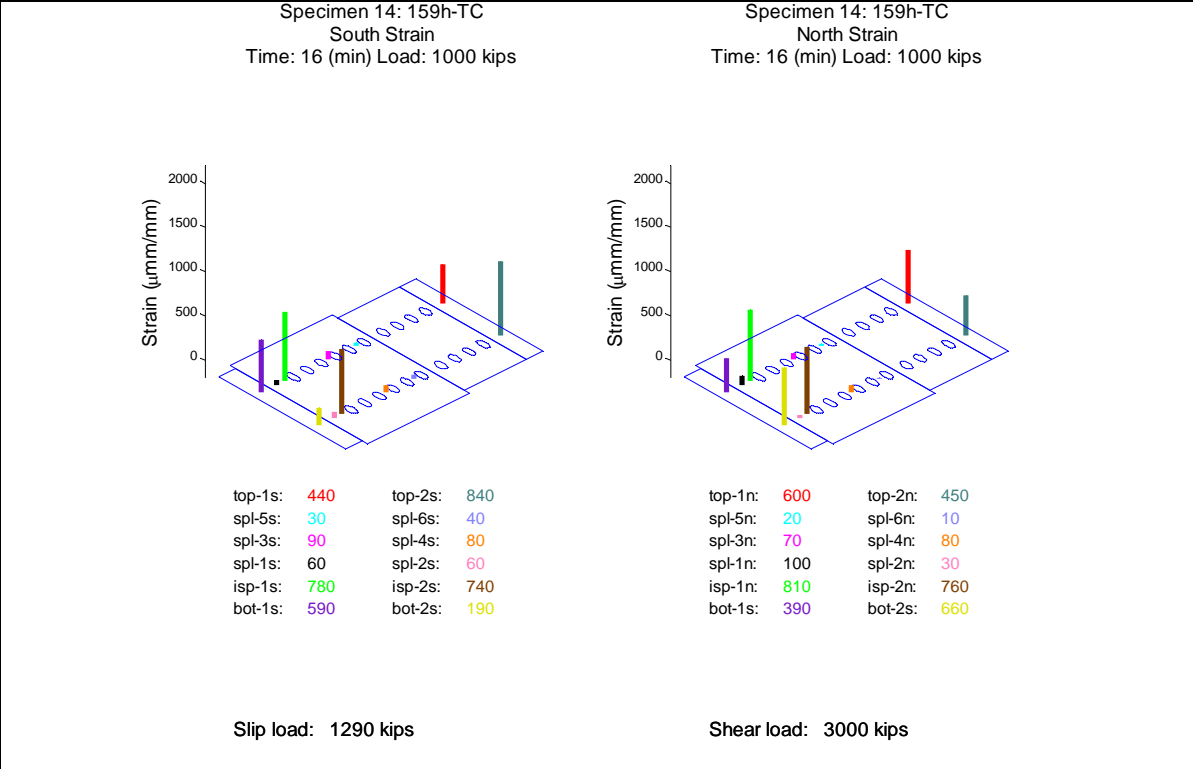


**Figure B.381 – 159n-TC: Strain distribution at 1,000 kips**

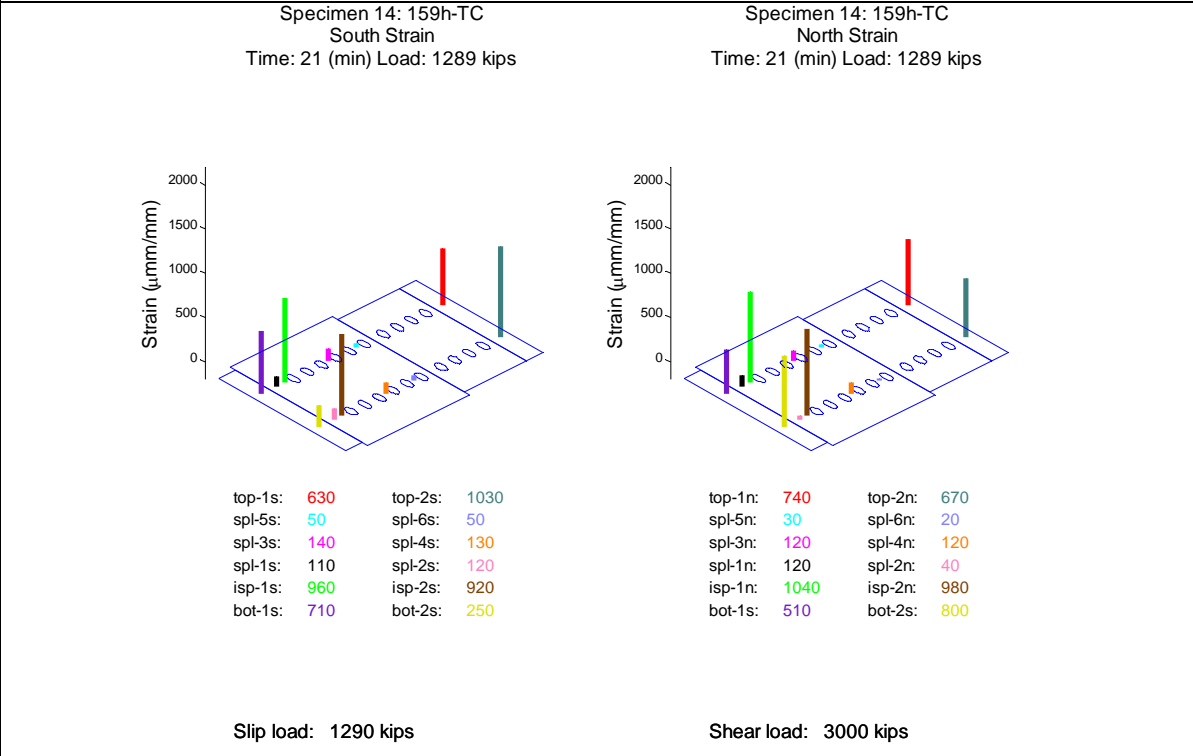
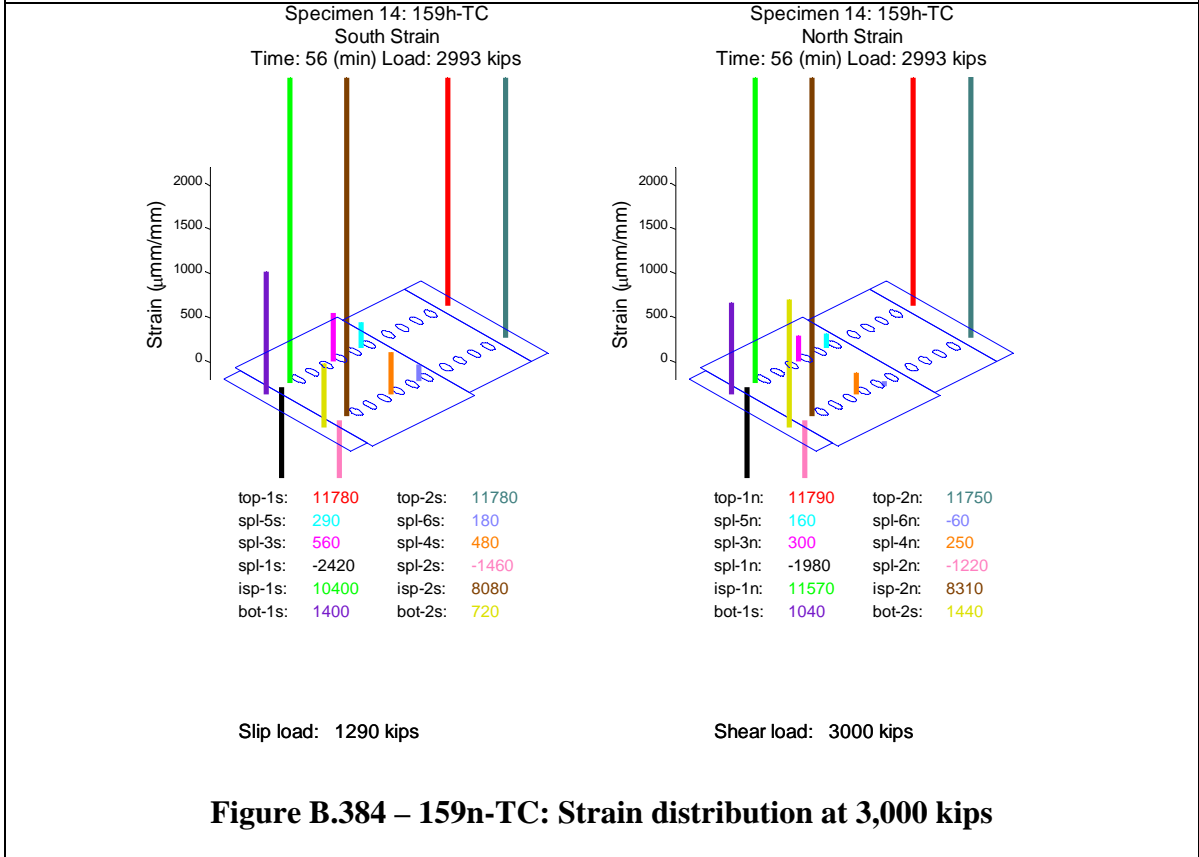
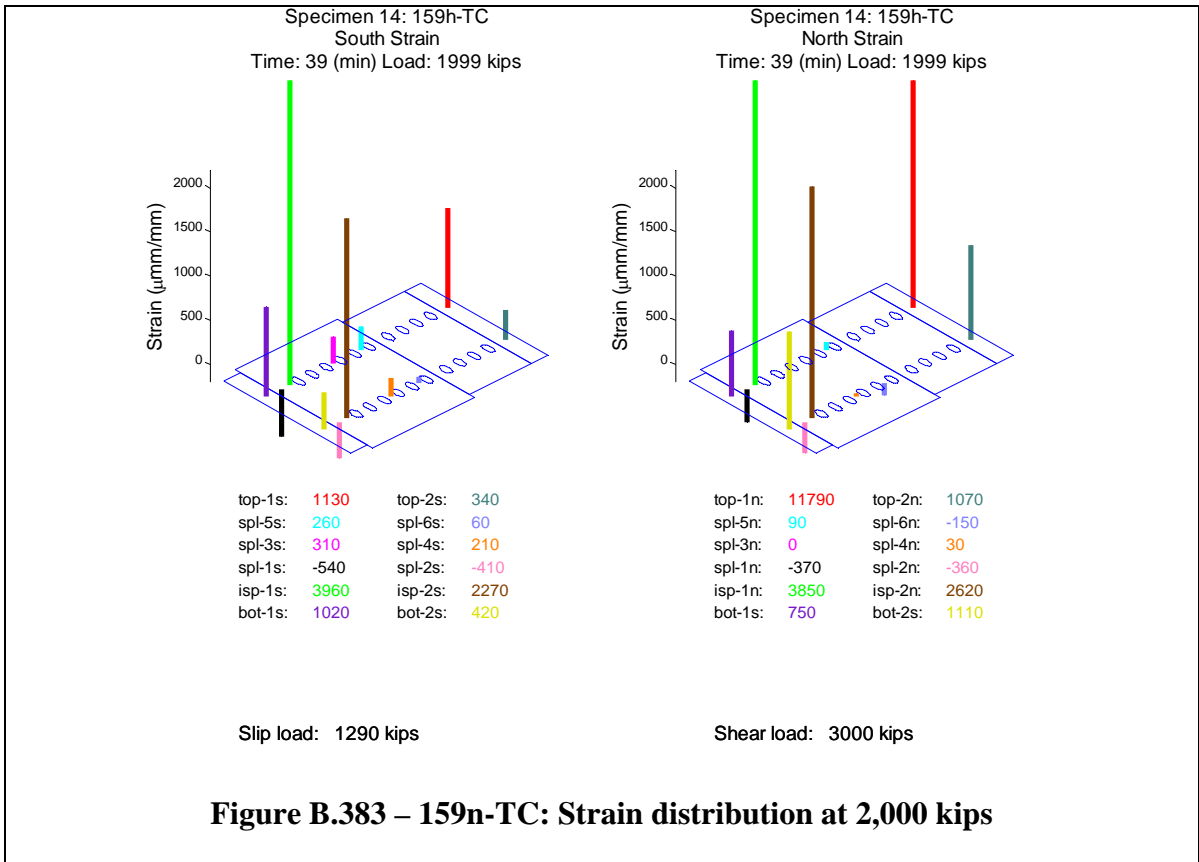


**Figure B.382 – 159n-TC: Strain distribution prior to slip at 1,290 kips**



## B.16 Specimen 159f-weld

Specimen 159f-weld (Figure B.385 to Figure B.412) behaved approximately linearly until the observed slip load (1,682 kips). During the slip event, the relative displacement between the splice plate and the filler plate increased suddenly. Slip initiated between the filler plate and the splice plate on both the north and south sides of the specimen. Over a period of 20 seconds, the relative displacements increased by the amounts shown in Table B.15. This is seen most clearly in the relative LVDTs (Figure B.401 and Figure B.402). During this dynamic event, the load dropped and increased several times. The lowest load measured was 835 kips (Figure B.391). The machine and specimen stabilized at 1,710 kips and the load was held for observation of the specimen (Figure B.392).

**Table B.15 – 159f-weld: Relative slip**

<b>Location</b>	<b>North</b>	<b>South</b>
<b>Between Splice And Filler</b>	0.65 in	0.59 in
<b>Between Filler and Top Column</b>	-	-
<b>Sum</b>	0.65 in	0.59 in

During this event the bolts likely slipped into bearing on the top column and splice plates, as seen by the increase in stiffness in Figure B.398 at approximately a load of 1,400 kips and a relative slip of 0.60 inches. The maximum expected clearance in the holes based on the assembly was nominally  $2 * (5/16 \text{ inches}) = 0.625 \text{ inches}$ .

There was no appreciable relative displacement between the top column and the filler plates (Figure B.397, Figure B.386). The weld did not exhibit any signs of fracture and the relative displacement is two orders of magnitude smaller than the primary slip displacements (Figure B.398).

The top column began to yield at approximately 2,200 kips. The top column experienced local buckling of the web and flanges up to a load of 2,517 kips. The test was stopped due to the inability of the top column to sustain additional load (Figure B.387, Figure B.388, Figure B.389 and Figure B.390). After which five bolts failed through the threads on the bottom column on the north side of the specimen, likely caused by rotation of the splice plate due to large deformations of the top column.

After slip, the specimen produced pinging noises at the following loads; 1840, 2050, 2143, 2226, 2303, 1471, 2482 and 2612 kips. Noises believed to be produced by the testing machine were neglected. The noises are likely associated with additional small slip events, bolts coming into bearing with the bolt holes, or possibly initiation of fractures within the bolts.

The splice plate LVDTs (Figure B.395 and Figure B.396) showed a dynamic increase or decrease in displacement during the slip events. This may be due to a number of reasons,

including stress relief in the splice plates after slip, very small slips relative to the column flanges, or small dynamic vibrations (with resulting small permanent offsets) of the LVDT holders, but the displacements are an order of magnitude smaller than the primary slip displacements (Figure B.398) and are not likely to indicate significant behavior.

Figure B.399 compares the LVDTs directly measuring relative slip between the top column and filler plates (Figure B.397) with the difference between the average of the two LVDTs on either filler plate at the same cross section as the LVDTs on the top column (Figure B.394) and the average of the two LVDTs at the bottom center of the top column (Figure B.393). The small displacements emphasize localized effects of the top column yielding. Therefore, the relative LVDTs do not correspond well to the difference between the corresponding absolute LVDTs.

Figure B.400 compares the LVDTs directly measuring relative slip between the filler plate and the splice plate (Figure B.398) with the difference between the average of the two LVDTs on either filler plate at that same cross section as the LVDTs on the top column (Figure B.394) and the average of the two LVDTs on either splice plate at that same cross section as the LVDTs on the top column (Figure B.395). The measurements of the relative LVDTs correspond well to the difference between the corresponding absolute LVDTs.

For this specimen, strain gages were attached to the inside face of the splice plate in the gap between the top and bottom columns (Figure B.407). These measurements, when compared to the measurements from the outside face of the splice plate (Figure B.406), indicate significant bending in the splice plates. Yielding was recorded on the inside of the splice plate.

The top column strain gages show that the localized introduction of load was approximately uniform (Figure B.403). The bottom column strain gages indicate that the localized reaction was more heavily load on the south side (Figure B.408).

After slip, the splice plate strains are generally small except for the flexural strains below bolt row 1. Snapshots of the specimen strain at 1000 kips, immediately prior to slip, 2000 kips and immediately prior to top column local buckling are visually presented in Figure B.409, Figure B.410, Figure B.411 and Figure B.412, respectively. These graphs show that the strain enters into the splice plate gradually and relatively uniformly from bolt row 6 to bolt row 1 throughout the experiment.

The experiment was executed in load control. The loading rate for the experiment was approximately 1 kip per second. One elastic cycle was executed prior to the test, going up to a load of 200 kips and returning to zero load, to verify instrumentation. The data collection rate for the experiment was held constant at 10 Hertz (10 sets of readings per second).

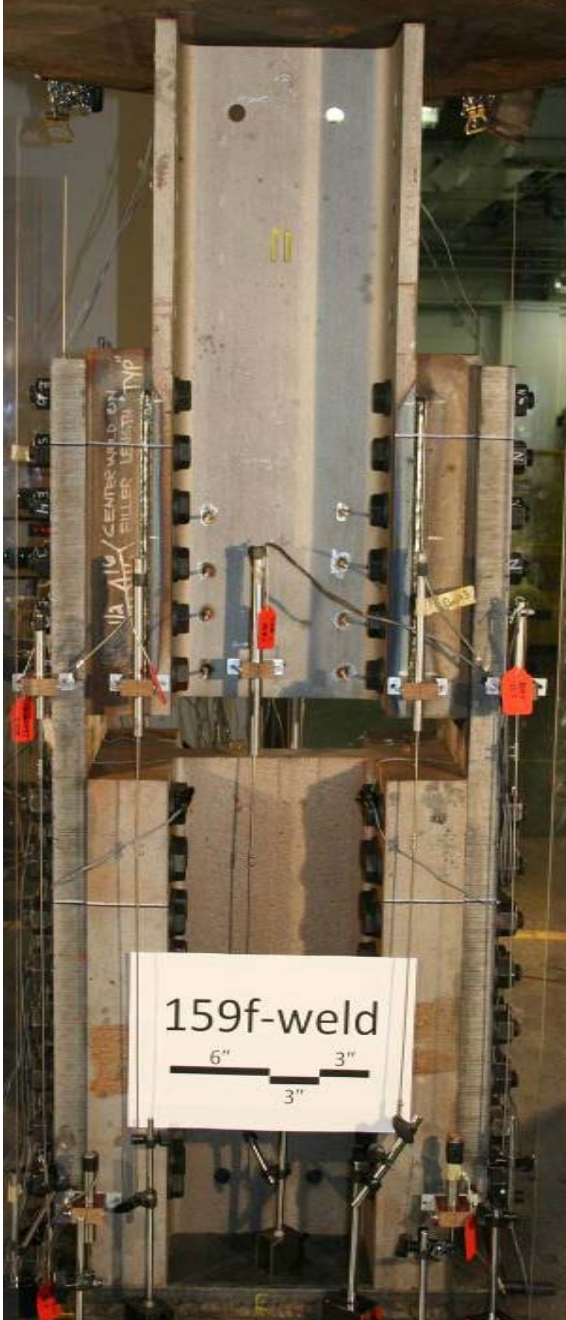


**Figure B.385 – 159f-weld: Before test (east side)**

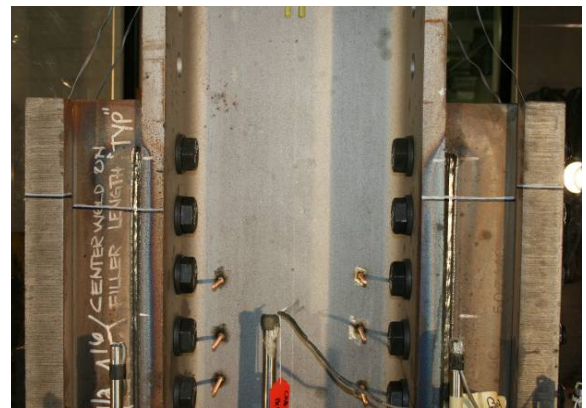


**Figure B.386 – 159f-weld: After slip (east side)**

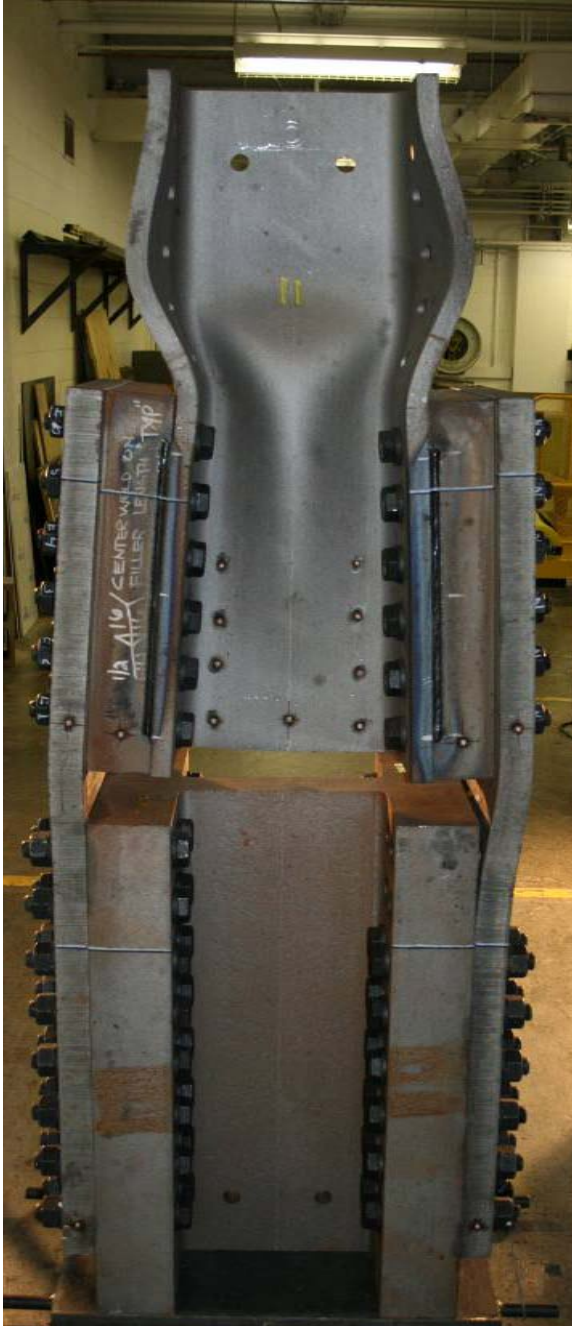
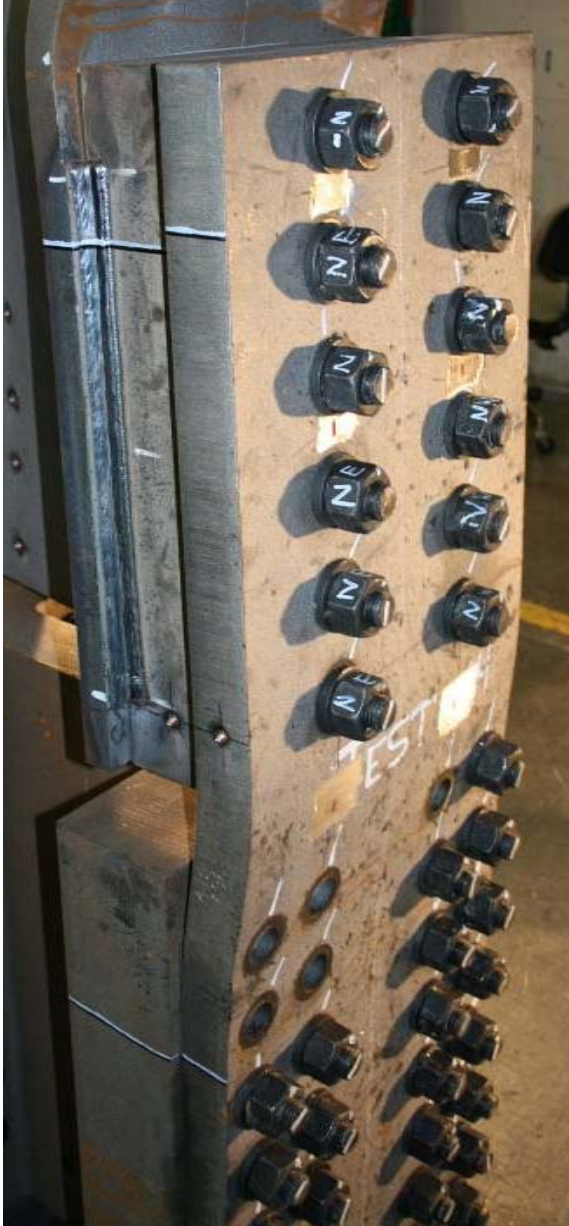


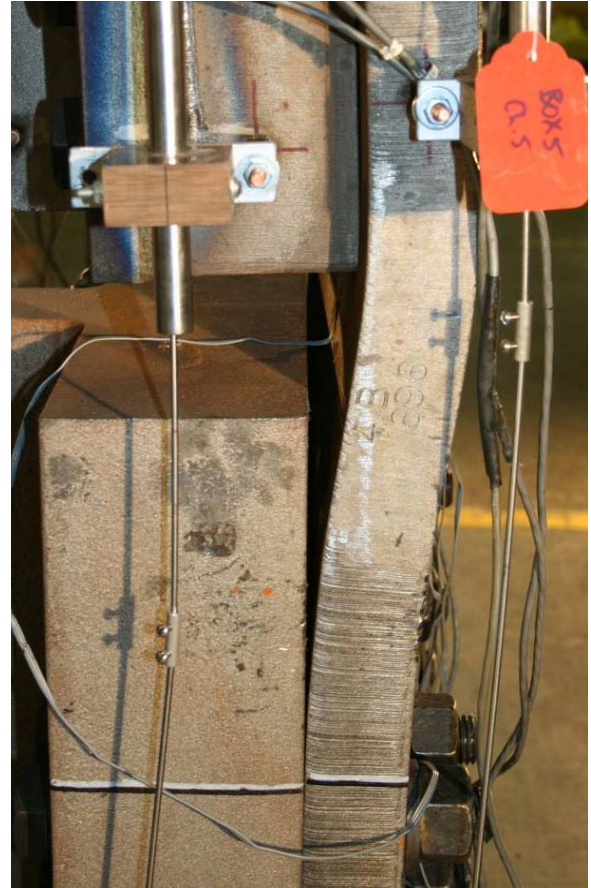
Figure B.387 – 159f-weld: After test (east side)



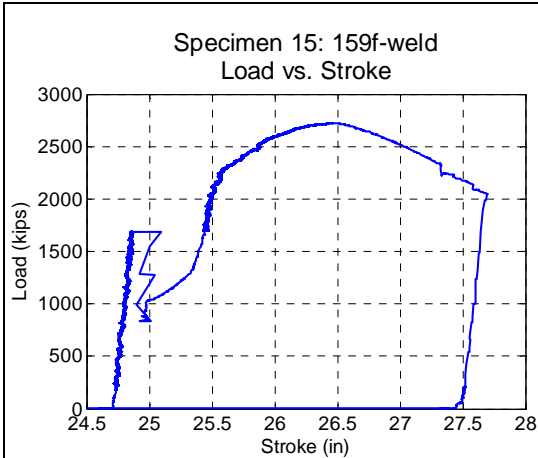
Figure B.388 – 159f-weld: After test (east side)



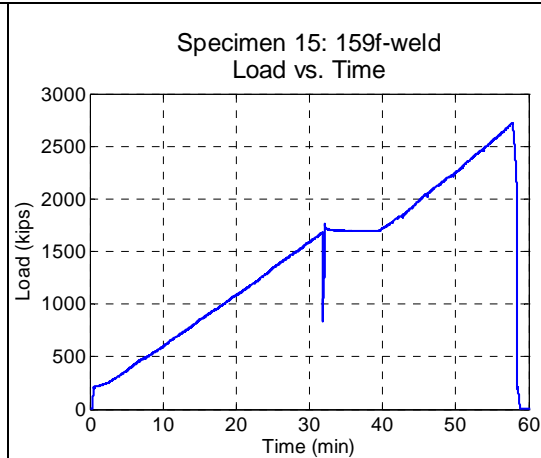
**Figure B.389 – 159f-weld: After test (north side)**



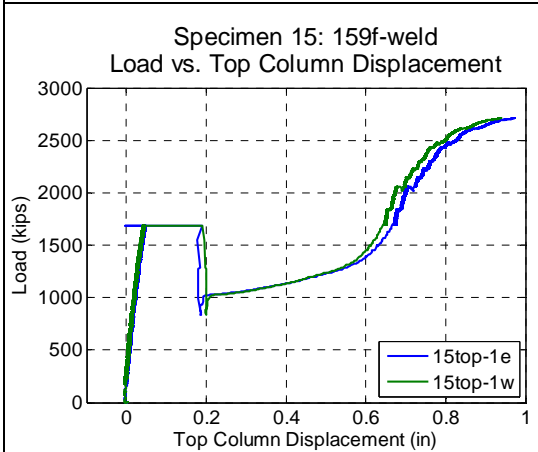
**Figure B.390 – 159f-weld: After test (east side)**



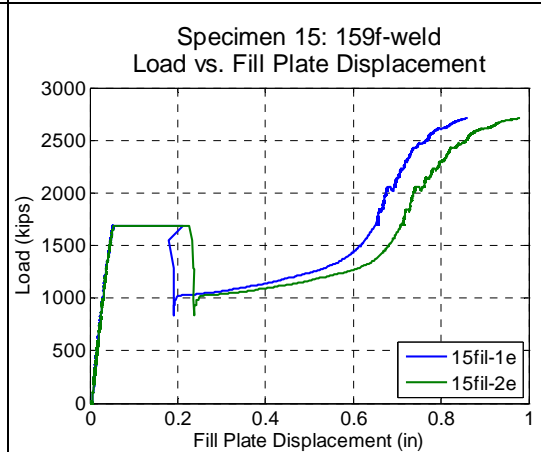
**Figure B.391 – 159f-weld: Load vs. stroke**



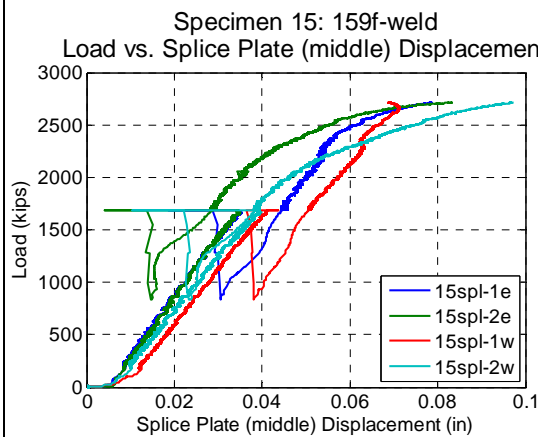
**Figure B.392 – 159f-weld: Load vs. time**



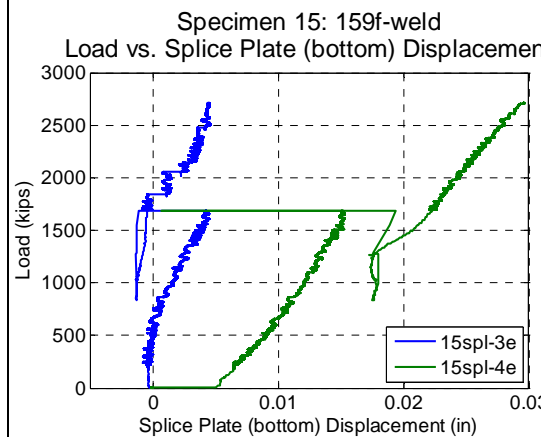
**Figure B.393 – 159f-weld: Load vs. top column displacement**



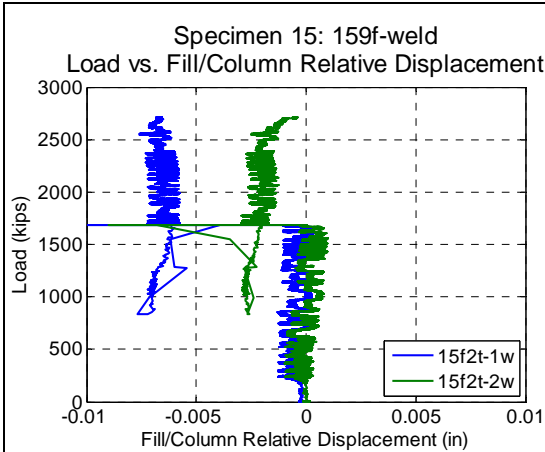
**Figure B.394 – 159f-weld: Load vs. filler plate displacement**



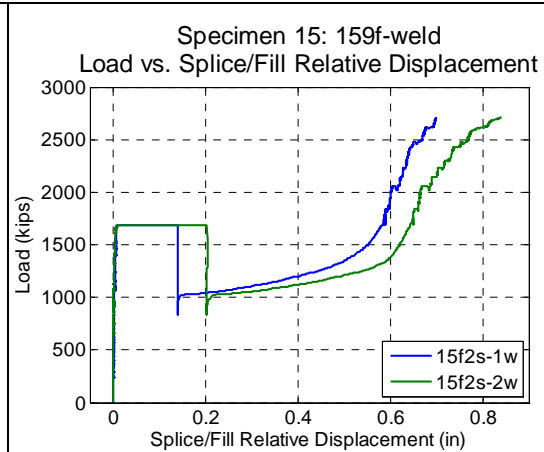
**Figure B.395 – 159f-weld: Load vs. splice plate (middle) displacement**



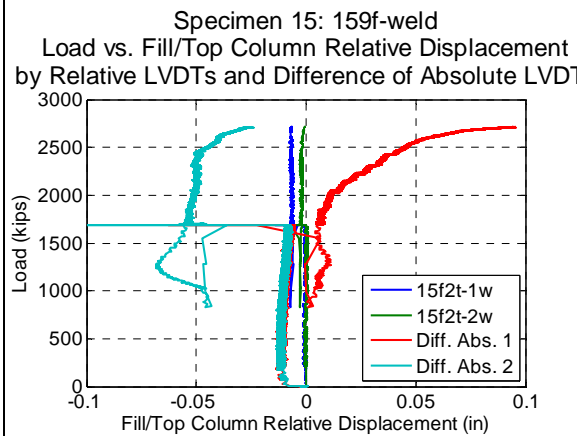
**Figure B.396 – 159f-weld: Load vs. splice plate (bottom) displacement**



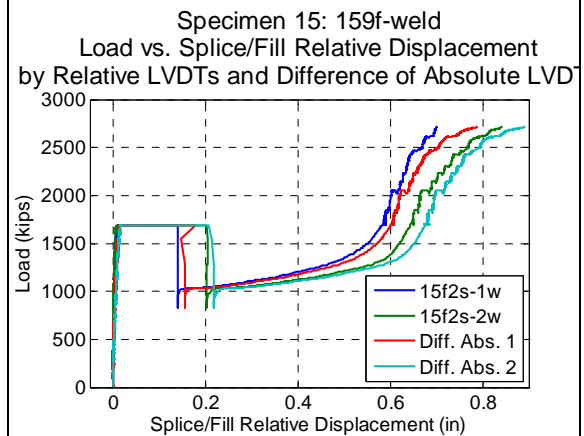
**Figure B.397 – 159f-weld: Load vs. filler/column relative displacement**



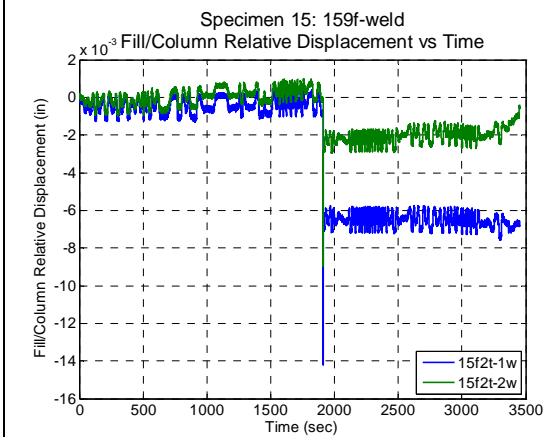
**Figure B.398 – 159f-weld: Load vs. splice/filler relative displacement**



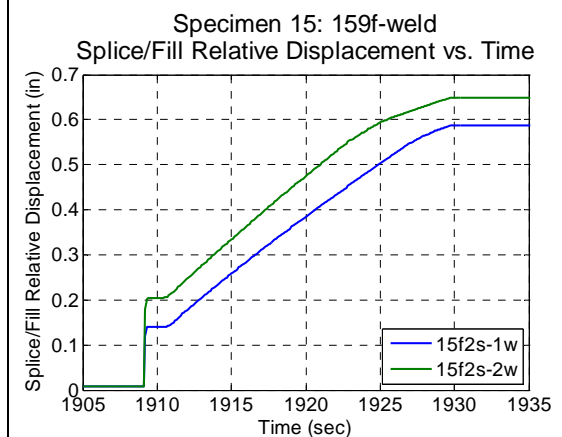
**Figure B.399 – 159f-weld: Comparison of filler/column relative and absolute LVDTs**



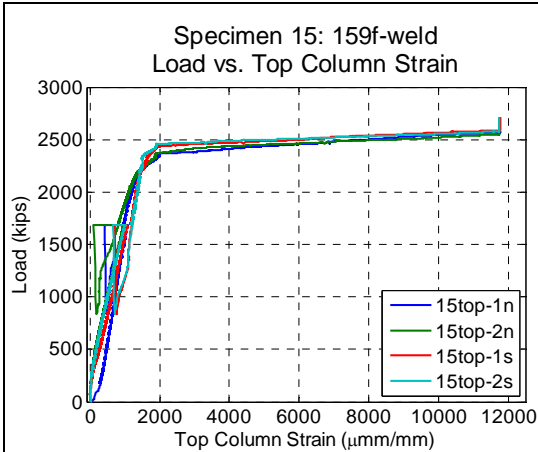
**Figure B.400 – 159f-weld: Comparison of splice/filler relative and absolute LVDTs**



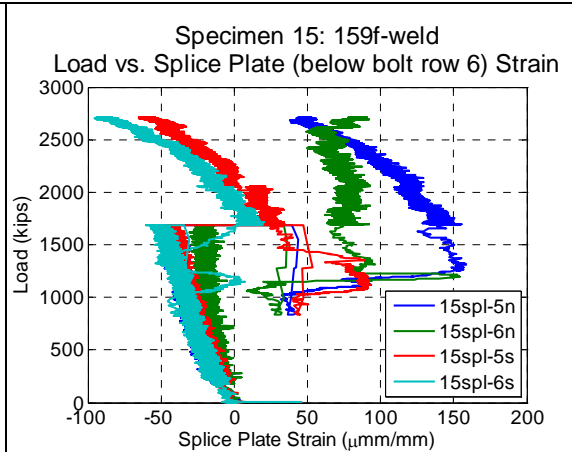
**Figure B.401 – 159f-weld: Filler/column relative displacement vs. time**



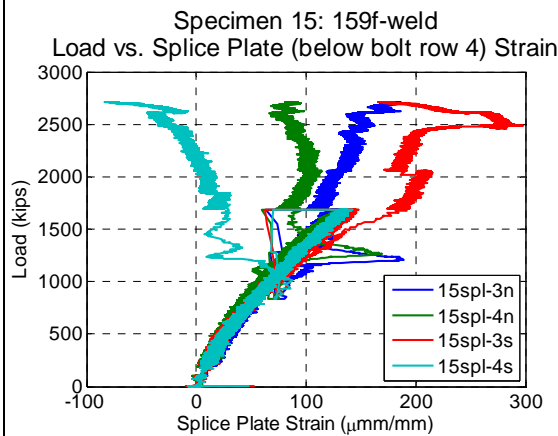
**Figure B.402 – 159f-weld: Splice/filler relative displacement vs. time**



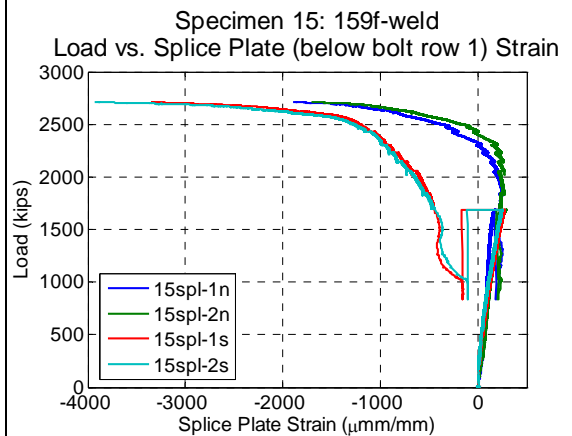
**Figure B.403 – 159f-weld: Load vs. top column strain**



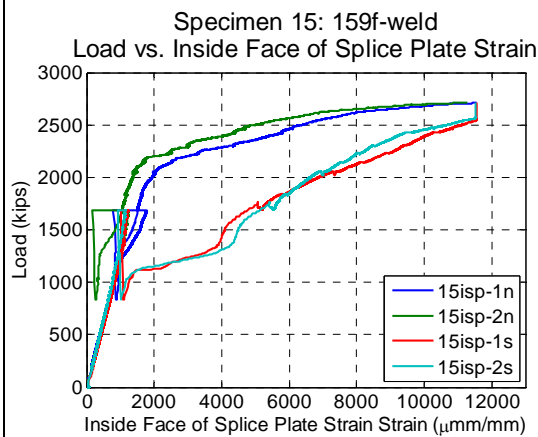
**Figure B.404 – 159f-weld: Load vs. splice plate (below bolt row 6) strain**



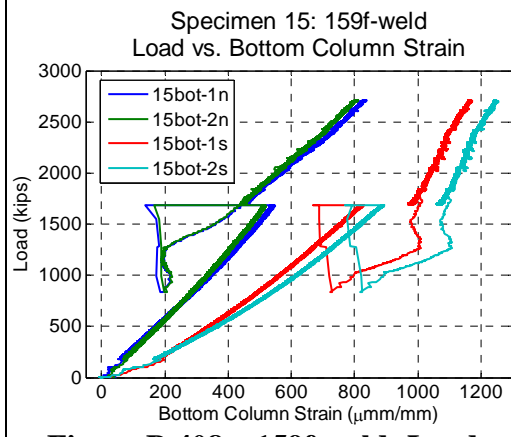
**Figure B.405 – 159f-weld: Load vs. splice plate (below bolt row 4) strain**



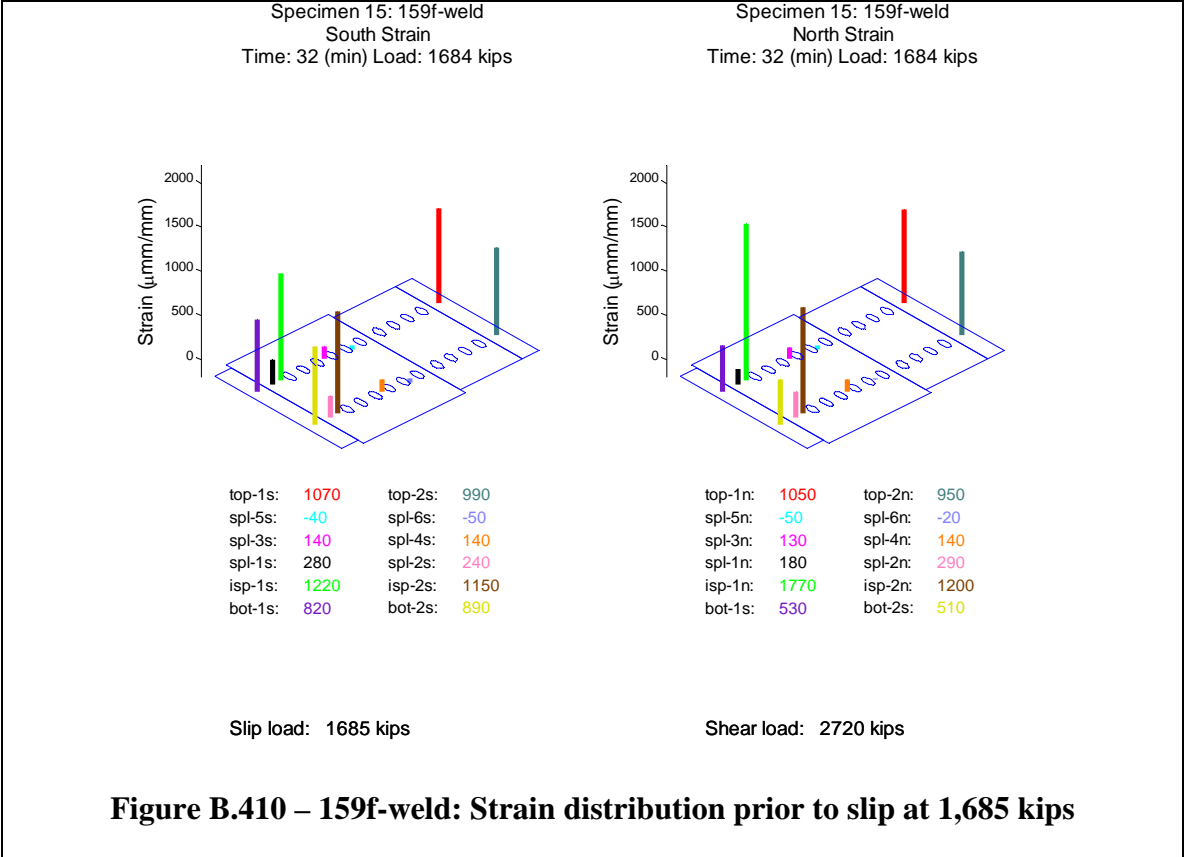
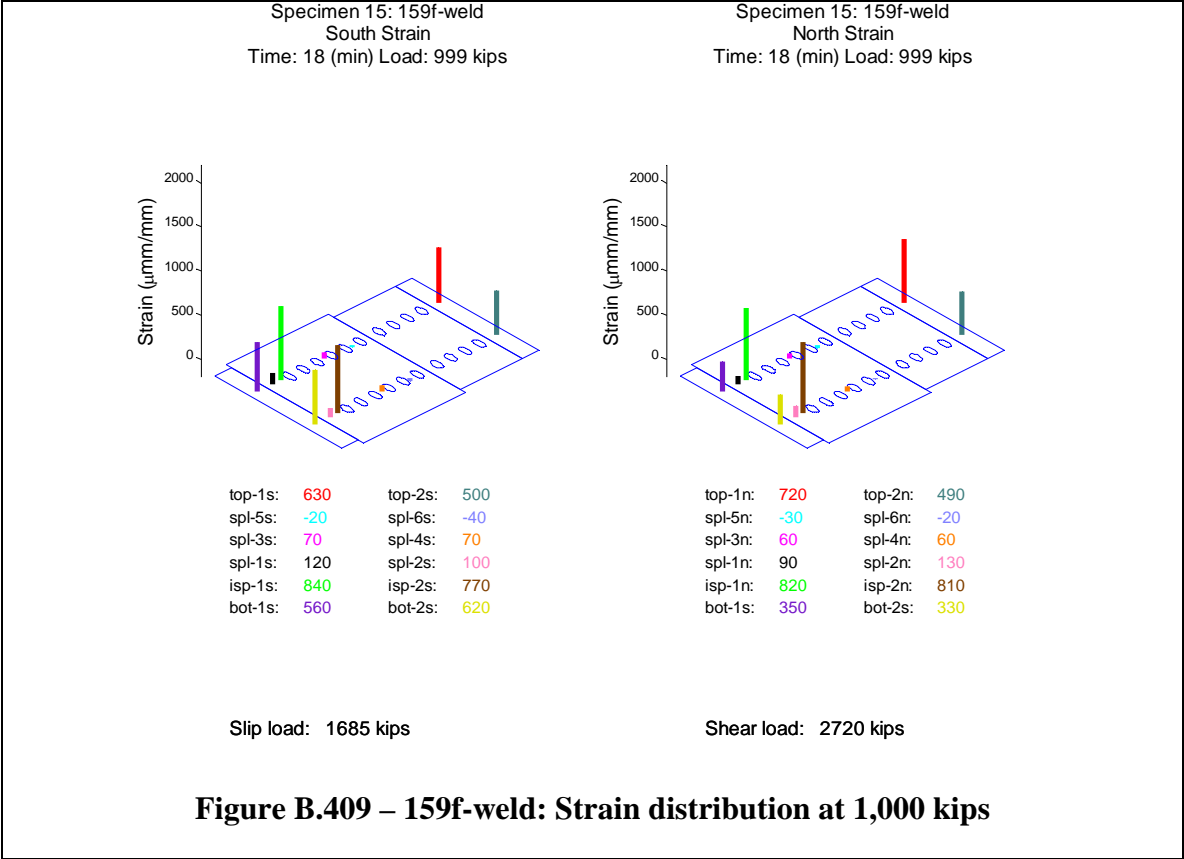
**Figure B.406 – 159f-weld: Load vs. splice plate (below bolt row 1) strain**



**Figure B.407 – 159f-weld: Load vs. inside face of splice plate strain**



**Figure B.408 – 159f-weld: Load vs. bottom column strain**



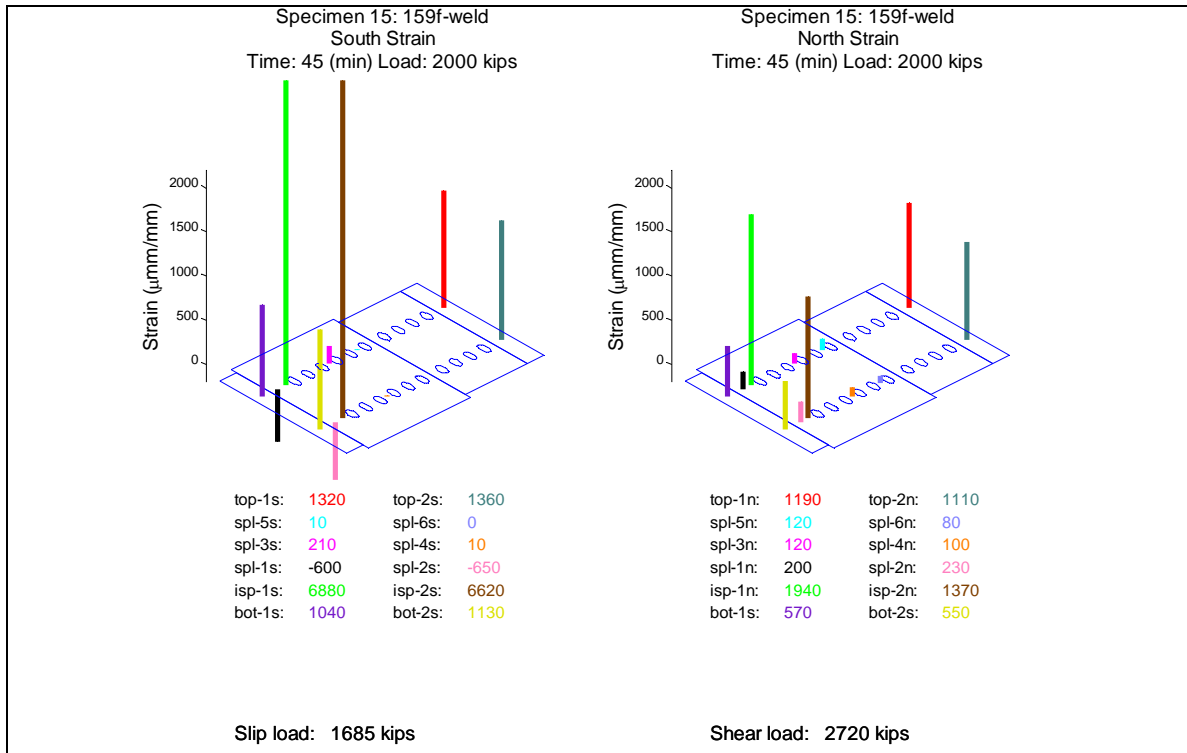


**Figure B.411 – 159f-weld: Strain distribution at 2,000 kips**

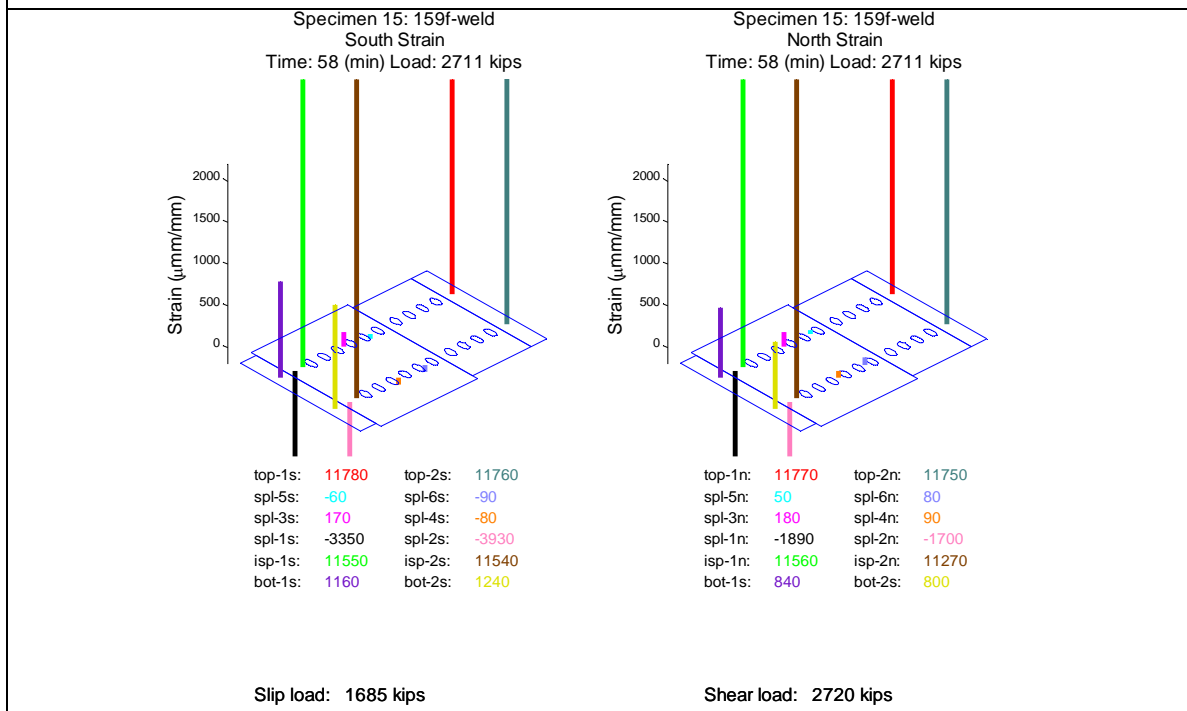


**Figure B.412 – 159f-weld: Strain distribution prior to top column local buckling at 2,720 kips**

## B.17 Specimen 159h-weld

Specimen 159h-weld (Figure B.413 to Figure B.440) behaved approximately linearly until the observed slip load (1,616 kips). During the slip event, the relative displacement between the filler plate and the splice plate on both the north and south side of the specimen increased suddenly and continued slipping for 20 seconds. Approximately 30 minutes later, at a load of 2,510 kips, slip was observed between the filler plate and the top column on both the north and south side of the specimen, indicating failure of the weld. The specimen continued slipping for 20 seconds. Table B.16 summarizes the slip events. The slip events are seen most clearly in the relative LVDTs (Figure B.429 and Figure B.430). During each dynamic slip event, the load dropped and increased several times. For the initial slip the lowest load measured was 876 kips (Figure B.419). The machine and specimen stabilized at 1,625 kips and the load was held for observation of the specimen (Figure B.420). For the secondary slip the lowest load measured was 1,537 kips (Figure B.419). The machine and specimen once again was stabilized at 2,500 kips and the load was held for observation of the specimen (Figure B.420).

**Table B.16 – 159h-weld: Relative slip**

<b>Location</b>	<b>North</b>	<b>South</b>
<b>Between Splice and Filler</b>	0.6 in	0.57 in
<b>Between Filler And Top Column</b>	0.46 in	0.51 in
<b>Sum</b>	1.06 in	1.08 in

During the first event the bolts likely slipped into bearing on the splice plates, as seen by the increase in stiffness in Figure B.422 at approximately a load of 1,600 kips and a relative slip of 0.60 inches (Figure B.415). The maximum expected clearance in the holes based on the assembly was nominally  $2 * (5/16 \text{ inches}) = 0.625 \text{ inches}$ .

The development welds failed through the throat during the second slip event, causing significant displacement between the top column and filler plate (Figure B.429).

After the slip event, one bolt on the southwest side of the specimen (SW3) failed through the threads, indicating a pretension failure. The bolt head and shank fell from the specimen. One bolt on the southeast side (SE4) was observed to no longer be flush. It failed, through the threads, during the failure of the welds. One bolt on the southwest side (SW2) failed through the threads at a load of 2,033 kips. The bolt head and shank remained in the specimen. This bolt provided some doweling action and failed a second time in shear at the ultimate load of the specimen. Three bolts were retorqued during assembly in this specimen, including bolts SE1, SW3, and SW6; bolt SE4 was likely not considered a neighboring bolt to those that were retorqued, but SW2 probably was, and SW3 was retorqued, as per Table B.2.

The top column began to yield at approximately 2,150 kips (Figure B.431). Upon further loading, the bolts, now experiencing shear, yielded and eventually failed at the observed bolt shear load (2,746 kips) (Figure B.416, Figure B.417 and Figure B.418). The remaining bolts through the splice plate on the south flange of the top column failed nearly simultaneously on the shear plane between the splice plate and the fill plate.

After slip, the specimen produced pinging noises at the following loads; 1721, 1804, 1872, 1943, 2033 (bolt SW2 failed), 2105, 2165, 2167, 2209, 2265, 2304, 2330, 2366, 2386, 2416, 2438, 2467, 2492, 2573, 2600, 2621, 2667, 2681 and 2693 kips. Noises believed to be produced by the testing machine were neglected. The noises are likely associated with additional small slip events, bolts coming into bearing with the bolt holes, or possibly initiation of fractures within the bolts.

Between the slip event and shear failure the west strain gage at bolt row 4 on the south splice plate (spl-3s) was damaged (Figure B.433)

The splice plate LVDTs (Figure B.423 and Figure B.424) showed a dynamic increase or decrease in displacement during the slip events. This may be due to a number of reasons, including stress relief in the splice plates after slip, very small slips relative to the column flanges, or small dynamic vibrations (with resulting small permanent offsets) of the LVDT holders, but the displacements are an order of magnitude smaller than the primary slip displacements (Figure B.425 and Figure B.426) and are not likely to indicate significant behavior.

Figure B.427 and Figure B.428 compare the LVDTs directly measuring relative slip between the filler plate and either the top column (Figure B.425) or the splice plate (Figure B.426) with the difference between the average of the two LVDTs on either filler plate at that same cross section as the LVDTs on the top column (Figure B.422) and either the average of the two LVDTs at the bottom center of the top column (Figure B.421) or the average of the two LVDTs on either splice plate at that same cross section as the LVDTs on the top column (Figure B.423). The measurements of the relative LVDTs correspond well to the difference between the corresponding absolute LVDTs.

For this specimen, strain gages were attached to the inside face of the splice plate in the gap between the top and bottom columns (Figure B.435). These measurements, when compared to the measurements from the outside face of the splice plate (Figure B.434), indicate significant bending in the splice plates. Yielding was recorded on the inside of the splice plate.

The top column strain gages show that the localized introduction of load had a bias towards the northwest (Figure B.431). The bottom column strain gages show that the localized reaction had a small bias to the south side (Figure B.436).

The splice plate was loaded uniformly throughout (Figure B.432, Figure B.433, Figure B.434 and Figure B.435). Snapshots of the specimen strain at 1000 kips, immediately prior to slip, 2000 kips and immediately prior to shear are visually presented in Figure B.437, Figure B.438, Figure B.439 and Figure B.440, respectively. These graphs show

that the strain enters into the splice plate gradually and relatively uniformly from bolt row 6 to bolt row 1 throughout the experiment.

To avoid local buckling of the top column, 3  $\frac{3}{4}$ " plates were bolted to the top column. These plates provided the top column flanges additional restraint similar to that provided by the filler plates of previous specimens. These plates performed adequately and prevented local buckling of the top column seen in specimen 159f-weld.

The experiment was executed in load control. The loading rate for the experiment was approximately 1 kip per second. The load was held at 2,393 kips and 2,727 kips to observe local buckling of the top column. One elastic cycle was executed prior to the test, going up to a load of 200 kips and returning to zero load, to verify instrumentation. The data collection rate for the experiment was held constant at 10 Hertz (10 sets of readings per second).

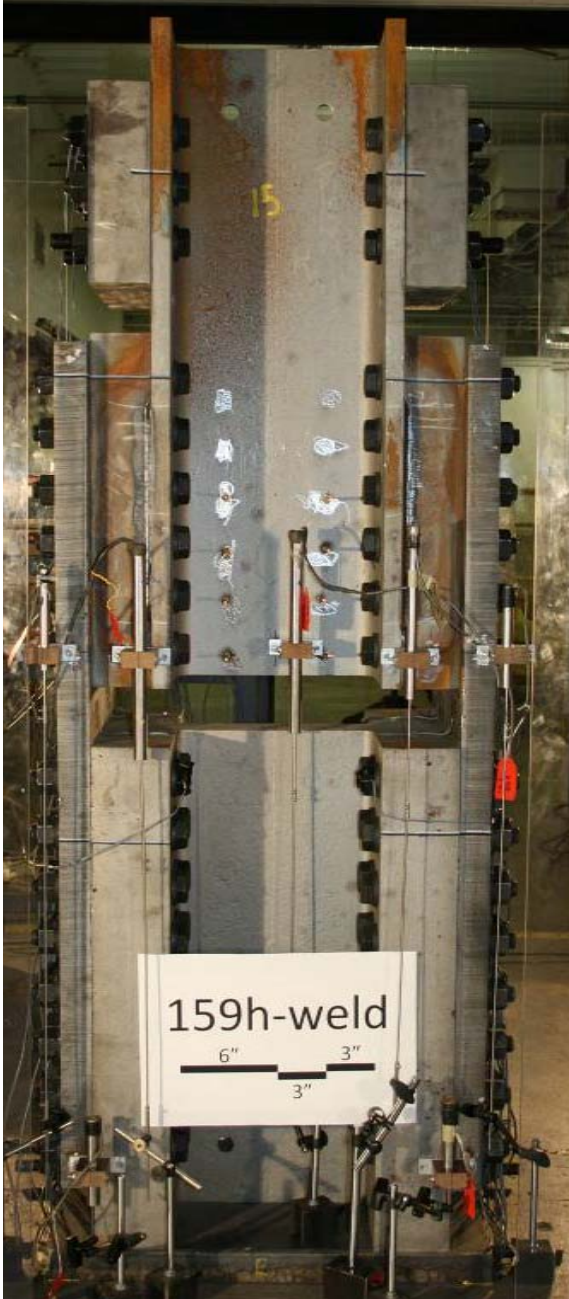


**Figure B.413 – 159h-weld: Before test  
(east side)**



**Figure B.414 – 159h-weld: Before test  
(southeast side)**

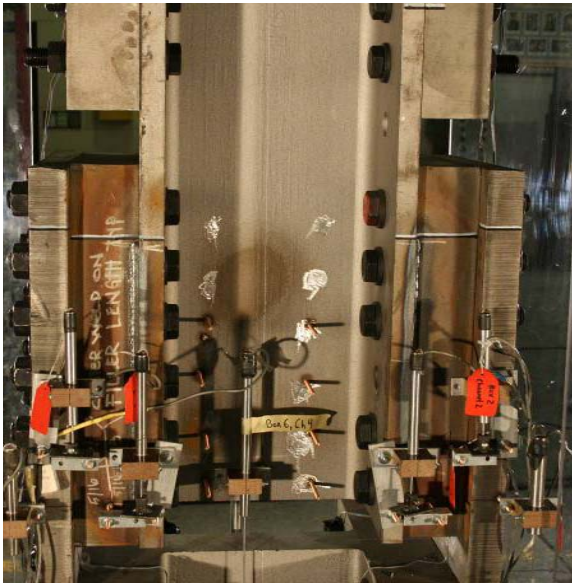


**Figure B.415 – 159h-weld: After slip  
(west side)**



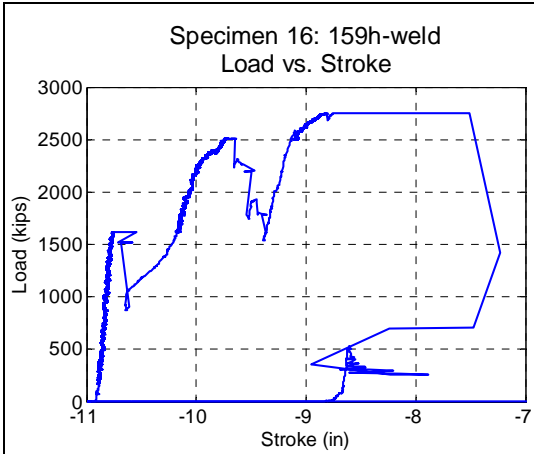
**Figure B.416 – 159h-weld: After test  
(east side)**



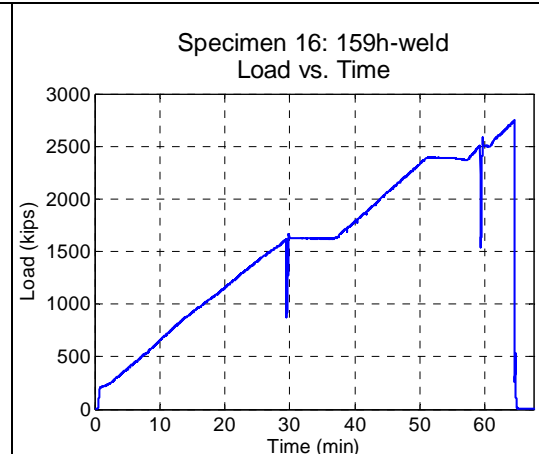
**Figure B.417 – 159h-weld: After test  
(west side)**



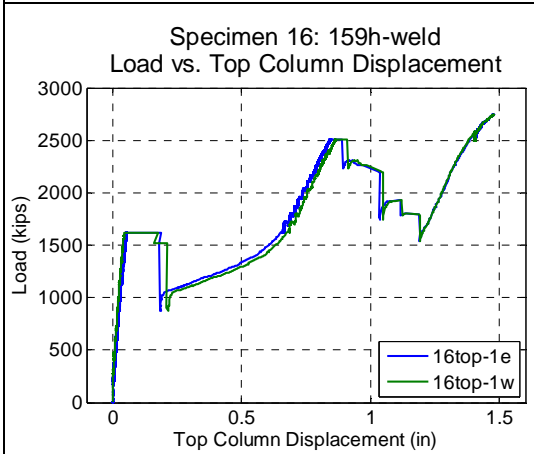
**Figure B.418 – 159h-weld: After test  
(northeast side)**



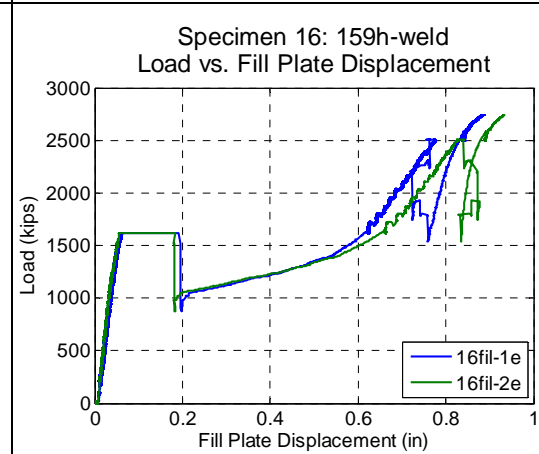
**Figure B.419 – 159h-weld: Load vs. stroke**



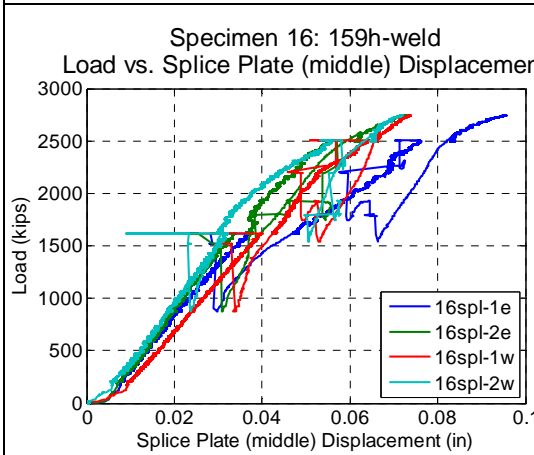
**Figure B.420 – 159h-weld: Load vs. time**



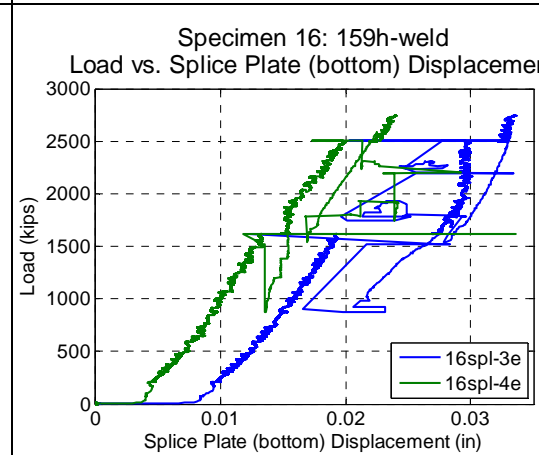
**Figure B.421 – 159h-weld: Load vs. top column displacement**



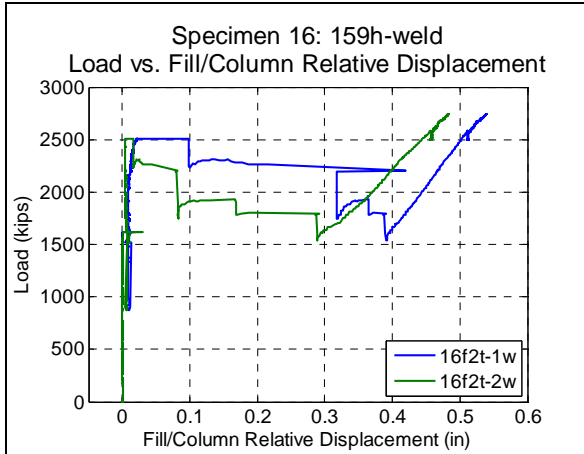
**Figure B.422 – 159h-weld: Load vs. filler plate displacement**



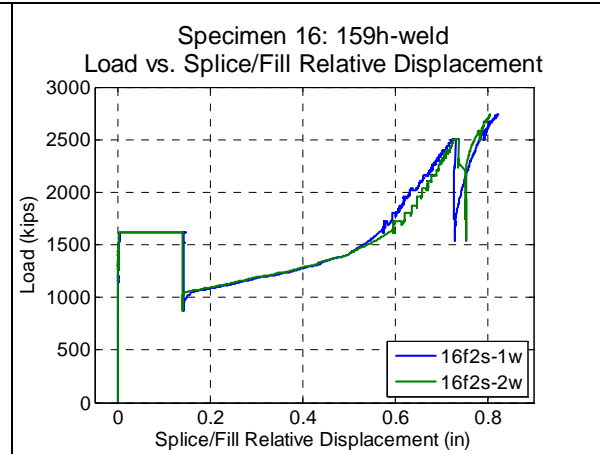
**Figure B.423 – 159h-weld: Load vs. splice plate (middle) displacement**



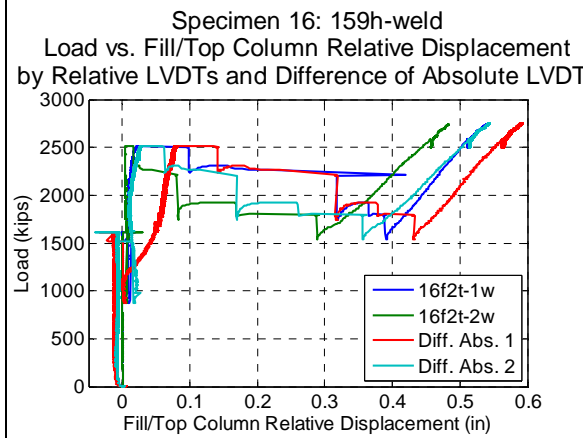
**Figure B.424 – 159h-weld: Load vs. splice plate (bottom) displacement**



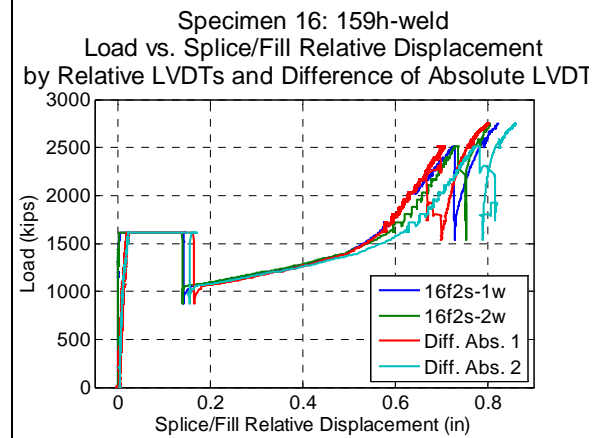
**Figure B.425 – 159h-weld: Load vs. filler/column relative displacement**



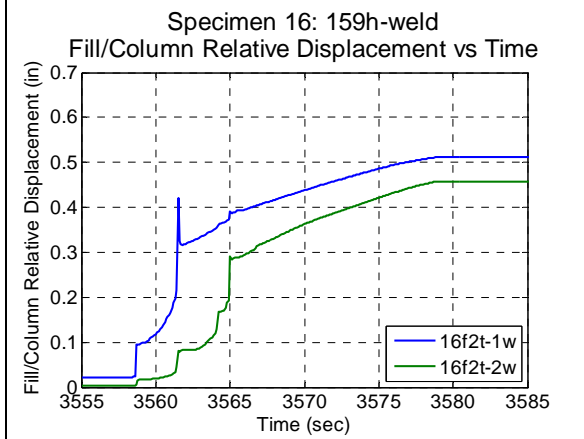
**Figure B.426 – 159h-weld: Load vs. splice/filler relative displacement**



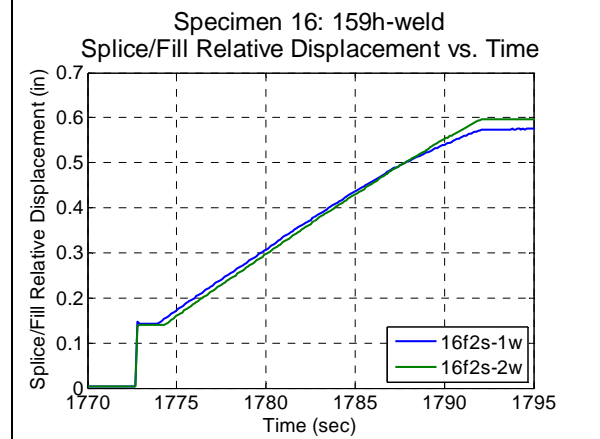
**Figure B.427 – 159h-weld: Comparison of filler/column relative and absolute LVDTs**



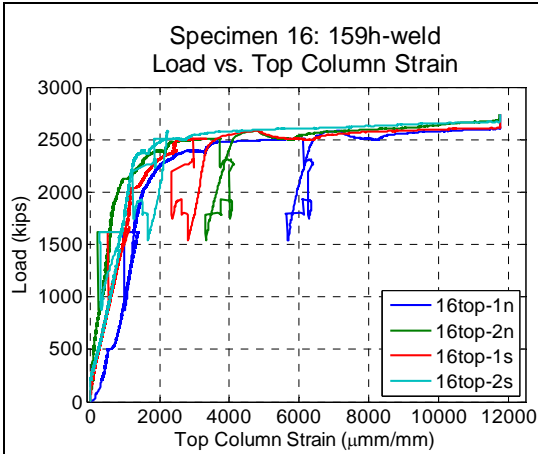
**Figure B.428 – 159h-weld: Comparison of splice/filler relative and absolute LVDTs**



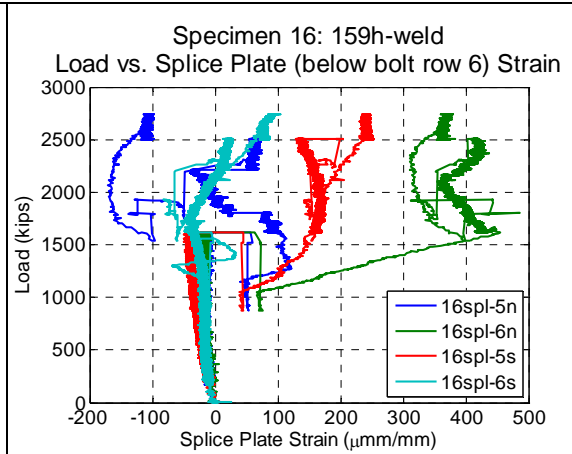
**Figure B.429 – 159h-weld: Filler/column relative displacement vs. time**



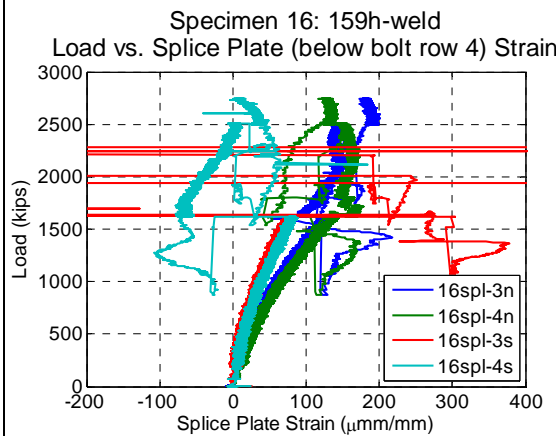
**Figure B.430 – 159h-weld: Splice/filler relative displacement vs. time**



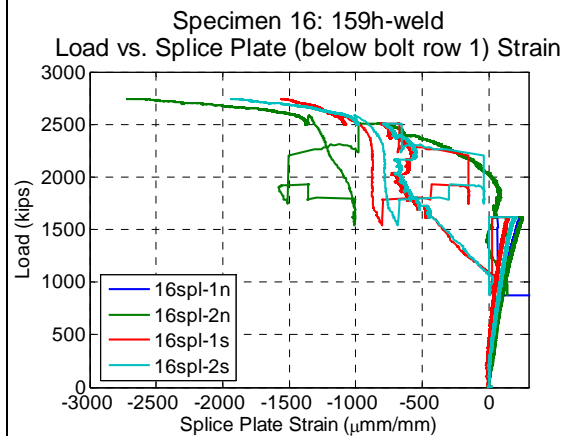
**Figure B.431 – 159h-weld: Load vs. top column strain**



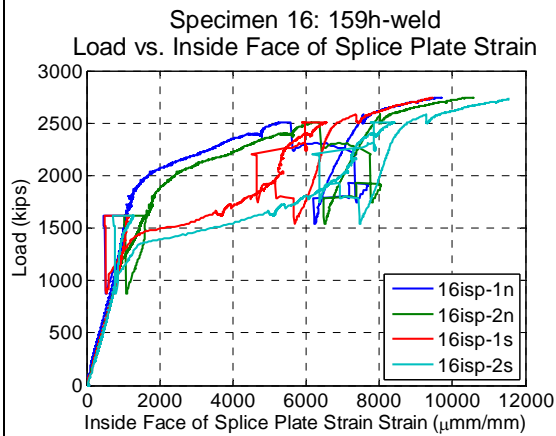
**Figure B.432 – 159h-weld: Load vs. splice plate (below bolt row 6) strain**



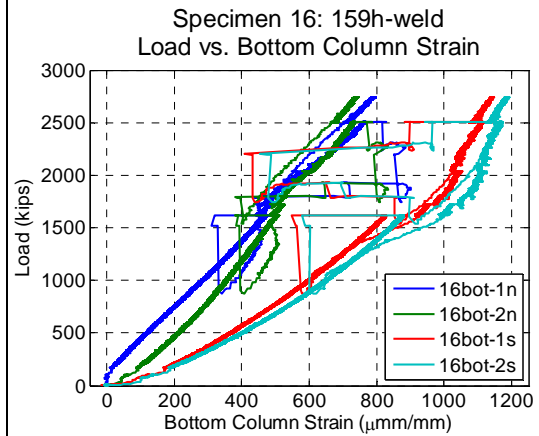
**Figure B.433 – 159h-weld: Load vs. splice plate (below bolt row 4) strain**



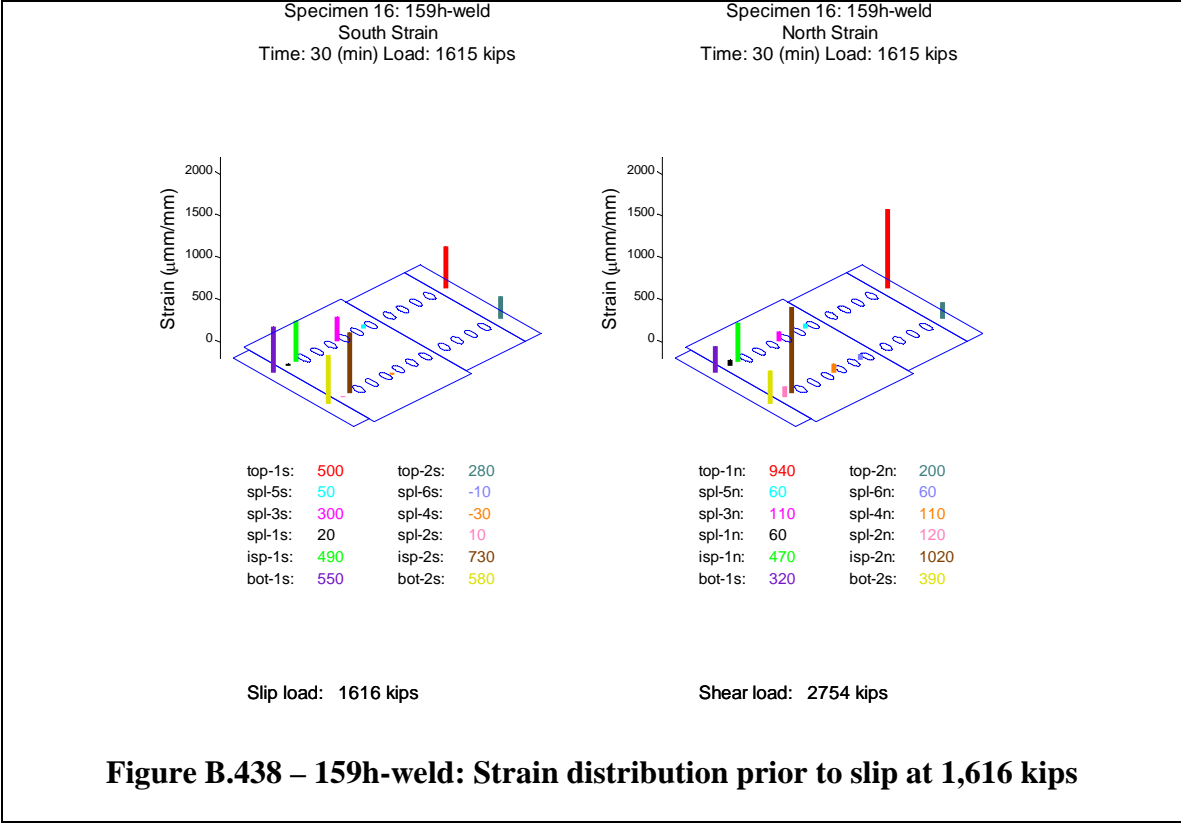
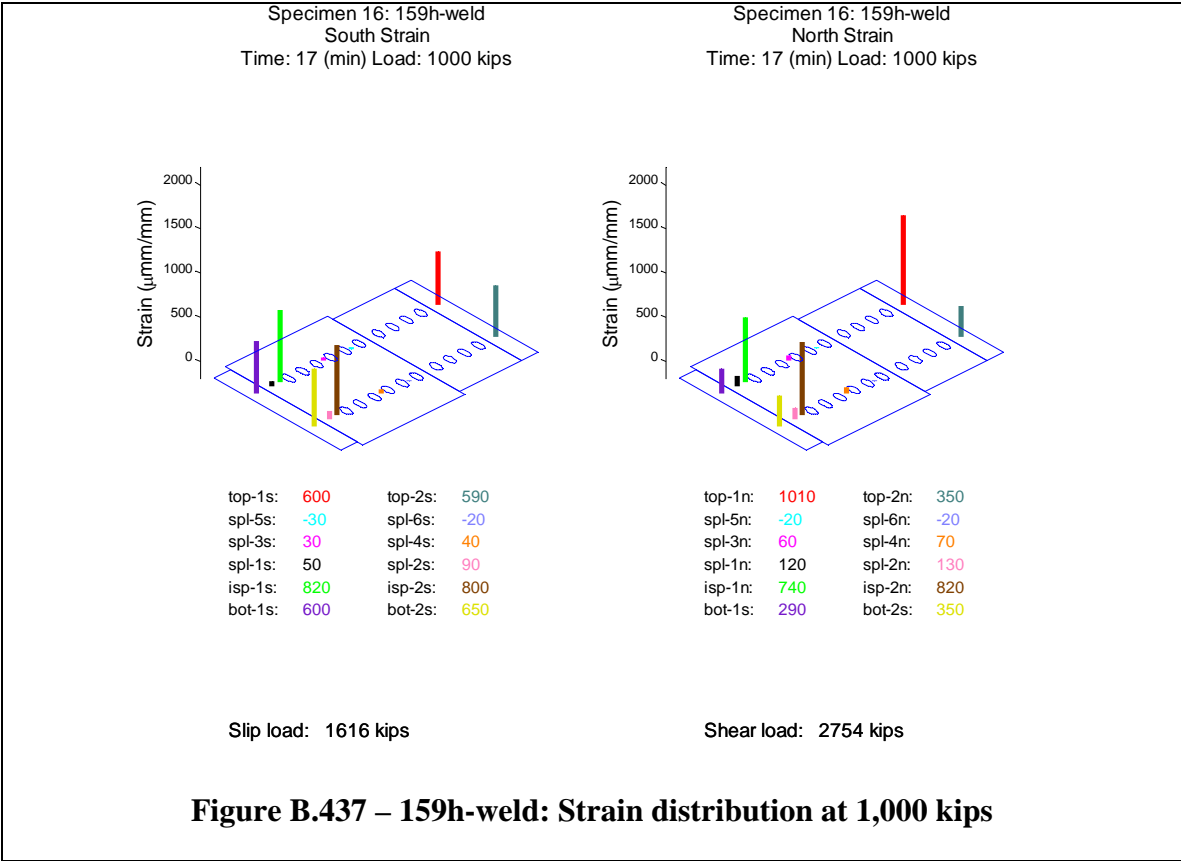
**Figure B.434 – 159h-weld: Load vs. splice plate (below bolt row 1) strain**

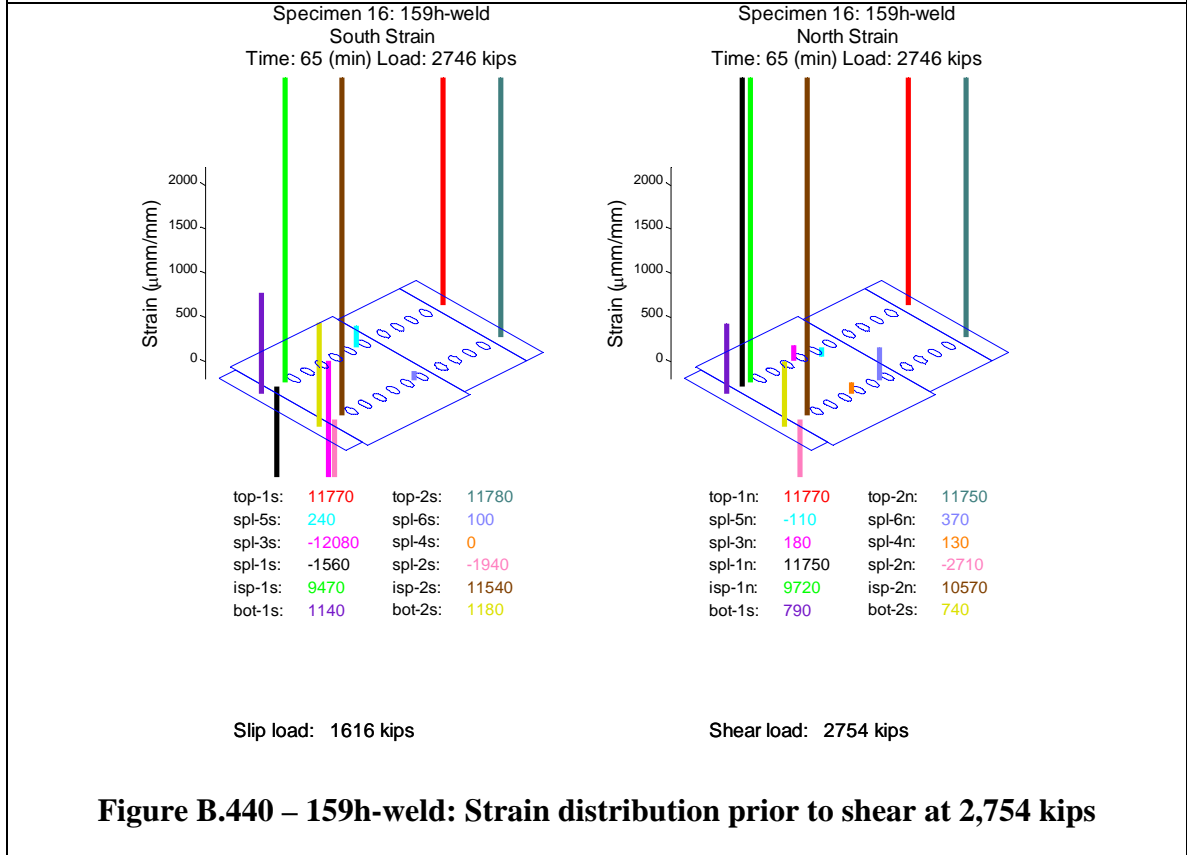
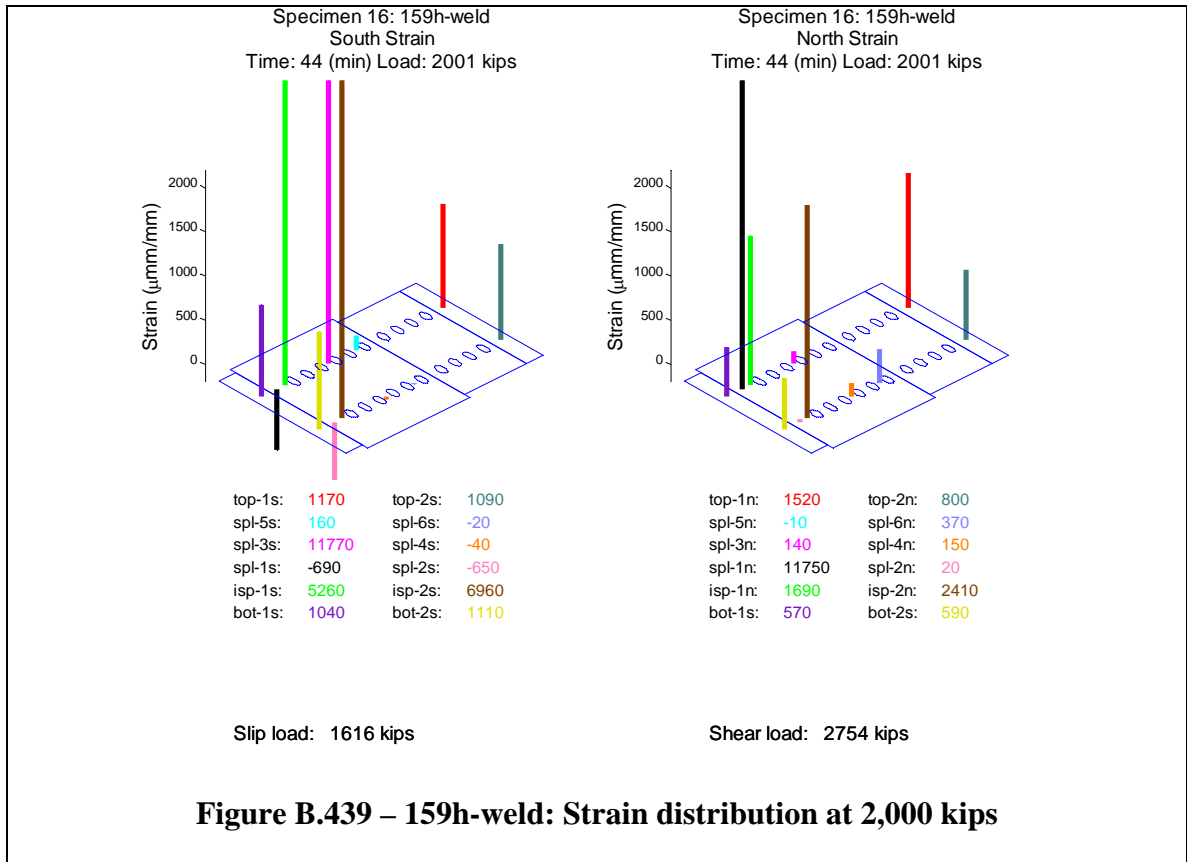


**Figure B.435 – 159h-weld: Load vs. inside face of splice plate strain**



**Figure B.436 – 159h-weld: Load vs. bottom column strain**





## **DETAILED COMPARISON OF SPECIMEN BEHAVIOR**

### **C.1 Introduction**

This appendix presents a number of comparative plots that enable comparing and contrasting the response of the specimens tested in this work. The information presented focuses on measured displacement data, and several different groupings are used for the investigation.

### **C.2 Effect of Hole Oversize**

The displacement of the load versus top column displacement for specimens 730-std and 730-over with standard and oversize bolt holes respectively is plotted in Figure C.7. After slip the specimens trace parallel paths, offset by approximately 0.5 in. The additional displacement is attributed to the additional bolt hole oversize, 0.25 in. in each hole, 0.5 in. cumulatively of the splice plate and top column bolt holes. The additional displacement does not effect the subsequent behavior. The slip and shear strength seem uninfluenced by the different bolt hole oversize.

### **C.3 Effect of Filler Presence**

With exception of specimen 730-std and 730-over, all specimens had oversize holes and fillers between the splice plate and top column. The presence of the filler decreased the stiffness and increased the deformation during slip for all of the specimens compared to specimen 730-over without a filler (Figure C.6 and Figure C.7). The two thicknesses of fillers in this report (1 5/8 in. and 3 3/4 in.) do not influence the top column displacement magnitude but the stiffness was lower for the 455 specimens. The additional displacement compared to specimen 730-over is attributed to the deformation of the bolt within the filler; which is approximately equal to the oversize of the filler bolt hole (5/16 in. in this study) and bearing deformation of the bolt hole of the filler plate (approximately 0.1 in. on each side). As demonstrated by specimen 159f, prior to slip of the surface between the top column and filler plate, the behavior is similar to the case without a filler plate (730-over, Figure C.6).

### **C.4 Influence of Filler Development**

The load versus top column displacement comparing development for the 159 and 455 specimens is shown in Figure C.1 and Figure C.2 respectively. In both cases, the undeveloped specimens demonstrate slightly higher displacement after slip than the developed specimens. Development of the filler adds resistance to displacement between

the top column and filler plate. Therefore, the development of the filler reduces the displacement between the top column and filler plate (Figure C.13 and Figure C.14). The larger the filler plate the more bolts required to develop the filler, providing additional resistance to displacement between the filler plate and top column. This explains the greater influence of development for the 159 specimens (3 3/4 in. filler) compared to the 455 (1 5/8 in. filler) specimens. Figure C.18 and Figure C.19 show the relative displacement between the splice plate and filler plate for the 159 and 455 specimens respectively. The 159 specimens show scatter without an identifiable influence of development. The 455 specimens show that all have similar behavior, again without an identifiable influence of development. The relative displacement between the splice plate and filler plate is uninfluenced by development, since the load and resistance across this plane is uninfluenced by development.

## **C.5 Influence of Multiple Plies**

The top column displacement for the two undeveloped 159 two-ply specimens is presented in Figure C.3 along with two undeveloped 159 specimens. After slip, the top column displacement is approximately 0.10 in. larger for the two-ply specimens compared to single-ply specimens. The relative displacement between the top column and filler plate (Figure C.15) does not show an influence of the additional ply. This is because the additional 1/4 in. ply is between the splice plate and filler plate, which does not influence the behavior of the surface between the thick filler plate (3 1/2 in.) and the top column. The relative displacement between the splice plate and filler plate (Figure C.20) is increased for the two-ply specimens. This is caused by the addition of the 1/4 in. ply between the two plates. The bolt is unrestrained within the 1/4 in. filler since the bolt oversize (5/16 in.) is large compared to the thickness of the plate, requiring a large bolt rotation to mobilize restraint from the plate. This allows the thick filler plate to displace further (Figure C.10). The additional ply does not influence the behavior prior to slip although statistical analysis indicates that it influences the expected slip load. The addition of the thin ply did not influence the ultimate strength of this connection with thick fillers. If the ratio of the ply thicknesses were changed closer to unity, the restraint provided by the thin filler would increase and the restraint provided by the thick filler would decrease.

## **C.6 Influence of TC Bolts**

Specimens 159h-TC and 159n-TC utilized tension-controlled bolts rather than typical heavy hex TN bolts. The ultimate strength of both specimens exceeded the capacity of the testing machine (3,000 kips). The load versus top column displacement for the TC specimens and the half developed and undeveloped TN 159 specimens for comparison is presented in Figure C.4. The undeveloped TC specimen behaves similarly to the undeveloped TN specimens. The reduced slip displacement due to development (discussed above) was even more pronounced for 159h-TC compared to 159h. These observations are valid for the filler plate displacement (Figure C.11), relative displacement between the top column and filler plate (Figure C.16) and relative

displacement between the filler plate and splice plate (Figure C.21). No evidence was revealed to support the high ultimate strength of the TC specimens.

## **C.7 Influence of Welded Development**

Specimens 159f-weld and 159h-weld developed the filler plate with an equivalent amount of weld as the slip strength of the corresponding development bolts. The top column of 159f-weld suffered detrimental local buckling prior the ultimate connection strength and the development welds did not fail. The load verses top column displacement is plotted for the two welded specimens with the corresponding bolted specimens with the same level of development in Figure C.5. Specimens 159f-weld and 159h-weld behave similar to 159f prior to slip between the top column and filler plate. The development weld on specimen 159h-weld eventually broke, tracing a path similar to 159f. The test for specimen 159f-weld ended prematurely so, the connection did not achieve deformation consistent with the rest of the tests. It is predicted that if the weld was broken the deformation would increase, becoming similar to the other specimens. The weld did not influence the displacement of the filler plate (Figure C.12). Since the weld did not break, the relative displacement between the top column and filler plate remained insignificant throughout the test for specimen 159f-weld (Figure C.17). Specimen 159h-weld had lower relative displacement between the top column and filler plate after slip as compared to Specimen 159h, perhaps due to some residual resistance provided by the fractured weld (Figure C.17). The weld did not influence the relative slip between the splice plate and filler plate (Figure C.22), which is logical since the effect of development was not detected at this surface.

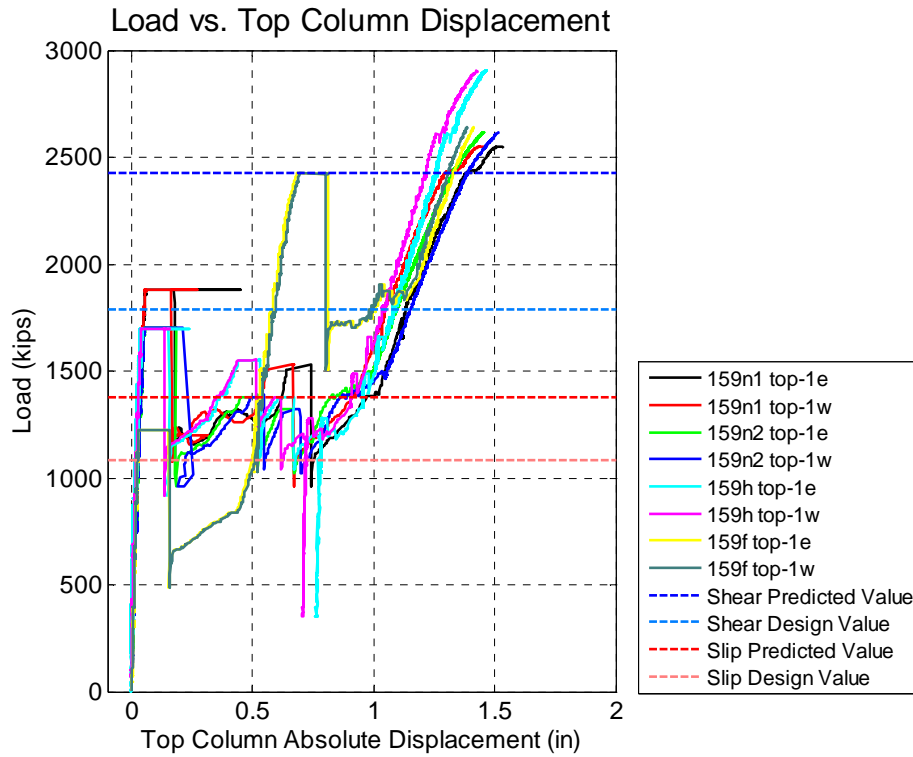


**Figure C.1 – 159 specimens effect of development: load vs. top column displacement**

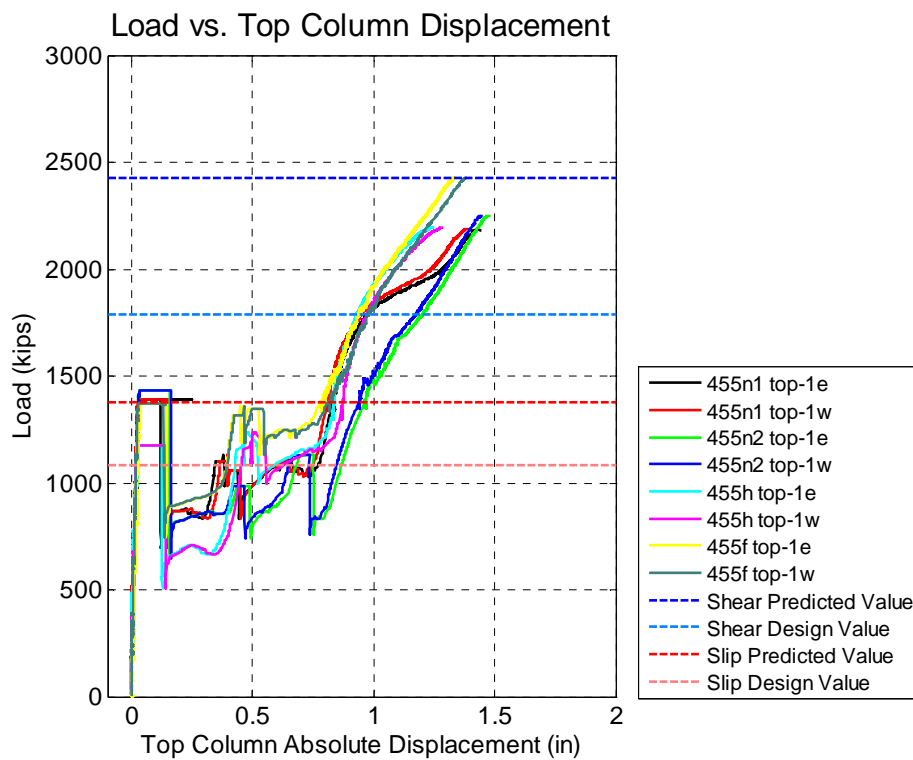


**Figure C.2 – 455 specimens effect of development: load vs. top column displacement**

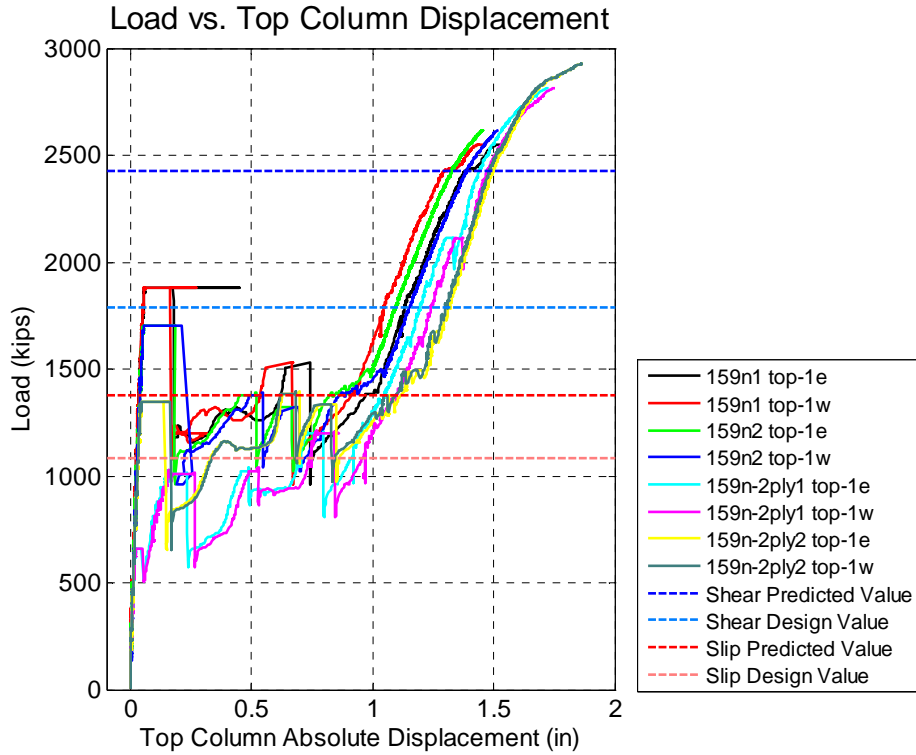


**Figure C.3 – Multi-ply 159 specimens: load vs. top column displacement**

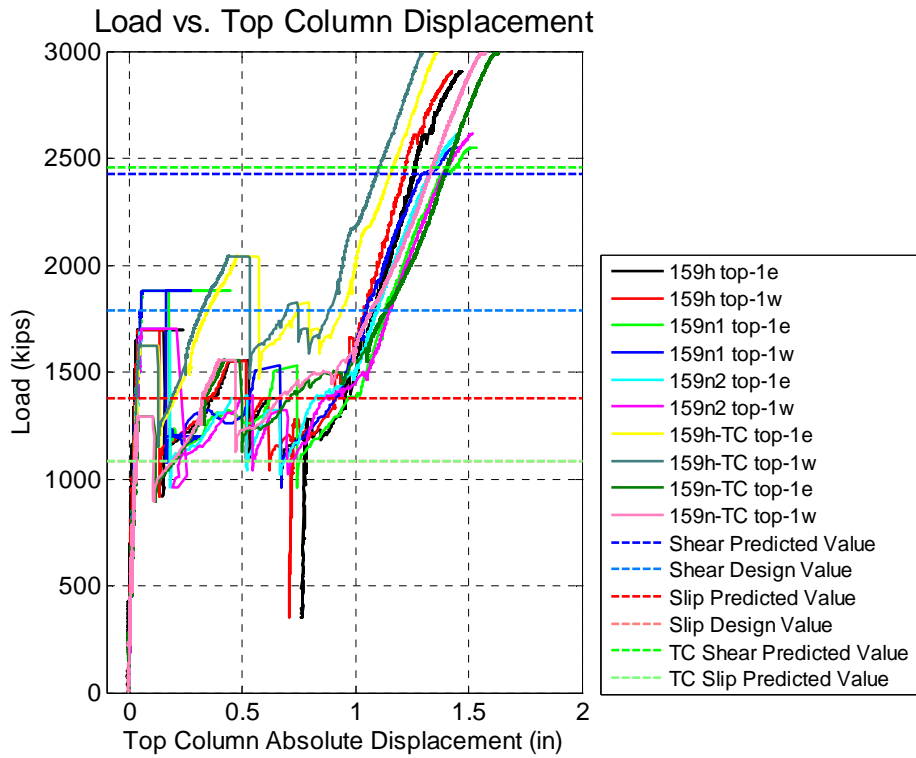


**Figure C.4 – TC 159 specimens: load vs. top column displacement**

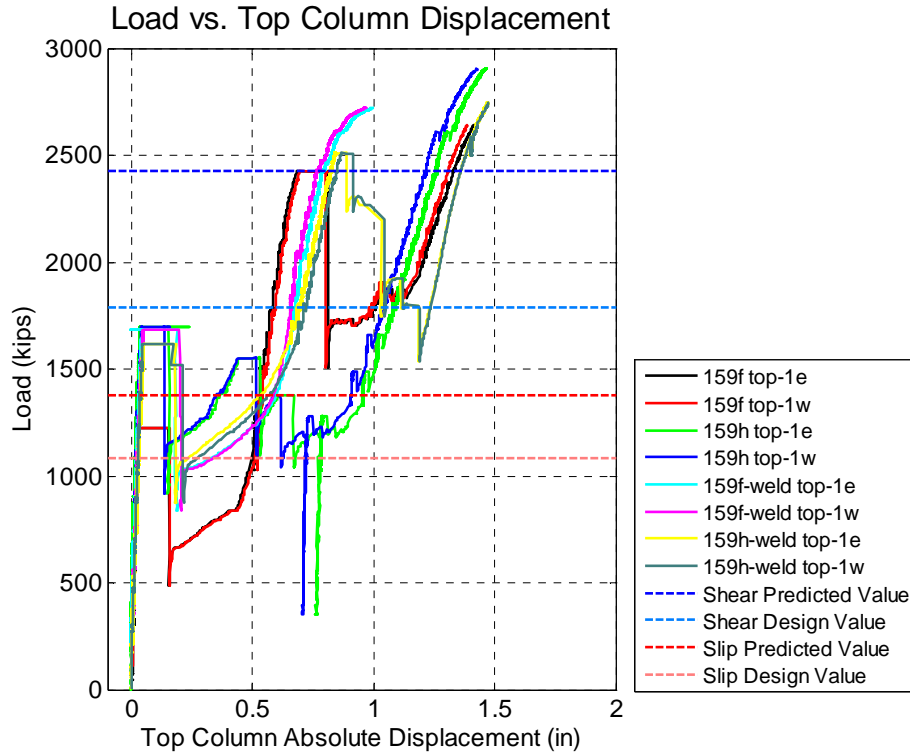


**Figure C.5 – Welded 159 specimens: load vs. top column displacement**

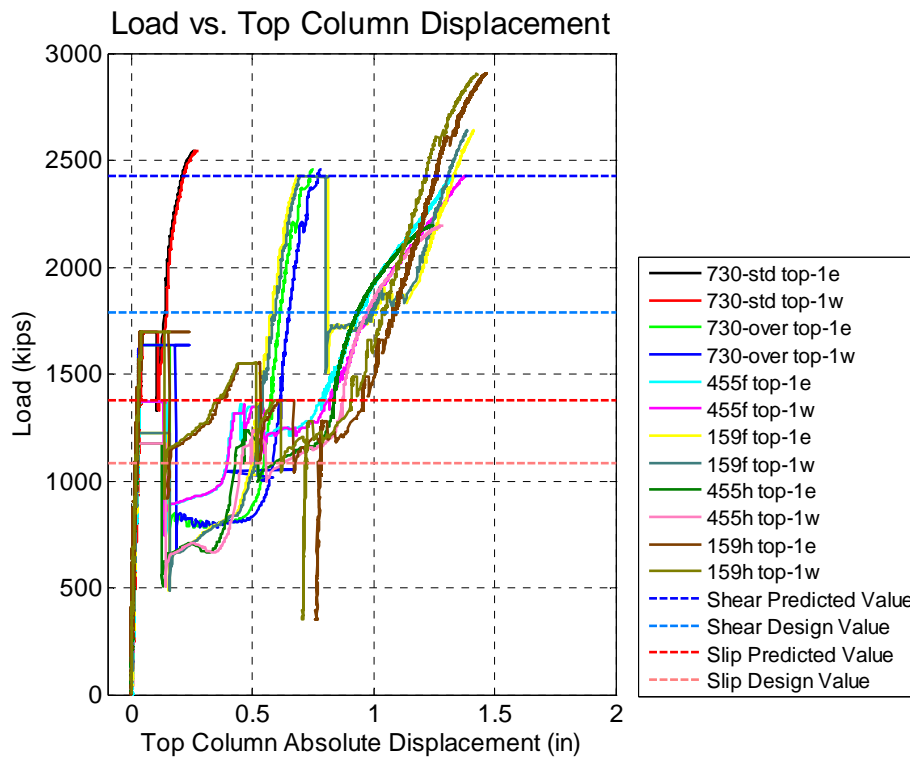


**Figure C.6 – Developed specimens: load vs. top column displacement**

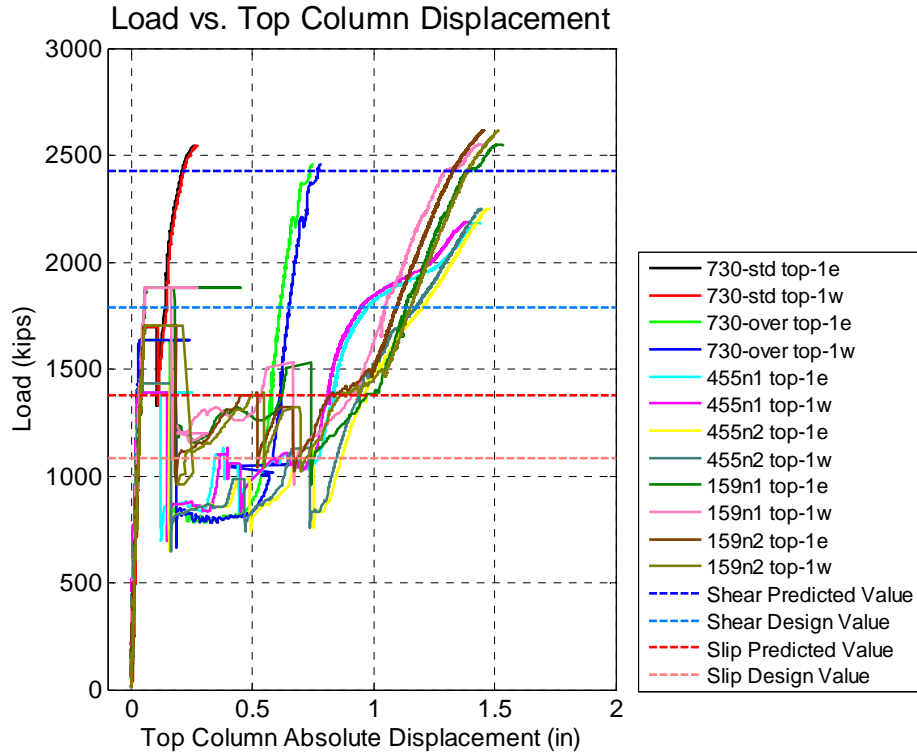


**Figure C.7 – Undeveloped specimens: load vs. top column displacement**

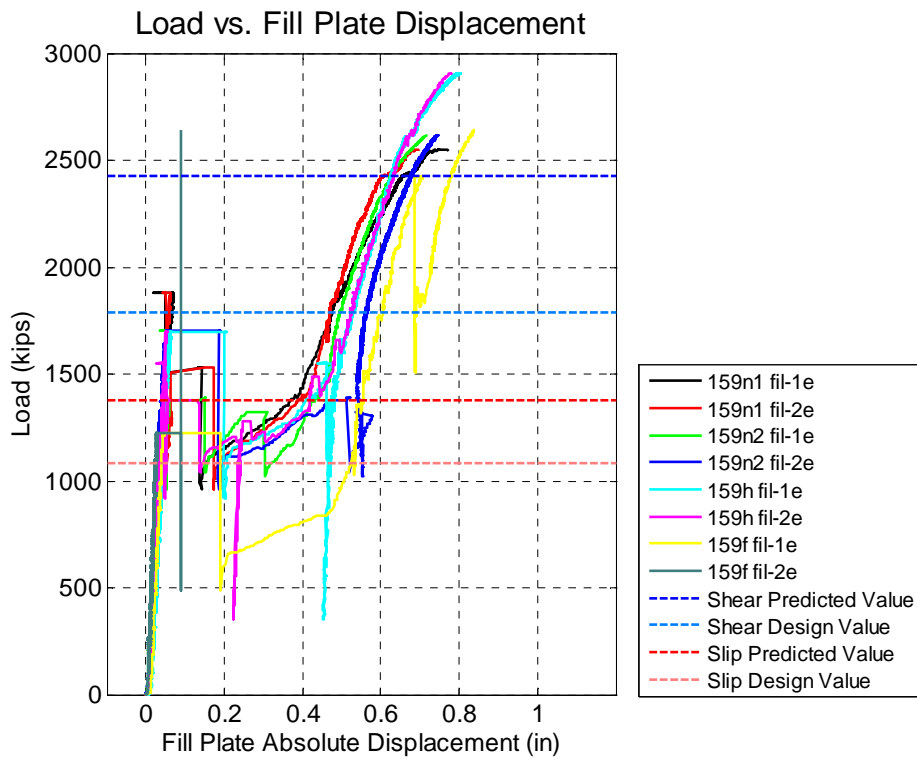


**Figure C.8 - 159 specimens effect of development: load vs. filler plate displacement**

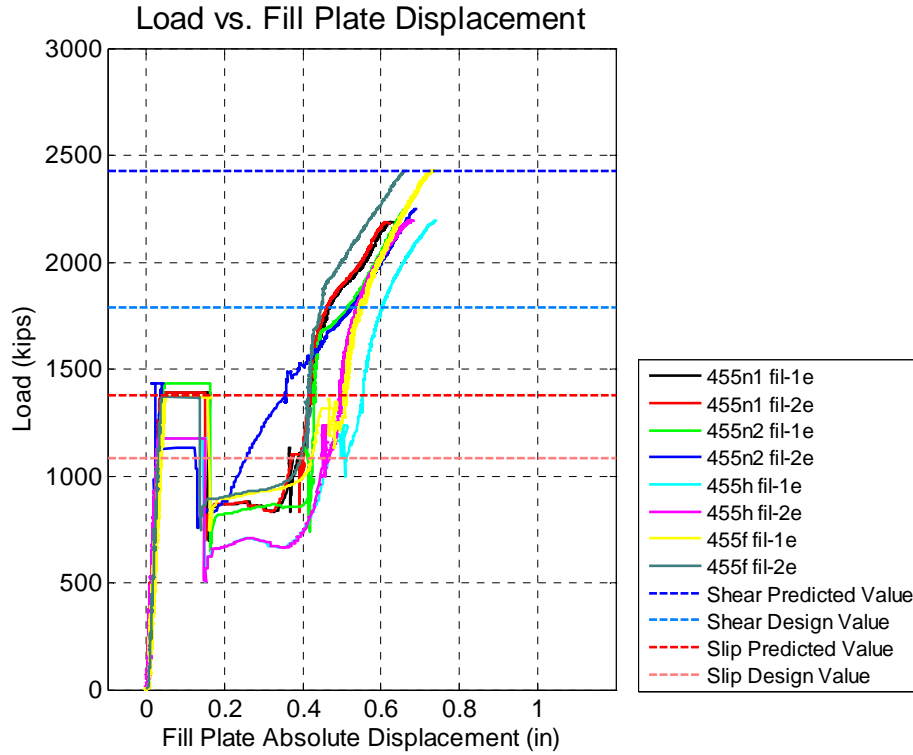


**Figure C.9 - 455 specimens effect of development: load vs. filler plate displacement**

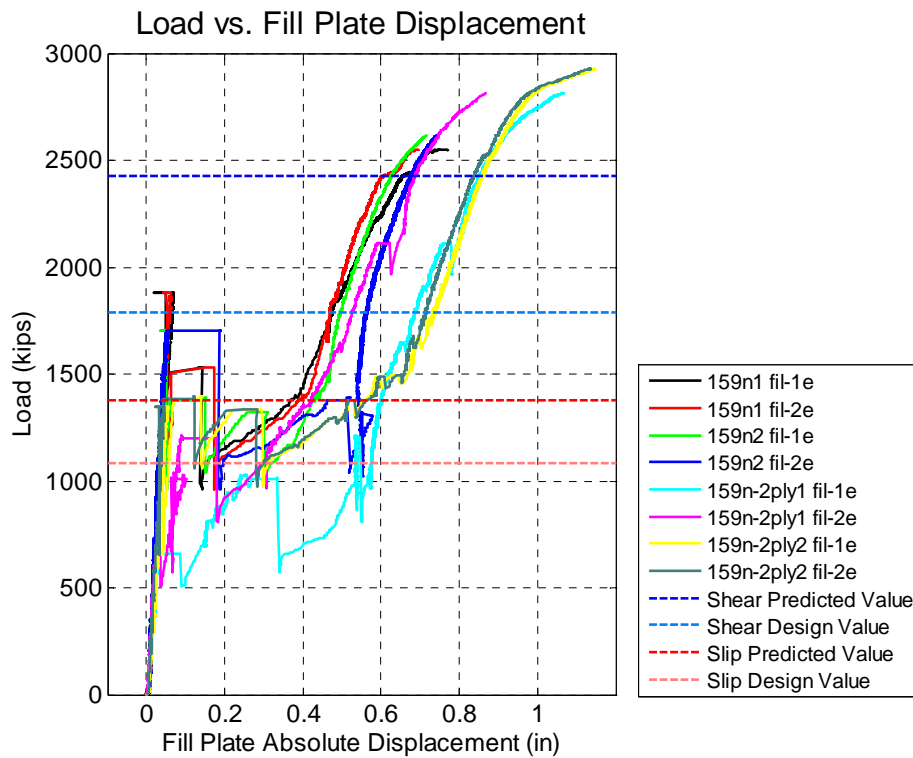


**Figure C.10 - Multi-ply 159 specimens: load vs. filler plate displacement**

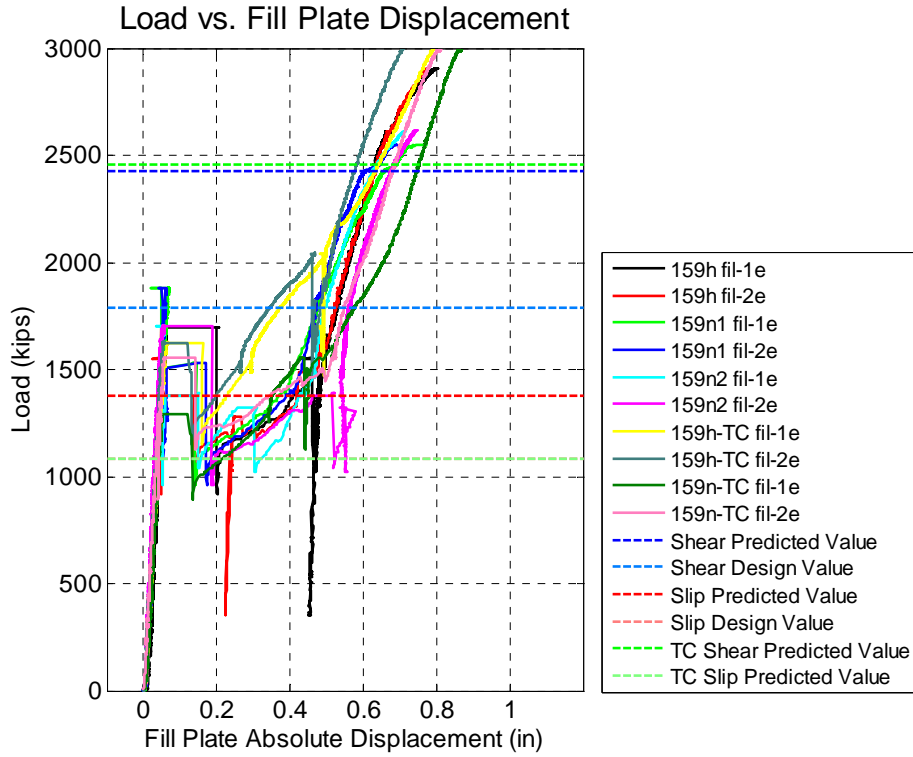


**Figure C.11 - TC 159 specimens: load vs. filler plate displacement**

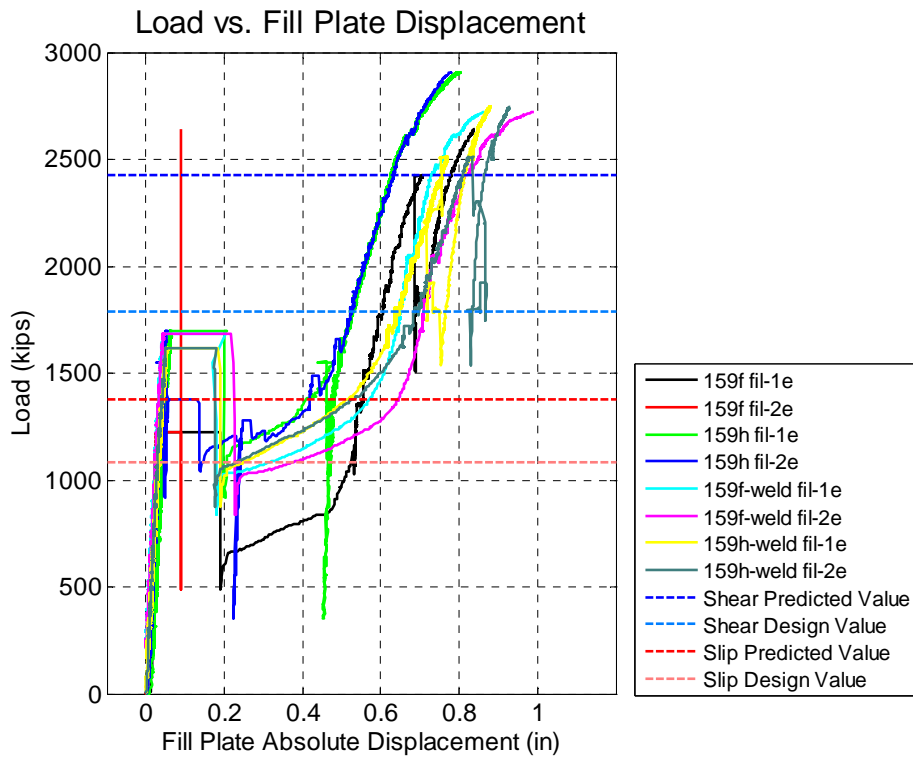


**Figure C.12 - Welded 159 specimens: load vs. filler plate displacement**

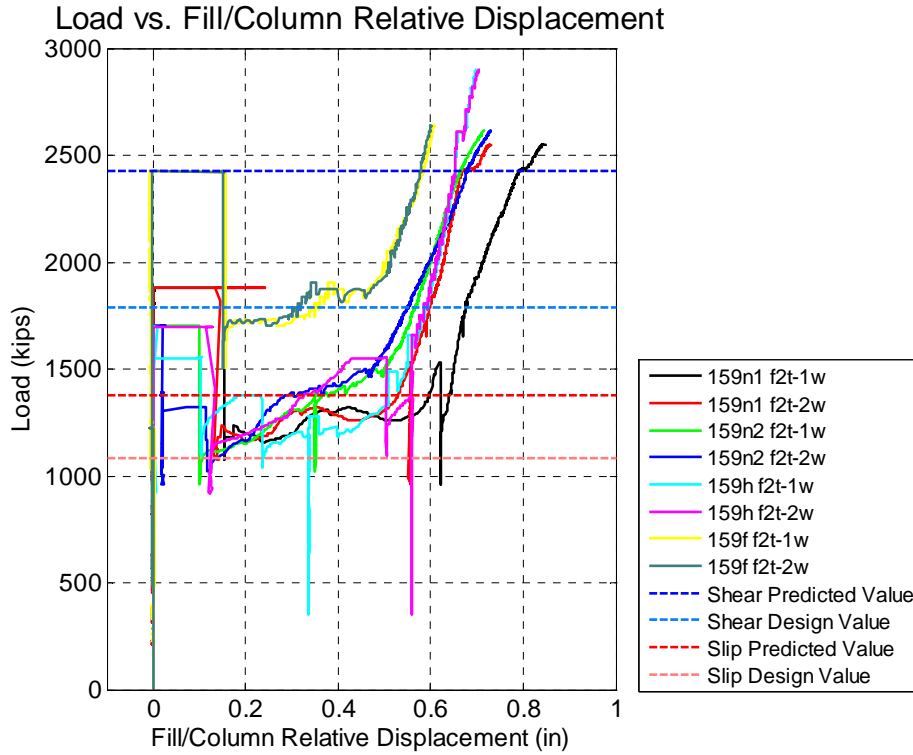


**Figure C.13 - 159 specimens effect of development: load vs. filler plate and top column relative displacement**

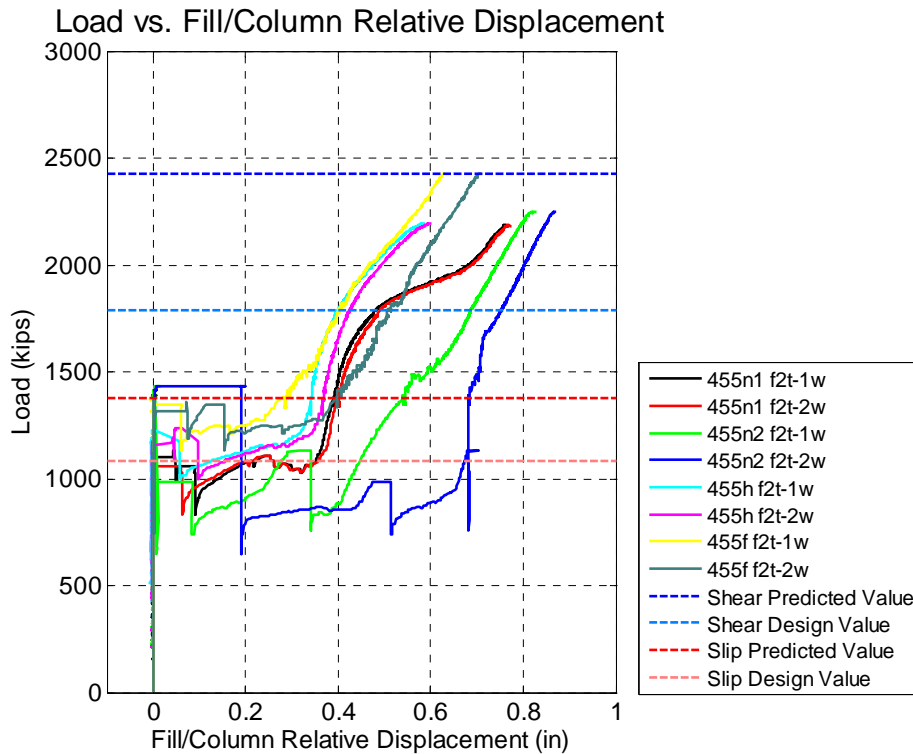


**Figure C.14 - 455 specimens effect of development: load vs. filler plate and top column relative displacement**

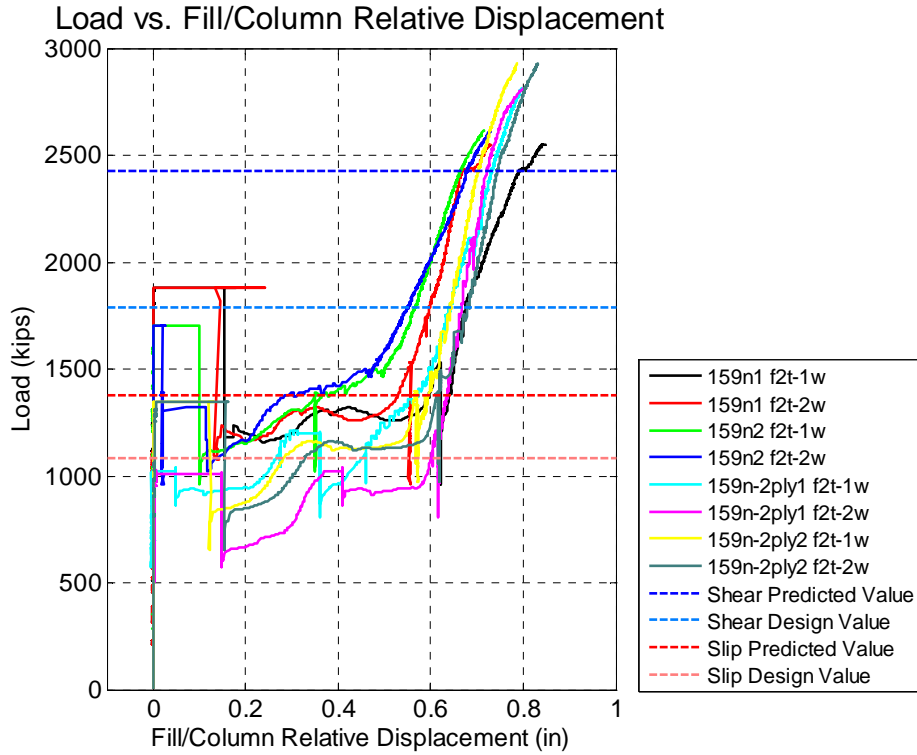


**Figure C.15 - Multi-ply 159 specimens: load vs. filler plate and top column relative displacement**

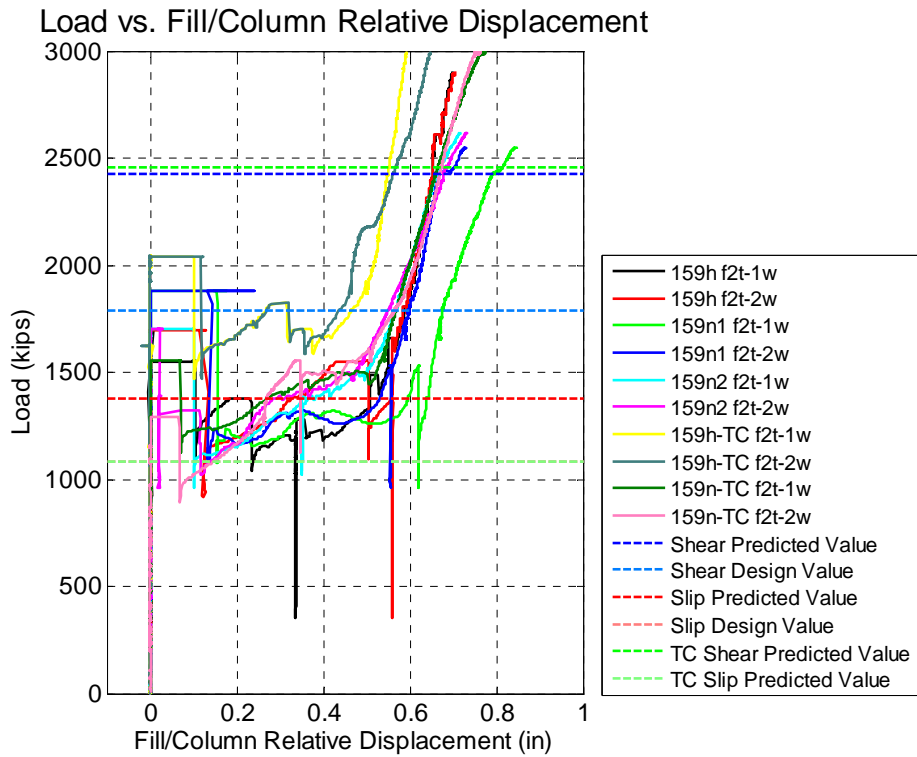


**Figure C.16 - TC 159 specimens: load vs. filler plate and top column relative displacement**

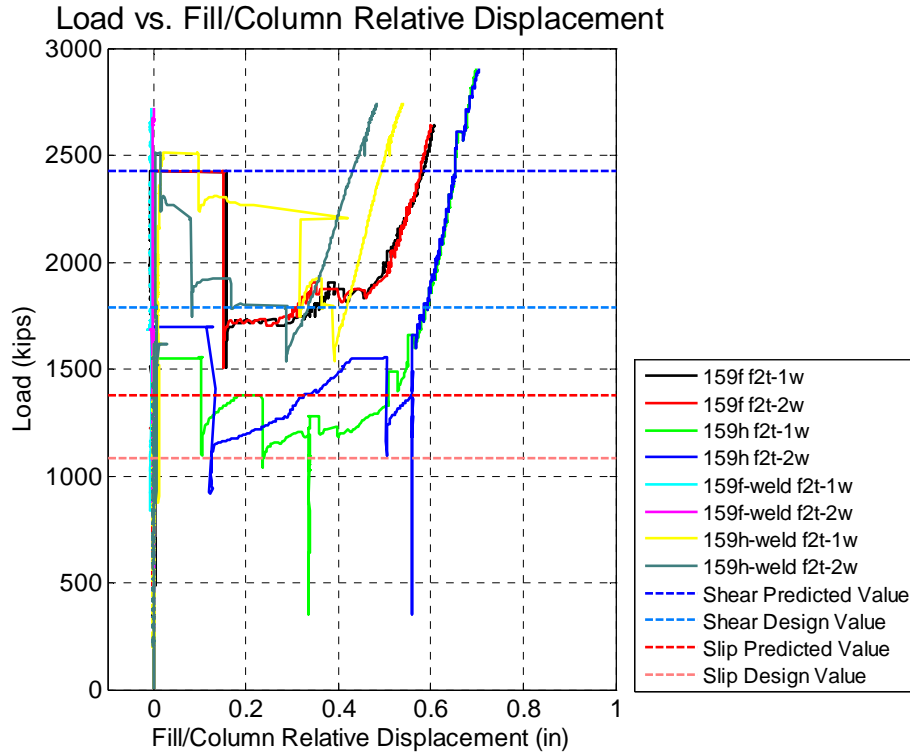


**Figure C.17 - Welded 159 specimens: load vs. filler plate and top column relative displacement**

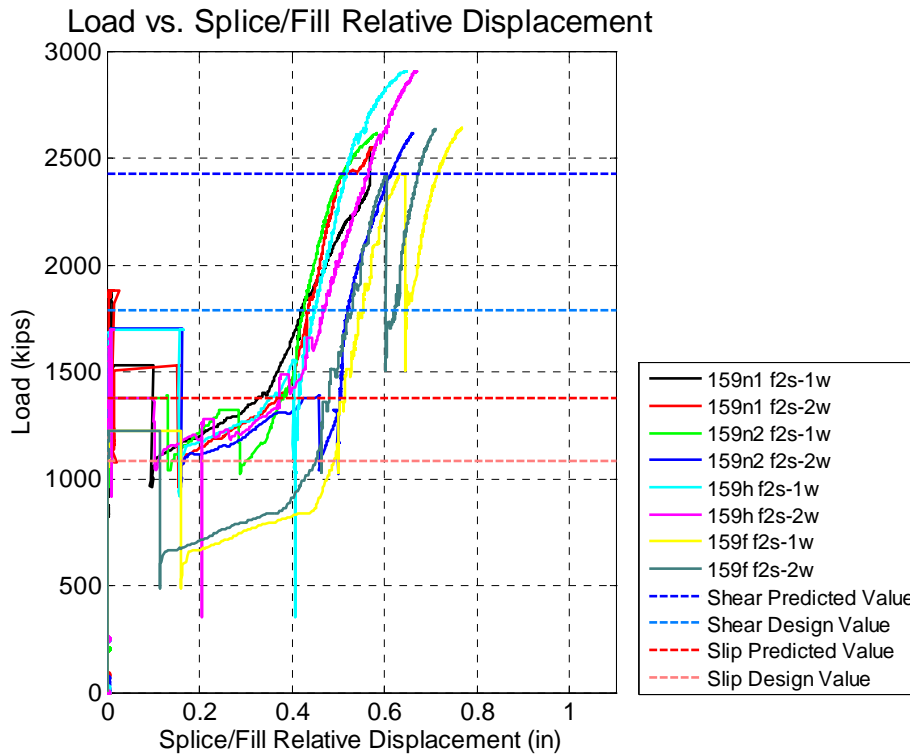


**Figure C.18 - 159 specimens effect of development: load vs. filler plate and splice plate relative displacement**

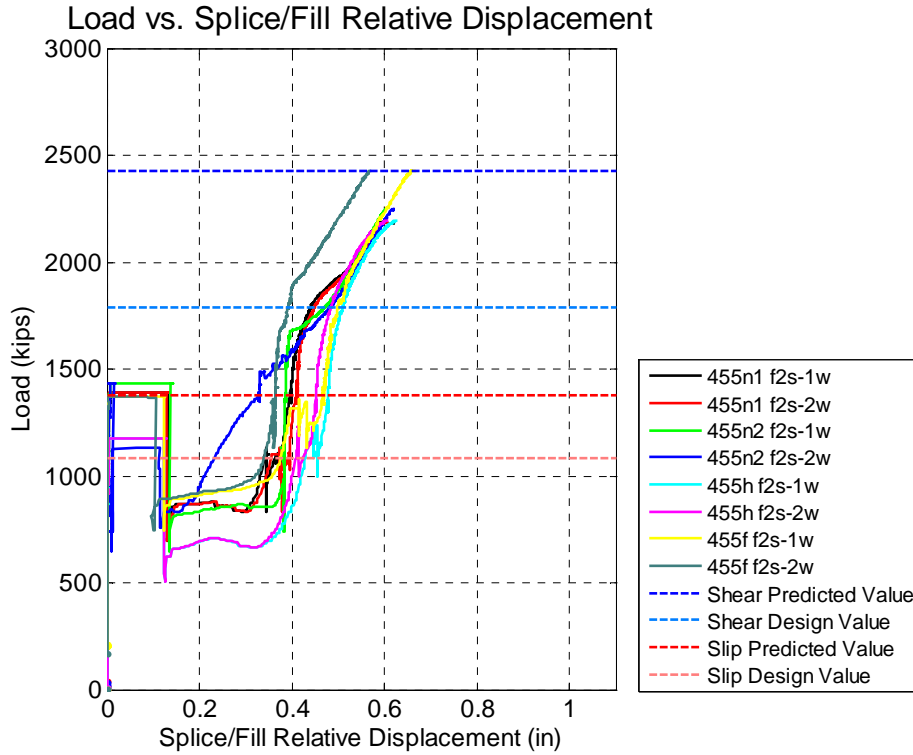


**Figure C.19 - 455 specimens effect of development: load vs. filler plate and splice plate relative displacement**

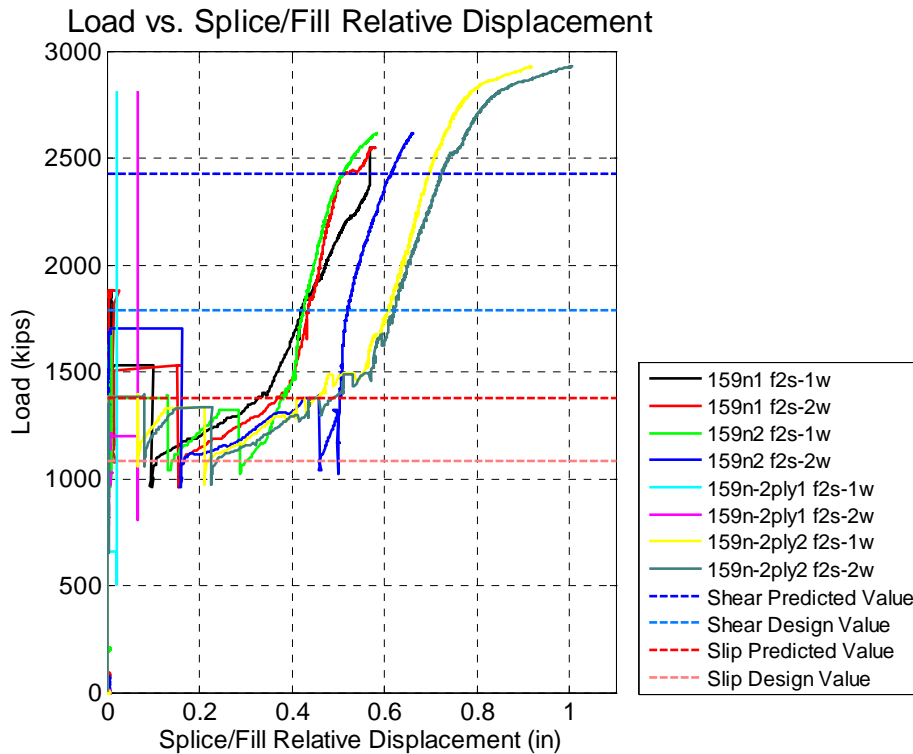


**Figure C.20 - Multi-ply 159 specimens: load vs. filler plate and splice plate relative displacement**

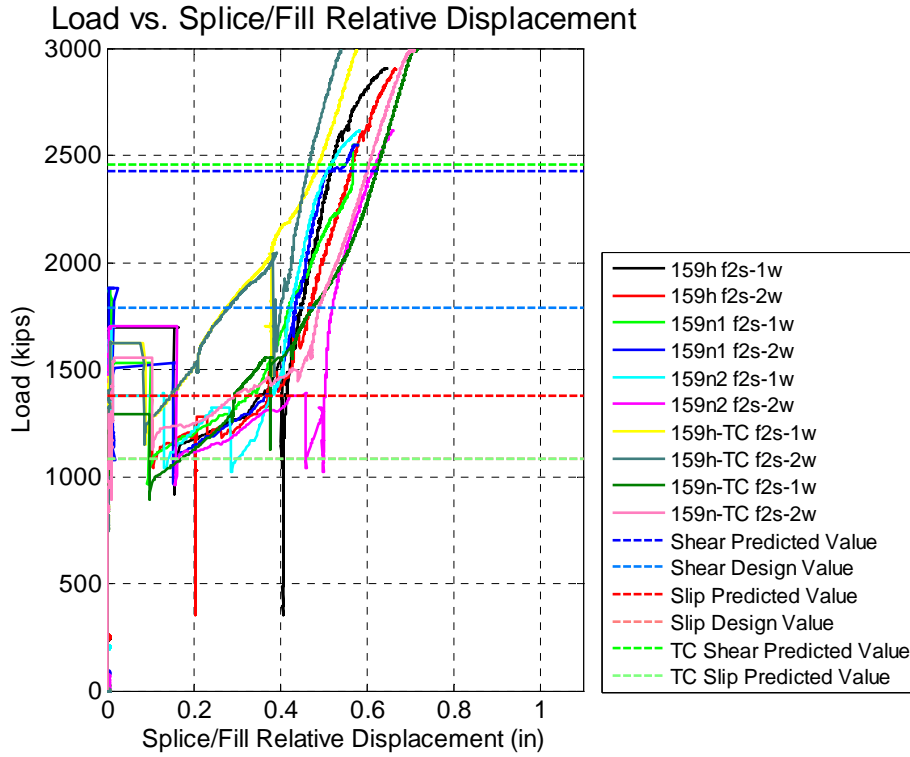


**Figure C.21 - TC 159 specimens: load vs. filler plate and splice plate relative displacement**

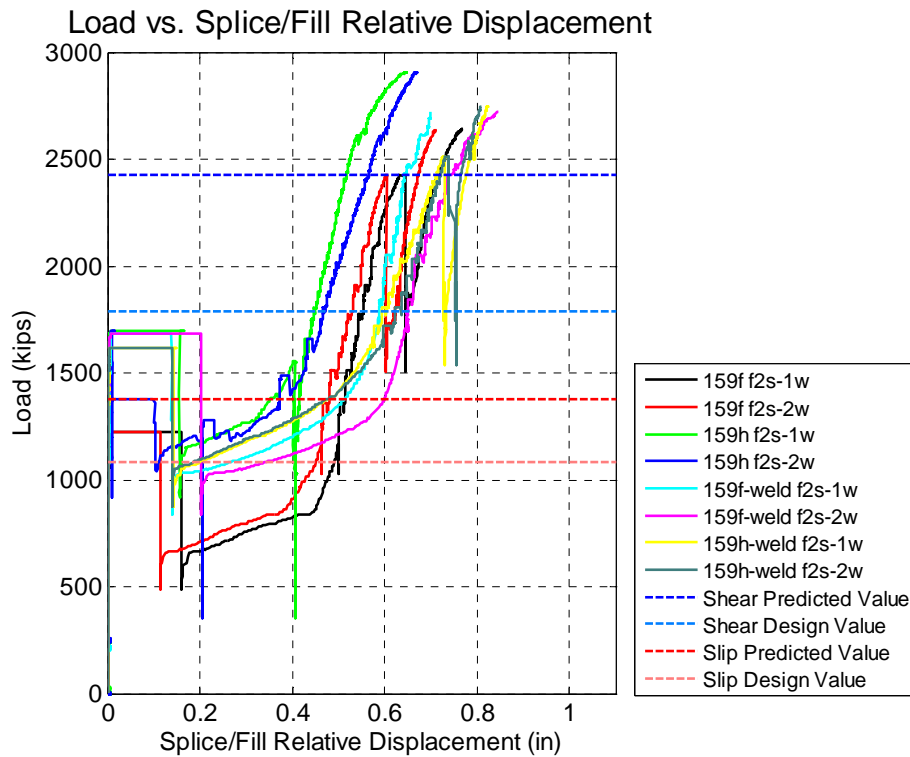


**Figure C.22 - Welded 159 specimens: load vs. filler plate and splice plate relative displacement**

# STATISTICAL ANALYSIS OF SLIP STRENGTH

## D.1 Introduction

Slip strength is the product of the clamping force and the slip coefficient, both of which are quantities that display random variation. Accounting for this in connections with fillers, where the strength of *all* surfaces need *not* be exceeded for failure to occur, the expected slip strength may be lower than may be indicated by a deterministic analysis. While a connection with only one slip surface will still show variation in strength due to the variation of the clamping force and slip coefficient, connections that have additional slip surfaces are more likely to slip at lower strengths since there are more slip surfaces that may exhibit these statistical variations. This potentially leads to a lower strength of the connection as a whole. For this analysis, the connection is assumed to have the same configuration as those examined in this report, however this concept can readily be extended to other connection configurations.

The concept of order statistics (David 1970 and Song and DerKiureghian 2003) can be utilized to determine the expected slip strength of a connection. The cumulative distribution function (CDF) of the lowest of a set of random variables can be written in terms of the cumulative distribution functions of the individual random variables:

$$F_{lowest}(x) = 1 - \prod_{i=1}^n \{1 - F_i(x)\} \quad (D.1)$$

where  $F_i(x)$  is the CDF of the one of the set of random variables.

A normal distribution is completely defined by a mean and standard deviation, and the CDF of a normal distribution is given in Equation (D.2). To avoid confusion with the slip coefficient, the mean of a random variable is designated by the symbol  $m$ , rather than the typical  $\mu$ .

$$F_x(x) = \frac{1}{2} \left( 1 + \operatorname{erf} \left( \frac{x - m_x}{\sigma_x \sqrt{2}} \right) \right) \quad (D.2)$$

The slip strength of a surface is the product of the slip coefficient and the clamping force, as shown in Equation (D.3). The clamping force is the product of the number of bolts and average bolt pretension. Both the slip coefficient and the average bolt pretension are random variables. In this study the random variation of the average bolt pretension is

neglected. Statistical data derived from Grondin (2008) regarding the slip coefficient and the bolt pretension indicates that the majority of uncertainty in slip strength arises from the variation in slip coefficient. Also, the statistical data on the average clamping force depends on the bolt type and method of pretensioning. Thus, the variable effect of bolt pretension is not addressed in this analysis. Note that for this analysis, neglecting the uncertainty in the average bolt pretension results in higher expected slip strengths.

$$S = \mu C = \mu N_b T_{b,avg} \quad (D.3)$$

where  $S$  is the slip strength,  $\mu$  is the slip coefficient,  $C$  is the clamp force,  $N_b$  is the number of bolts, and  $T_{b,avg}$  is the average bolt pretension. The mean and standard deviation of the slip strength can be found by Equation (D.4):

$$\begin{aligned} m_{S,one\ surface} &= m_{\mu,one\ surface} N_b T_{b,avg} \\ \sigma_{S,one\ surface} &= \sigma_{\mu,one\ surface} N_b T_{b,avg} \end{aligned} \quad (D.4)$$

The slip coefficient, and hence slip strength, is assumed to follow a normal distribution. This matches well with available data, particularly for Class B surfaces (Grondin, 2008). Statistical data of the slip coefficient is obtained from measured values from experimental ancillary tests such as those found in RCSC Appendix A (RCSC, 2004). These tests are, in general, conducted with two slip surfaces. If one assumes the measured slip coefficient from the experimental tests is the lowest of the two surfaces (Option A), then the mean and standard deviation for one surface is determined such that when order statistics are employed, the mean and standard deviation for the lowest slip coefficient of two surfaces are calculated to be the same as published results. Conversely, if one assumes the measured slip is the average of the two surfaces (Option B), then the mean and standard deviation of the slip strength of one surface are:

$$\begin{aligned} m_{\mu,one\ surface} &= m_{\mu,two\ surfaces} \\ \sigma_{\mu,one\ surface} &= \sqrt{2} \sigma_{\mu,two\ surfaces} \end{aligned} \quad (D.5)$$

In the current research, observation of ancillary tests indicates that Option B better characterizes the slip strength, in that it is rare in the ancillary tests that one slide slips noticeably before the other.

It is also necessary in this analysis to characterize the slip failure of the structural connections (such as the main specimens in this research). One definition characterizes failure as when the lowest slip strength of any surface in the connection is exceeded (Option C). Another definition characterizes failure as when the sum of the lowest slip strengths from either side of the connections is exceeded (Option D) (this assumes the connection is a double lap splice such as those tests in this research). In the case of Option D, when the strength of one side, but not the other, has been exceeded, eccentricities are introduced to the connection. If the connection is capable of supporting those eccentricities (i.e., has thick splice plates) then the slip strength is not realized until the slip resistance of the other side is reached and movement occurs on both side. If the

connection is not capable of supporting those eccentricities (i.e., has thin splice plates) then movement occurs on one surface when the lowest slip resistance of either side is reached. The experimental data presented in this report indicates that, in general, Option D is a reasonable choice for definition of failure since all but one of the first slip events occurred with movement of at least one surface from each side. However, one specimen (159n-2ply1) experienced first slip on only one surface, indicating that Option C would have been an appropriate definition of failure. Connections with thinner splice plates may also be better modeled by Option C. Section 4.3 of this report highlights the use of the analyses in this appendix to assess the slip strengths of the connections tested in this work.

## D.2 Undeveloped Filler with Multiple Plies

Utilizing the various options, the expected slip strength for a connection can be calculated. A connection with undeveloped fillers consisting of different numbers of plies is examined. For this example, a connection like that presented in this report will be examined and the following data will be used: the number of bolts is 12 for each of the two sides; the average bolt pretension is 115 k for all bolts; the slip coefficient for blast cleaned surfaces is given by Grondin (2008) as:

$$\begin{aligned}
 m_{\mu, two\ surfaces} &= 0.525 \\
 COV_{\mu, two\ surfaces} &= 0.193 \\
 \sigma_{\mu, two\ surfaces} &= 0.193 \times 0.525 = 0.101
 \end{aligned}
 \tag{D.6}$$

This would indicate a deterministic slip strength of 724 k ( $S = \mu N_b T_{b,avg} = (0.525)(12)(115) = 724.5k$ ) for each side and 1449 k for the connection. The expected slip strength from these analyses will be compared to this value. Utilizing Option A, for these values to be accurate for two surfaces, the slip coefficient of one surface needs to be defined by:

$$\begin{aligned}
 m_{\mu, one\ surface} &= 0.593 \\
 \sigma_{\mu, one\ surface} &= 0.108
 \end{aligned}
 \tag{D.7}$$

These values were obtained by an iterative procedure in which the mean and standard deviation of one surfaces was varied until the mean and standard deviation of the minimum of two surfaces was equal to the published data. This results in the following statistical data for the slip strength (subscript “S”) of one surface.

$$\begin{aligned}
 m_{S, one\ surface} &= m_{\mu, one\ surface} N_b T_{b,avg} = (0.593)(12)(115) = 818k \\
 \sigma_{S, one\ surface} &= \sigma_{\mu, one\ surface} N_b T_{b,avg} = (0.108)(12)(115) = 149k
 \end{aligned}
 \tag{D.8}$$

Utilizing Option B, the slip coefficient of one surface is defined by

$$\begin{aligned}
m_{\mu,one\ surface} &= 0.525 \\
\sigma_{\mu,one\ surface} &= 0.101\sqrt{2} = 0.143
\end{aligned}
\tag{D.9}$$

This results in the following statistical data for the slip strength of one surface.

$$\begin{aligned}
m_{S,one\ surface} &= m_{\mu,one\ surface} N_b T_{b,avg} = (0.525)(12)(115) = 724k \\
\sigma_{S,one\ surface} &= \sigma_{\mu,one\ surface} N_b T_{b,avg} = (0.143)(12)(115) = 197k
\end{aligned}
\tag{D.10}$$

Since in an undeveloped filler connection the random variable describing the slip strength is the same for all surfaces, Equation (D.1) reduces to Equation (D.11).

$$F_{S,one\ side}(x) = 1 - \left\{1 - F_{S,one\ surface}(x)\right\}^n
\tag{D.11}$$

For option C,  $n$  in Equation (D.11) is taken as the number of slip surfaces in the entire connection, since the lowest slip strength of all surfaces is significant. For option D,  $n$  in Equation (D.11) is taken as the number of slip surfaces in one side of the connection, since the lowest slip strength from either side is significant. In either case the CDF of a lowest slip strength is determined and from the CDF, the PDF, mean, and standard deviation are all determined as in Equation (D.12) (David, 1970).

$$\begin{aligned}
f_X(x) &= \frac{d}{dx} F_X(x) \\
m_X &= \int_{-\infty}^{\infty} x f_X(x) dx \\
\sigma_X^2 &= \int_{-\infty}^{\infty} (x - m_X)^2 f_X(x) dx
\end{aligned}
\tag{D.12}$$

The mean and standard deviation of the connection strength is determined as follows for Option C, Equation (D.13) and Option D, Equation (D.14).

$$\begin{aligned}
m_{S,connection} &= 2m_{S,one\ side} \\
\sigma_{S,connection} &= 2\sigma_{S,one\ side}
\end{aligned}
\tag{D.13}$$

$$\begin{aligned}
m_{S,connection} &= 2m_{S,one\ side} \\
\sigma_{S,connection} &= \sqrt{2}\sigma_{S,one\ side}
\end{aligned}
\tag{D.14}$$

where  $m_{S,connection}$  is the expected slip strength of the connection. The expected slip strength for the four options (A/C, A/D, B/C, B/D) is presented in Figure D.1, noting the definitions of the options in Table D.1. Only options A/C and B/D predict zero reduction for no filler. In this research, observation of the experimental results of the connection tests indicate that Option D is most representative of the behavior of the connection. Thus, this research assumes a theoretical reduction for multiple plies is best represented by Option B/D. However, recognizing also that some connections may slip on one side

first, Option B/C may also be assumed. The results shown in Section 4.3 indicate that these theoretical predictions bracket well the results seen in experimental tests.

**Table D.1- Options for slip resistance assumptions in ancillary and connection tests**

Option	Description
A	Ancillary experiments provide the lowest of two slip coefficients
B	Ancillary experiments provide the average of two slip coefficients
C	Connection failure is defined by lowest slip resistance on either side
D	Connection failure is defined by sum of lowest slip resistance from both sides

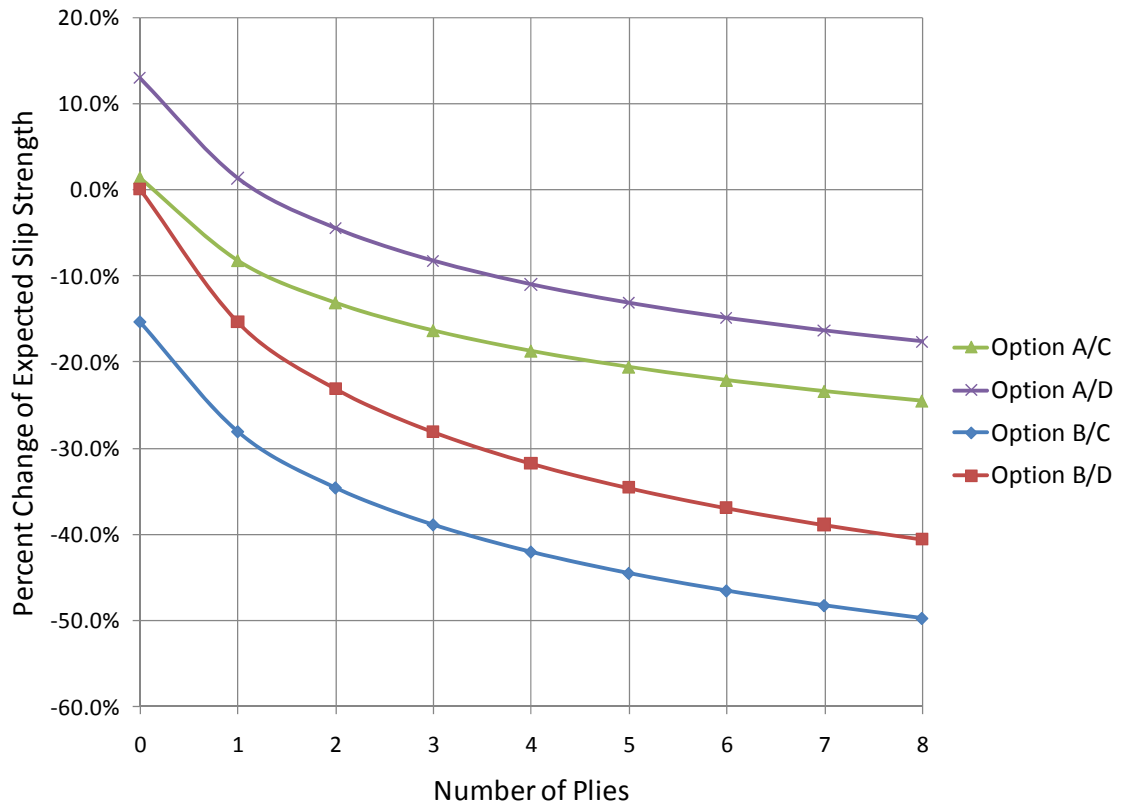


**Figure D.1 - Percent change of expected slip strength for connection with undeveloped fillers**

### D.3 Developed Filler

Developing the filler has the result of increasing the number of bolts between the filler and connected element. The number of bolts required to develop the filler is based on the thickness of the filler in relation to the connected element, Equation (D.15).

$$N_{b,develop} = \frac{\rho}{1 + \rho} N_{b,connection} \tag{D.15}$$

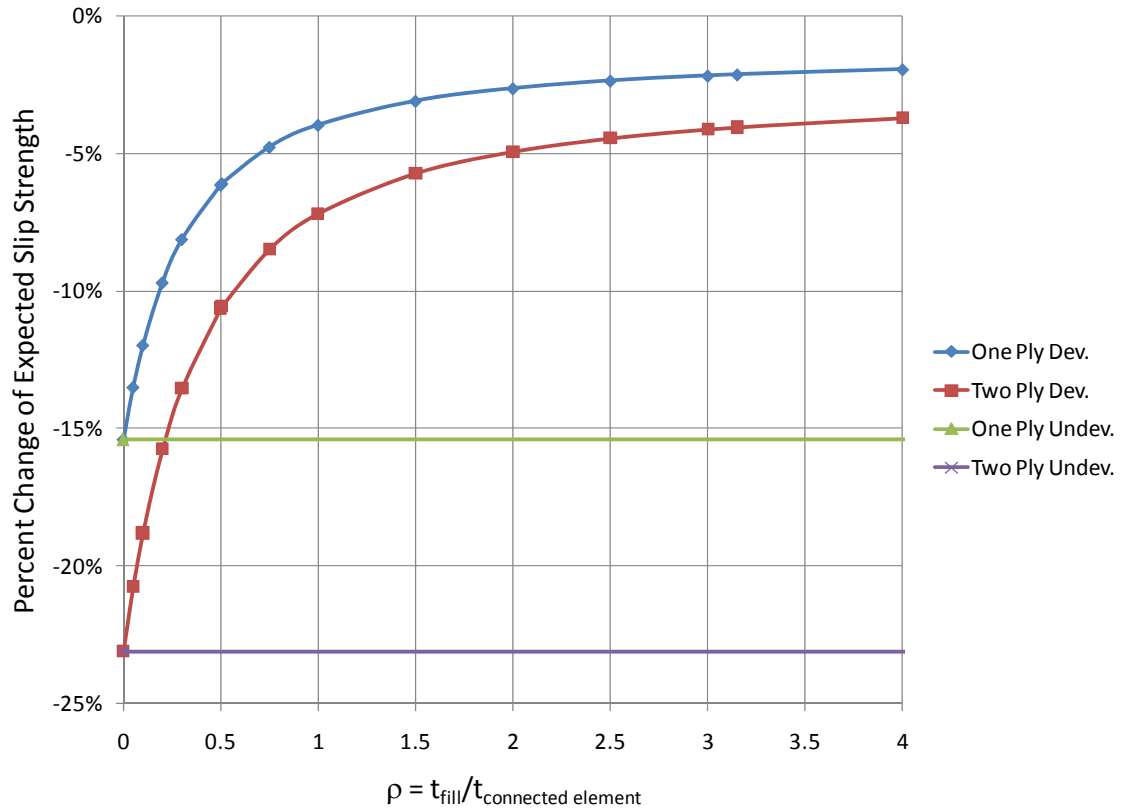
Where  $\rho$  is the ratio of filler thickness to connected element thickness. These extra bolts are intended to allow for a uniform distribution of stress across the combined cross section, but they also increase the clamping force between the filler and the connected element. This added clamping force can be modeled in the statistical model by modifying Equation (D.1) as Equation (D.16).

$$F_{S,one\ side}(x) = 1 - \left\{1 - F_{S,undeveloped}(x)\right\} \left\{1 - F_{S,developed}(x)\right\}^n \quad (D.16)$$

Where  $n$  is the number of plies of developed filler and the mean and standard deviation of the CDF for each developed surface reflects the increase clamping force, Equation (D.17)

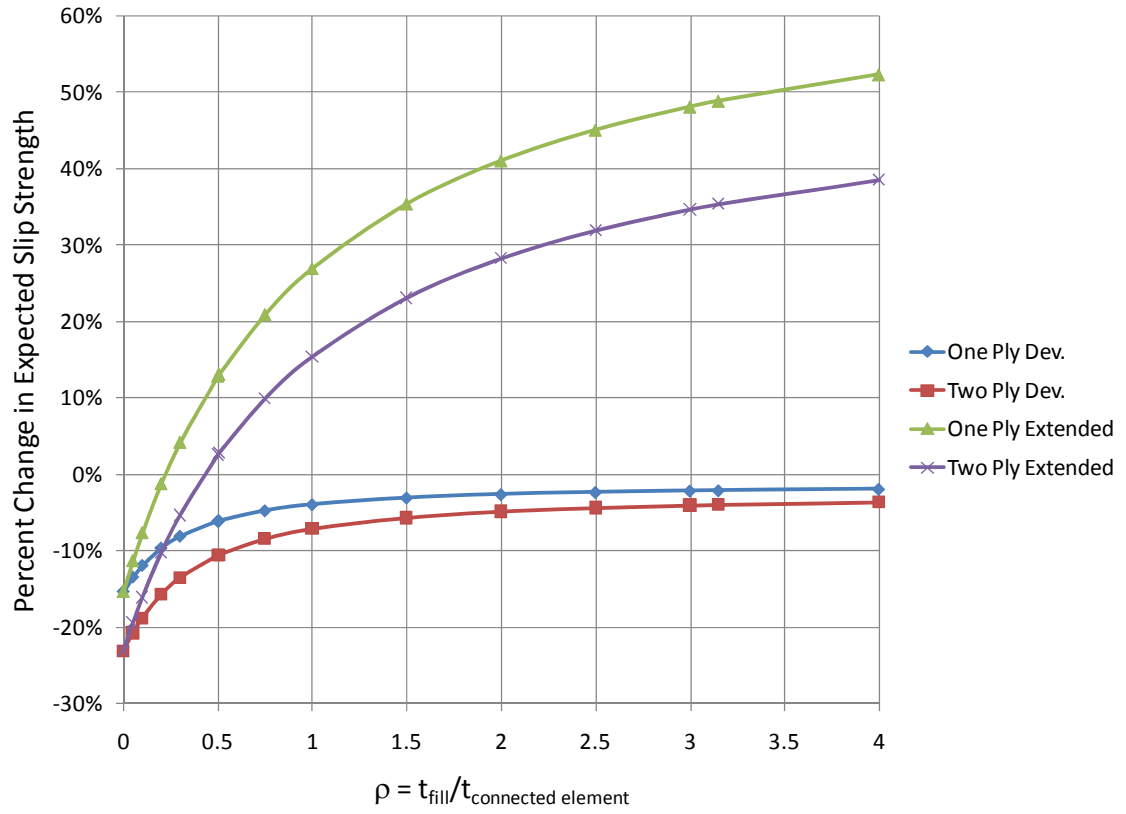
$$\begin{aligned} m_{S,developed} &= m_{\mu,one\ surface} \frac{1+2\rho}{1+\rho} N_b T_{b,avg} \\ \sigma_{S,developed} &= \sigma_{\mu,one\ surface} \frac{1+2\rho}{1+\rho} N_b T_{b,avg} \end{aligned} \quad (D.17)$$

Figure D.2 shows the results of statistical analyses with one and two ply developed fillers of varying thicknesses. The results of statistical analyses with one and two ply undeveloped fillers are shown as horizontal lines, since these values do not change with filler thickness. Option B/D was used for these analyses. For filler thicknesses approaching zero, the percent reduction of expected slip strength approaches the expected strength of an undeveloped filler, since very few additional bolts are required and hence the added clamping force is very little. As the filler thickness becomes very large, the percent reduction of expected slip strength becomes relatively small. For these connections, although the number of added bolts is substantial, there is still a statistical possibility that slip will occur on the developed surface, thus the percent reduction does not reach zero.



**Figure D.2 - Percentage change of expected slip strength for connection with developed fillers**

Figure D.3 shows a comparison of percentage change in expected strength between a connection with a developed filler and one where the joint has been extended to accommodate the additional development bolts. As a conservative action, it is expected that extending the joint will result in a larger expected strength for all cases, since all surfaces benefit from the additional clamping force. While the difference is modest for very thin fillers, extending the joint provides a significant strength increase above only developing the filler for thick fillers. The extended joint exceeds the deterministic strength of the connection for thick fillers, in that the percentage change is positive.



**Figure D.3 - Percentage change of expected slip strength for connection with developed fillers or extended connections**

## STEEL AND BOLT MATERIAL AND CALIBRATION REPORTS

### Specimen plate properties

Plate Thickness (in)	Heat ID	Yield Strength (ksi)	Ultimate Strength (ksi)
1/4	533713	53	75
1-5/8	3105972	58	84
2	7102887	59	82
	7102892	53	82
3-1/2	307461	50	71
3-3/4	S07446	51	74

### Specimen column properties

Column	Hole Size	Heat Number	Yield Strength (ksi)	Ultimate Strength (ksi)
Top Columns				
W14x730	Standard	40694	71	91
W14x730	Oversize	27725	60	82
W14x455	Oversize	24788	65	82
W14x159	Oversize	287830	56	73
Bottom Columns				
W14x730	Standard	40694	71	91
W14x730	Oversize	27723	60	82
		27725	60	82
		27726	61	81
		41099	70	89

Tag #:  
P/O #:  
Qty:

P/N #:

Job #:  
W/O #:

# METALLURGICAL TEST REPORT



SPS Coil Processing Tulsa  
5275 Bird Creek Ave.  
Port of Catoosa, OK 74015

**RECEIVED**

S  
O  
L  
D  
T  
O

12986  
W & W Steel LLC  
25369  
Oklahoma City OK 73125

SEP 18 2007

REC. DEPT.

S  
H  
I  
P  
T  
O

12986  
W & W Steel LLC  
1730 West Reno  
Oklahoma City OK 73125

PAGE 2 of 3  
DATE 09/18/2007  
TIME 08:18:40  
USER WILLIAMR

Order	Material No.	Description	1/4	60 X 240	A36	STP MIL PLT	Quantity	Weight	Customer Part	Customer PO	Ship Date
791456-0020	70860240	1/4	60 X 240	A36	STP MIL PLT	36,735.000	35,735.000		20729	09/18/2007	

(5th)

### Chemical Analysis

Heat No.	Vendor	Phosphorus	Sulphur	Silicon	Chromium	Molybdenum	Boron	Copper	Aluminum	Titanium	Vanadium	Nitrogen	Tin
533713	CARGILL FERROUS INT'L	0.0120	0.0040	0.0700	0.0000	0.0000	0.0000	0.0000	0.0430	0.0000	0.0000	0.0000	0.0000
Batch 0000376061	10 EA			10,210 LB									

### Mechanical/ Physical Properties

Mill Coil No.	Tensile	Yield	Elong	Rckwl	Charpy	Charpy Dr	Charpy Sz	Olsen
300691	75,000.000	53,000.000	24.00	0	0	0	0	0
	0.000	0.000	0.00	0	0	0	0	0
	0.000	0.000	0.00	0	0	0	0	0
	0.000	0.000	0.00	0	0	0	0	0

### Chemical Analysis

Heat No.	Vendor	Phosphorus	Sulphur	Silicon	Chromium	Molybdenum	Boron	Copper	Aluminum	Titanium	Vanadium	Nitrogen	Tin
533713	CARGILL FERROUS INT'L	0.0120	0.0040	0.0700	0.0000	0.0000	0.0000	0.0000	0.0430	0.0000	0.0000	0.0000	0.0000
Batch 0000376062	10 EA			10,210 LB									

### Mechanical/ Physical Properties

Mill Coil No.	Tensile	Yield	Elong	Rckwl	Charpy	Charpy Dr	Charpy Sz	Olsen
300691	75,000.000	53,000.000	24.00	0	0	0	0	0
	0.000	0.000	0.00	0	0	0	0	0
	0.000	0.000	0.00	0	0	0	0	0
	0.000	0.000	0.00	0	0	0	0	0

THE CHEMICAL, PHYSICAL, OR MECHANICAL TESTS REPORTED ABOVE ACCURATELY REFLECT INFORMATION AS CONTAINED IN THE RECORDS OF THE CORPORATION.

Tag #:  
P/O #:  
Qty:

P/N #:

Job #:  
W/O #:



# Mill Test Report

Page 6

P. O. Box 279  
Winton, NC 27986  
(252) 356-3700

**NUCOR**  
**PLATE MILL**

Insulating Date: 12/09/2003  
Vehicle No: TTPX 804210  
B/L No.: 57696  
Load No.: 59144  
Our Order No.: 20557/3  
Cust. Order No.: 6851

Specification: 1.625" x 96.000" x 240.000"  
ASTM A572 Grade 50-01/ASTM A709 Grade 50-01b Type 2  
Sold To: RANGER STEEL SUPPLY CORPORATION  
1225 NORTH LOOP WEST, SUITE 200  
Ship To: A+L TRUCKING/RANGER STEEL  
ZONE 23 TRACK 415

Marking:

Test Note: HOUSTON, TX 77008 HOUSTON, TX 77029

Heat No.	C	Mn	P	S	Si	Cu	Ni	Cr	Mo	Al	V	Nb	Ti	N	Ca	B	Sn	Ceq	pcm
3105972	0.17	1.17	0.005	0.007	0.30	0.35	0.12	0.10	0.02	0.009	0.050	0.001	0.000	0.0072	0.0016	0.0000	0.000	0.433	0.272

Plate Serial No.	Pieces	Yield (psi)	Tensile (psi)	Elongation		Charpy Impacts (ft-lbs)		Temp (deg F)	Min Ave
				(% in 2")	(% in 8")	5	2		
3105972 - 04	4	55,600	82,800	19.8	17.4				
		60,900	85,500						

RECEIVED  
MAY 04 2004  
REC. DEPT.

PO # 11926

RANGER STEEL SUPPLY CORP.  
20557/3

Manufactured to fully killed practice. Welding or weld repair was not performed on this material.  
Mercury has not been used in the direct manufacturing of this material. Yield by 0.5EUL method. Produced as discrete plate.  
Ceq = C + (Mn / 5) + (Cr + Mo + V) / 5 + ((Cu + Ni) / 15)  
pcm = C + (Sb / 30) + (Mn / 20) + (Cu / 20) + (Ni / 60) + (Cr / 20) + (Mo / 15) + (V / 10) + Sb  
Metall and manufactured in the USA. ISO 9001:2000 certified (#12443-0) by SRI Quality System Register (#0665-09).  
DIN 5049 3.1, EN 10204 3.1.3 compliant. Produced under ABS Quality Assurance certificate No. 03-MIPQA-182.

We hereby certify that the contents of this report are accurate and correct. All test results and operations performed by this material manufacturer are in compliance with the applicable specifications.

T. A. Deparis, Metallurgist

Tag #:  
P/O #:  
Qty:

P/N #:

Job #:  
W/O #:



# Mill Test Report

Page 1

**NUCOR**  
P.O. Box 279  
Winston, NC 27386  
(252) 356-3700

Issuing Date: 04/30/2007  
Vehicle No: LW 62111  
Specification: 2.0000" x 96.000" x 240.000"  
ASTM A572 Grade 50-60/ASTM A709 Grade 50-70/AASHTO M270-50  
Type 2 AI R116g

Load No.: 163948  
Our Order No.: 53685711  
Cust. Order No.: 433606-4

Sold To: SUPERIOR SUPPLY & STEEL  
5430 MW CENTRAL, SUITE 200  
HOUSTON, TX 77062

Ship To: SUPERIOR SUPPLY & STEEL (1)  
C/O RICHARDSON STEEL  
8500 CLINTON DRIVE  
AD590 PYRA TRACK #200  
HOUSTON, TX 77248

Marking:

Heat No	C	Mn	P	S	Si	Cu	Ni	Cr	Mo	Alz	V	Nb	Ti	N	Ca	B	Sn	CEQ	PCM
7102887	0.17	1.15	0.018	0.003	0.16	0.24	0.06	0.11	0.01	0.026	0.041	0.001	0.001	0.0015	0.0001	0.0011	0.011	0.41	0.25
7102892	0.18	1.15	0.019	0.003	0.23	0.24	0.07	0.13	0.01	0.029	0.038	0.001	0.001	0.0011	0.0001	0.0010	0.010	0.43	0.27

Plate Serial No	Tensile Test			Charpy Impacts											
	Pieces	Tons	Dir.	(ft-lb) Yield	(ft-lb) Tensile	(ft-lb) Dir.	(ft-lb) shear 1	(ft-lb) shear 2	(ft-lb) shear 3	(ft-lb) shear Ave.	(ft-lb) shear	Size	Temp (°F)	Min	Ave.
7102887-06	1	6.53	T	63,400	83,400	H-L	30.6	30.1	28.9	29.9	29.9	10mm	-22	25	25
7102892-06	3	19.60	T	53,400	80,900	H-L	42.4	30.7	30.9	34.7	34.7	10mm	-22	25	25
			T	53,100	82,500	H-L	27.3	41.4	33.7	34.1	34.1	10mm	-22	25	25

*PO. # 20694 (STK)*

**RECEIVED**  
AUG 29 2007  
REC. DEPT.

Manufactured to fully killed fine grain practice by Electric Arc Furnace. Welding or weld repair was not performed on this material. We hereby certify that the contents of this report are accurate and correct. All test results and operations performed by the material manufacturer are in compliance with the applicable specifications.

Mercury has not been used in the direct manufacturing of this material. Produced as continuous cast as-cast discrete plate.

Yield by 0.5ELU method unless otherwise specified. Ceq = C+(Mn/6)+(Cr+Mo+V/6)+(Cu+Ni/15)

Pcm = C+(Si/20)+(Mn/20)+(Cu/20)+(Nb/50)+(V/10)+58

Melted and manufactured in the USA. ISO 9001:2000 certified (#12443-0) by SRI Quality System Registrar (#0985-09). PED 9723/JEC 712 Annex 1, Para. 4.3 Compliant.

DIN 90049 3.1.BEN 10204 3.1.B(2004) compliant. For ABS grades only. Quality Assurance certificate No. 03-MMPQA-182

T. A. Deparis, Metallurgist  
05/07/2007 11:56:03 AM

Tag #:

P/N #:

Job #:

P/O #:

W/O #:

Qty:

PO-172516702



Jindal United Steel Corporation

TC No.: BR164961-7461-02

5200 E. McKinney Road

3/2 A572-50

Baytown, TX 77520

METALLURGICAL TEST REPORT

Said To:		Order No: JUS762-05		This is to certify that the product described herein was manufactured, sampled, and tested in accordance with the specifications and requirements in such specifications. Fine Grain, Si-Al Fully Killed Steel		Bulletin Num. 104961	
Place Manufactured in the USA		F.O. Number 439048-4		Approved By: <i>Helen Green</i>			
Certified by ISO 9001:2000		Shipping Mode: DIRECT TRUCK		DIN 50849 3.1.B / EN 10204 2.09 3.1			
Specifications: HOT ROLLED PLATE CUT EDGES ASTM A572-04 GR 50 DUAL TO A709-01 GR 50 WITH LCVN HIGH STRENGTH LOW ALLOY		Insp.		1470000			

Item No.	Material Description			Bulletin		Heat No.	Gauge Tested	Test Plate Identity	Test Cond	Yield Point (KSI)	Tensile Strength (KSI)	Elongation (%)		Yield Strength Determined at	LCVN FULL min @ -220°F
	Gauge	Width	Length	Qty	Wgt							in 2"	in 4"		
05	3.5000	96.0000	240.0000	1	22.870	807461	3.500	01A	AR	50	71	33	0.2%	158 - 235 - 237 FULL min @ -22°F	

Heat No. 507461	CE-A-01																
Test Type	C	Mn	P	S	Si	Cu	Ni	Cr	Mg	Sn	Al	N	V	B	Ti	Ca	
LADLE	0.16	1.40	0.015	0.004	0.28	0.01	0.01	0.02	0.003	0.001	0.043	0.005	0.009	0.0001	0.003	0.002	

w-55747 from O'neal

4

Tag #:

P/N #:

Job #:

P/O #:

W/O #:

Qty:

TC No.: BR104955-7446-0

# Jindal United Steel Corporation

5200 E. McKinney Road  
Baytown, TX 77520

PO-MS10R02

## METALLURGICAL TEST REPORT

<b>Sold To:</b> SUPERIOR SUPPLY & STEEL PO BOX 2087 LAKE CHARLES, LA 70602		<b>Ship To:</b> SUPERIOR SUPPLY & STEEL 9640 CLINTON DRIVE PORT OF HOUSTON HOUSTON, TX 77091		This is to certify that the product described herein was manufactured, sampled, and tested in accordance with the specifications and requirements in such specifications. Fine Grain, Si-AL Fully Killed Steel	
<b>Plates Manufactured in the USA</b> Certified by ISO 9001:2000		Order No: JUS2762-06 Date: 8/27/2007		Approved By: <i>Helen Green</i> Shipping Mode: DIRECT TRUCK DIN 50049 3.1.B / EN 10204:2004 3.1	
Specifications: HOT ROLLED PLATE CUT EDGE ASTM A572-04 GR 50 DUAL TO A709-05 GR50 WITH LCVN HIGH STRENGTH LOW ALLOY		P.O. Number: 439048-4		Bulletin Num. 104955	

PO# 07-A0

PO # 65051

Item No.	Material Description		Bulletin		Gauge Tested	Heat No.	Test/Plate Identity	Test Cond	Yield Point (KSI)	Tensile Strength (KSI)	Elongation (%)		Yield Strength Determined at	LCVN FULL min @ -22DEG F
	Gauge	Width	Length	Qty							Wgt	in 8"		
06	3.7500	96.0000	235.0000	1	23,993	S07446	01A	AR	51	74	28	0.2%	25 FT/LBS	81 - 88 - 70 FULL min @ -22°F

UNITED STEEL  
MILL TEST REPORT  
DATE: 10/25/07  
ORDER NO: 102510R02  
CUST PO: 07-A0

Heat No.: S07446 CE: 0.40

Test Type	C	Mn	P	S	SI	Cu	Ni	Cr	Mo	Sn	Al	N	V	B	Ti	Ch
LADLE	0.15	1.39	0.011	0.003	0.27	0.02	0.01	0.02	0.003	0.001	0.036	0.005	0.065	0.0001	0.003	0.007

# INSPECTION CERTIFICATE



Certificate No. : J420070607006

P/O No. : 10017/1

L/C No. : 000-LOHR STRUCTURAL

Date issued : 2007/06/07 QS : 450SETS

Date Shipped: 2007/06/05

Date Tested: 2007/05/29

Date Manufactured: 2007/05/28

Specifications : Set : ASTM F2280 ~ 06

Bolt : ASTM F2280 ~ 06

Nut : ASTM A563 ~ 04

Washer : ASTM F436 ~ 04

Customer : LOHR STRUCTURAL FASTENERS, INC.

Description : A490 SMART HEX T/C BOLTS, NUTS, WASHER, PLAIN (5/16" THICK WASHER FACE)

Size : 1 1/8-7UNCX9

Surface Condition : PLAIN

Set Lot No. : F2J0910300

Q'ty Manufactured : 460 SETS

Marking : Bolt : A490TC, LSF, KCA, KPF LOGO

Nut : DH, KPF LOGO

Washer : F436, KPF LOGO

FACTORY : 601 YONGTAN-DONG, CHUNGJU-CITY,

CHUNGCHEONGBUK-DO, KOREA 380-250

TEL: (043) 849 - 1114 FAX: (043) 849 - 1234

FIELD OF TESTING : MECHANICAL TESTING

LAB. ID. : 111983

CERT. NO. : 882-01



STANDARD OF CERTIFIED : ISO/TS 16949, ISO 9001, ISO 14001

CERT. NO. : TS-01699, AC-01699, EAC-01699

## 1. Chemical Composition (%)

Division	Spec.	C		Si		Mn		P		S		Cr		Ni		B		Cu	
		Min.	Max.																
Bolt		30	48																
Heat No.	1H7303	35	17	20	60	77	11	5	114	19	2								
Nut																			
Heat No.	312226	44	24	77	14	10	14												
Washer																			
Heat No.	S839586	46	19	65	19	4	2												

## 2.2 Nut

- Lot No : F2J0901800

- Grade : CR, DH

Division	Hardness		Proof Load	
	Min.	Max.	Min.	Max.
Unit	HRC	HRC	lbf	lbf
Spec.	24	33	133,530	
Results.	HRC 30	31	6000	6000
Tested By	G.Y. HWANG		G.Y. HWANG	

## 2.3 Washer

- Lot No : F2J0435420

- Grade : TYPE 1

Division	Hardness		Axial Tension	
	Min.	Max.	Min.	Max.
Unit	HRC	HRC	lbf	lbf
Spec.	38	45	94,000	
Results.	HRC 40	41	92,250	98,650
Tested By	G.Y. HWANG		C.I. LEE	

## 2. Mechanical Properties

### 2.1 Bolt

- Lot No : F2J0910200

- Grade : TYPE 1

Division	Hardness		Specimen Tensile				Proof Load		Wedge Tensile Load	
	Min.	Max.	Yield Strength	Tensile Strength	Elongation	Reduction of Area	Load	Elongation	n=3	n=3
Unit	HRC	HRC					lbf	in	lbf	lbf
Spec.	38	35	N/A	N/A	N/A	N/A	91,550		114,450	132,000
Results.	HRC 35	36	N/A	N/A	N/A	N/A	92,590		92,590	129,870
Tested By	J.W. JU						J.W. JU		J.W. JU	

## 3. Assembly Lot Tension Test

- Lot No : F2J0910200

- Grade : TYPE 1

Division	Hardness		Axial Tension	
	Min.	Max.	Min.	Max.
Unit	HRC	HRC	lbf	lbf
Spec.	38	45	94,000	
Results.	HRC 40	41	92,250	98,650
Tested By	G.Y. HWANG		C.I. LEE	

## 4. Visual & Thread Inspection

- Lot No : F2J0910200

- Grade : TYPE 1

Division	Appearance		Thread	
	Min.	Max.	Min.	Max.
Unit	OK	OK	OK	OK
Spec.	OK	OK	OK	OK
Results.	OK	OK	OK	OK
Tested By	G.Y. HWANG		C.I. LEE	

Reference : 1. MAGNETIC PARTICLE INSPECTION PER ASTM F2280 SEC.13 WAS PERFORMED AS REQUIRED BY ASTM E709 AND PASSED. 2. RESULT OF CARBURIZATION AND DECARBURIZATION TEST PER SEC.10 ASTM F2280. O.K

This is to certify that the above results are true and correct in every detail.

Chief of Quality Management Dept.

IN-SUB CHOIE

# INSPECTION CERTIFICATE



Certificate No. : J420070806077

P/O No. : 10048

L/C No. : COD-LOHR STRUCTURAL

Date issued : 2007/08/06 QS : 1.570SETS

Date Shipped: 2007/07/31

Date Tested: 2007/07/23

Date Manufactured: 2007/07/21

Specifications : Set : ASTM F2280 ~ 06

Bolt : ASTM F2280 ~ 06

Nut : ASTM A563 ~ 04

Washer : ASTM F436 ~ 04

Customer : LOHR STRUCTURAL FASTENERS, INC.

Description : A490 SMART HEX T/C BOLTS, NUTS, WASHER, PLAIN (5/16" THICK WASHER FACE)

Size : 1 1/8-7UNCx7

Surface Condition : PLAIN

Set Lot No. : F2J1603601

Q'ty Manufactured : 1,650 SETS

Marking : Bolt : A490TC,LSF,KCH,KPF LOGO

Nut : DH,KPF LOGO

Washer : F436,KPF LOGO

FACTORY : 601 YONGTAN-DONG, CHUNGJU-CITY,  
CHUNGCHONGNGBUK-DO, KOREA 380-250

TEL.:(043) 849 - 1114 FAX:(043) 849 - 1234



FIELD OF TESTING : MECHANICAL TESTING  
LAB. ID. : 111983  
CERT. NO. : 882-01

STANDARD OF CERTIFIED : ISO/TS 16949, ISO 9001, ISO 14001  
CERT. NO. : TS-01899, AC-01899, EAC-01899

## 2. Mechanical Properties

### 2.1 Bolt

- Lot No : F2J1603501

- Grade : TYPE 1

## 1. Chemical Composition (%)

Division	Spec.	C x100	Si x100	Mn x100	P x10000	S x10000	Cr x100	Ni x100	B x10000	Cu x100
Bolt	100125	37	17	75	12	8	113	18	2	3
Nut	754-1351	20	55	60	40	50				
Washer	754-1351	46	26	66	11	10	15	7	14	
Heat No.	SB39586	46	19	65	19	4	2	2	1	

### 2.2 Nut

- Lot No : F2J1610700

- Grade : GR.DH

### 2.3 Washer

- Lot No : F2J1522320

- Grade : TYPE 1

Division	Spec.	Hardness n=5		Proof Load n=5
		Min.	Max.	
Unit		HRC	HRC	lbf
Spec.		24	38	133,530
Results.		31	32	GOOD
Tested By		G.Y. HWANG		G.Y. HWANG

Division	Unit	Hardness n=13		Core	Specimen Tensile			Proof Load n=3		Wedge Tensile Load n=3
		Surface	HRC		Yield Strength	Tensile Strength	Elongation	Reduction of Area	Load	
Unit		HRC	HRC							lbf
Spec.		39	35	N/A	N/A	N/A	N/A	91,550	0.0005	114,450
Results.		37	36					92,150	0.0001	131,840
Tested By		J.W. JU						92,150	0.0001	131,900

## 3. Assembly Lot Tension Test

Division	Unit	Axial Tension n=4	
		Min.	Max.
Spec.		84,000	94,710
Results.		97,090	96,400
Tested By		C.I. LEE	

## 4. Visual & Thread Inspection

Division	Appearance	Thread
Bolt	OK	OK
Nut	OK	OK
Washer	OK	---

Reference : 1. MAGNETIC PARTICLE INSPECTION PER ASTM F2280 SEC.13 WAS PERFORMED AS REQUIRED BY ASTM E709 AND PASSED. 2. RESULT OF CARBURIZATION AND DECARBURIZATION TEST PER SEC.10 ASTM F2280. 0.K

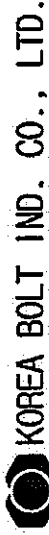
This is to certify that the above results are true and correct in every details

Chief of Quality Management Dept.

IN-SUB CHO

KPF

# INSPECTION CERTIFICATE



FACTORY : 731-3, WONSU-DONG, DANWON-GU,  
ANSAN-CITY, KYUNGGI-DO, KOREA 425-090  
TEL : (031)4891 - 500  
FAX : (031)492 - 7034

Certificate No. : J420040923007

P/O No. : 8588

L/C No. : COD-LOHR STRUCTURAL

Date Issued : 2004/09/23

Date Shipped : 2004/09/23

Date Tested : 2004/09/22

Date Manufactured : 2004/08/31

Specifications : ASTM F436 - 93(2000)

Customer : LOHR STRUCTURAL FASTENERS, INC.

Description : F436 WASHERS

Grade : TYPE 1

Size : 1 1/8(T=5/16)

Marking : F436,KOREA BOLT L060

Surface Condition : PLAIN

Lot No. : F2F2134250

Q'ty Shipped : 50,000 PCS

FIELD OF TESTING : MECHANICAL, CHEMICAL  
LAB. ID. : 111983  
CERT. NO. : 0882-01, 0882-02

## 1. Chemical Composition (%)

Heat No.	C		Si		Mn		P		S		Cr		Ni		Cu		Ti		V		Al	
	Min.	Max.																				
Y92361	44		20		67		14		6		1		1		1		1					

## 2. Macroetch Meet

Division	Surface Condition	Random Condition	Center Segregation	Spec. of Test Method

## 3. Mechanical Properties

Division	Hardness		Core		Yield Strength		Tensile Strength		Elongation		Reduction of Area		Proof Load		Sample Nut Hardness	Tensile Load	Bolt Retaining Hardness	Bonding Test	Tap Wrench Fit Test	Decarburization Test By Hardness
	Surface	n = 5	HRC	HRC	Min.	Max.	Min.	Max.	Min.	Max.	Min.	Max.	Load	Elongation						
Unit																				
Spec. 1	HRC																			
Results 1	42																			
Results 2	42																			
Results 3	41																			
Results 4	41																			
Results 5	40																			
Results 6	41																			
Results 7																				
Results 8																				
Results 9																				
Results 10																				
Results Avg.																				
Tested By	J.H. LIM																			
Spec. of Test Method	ASTM F606 -																			

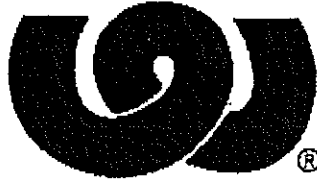
Reference : This is to certify that the above results are true and correct in every details

*[Signature]*  
IN-SUB CHOE  
Chief of Quality Assurance Dept.

KOREA BOLT, IND. CO., LTD.

STAMPING THE FUTURE  
WROUGHT WASHER MFG., INC.

PO# 65342  
JOB# 07-X6



June 14, 2007

Certification of Compliance

012476  
ALBRITTON & GROVES - HOUSTON  
3605 WILLOWBEND BLVD. #550  
HOUSTON, TX 77054

Wrought Washer  
Order/Lot Number  
219194

Heat Number 163983	Chemical Analysis				
	C	Mn	P	S	Si
	0.370	0.680	0.008	0.005	0.213

Purchase Order Number	Part Description	Date Shipped	Quantity Shipped
HARDENED	1 1/8 S MARK HT	06/13/2007	18,000

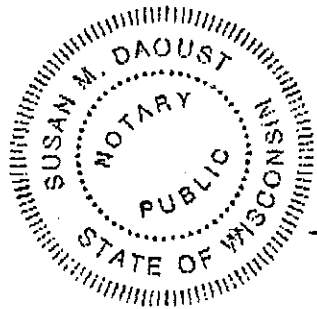
We hereby certify that the subject parts conform to the requirements of the applicable specification indicated for the subject parts and are in complete conformance to F436-04. We hereby certify that the subject parts were hardened to RC 38-45.

We hereby certify that all statutory requirements as to American Production and Labor Standards and all conditions of purchase applicable to the transaction have been complied with and that the subject parts were melted and manufactured in the U.S.A.

Truly yours,  
Wrought Washer Mfg., Inc.

Paul Schaefer  
Q.C. Manager

Sworn and subscribed before me on June 14, 2007  
My commission expires June 21, 2009



(070) SMARK, ITT, F436  
WW INTERNAL USE: 50881101/010/017328/34836

# INSPECTION CERTIFICATE



FACTORY : 601 YONGTAN-DONG, CHUNGJU-CITY,  
CHUNGCHONG-DO, KOREA 380-250  
TEL : (043) 849 - 1114  
FAX : (043) 849 - 1234

FIELD OF TESTING : MECHANICAL TESTING  
LAB. ID : 111983  
CERT. NO. : 882-01

STANDARD OF CERTIFICATION : ISO/TS 16949, ISO 9001, ISO 14001  
CERT. NO. : TS-01899, AC-01899, EAC-01899

Customer : LOHR STRUCTURAL FASTENERS, INC.

Description : GR,DH HEAVY HEX NUTS, PLAIN

Grade : GR,DH

Size : 1 1/8-7UNC

Marking : DH,KPF LOGO

Surface Condition : WAX COATING TC-2 TYPE

Lot No. : F2J1051800

Q'ty Shipped : 18,900 PCS

Certificate No. : J420070511049

P/O No. : 0412

L/C No. : C0D-LOHR STRUCTURAL

Date Issued : 2007/05/11

Date Shipped : 2007/05/09

Date Tested : 2007/04/14

Date Manufactured : 2007/04/12

Specifications : ASTM A563 - 04

## 1. Chemical Composition (%)

Heat No.	C	Si	Mn	P	S	Cr	Ni	Mo	Al	B	Cu	Ti	V	Al
	x100	x100	x100	x10000	x10000	x100	x100	x100	x10000	x10000	x100	x100	x100	x10000
312226	20	44	24	77	14	10	2	6	11					

## 2. Macroetch Meet

Division	Surface Condition	Random Condition	Center Segregation	Spec. of Test Method
Spec.				
Results				
Tested By				

## 3. Mechanical Properties

Division	Hardness		Specimen Tensile		Proof Load		Tensile Load	Sample Nut Hardness	Impact Test	Bend Test	Bolt Retention Hardness	Tap Wrench Fit Test	Decorburization Test By Hardness
	Surface	Core	Yield Strength	Tensile Strength	Load	Elongation							
Unit	n = 3												
Min.	HRC												
Max.	HRC												
Min.	24												
Max.	38												
1	HRC	30											
2		30											
3		30											
4		30											
5													
6													
7													
8													
9													
10													
Avg.													
Tested By	G. Y. HWANG												
Spec. of Test Method	ASTM F606 -												

Reference :

This is to certify that the above results are true and correct in every details

*G. Y. Hwang*

IN-SUB CHOICE  
Chief of Quality Management Dept.

PO# 60045  
SO# 07-16

**Cert Summary Page** SLSB, LLC dba ST. LOUIS SCREW & BOLT

W & W STEEL COMPANY

Customer PO 65045

**Invoice No.**

Sales Order S18022

Cert No	Inv Line No	Item No	Invoice Date	Quantity	Lot No	Heat	Assembly No	SLSB PO
26040	150000	AFA113900		1,425	028135			HAYDON
	Description: 1-1/8(7)X 9" A490-1 BOLT							
25762	180000	AAW113		1,565	219936	279888		SL14738
	Description: 1-1/8 F436-1 STRUCTURAL WASHER - <i>NOT USED</i>							
26041	250000	AAA088250		4	028103			HAYDON
	Description: 7/8(9)X 12-1/2 A325-1 BOLT							



# SLSB, LLC dba ST. LOUIS SCREW & BOLT

W & W STEEL COMPANY

Customer PO 65045

Invoice No. S18022

Invoice Date 10/04/07

Sales Order S18022

Cert No Inv Line No Item No

Quantity Lot No

Heat

26040 150000 AFA113900

1,425 028135

Assembly No

SLSB PO  
HAYDON

# TEST REPORT

**LOT #:** 028135  
**PH:** 800-237-7059  
**FAX:** 314-389-7510  
 SLSB, LLC dba St. Louis Screw & Bolt  
 2000 Access Blvd  
 PO Box 260  
 Madison, IL 62060  
 1887  
 St. Louis  
 Screw & Bolt

<b>PRODUCTION INFORMATION:</b>	
<b>PART#:</b> AFA113900	<b>DESCRIPTION:</b> HHS
<b>SIZE:</b> 1-1/8(7)UNC2AX9	<b>ASTM SPEC:</b> A490-1 06
<b>LOT#:</b> 028135	<b>FINISH:</b> BLANK
<b>ISSUE DATE:</b> 10/12/07	<b>MFG DATE:</b> 10/4/07

**CHEMISTRY FROM RAW MATERIAL SUPPLIER:**  
**HEAT NO:** M24431  
**ASTM SPEC:** A29  
**STEEL MILL SUPPLIER:** TURRET

**CHEMICAL CONTENTS**

<b>C</b>	<b>MN</b>	<b>P</b>	<b>S</b>	<b>Si</b>	<b>Ni</b>	<b>Cr</b>	<b>Mo</b>	<b>Cu</b>	<b>Sn</b>	<b>Al</b>	<b>N</b>
0.40	0.85	0.016	0.030	0.26	0.94	0.18				0.027	

**MECHANICAL PROPERTIES:**

<b>PRODUCTION QTY</b>	<b>PCS SAMPLED</b>	<b>ISSUE DATE</b>	<b>SAMPLED BY</b>	<b>TESTED BY</b>	<b>H.T. PO#</b>	<b>TEST METHODS</b>	<b>VISUAL INSPECTION PER</b>	<b>PCS SAMPLED</b>	<b>LOT PASSED</b>
1552	3	10/12/07	DH	DH	783620-01	ASTM F606	ASTM F788	3	PASSED

**TENSILE STRENGTH**

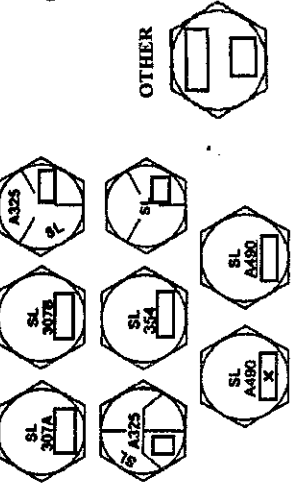
<b>WEDGE</b>	<b>DEGREE</b>	<b>LBS.</b>	<b>LBS.</b>	<b>PROOF LOAD TEST</b>	<b>HARDNESS</b>	<b>CORE</b>
6		114450-132000	91550	SURFACE	36	N/A

**SAMPLES**

	<b>1</b>	<b>2</b>	<b>3</b>	<b>4</b>	<b>5</b>	<b>6</b>	<b>7</b>	<b>8</b>	<b>AVG.</b>
<b>TENSILE LOAD</b>	131535	128260	129990						129928
<b>PROOF LOAD</b>	.0000	.0001	.0000						.0001
<b>HRC- SURF</b>	35.2	36.8	35.7						36
<b>HRBW-CORE</b>									

The SLSB LLC Laboratory has been accredited by the American Association for Laboratory Accreditation in the field of mechanical and fastener testing for the tests listed above, certificate# 0696-01. The sampling plan meets or exceeds that which is required by the bolt spec or the FQA. The steel was made and melted in the USA, and the product was tested by SLSB LLC, St. Louis, MO, USA, free of mercury contamination. We certify that the samples tested conform to the ASTM specification listed above, and the date is a true representation of the information provided by the material supplier and our testing laboratory. This test certificate relates only to the items listed on this document and may not be reported or distributed except in full. Thread fit and dimensional requirements are compliant to ANSI B18.2.6 specification.

**MANUFACTURERS ID HEAD MARKING: SL**



**AMENDED**  **DATE:** 10/12/07 **INITIAL:**  
 Signed: *Rachael Holden*

\*Heats of steel used have not had the following materials intentionally added: bismuth, selenium, tellurium, or lead.



- Manufacturers of Quality Fasteners -  
Hot Heading Cold Heading CNC Machining

4210 SHIRLEY LANE • ALSIP, IL 60803  
708-597-9100 • 800-323-1347 • FAX 708-597-0423  
WEBSITE www.bbcfasteners.com

SLSB LLC  
dba ST. LOUIS SCREW AND BOLT  
P.O. BOX 260  
MADISON, IL 62060-0260

OCTOBER 5, 2007

SHIP TO: PAULO PRODUCTS COMPANY  
5711 WEST PARK AVENUE  
ST. LOUIS, MO 63110-1890

**MATERIAL AND TEST CERTIFICATE**  
**DESCRIPTION OF MATERIAL AND SPECIFICATIONS**

ITEM NO.	QUANTITY	DESCRIPTION	CUSTOMER ORDER NO.	INVOICE NO.	SPECIFICATION	SHIPPING DATE	SAMPLE PLAN
1	1552	BHR112C090046PLD 1 1/8 -7X9" HVY. HEX SOFT BOLT, A490-1	SL14721	043522	ASTM A490-06	10-4-07	ASTM A490

"Material was melted and manufactured 100% in the U.S.A."

**CHEMICAL ANALYSIS**

ITEM NO.	AISI NO.	HEAT NO.	C	Mn	P	S	SI	NI	Cr	Mo	Cu	Al	V
1	4140	M24431	.40	.85	.016	.030	.26		.94	.18		.027	

"Certification of chemical analysis as supplied by our steel supplier"

**MECHANICAL PROPERTIES**

ITEM NO.	TENSILE STRENGTH LBF	YIELD PSI	PROOF LOAD	ELONGATION % IN 2"	SURFACE HARDNESS HR 30N	HARDNESS BHN R/C

We hereby certify that the above test results are correct and that all the parts or material identified have been manufactured and inspected in accordance with applicable quality requirements. We also certify that all parts or material conform to the applicable drawings, specifications, and conditions set forth on the purchase order.

David Aron  
Quality Assurance

Sworn to and subscribed before me this 5th day of October, 2007.

Margaret Ann Murray  
Notary Public

THIS TEST REPORT CANNOT BE REPRODUCED EXCEPT IN FULL WITHOUT WRITTEN APPROVAL OF BBC FASTENERS, INC.

Tested by: BBC Fasteners A2LA Testing Laboratory Accreditation #0234-01, expires





(724) 266-8200  
800-245-4800  
Fax (724) 266-5702

P. O. Box 55 • Leetsdale, PA 15056-0055

800-STL-BARS

**MATERIAL CERTIFICATION**

**DATE PRINTED 9/24/2007**

ACCT# 2927

SOLD TO: BBC FASTENERS  
4210 SHIRLEY LANE  
ALSIP IL 60803

INVOICE#: SHIPMENT  
DATE: PO#:  
47871 9/21/2007 S40567

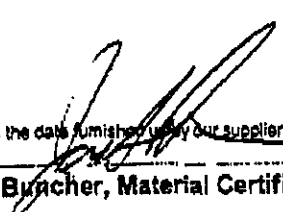
**DESCRIPTION OF MATERIAL AND SPECIFICATIONS**

ITEM#: 81541 1.125 HR RD 4140 22

HEAT#: M24431 PRODUCER:

C: .40 MN: .85 P: .016 S: .030 SI: .26 NI:  
CR: .94 MO: .18 CU: AL: .027 PB: SN:  
V: CB: CA: SE: FE: O:  
N: H: MISC:

We hereby certify that the above is the same as the data furnished by our supplier or resulting from tests performed in a recognized laboratory.

  
Jay Buncher, Material Certification Clerk

PO# 60010  
PO# 07-X6

**C. NELMS**

**Cert Summary Page SLSB, LLC dba ST. LOUIS SCREW & BOLT**

W & W STEEL COMPANY

Customer PO 65045

Invoice No. Invoice Date Sales Order S18022

Cert No	Inv Line No	Item No	Quantity	Lot No	Heat	Assembly No	SLSB PO
17404	160000	AFA113700	140	499163	RT7306921		SL13135
	Description: 1-1/8(7)X 7" A490-1 BOLT						
20974	170000	VDH113	1,565	JK721			SL13650
	Description: 1-1/8(7) HVY HEX NUT A563-DH — NOT USED						
25562	190000	AAA087600	4	570186			SL14348
	Description: 7/8(9)X 6" A325-1 BOLT						
20627	200000	AAA087700	4	508335			SL13929
	Description: 7/8(9)X 7" A325-1 BOLT						
22625	210000	AAA087750	7	508392			SL13805
	Description: 7/8(9)X 7-1/2 A325-1 BOLT						
25243	220000	AAA087850	4	588050			SL14348
	Description: 7/8(9)X 8-1/2 A325-1 BOLT						
14112	230000	AAA087900	8	526507	414420		SL12260
	Description: 7/8(9)X 9" A325-1 BOLT						
23725	240000	AAA087950	4	526595			SL13805
	Description: 7/8(9)X 9-1/2 A325-1 BOLT						
25088	260000	VDH087	31	KQ031			SL14244
	Description: 7/8(9) HVY HEX NUT A563-DH						
24496	270000	AAW087	62	B8982	20641160		SL14457
	Description: 7/8 F436-1 STRUCTURAL WASHER						
							PRESTIGE STAMPING INC.

# SLSB, LLC dba ST. LOUIS SCREW & BOLT

W & W STEEL COMPANY

Customer PO 65045

Invoice No. S18022

Invoice Date 09/27/07

Sales Order S18022

Cert No 17404

Inv Line No 160000

Item No AFA113700

Quantity 140

Lot No 499163

Heat RT7306921

Assembly No

SLSB PO

SL13135



# LAKE ERIE PRODUCTS

CUSTOM ENGINEERED FASTENERS

Ship Date: 10-27-06  
A TimMas Company

Certification: 170100\*7\*1  
Report Date: 10-27-06

## TEST REPORT

13001 ATHENS AVENUE  
CLEVELAND, OHIO 44107  
T. 216.521.1800  
F. 216.228.4520

3281 WEST COUNTY ROAD O NS  
FRANKFORT, INDIANA 46041-6966  
T. 765.654.0477  
F. 765.654.0857

Cust PO: SL13135

Lot Nbr: 499163  
Quantity: 420 Pieces  
MEg Date: 02-24-06

St. Louis Screw & Bolt  
PO Box 470037  
2000 ACCESS BLVD  
MADISON, IL 62060

### PART INFORMATION

Part Number: AFA113700  
Description: 1 1/8-7 X 7 A490-1  
Finish: PLAIN

Head marking: A490 TYPE 1 - 1 DOT SL

### RAW MATERIAL ANALYSIS

Steel Heat Nbr: RT7306921  
Steel Supplier: REPUBLIC TECHNOLOGIES INTL.      Steel Grade: 50B35 SKFG

C	Mn	P	S	Si	Ni	Cr	Mo	Cu	Sn
0.3400	1.0300	0.0100	0.0070	0.2300	0.0400	0.5400	0.1200	0.0500	0.0040
V	Al	N	B	Ti					
0.0050	0.0290	0.0049	0.0014	0.0000					

### MECHANICAL PROPERTIES

Wedge Angle: 6 Test Performed Tensile, PSI	Proof Load (lbs/Psi): 91560/120000			Samples
	High	Low	Average	
	158000	155000	156400	5
Proof Load Elongation	0.0002	0.0000	0.0001	5
Superficial R30N	54.0	53.0	53.2	5
Core Hardness, HRC	34.0	33.0	33.6	5

Certification test results include those reported by the following laboratories:  
Republic Technologies Int'l, A2LA, 10-31-07  
Lake Erie Products, Inc., A2LA 0122.02, 05-31-08

### Applicable Standards, Specifications, and Sampling Schemes:

THE FOLLOWING STATEMENTS APPLY TO:

ASTM A-325-04b, TYPE 1 and TYPE 3 BOLTS  
ASTM A-490-04a, TYPE 1 and TYPE 3 BOLTS

Test Methods are in accordance with ASTM F606-05.

Thread Fit and Dimensional Properties are compliant to ASTM B18.2.6.

These bolts passed inspection for surface discontinuities, per ASTM F788.

These bolts were not produced from heats in which Bismuth, Selenium,

Tellurium, or Lead was intentionally added.

These bolts were not exposed to Mercury or any other metal alloy that

is liquid at ambient temp during processing or while in our possession.

Material is of U.S. origin, and was melted and manufactured in the U.S.A.

Page: 1 of 2

We certify: The product furnished by Lake Erie Products was manufactured, sampled, tested, and inspected in accordance with the standards and specifications listed above and with Lake Erie Products Quality Manual in effect as of the date of manufacture. The above data accurately represents values provided by Lake Erie Products suppliers and/or values generated in one of Lake Erie Products A2LA accredited laboratories. Statistical process control data is on file.

This test report relates only to the sample tested above. This document may only be reproduced unaltered and may not be used for any purpose other than the purpose of certifying the same or lesser quantity of the product specified herein. Reproduction, alteration or use of this document for any other purpose is prohibited. Except as expressly provided in this certification, Lake Erie Products makes no (and disclaims all) representations, warranties and guarantees whatsoever, whether express, implied or statutory, including, without limitation, any warranty of merchantability or fitness for a particular purpose.

Lake Erie Products

*Gerald E. Simons*  
Gerald E. Simons  
Quality Manager



334  
CERT #0122-01 / #0122-02  
"MECHANICAL FIELD OF TESTING"

18



# LAKE ERIE PRODUCTS

CUSTOM ENGINEERED FASTENERS

## TEST REPORT

13001 ATHENS AVENUE  
CLEVELAND, OHIO 44107  
T. 216.521.1800  
F. 216.228.4520

3281 WEST COUNTY ROAD O NS  
FRANKFORT, INDIANA 46041-6966  
T. 765.654.0477  
F. 765.654.0857

Ship Date: 10-27-06  
A Trivias Company

Cust PO: SL13135

Certification: 170100\*7\*1  
Report Date: 10-27-06

Lot Nbr: 499163  
Quantity: 420 Pieces  
Mfg Date: 02-24-06

-----  
THE FOLLOWING STATEMENTS APPLY TO:

ASTM A-490-04a, TYPE 1 and TYPE 3 BOLTS

These bolts passed carburization and decarburization tests, per SAE J121.  
\*These bolts passed magnetic particle inspection for longitudinal discontinuities and transverse cracks, per ASTM A490-04a, E709, and E1444 Test Methods.

-----  
\*Magnetic particle inspection is not included on Lake Eries Laboratory scope of accreditation.

The listed standards, specifications, and sampling schemes are of the revision in effect on the date of manufacture unless noted otherwise. Only those standards specifically noted under "test methods" or "additional test methods" are included on LE's scope of laboratory accreditation.

-----  
DEVIATIONS FROM THE TEST METHODS

13.01

-----  
This lot has been found to conform to the requirements of the above standards and specifications

-----  
Original Mill Certification Attached  
Scan Certifications to PDF and email to:  
certs@stlouisscrewbolt.com

Page: 2 of 2

We certify: The product furnished by Lake Erie Products was manufactured, sampled, tested, and inspected in accordance with the standards and specifications listed above and with Lake Erie Products Quality Manual in effect as of the date of manufacture. The above data accurately represents values provided by Lake Erie Products suppliers and/or values generated in one of Lake Erie Products A2LA accredited laboratories. Statistical process control data is on file.

This test report relates only to the sample tested above. This document may only be reproduced unaltered and may not be used for any purpose other than the purpose of certifying the same or lesser quantity of the product specified herein. Reproduction, alteration or use of this document or any other purpose is prohibited. Except as expressly provided in this certification, Lake Erie Products makes no (and disclaims all) representations, warranties and guarantees whatsoever, whether express, implied or statutory, including, without limitation, any warranty of merchantability or fitness for a particular purpose.

Lake Erie Products

Gerald E. Simons  
Gerald E. Simons  
Quality Manager



335  
CERT #0122-01 / #0122-02  
"MECHANICAL FIELD OF TESTING"

19



1807 EAST 28TH ST. LORAIN, OH 44055  
 PHONE: 330-438-5694 FAX: 330-438-5905

CERTIFICATE OF TESTS

REPUBLIC ENGINEERED PRODUCTS

DECEMBER 21, 2005  
 PAGE: 1 OF 2

=====  
 PURCHASE ORDER: 32922  
 PART NUMBER : G364074  
 ORDER NUMBER: 05-42850-01 403  
 HEAT : 7306921  
 CHARGE ADDRESS =====

PURCHASE ORDER DATE: 10/19/05  
 ACCOUNT NUMBER : 42986302  
 SCHEDULE : 07282-81

SHIP TO =====

LAKE ERIE SCREW CORP  
 3595 W STATE RD 28  
 FRANKFORT IN 460416708

LAKE ERIE SCREW CORP  
 KEELY LEACH  
 13001 ATHENS AVE WEST DRIVE  
 LAKWOOD OH 44107

----- MATERIAL DESCRIPTION -----  
 HOT ROLLED STEEL COILS ALLOY LAKE ERIE SCREW SPEC LE 1.1 REV 6 DTD 07/06/99 EXC  
 DECARB & NI GRADE-50B35-MOD FINE GRAIN COLD WORK Q CRITICAL SURFACE SENSITIVE  
 FIXED PRACTICE PART REST CHEM REST MAX INCID ELEM

SIZE: RDS 1-5/32 X COILS  
 COIL WT 3800/4600 ID 37 MN OD 54 MX

LADLE CHEMISTRY %										
C	MN	P	S	SI	CU	NI	CR	MO	AL	
0.34	01.03	.010	.007	0.23	0.05	00.04	00.54	0.12	00.029	
V	N	CB	B	SN						
0.006	.0049	0.001	.0014	.004						

SEMI-FINISH RESULTS-----

AUSTENITIC GRAIN SIZE  
 AUST GRAIN SZ 7.

JOMINY STD													SAE J406				ASTM A255						
1	2	3	4	5	6	7	8	9	10	11	12	13	14	15	16	18	20	22	24	26	28	30	32
55	54	53	52	52	52	52	51	51	50	49	48	47	45	44	42	39	36	34	33	32	30	30	29
55	54	53	52	52	52	52	51	51	50	49	48	47	45	44	42	39	36	34	33	32	30	30	29

----- FINISH SIZE RESULTS SCHEDULE: 0728281 -----  
 DECARBURIZATION SAE J419 ASTM E1077  
 COMPLETE TOTAL DEPTH  
 INCHES INCHES  
 PCE 01 .000 .003

REDUCTION RATIO 34.2 TO 1

----- NOTES -----  
 MELT SOURCE: REP-LORAIN MELT COUNTRY: U.S.A.  
 HOT ROLL SRCE: REP-LORAIN HOT ROLL COUNTRY: U.S.A.  
 MELT METHOD: STRAND CAST

CHEMICAL ANALYSIS CONFORMS TO APPLICABLE SPECS: ASTM E415, ASTM E1019,  
 AND ASTM E1085.

REPUBLIC ENGINEERED PRODUCTS LORAIN HOT ROLLED BAR PLANT IS ISO/TS  
 16949 REGISTERED

WHEN EVALUATED, MACRO ETCHES WERE VISUALLY RATED ON SAMPLES ETCHED  
 USING HYDROCHLORIC ACID AT A TEMPERATURE OF 170 DEGREES (F)  
 (+/-10 DEGREES F)

WHEN PERFORMED, MICROSCOPIC TESTS WERE UTILIZED TO DETERMINE  
 DECARBURIZATION USING NITAL AS THE ETCHANT AND WERE RATED AT 100X  
 MAGNIFICATION

R A SZELIGA  
 MANAGER TECH. SERVICES

*R. A. Szeliga*

BY D. BARTON

336



1807 EAST 28TH ST. LORAIN, OH 44055  
PHONE: 330-438-5694 FAX: 330-438-5905

CERTIFICATE OF TESTS

REPUBLIC ENGINEERED PRODUCTS

DECEMBER 21, 2005  
PAGE: 2 OF 2

=====  
PURCHASE ORDER: 32922  
PART NUMBER : G364074  
ORDER NUMBER: 05-42850-01 403  
HEAT : 7306921

=====  
PURCHASE ORDER DATE: 10/19/05  
ACCOUNT NUMBER : 42986302  
SCHEDULE : 07282-81

----- NOTES (CONTINUED) -----

REPUBLIC ENGINEERED PRODUCTS HEREBY CERTIFY THAT THE MATERIAL LISTED HEREIN HAS BEEN INSPECTED AND TESTED IN ACCORDANCE WITH THE METHODS PRESCRIBED IN THE GOVERNING SPECIFICATION AND BASED UPON THE RESULTS OF SUCH INSPECTION AND TESTING HAS BEEN APPROVED FOR CONFORMANCE TO THE SPECIFICATION.  
THE RESULTS RELATE ONLY TO THE ITEMS TESTED

CERTIFICATION OF TESTS SHALL NOT BE REPRODUCED EXCEPT IN FULL

THE MATERIAL WAS NOT EXPOSED TO MERCURY OR ANY METAL ALLOY THAT IS LIQUID AT AMBIENT TEMPERATURE DURING PROCESSING OR WHILE IN OUR POSSESSION. NO WELDING OR WELD REPAIR WAS PERFORMED ON THIS MATERIAL

ALL TESTING HAS BEEN PERFORMED USING THE CURRENT REVISION OF THE TESTING SPECIFICATION

RECORDING OF FALSE, FICTITIOUS OR FRAUDULENT STATEMENT OR ENTRIES ON THIS DOCUMENT MAY BE PUNISHED AS A FELONY UNDER FED STATUES TITLE 18 CHAPTER 47.

MATERIAL IS OF U. S. ORIGIN AND WAS MELTED AND MANUFACTURED IN THE U.S.A.

----- END OF DATA ----- CC ----- END OF DATA -----  
FAX SHIP TO 1 COPY ATTENTION KEELY LEACH 765-654-0857  
FILE 1 COPY  
WITH SHIPMENT 1 COPY SHIPPING AREA:

R A SZELIGA  
MANAGER TECH. SERVICES

*R. A. Szeliga*

BY D. BARTON

337



**SKIDMORE-WILHELM**  
Manufacturing Company

422 South Green Rd  
South Euclid, OH 44121  
216-481-4774  
216-481-2427 fax  
www.skidmore-wilhelm.com

# Certificate of Calibration

Date of Calibration	10/3/2007
Model/Serial Number	H1090
Technician	William Robinson
Temperature (°F):	72

Actual Load	Gage Reading	% Deviation
50,000	50,000	0.00%
75,000	75,000	0.00%
100,000	100,000	0.00%
125,000	125,000	0.00%
150,000	150,500	0.33%

Calibration was performed on Skidmore-Wilhelm's Compression Press S/N 4804. The Calibration of the applied test loads is maintained by Morehouse Instrument Co. Proving Ring S/N 3704. The calibration of this ring is traceable to NIST through Report No. 3074F0906, dtd. 6/9/06.

# Stanley Proto Industrial Tools™

## Torque Wrench Calibration Verification Report

This Torque Wrench, Model # J6020 AB Serial # DGK 29466 has been calibrated with test equipment with a certified accuracy of  $\pm 1/2\%$ , traceable to the United States National Institute of Standards and Technology. Stanley Proto certifies this torque wrench has been found to conform to the accuracy requirements of the American National Standard, ASME B107.14M-1994.

Certified Accuracy $\pm 3\%$ Clockwise			$\pm 6\%$ Counter Clockwise		
Capacity of Wrench	Wrench Setting	Average Reading	Capacity of Wrench	Wrench Setting	Average Reading
20%	<u>120</u>	<u>120.6</u>	20%	<u>120</u>	<u>123.4</u>
60%	<u>360</u>	<u>364.9</u>	60%	<u>360</u>	<u>370.1</u>
100%	<u>600</u>	<u>608.5</u>	100%	<u>600</u>	<u>616.2</u>

Authorized Repair Center  
 Stanley Proto Industrial Tools  
 2195 East View Parkway, Suite 103  
 Conyers, GA 30013  
 FORM 75-3175-2 REV2

Inspector: [Signature]  
 Date: 11/1/07  
 Customer "In Service Date": \_\_\_\_\_  
 Calibration Due Date: \_\_\_\_\_



# CUTTING ORDER

RECORD COPY  
CUTTING ORDER

WAREHOUSE = 1

MAT'L PREP = 2

PATTIE = 1

EAST YARD = 2

COPIES TO:

STOCK REQUIREMENTS				REQUIREMENTS PER STOCK				INVENTORY CONTROL			PRODUCTION REMARKS	OFFER	ROUTE TO	SHOP REMARKS	
S	NO. REQ'D	STOCK LENGTH	SHAPE	SIZE	GR.	NO. REQ'D	LENGTH	MARK	TOTAL PCS TO SHOP	FALLOFF					FROM BAY
S	1	13-6	W	14 x 730		1	3-4'4	D1	1	2	41		DL	F	27725
S	1	11-2	W			3	2-8'8	B1	3	2 3 4 5 6 14 15 7 8 9 10 11 12 13 14					27725
S	1	11-2	W			3	2-8'8	B1	3		41				27726
S	1	11-1	W			4	2-8'8	B1	4		41				27723
S	1	8-0	W			1	3-4'4	C1	1		45				40694
S	1	8-0	W			1	2-8'8	A1	1						40694
S	1	F.O. 7-2	W			2	0-4	f6	2				SAW	F	40694
S	1	20-9	W	14 x 455		1	2-8'8	B1	1		45		DL	F	41099
S	1	20-9	W	14 x 455		4	3-4'4	BZ	4	7 8 9 10	33		DL	F	24788
S	1	37-0	W	14 x 159		2	0-4	g7	2				SAW	F	24788
S	1	37-0	W	14 x 159		10	3-4'4	c3	10	3 4 5 6 14 15 11 12 13 14	HLE		DL	F	287830
S	1	37-0	W	14 x 159		3	0-4	c7	3				SAW	F	287830

GRADE 50

GRADE 50

GRADE 50

**ENTERED**

OCT 12 2007

CONTRACT NO. 55747

GROUP NO. 1

PAGE 1

DATE TO SHOP

DRAWING NO.

DESCRIPTION OF WORK

Tag #:

P/N #:

Job #:

P/O #:

W/O #:

Qty:

**Sales Agent:**  
 Arcelor Commercial Sections S.A.  
 66, rue de Luxembourg  
 L-4221 ESCH-SUR-ALZETTE

**Plant:**  
 Differdange



**Arcelor Commercial Sections S.A.**  
 66, rue de Luxembourg, L-4221 Esch-sur-Alzette  
 R.C. Luxembourg Section B 36177

**Certificate Nr X 1061588**  
 Delivery note number 1061588 from 22 February 2007

Our reference : 1700005552  
 Your reference : 70086 *50#6-13*  
 17.11.2006  
 Consignee : W & W Steel Co.

Arcelor International America, LLC  
 Mill business, Long Products  
 350 Hudson Street  
 NEW YORK NY 10014  
 USA

ASTM A913 GRADE 65 / FINE GRAIN SILICON KILLED

Manufacturer's test certificate acc. to ASTM A 6

Ord. Item	Product	Length	Weight	Heat nr	Weight	Sund.	Bars
000001	W 14 X 16 X 730 W 360 X 410 X 1086	54' 16.459 mm	17,881 mt	40694	17,881 mt		1

Heat nr	Heat analysis (%)												
	C	Mn	P	S	Si	Cu	Ni	Cr	V	Nb	Mo	CEV	
	Min 0,10												
	Max 0,16 1,60 0,030 0,030 0,40 0,35 0,25 0,25 0,060 0,050 0,070 0,43												
40694	0,09 1,52 0,016 0,030 0,19 0,28 0,14 0,13 0,059 0,003 0,035 0,42												

Heat nr	Tensile test		
	PSI	PSI 200 mm	
	Ys	UTS	El. (%)
	Min 65.000 80.000 15,00		
	Max 71.340 91.350 20,81		
40694	71.340 91.350 20,81		
40694	71.050 90.625 20,11		

**C. NELMS**

Bettendorff Julien  
 Porteur de signature spéciale



Tag #:

P/N #:

Job #:

P/O #:

W/O #:

Qty:

<b>Sales Agent:</b> Arcelor Commercial Sections S.A. 66, rue de Luxembourg L-4221 ESCH-SUR-ALZETTE		 <b>Arcelor Commercial Sections S.A.</b> 66, rue de Luxembourg, L-4221 Esch-sur-Alzette R.C. Luxembourg Section B 36.177																																	
<b>Plant:</b> Differdange																																			
Our reference : 1700005377 Your reference : 70036 11.09.2006 Consignee : W & W Steel Co.		<b>Certificate Nr X 1022355</b> Delivery note number 1022355 from 22 December 2006																																	
ASTM A 992 - FINE GRAIN SILICOM KILLED.		Arcelor International America, LLC Mill business, Long Products 350 Hudson Street NEW YORK NY 10014 USA																																	
Manufacturer's test certificate acc. to ASTM A 6																																			
<table border="1"> <thead> <tr> <th>Ord. Item</th> <th>Product</th> <th>Length</th> <th>Weight</th> <th>Heat nr</th> <th>Weight</th> <th>Bund.</th> <th>Bars</th> </tr> </thead> <tbody> <tr> <td>000004</td> <td>W 40 X 16 X 593 W 1000 X 400 X 883</td> <td>60' 18.288 mm</td> <td>16,139 mt</td> <td>27214</td> <td>16,139 mt</td> <td></td> <td>1</td> </tr> <tr> <td>000005</td> <td>W 40 X 16 X 503 W 1000 X 400 X 748</td> <td>61' 18.593 mm</td> <td>13,918 mt</td> <td>27669</td> <td>13,918 mt</td> <td></td> <td>1</td> </tr> <tr> <td>000006</td> <td>W 14 X 16 X 730 W 360 X 410 X 1086</td> <td>52' 15.850 mm</td> <td>34,438 mt</td> <td>27723 27725</td> <td>17,219 mt 17,219 mt</td> <td></td> <td>1 1</td> </tr> </tbody> </table>				Ord. Item	Product	Length	Weight	Heat nr	Weight	Bund.	Bars	000004	W 40 X 16 X 593 W 1000 X 400 X 883	60' 18.288 mm	16,139 mt	27214	16,139 mt		1	000005	W 40 X 16 X 503 W 1000 X 400 X 748	61' 18.593 mm	13,918 mt	27669	13,918 mt		1	000006	W 14 X 16 X 730 W 360 X 410 X 1086	52' 15.850 mm	34,438 mt	27723 27725	17,219 mt 17,219 mt		1 1
Ord. Item	Product	Length	Weight	Heat nr	Weight	Bund.	Bars																												
000004	W 40 X 16 X 593 W 1000 X 400 X 883	60' 18.288 mm	16,139 mt	27214	16,139 mt		1																												
000005	W 40 X 16 X 503 W 1000 X 400 X 748	61' 18.593 mm	13,918 mt	27669	13,918 mt		1																												
000006	W 14 X 16 X 730 W 360 X 410 X 1086	52' 15.850 mm	34,438 mt	27723 27725	17,219 mt 17,219 mt		1 1																												
<b>Heat nr</b>		<b>Heat analysis (%)</b>																																	
		C	Mn	P	S	Si	N	Cu	Ni	Cr	V	Nb	Mo	CEV	Sn	Nb+V																			
Min		0,50		0,10																															
Max		0,23	1,50	0,035	0,045	0,40		0,60	0,45	0,35	0,150	0,050	0,150	0,47	0,150																				
27214		0,16	1,35	0,019	0,031	0,19	0,011	0,15	0,10	0,14	0,089	0,000	0,040	0,46	0,01	0,089																			
27669		0,08	1,08	0,017	0,030	0,15	0,008	0,15	0,12	0,15	0,003	0,004	0,070	0,32	0,01	0,007																			
27723		0,09	1,06	0,016	0,030	0,18	0,011	0,19	0,10	0,11	0,036	0,001	0,025	0,33	0,01	0,037																			
27725		0,09	1,07	0,013	0,026	0,17	0,009	0,22	0,10	0,07	0,037	0,001	0,020	0,32	0,01	0,038																			
<b>Heat nr</b>		<b>Tensile test</b>																																	
		PSI	PSI 200 mm																																
		Ys	UTS	El. (%)	Y/U																														
Min		50.000	65.000	18,00																															
Max		65.000		0,85																															
27214		61.480	87.725	20,71	0,70																														
27214		60.320	85.985	20,00	0,70																														
27669		59.595	80.185	22,45	0,74																														
27669		55.245	74.965	23,83	0,74																														
27723		59.450	82.215	18,48	0,72																														
27723		59.885	81.780	20,79	0,73																														
Bettendorff Julien Porteur de signature spéciale 		6-13																																	

Tag #:  
P/O #:  
Qty:

P/N #:

Job #:  
W/O #:

<b>Sales Agent:</b> Arcelor Commercial Sections S.A. 66, rue de Luxembourg L-4221 ESCH-SUR-ALZETTE	 Arcelor Commercial Sections S.A. 66, rue de Luxembourg, L-4221 Esch-sur-Alzette B.C. Luxembourg, Section B-35.177
<b>Plant:</b> Differdange	<b>Certificate Nr X 1020817</b> Delivery note number 1020817 from 20 December 2008

Our reference : 1700005377  
 Your reference : 70038 *Job # 6-13*  
 11.09.2006  
 Consignee : W & W Steel Co.

ASTM A 992 - FINE GRAIN SILICON KILLED.

Manufacturer's test certificate acc. to ASTM A 6

Arcelor International America, LLC  
 Mill business, Long Products  
 350 Hudson Street  
 NEW YORK NY 10014  
 USA

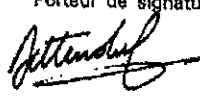
**C. NELMS**

Ord. Item	Product	Length	Weight	Heat nr	Weight	Bund.	Bars
000004	W 40 X 16 X 593 W 1000 X 400 X 883	60' 18.288 mm	16,139 mt	27658	16,139 mt		1
000008	W 14 X 16 X 730 W 360 X 410 X 1086	52' 15.850 mm	51,657 mt	27709 27724 27725	17,219 mt 17,219 mt 17,219 mt		1 1 1

Heat nr	Heat analysis (%)														
	C	Mn	P	S	Si	N	Cu	Ni	Cr	V	Nb	Mo	CEV	Sn	Nb+V
	Min	0,50			0,10										
	Max	0,23	1,50	0,035	0,045	0,40	0,60	0,45	0,35	0,150	0,050	0,150	0,47	0,150	
27658		0,17	1,35	0,013	0,024	0,19	0,012	0,12	0,10	0,10	0,088	0,001	0,038	0,45	0,01
27709		0,09	1,08	0,012	0,029	0,18	0,007	0,16	0,11	0,08	0,038	0,002	0,031	0,32	0,01
27724		0,11	1,07	0,014	0,030	0,19	0,010	0,18	0,11	0,09	0,036	0,001	0,022	0,33	0,01
27725		0,09	1,07	0,013	0,026	0,17	0,009	0,22	0,10	0,07	0,037	0,001	0,020	0,32	0,01

Heat nr	Tensile test				
	PSI	PSI 200 mm	UTS	EL. (%)	
	Ys	Y/T			
	Min	50.000	65.000	18,00	
	Max	65.000			0,85
27658		63.655	87.000	19,40	0,73
27658		61.190	86.710	18,63	0,71
27709		58.580	79.170	21,07	0,74
27709		57.420	77.575	21,00	0,74
27724		62.350	83.955	21,47	0,74
27724		60.320	80.910	21,63	0,75
27725		58.000	78.445	20,19	0,74
27725		61.625	84.680	19,13	0,73

Bettendorff Julien  
 Porteur de signature spéciale



*6-13*

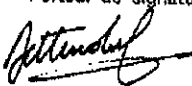
Tag #:  
P/O #:  
Qty:

P/N #:

Job #:  
W/O #:

<p><b>Sales Agent:</b> Arcelor Commercial Sections S.A. 66, rue de Luxembourg L-4221 ESCH-SUR-ALZETTE</p> <p><b>Plant:</b> Differdange</p>	 <b>Arcelor Commercial Sections S.A.</b> 66, rue de Luxembourg, L-4221 Esch-sur-Alzette P.O. Luxembourg Section B 36177																																																				
<p><b>Certificate Nr X 1022515</b> Delivery note number 1022515 from 22 December 2006</p>																																																					
<p>Our reference : 1700005377 Your reference : 70036 11.09.2006 Consignee : W &amp; W Steel Co.</p>	<p><b>Arcelor International America, LLC</b> Mill business, Long Products 350 Hudson Street NEW YORK NY 10014 USA</p>																																																				
<p><b>ASTM A 992 - FINE GRAIN SILICON KILLED.</b></p>																																																					
<p>Manufacturer's test certificate acc. to ASTM A 6</p>																																																					
<table border="1" style="width:100%; border-collapse: collapse;"> <thead> <tr> <th>Ord.item</th> <th>Product</th> <th>Length</th> <th>Weight</th> <th>Heat nr</th> <th>Weight</th> <th>Bund.</th> <th>Bars</th> </tr> </thead> <tbody> <tr> <td rowspan="2">000005</td> <td>W 40 X 18 X 503</td> <td>61'</td> <td rowspan="2">27,836 mt</td> <td></td> <td></td> <td></td> <td></td> </tr> <tr> <td>W 1000 X 400 X 748</td> <td>18.593 mm</td> <td>27668</td> <td>13,918 mt</td> <td></td> <td>1</td> </tr> <tr> <td></td> <td></td> <td></td> <td></td> <td>27669</td> <td>13,918 mt</td> <td></td> <td>1</td> </tr> <tr> <td rowspan="2">000006</td> <td>W 14 X 16 X 730</td> <td>52'</td> <td rowspan="2">34,438 mt</td> <td></td> <td></td> <td></td> <td></td> </tr> <tr> <td>W 360 X 410 X 1086</td> <td>15.850 mm</td> <td>27725</td> <td>17,219 mt</td> <td></td> <td>1</td> </tr> <tr> <td></td> <td></td> <td></td> <td></td> <td>27726</td> <td>17,219 mt</td> <td></td> <td>1</td> </tr> </tbody> </table>		Ord.item	Product	Length	Weight	Heat nr	Weight	Bund.	Bars	000005	W 40 X 18 X 503	61'	27,836 mt					W 1000 X 400 X 748	18.593 mm	27668	13,918 mt		1					27669	13,918 mt		1	000006	W 14 X 16 X 730	52'	34,438 mt					W 360 X 410 X 1086	15.850 mm	27725	17,219 mt		1					27726	17,219 mt		1
Ord.item	Product	Length	Weight	Heat nr	Weight	Bund.	Bars																																														
000005	W 40 X 18 X 503	61'	27,836 mt																																																		
	W 1000 X 400 X 748	18.593 mm		27668	13,918 mt		1																																														
				27669	13,918 mt		1																																														
000006	W 14 X 16 X 730	52'	34,438 mt																																																		
	W 360 X 410 X 1086	15.850 mm		27725	17,219 mt		1																																														
				27726	17,219 mt		1																																														
Heat nr	Heat analysis (%)																																																				
	C	Mn	P	S	Si	N	Cu	Ni	Cr	V	Nb	Mo	CEV	Sn	Nb+V																																						
	Min	0,50			0,10																																																
	Max	0,23	1,50	0,035	0,045	0,40	0,60	0,45	0,35	0,150	0,050	0,150	0,47	0,150																																							
27668		0,09	1,00	0,017	0,025	0,24	0,010	0,17	0,16	0,16	0,003	0,007	0,055	0,32	0,01																																						
27669		0,08	1,08	0,017	0,030	0,16	0,008	0,15	0,12	0,15	0,003	0,004	0,070	0,32	0,01																																						
27725		0,09	1,07	0,013	0,026	0,17	0,009	0,22	0,10	0,07	0,037	0,001	0,020	0,32	0,01																																						
27726		0,09	1,11	0,016	0,028	0,19	0,010	0,31	0,15	0,08	0,038	0,001	0,028	0,34	0,01																																						
Heat nr	Tensile test																																																				
	PSI	PSI 200 mm																																																			
	Ys	UTS El. (%)		Y/U																																																	
	Min	50.000	65.000	18,00																																																	
	Max	65.000		0,85																																																	
27668		59.740	79.750	21,28	0,75																																																
27668		62.930	82.650	18,68	0,76																																																
27669		59.595	80.185	22,45	0,74																																																
27669		55.245	74.965	23,83	0,74																																																
27725		58.000	78.445	20,19	0,74																																																
27725		61.625	84.680	19,13	0,73																																																
27726		59.885	80.910	25,24	0,74																																																
27726		61.770	82.070	23,45	0,75																																																

Bettendorff Julien  
Porteur de signature spéciale



6-13

Tag #:

P/N #:

Job #:

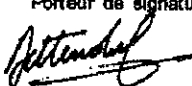
P/O #:

W/O #:

Qty:

<b>Représentant:</b> Arcelor Commercial Sections S.A. 66, rue de Luxembourg L-4221 ESCH-SUR-ALZETTE  <b>Site:</b> Differdange		 <b>Arcelor Commercial Sections S.A.</b> 66, rue de Luxembourg, L-4221 Esch-sur-Alzette R.C. Luxembourg Section B 36.177													
Our reference : 1700005677 Your reference : 70112 18.12.2006 Consignee : W & W Steel Co.		<b>Certificate Nr X 1071933</b> Delivery note number 1071933 from 8 March 2007													
<b>ASTM A913 GRADE 55 / FINE GRAIN SILICON KILLED</b>		Arcelor International America, LLC Mill business, Long Products 350 Hudson Street NEW YORK NY 10014 USA													
Manufacturer's test certificate acc. to ASTM A 8															
Ord. Num	Product	Length	Weight	Heat nr	Weight	Bund.	Bars								
000024	W 14 X 16 X 730 W 360 X 410 X 1086	36' 10.973 mm	11,921 mt	41099	11,921 mt		1								
Heat nr	Heat analysis (%)														
	C	Mn	P	S	Si	Cu	Ni	Cr	V	Nb	Mo	CEV			
	Min	0,10													
	Max	0,16	1,60	0,030	0,030	0,40	0,25	0,25	0,060	0,050	0,070	0,43			
41099		0,10	1,56	0,015	0,030	0,22	0,18	0,14	0,11	0,059	0,002	0,040	0,42		
Heat nr	Tensile test														
	PSI	PSI 200 mm	Ys	UTS El. (%)											
	Min	65.000	60.000	15,00											
	Max														
41099		69.890	89.900	20,94											
41099		69.455	88.595	21,17											

6-13

Bettendorff Julien  
 Porteur de signature spéciale  


Tag #:

P/N #:

Job #:

P/O #:

W/O #:

Qty:

RELEVÉ DE CONTROLE - MILL'S TEST CERTIFICATE WERKSZEUGNIS		PAGE 1																					
PROFILARBED GESTION QUALITE(5) L 4503 DIFFERDANGE GRAND-DUCHE DE LUXEMBOURG		ADVICE NR : 550300 20010802																					
MANUFACTURER'S TEST CERTIFICATE TO ASTM A 6 - PAR. 18. ASTM A992/98 - ASTM A572/99A GR50 FINE GRAIN SILICON KILLED ORDER NO. : 01 ZE 3015 001 CUSTOMER NR : 40097 UTILISATEUR : WMSTEEL W & W STEEL CO.																							
TRADEARBED INC., NEW YORK THIRD AVENUE, 825 US-NEW YORK, NY 10022 U.S.A. (EAST C)																							
ITEM NR ADV./ORDER	PRODUCT	SIZE	LENGTH	WEIGHT	KG	PA	LI	BUN	PCS														
001-003	W-BEAMS	W 14 X 16 X 455	42,33'	8737					1														
002-001	W-BEAMS	W 14 X 16 X 500	48,33'	10962					1														
003-003	W-BEAMS	W 14 X 16 X 455	42,33'	8737					1														
004-003	W-BEAMS	W 14 X 16 X 455	42,33'	8737					1														
NO/NR HEAT	C	MN	P	S	SI	HEAT	A	N	A	L	V	S	I	S	CR	V	NI	CR	( % ) MO	NB	CEQ	WEIGHT KG	PCS
24788	0,08	1,10	0,025	0,007	0,18	0,17	0,07	0,13	0,002	0,014	0,018	0,31	8737	1									
24745	0,08	1,11	0,017	0,008	0,19	0,13	0,05	0,09	0,002	0,015	0,008	0,30	10962	1									
24744	0,09	1,20	0,023	0,007	0,19	0,27	0,12	0,12	0,003	0,016	0,025	0,35	8737	1									
24788	0,08	1,10	0,025	0,007	0,18	0,17	0,07	0,13	0,002	0,014	0,018	0,31	8737	1									
NO/NR HEAT	TENSILE TEST																						
	PSI	PSI	200MM	E/R																			
	YS	UTS	EL.(%)	%																			
001-WA0621	64.670	82.360	22,0	0,78																			
002-WA0301	60.030	74.820	26,0	0,80																			
003-WA0171	63.510	81.635	22,0	0,78																			
004-WA0621	64.670	82.360	22,0	0,79																			

P.O. 40097  
L1-18



MULLER GAETAN  
PORTEUR DE SIGNATURE SPECIALE

Tag #:

P/N #:

Job #:

P/O #:

W/O #:

Qty:

2-

RELEVÉ DE CONTRÔLE - MILL'S TEST CERTIFICATE WERKSZEUGNIS		PAGE 2 ADVICE NR : 550300 20010802
MANUFACTURER'S TEST CERTIFICATE TO ASTM A 8 - PAR. 18. ASTM A992/98 - ASTM A572/99A GR50 FINE GRAIN SILICON KILLED		
ORDER NO. : 01 ZE 3015 001 CUSTOMER NR : 40097 UTILISATEUR : WASTEEL W & W STEEL CO.	TRADEARBED INC., NEW YORK THIRD AVENUE, 825 US-NEW YORK, NY 10022 U.S.A. (EAST C)	
PROFILARBED GESTION QUALITE(S) L 4503 DIFFERDANGE GRAND-DUCHE DE LUXEMBOURG		
ITEM NR ADV./ORDER	NO/NR HEAT	COMPLEMENTARY HEAT ANALYSIS ( % )
001-003	24788	0.024 SN NB + V
001-003	24788	0.016 SN NB + V
002-001	24745	0.007 SN NB + V
002-001	24745	0.017 SN NB + V
003-003	24744	0.014 SN NB + V
003-003	24744	0.019 SN NB + V
004-003	24788	0.024 SN NB + V
004-003	24788	0.016 SN NB + V



MULLER GAETAN

PORTEUR DE SIGNATURE SPECIALE

Tag #:

P/N #:

Job #:

P/O #:

W/O #:

Qty:

**NUCOR-YAMATO STEEL CO.**

P O BOX 1228  
BLYTHEVILLE AR 72316

DATE  
12/22/06

**CERTIFIED MILL TEST REPORT**

100% MELTED AND MANUFACTURED IN U.S.A

All shapes produced by Nucor-Yamato Steel are cast and rolled to a fully killed and fine grain practice.

**SOLD TO**

W & W STEEL CO.-OKC  
1730 W. RENO  
PO BOX 25369  
OKLAHOMA CITY, OK 73125

**SHIP TO**

W & W STEEL CO.-OKC  
1730 W. RENO  
PO BOX 25369  
OKLAHOMA CITY, OK 73125

INVOICE 104035	CUSTOMER NO. 1549
BILL OF LADING 822881	CUSTOMER NO. 70067

*Handwritten:* 104035

**SPECIFICATIONS GRADE:** ASTM A992/A992M-06a A572/A572M GR50-04 ASTM A709/A709M-03a GR50 (345)  
ASTM A709/A709M-03a GR50S (345S) ASTM A6/A6M-05a

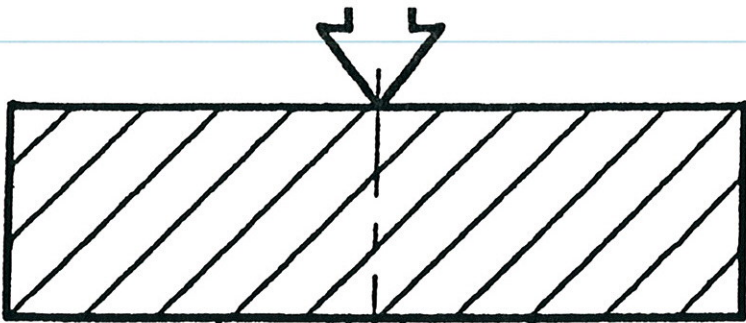
ITEM	ITEM DESCRIPTION	QTY	HEAT #	MECHANICAL PROPERTIES								CHEMICAL PROPERTIES											
				TENSILE TO TENSILE EXTEN	YIELD STRENGTH F <sub>0.2</sub> MPa	TENSILE STRENGTH F <sub>T</sub> MPa	ELONG % K	CHARPY IMPACT		C	Mn	P	S	Si	Cu	Ni	Cr	Mo	V	Cb	CE		
								TEMP F	IMPACT ENERGY FT-LBS Joules														
1	W14 -159.0 35' 4" W360 x237.0 10.770 M	1	287828	.78	58000	74000	29					.081	.30	.022	.024	.19	.32	.12	.16	.03	.00	.019	.37
2	W14 -159.0 37' W360 x237.0 11.278 M	3	287830	.77	56000	73000	29					.071	.32	.023	.025	.20	.32	.11	.18	.03	.00	.018	.36
3	W14 -159.0 37' W360 x237.0 11.278 M	2	287840	.77	58000	75000	29					.081	.31	.016	.021	.20	.27	.10	.12	.03	.00	.020	.35

ELONGATION BASED ON 8.00 INCH GAUGE LENGTH  
 $CE = C + Mn/6 + (Cr+Mo+V) / 5 + (Ni+Cu) / 15$   
 $Pcm = C+Si / 30 + Mn / 20 + Cu / 20 + Ni / 60 + Cr / 20 + Mo / 15 + V / 10 + 5B \approx .005$   
 Corrosion Index:  $CI = 26.01(\%Cu) + 3.88(\%Ni) + 1.2(\%Cr) + 1.49(\%Si) + 17.28(\%P) - 7.29(\%Cu)(\%Ni) - 9.10(\%Ni)(\%P) - 33.39(\%Cu)^2$

I hereby certify that the contents of this report are accurate and correct. All test results and evaluations performed by this material manufacturer are in compliance with the requirements of the material specifications, and when designated by the purchaser, meet the applicable specifications.

GARY PENNELL  
QUALITY ASSURANCE

STATE OF ARKANSAS  
COUNTY OF MISSISSIPPI  
SWORN TO AND SUBSCRIBED BEFORE ME THIS  
Day of \_\_\_\_\_



"CONTROL" BOLTS

MK - 1C  
W14x73Ø A992

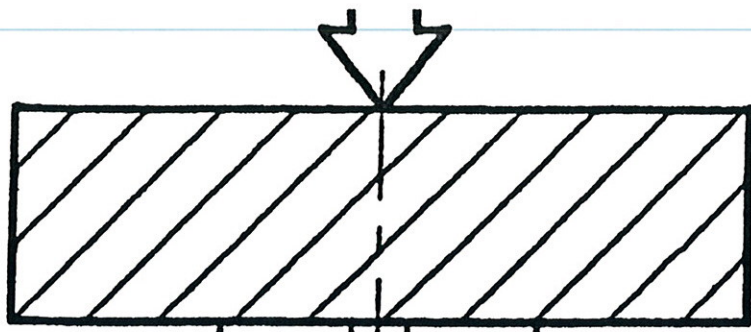
MK - 1A  
W14x73Ø A992

MK - 4A  
PL2x16<sup>3</sup>/<sub>4</sub>x4'-4<sup>1</sup>/<sub>2</sub>'  
GR 5Ø (TYP)

3 3<sup>3</sup>/<sub>4</sub> 3<sup>3</sup>/<sub>4</sub> 3

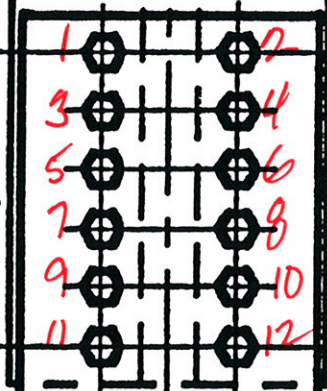
88-1<sup>1</sup>/<sub>8</sub>x9' A4  
w/ (2) 3<sup>3</sup>/<sub>16</sub>"

WISC SLIP CRITICAL TEST CONNE

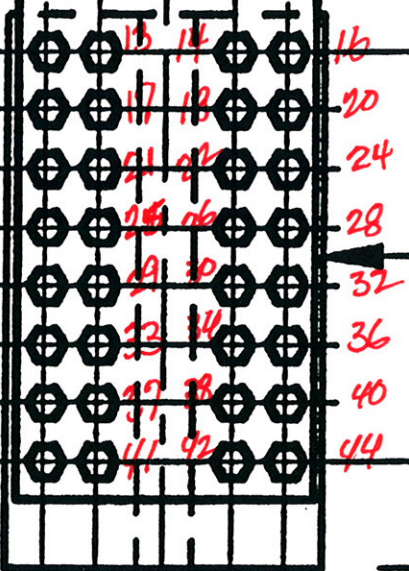


BOLT TORQUING SEQUENCE

MK - 1C  
W14x73Ø A992



MK - 1A  
W14x73Ø A992

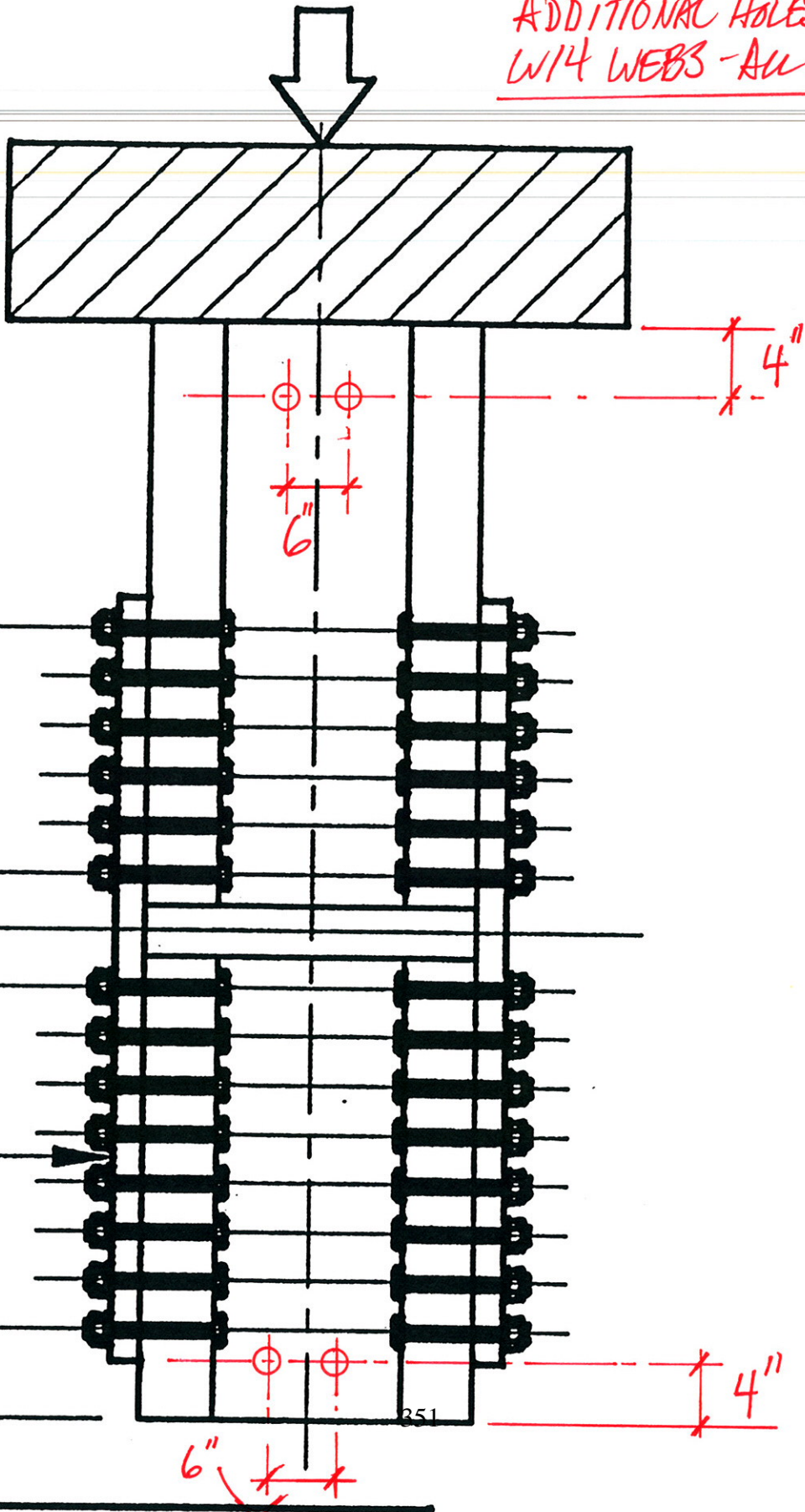


MK - 4A  
PL2x16<sup>3</sup>/<sub>4</sub>x4'-4<sup>1</sup>/<sub>2</sub>  
GR 50 (TYP)

3    3<sup>3</sup>/<sub>4</sub>    3<sup>3</sup>/<sub>4</sub>    3

88-1<sup>1</sup>/<sub>2</sub>x9' A4  
w/ (2) <sup>3</sup>/<sub>16</sub>"

ADDITIONAL HOLES FOR  
W/4 WEBS - ALL SPECIMENS



K - 4A  
6<sup>3</sup>/<sub>4</sub> x 4' - 4<sup>1</sup>/<sub>2</sub>  
3Ø (TYP)

**3,000,000-LB SOUTHWARK-EMERY TESTING  
MACHINE CALIBRATION REPORT**

UNIVERSITY OF ILLINOIS  
AT URBANA-CHAMPAIGN

James W. Phillips, Ph.D., P.E.  
Department of Mechanical Science and Engineering  
158 Mechanical Engineering Building  
1206 West Green Street  
Urbana, IL 61801-2906

## 2007 Calibration Report on the 3,000,000-lb Southwark-Emery Tension/Compression Machine

On January 9, 2007, the 1,000,000-lb hydraulic gage, the 3,000,000-lb hydraulic gage, and a Sensotec pressure transducer (Model A-5/743-03, 0–3000 psia) with an Omega strain-gage indicator (Model DP41-S) connected to the Tate-Emery hydraulic load cell on the 3,000,000-lb Southwark-Emery universal testing machine in Talbot Laboratory were calibrated by means of a strain-gaged load cell that had been calibrated by the National Institute of Standards and Technology, Gaithersburg, Md., in 2002, according to ASTM standard procedures E4-91 and E74-91, as applicable to load cells exceeding 1,000,000-lb capacity. This memorandum sets forth the procedures and results of the calibration.

### Procedure

1. The load-cell indicator (Interface Model 9840, Serial No. 90070) was first calibrated by means of an NIST-calibrated precision resistor box (Micromeritics Model 1550A, Serial No. 135879), which was certified to be calibrated by Micro-Measurements in June 2005. The load-cell indicator was set so as to read directly in millivolts per volt (mV/V), from zero to approximately 4.9 mV/V in steps of 0.0001 mV/V. The results of this preliminary calibration are indicated in the accompanying table.

Calibration value, mV/V		Value read on indicator, mV/V
Nominal	Exact	
0	0.0000	0.0000
1	1.0000	1.0000
2	2.0000	2.0000
3	3.0000	3.0000
4	4.0000	3.9999
4.5	4.5000	4.5001

2. The load-cell indicator was connected to the NIST-calibrated load cell with the same 6-wire cable that was used by the National Institute of Standards and Technology during its calibration. Values of the compressive load applied to the load cell are determined from the relation

$$x = A + BP_1 + CP_1^2, \quad (1)$$

where  $x$  is the indicated reading in mV/V, and  $P_1$  is the temperature-uncorrected NIST-applied load, in kips. (One kip equals 1000 lb.) The coefficients  $A$ ,  $B$ , and  $C$  are given by the 2002 NIST calibration data as follows:

Load range, kips	$A$ mV/V	$B$ mV/V/kip	$C$ mV/V/kip <sup>2</sup>
0–1000	–0.00011	$1.51527 \times 10^{-3}$	$-0.00377 \times 10^{-6}$
0–3000	–0.00027	$1.51779 \times 10^{-3}$	$-0.004311 \times 10^{-6}$

For example, if a load cell not exceeding 1,000,000-lb capacity is being calibrated, the value of  $P_1$  for  $x = 1.5000$  mV/V is  $P_1 = 992.4$  kips; whereas if a load cell exceeding 1,000,000 lb capacity is being calibrated, the value of  $P_1$  for  $x = 1.5000$  mV/V is  $P_1 = 991.2$  kips. These values are determined by writing the solution to Eqn. (1) as:

$$P_1 = \frac{-B \pm \sqrt{B^2 - 4C(A-x)}}{2C}, \tag{2}$$

where the plus (+) sign should be used since  $P_1 = 0$  when  $x \cong A$ .

3. The actual load  $P$  acting on the load cell at the UIUC calibration temperature  $T$  was found by the relation

$$P = F \cdot P_1, \tag{3a}$$

where  $F$  is the ASTM E74-91 temperature correction factor

$$F = 1 - 0.000270(T - T_{NIST}) \tag{3b}$$

and  $T_{NIST}$  is the temperature at which the load cell was calibrated at the National Institute of Standards and Technology:

Load range, kips	UIUC temperature, $T$ (°C)	NIST temperature, $T_{NIST}$ (°C)	ASTM correction factor, $F$
0-1000	24.6	23.0	0.99957
0-3000	24.8	25.2	1.00016

For example, for the 1,000,000-lb load range at  $T = 24.6^\circ\text{C}$ , the corrected value  $P$  for  $x = 1.5000$  mV/V is  $P = (0.99957)(992.4) = 992.0$  kips; whereas, for the 3,000,000-lb load range at  $T = 24.6^\circ\text{C}$ , the corrected value  $P$  for  $x = 1.5000$  mV/V is  $P = (1.00016)(991.2) = 991.4$  kips.

A Hewlett-Packard calculator using reverse-Polish notation can be programmed to yield the value of the temperature-corrected  $P$  for any  $x$  as follows:

```

sto 0   Store x in Register 0 for recall if      +
necessary
ch $\sqrt{x}$ 
chs
rcl 1   Assume A is in Register 1              -
+
rcl 3   Assume C is in Register 3              2
 $\times$ 
 $\times$ 
4
 $\times$ 
ch $\div$ 
rcl 2   Assume B is in Register 2               $\times$ 
 $x^2$ 
f fix 1  $P$  is displayed in kips to the nearest 0.1 kip

```

4. Calibration data were taken at load increments according to the following table:

Load range, kips	Number of readings, including zero load	Load increment, kips
0-1000	11	100
0-3000	13	250

For each value of the Tate-Emery indicated load, the actual load  $P$  was determined from Eqns. (2) and (3) after the value of  $x$  had been read from the load-cell indicator.

**Results of the August 1983 Calibration using the First UIUC Reference Load Cell**

The August 1983 calibration of the Tate-Emery cell was the first known NIST (formerly National Bureau of Standards)-traceable calibration ever to be performed on the Southwark-Emery. Prior to 1983, annual consistency checks had been performed by means of a 0.0001-inch dial-gage indicator on a solid circular steel bar kept in Talbot Laboratory’s crane bay. The consistency checks showed that the Tate-Emery cell response had not changed over a 41-year period (1942–1983), even after the Tate-Emery diaphragm was replaced in the Spring of 1983.

It was found, in the 1983 calibration, that both the 1,000,000-lb gage and the 3,000,000-lb gage were extremely linear in their response to the load. Any nonlinearity in either gage’s response was masked by a seemingly reproducible deviation perhaps related to the pitch of the rack-and-pinion mechanism in

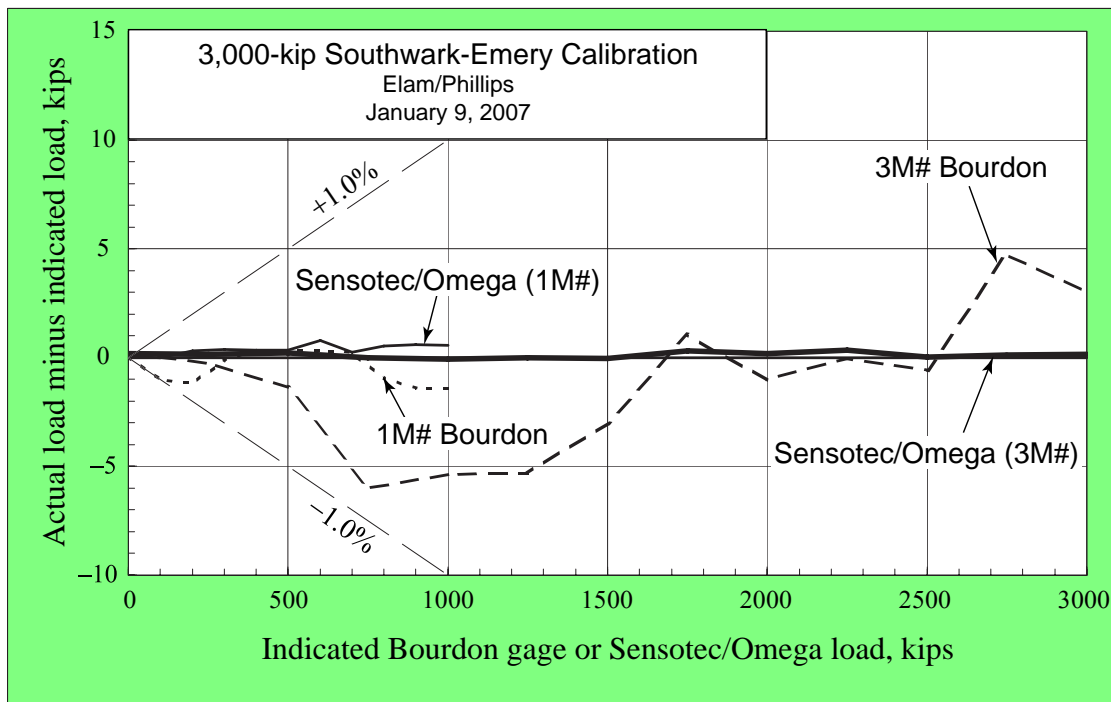


**Fig. 1. Plots of the deviation (actual load minus indicated load) as functions of the indicated load, for the 1,000,000-lb and 3,000,000-lb Bourdon gages and Sensotec transducer, after the January 9, 2007, calibration.**

each gage. This deviation was approximately  $\pm 1$  kip on the 1,000,000-lb gage and  $\pm 3$  kips on the 3,000,000-lb gage. Consequently, it can be stated that the precision of either gage is approximately 0.1% of the full-scale value.

As for accuracy, it was determined in the 1983 calibration that the 1,000,000-lb gage was reading low by approximately 0.5%, and that the 3,000,000-lb gage was reading low by approximately 1.2%, prior to calibration. The pre-calibration readings of the Tate-Emery gages were found to be conservative: if the indicated load on the 3,000,000-lb gage was 2.000 million pounds, for example, the actual load on the specimen was approximately  $1.012 \times 2.000$  million pounds or 2.024 million pounds. The indicated values on the 1,000,000-lb gage were also conservative, but to a lesser degree.

Both the 1,000,000-lb gage and the 3,000,000-lb gage were opened for inspection. The mechanisms were determined to be in good working order, although the 3,000,000-lb mechanism showed some bearing wear. For each gage, the lever-arm of the rack gear was adjusted with the aid of a vernier caliper to correct the scale factor. It was easier to adjust the 1,000,000-lb gage because its mechanism has

a lever-arm considerably longer than that of the 3,000,000-lb gage. Corrections to the lever-arm lengths are of the order of 0.001 inch, and fine adjustment of the 3,000,000-lb gage was found to be tedious.

As a result of the 1983 adjustment, the scale-factor errors were reduced to approximately 0.04% and 0.20%, respectively, for the 1,000,000-lb and 3,000,000-lb gages. The errors in both cases remained conservative, in the sense mentioned previously.

**Results of the January 2002 Calibration using a New UIUC Reference Load Cell**

In 2001, Mr. David Foley machined a new reference load cell—more compact than the first one—from Viscount 44, and instrumented it with sixteen 350Ω strain gages. It was sent to the National Institute of Standards and Technology for calibration by Mr. Rick Seifarth and returned in January 2002. Although the values of the *B* coefficients were somewhat larger than those of the first cell (since the cross-sectional

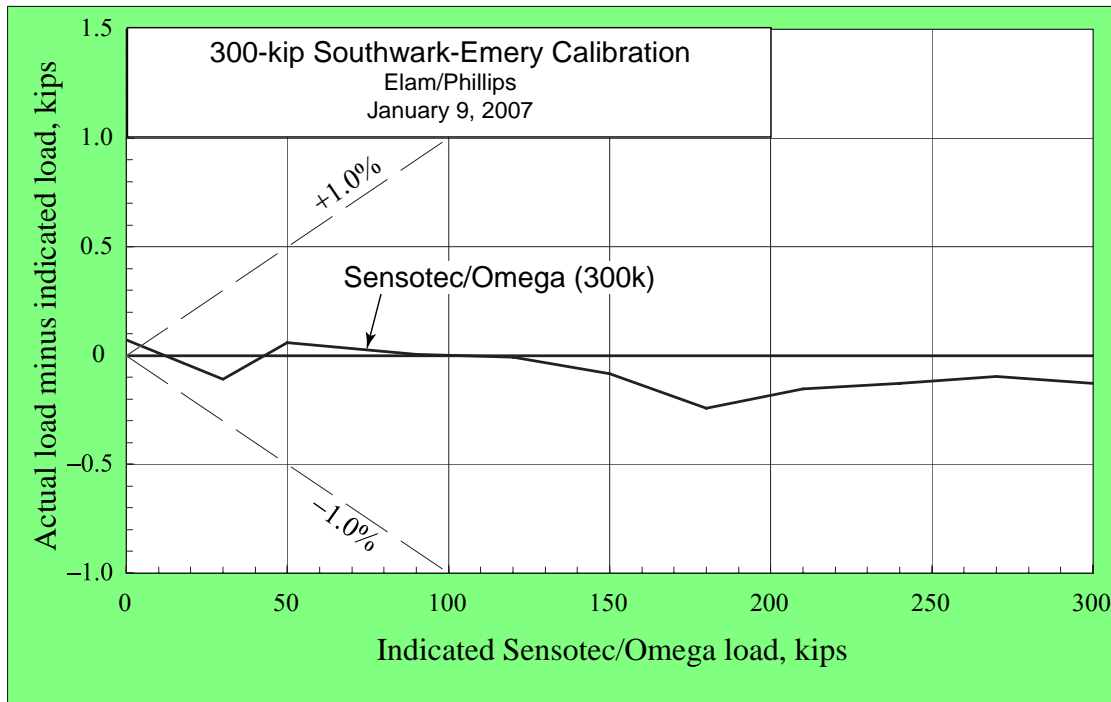


**Fig. 2. Plot of the deviation (actual load minus indicated load) as a function of the indicated load, for the 0–300-kip Sensotec transducer, after the January 9, 2007, calibration.**

area was smaller and the working stress correspondingly greater), the subsequent calibration of the Tate-Emery load cell produced essentially the same results as those of January 2001 using the former load cell. The former cell had been recalibrated by Mr. Seifarth in 1992, with less than 0.1% change in response from its 1983 calibration.

**Results of the Most Recent Tate-Emery Calibration**

The results of the calibration of the Tate-Emery load cell in the Southwark-Emery testing machine on January 9, 2007, are shown in Fig. 1. It will be seen that the response of the 1,000,000-lb Bourdon gage is characterized approximately by the relation

$$P = 1.000 I \pm 1 \text{ kip},$$

where *P* is the actual load on the specimen, and *I* is the indicated load on the gage. The corresponding relation for the 3,000,000-lb Bourdon gage is

$$P = 1.000 I \pm 5 \text{ kip}.$$

The Sensotec pressure transducer, installed in 1988 for the purpose of automated data acquisition, and augmented in July 1997 with an Omega DP41-S strain-gage indicator, has a nearly linear response given approximately by

$$P = 1.000 I \pm 1 \text{ kip} .$$

For both hydraulic gages, the precision of the readings is less than or equal to the smallest dial division. For the Sensotec/Omega readout, the precision is limited to 0.5 kip. The procedures in ASTM E4 (Load Verification of Testing Machines) require that the accuracy be stated as a percentage of the indicated reading, and that the range over which this accuracy holds also be stated. Accordingly, it can be stated that without any correction, the 1,000,000-lb Bourdon gage is accurate to within 0.5% over the range of 100 kips to 1000 kips. The 3,000,000-lb Bourdon gage is accurate to within 0.5% over the range of 300 kips to 3000 kips. The Sensotec/Omega readout system is accurate to within 1 kip, or 0.1% of the indicated load, whichever is larger, over the range from 0 to 3000 kips. It should be noted that ASTM E4 requires that the stated accuracy shall not exceed 1.0%.

**Low-range Calibration (0–300 kips)**

In January 2005, a separate load cell and readout were added to the common load-cell pressure manifold. The range of the new device, a Sensotec pressure transducer (Model A-5/8246-15, 0–300 psia) with an Omega strain-gage indicator (also a Model DP41-S), is 0–300 kips. The new device was then calibrated using the procedure outlined above, using the NIST calibration parameters for the 1,000,000-lb range of the UIUC reference load cell. The results for the January 9, 2007, calibration of this device are given in Fig. 2.

The response of the 0–300 kip readout is seen to be approximately

$$P = 0.999 I \pm 0.2 \text{ kip} ,$$

where, as before,  $I$  denotes the indicated load on the load-cell readout and  $P$  denotes the NIST-traceable load being applied. This readout system is accurate to within 0.2 kip, or 0.1% of the indicated load, whichever is larger, over the range from 0 to 300 kips.

The calibration procedure outlined in this memorandum meets the requirements of ASTM E4 and ASTM E74 (Calibration of Force-Measuring Instruments for Verifying the Load Indication of Testing Machines). It is recommended that the Tate-Emery load cell be recalibrated yearly.

  
\_\_\_\_\_  
James W. Phillips  
\_\_\_\_\_  
\_\_\_\_\_



## List of Recent NSEL Reports

<i>No.</i>	<i>Authors</i>	<i>Title</i>	<i>Date</i>
001	Nagayama, T. and Spencer, B.F.	Structural Health Monitoring Using Smart Sensors	Nov. 2007
002	Sun, S. and Kuchma, D.A.	Shear Behavior and Capacity of Large-Scale Prestressed High-Strength Concrete Bulb-Tee Girders	Nov. 2007
003	Nagle, T.J. and Kuchma, D.A.	Nontraditional Limitations on the Shear Capacity of Prestressed, Concrete Girders	Dec. 2007
004	Kwon, O-S. and Elnashai, A.S.	Probabilistic Seismic Assessment of Structure, Foundation, and Soil Interacting Systems	Dec. 2007
005	Nakata, N., Spencer, B.F., and Elnashai, A.S.	Multi-dimensional Mixed-mode Hybrid Simulation: Control and Applications	Dec. 2007
006	Carrion, J. and Spencer, B.F.	Model-based Strategies for Real-time Hybrid Testing	Dec. 2007
007	Kim, Y.S., Spencer, B.F., and Elnashai, A.S.	Seismic Loss Assessment and Mitigation for Critical Urban Infrastructure Systems	Jan. 2008
008	Gourley, B.C., Tort, C., Denavit, M.D., Schiller, P.H., and Hajjar, J.F.	A Synopsis of Studies of the Monotonic and Cyclic Behavior of Concrete-Filled Steel Tube Members, Connections, and Frames	April 2008
009	Xu, D. and Hjelmstad, K.D.	A New Node-to-node Approach to Contact/Impact Problems for Two Dimensional Elastic Solids Subject to Finite Deformation	May 2008
010	Zhu, J. and Popovics, J.S.	Non-contact NDT of Concrete Structures Using Air Coupled Sensors	May 2008
011	Gao, Y. and Spencer, B.F.	Structural Health Monitoring Strategies for Smart Sensor Networks	May 2008
012	Andrews, B., Fahnestock, L.A. and Song, J.	Performance-based Engineering Framework and Ductility Capacity Models for Buckling-Restrained Braces	July 2008
013	Pallarés, L. and Hajjar, J.F.	Headed Steel Stud Anchors in Composite Structures: Part I – Shear	April 2009
014	Pallarés, L. and Hajjar, J.F.	Headed Steel Stud Anchors in Composite Structures: Part II – Tension and Interaction	April 2009
015	Walsh, S. and Hajjar, J.F.	Data Processing of Laser Scans Towards Applications in Structural Engineering	June 2009
016	Reneckis, D. and LaFave, J.M.	Seismic Performance of Anchored Brick Veneer	August 2009
017	Borello, D.J., Denavit, M.D., and Hajjar, J.F.	Behavior of Bolted Steel Slip-critical Connections with Fillers	August 2009